RECEIVED BY TIC MAR 0 5 1984

CONF-830483--Vol.2

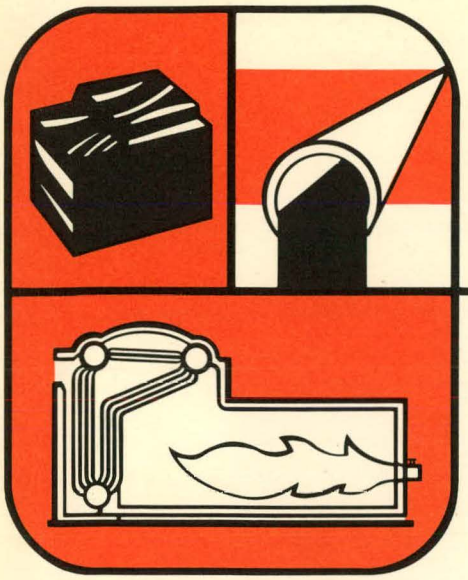

PROCEEDINGS
Volume 2

DO NOT MICROFILM
COVER

Fifth International Symposium on

Coal Slurry Combustion and Technology

April 25-27, 1983
Tampa, Florida

MASTER

United States Department of Energy
Pittsburgh Energy Technology Center
Pittsburgh, Pennsylvania

DISTRIBUTION OF THIS DOCUMENT IS UNLIMITED

DISCLAIMER

This report was prepared as an account of work sponsored by an agency of the United States Government. Neither the United States Government nor any agency Thereof, nor any of their employees, makes any warranty, express or implied, or assumes any legal liability or responsibility for the accuracy, completeness, or usefulness of any information, apparatus, product, or process disclosed, or represents that its use would not infringe privately owned rights. Reference herein to any specific commercial product, process, or service by trade name, trademark, manufacturer, or otherwise does not necessarily constitute or imply its endorsement, recommendation, or favoring by the United States Government or any agency thereof. The views and opinions of authors expressed herein do not necessarily state or reflect those of the United States Government or any agency thereof.

DISCLAIMER

Portions of this document may be illegible in electronic image products. Images are produced from the best available original document.

DO NOT MICROFILM
COVER

United States Department of Energy
Pittsburgh Energy Technology Center
Dr. Sun W. Chun, Director

For additional symposium information, contact:
Charles A. Thomas, Symposium Chairman
Pittsburgh Energy Technology Center
United States Department of Energy
P.O. Box 10940
Pittsburgh, Pennsylvania 15236
(412) 675-5731

CONF-830483--Vol.2

DE84 007931

NOTICE
PORTIONS OF THIS REPORT ARE ILLEGIBLE
It has been reproduced from the best available copy to permit the broadest possible availability.

FIFTH INTERNATIONAL SYMPOSIUM

ON

COAL SLURRY COMBUSTION

Hyatt Regency, Tampa, Florida

April 25-27, 1983

OPENING REMARKS
Charles A. Thomas, *Symposium Chairman*
Pittsburgh Energy Technology Center, DOE

WELCOMING ADDRESS
Dr. Sun W. Chun, *Director*
Pittsburgh Energy Technology Center, DOE

KEYNOTE SPEAKER
Donald L. Bauer, *Deputy Assistant Secretary*
for Fossil Energy, DOE

PROCEEDINGS OVERVIEW
(Gray Pages Divide Sessions)

VOLUME I SESSIONS

I Slurry Preparation and Handling Techniques—Laboratory and Commercial-Scale

II Additives Considerations

III Beneficiation

IV Economics and Commercialization

V Demonstration Projects

VI Equipment

VOLUME II SESSIONS

VII Bench Scale Testing

VIII Pilot Testing

IX Combustion

X Rheology and Characterization

DISCLAIMER

This report was prepared as an account of work sponsored by an agency of the United States Government. Neither the United States Government nor any agency thereof, nor any of their employees, makes any warranty, express or implied, or assumes any legal liability or responsibility for the accuracy, completeness, or usefulness of any information, apparatus, product, or process disclosed, or represents that its use would not infringe privately owned rights. Reference herein to any specific commercial product, process, or service by trade name, trademark, manufacturer, or otherwise does not necessarily constitute or imply its endorsement, recommendation, or favoring by the United States Government or any agency thereof. The views and opinions of authors expressed herein do not necessarily state or reflect those of the United States Government or any agency thereof.

DISTRIBUTION OF THIS DOCUMENT IS UNLIMITED

TABLE OF CONTENTS
VOLUMES I and II

Volume I

SESSION I—SLURRY PREPARATION AND HANDLING TECHNIQUES
LABORATORY AND COMMERCIAL—SCALE
Monday, April 25, 1983
Chairman: Gary E. Voelker, Department of Energy

CoaLiquid Coal Slurry Program—1983
G. T. Hawkins—CoaLiquid, Inc. 3
Coal—#2 Oil Mixtures—Pipelining and Combustion Tests
V. P. Singh—Ontario Hydro 17
Coal Slurry Utilization In Small Industrial Fire Tube Boilers
R. L. Savage, W. R. Warfield, A. M. Mengon and S. C. Zronek—Ohio University 37
Ultra Fine Grinding of Australian Brown Coal For Use in Diesel Engines
J. J. Kowalczewski, P. C. Bandopadhayay, R. J. Downie and W. R. Read—CSIRO 46
Studies on Additives For Coal Water Mixture
A. Naka and Y. Mizuno—Dai-Ichi Kogyo Seiyaku Co., Ltd., Neos Co., Ltd. 58
***CWM Development: Pilot Plant to Commercial Scale**
R. J. McCormick, F. Ford, R. Moore and A. J. Madgavkar—Occidental Research Corporation 75

SESSION II—ADDITIVES CONSIDERATIONS
Monday, April 25, 1983
Chairman: Howard Feibus, Department of Energy

Rheological Characteristics of Coal-Water Mixture With High Coal Content
Li Xing-Chang, Yun Hong-Nian, Yang Li-Xian and Jiang Long—Institute of Photographic Chemistry 79
Studies On Additive For CWS
Shin-ichi Watanabe, Masaaki Yamamura, Ken-ichi Katabe and Yasuhiro Kiyonaga
—Kao Corporation, Lion Corporation 88
Research Establishing The Benefits of Oxygen-Enriched Air In Firing Coal-Water Slurries In Oil-Capable Boilers
J. J. Reuther and E. J. Greskovich—The Pennsylvania State University, Air Products and Chemicals, Inc. 109
Studies On Additives For Coal Slurries
Y. Song, T. Wei, C. Zhang, X. Li and C. Luo—Institute of Coal Chemistry 112
The Effect Of Additive Selection On Coal Water Mixture
H. Kuo, S. L. Lee and Y. S. Huang—Imperial Dynasty, Inc. 127
Effects Of Coal Type, Surfactant, And Coal Cleaning On The Rheological Properties Of Coal Water Mixture
R. Kaji, Y. Muranaka, K. Otsuka, Y. Hishinuma, T. Kawamura, M. Murata, Y. Takahashi, Y. Arikawa, H. Kikkawa, T. Igarashi and H. Higuchi—Hitachi, Ltd., Babcock-Hitachi, K. K., Nippon Oil & Fats Co., Ltd. 151

SESSION III—BENEFICIATION
Monday, April 25, 1983
Chairman: Albert W. Deurbrouck, Pittsburgh Energy Technology Center, DOE

New Deashed COM Technique And Demonstration Test Program
Y. Matsuura, Y. Sugino, N. Sato, Y. Nakamura, K. Muroi, Y. Kamijo and K. Shinano
—Electric Power Development Co., Ltd., Kawasaki Heavy Industries, Ltd., Hitachi, Ltd., Tsukishima Kikai Co., Ltd., Sumitomo Heavy Industries, Ltd. 179
Effects of Coal Beneficiation On Handling Properties of Coal-Water Mixtures
A. C. Ekmann—Pittsburgh Energy Technology Center 214

*Papers were not available at time of publication.

The Availability of Very Low Ash Coal For Coal-Based Fuels
P. J. Bethell and F. R. Sell—A. T. Massey Coal Company, COMCO 238
***Spray Flotation, A New Way to Clean Coal**
L. Burgess, P. McGarry and D. Herman—Gulf+Western 255
Ultrasonically Enhanced Size Reduction of Coal
S. R. Taylor, W. B. Tarpley, Jr. and G. R. Moulder—Energy & Minerals Research Company 256
Coal Refining by Physical Methods for the Preparation of Coal Slurries With Less Than One Weight Percent Ash
D. V. Keller, Jr.—Otisca Industries, Ltd. 269
***Mineral Matter Composition and Economic Considerations in Coal Beneficiation for CWM**
E. T. McHale, E. G. Skolnik, J. H. Lippold, R. S. Scheffee and C. B. Henderson
—Atlantic Research Corporation 279
***Economics and Technical Feasibility of CWM on Rotary Rock Dryers and Other Industrial Applications**
W. K. Fox, J. T. Clements, D. R. Gallagher, W. N. Poundstone and L. Rheinfrank, Jr.
—Standard Havens Research Corporation, Standard Havens, Inc., Gallagher Asphalt Co. 280

SESSION IV—ECONOMICS AND COMMERCIALIZATION
Monday, April 25, 1983
Chairman: Norbert E. Methven, Weyerhaeuser Corporation

The Development and Commercialization of A Low-Cost Petroleum Coke-Oil Slurry Fuel For The Marine Industry
D. G. Beshore and A. S. Yagiela—Cities Service Research and Development Company, COMCO 283
***U.S. Military Academy Coal-Oil Mixture Conversion Study**
J. F. Thompson, Jr.—U.S. Army Corps of Engineers 304
COMCO's Composite Fuels Preparation Plant, Port Sutton, Tampa, Florida
J. C. Wilda—COMCO 305
Commercial Operation of The Paul L. Bartow Unit 1 Coal-Oil Mixture
M. E. Higgins—Florida Power Corporation 314
COM Burner Development, Paul L. Bartow Unit 1
W. E. Dudley, M. E. Higgins and D. K. Meyer—Florida Power Corporation 318
Operation and Testing of The Paul L. Bartow Unit 1 on Coal-Oil Mixture
G. L. Petersen, D. T. Buell, S. A. Scavuzzo and J. Neidert, Jr.
—Florida Power Corporation, Babcock & Wilcox Company 323
***Experience With Precipitator Performance on COM Fuel at Florida Power Bartow Unit #1**
N. Shilling, W. Morris, J. Brummer and W. C. Love—General Electric Environmental Services, Florida Power Corporation 336
Design and Economics of Utility Power Plants Utilizing Deep Cleaned Coal Water Slurries
J. C. Cutting, S. S. Strom and R. E. Waryacz—Gilbert/Commonwealth, Combustion Engineering 337
***Performance Predictions for Coal Water Slurry Firing in Utility Steam Generators**
M. J. Hargrove and G. N. Liljedahl—Combustion Engineering Inc. 356
***Coal Water Slurry Pilot Facility**
R. A. Passman—Atlantic Research Corporation 357
***Performance and Economic Analysis of Turbine Cycles Fueled With Ultra-Clean Coal-Water Mixtures**
R. A. Bajura, L. H. Berkshire, W. C. Morel and J. E. Notestein
—Morgantown Energy Technology Center 358

SESSION V—DEMONSTRATION PROJECTS
Tuesday, April 26, 1983
Chairman: Michael E. Higgins, Florida Power Corporation

***Commercial Demonstration Of A Coal-Oil Mixture In Industrial Applications**
D. R. Adams—Island Creek Coal Sales Company 3

*Papers were not available at time of publication.

OM Injection Into All Tuyeres of Kashima No. 3 Blast Furnace
I. Kurashige, T. Iba, T. Miyazaki, K. Satoh, M. Kojima and Y. Aminaga
—Sumitomo Metal Industries, Ltd. 362
Shoreside Testing Of A Coal/Oil Mixture As A Marine Boiler Fuel
C. F. Eckhart and C. L. Wagoner—The Babcock & Wilcox Company 381
Test Results of COM At An Actual Utility Boiler
Y. Matsuura, Y. Sugino, K. Yamaguchi, I. Koyama, T. Shinohara and M. Nishizawa
—Electric Power Development Co., Ltd., Kawasaki Heavy Industries, Ltd., Babcock Hitachi K. K., Tsukishima Kikai Co., Ltd., Hitachi Zosen Corporation 409
COM Test Program At Yang Shupu Power Plant
Zhao Xiao, Hou En-Hai and Xu Fang-Jie
—Yang Shupu Power Plant, Xian Thermal Power Research Institute 478
Is Coal-Oil Slurry A Suitable Alternate Process Fuel For The Iron Ore Industry?
A. Bedrossian, J. S. Burgess, Y. Duret and M. Gausachs—Iron Ore Company of Canada 489
Combustion Of Coal-Water Slurry In A Multiple-Burner Furnace
H. Kuroda, T. Masai, Y. Takahashi and S. Watanabe—Kure Works, Babcock-Hitachi K. K. 502
***Combustion of Coal-Water Slurries in Sweden**
L. Stigsson—Fluidcarbon Sweden AB 522

SESSION VI—EQUIPMENT
Tuesday, April 26, 1983
Chairman: Eugene Chao, EBASCO Services, Inc.

Burner Development For Coal and Water Slurry Fuel
R. H. Hickman and F. P. Buckingham—Forney Engineering Company 525
Ultrasonic Technique For Measuring Coal Concentration In COM
L. Yuying, X. Yang and J. Luo—Institute of Coal Chemistry 533
A Method For Predicting Flow Rate In Positive Displacement Rotary Pumps
M. L. Dillon and K. A. St. Clair—Robbins & Myers, Inc. 542
Direct Wet-Grinding and Dispersion of Coal For Preparation of Coal-Water Mixtures
G. Schall—Draiswerke, Inc. 558
Conversion of Oil-Designed Power Plants Using Advanced Coal Cleaning and Slurrying Technologies
R. C. Furman—Consulting Engineer 579
Front End Boiler Equipment Selection, Performance and Hydraulics For Using Coal Water Mixtures
J. F. Jones, R. A. Meyers, L. C. McClanathan, and J. L. Anastasi—TRW Inc. 595
Evaluation of CWM Use In Ironmaking
G. Malgarini, M. Giuli, L. Palumbo and S. Palella—Centro Sperimentale Metallurgico 606
A New Burner Design For CWS Combustion
S. K. Batra and W. A. Walsh, Jr.—GIMRET International, Inc., The Lezzon Group 625
***Performance and Scale-Up of the Szego Mill for Coal-Slurry Fuels Preparation**
O. Trass, E. A. J. Gandolfi and G. Papachristodoulou—University of Toronto, General Comminution, Inc. 656

Volume II

SESSION VII—BENCH SCALE TESTING
Wednesday, April 27, 1983
Chairman: Richard C. Furman, Consultant Engineer (Miami)

An Erosion Study of Flosonic and Peabody Atomizers in A Coal Liquid Mixture Environment
A. Bennett, C. E. Capes, K. A. Jonasson, W. L. Thayer, S. G. Whiteway, K. F. Burrill and V. Zeitz
—National Research Council of Canada, Scotia Liquicoal Ltd. 659
Atomization of Coal/Methanol and Coal/Oil Slurries
S. J. Kim and C. T. Crowe—Washington State University 677

*Papers were not available at time of publication.

*Performance Characterization of an Atmospheric Pressure Combustor for Ultra-Clean Coal Water Mixtures
D. M. Waltermire, U. Grimm and R. J. Anderson—Morgantown Energy Technology Center 692
*Determinations of Coal-Water Mixture Properties for Predictions of Products of Combustion Characteristics
R. R. Romanosky, Jr., J. J. Kovach and R. J. Anderson—Morgantown Energy Technology Center 693
*Flow Properties of Coal-Water Mixtures
J. Ekmann and D. J. Wildman—Pittsburgh Energy Technology Center 694
Effect of Coal Ash Content on Performance of A CWM-Fired Boiler
Y.S. Pan, G. T. Bellas, R. B. Snedden, D. J. Wildman and J. I. Joubert
—Pittsburgh Energy Technology Center 695
Combustion Characteristics and Air Pollution Emissions from Various Coal-Oil Dispersions
J. S. Alabaf—University of Surrey 718
*A Procedure for the Evaluation of the Combustion Performance of Coal-Water Slurries
S. L. Chen, R. Payne, W. Richter and J. Wilborn
—Energy and Environmental Research Corporation, Southern California Edison 756
Coal Slurry Characteristics of Bituminous and Korean Anthracite
D. C. Kim, S. H. Cho, S. K. Kang and D. H. Shin—Korea Institute of Energy and Resources 757

SESSION VIII—PILOT TESTING
Wednesday, April 27, 1983
Chairman: Horace Whaley, Canada Centre for Mineral and Energy Technology

The Swedish Straw-Oil-Mixture Project (SOM Project)
A. Haag—The Swedish National Board for Energy Source Development 777
The Development of Coal-Water Mixture Technology for Utility Boilers in Eastern Canada
H. Whaley, D. M. Rankin, R. P. Nicholson and I. D. Covill
—Energy, Mines and Resources Canada, New Brunswick Electric Power Commission, Cape Breton Development Corporation, Nova Scotia Power Commission 809
Mixing Tank Tests for Enlightened Coal Slurries
R. R. Faddick—Colorado School of Mines 826
Recent Study on Highly Loaded Coal Water Slurry
Y. Nakabayashi, N. Sato, K. Fujii, S. Takao and N. Suzuki
—Electric Power Development Co., Ltd., Kawasaki Heavy Industries, Ltd. 842
Coal Slurry Fuels: Moving Toward Commercial Utilization
G. A. Maier, R. E. Barrett, B. W. Rising and R. D. Giammar
—Florida Power and Light Company, Battelle Columbus Laboratories 872
Comparison of Coal Conversion Alternatives
E. Kimel and R. Kurtzrock—Burns and Roe, Inc., Pittsburgh Energy Technology Center 897
An Examination of the Behaviour and Structure of Single Droplets of Coal-Oil Fuels During Combustion
K. J. Lapwood, P. J. Street and F. D. Moles
—University of Surrey, Marchwood Engineering Laboratories, Central Electricity Generating Board 924

SESSION IX—COMBUSTION
Wednesday, April 27, 1983
Chairman: Roy C. Kurtzrock, Pittsburgh Energy Technology Center, DOE

Size Distribution, Density and Yield of Carbon Particles Generated in Coal-Oil Slurry Flames
R. P. Cossee and A. B. Hedley—SHELL/NCB Coal Technology Research Group, University of Sheffield 949
*Coal-Methanol Mixture Combustion Tests with Coals of Different Ranks
Y. S. Pan, G. T. Bellas, R. B. Snedden and J. I. Joubert—Pittsburgh Energy Technology Center 972

*Papers were not available at time of publication.

al-Water Mixture Laboratory Combustion Studies
G. J. Germane, L. D. Smoot, S. P. Diehl, K. H. Richardson and D. C. Rawlins—Brigham Young University 973
Some Aspects on Preparation Technique of Coal Water Slurry and Its Combustion Performance
Huang Zhaoxiang, Wu Yifeng, Wang Yizhen, Li Zhangjie, and Zhai Wenhui
—Institute of Engineering Thermophysics, Institute of Chemistry 1000
Combustion and Fuel Characterization of Coal-Water Mixtures
M. J. Hargrove, A. A. Levasseur and B. E. Davis
—Combustion Engineering, Inc., Gulf Research and Development Company 1023
A Thermodynamic Analysis of the Gas Turbine/Steam Turbine Combined Cycle With Coal-Water Slurry As Fuel
Wang Ying-shi, Gao Li-jun and Zhang Ya-nan—Institute of Engineering Thermophysics 1038
Large Scale CWS Firing Tests at the S. Barbara Power Station
G. DeMichele, M. Graziadio, S. Ligasacchi, G. Saccenti and G. Salvi
—Enel-CRTN Pisa, SNAMPROGETTI 1053
On the Ignition Characteristics of Coal/Water Slurries
K. C. Adiga, V. R. Pai Verneker, G. Gettinger, B. M. Moudgil and D. O. Shah
—University of Florida 1070
***Co-Firing of CWS With Natural Gas**
J. Dooher, T. Kanabrocki and D. Wright—Adelphi University 1091
Some Information on Combustion of CWS
Chen Yunsien, Cen Kefa, Xie Minghu, Ni Mingjiang, Cao Xinyu, Yuan Zhenfu, Huang Guoquan, Lu Chongqing, and Lu Deshou—Zhejiang University 1092

SESSION X—RHEOLOGY AND CHARACTERIZATION
Wednesday, April 27, 1983
Chairman: Geoffrey Parfitt, Carnegie-Mellon University

The Specific Volume of Coal Slurries in Aqueous and Non-Aqueous Media
R. L. Rowell—University of Massachusetts 1111
Rheology and Pumping Characteristics of Coal-Water Slurry Fuels Prepared in a Columbia Chase Integrator
S. K. Batra, R. B. Kenney and A. O'Toole—GIMRET International, Inc., Columbia Chase Corporation 1119
Handling Properties of Coal/Water Slurries
J. Dooher, B. Gilmartin, D. Albert, N. Chuisano, D. Cote, J. Gozelski, M. Grasso, T. Kanabrocki, P. Malicki, D. Wright and M. Mullarkey—Adelphi Center for Energy Studies, Adelphi University, Long Island Lighting Company 1142
Rheological Characteristics of Coal Water Mixture
Y. Kiyonaga and S. Watanabe—Lion Corporation, Kao Corporation 1157
***Rheology of Highly Concentrated Coal Slurries**
G. D. Botsaris and Y. Glazman—Tufts University 1181
Coal/Water Slurry Rotating Cup Atomization
R. J. Marnicio and H. T. Sommer—Carnegie-Mellon University 1182
***Properties and Performance Characteristics of Coal-Water Fuels**
G. A. Farthing, Jr., R. D. Daley, S. J. Vecci, E. R. Michaud and R. Manfred
—The Babcock & Wilcox Company, Electric Power Research Institute 1204
Rheology of Coal/Water Slurries
E. Z. Casassa, G. D. Parfitt, A. S. Rao and E. W. Toor—Carnegie-Mellon University 1205
Some Rheological Data and Atomization Behaviour of CWM's Containing 68 to 83% Coal
L. Gillberg, N. Larsson, M. Mathiesen, O. Nystrom and J. Persson—AB Carbogel 1229

Authors Index located at the end of each volume.

*Papers were not available at time of publication.

Session VII

BENCH SCALE TESTING

Wednesday, April 27, 1983

Chairman: Richard C. Furman,
Consultant (Miami)

AN EROSION STUDY OF FLOSONIC AND PEABODY ATOMIZERS IN A COAL LIQUID MIXTURE ENVIRONMENT.

A. BENNETT, C.E. CAPES, K.A. JONASSON, W.L. THAYER, S.G. WHITEWAY,
NATIONAL RESEARCH COUNCIL OF CANADA, OTTAWA, ONTARIO, CANADA K1A OR9

K.F. BURRILL AND V. ZEITZ,
SCOTIA LIQUICOAL LTD., HALIFAX, N.S., CANADA B3J 2X1

SUMMARY

Parallel two hundred hour erosion tests, utilizing 55:30:15/Coal:Oil:Water fuel, on a Flosonic DX3 burner tip containing ceramic wear parts and on a Peabody burner tip have been completed in the Halifax facilities of Scotia Liquicoal Ltd. Costly and complex combustion trials were replaced by a fuel recirculating, hot spray technique.

Comparison of the hot spray Peabody wear rate with that observed previously in combustion tests showed the former method to be a valid screening technique for evaluating burner tip erosion effects of CLM fuels. Based on visual observations of atomization and relative erosion characteristics the ceramic modified Flosonic DX3 shows promise as being a low wear CLM burner tip.

INTRODUCTION

Since the mid 1970's a growing interest has developed throughout the world in Coal Liquid Mixture (CLM) technology. Much work has been accomplished characterizing rheology, combustion and the economics of CLM fuels. Large scale demonstration burns costing millions of dollars have taken place. One facet of this technology that remains as a roadblock to commercialization is the development of hardware to handle adequately the erosive nature of CLM. This erosion problem is particularly important when specifying a burner tip. To address this problem, the burner tip test program described herein was initiated in joint effort between the National Research Council of Canada (NRC) and Scotia Liquicoal Ltd. (SLC) with the cooperation of Energy Mines and Resources Canada (EMR), The Center for Energy Studies (CES)/Technical University of Nova Scotia (TUNS) and MBB Mechanical Services Ltd.

OBJECTIVES OF TEST PROGRAM

The philosophy of the program was to screen inexpensively a candidate nozzle before moving on to costly demonstration burns. The program involves three phases:

1. Screen burner tips on the basis of atomization and erosive wear.

2. Preliminary combustion characterization.

3. Demonstration burn.

Once a burner tip had shown the ability to atomize adequately and withstand the erosive nature of the fuel, characterization of the nozzle under burn conditions would begin. Preliminary testing of the nozzle in a flame tunnel would prove the nozzle under actual burn conditions and yield operating characteristics of the burner assembly useful in a commercial boiler. Having successfully completed the first two phases of the program, the candidate will undergo a commercial-scale demonstration burn to show the viability of a CLM fuel coupled with a capable burner.

In development of the first phase, a simple procedure was sought that would provide a representative CLM erosion environment. Thus, the hot spray technique was developed to recirculate heated coal slurry fuel through a candidate burner tip using air as the atomizing medium. This method permitted the measurement of erosive wear and provided observations on the atomization ability of the nozzle using much smaller quantities of fuel than that needed for a once-through burner test.

To validate the hot spray technique a burner tip with known CLM erosion characteristics was similarly tested. The nozzle chosen was the internally mixed Peabody tip with which the Ontario Research Foundation (ORF) produced erosion data in a 300 hour burn of 40:60/Coal:No.6 Oil slurry (1). Data provided by testing the Peabody tip in the hot spray chamber compared with the ORF data yielded a point of departure from which the relative erosion characteristics of other burner tips could be evaluated.

After verification of the hot spray technique as a test of burner tip erosion, a candidate low-wear nozzle was sought. The following factors were kept in mind during the selection:

1. Low fuel velocities to the point of atomization

2. Good atomization of viscous fluids

3. Wear resistance to CLM fuels.

Based on these criteria, the selected burner tip was the Flosonic DX3. Through the joint efforts of SLC, NRC and the manufacturer, Fluid Kinetics, a ceramic modified Flosonic nozzle was designed and manufactured to effectively satisfy these criteria.

FUEL PROCESSING

COW fuel used in the test was provided by SLC's demonstration plant in Dartmouth, N.S. A four step method is used in the production.

1. Grinding of the coal in water.

2. Recovery of the coal and rejection of ash in the water phase using the Spherical Agglomeration technique developed at NRC.

3. Blending the beneficiated agglomerates with No.6 fuel oil.

4. Stabilization of the mixture with a proprietary ultrasonic process.

Figure 1 shows a schematic representation of the fuel processing facility. The heavy line indicates the progression of the coal through the plant. The coal employed was Devco metallurgical, ground to a mean particle size of 25 μm employing Szego mills. This newly surfaced coal then proceeded through the Spherical Agglomeration circuit where coal agglomerates were formed in a process that beneficiates the coal with respect to ash and sulphur. Enough No.6 fuel oil and water were then added to the agglomerates to bring the fuel to a composition of 55% coal, 30% oil and 15% water. In this manner 4,000 gallons of COW fuel were produced by SLC for the hot spray testing program.

The ash content of the COW was 1.5%, total sulphur 1.3% and the calorific value 14,300 Btu/lb.

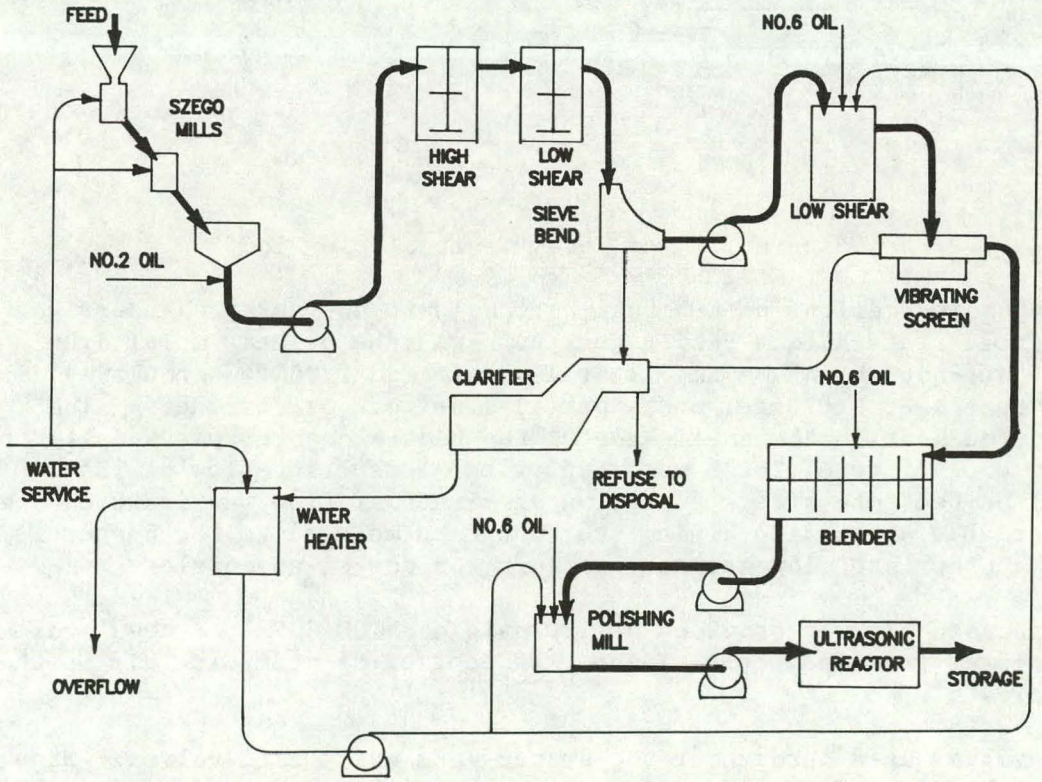

Figure 1. Scotia Liquicoal Fuel Preparation Circuit

HOT SPRAY TESTING

A schematic of the hot spray loop as used in this study is shown in Figure 2.

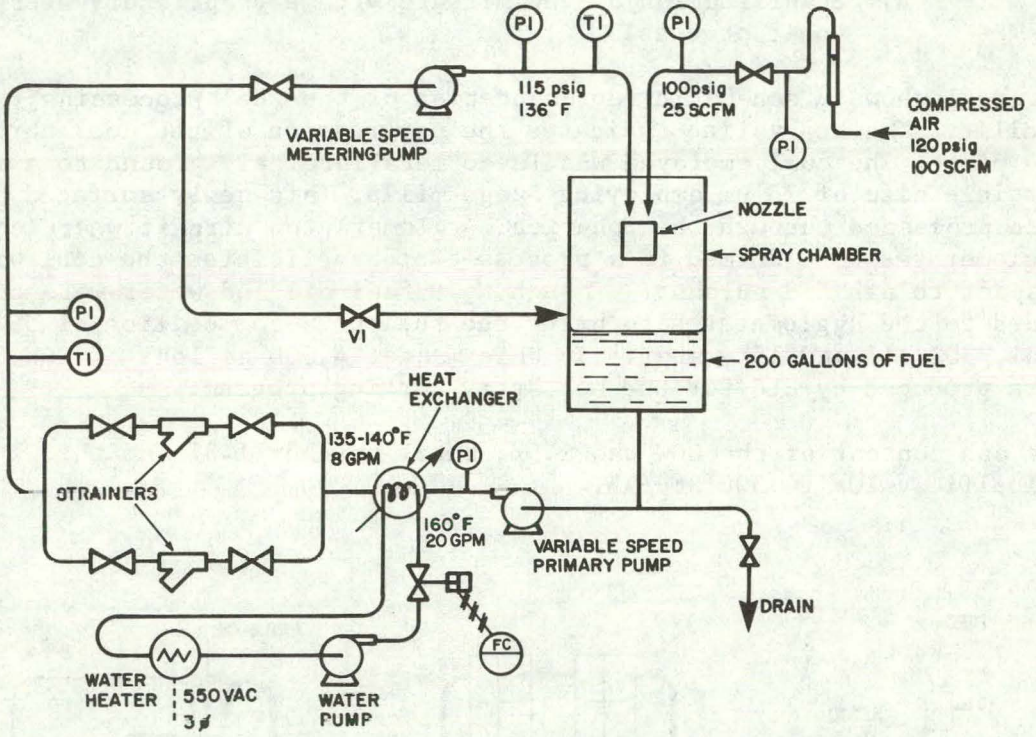

Figure 2. Hot Spray Recirculating Loop

Two hundred gallons of COW fuel were held in the spray chamber. A variable speed KK 124 Viking gear pump was the primary mover drawing fuel off-bottom and moving it at 100 psig and 8 USGPM through a shell and tube heat exchanger and a parallel network of strainers. The required heat to the shell side of the heat exchanger was supplied by a 20 USGPM flow of 160°F water ensuring a resulting flow of 135-140°F fuel on the tube side. A portion of this fuel flow was drawn through a variable speed J124 Viking gear pump and metered to the burnertip at the appropriate flowrate and pressure for the given nozzle.

Compressed air was provided at 120 psig and 100 SCFM. A regulator and rotameter provided pressure and flow control of atomizing air to the nozzle.

The valves used throughout the system were brass ball valves. With the exception of VI all valves were subjected to on-off service only. VI was used as a control valve, in that it provided an increased inlet pressure to the metering pump when throttling the flow from the primary pump. This configuration enabled trouble free operation of the

metering pump throughout the test. A deteriorating performance of VI supported by visual inspection showed erosion of valve surfaces in this service.

As shown in Figure 2 pressure and temperature of the fuel were monitored throughout the test loop. Conventional bourdon tube pressure gauges proved unsuccessful and were replaced with solid state semiconductor pressure indicators. Fuel flow was calibrated by a bucket and stopwatch method.

The spray chamber was equipped with a large window that provided easy access to the nozzle being tested, yielding a simple method of fuel calibration and visual observation of the resulting spray pattern.

Since fuel was recirculated in the test, it was anticipated that such recirculation might alter the character of the fuel. Specifically, a change in fuel composition through the loss of more volatile components and particle size reduction due to autogenous grinding effects throughout the pumping loop, were anticipated. To monitor any such changes a rigid fuel analysis schedule was incorporated into the test program. Throughout the first 50 hours of the 200 hour run fuel samples were taken every 5 hours. At the end of the 50 hours an evaluation was made to determine any action necessary to overcome fuel degradation.

The hot spray procedure was begun by first charging the spray chamber with No. 6 fuel oil and recirculating it through the heat exchanger and valve VI until the temperature stabilized at 135-140°F. Upon reaching the desired fuel temperature, atomizing air was sent to the nozzle with the fuel then directed through the metering pump to the nozzle. Fuel and air flowrates and pressures were adjusted to achieve an adequate spray thus yielding approximate conditions to which the nozzle was set when spraying COW.

The No. 6 oil was pumped out and replaced with 200 gallons of COW fuel. After this fuel had reached temperature, through recirculation, air and fuel were metered to the nozzle and the 200 hour erosion test was begun.

A schedule to monitor nozzle erosion was established whereby the spray testing was interrupted at 10, 25, 50 and 100 hours. Complete inspection of the nozzle, as described later, took place at this time. Coinciding with the erosion evaluation were the spray pattern observations. Two spot lights inside the spray chamber provided adequate lighting to record the spray pattern photographically.

Peabody Nozzle

The Peabody atomizing nozzle used was the model F14.1-0-75-F9 HZ as fabricated and supplied by the Ontario Research Foundation. The burner tip is internally atomized and designed for oil firing at 10 MM btu/hr using steam as the atomizing medium.

As shown in Figure 3, the Peabody consists of 3 major component

pieces. The fuel enters the center opening of the mixing chamber and is directed out to a surrounding annular space in an encompassing nozzle body. This annulus in turn feeds the fuel to the high velocity atomizing medium where the liquid is sheared and atomized. This dispersed fuel/air mix enters the tangentially drilled holes of the swirler and then finally exits through the ten 0.081 inch diameter holes of the end cap.

The end cap was machined from M2 general purpose tool steel. Following a heat treatment the surface was nitrided to a hardness of 65 Rockwell C.

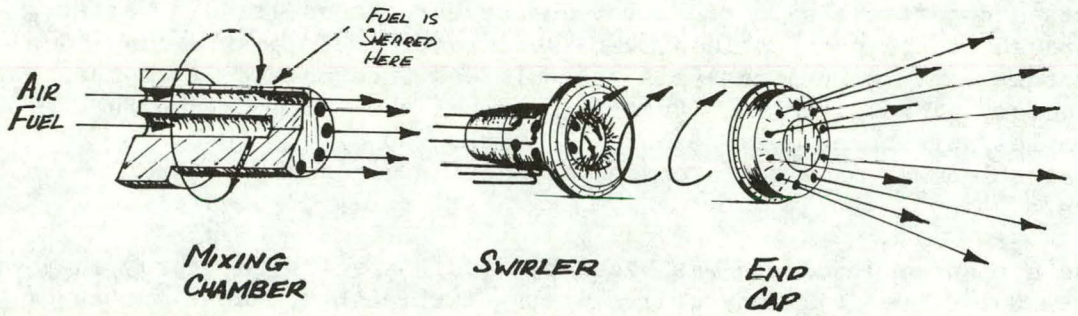

Figure 3. Peabody Atomizer

Flosonic Nozzle

The Flosonic nozzle tested was the model DX3 manufactured by Fluid Kinetics Inc. of Fairfield, Ohio. As shown in Figures 4 and 5 the atomizer consists of three components: spray deflector, cap nut and distributor.

Fuel is introduced to the distributor through six 0.173 inch diameter holes. The atomizing medium moves through the distributor via the center opening and is delivered to a plenum formed by the spray deflector and the distributor. An accurately tapered annular opening accelerates the atomizing medium to sonic velocities. The liquid stream merging through a concentric annular space created between the cap nut and the distributor body is sheared by the accelerated air stream.

The compressed air expands during this stage forcing the fuel away from the spray deflector. Due to the attainment of supersonic velocities, shock waves are set up which vibrate and further shear the liquid droplets. The resulting spray then diverges at an angle determined by the shape of the spray deflector.

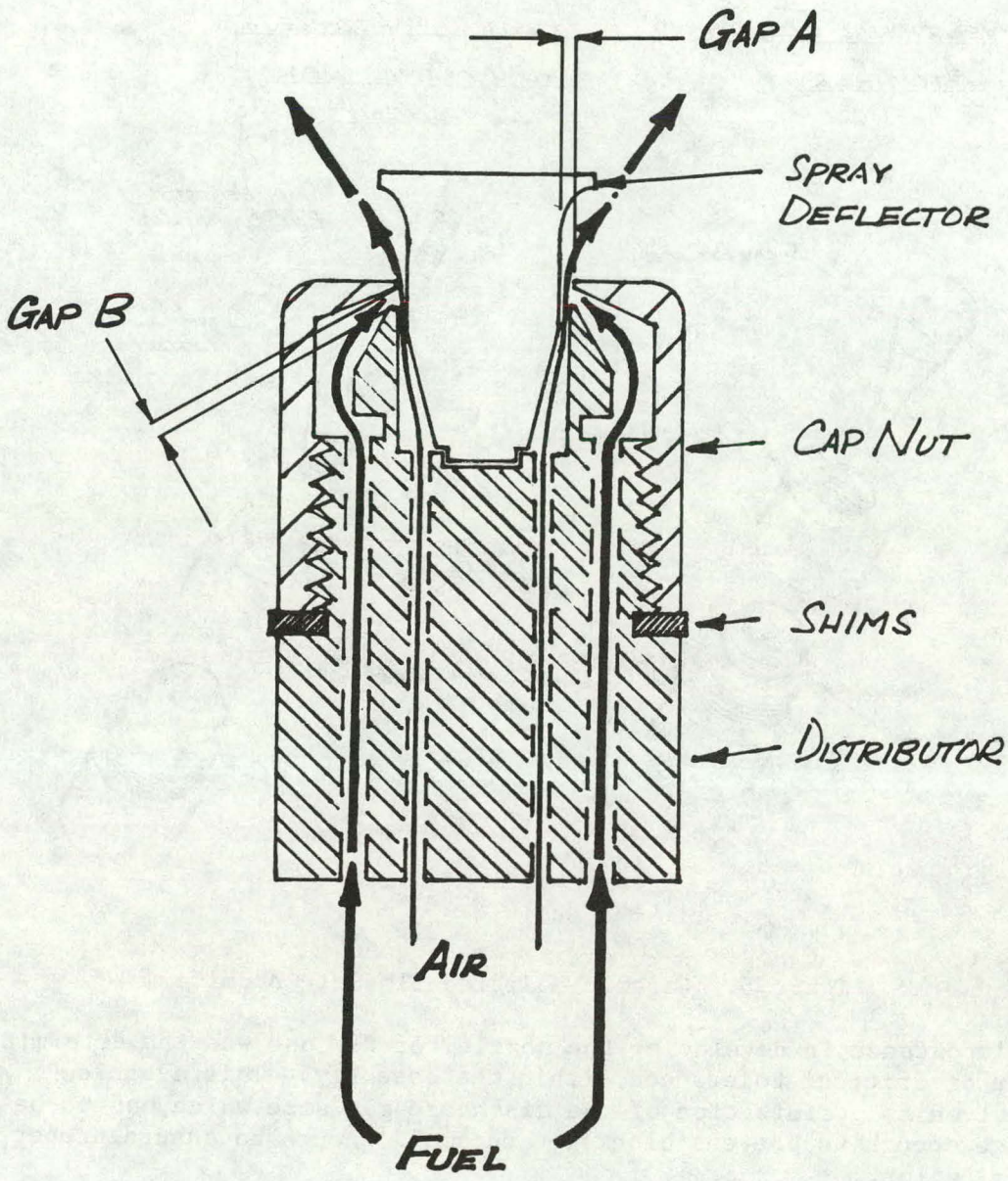

Figure 4. Flosonic Atomizer

Figure 5 diagrammetically documents the development of the ceramic modified Flosonic atomizer during the present work. A ceramic ring was inserted in the cap nut and the spray deflector was entirely fabricated from ceramic in an attempt to alleviate erosion of these wear-prone areas. The ceramic employed was a high density aluminum oxide supplied by Fluid Kinetics.

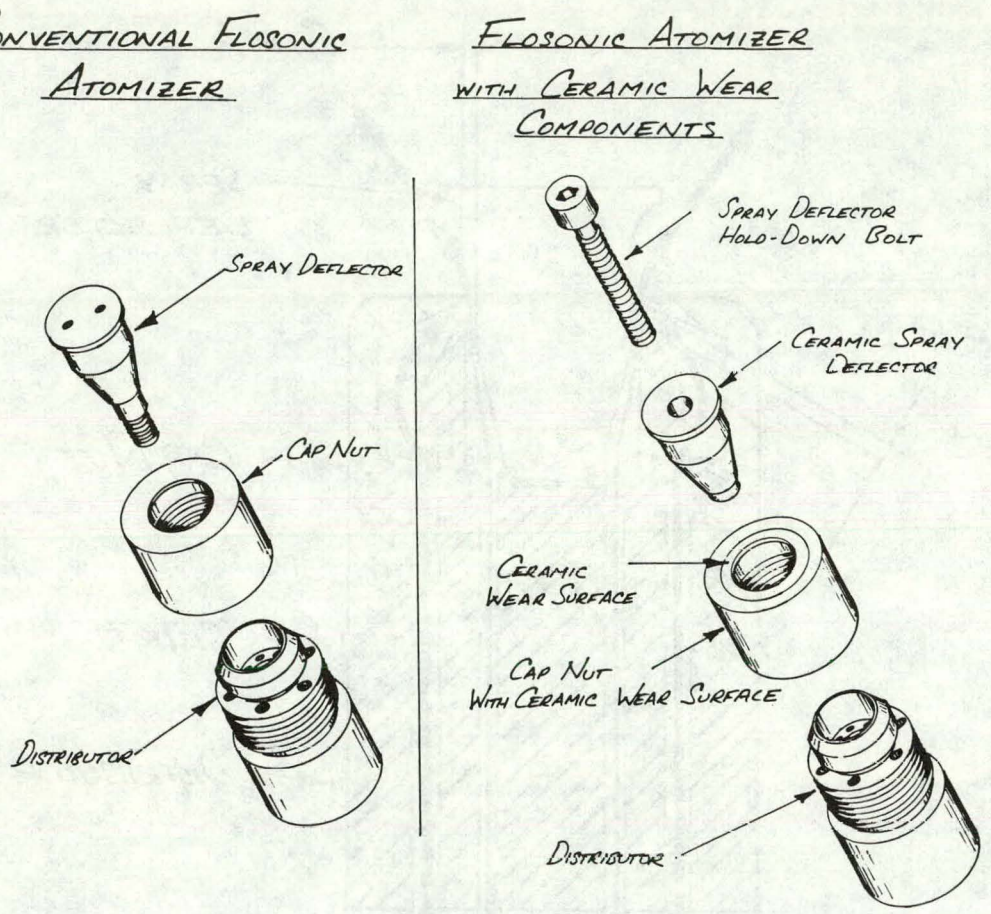

Figure 5. Ceramic Modified Flosonic Atomizer

Of importance in developing the nozzle for CLM use was the determination of critical tolerances within the assembly. This exercise involved an optimization of the discharge gap size which had to be large enough to prevent blockage and small enough to ensure proper atomization.

WEAR EVALUATION

Burner tip wear evaluation was performed at 0, 10, 25, 50, 100 and 200 hours into the test program for both the Peabody and Flosonic nozzles. The wear evaluation program was divided into three parts:

1. Gravimetric
2. Optical
3. Mass flow resistance

Gravimetric

Component parts of the nozzle assemblies were weighed accurately at each test stage. Before weighing, the components were subjected to a rigorous cleaning procedure.

Optical

Critical wear areas of the two nozzles were optically measured on a Mictrotechnica, Cyclop 1 comparator. The magnification employed was 20x and 50x for the Flosonic and Peabody nozzles, respectively.

Peabody: The diameters of each of the ten 0.081 orifices of the end cap (see Figure 3) were measured in X and Y orientations.

Flosonic: The cap nut, distributor and dispersion cone were all measured at points of anticipated wear. Figure 6 shows the dimensions measured on the distributor and dispersion cone.

Mass Flow Resistance

The third method used to quantify resulting wear was to measure a discharge of water through the atomizers at a specified head, on the premise that any erosive wear would result in an increase in water flowrate. Figure 7 is a schematic of the test apparatus.

One hundred and twenty-five U.S. gallons of 25°C water were held 6 ft. above the nozzle tip. The discharge valve was opened and the discharged water was collected in a 45 gallon drum mounted on a scale. A 400 lb. discharge of water was timed at 20 lb. intervals with resulting rates recorded.

This same procedure was repeated with the tip removed from the end of the water delivery system to allow calculation of any head losses in the apparatus. These losses were then subtracted from the total static head to allow the nozzle discharge coefficient to be calculated. Due to the curved annular internal shape of the Flosonic nozzle, the actual cross sectional area of discharge was not easily defined nor measured. Thus a combined discharge coefficient, C_dA_o (discharge coefficient x area of orifice), was determined.

The following equation (2) was used to calculate the combined discharge coefficient, C_dA_o, from the flow resistance data:

$$C_dA_o = \frac{2A_T}{t\sqrt{2g}} \left(\sqrt{H_1} - \sqrt{H_2}\right)$$

where A_T is the cross-sectional area of the water storage tank and t is the time to discharge from head H_1 to head H_2. H_1 and H_2 represent the actual pressure operating at the nozzle, that is, the effects of frictional losses in the apparatus have already been taken into account in these heads.

DISPERSION CONE

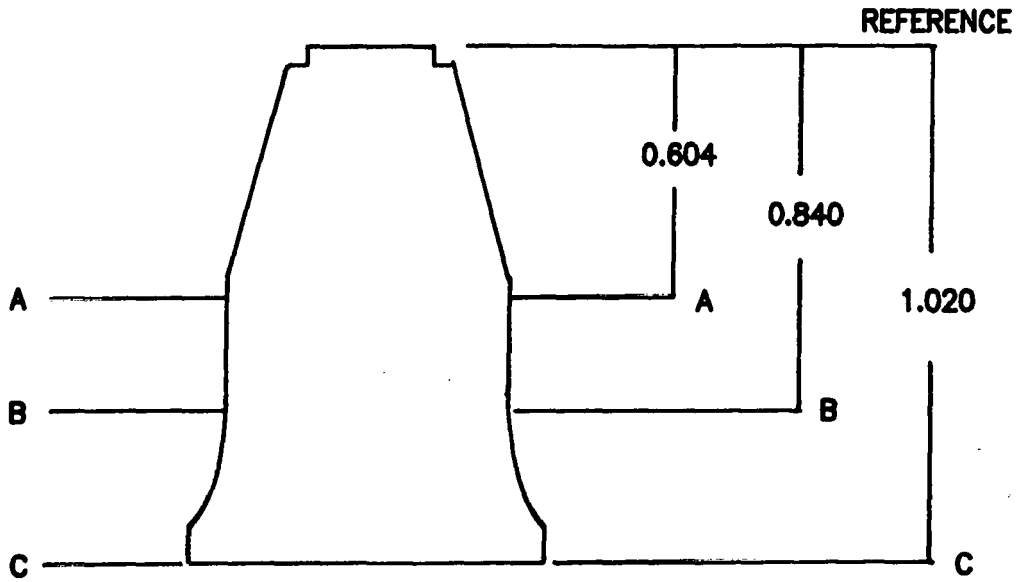

DISTRIBUTOR

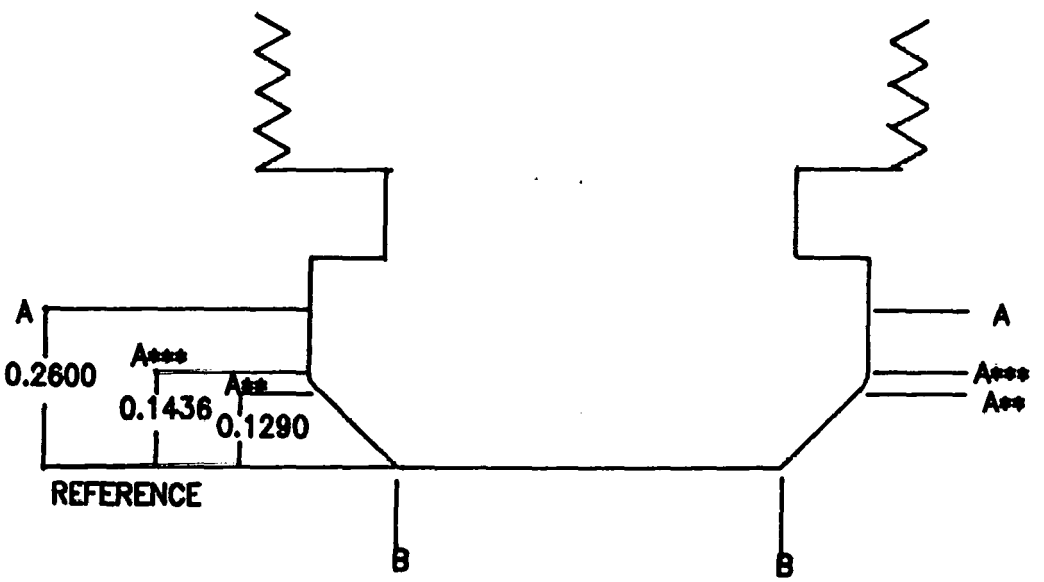

Figure 6. Optical measurements made on Flosonic Components

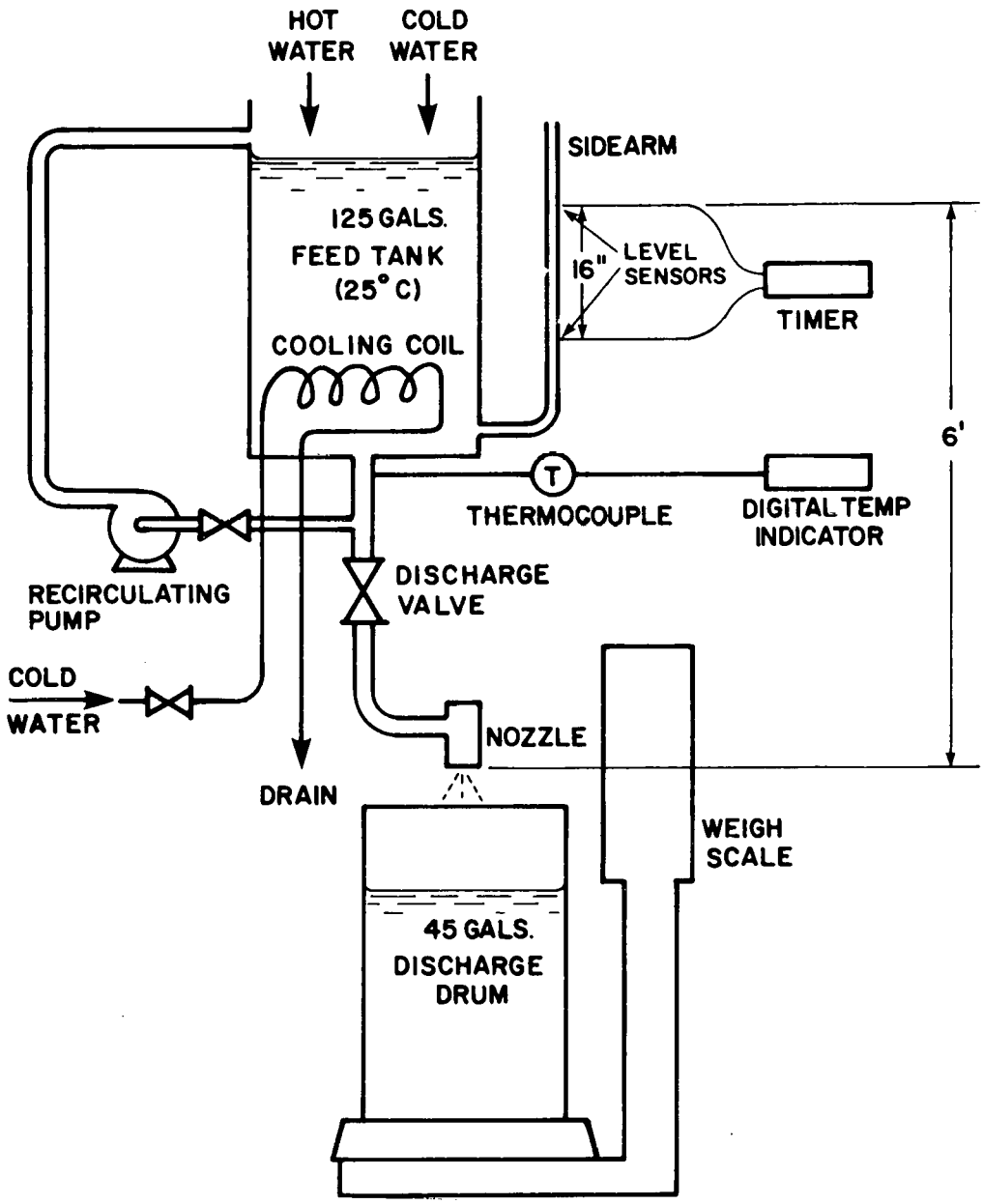

Figure 7. Water Flow Resistance Apparatus

It was felt that any erosive wear would be detectable in this coefficient, resulting either from polishing of internal nozzle surfaces or from removal of major amounts of material.

HOT SPRAY TEST LOG

Throughout the 200 hour Peabody and Flosonic hot spray tests the test loop was monitored hourly from start to finish. Tables 1 and 2 contain time weighted averages of fuel temperature, fuel pressure, air pressure and volumetric flowrates of air and fuel.

In both cases the fuel temperature was maintained at 135-140°F. The necessary fuel pressures to achieve good atomization were slightly higher for the Peabody tip, which required 135 psig versus 115 psig for the Flosonic. On the other hand, the Flosonic demanded higher atomization air pressure to perform satisfactorily. One anomaly in the fuel pressure data is the increased flowrate of fuel through the Flosonic in the 100-200 hour period. To achieve this increased flow no corresponding increase in fuel pressure was applied. This can be explained by an alteration in fuel preparation at this point which resulted in a lower viscosity mixture.

The operating conditions chosen were arrived at based on two criteria. Of primary importance was adequate atomization determined by visual observations. The second was to operate the two nozzles at their designed operating conditions of 1 USGPM and 2 USGPM for the Peabody and Flosonic atomizers respectively. Operation of the Peabody at 1.29 USGPM required an air/fuel ratio of 0.19 lb. air/lb. fuel while the Flosonic needed 0.11 lb. air/lb. fuel to atomize a 1.8 USGPM flowrate of fuel.

TABLE 1: PEABODY TEST LOG

TEST PERIOD	FUEL TEMPERATURE AT NOZZLE (°F)	FUEL PRESSURE (psig)	FUEL MASS FLOWRATE (lb/min)	AIR PRESSURE (psig)	AIR VOLUMETRIC FLOWRATE (SCFM)
0-10 Hrs	134	119.6	11.35	72.1	33.8
10-25 Hrs	133	118.9	10.91	70.9	32.1
25-50 Hrs	137	141.5	11.86	81.4	26.7
50-100 Hrs	139	133.1	12.12	81.4	31.4
100-200 Hrs	141	139.2	11.70	78.6	29.4
AVERAGE	139.1	135.5	11.75 (1.29 USGPM)	78.7	29.9

TABLE 2: FLOSONIC TEST LOG

TEST PERIOD	FUEL TEMPERATURE AT NOZZLE (°F)	FUEL PRESSURE (psig)	FUEL MASS FLOWRATE (lb/min)	AIR PRESSURE (psig)	AIR VOLUMETRIC FLOWRATE (SCFM)
0-10 Hrs	141	98.5		100.0	25.56
10-25 Hrs	135	101.7		101.2	25.72
25-50 Hrs	134	106.1	11.12	100.4	25.61
50-100 Hrs	135	126.3	11.88	98.3	24.57
100-200 Hrs	135	116.4	21.42	100.2	24.04
AVERAGE	135.2	115.6	16.46 (1.80 USGPM)	99.8	24.57

FUEL COMPOSITION AND SIZE ANALYSIS

Table 3 contains the average values of the fuel composition and particle size analyses. A combined Dean and Stark/Soxhlet extraction procedure was used to evaluate fuel composition (3). For particle size, NRC employed a combined Sieve/Coulter Counter technique while TUNS used a combined Sieve/Sedimentation balance procedure.

The mean particle sizes reported in Table 3 indicate no appreciable attrition of solid particles due to recirculation of the fuel throughout the loop. This observation is also supported by microscopic examination of the sampled fuel.

Table 3 also shows the effects of recirculation on the composition. As feared, the more volatile components had been escaping during recirculation. This was most apparent in the dramatic drop in water content from 16.7% to 12.4% in the case of the Peabody results. The loss of water, as well as No. 2 oil, resulted in a significant increase in viscosity.

The rising fuel viscosity made pumping and subsequent loop control difficult after about 17 hours on the first run. Thus a 20 hour fuel change cycle was incorporated into the procedure for the remainder of the hot spray testing.

TABLE 3: FUEL ANALYSIS

		Coal (%)	Water (%)	Oil (%)	Mean Particle Diameter (μm) TUNS	NRC
PEABODY	Initial	51.6(1.6)	16.7(1.4)	31.7(0.7)	30.5(3.5)	25.4(0.4)
	Final	54.9(1.3)	12.4(2.4)	32.8(2.0)	31.0(4.4)	25.8(1.7)
FLOSONIC	Initial	54.2(2.3)	13.9(3.0)	31.6(1.7)	33.3(4.6)	23.3(4.1)
	Final	57.5(1.9)	11.3(2.2)	31.1(2.3)	31.0(1.4)	22.5(4.7)

( ) denotes one standard deviation

DISCUSSION OF RESULTS

Tables 4 and 5 contain all the raw data pertinent to the wear evaluations of both the Peabody and Flosonic nozzles.

The operating principles and configurations of the Peabody and Flosonic nozzles differ widely. Thus, the character of the surface exposed in each case to wear is significantly different. This realization makes the simple comparison of the nozzle erosion rates by means of weight loss and dimensional change data meaningless. Thus the decision was made to use changes in the C_dA_o as the means of evalu-

ating wear. If possible, interpretation of any resulting trends would be supported by gravimetric and optical measurements.

Figure 8 depicts the per cent increase in C_dA_o versus solids discharged for the Peabody hot spray erosion test and the ORF Peabody combustion erosion test (1). As the nozzles were operated under different conditions in these tests (1.3 vs. 0.5 USGPM and 60% vs. 40% solids, respectively) a simplified method of normalizing and comparing results was sought. The method employed as shown in Figures 8 and 9 was to relate the per cent increase in C_dA_o to the weight of solids discharged through the nozzle. The results for the two different tests on the Peabody nozzle can be seen to compare well, so that this method of normalization is deemed to be reasonable for normalizing this type of data.

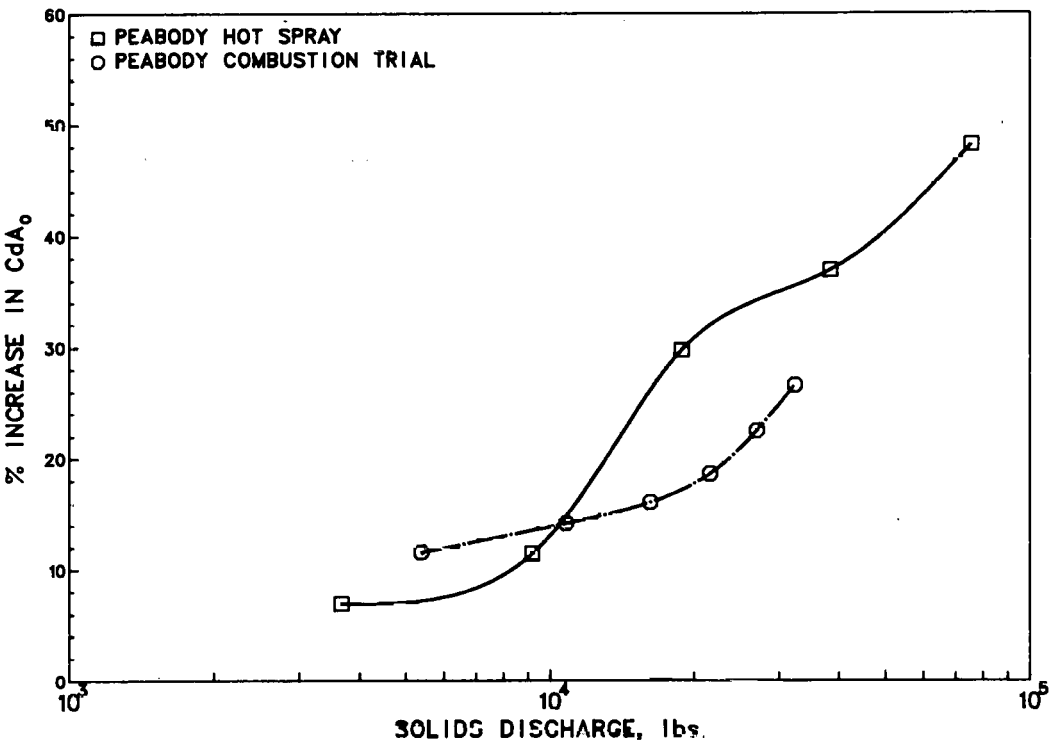

Figure 8. Increase in C_dA_o versus Solids Discharged for Peabody Nozzle

As the Peabody atomizer eroded similarly in the combustion and hot spray recirculation tests, it follows that the hot spray test provides a suitable environment for evaluating the CLM erosion of burner tips.

Following 200 hours of hot spray testing with a 55:30:15/COW fuel the Peabody exhibited a 48% increase in the C_dA_o coefficient of discharge. Visual observations of the spray pattern as the test progressed indicated a significant deterioration in spray pattern.

Figure 9 depicts the Flosonic erosion behaviour as described by the per cent increase of C_dA_o versus the weight of solids discharged. As a reference curve the Peabody data from Figure 8 is shown in a generalized form in Figure 9. Following 200 hours of hot spray (1.52×10^5 lbs solids discharged) the Flosonic showed a 5.0% increase in the parameter C_dA_o. No deterioration in spray pattern was noted throughout the 200 hours.

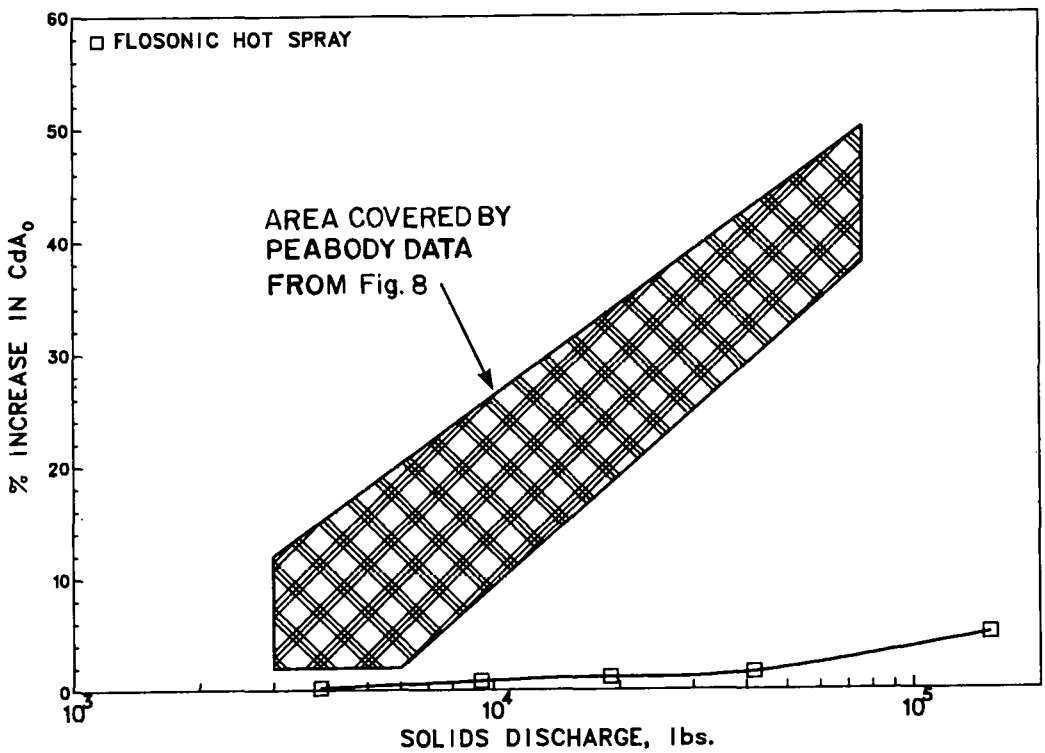

Figure 9. Increase in C_dA_o versus Solids Discharged for Flosonic Nozzle

To correlate the change in C_dA_o to actual dimensional changes within the Flosonic atomizer a mass flow resistance sensitivity study was performed. Wear was synthetically produced in a stainless steel Flosonic atomizer of the same configuration as that used in the hot spray test. The two critical tolerances within the tip shown in Figure 4 as gaps A and B were altered and resulting water rates were measured. The collected data shown in Figure 10 show an average increase of 1.26% of C_dA_o for every one thousandth of an inch change in either of the critical dimensions.

While no change was realized in the Flosonic spray pattern, a rise of 3.29% in C_dA_o was reported in the last segment of the curve in Figure 9. If this rise in C_dA_o were due entirely to dimensional changes, the above results from introduction of synthetic wear indicate that a 0.0026 inch increase should have been realized in measurements of the ceramic ring diameter, cross-section BB of the

dispersion cone, or cross-section AA of the distributor during the 100-200 hour test segment. Optical and gravimetric results indicated that no such significant dimensional changes took place over this last segment of the test. However, a red/brown coloured deposit did develop on the surfaces of both the spray deflector and the ceramic ring, which may have resulted in surface smoothing and a subsequent increase in C_dA_o in the water tests.

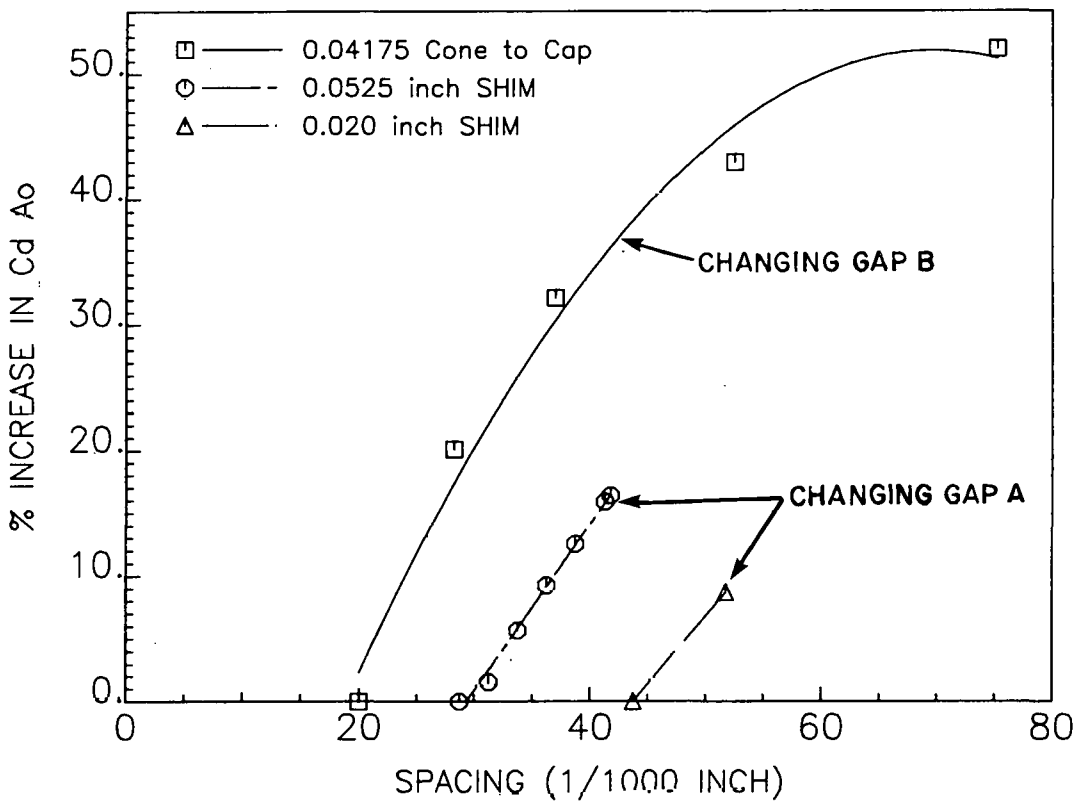

Figure 10. Mass Flow Resistance Sensitivity

It should be noted that Flosonic and Peabody nozzles required very different atomizing air velocities to operate satisfactorily. The Flosonic design employs air velocities of the order of 1200 ft/sec whereas the Peabody atomizing air discharges at 250 ft/sec. This difference has not been taken into account in the normalization of the water discharge data used in Figure 9. Considering the much higher air velocity in the Flosonic nozzle, its very low rate of wear compared with that of the Peabody nozzle, as indicated by the discharge data in Figure 9, is even more remarkable.

TABLE 4: ATOMIZER WEAR DATA

			Test Period (hrs.)	0	0-10	10-25	25-50	50-100	100-200
FLOSONIC	Solids discharged at end of period (lbs.)			NA	3876	9366	19026	41736	152170
	Cap Nut		AA (in.)	0.8461	0.8465	0.8482	0.8476	0.8477	0.8482
			BB (in.)	-	0.8471	0.8480	0.8486	0.8476	0.8480
			CC (in.)	0.9596	0.9592	0.9590	0.9580	0.9590	0.9592
			Weight (grams)	23.6116	23.6100	23.6098	23.5919	23.5915	23.5786
			XX (in.)	0.9290	0.9291	0.9289	0.9291	0.9286	0.9290
			YY (in.)	0.9295	0.9292	0.9290	0.9291	0.9297	0.9289
			Weight (grams)	123.2575	123.2566	123.2555	123.2518	123.2527	123.2561
			AA (in.)	1.1893	1.1876	1.1870	1.1889	1.1884	1.1886
			AA*** (in.)	-	-	1.1851	1.1868	1.1858	1.1858
			AA** (in.)	-	-	1.1866	1.1778	1.1770	1.1770
			Weight (grams)	293.21	293.19	293.18	293.21	293.19	293.16
	$CdA_o \times 10^4$			3.1758	3.1825	3.2019	3.2129	3.2261	3.3347
PEABODY	Solids discharged at end of period (lbs.)			NA	3666	9165	18825	38475	75615
	End Cap		Orifice Area ($in^2 \times 10^2$)	5.0140	5.1403	5.1657	5.3846	5.6611	5.8494
			Weight (grams)	40.6296	40.6127	40.6082	40.5631	40.5507	40.5253
	$CdA_o \times 10^4$			2.6750	2.8607	2.9800	3.4685	3.6607	3.9632

TABLE 5: ONTARIO RESEARCH FOUNDATION PEABODY COMBUSTION TRIAL WEAR DATA (1)

Test Period (hrs.)	0	0-50	50-105	105-150	150-195	195-250	250-292
C_dA_o ($ft.^2 \times 10^4$)	2.1364	2.3838	2.4392	2.4793	2.5340	2.6167	2.7041
Total Area of Orifice ($in^2 \times 10^2$)	5.1274	5.5367	5.6652	5.7583	5.8854	6.0775	6.2806

CONCLUSIONS

It has been shown through a rigorous test program that a recirculating spray of COW fuel can provide an erosive environment similar to that in an actual combustion environment.

The Flosonic DX3 atomizer showed a much better ability to resist CLM erosive wear than the Peabody nozzle. The Peabody showed a deteriorating spray pattern and an order of magnitude greater increase in C_dA_o than did the Flosonic atomizer which demonstrated no change in spray pattern over the course of the test.

REFERENCES

1. Bruno, L., Deshpande, A.S., Whaley, H., Coal/Oil Slurry Combustion and Tribology - A Canadian Experience, Fourth International Symposium on Coal Slurry Combustion and Technology, Vol. 2, Session III, May 10-12, 1982. Orlando, Florida.

2. Streeter, V.L., Fluid Mechanics, 4th ed., p.424, McGraw-Hill, New York, 1966.

3. See ASTM D244.

ACKNOWLEDGEMENT

R. D. Coleman and S. Croteau performed the analytical work at NRC.

ATOMIZATION OF COAL/METHANOL AND COAL/OIL SLURRIES

by

S. J. Kim and C. T. Crowe
Mechanical Engineering Department, Washington State University
Pullman, WA 99164-2920

Abstract

The combustion process of a coal/oil slurry begins by atomization of the slurry. This paper is a presentation of results on atomization of coal/oil and coal/methanol mixtures with a two fluid and a wheel atomizer. The slurries consisted of coal/methanol and coal/oil mixtures with two different concentrations and two coal particle sizes. The volume median diameters of the coal particles, as measured by a Coulter counter, were 50 and 130 microns. The oil was No. 2 diesel oil. The droplet size was determined by photographing the spray and analyzing the photographs to determine droplet size and distribution. The results show that the inclusion of particles in the liquid (both methanol and diesel oil) does not appreciably affect the atomized droplet size. The tendency is for the slurry droplets to be somewhat smaller than the droplets atomized with the pure liquid. In some instances, one would observe a complete separation of the coal particles from the liquid. The nominal droplet produced by the wheel atomizer was larger than that for the two-fluid atomizer and separation of the coal from the fluid was not observed.

1. INTRODUCTION

It is essential for the well-being of the nation that the energy resources of the country be used effectively and efficiently. Coal is the only fossil fuel available in sufficient quantities which, if developed properly, could reduce dependence on petroleum imports. Of the total coal reserves in the world, 20% lie within the United States and only 3% of this quantity has been extracted prior to 1974. Even with the current usage growth rate, it is estimated that reserves will last 350 years.

Increased development of coal requires solutions to technical problems associated with mining, processing, transporting, and utilization. Many directions for coal processing, including liquification and gasification, have been proposed. Another one, the genesis of this project, is the direct mixing of solid coal particles with liquid fuels. This approach is attractive in the short run because it could replace a sizeable percentage of petroleum used in oil-fired power plants with minimum modification to the furnace. Before an assessment can be made of the types of retrofit modifications necessary, information is needed about the effect of the presence of coal particles on the fundamentals of atomization, vaporization, and combustion of coal-liquid suspensions.

Each of these processes may be affected by parameters such as loading ratio, coal and droplets size and fluid properties.

Although the spraying of slurries has been a routine process in the spray drying industry [1], there appears to be little data on the effect of slurry properties on droplet size. Fundamental studies performed at Brookhaven laboratory [2], using a twin-fluid atomizer, have shown that the Sauter mean diameter for 20% coal-oil mixtures was not significantly different than that for pure oil. The argument is made that the influence of coal should increase drop size as concentration increases. The effects of coal particle size and atomizer type were not reported. The objective of this project was to obtain fundamental information of the atomization of coal-methanol and coal-oil slurries.

2. SLURRY HANDLING SYSTEM

There were several criteria [3] for the design of the slurry handling system. (a) The photographic technique required steady state run times on the order of four minutes to allow approximately 20 exposures to be taken. (b) Steady state operation with constant flow conditions was necessary. These conditions include uniformity of slurry delivery to the atomizer (constant loading), symmetry of the hollow-cone spray in the test section, and constant slurry supply pressure and air pressure. (c) The apparatus was to be convenient and easy to operate. These features included a straightforward method for slurry transfer to and from the apparatus, good access for maintenance and clean up, and ample room for set-up of the photographic apparatus.

The layout for the system is shown in Fig. 1. This system consisted of a mixing tank connected with gear pumps, a spray chamber, and a collecting tank for the atomized slurry. In the set-up, two pumping circuits with two gear pumps were attached to the mixing tank. One circuit was used for filling and continuous mixing in the tank. The second circuit was for the delivery of the slurry to the atomizer. It was quickly found, however, that the gear pump could not deliver the slurry at the required pressure to the atomizer. Also, a rotameter had been installed in the delivery line to measure the flow rate but the slurry was too dark for the float to be seen. The pump was removed and a nitrogen bottle was attached to the tank to pressurize the tank and deliver the slurry to the atomizer. A rotameter on the nitrogen line measured the slurry flow rate. This arrangement is shown in Fig. 2.

The mixing tank had four copper tubes inside as shown in Fig. 3. The first two openings on the mixing tank served as the inlet and outlet for the pumping circuit. Copper tubing (5/8 in. diameter) bent in a radius equal to the inside diameter of the mixing tank entered each of the three ports and terminated at the tank bottom. Through this design, the slurry is mixed by the tangential injection and continuous recirculation through the pumping loop. However, after operation of the system, a sludge of coal particles was noticed inside the mixing tank which reduced the effective loading of the slurry. Also, it was presumed that the gear pump further crushed the coal particles.

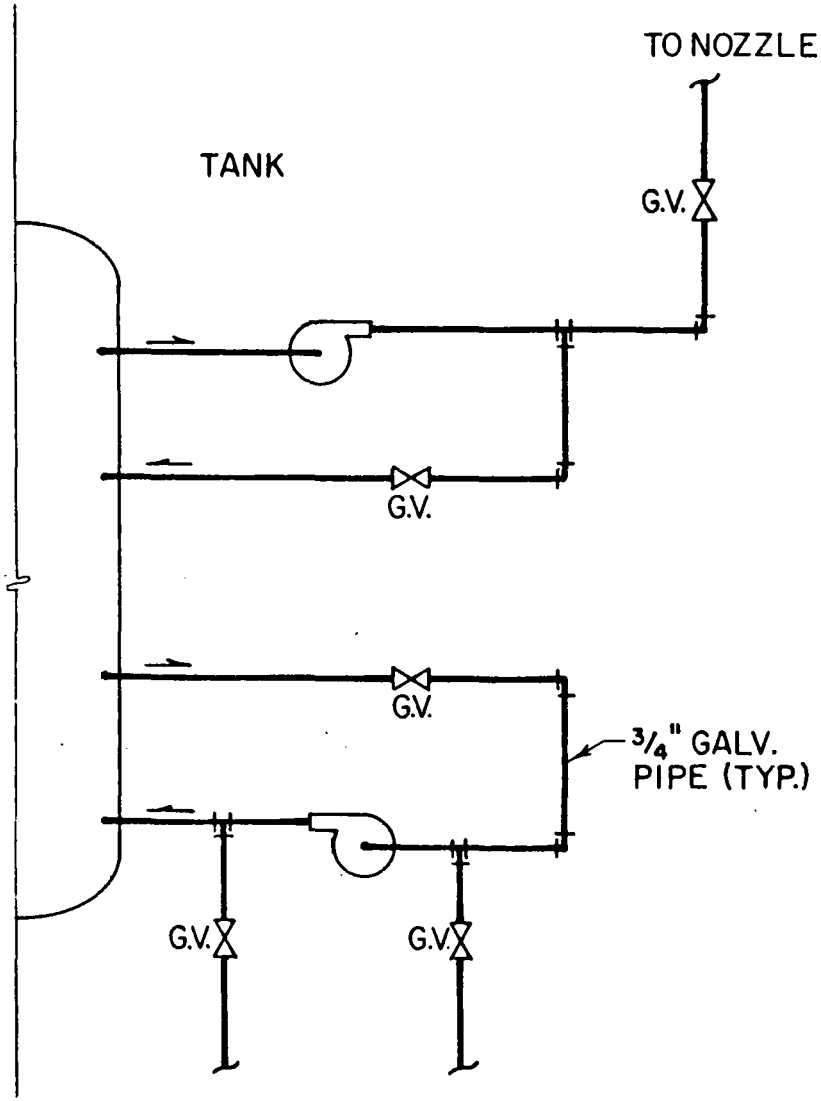

Figure 1. Slurry handling system with initian piping arrangement

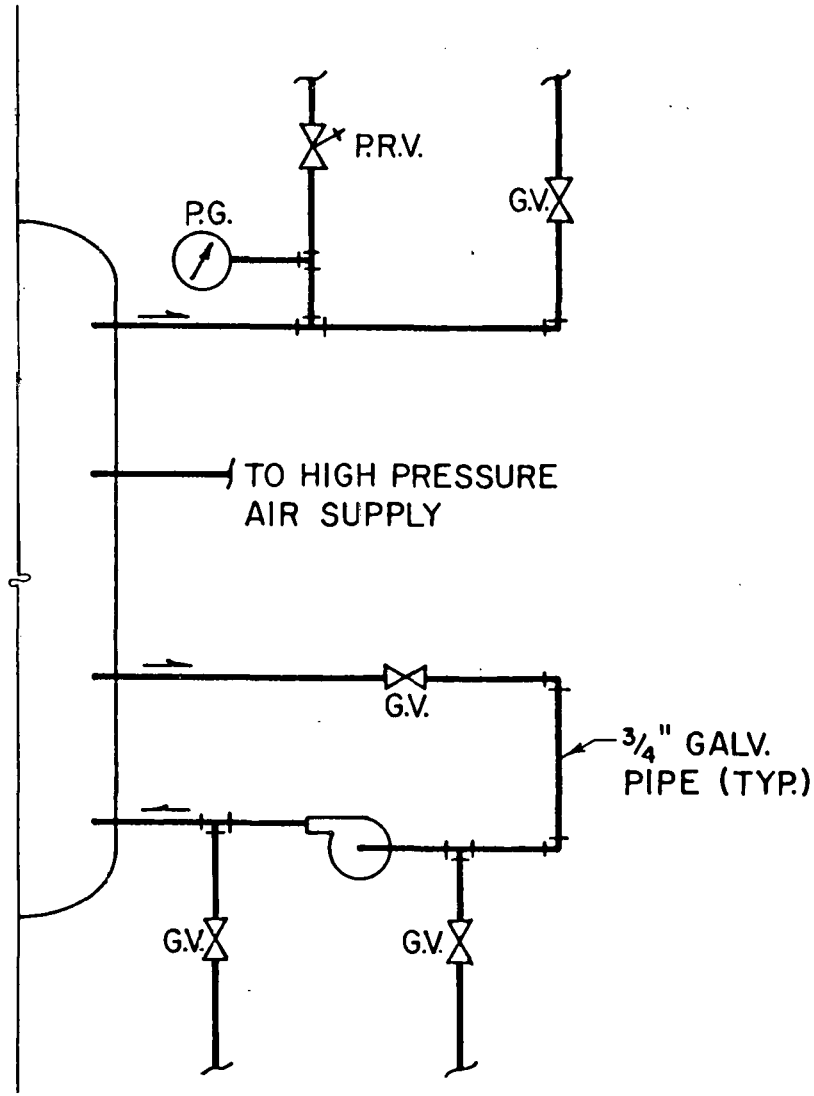

Figure 2. Slurry handling system with modified piping arrangement

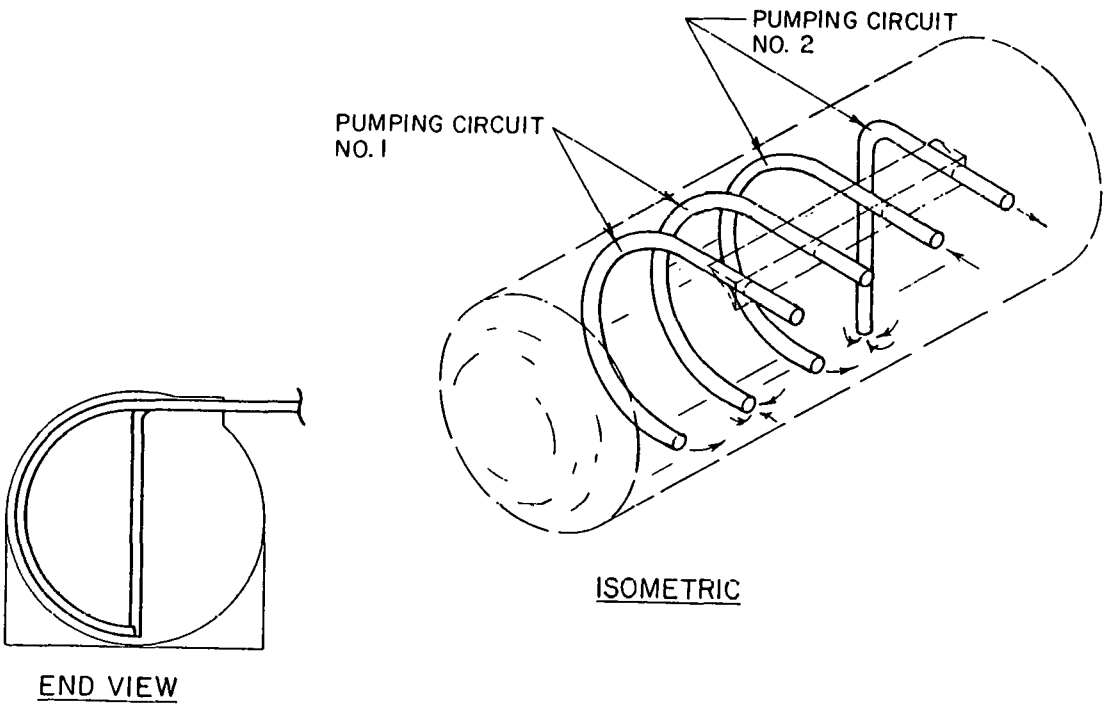

Figure 3. Arrangement of copper tubing within mixing tank

These difficulties led to the design of a new system. After considering several designs and arrangements, it was decided to modify the tank and pumping system as shown in Fig. 4. The tank was oriented vertically with an access port for cleaning located in the top. The gear pump was replaced with a rotary type pump. The rotary pump selected was manufactured by Oberdorfer. It had a pumping capability of about 30 gallons/min. To reduce pressure drop in the mixing lines, the 1 in. pipes were replaced with 4 in. pipes and the copper tubes were removed from inside of the tank.

3. SLURRY PREPARATION

The pulverized coal was prepared by obtaining lump coal from the Washington State University steam heating plant, crushing the coal with a jaw crusher and a roll crusher at the University of Idaho, and, finally, pulverizing the coal with a laboratory grinder (Alpine LU 100). The coal particles were cut at 100 microns with an Alpine MZ-100 classifier. The coal smaller than 100 microns had a mass median diameter of 45 microns as measured by a Coulter counter (model TAII). The above 100 micron coal was further cut with a 200 micron sieve to yield a mass median diameter of 130 microns. The distributions are shown in Fig. 5.

4. PNEUMATIC (TWO-FLUID) NOZZLE ATOMIZATION

The Delevan model 32668 in-line swirl air atomizing nozzle was selected based on the following features:

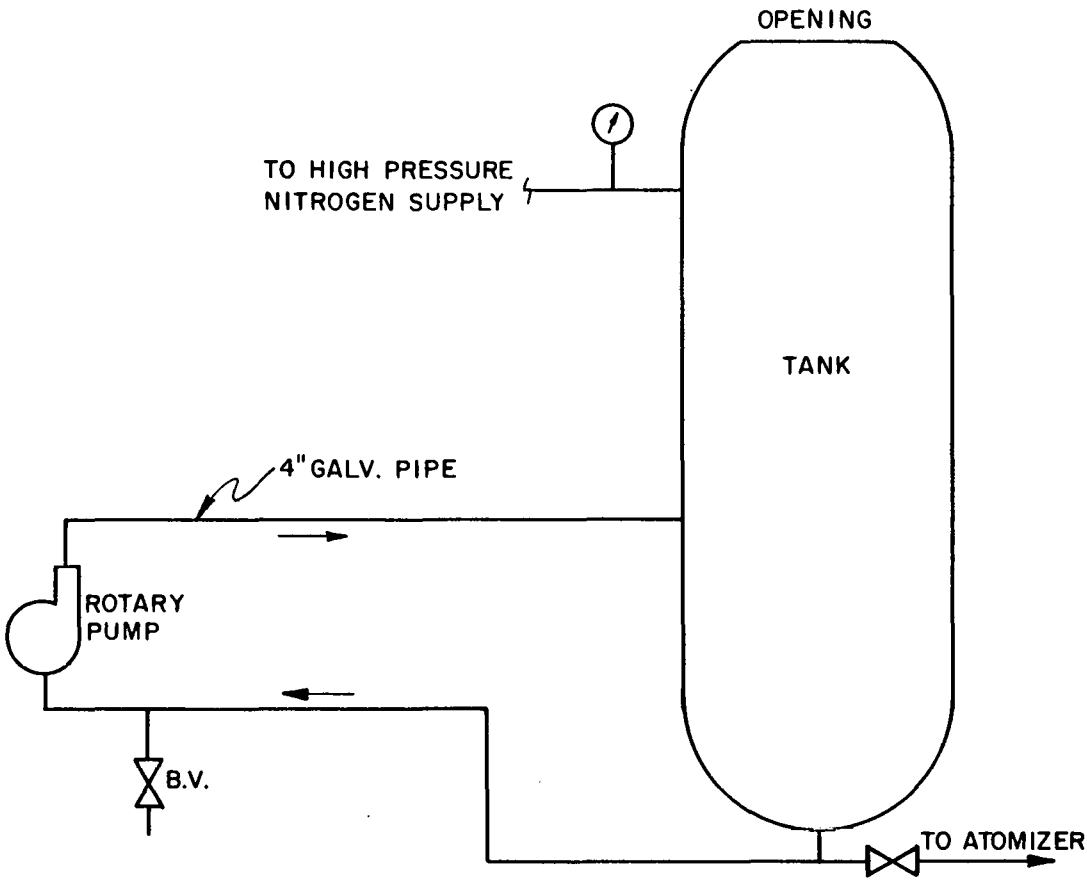

Figure 4. Modified slurry handling system

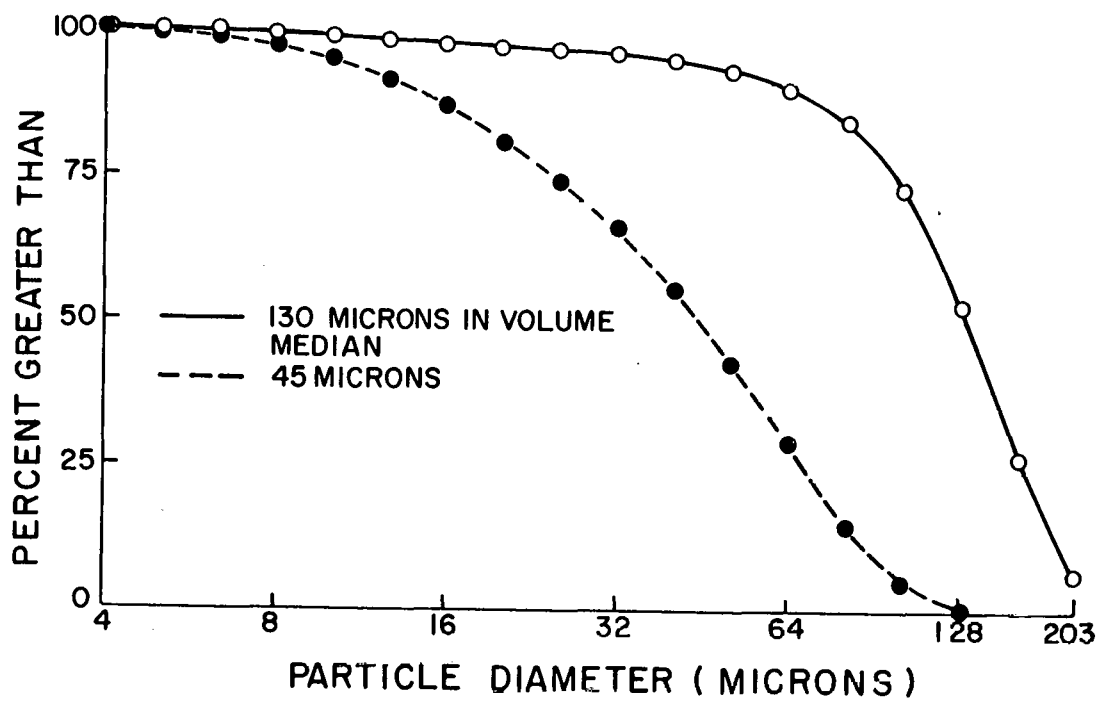

Figure 5. Distribution of coal particle sizes

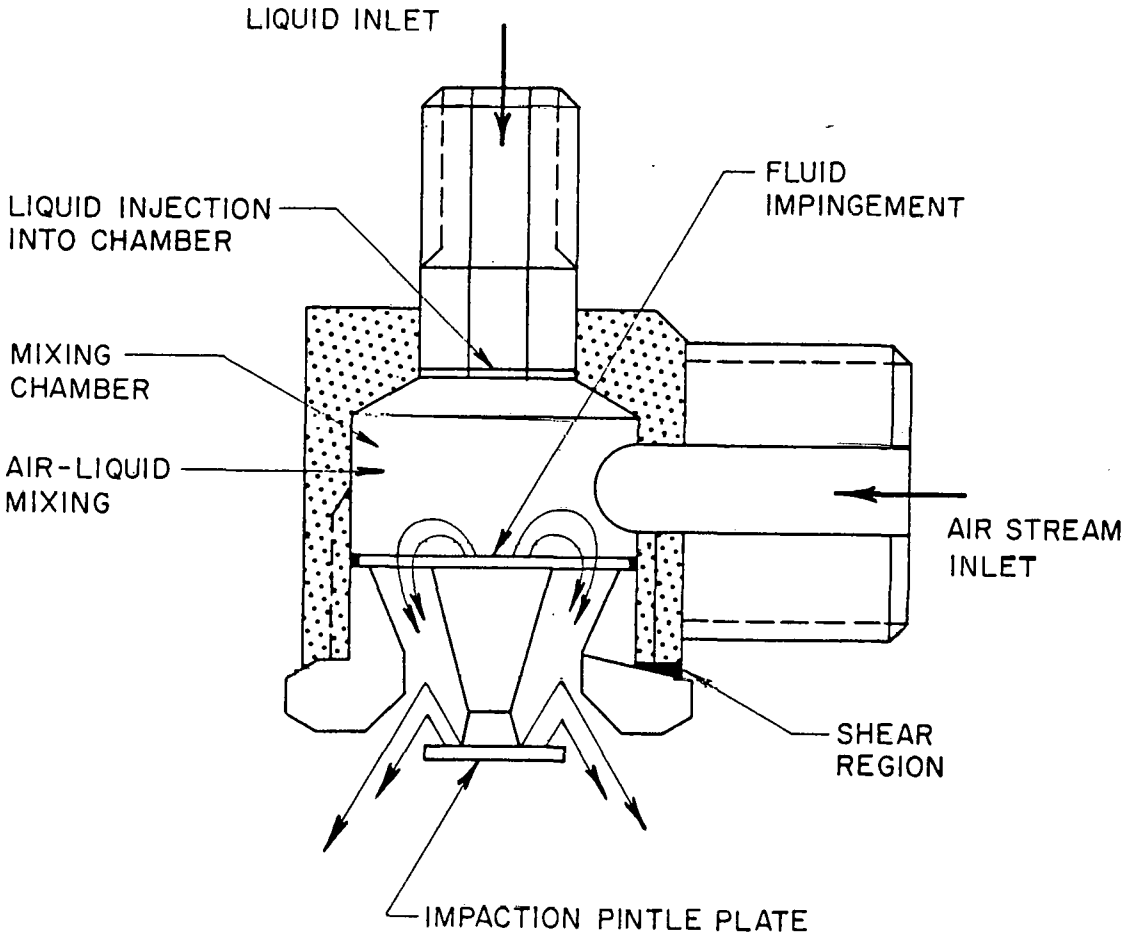

Figure 6. Internal design of nozzle

- droplet size control provided by minor changes in air supply pressures
- large fluid passages allowing flow of coal particles
- adjustable spray angle through interchangeable nozzle caps
- vortex mixing, primary gas impingement, even fluid distribution, and external air impingement yielding fine atomization

The internal design of the nozzle is shown in Fig. 6. Air is introduced tangentially into the mixing chamber in a low pressure region of the swirling liquid creating high turbulence conditions and primary atomization. As the slurry leaves the orifice, it impinges against the pintle plate which serves a dual purpose; fine control of spray angle and secondary air atomization causing even further break-up to finer droplets. The capacity of the nozzle was normally 4 gal/min achievable with a maximum air supply pressure of 70 psig and slurry supply pressure of 106 psig. These values represent factory calibrations using water only. The nozzle cap and pintle plate were made of wear-resistant 440 stainless steel, chosen for maximum survivability in this abrasive environment.

5. PHOTOGRAPHY METHOD FOR PNEUMATIC NOZZLE ATOMIZATION

The original scheme was to use photography of the droplets in which optical access to the chamber was provided by windows purged with a high velocity air stream issuing from a planar nozzle at the top of the window. The original photographic system shown in Fig. 7 consisted of a camera mounted on a microscope, a short duration, high-intensity light source, coupled with a condensing lens and a big spray chamber (24 in x 24 in x 36 in). The film used for this photography was 24 mm x 36 mm, which covered a spray field 2.4 mm x 3.6 mm at a magnification ratio of 40X. These large magnifications severely restrict the field of view. After many trials, the photography of the original system was abandoned. But further studies with another experiment encouraged another attempt at photography with a smaller spray chamber and a modified air cleaning system.

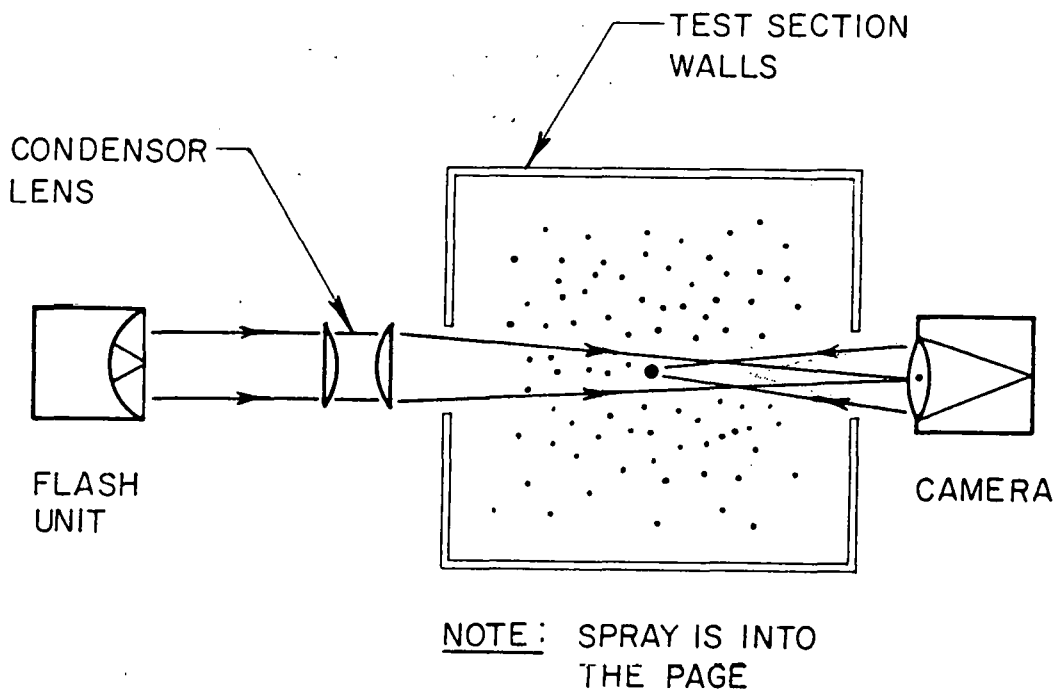

Figure 7. Original photographic system

5.1 Modified Spray Chamber and Air Purging System

Redesign of the chamber was based on having a sufficient number of droplets in the sample volume for photography and analysis and ensuring a clean microscope lens. The spray from two-fluid atomizers has a cone-type configuration so the number density of droplets increased rapidly as the sampling volume approached the nozzle. If the sampling, however, is too close to the nozzle, incomplete atomization occurs. The distance of 4 in. between nozzle and test section was chosen based on previous experience with the impression method [4]. The dimensions of the chamber shown in Fig. 8 were 4 in. x 8 in. and 20 in. high. An air purging system which produced a cyclonic flow was designed to clean the

two windows of the spray chamber. The air was directed toward the inside surface of the glass window. A cylinder was connected to the window to penetrate the spray and prevent excessive attenuation of the light by the dark spray. It was found, however, that this cylinder seriously affected the flow field in the chamber and created undesirable liquid flow patterns on the chamber wall. After many futile attempts, the cylinder and two windows were removed from the spray chamber, leaving two holes and an air-purge system on the microscope-camera side. The air-purge was directed toward the inside of the chamber. These modifications maintained a very clean microscope lens and a sufficient intensity of the incident light. The diameter of the hole for the microscope was 1 in. and the hole for the light source was 2 in. The purge air flow rate was controlled by a ball valve at a rate which did not disturb the spray field inside the chamber and which maintained a clean microscope lens.

The overall set-up is shown in Fig. 8. A two-fluid atomizer, attached with moveable holder, was positioned at the mid-point of the top cover of the spray chamber. This atomizer was connected directly to the slurry delivery line. The same camera-microscope combination as was used previously was used here. This microscope had five magnification ratios of which 30X was used most frequently. Two film types were used. ASA 30 film was used for the pure liquid spray and ASA 400 for slurries because the dark slurry attenuates the incident light significantly. A microscope, a light and two holes were carefully aligned. The distance from the axis of spray cone to the lens of microscope has to be greater than 4 in. owing to 4 in. focal length of microscope and a hollow cone type of spray. The light source is a half microsecond duration, high intensity EGG type light with a condensing lens. It is located at about 8 in. from the axis of spray cone. But this distance is not a critical factor for good droplets images.

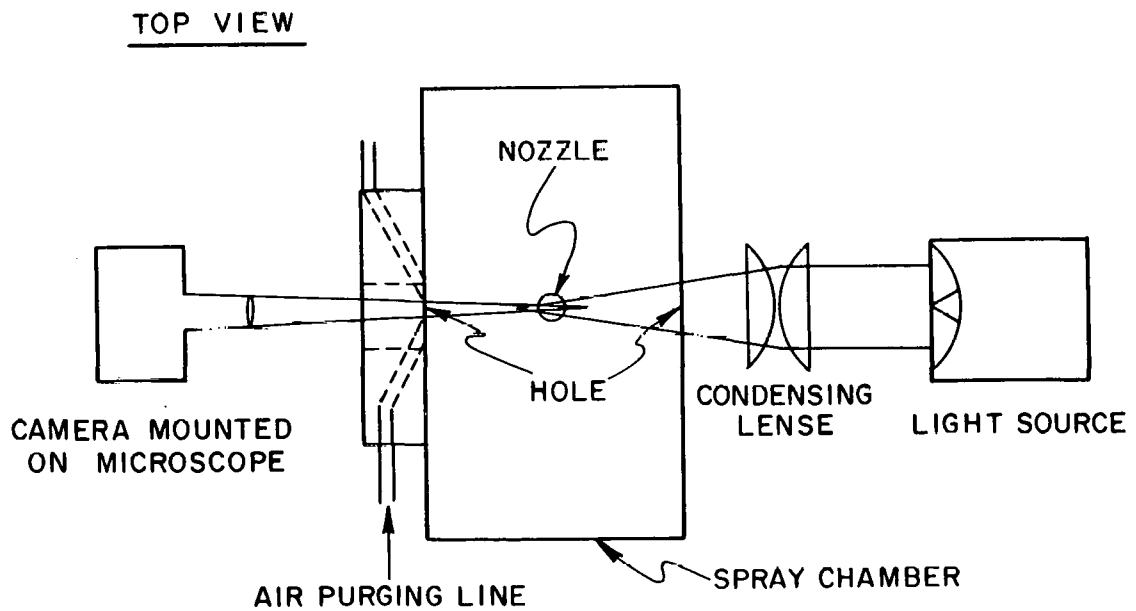

Figure 8. Set-up of photographic system

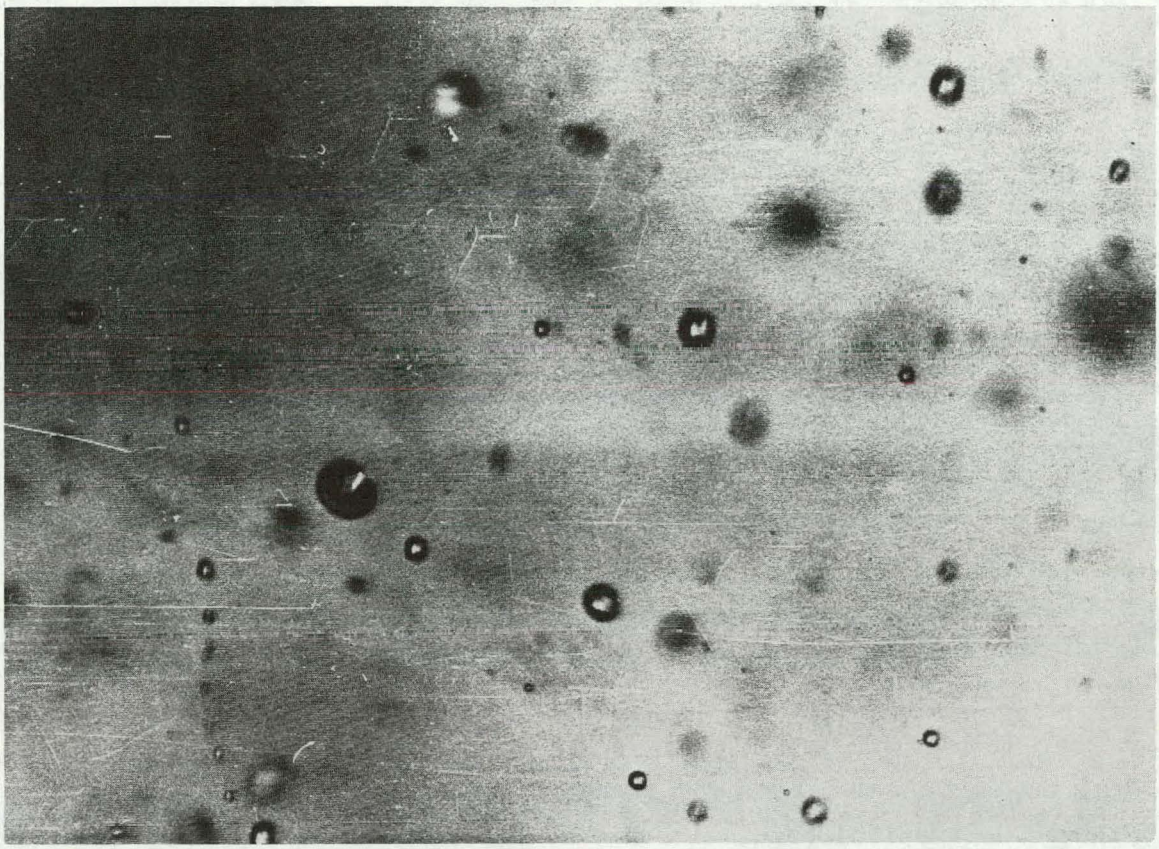

Figure 9. Picture of droplets from pneumatic atomizer

5.2 Data Analysis

With this arrangement of the system, many pictures were taken directly of the spray field. These pictures are shown in Fig. 9. The lens was opened so the exposure time was determined by the duration of the flash. Data on droplet size was accumulated and plotted in a probability graph as shown in Fig. 10.

5.3 Experimental Results

The following table summarizes the experimental results. The nominal liquid flow rate was 4 galllons per minute.

Coal Particle Size in Volume Median	Number Median Diameter in microns			
	45 microns		130 microns	
	Air-atomizing pressure		Air-atomizing pressure	
Fluid	30 psi	60 psi	30 psi	60 psi
methanol	76	60	76	60
10% coal-methanol	66	49	66	60
20% coal-methanol	63	46	60	52
D-2 diesel oil	87	69	87	69
10% coal-oil	84	59	91	79
20% coal-oil	84	60	93	73

Table 1. Experimental results for the two-fluid atomizer

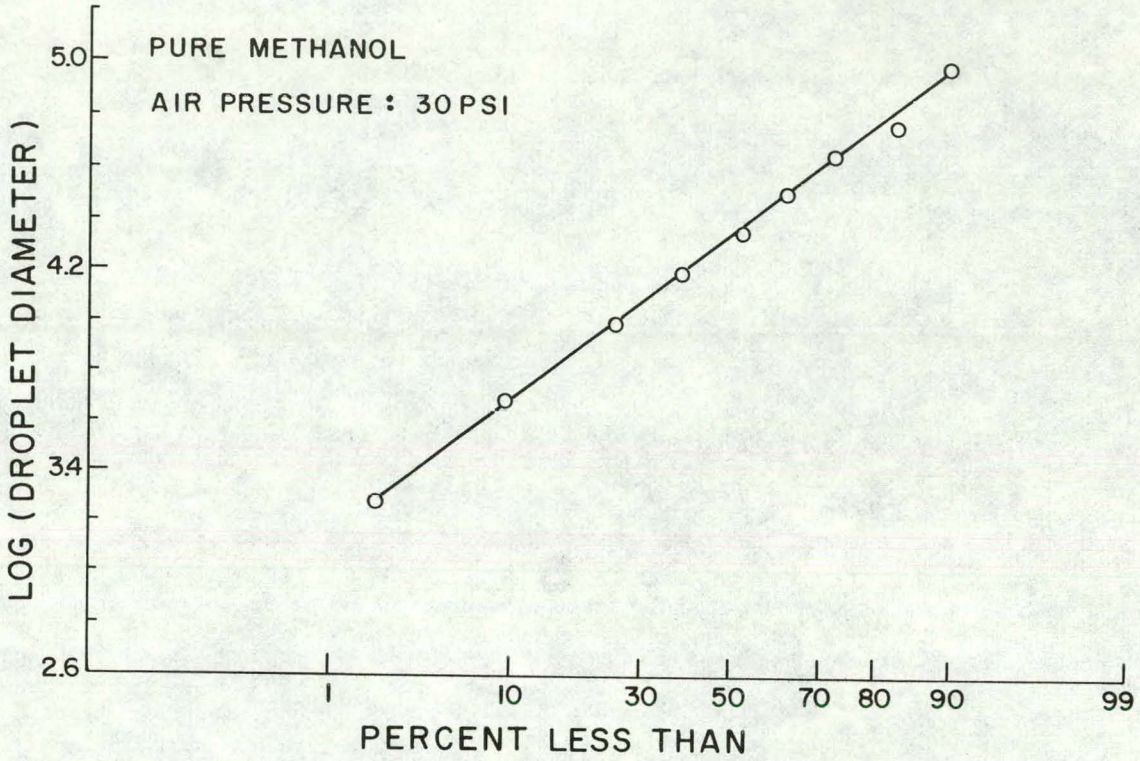

Figure 10. Typical cumulative number distribution of droplets from two-fluid atomizer as measured by the photographic method

6. WHEEL ATOMIZATION

Wheel atomization is a rotary atomization in which the liquid is disintegrated into many droplets by accelerating centrifugally the feed liquid to a high velocity before discharge. The ligaments of liquid are equally distributed along the wheel and these ligaments disintegrate into many droplets due to the kinetic energy of the liquid. The degree of atomization depends on wheel speed, feed rate, liquid properties and atomizer design.

Upon consulting with a large number of manufacturers, it was discovered that purchase of a wheel atomizer alone was not possible. Wheel atomizers must be purchased as part of a complete unit, such as a spray dryer. Hence, it was necessary to design and fabricate our own atomizer.

The wheel atomizer unit is shown in Fig. 11. The wheel, fabricated from aluminum, was 4 in. diameter and had forty 3/32 in holes. It was connected with an A.C. motor originally used for hand drill and manufactured by Dayton Electric Mfg. Co. The variable speed motor had a maximum rotational rate of 1450 rpm. The slurry was supplied through a stationary tube to the inner part of the rotating wheel and expanded radially towards the rim. In the central portion of a wheel, friction between the slurry and the inner surfaces of the wheel cause the slurry to rotate. The slurry ultimately rotates at the wheel speed when it escapes through the holes.

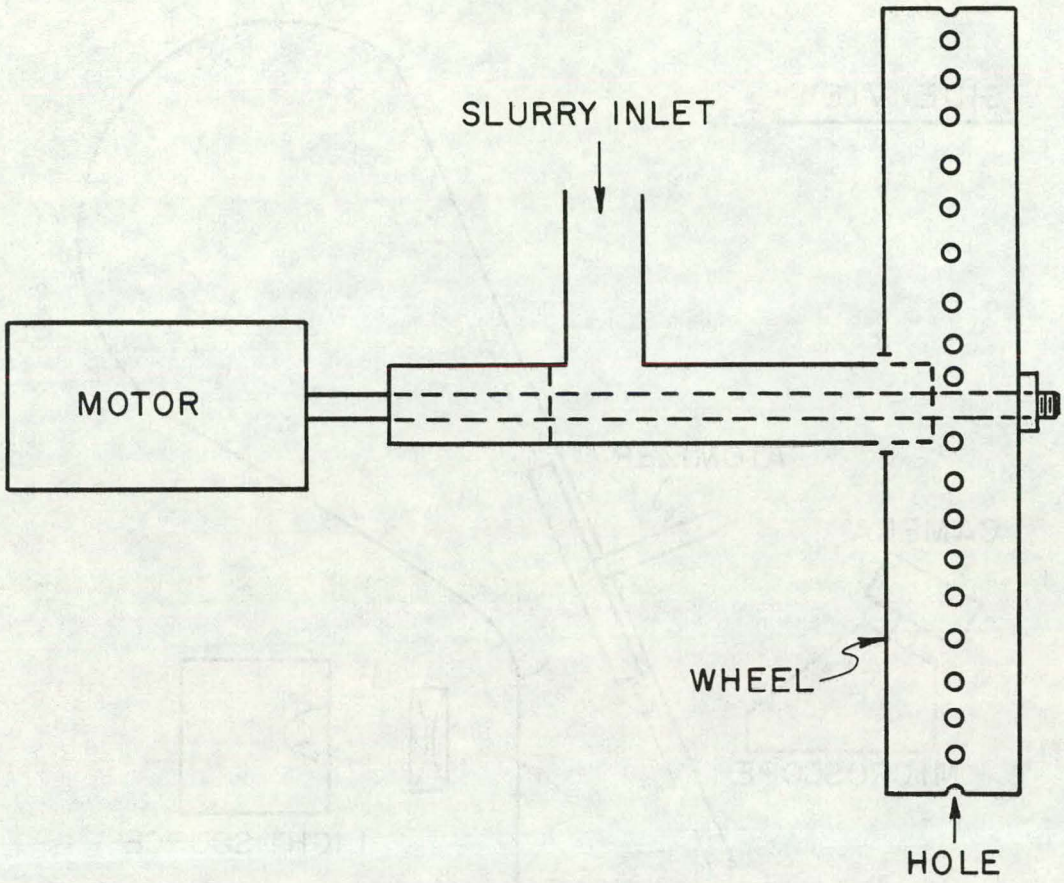

Figure 11. Wheel atomizer

7. PHOTOGRAPHY METHOD FOR WHEEL ATOMIZATION

7.1 Modified Spray Chamber

The pattern of spray produced by a wheel atomizer is a very flat circular sheet. The problem in the spray chamber design was how to confine whole spray to a limited space in such a way as to not disturb the spray at the test section. The resulting design is shown in Fig. 12. The chamber had two holes for photography without any purge air. An adjustable mounting for the atomizer permitted positioning the atomizer an adequate distance from the test section. The chamber design inhibited the splashing of the droplets and allowed the liquid to flow smoothly down the side opposite the camera. This design prevented droplets, other than those issued directly by the wheel, from entering the sample volume.

The distance between the periphery of the wheel and the test section was 5 in., which was found, through several trial positions, to be optimum. If an atomizer is located too close to the test section, only ligaments appear at the test section. On the other hand, if it is too far from the atomizer, too few droplets appear in the field of vision to yield sufficient data per frame. The overall set-up is shown in Fig. 12.

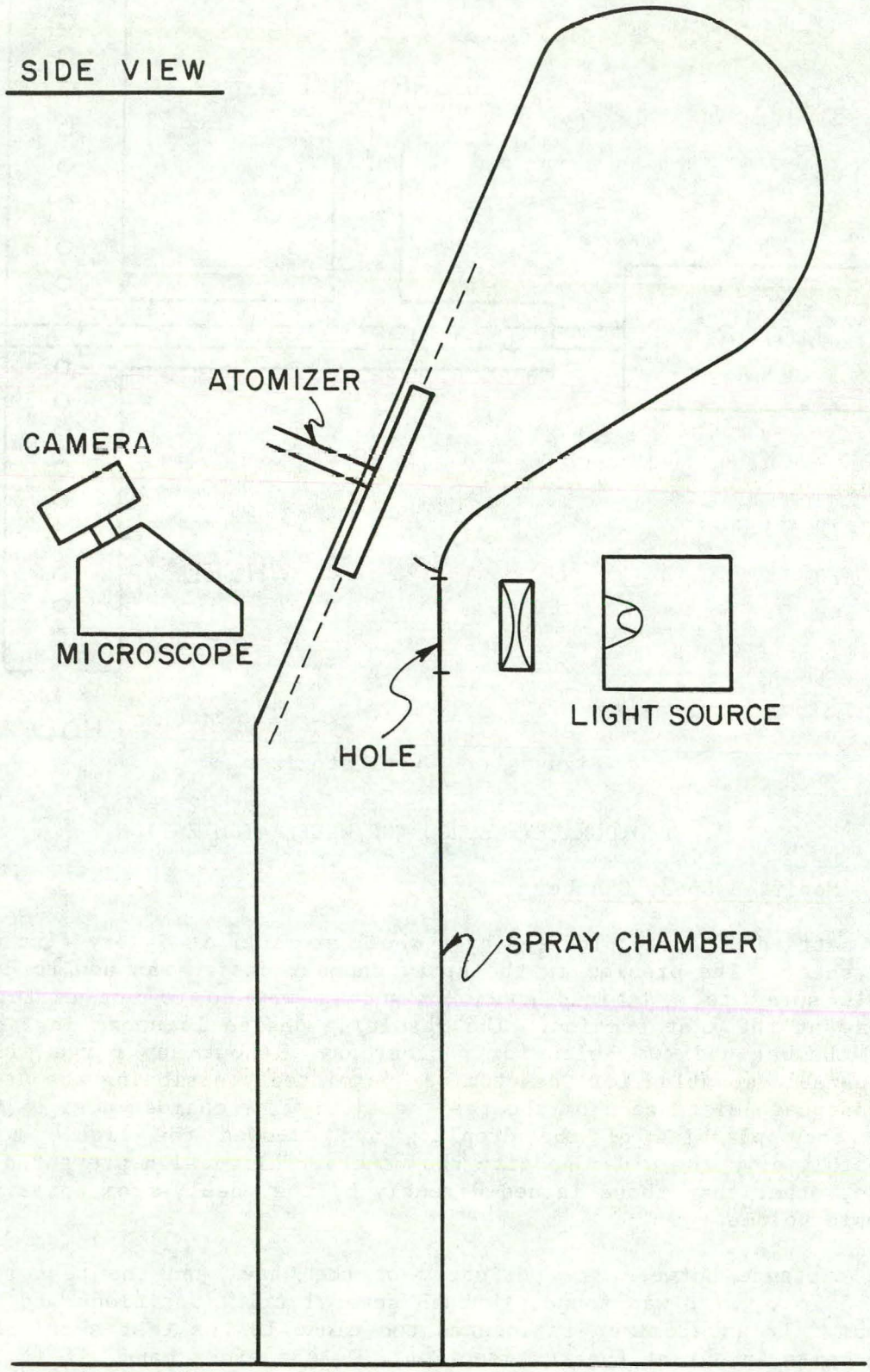

Figure 12. Modified spray chamber with camera and light source for wheel atomizer

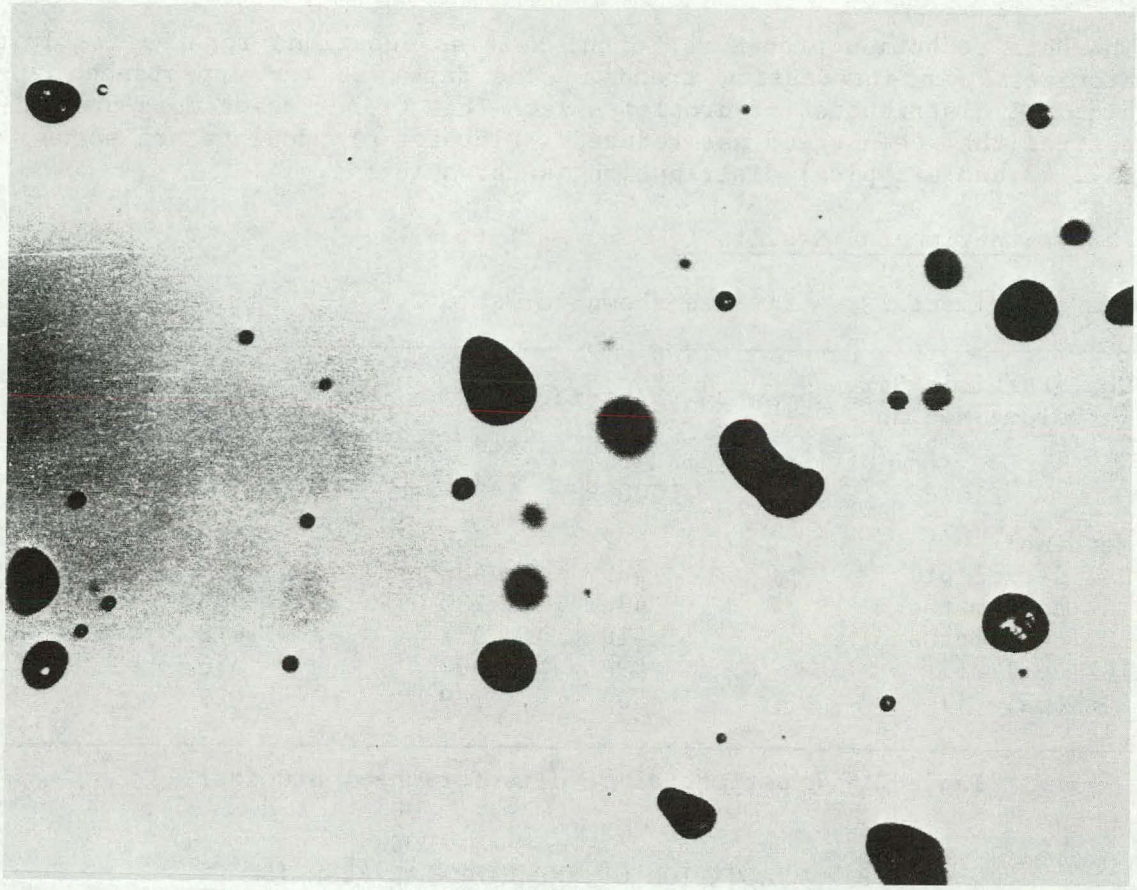

Figure 13. Picture of droplets from wheel atomizer

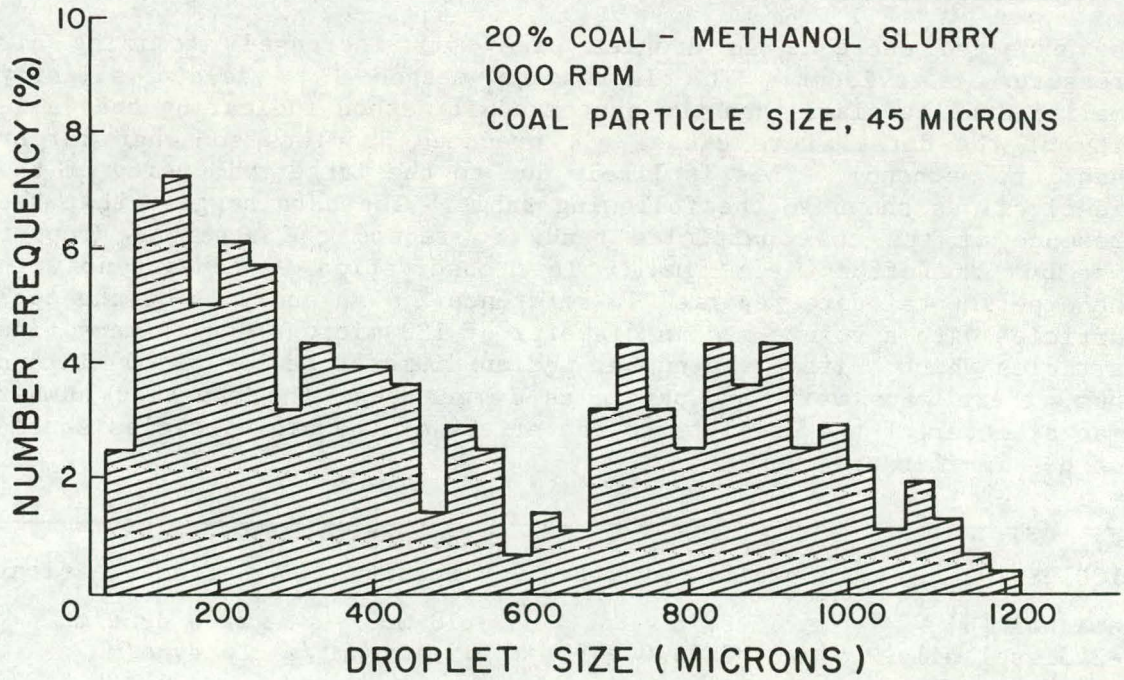

Figure 14. Typical number frequency distribution of droplets generated by wheel atomizer

7.2 Data Analysis

The data reduction procedure is the same as described for the twofluid atomizer. An interesting trend in the data was the appearance of a binomial distribution of droplet size. This trend became more predominant as the wheel speed was reduced. Pictures of droplets are shown in Fig. 13 and a typical distribution is shown in Fig. 14.

7.3 Experimental Results

The experimental results are shown in Table 2.

Coal Particle Size in Volume Median	Number Mean Diameter in microns			
	45 microns		130 microns	
	Wheel speed		Wheel speed	
Fluid	1000 RPM	1400 RPM	1000 RPM	1400 RPM
methanol	472	360	472	360
D-2 diesel oil	509	436	509	436
10% coal-methanol	436	290	345	254
20% coal-methanol	418	327	418	298
10% coal-oil	494	404	356	323
20% coal-oil	509	389	429	362

Table 2. Experimental results for wheel atomizer.

8. EVALUATION OF EXPERIMENTAL RESULTS

8.1 Two-Fluid Atomization

The expected decrease in droplet size with increased atomizing air pressures is evident. The impression method [4] yielded slightly smaller droplet sizes than the photographic method indicating the validity of the data. Pure diesel oil produced droplets somewhat larger than pure methanol. This is likely due to the larger viscosity of the diesel oil as shown in the following table. The data suggest that the presence of the coal particles tends to reduce the atomized droplet size but the effect is minimal. This observation is consistent with the experimental data reported in reference 2. An analysis of the coal particles with a volume median diameter of 130 microns showed many fine particles which shifted the number median diameter as low as 10 microns. Thus, there were very few particles larger than the observed number mean diameter of the droplets so the effect of the big particles should not be significant.

LIQUIDS	Specific gravity	Kinematic Viscosity	Surface tension
Methanol [6]	0.76	0.78 mm^2/s	22.6 dyne/m
D-2 diesel oil [2,5]	0.76-0.935	1.9-4.1 mm^2/s	26 dyne/m

Table 3. Comparison of properties of methanol and diesel oil

8.2 Wheel Atomization

Increasing the rotational speed of the wheel produces smaller droplets of pure liquid and slurry. The droplets produced by the wheel atomizer are an order of magnitude larger than those generated by the two-fluid atomizer. Commercial wheel atomizers produce smaller droplets because of the higher wheel speeds achievable. The data show, as expected, that increasing the wheel speed leads to smaller droplets. The presence of the coal in the methanol slurries appears to reduce the droplet size but the trend is not significant. The effect of coal on the droplet size of the coal/oil slurry follows a similar trend but, once again, is not significant.

9. CONCLUSION

The presence of coal in coal/methanol and coal/oil slurries at concentrations up to 20 percent does not appreciably affect the droplet size generated by two-fluid and wheel atomizers. The trend is a reduction in droplet size due to the presence of coal. These data suggest that a coal/oil or coal/methanol slurry could be burned in an oil burning furnace with little or no modifications.

REFERENCES

1. Masters, Spray Drying, John Wiley and Sons, 1976, New York, NY

2. Butcher, T., Pucci, A. and Krishna, C.R., "Atomization of Coal Slurry Jets," Conference on Coal-Oil Mixture Combustion, sponsored by Pittsburgh Energy Technology Center, November 27-29, 1979, Danvers, Massachusetts.

3. Crow, Eddie C.,Jr., "The Experimental Simulation of the Atomization of a Coal-Methanol Slurry," M.S. Thesis, Washington State University, 1981.

4. S.J. Kim, "Experimental Study of Slurry Atomization," M.S. Special Project, Washington State University, 1982.

5. Annual Books of ASTM Standards (part 23), Standard Specification for Diesel Fuel Oil, p.452, 1979.

6. Lange's Handbook of Chemistry, J. A. Dean, ed., 11th edition, McGraw-Hill Book Company, 1973.

The following manuscript was unavailable at time of publication:

Performance Characterization of an Atmospheric Pressure Combustor for Ultra-Clean Coal-Water Mixtures

D. M. Waltermire, U. Grimm and R. J. Anderson
Morgantown Energy Technology Center

DO NOT MICROFILM THIS PAGE

The following manuscript was unavailable at time of publication:

Determinations of Coal-Water Mixture Properties for Predictions of Products of Combustion Characteristics

R. R. Romanosky, Jr., J. J. Kovach and R. J. Anderson
Morgantown Energy Technology Center

DO NOT MICROFILM THIS PAGE

The following manuscript was unavailable at time of publication:

Flow Properties of Coal-Water Mixtures

J. Ekmann and D. J. Wildman
Pittsburgh Energy Technology Center

DO NOT MICROFILM THIS PAGE

EFFECT OF COAL ASH CONTENT ON PERFORMANCE OF A CWM-FIRED BOILER

Y.S. Pan, G.T. Bellas, R.B. Snedden,
D.J. Wildman, and J.I. Joubert
U.S. Department of Energy
Pittsburgh Energy Technology Center
Pittsburgh, Pennsylvania 15236

ABSTRACT

A series of parametric tests was conducted to determine the effect of fuel ash content on boiler performance when burning CWMs containing about 60 percent coal. Three types of coal -- Pittsburgh seam coal containing 11.4 percent ash, a Virginia coal containing 6.9 percent ash, and an Eastern Kentucky coal containing 2.6 percent ash -- were evaluated. The CWMs prepared with each coal could be burned at carbon conversion efficiencies in excess of 97 percent using preheated air at 500°F. As expected, the amounts of particulate emissions and boiler ash deposition were directly related to the ash content in the coals used.

INTRODUCTION

Since 1981, an evaluation of coal-water mixtures as alternate fuels for oil-designed boilers has been underway at the Pittsburgh Energy Technology Center (PETC). The initial exploratory CWM test results obtained in a 100-hp firetube boiler and a 700-hp watertube boiler were reported at the Fourth International Symposium on Coal Slurry Combustion at Orlando, Florida, in May 1982.[1] A comprehensive CWM combustion program is now being conducted using the 700-hp boiler (Figure 1), which generates 24,000 pounds of steam per hour at its full capacity.

The initial phase of the CWM tests in the 700-hp boiler was carried out using a modified dual-air-zone register.[1,2] Because of limitations on the preheated-air supply available to the boiler, the boiler could not be operated at its full capacity. A larger forced-draft fan was installed, and the air register was changed to a single-air-zone design with a concentric center-tube surrounding the burner nozzle that introduced a separately controllable air stream (Figure 2). In addition, the original 13.5-inch-long refractory tile throat in the boiler was extended to 22.5 inches. These modifications have allowed the 700-hp boiler to be operated routinely on CWM at full capacity.[3]

A series of parametric tests was conducted to evaluate the effect of coal ash content on boiler performance. The CWM fuels were prepared

at PETC with the highest coal concentrations that resulted in acceptable mixing and transport characteristics. The CWMs tested generally contained approximately 60 percent dry coal, pulverized to a nominal size consist of 90 percent minus 200 mesh, and 0.5 percent Lomar-D* (a viscosity reducing agent); the balance was water. Three types of coal -- Pittsburgh seam coal containing 11.4-percent ash, a beneficiated Virginia coal containing 6.9-percent ash, and a beneficiated Eastern Kentucky coal containing 2.6-percent ash -- were evaluated. Typical analyses of these three coals are given in Table 1.

The Pittsburgh seam coal was obtained from the Consolidation Coal Company, Pittsburgh, Pennsylvania, and is an equal blend of high volatile A bituminous coals from Westlen Mine No. 2 (a deep mine) and strip mines in either Deroy, Ledersville, or Laudersville, Pennsylvania. The resultant blend of coal is washed and crushed to 3/4-inch by 3/16-inch size and sold as "Junior Stoker" coal mainly to the utility market. The beneficiated Virginia and Eastern Kentucky coals were obtained from the United Coal Company, Bristol, Virginia, and both are high volatile A bituminous coals. The Virginia coal is termed a Wellmore blend and consists of Virginia Blair seam and Virginia Hagy seam coals. The Eastern Kentucky coal is a highly cleaned coal produced by United Coal on special order only.

COMBUSTION TEST FACILITY

The 700-hp Combustion Test Facility, as arranged for firing CWM, is shown in Figure 3. Central to this facility is the 700-hp, two-pass, watertube, industrial boiler, originally designed for oil firing. The facility has a complete fuel preparation system, a dry sorbent injection system for SO_2 removal, and a baghouse for particulate control. The facility is also equipped with extensive instrumentation and a computer-controlled data acquisition system. A detailed description of the test facility can be found in previous publications.[4,5]

Coal-water mixtures are prepared in an 1800-gallon-capacity mix tank, using predetermined amounts of water, pulverized coal, and viscosity reducing agent. Before use, the mixtures are transferred to a 2800-gallon hold tank. Both the mix tank and the hold tank are steam-jacketed and equipped with turbine-blade-type agitators. External recirculation of mixtures, using compressed-air-powered diaphragm pumps, from the bottom of the tanks to the top maintains the consistency of the mixtures.

---

*Reference in this paper to any specific commercial product, process, or service is to facilitate understanding and does not necessarily imply its endorsement or favoring by the United States Department of Energy.

The CWM fuel train includes a variable-speed progressing-cavity feed pump that controls the fuel flow rate to the boiler, a Micro-Motion mass flowmeter, and a pneumatically actuated three-way pinch valve that replaces safety shutoff and fuel return valves that were part of the original fuel train for No. 6 oil firing.

The burner nozzle (Figure 4) used in carrying out all CWM tests is only slightly different from the oil-designed, inside-mix, steam-atomized burner nozzles used in previous coal-oil mixture tests. The changes are the enlargement of the nozzle hole cross-section area, the reduction of the burner spray angle, and the utilization of air atomization. Preheated combustion air at 500°F is normally used to maintain stable combustion, and natural gas is used as a start-up fuel.

COMBUSTION TEST PROCEDURES

For each CWM combustion test, pulverized coal with a specified particle size consist is first prepared and then mixed with water in the mix tank. Mixture concentration is checked and the mixture is transferred to the hold tank.

Prior to each test, the furnace is cleaned, and then the boiler is brought up to one quarter of its full firing rate overnight with natural gas to allow the boiler skin temperature to reach its steady-state value. The heat transfer surface of the convection bank of the boiler is cleaned by activating the soot blower several times before a test. The soot blower is not activated during a test to avoid interference with data acquisition. At the start of a test, CWM and preheated combustion air are introduced to bring the boiler to the proper firing rate; at the same time, natural gas is gradually shut off. The time duration for switching from natural gas to CWM and bringing the boiler to the proper firing rate is about 20 minutes.

Upon reaching the proper boiler firing rate, the excess air level is set at the specified condition. The atomizing air flow and pressure, combustion air swirl, center-tube air flow, and the burner nozzle position are adjusted so that a good flame pattern is obtained without flame impingement on the furnace wall. The boiler is operated at steady-state test conditions for at least one hour before acquisition of test data is initiated. The duration of each test is about 4 hours.

After completion of the test, the boiler is switched back to natural gas and brought down with minimal disturbance to the furnace ash accumulation. The furnace is allowed to cool and then is opened for inspection. Furnace deposits are collected, weighed, and analyzed.

COMBUSTION TEST RESULTS

Prior to the series of CWM tests, a baseline No. 6 oil test was performed. A typical No. 6 oil analysis and test results are given in Table 2.

The CWM tests with Pittsburgh seam coal and Virginia coal were conducted using a burner assembly (Figure 2) without the diffuser at the exit of the center air tube; during the tests with Eastern Kentucky coal, the diffuser was installed. All of the CWM tests were carried out with preheated air at a temperature of approximately 500°F.

Pittsburgh Seam Coal

Analyses of CWMs prepared with 11.4-percent-ash Pittsburgh seam coal are given in Table 3. Boiler operating conditions and performance on CWM are given in Table 4. At full boiler load, tests were conducted at three excess air levels ranging from 8.7 to 15.2 percent (Tests No. 1, 2, and 3); a half-load test was carried out at an excess air of 19.4 percent (Test No. 4). The carbon conversion efficiencies at full load were found to be 95.5 to 97.1 percent, increasing with the increase of excess air; the calculated boiler efficiencies based on the heat-loss method of the ASME Steam Power Code were approximately 75 percent, which were about 7 percent lower than the boiler efficiency attained during the No. 6 oil baseline test (Table 2) conducted with 11.8 percent excess air at ambient temperature. Of the total thermal input, 5.92 to 6.15 percent was consumed in evaporating the water in the CWM. At half load, both carbon conversion efficiency (98.8 percent) and boiler efficiency (76.6 percent) were higher than levels achieved in the full-load tests.

Table 5 compares flue gas emissions and furnace deposits during the CWM tests. The SO_2 emissions generally corresponded to the sulfur content of the fuel. The NO_x emissions ranged from 375 to 452 ppm or 0.52 to 0.61 lb/MBtu at full load. Uncontrolled particulate emissions and furnace deposition, as expected, were also substantially higher when burning CWM in comparison to burning No. 6 fuel oil (Table 2).

Beneficiated Virginia Coal

The CWM combustion tests with 6.9-percent-ash beneficiated Virginia coal were performed at full load with three different excess air levels (4.8 to 15.4 percent) and at the lowest boiler load achievable with and without a diffuser at the exit of the center air tube. Table 6 gives the analyses of CWM used during these tests.

Boiler operating conditions and performance during the CWM tests are given in Table 7. At full load, the carbon conversion efficiencies varied from 95.1 to 97.5 percent; the boiler efficiencies were about 77 percent. Of the total thermal input, 5.13 to 5.50 percent was consumed in evaporating the water in the CWM. The lowest stable firing rate of the boiler on CWM prepared with Virginia coal corresponded to 16,710 pounds of steam per hour with no diffuser in the center air tube. Upon installation of a diffuser that creates additional air swirl close to the burner and acts as a flame holder, the lowest boiler load achieved was 14,150 pounds of steam per hour. However, the carbon conversion efficiencies were only 97.2 and 98.7

percent, respectively, with and without the diffuser at the two lowest loads. Table 8 gives flue gas emissions and furnace deposition during CWM tests using the Virginia coal.

Beneficiated Eastern Kentucky Coal

The series of CWM tests with 2.6-percent-ash beneficiated Eastern Kentucky coal was conducted with the diffuser at the exit of the center air tube. Tests were performed at full load with three excess air levels (6.5 to 17.2 percent) and at the lowest achievable boiler load. Table 9 gives the analyses of the CWMs used in these tests. The boiler operating conditions and performance during the tests are given in Table 10. The carbon conversion efficiencies increased from 95.7 to 97.4 percent with the increase in excess air level; the boiler efficiencies were about 77.6 percent at full load. The lowest load was achieved at a steam generation of 14,960 pounds per hour, which was slightly higher than that with Virginia coal. Table 11 gives flue gas emissions and furnace deposition during CWM tests using the Eastern Kentucky coal.

Comparison of Test Results

A comparison of carbon conversion and boiler efficiencies obtained during full-load tests with CWMs prepared with the three coals of different ash contents is given in Figure 5. For each coal, carbon conversion efficiencies increased slightly with the increase in excess air. Carbon conversion efficiencies achieved with CWMs prepared with the Virginia and Eastern Kentucky coals were about the same and were slightly higher than the carbon conversions obtained with the Pittsburgh seam CWMs. No apparent correlation between coal ash-content and carbon conversion achieved was discernible, indicating that other coal properties are of more importance in relation to coal reactivity.[6-8]

For each coal, the boiler efficiency remained about the same over the range of excess air levels employed, reflecting the counterbalancing effects of increasing carbon conversion and increasing stack heat losses with increasing excess air. Boiler efficiency for a given set of conditions increased with decreasing coal ash-content. This was a result of the lowering of boiler ash deposition rates (Figure 6) as coal ash-content decreased, which in turn resulted in lower average flue-gas temperature and lower stack heat losses over the period of a test. As indicated in Figure 6, measured ash deposition in the furnace section of the boiler and deposition in the convective section, calculated by material balance, increased monotonically with ash content in the coal.

CONCLUDING REMARKS

The results of the CWM combustion tests conducted in the PETC oil-designed 700 HP boiler lead to the following observations: (1) CWMs containing 60 percent by weight of three different hvAb coals could be burned at carbon conversion efficiencies in excess of 97 percent using preheated air at 500°F (coal particle size consists were

90 percent minus 200 mesh, only slightly finer than typical utility boiler grind). (2) The ash content of the coal had a marked effect on the rate of deposition in both the radiant and convective sections of the boiler, resulting in a significant lowering of the average flue-gas temperature and increase in boiler efficiency during the period of a test as ash-content of the coal decreased from 11.4 to 2.6 percent. (3) Even when burning CWMs prepared with coal containing only 2.6 percent ash, deposition in both the radiant and the convective sections of the boiler was significant. Beneficiated coals with substantially less ash content will be required if CWMs are to be burned without the assistance of ash removal equipment (such as soot blowers) in a boiler of the same general configuration as the PETC unit.

REFERENCES

1. Pan, Y.S., G.T. Bellas, R.B. Snedden, D.E. Wieczenski, and J.I. Joubert. "Exploratory Coal-Water and Coal-Methanol Mixture Combustion Tests in Oil-Designed Boilers," presented at the Fourth International Symposium on Coal Slurry Combustion, Orlando, Florida, May 10-12, 1982.

2. Pan, Y.S., G.T. Bellas, and J.I. Joubert. "Coal-Liquid Mixture Combustion Tests in Oil-Designed Boilers," ASME paper 82-IPC-Fu-2, presented at 1982 ASME Industrial Power Conference, New Orleans, Louisiana, October 3-6, 1982.

3. Pan, Y.S., G.T. Bellas, R.B. Snedden, and J.I. Joubert. "Coal Slurries on Alternate Fuels for Oil-Designed Boilers," presented at American Flame Research Committee's International Symposium on Conversion to Solid Fuels, Newport Beach, California, October 26-28, 1982.

4. Pan, Y.S., G.T. Bellas, D. Lunifeld, and J.I. Joubert. "Coal-Oil Mixtures: A Near-Term Approach to Conserving Petroleum," ASME paper 81-Pet-22, presented at ASME Energy-Sources Technology Conference and Exhibition, Houston, Texas, January 18-22, 1981.

5. Pan, Y.S., G.T. Bellas, M.P. Mathur, J.I. Joubert, and D. Bienstock. "Recent Coal-Oil Mixture Combustion Tests at PETC," DOE/PETC/TR-80/5, Pittsburgh Energy Technology Center, Pittsburgh, Pennsylvania, June 1980.

6. Field, M.A., D.W. Gill, B.B. Morgan, and P.G.W. Hawksley, Combustion of Pulverized Coal, The British Coal Utilization Research Association, Leatherhead, Surrey, England, Chapters 4-6, John Wiley and Sons, 1967.

7. Essenhigh, R.H. Fundamentals of Coal Combustion, in Chemistry of Coal Utilization, 2nd Supplementary Volume, ed. by M.A. Elliott, Chapter 19, John Wiley and Sons, 1981.

8. Howard, J.B. Fundamentals of Coal Pyrolysis and Hydropyrolysis, in Chemistry of Coal Utilization, 2nd Supplementary Volume, ed. by M.A. Elliott, Chapter 12, John Wiley and Sons, 1981.

TABLE 1. TYPICAL ANALYSES OF PITTSBURGH SEAM COAL AND BENEFICIATED VIRGINIA AND EASTERN KENTUCKY COALS

Coal Type	Pittsburgh Seam	Beneficiated Virginia	Beneficiated Eastern Kentucky
Proximate Analysis (%) - As Fired			
Moisture	1.5	1.6	1.9
Volatile Matter	37.3	33.5	40.0
Fixed Carbon	50.0	58.1	55.5
Ash	11.2	6.8	2.6
Ultimate Analysis (%) - Moisture Free			
Hydrogen	5.0	5.2	5.6
Carbon	72.7	78.6	82.2
Nitrogen	1.5	1.6	1.6
Sulfur	2.1	1.4	1.2
Oxygen (ind.)	7.3	6.3	6.8
Ash	11.4	6.9	2.6
Heating Value (Btu/lb) - Moisture Free	13,333	14,108	14,829
Ash Fusion Temperatures (^{o}F)			
Initial Deformation Temp.	2,440	2,050	2,210
Softening Temp.	2,530	2,300	2,330
Fluid Temp.	2,610	2,420	2,480
Major Constituents in Ash (%)			
SiO_2	51.81	47.64	38.88
Al_2O_3	25.99	29.82	32.97
Fe_2O_3	15.49	14.62	18.79
TiO_2	1.30	1.48	1.56
CaO	1.12	1.82	5.49
MgO	0.91	1.11	0.48
Na_2O	0.45	0.72	1.47
K_2O	1.90	1.28	1.68
SO_3	0.45	0.94	1.36

TABLE 2. NO. 6 FUEL OIL BASELINE TEST

Fuel Analysis

Ultimate Analysis (%)

Hydrogen	11.5
Carbon	87.0
Nitrogen	0.2
Sulfur	0.8
Oxygen (ind.)	0.3
Ash	0.2
Heating Value (Btu/lb)	18,695

Operating Conditions and Boiler Performance

Load	Full
Flue Gas O_2 (%)	2.4
Excess Air (%)	11.8
Steam Flow (lb/hr)	24,140
Fuel Flow (lb/hr)	1,511
Thermal Input (MBtu/hr)	28.4
Combustion Air Temp. (^{o}F)	81
Total Air Flow (lb/hr)	23,630
Atomizing Air Flow (lb/hr)	369
Atomizing Air Pressure (psig)	113
Center-Tube Air Flow (lb/hr)	0
Average Flue Gas Temp. (^{o}F)	544
Carbon Conversion Efficiency (%)	~100
Boiler Efficiency (%) (Heat Loss Method)	81.8

Emissions

Flue Gas Analysis

O_2	(%)	2.4
CO_2	(%)	13.6
CO	(ppm)	24
SO_2	(ppm)	484
	(lb/MBtu)	0.88
NO_x	(ppm)	165
	(lb/MBtu)	0.22
THC*	(ppm)	0

Particulate

Emissions	(lb/hr)	1.9
	(lb/MBtu)	0.07
Analysis (%)		
Carbon		----
Sulfur		----
Ash		89.3

*Total hydrocarbons

TABLE 3. ANALYSES OF COAL-WATER MIXTURES PREPARED WITH PITTSBURGH SEAM COAL

Test Number	1	2	3	4
Weight Percent Coal	59.6	60.2	60.6	58.6
Coal Size Consist (% minus 200 mesh)	90	90	91	90
Ultimate Analysis (%)				
Hydrogen	7.6	7.5	7.5	7.6
Carbon	43.2	43.6	43.9	42.5
Nitrogen	0.8	0.8	0.9	0.8
Sulfur	1.5	1.5	1.5	1.5
Oxygen	39.7	39.3	38.8	40.5
Ash	7.2	7.3	7.4	7.1
Heating Value (Btu/lb)	7,729	7,807	7,859	7,599

TABLE 4. OPERATING CONDITIONS AND BOILER PERFORMANCE, COAL-WATER MIXTURE TESTS WITH PITTSBURGH SEAM COAL

Test Number	1	2	3	4
Load	Full	Full	Full	Half
Flue Gas O_2 (%)	2.5	2.9	3.3	3.7
Excess Air (%)	8.7	12.0	15.2	19.4
Steam Flow (lb/hr)	23,980	24,120	24,040	12,400
Fuel Flow (lb/hr)	3,697	3,660	3,605	1,860
Thermal Input (MBtu/hr)	31.1	31.2	31.0	15.5
Combustion Air Temp. (°F)	493	492	501	508
Total Air Flow (lb/hr)	23,750	24,490	24,970	12,920
Atomizing Air Flow (lb/hr)	1,129	1,137	1,077	1,038
Atomizing Air Pressure (psig)	94	93	94	80
Center-Tube Air Flow (lb/hr)	4,677	4,880	5,045	2,047
Center-Tube Air Temp. (°F)	404	389	407	445
Average Flue Gas Temp. (°F)	570	592	599	532
Carbon Conversion Efficiency (%)	95.5	96.5	97.1	98.8
Boiler Efficiency (%) (Heat Loss Method)	75.0	74.9	75.3	76.6
Heat Loss due to Water in Fuel (%)	6.15	6.03	5.92	6.25

TABLE 5. EMISSIONS AND FURNACE ASH DEPOSITION, COAL-WATER MIXTURE TESTS WITH PITTSBURGH SEAM COAL

Test Number	1	2	3	4
Flue Gas Analysis				
O_2 (%)	2.5	2.9	3.3	3.7
CO_2 (%)	15.3	14.8	14.7	14.2
CO (ppm)	86	101	90	143
SO_2 (ppm)	1,981	1,814	1,906	1,743
(lb/MBtu)	3.69	3.53	3.95	3.60
NO_x (ppm)	452	375	382	423
(lb/MBtu)	0.61	0.52	0.57	0.63
THC* (ppm)	9	7	4	1
Particulate				
Emissions (lb/hr)	249	228	195	61
(lb/MBtu)	8.01	7.31	7.09	3.93
Mean Particle Size (μm)	31.8	13.7	12.3	18.1
Analysis (%)				
Carbon	28.3	23.3	22.5	15.9
Sulfur	0.4	0.3	0.4	0.3
Ash	69.5	75.0	75.6	82.4
Furnace Deposits (lb/hr)	14.5	18.9	19.2	12.4
Analysis (%)				
Carbon	5.2	17.4	10.9	0.3
Sulfur	0.5	0.6	0.7	0.2
Ash	93.3	78.9	87.8	99.2

*Total hydrocarbons

TABLE 6. ANALYSES OF COAL-WATER MIXTURES PREPARED WITH BENEFICIATED VIRGINIA COAL

Test Number	1	2	3	4	5
Weight Percent Coal	60.7	60.1	61.9	60.3	60.1
Coal Size Consist (% minus 200 mesh)	92	89	93	88	89
Ultimate Analysis (%)					
Hydrogen	7.6	7.6	7.5	7.6	7.6
Carbon	47.7	47.2	48.7	47.4	47.0
Nitrogen	1.0	0.9	1.0	0.9	0.9
Sulfur	0.8	0.8	0.9	0.8	0.8
Oxygen	38.7	39.4	37.6	39.1	39.6
Ash	4.2	4.1	4.3	4.2	4.1
Heating Value (Btu/lb)	8,564	8,479	8,733	8,507	8,436

TABLE 7. OPERATING CONDITIONS AND BOILER PERFORMANCE, COAL-WATER MIXTURE TESTS WITH BENEFICIATED VIRGINIA COAL

Test Number	1	2	3	4	5*
Load	Full	Full	Full	Lowest	Lowest
Flue Gas O_2 (%)	1.8	2.9	3.3	2.8	3.5
Excess Air (%)	4.8	13.2	15.4	12.0	16.4
Steam Flow (lb/hr)	24,107	24,200	23,800	16,710	14,150
Fuel Flow (lb/hr)	3,443	3,330	3,235	2,364	2,014
Thermal Input (MBtu/hr)	31.9	30.8	30.9	21.9	18.7
Combustion Air Temp. (°F)	501	498	497	505	502
Total Air Flow (lb/hr)	23,250	24,780	25,580	16,900	14,950
Atomizing Air Flow (lb/hr)	1,109	1,128	1,093	1,032	1,041
Atomizing Air Pressure (psig)	90	105	90	76	72
Center-Tube Air Flow (lb/hr)	4,726	4,882	4,929	2,674	3,141
Center-Tube Air Temp. (°F)	406	415	411	432	443
Average Flue Gas Temp. (°F)	539	563	584	489	481
Carbon Conversion Efficiency (%)	95.1	97.5	97.5	96.7	97.2
Boiler Efficiency (%) (Heat Loss Method)	77.0	77.3	76.9	78.2	78.0
Heat Loss due to Water in Fuel (%)	5.35	5.50	5.13	5.30	5.30

*With a diffuser at the exit of the center-air tube.

TABLE 8. EMISSIONS AND FURNACE ASH DEPOSITION, COAL-WATER MIXTURE TESTS WITH BENEFICIATED VIRGINIA COAL

Test Number	1	2	3	4	5
Flue Gas Analysis					
O_2 (%)	1.8	2.9	3.3	2.8	3.5
CO_2 (%)	16.4	15.1	14.7	15.2	14.1
CO (ppm)	93	90	87	93	100
SO_2 (ppm)	1,244	1,159	1,096	1,161	1.048
(lb/MBtu)	2.14	2.23	2.15	2.20	2.15
NO_x (ppm)	477	490	474	339	334
(lb/MBtu)	0.59	0.68	0.67	0.46	0.49
THC* (ppm)	0.2	0.7	0.3	0.9	1.2
Particulate					
Emissions (lb/hr)	177	108	120	95	68
(lb/MBtu)	5.56	3.51	3.89	4.35	3.61
Mean Particle Size (μm)	17.4	17.6	26.6	19.6	33.3
Analysis (%)					
Carbon	45.1	35.7	32.6	37.9	38.7
Sulfur	0.5	0.5	0.4	0.5	0.5
Ash	53.2	62.2	65.6	59.6	58.5
Furnace Deposits (lb/hr)	12.2	14.9	8.9	5.4	8.7
Analysis (%)					
Carbon	5.2	7.3	4.9	9.5	13.0
Sulfur	0.5	0.4	0.3	0.5	0.9
Ash	93.3	91.9	93.4	88.6	85.0

*Total hydrocarbons

TABLE 9. ANALYSES OF COAL-WATER MIXTURES PREPARED WITH BENEFICIATED EASTERN KENTUCKY COAL

Test Number	1	2	3	4
Weight Percent Coal	59.4	61.4	60.1	60.5
Coal Size Consist (% minus 200 mesh)	88	87	89	88
Ultimate Analysis (%)				
Hydrogen	7.9	7.8	7.8	7.8
Carbon	48.8	50.5	49.4	49.8
Nitrogen	1.0	1.0	1.0	1.0
Sulfur	0.7	0.7	0.7	0.7
Oxygen	40.0	38.4	39.5	39.1
Ash	1.6	1.6	1.6	1.6
Heating Value (Btu/lb)	8,808	9,105	8,912	8,972

TABLE 10. OPERATING CONDITIONS AND BOILER PERFORMANCE, COAL-WATER MIXTURE TESTS WITH BENEFICIATED EASTERN KENTUCKY COAL

Test Number	1	2	3	4
Load	Full	Full	Full	Lowest
Flue Gas O_2 (%)	2.0	2.8	3.6	2.9
Excess Air (%)	6.5	12.3	17.2	14.6
Steam Flow (lb/hr)	24,020	23,930	24,060	14,960
Fuel Flow (lb/hr)	3,250	3,087	3,111	1,918
Thermal Input (MBtu/hr)	31.0	30.6	30.3	18.8
Combustion Air Temp. (°F)	501	493	489	493
Total Air Flow (lb/hr)	22,290	23,710	24,430	14,820
Atomizing Air Flow (lb/hr)	1,060	1,111	1,005	1,070
Atomizing Air Pressure (psig)	84	90	78	90
Center-Tube Air Flow (lb/hr)	4,234	4,448	4,545	2,611
Center-Tube Air Temp. (°F)	414	411	400	432
Average Flue Gas Temp. (°F)	522	549	538	480
Carbon Conversion Efficiency (%)	95.7	97.0	97.4	99.1
Boiler Efficiency (%) (Heat Loss Method)	77.4	77.6	77.6	80.0
Heat Loss due to Water in Fuel (%)	5.34	4.94	5.19	4.97

TABLE 11. EMISSIONS AND FURNACE ASH DEPOSITION,
COAL-WATER MIXTURE TESTS WITH BENEFICIATED EASTERN KENTUCKY COAL

Test Number	1	2	3	4
Flue Gas Analysis				
O_2 (%)	2.0	2.8	3.6	2.9
CO_2 (%)	15.7	14.8	14.3	14.8
CO (ppm)	198	138	103	114
SO_2 (ppm)	916	1,044	861	856
(lb/MBtu)	1.65	2.03	1.71	1.67
NO_x (ppm)	293	275	308	446
(lb/MBtu)	0.39	0.39	0.44	0.63
THC* (ppm)	3	2	2	2
Particulate				
Emissions (lb/hr)	110	84	79	22
(lb/MBtu)	3.27	2.76	2.62	1.16
Mean Particle Size (μm)	22.9	16.9	29.4	39.2
Analysis (%)				
Carbon	60.1	54.2	50.0	36.6
Sulfur	0.9	0.9	0.9	0.9
Ash	36.7	43.6	46.8	62.5
Furnace Deposits (lb/hr)	3.3	4.0	2.3	4.1
Analysis (%)				
Carbon	35.7	32.7	16.6	16.2
Sulfur	2.7	1.6	1.5	1.4
Ash	55.3	60.0	81.6	80.6

*Total hydrocarbons

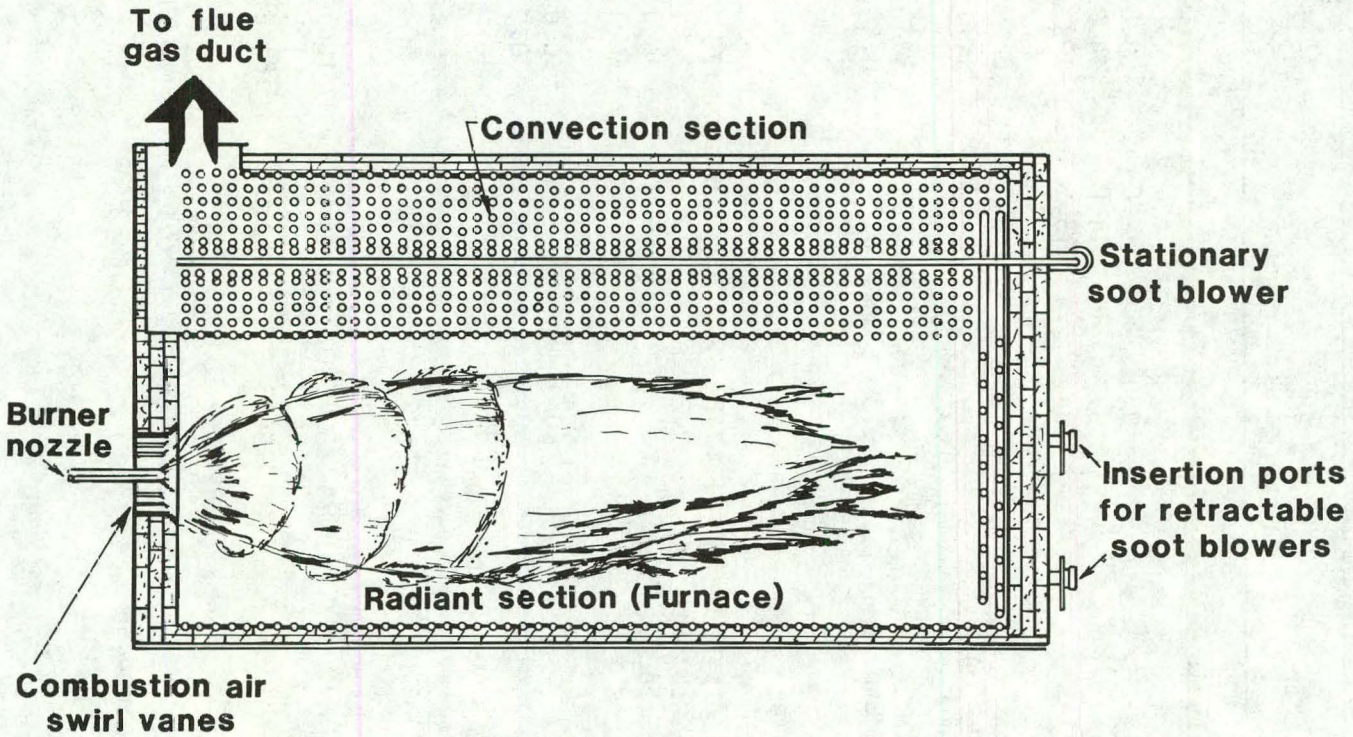

FIGURE 1. Horizontal Cross-Section View of the 700-hp Watertube Boiler

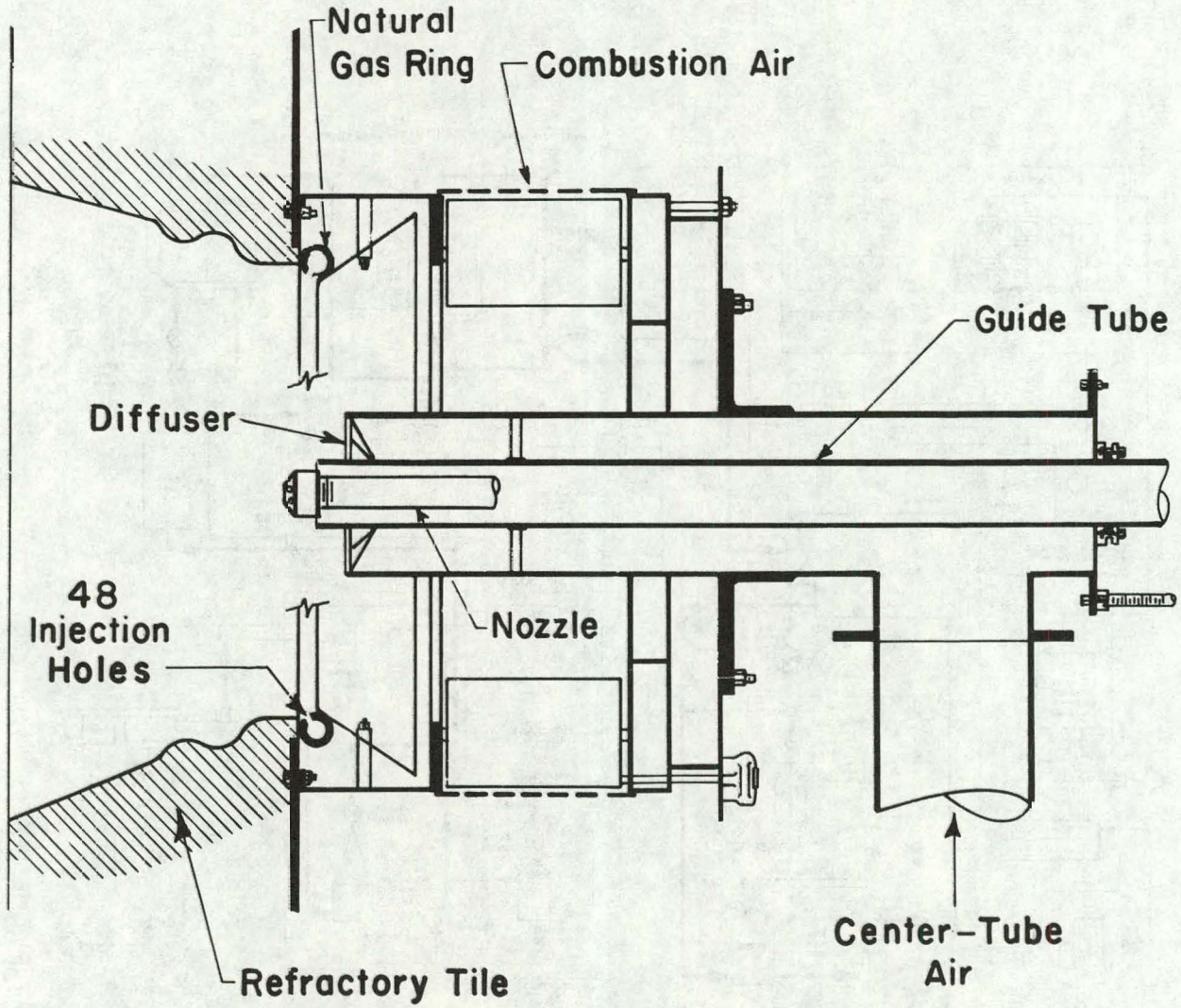

FIGURE 2. Burner Assembly used for CWM Tests

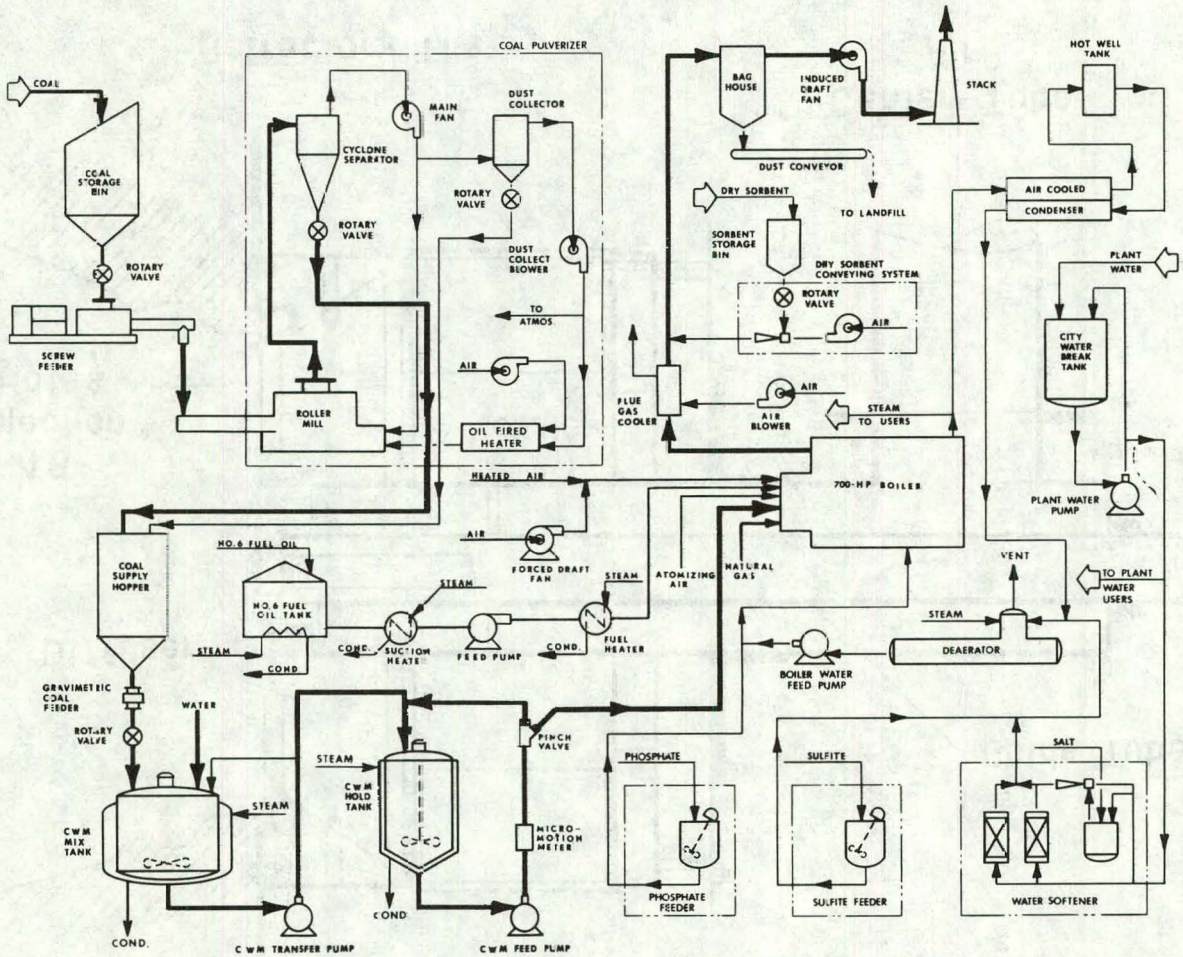

FIGURE 3. Flow Diagram of the 700-hp Combustion Test Facility

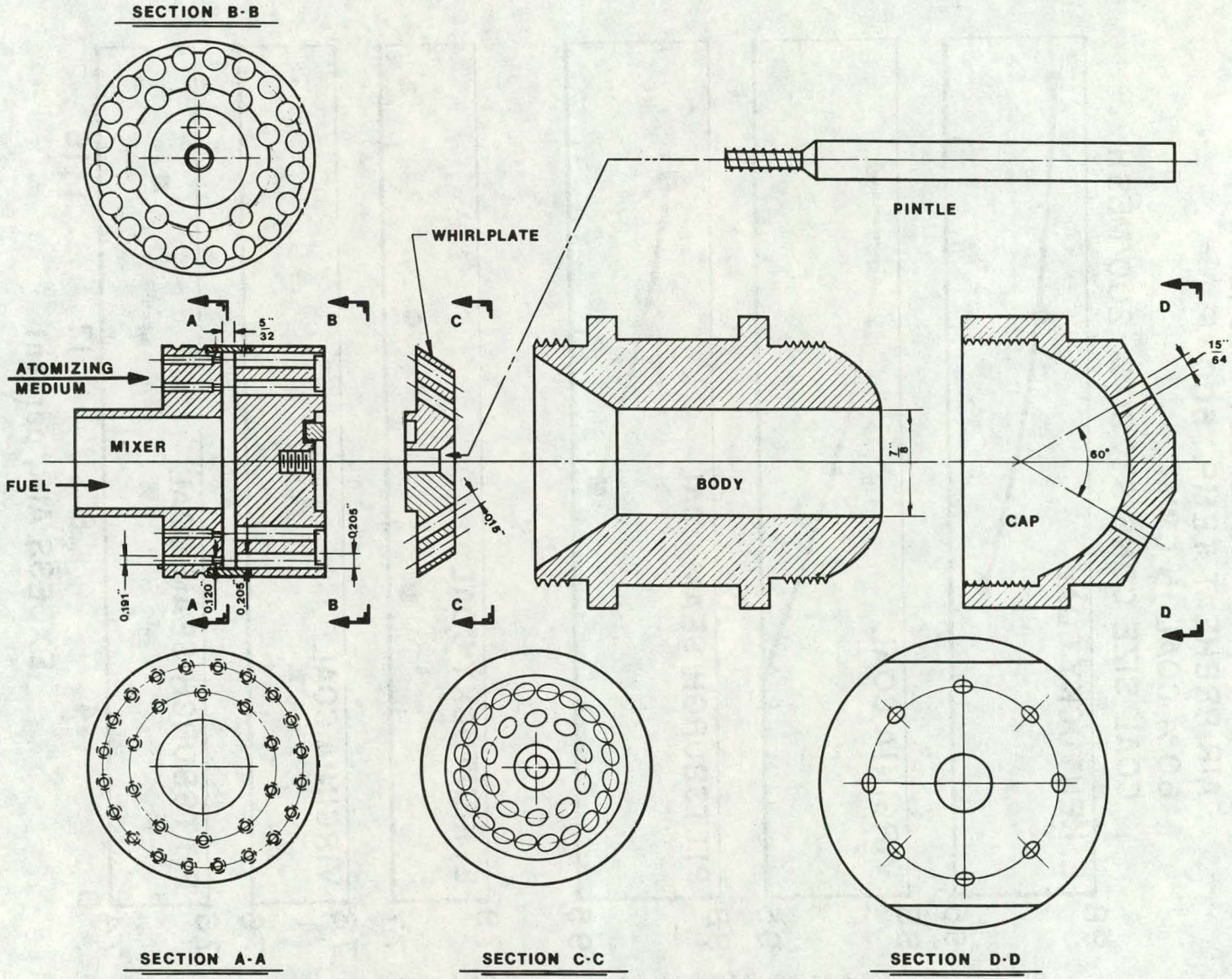

FIGURE 4. Assembly of the Burner Nozzle used for CWM Tests

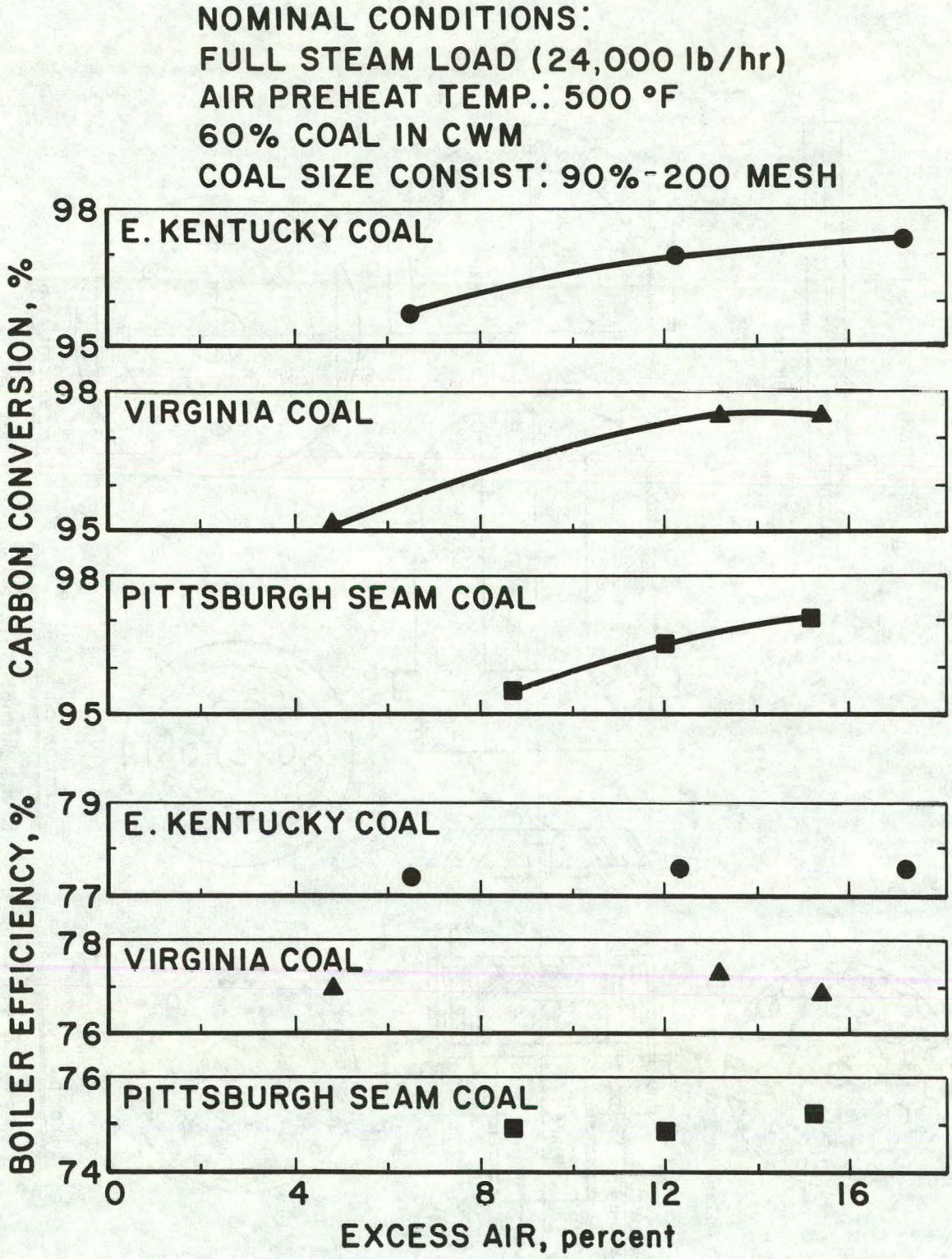

FIGURE 5. Carbon Conversion and Boiler Efficiencies during CWM Full-Load Tests with Three Different Coals

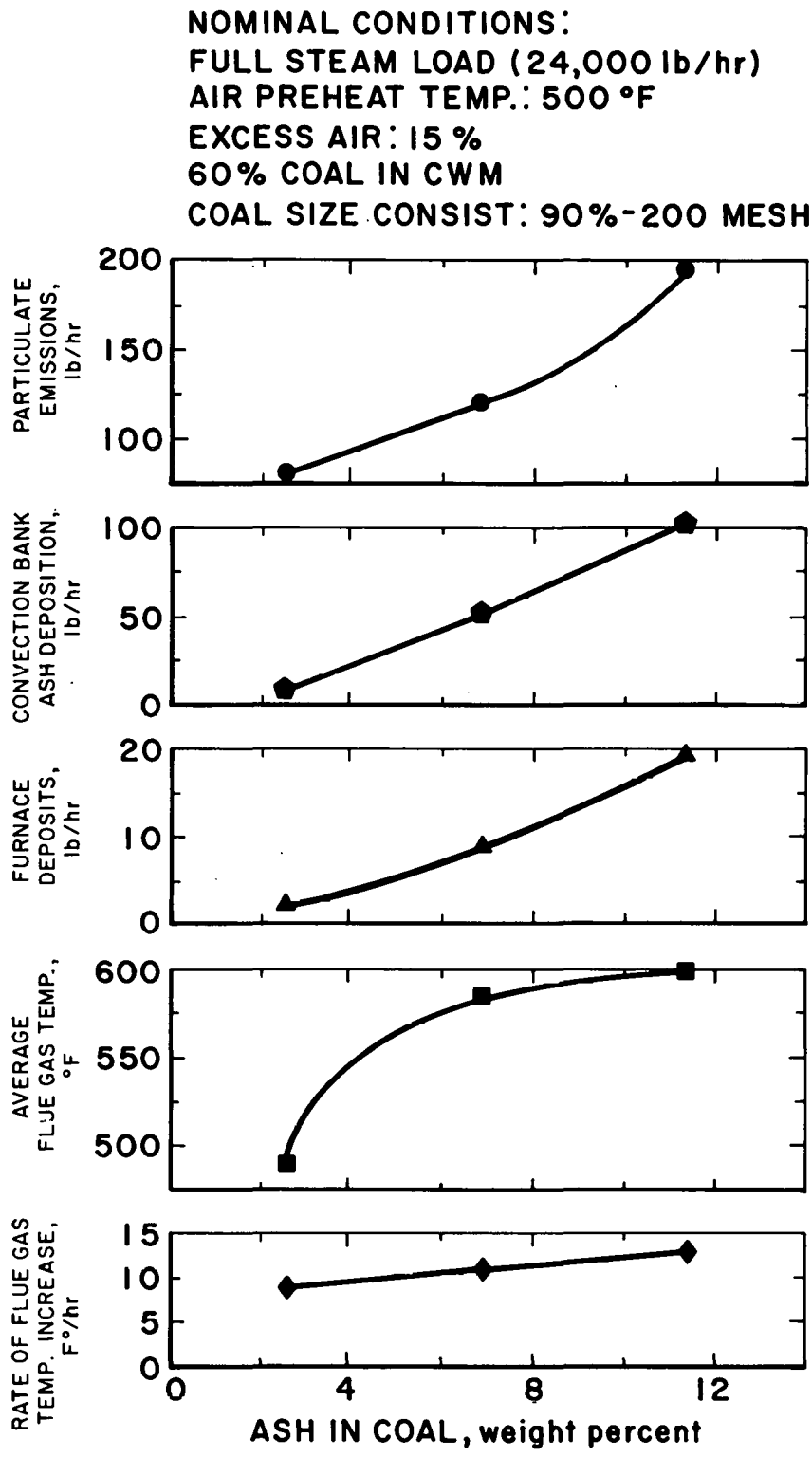

FIGURE 6. Effect of Coal Ash-Content on Particulate Emissions, Deposition Rates, and Flue Gas Temperature during CWM Combustion Tests

COMBUSTION CHARACTERISTICS AND AIR POLLUTION EMISSIONS FROM VARIOUS COAL-OIL DISPERSIONS

by

J.S. ALABAF

UNIVERSITY OF SURREY
DEPARTMENT OF CHEMICAL ENGINEERING
Guildford, Surrey, GU2 5XH, England

A B S T R A C T

Combustion and emissions research on 35% dispersions of low, medium and high volatile coals in 950 Redwood second fuel oil have been carried out using a low pressure air atomised Stordy-Hauck burner in a refractory lined flame tunnel, 3050 mm. in length and 610 mm. internal diameter. Differences between the combustion behaviour of these fuels are described.

A paper of recent research work on combustion characteristics of flame, emissions of nitrogen and sulphur oxides over a range of excess air from 2% to 30% is outlined. Flame burn-out time is increased by the presence of coal in the oil, except in the case of the low volatile anthracite, (low reactivity 101 NCB rank coal). The emissions of sulphur oxides are reduced, nitrogen oxides are increased, when compared to those from the constituent fuel oil.

The present paper deals principally with NO_x and SO_x emissions. Measured NO concentrations in the flue gas were found to be higher than would be expected from equilibrium calculations at those temperatures. The SO_2 and SO_3 concentrations agreed with those which would be expected at flue gas temperatures.

The chemical pathway has been developed to explain the differences between NO formation from atmospheric nitrogen, chemically bound fuel nitrogen and prompt NO, during the combustion process.

Electronic and optical microscopic investigations on the char particles throw light on the possible reasons for the combustion difference, and a combustion mechanism is proposed.

1. INTRODUCTION

The 1973 and 1979 oil crises followed by high cost of fuel oil is forcing many oil burning boiler plants to consider the use of coal. The cost of installing coal burning equipment frequently is quite high. Conversion methods of burning coal in the form of lumps is both mechanically difficult and thermally inefficient. If, however, the coal is finely powdered, it then behaves as a semi-fluid, which can be both transported and burnt far more easily. Powdered or as it is more commonly called pulverised coal, on account of both ignition and safety problems, cannot normally be burned at rates much less than one ton/hr. However, if the powdered coal is dispersed in an oil this serious limitation to its use is eliminated. The huge handling cost, one of the most significant elements in the transportation of coal, can only be reduced when coal is finely powdered and transported as a liquid or as a semi-liquid at ordinary atmospheric temperatures. Coal-in-oil fuels (dispersions and mixtures)[1] also have the same advantages as liquid fuels, and savings in oil consumption of up to 70% are possible.

The time required for the complete combustion of coal-in-oil fuel is greater than that for liquid or gaseous fuels, due to the presence of carbonaceous char which is left after combustion of the volatile matter.

Apart from the purely technical advantages of coal-in-oil fuels there are the economic considerations. Their use would tend to diminish the western nations imports of oil and find an outlet for a corresponding quantity of coal, with attendant advantages to the coal and other industries.

Coal-in-oil fuel appeared over a century ago. Since then, many different terms have been used to describe such fuels, which have never been adequately defined by the manufacturers. In order to clarify the definitions, which are largely the result of historical accident, the author proposes the following classifications for coil-in-oil fuels[1].

1.1. Coal-oil dispersions

Coal-oil dispersions, can be sub-classified into five groups:

(a) Coarse coal-oil suspensions with a pulverised coal particle size <80 μm (moderate proportion of additives or no additives required to stabilise the suspension).

(b) Medium coal-oil suspensions with a pulverised coal particle size <80 μm (very small proportion or no additives required to stabilize the suspension).

(c) Fine coal-oil suspensions with a pulverised coal particle size <80 μm (no additives required).

(d) Colloidal fuel with a pulverised coal particle size <1 μm (no additives required).

(e) Molecular coal-oil solution with a pulverised coal particle size <10 nm (no additives required).

1.2. Coal-oil mixtures

Coal-oil mixtures with a pulverised coal particle size 80 mass % <80 μm (large proportion of additives required to stabilize the coal-oil mixture). More details can be found elsewhere[1].

2. COMBUSTION CHARACTERISTICS OF VARIOUS COAL-OIL DISPERSIONS

Combustion tests were run for some 200 hours, burning approximately 4200 litres in total of four types of fuel; low, medium and high volatile coal-oil dispersions and the 950 Redwood second constituent fuel oil. The dispersions have been burned successfully without major difficulties in the modified oil firing low pressure air atomised Stordy-Hauck burner[2]. The combustion performance was satisfactory for these fuels and indicates that these can be burned in suitable industrial oil burning equipment. The combustion studies have indicated that there are fundamental differences between the burn-out mechanism of coal-oil dispersions compared to that of their constituent fuel oil, and also that the coal type is a significant factor in combustion performance. The burn-out time of the 950 second fuel oil is shorter than for the coal-oil dispersions, and this time becomes longer as the coal volatile content is increased. It would appear that the flame lengths from the medium and high volatile coal dispersions are longer, and more complete combustion is achieved. The dispersions flame was much brighter than that of the constituent fuel oil due to coal particles.

During the combustion of low volatile coal-oil dispersions, a cloud of fine particles was observed in the downstream end of the furnace indicating that the anthracite coal particles undergo a different combustion process to that of the medium and high volatile coals. More details can be found elsewhere[2].

2.1. Microscopic investigations of the particulates emissions

Stereoscan electron and optical microscopic studies on char particles produced by the combustion of the various coal-oil dispersions, shown in plates 1-6, have indicated that fundamental structural differences exist between the char particles from low and high volatile fuel. These show that the anthracite char particles are partially fused or possibly stuck together to form roughly spherical, loose agglomerates with angular particles of anthracite on the surface of a rounded, pitted solid. The small, rounded spheres visible on the particle surface shows no indication of swelling.

The char particles from medium and high volatile rank coal-in-oil dispersions show large internal cavities, and holes in their surfaces. Plates 2 and 3 show char particles from medium and high volatile coal-oil dispersions containing partially burned-out cenospheres which are similar in appearance to those produced by single particle pulverised coal combustion. The volatiles in the coal cause swelling, the mean char particle diameter of the particulates being greater than the starting mean size of the coals as ground. The chars produced by the combustion of the high volatile 501 NCB rank coal-in-oil dispersion show that the particles were very similar to those from the medium volatile 301 NCB rank coal-in-oil dispersion, but more uniformly burnt-out and more fragmented[2].

2.2. Mechanism for the combustion of droplets of coal-oil dispersions

The combustion of various coal-oil dispersions is a complex process, and takes place in two stages[2]. (See Figures 1 and 2.)

(i) Combustion of volatile matter

In the first stage, coal-oil dispersion fuel atomises through the burner nozzle. As the fuel enters the furnace, it is heated by convection from the surrounding gas and radiation from the flame and furnace walls, and begins to volatilise. Both physical and chemical changes occur.

Coal particles in the dispersion become plastic, and as the fuel evaporates the coal particles coalesce. The coal volatiles produce swelling as a result of bubble formation.

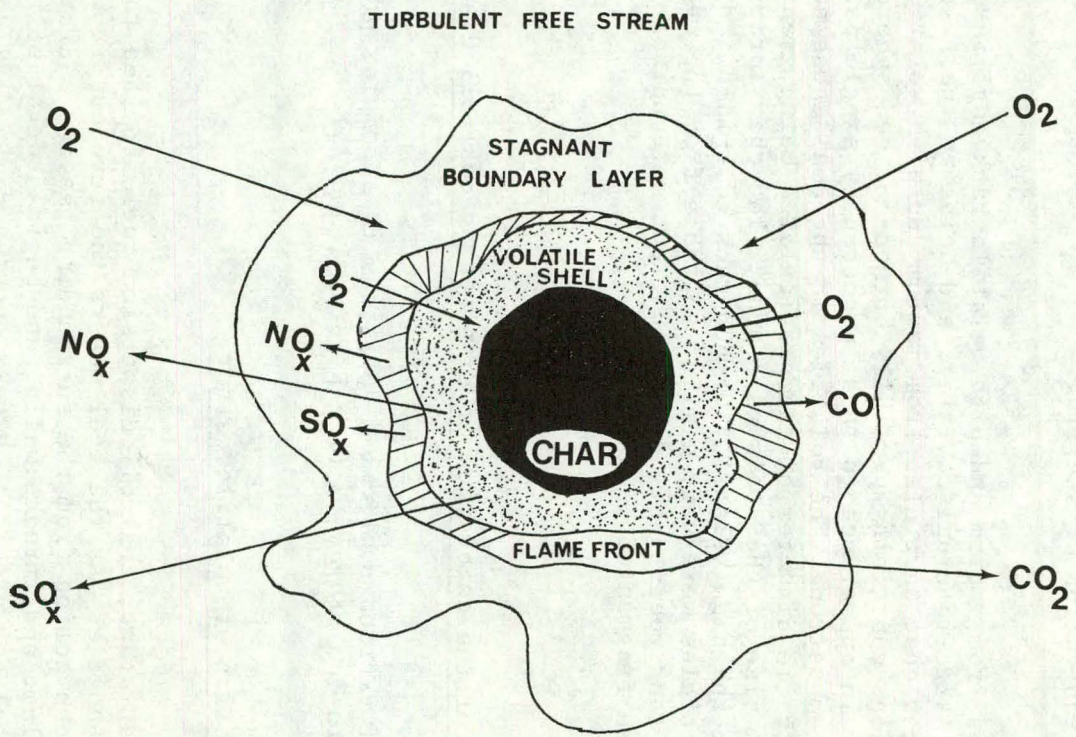

Figure 1. Proposed burning droplet for Coal-in-Oil fuels (coal-oil dispersions and coal-oil mixtures).

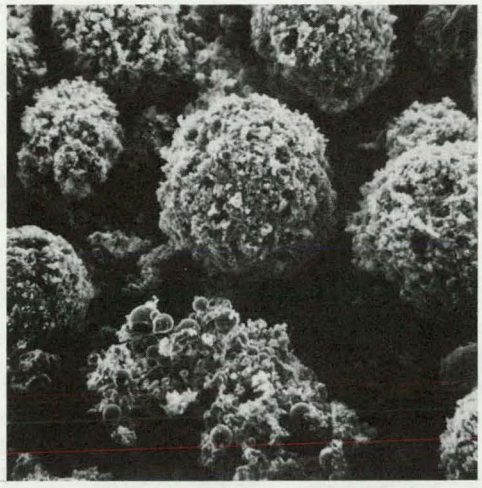

General view of char population
(×122). Exterior.

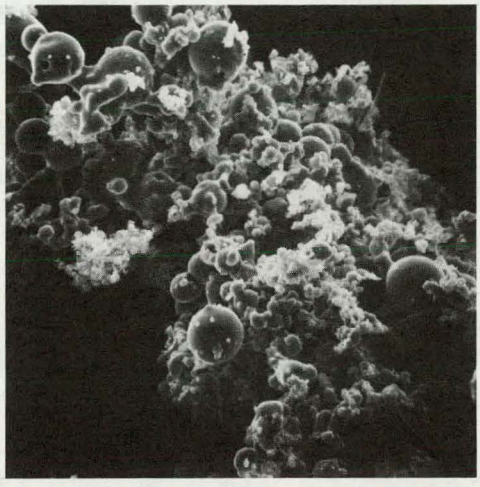

Surface detail showing
agglomerated ash particles
(× 305). Exterior.

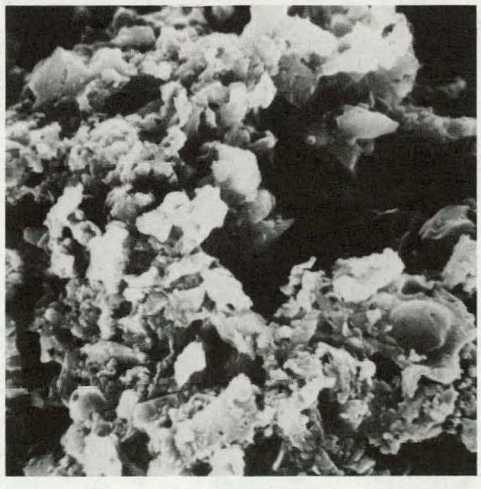

Surface detail showing
discrete angular anthracitic
coal char
(× 1463). Exterior.

Plate 1. Electron micrographs of NCB Rank 101/950 sec. fuel oil char.

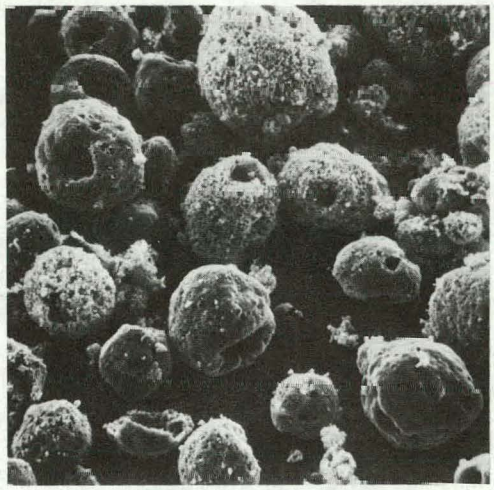

General view of char population (×135). Exterior.

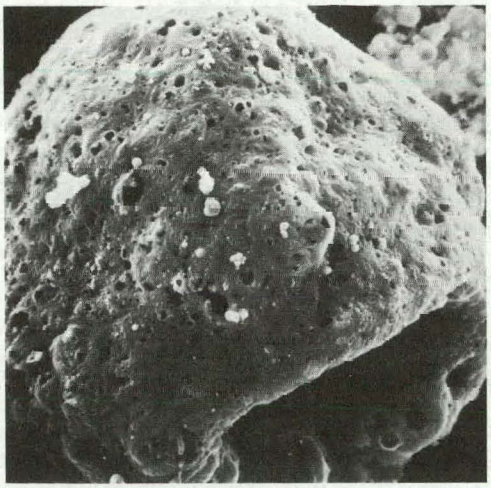

Typical char sphere showing open pore structure of cenosphere, with no evidence of individual coal particles (×670). Exterior.

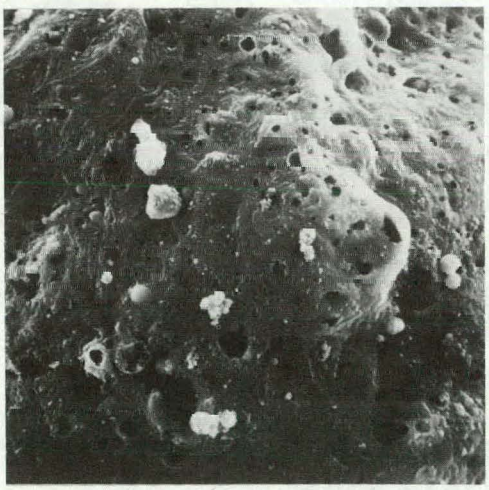

Surface detail showing fused open pore structure with ash particles evident (×1340). Exterior.

Plate 2. Electron micrographs of NCB Rank 301/950 sec. fuel oil char.

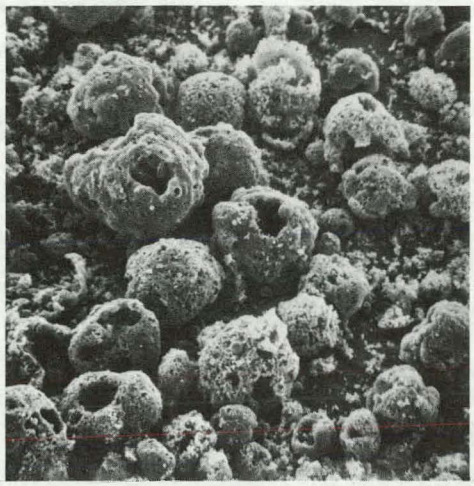

General view of char population
(×110). Exterior.

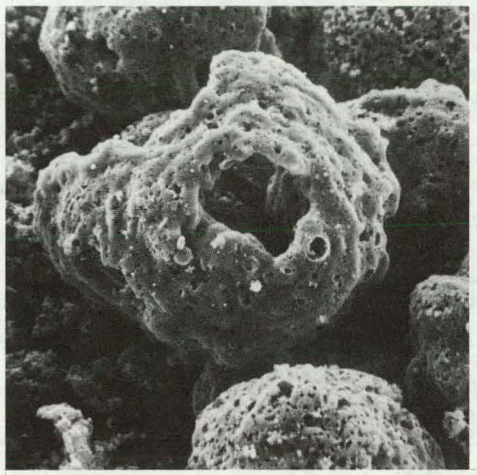

Typical char sphere showing open pore structure of cenosphere, with no evidence of individual coal particles
(×275). Exterior.

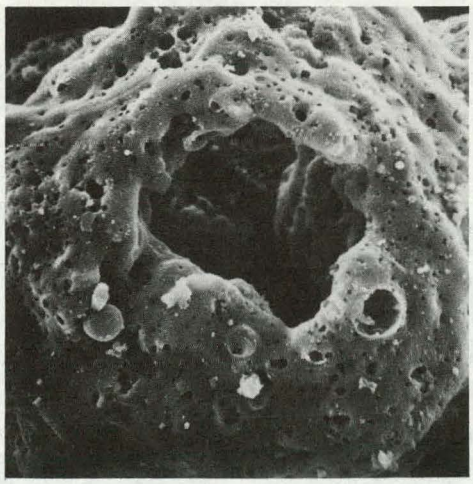

Surface detail showing fused nature of char cenosphere
(×550). Exterior.

Plate 3. Electron micrographs of NCB Rank 501/950 sec. fuel oil char.

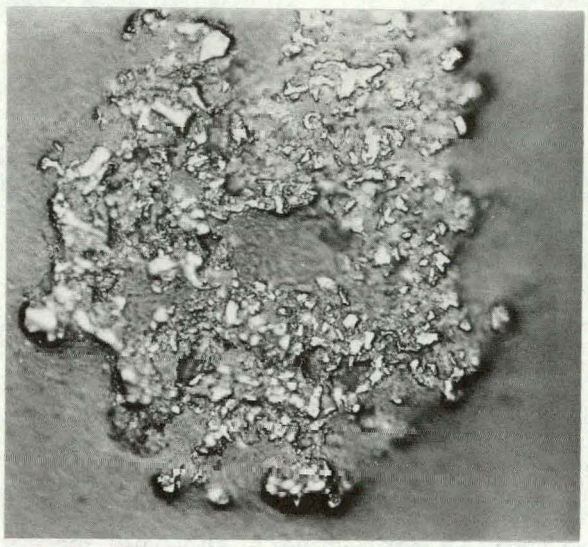

Cross section ×335
Agglomerate with internal spaces

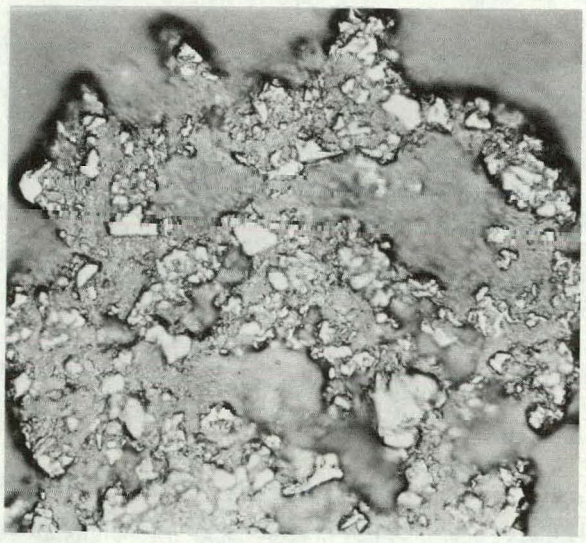

Cross section ×335
Large Agglomerate with Internal spaces

Plate 4. Optical micrographs of NCB Rank 101/950 sec. fuel oil char.

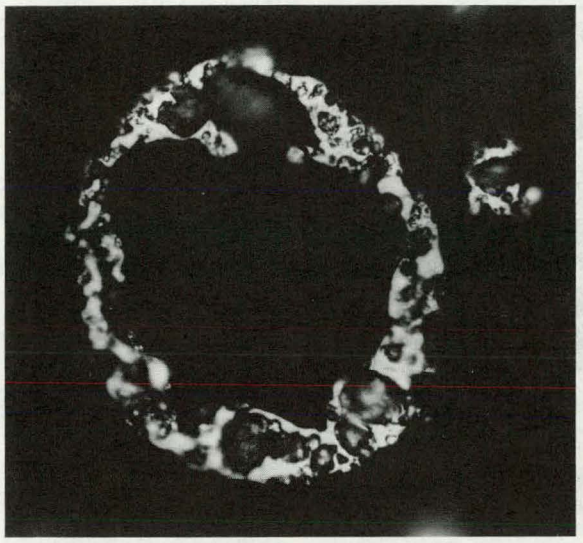

Cross section ×400
Balloon sphere/lacy char

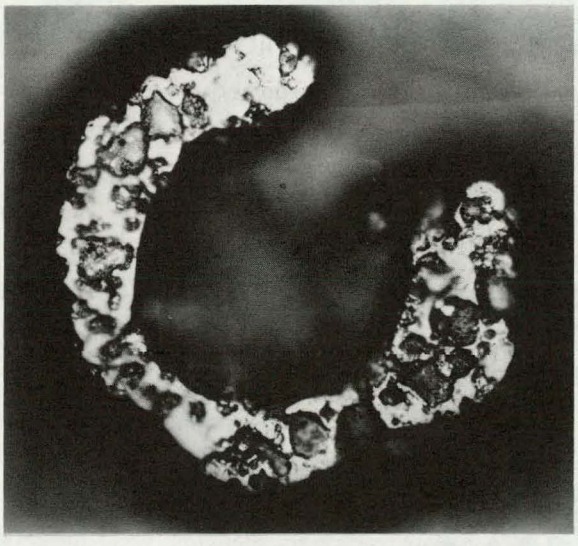

Cross section ×400
Typical c-shaped and
C-shaped/lacy char

Plate 5. Optical micrographs of NCB Rank 301/950 sec. fuel oil char.

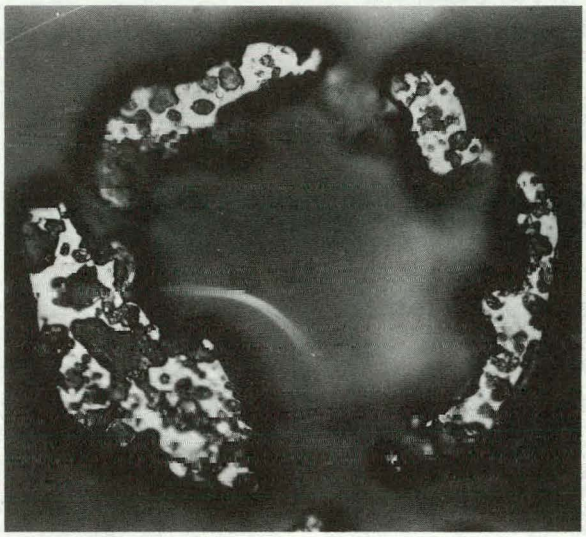

Cross section ×335
C-shaped and
C-shaped/lacy char

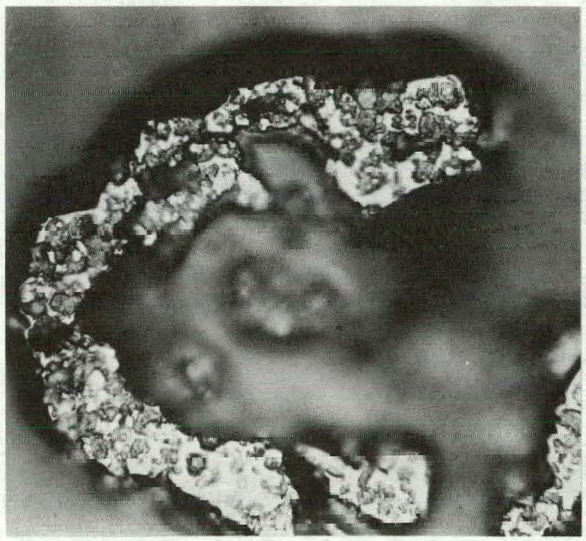

Cross section ×335
Typical c-shaped and
C-shaped/lacy char

Plate 6. Optical micrographs of NCB Rank 501/950 sec. fuel oil char.

Some of these burst at the outer surface, and some internally to produce a hollow sphere. The release of gases internally, which cannot escape fast enough through the pores of the outer shell, eventually burst out of the sphere producing a large hole. By this time the shell is sufficiently firm to prevent collapse, and any remaining volatiles are released more easily.

As a result of the volatilisation, a flame front is initiated and the combustion of the volatile shell surrounding each fuel droplet starts (Figure 1). The volatile shell consists of a mixture of combustible gases, carbon dioxide, and water vapour. Apart from carbon monoxide and hydrogen, the combustible gases are mainly hydrocarbons and hence burn rapidly. After the combustion of the volatile matter in the dispersion is complete, a carbon char is left.

(ii) Combustion of carbon char

The second stage of combustion involves the burning of this carbon char. The burning out of carbon particles in the dispersions is the primary reason for significant differences of flame length, emissivity, heat release and flame temperature between fuels. The combustion of the carbon char of medium and high volatile coal-oil dispersions takes place at the surface of the oil droplet size fused cenospheres. Volatile combustion in the earlier stages of combustion causes pores to be formed in the surface of the char particles, and combustion takes place on both the internal and external surface of the char, with oxygen diffusing through the pores. The combustion of these chars is slow, due to their relatively low external surface area to volume ratio, giving rise to longer flames than for the constituent fuel oil which burns to smaller particles.

In the case of the low volatile coal-oil dispersions, the low reactivity of the anthracite inhibits the formation of fused droplet size cenospheres, and the coal particles remain loosely bonded by any residual tar or oil ash at the end of the volatile combustion stage. These spherical agglomerates break up into small char particles, giving a relatively high external surface area to volume ratio in total. This more rapid combustion gives a shorter flame than with other disperions. The increased total surface area also gives rise to higher combustion at the end of the flame.

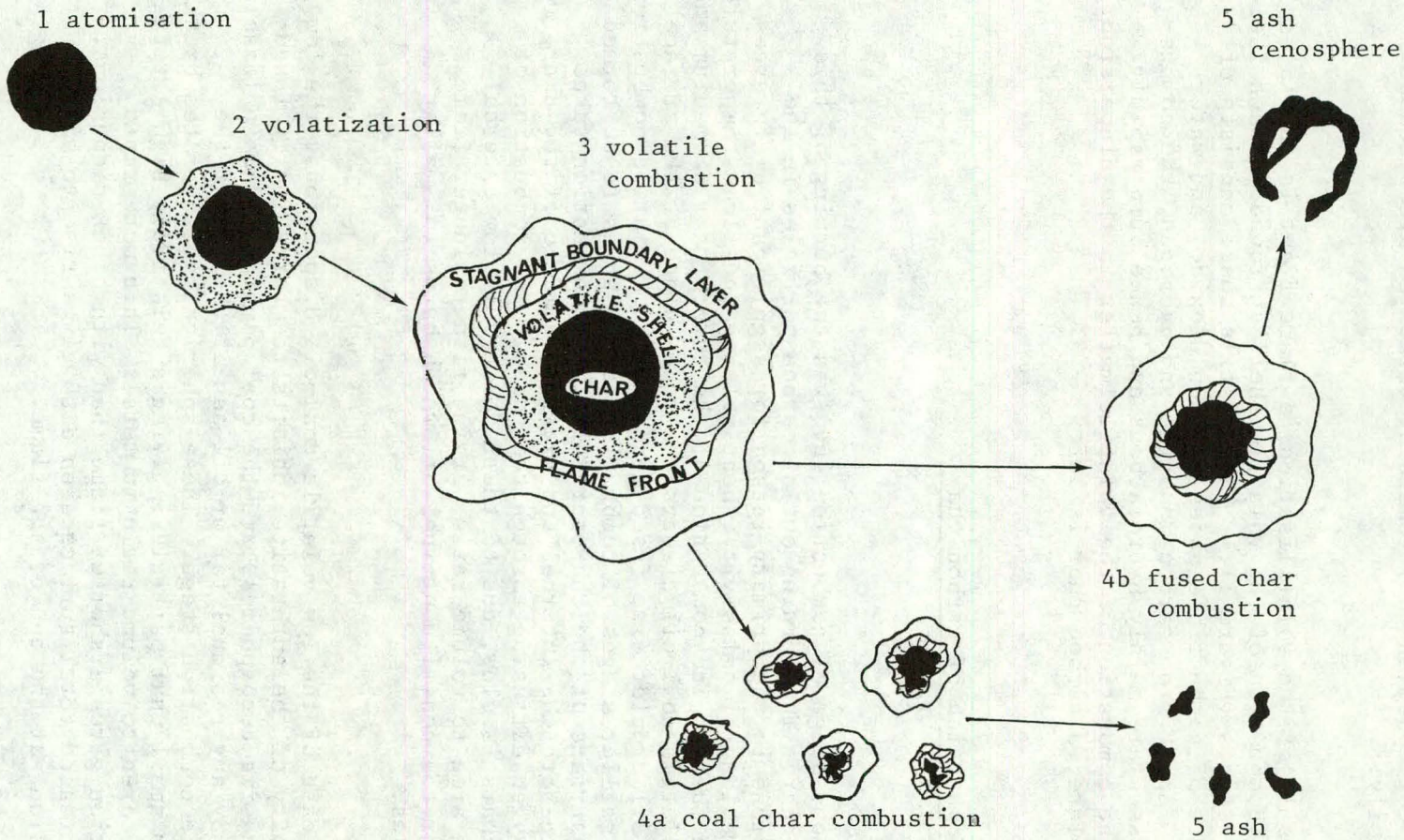

Figure 2. Proposed combustion pathways for Coal-in-Oil fuels (dispersions and the mixtures).

3. EMISSIONS OF NITROGEN OXIDES (NO_x)

The experimental test shows that in the combustion of various coal-oil dispersions, fuel-nitrogen oxidation is the major source of NO formation[2]. However the atmospheric nitrogen makes some contribution to NO formation. Section 3.4 indicates that rank of coal in the dispersion fuel and temperature play an important part in the nitric oxide formation.

3.1. Mechanism of NO_x formation

The formation of nitrogen oxides is a complex process involving the high temperature fixation of atmospheric nitrogen (thermal NO) and the fuel-bound nitrogen (Fuel NO). The formation of NO_x involves several chemical reactions in both equilibrium and non-equilibrium (kinetic) processes that take place in the pre-combustion, combustion and post-flame regions.

(i) Atmospheric nitrogen

$$O_2 \rightleftarrows O + O \qquad (1)$$

$$O + N_2 \rightleftarrows NO + N \qquad (2)$$

$$N + O_2 \rightleftarrows NO + O \qquad (3)$$

$$N_2 \rightleftarrows N + N \qquad (4)$$

$$N + OH \rightleftarrows NO + H \qquad (5)$$

$$NO + O \rightleftarrows NO_2 \qquad (6)$$

The equilibrium of each of these reactions is a function of temperature and concentration. At high temperatures atomic

species will exist in significant concentrations. At low temperatures NO_2 does not dissociate to NO and oxygen.

Kinetically the chain reactions (2) and (3) are important in the formation of NO with the chain being initiated by dissociation reactions (1) and (4). The rate of the reactions (2) and (3) increase rapidly as the flame temperature increases, because high activation energies are required to break the oxygen and nitrogen molecular bond in equation (1) and (4).

The actual rate of production of NO and NO_2 from air in a combustion system will obviously depend on the temperature profile, concentration profile and residence time. These factors are closely linked to the design of the burner and combustion space, being dependent on how the fuel and oxidant are mixed, how heat is abstracted from the combustion zone and the degree of mixing in the system.

(ii) Fuel-bound nitrogen

Nitrogen present in the fuel is usually chemically bound in groups such as $- NH_2$, $= NH$, $- CN$, $= N -$ which on pyrolysis in the combustion process produces radicals which are oxidised to NO. In general, the reactivity of these radicals is greater than that of atmospheric nitrogen, and require much lower bond energies to break the nitrogen bond. There is evidence[3] that nitrogen bond energies in coals are typically 80-100 Kcal/mole, compared to 225 Kcal/mole for atmospheric nitrogen, with the consequence that much more NO arises from fuel-bound nitrogen than from atmospheric nitrogen, when the fuel has a significant nitrogen content.

(iii) Prompt NO

As well as the mechanism indicated above, there is also evidence[4] for the formation of NO via a fixation of atmospheric nitrogen by carbon in hydrocarbon fuels.

$$\text{Fuel carbon} + N_2 \rightarrow - CN + N \qquad (7)$$

$$C_2 + N_2 \rightarrow 2CN \qquad (8)$$

$$CH + N_2 \rightarrow HCN + N \qquad (9)$$

$$HCN + O \rightarrow NO + HC \qquad (10)$$

Fine et al[4] reported the formation of HCN, NH_2 and NH

$$CH_3 + N_2 \rightarrow HCN + NH_2 \qquad (11)$$

$$CH_2 + N_2 \rightarrow HCN + NH \qquad (12)$$

The oxidation of these nitrogen containing species will produce prompt NO.(For further details see section 3.4.)

3.2. Thermodynamics of formation of NO_x emissions and percentage conversion at equilibrium

The following method theoretically predicts the equilibrium NO_x levels produced by the combustion. In the following section (3.3) a comparison is made with experimental data at a sampling point.

The theoretical NO_x formation is based upon the assumption that:

(i) The major chemical species of NO_x in flue gases can be considered to be in thermodynamic equilibrium.

(ii) The major NO formation process can be assumed to be from the nitrogen in the fuel.

During the combustion process, the reactions involved in the oxidation of nitrogen to nitrogen oxides with combustion air are expressed by the following equations at equilibrium:

(a) consider the nitric oxide (NO) reaction.

$$\tfrac{1}{2}\, N_2 + \tfrac{1}{2}\, O_2 \rightleftharpoons NO \qquad (13)$$

$$K_p = \frac{[NO]}{[N_2]^{\frac{1}{2}}[O_2]^{\frac{1}{2}}} \qquad (14)$$

where K_p is the equilibrium constant. The free energy ($\Delta\overset{\theta}{G}$) of formation of NO for this reaction is given by Nernst[6].

$$\Delta\overset{\theta}{G} = 21600 - 2.5\ T \qquad (15)$$

where

$$\Delta\overset{\theta}{G} = -\ RT\ \ln K_p \qquad (16)$$

$$\log K_p = \frac{-4720}{T} + 0.55 \qquad (17)$$

where

$$K_p = \frac{P_{NO}}{P_{N_2}^{\frac{1}{2}} \times P_{O_2}^{\frac{1}{2}}} \qquad (18)$$

$$K_p \times P_{O_2}^{\frac{1}{2}} = \frac{P_{NO}}{P_{N_2}^{\frac{1}{2}}}$$

$$\frac{P_{NO}}{P_{N_2}^{\frac{1}{2}} + P_{NO}} = \frac{K_p \times P_{O_2}^{\frac{1}{2}}}{1 + (K_p \times P_{O_2}^{\frac{1}{2}})} \qquad (19)$$

The theoretical percentage conversion of atmospheric nitrogen to NO at lower flue gas temperatures will be negligible because there is

evidence[4] that the formation of NO from atmospheric nitrogen can only occur at temperatures in excess of 1700°C. However despite the fact that the experimental tests for NO on the fuels used were made in combustion flue gases at which the temperature was lower, the NO was formed at flame temperatures and it is the equilibrium concentration of NO at these which should be considered. This leads to the conclusion that the elapsed time between the flame and the sampling point is too short for re-establishment of equilibrium at the lower temperature. Therefore one can assume some NO from atmospheric nitrogen will be found in the sample analysed.

(b) Consider the nitrogen dioxide (NO_2) reaction at equilibrium in combustion flue gases. As the combustion flue gases cool, the NO is oxidised further with oxygen to NO_2.

$$NO + \tfrac{1}{2} O_2 \rightleftharpoons NO_2 \tag{22}$$

$$K_p = \frac{[NO_2]}{[NO]\ [O_2]^{\frac{1}{2}}} \tag{23}$$

The free energy for the reaction (21) is given Bodenstein and Katayamon [8,9].

$$\Delta G^{\theta} = 14170 + 2.75T \ln T - 0.0028T^2 + 0.00000031T^3 + 2.73T. \tag{24}$$

When substituted in equation (16), the following results;

$$\log K_p = \frac{3097}{T} - 1.384 \log T + 6.12\times10^{-4}\ T - 6.77\times10^{-8}T^2 - 0.596, \tag{25}$$

where

$$K_p = \frac{P_{NO_2}}{P_{N_2}^{\frac{1}{2}} \times P_{O_2}^{\frac{1}{8}}} \tag{26}$$

$$K_p \times P_{O_2}^{\frac{1}{2}} = \frac{P_{NO_2}}{P_{NO}} \tag{27}$$

$$\frac{P_{NO_2}}{P_{NO} + P_{NO_2}} = \frac{K_p \times P_{O_2}^{\frac{1}{2}}}{1 + (K_p \times P_{O_2}^{\frac{1}{2}})} \tag{28}$$

NO_2 is thermodynamically unstable at high temperatures, and there is evidence[10], that above 150°C, NO_2 dissociates into NO and oxygen. The experimental tests on NO_x in combustion flue gases showed that only NO was formed.

3.3 Comparison of measured NO emission with theoretical predictions

Figures 4-8 shows that calculated equilibrium NO concentrations at flue gas temperatures correspond approximately with those which were measured. These are considerably higher than those which would be expected from the equilibrium concentrations at the temperature of approximately 100°C at which analysis was made. This would indicate that the dissociation of NO to N_2 and O_2 is slow. The precise temperature at which NO is formed is difficult to assess in view of the varied histories of the nitrogen molecules in the combustion process. Therefore one can conclude that equilibrium calculations are unreliable for calculating NO in the flue gas, and that NO production may be strongly influenced by maximum flame temperatures. This may be an important factor in the design of burners and their operation to minimise NO_x emissions.

3.4. Chemical pathways to NO_x formation from combustion of various coal-oil dispersions

From Tables A.1 and A.2 it can be seen that 74-83% of the total nitrogen initially present in the coal-oil dispersions were released during the volatilization process, 17-26% of that remaining in the char and 20-30% in unburned solids. Because the unburnt nitrogen content of the solids remaining from the combustion are greater than those obtained from the devolatilization tests, it is probable that the former contains atmospheric nitrogen. The tables also show that the nitrogen left in the char decreases as the devolatilization temperature increases. Increasing the rank produces the same effect, showing that the nitrogen is more easily released with higher rank coals.

During the combustion of various coal-oil dispersions the fuel-nitrogen is thermally decomposed into volatiles and char. NO is formed both by the volatile and char combustion. Therefore it would appear that there are two distinct pathways to the formation of NO from fuel-bound nitrogen.

(i) The combustion of volatile-nitrogen compounds

(ii) The combustion of char-nitrogen compounds

Figure 3· shows the proposed chemical pathways for NO_x formation.

(i) The combustion of volatile nitrogen compounds occurs as the atomised coal-oil dispersion fuel is decomposed by heat, and the volatilization reactions occur. The nitrogen compounds released in the volatile shell at this stage consist of vapour tar based compounds such as pyridines, pyrroles, quinoline, amines (aniline, naphthylamine, diphenylamine) and amides (benzamide). The released nitrogen from

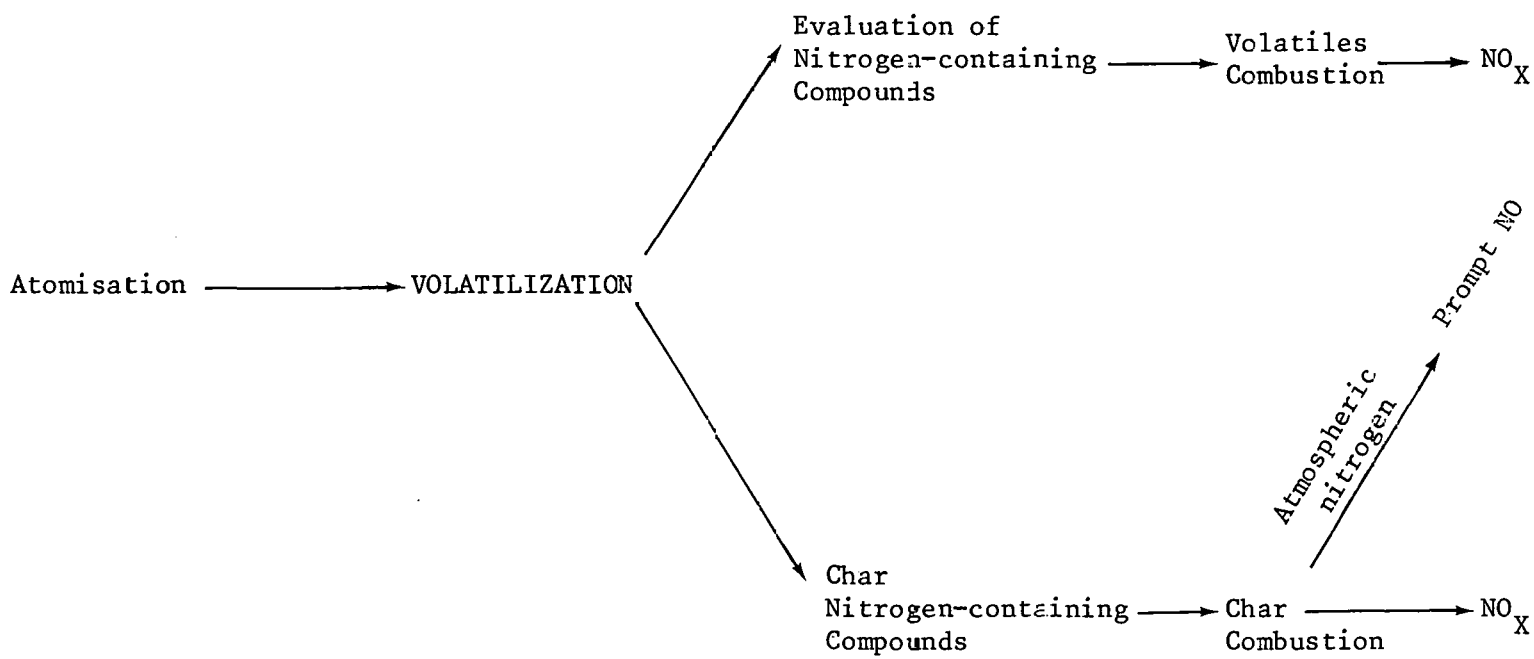

Figure 3. Proposed chemical pathways for NO_X production resulting from the oxidation and combustion of various coal-oil dispersions.

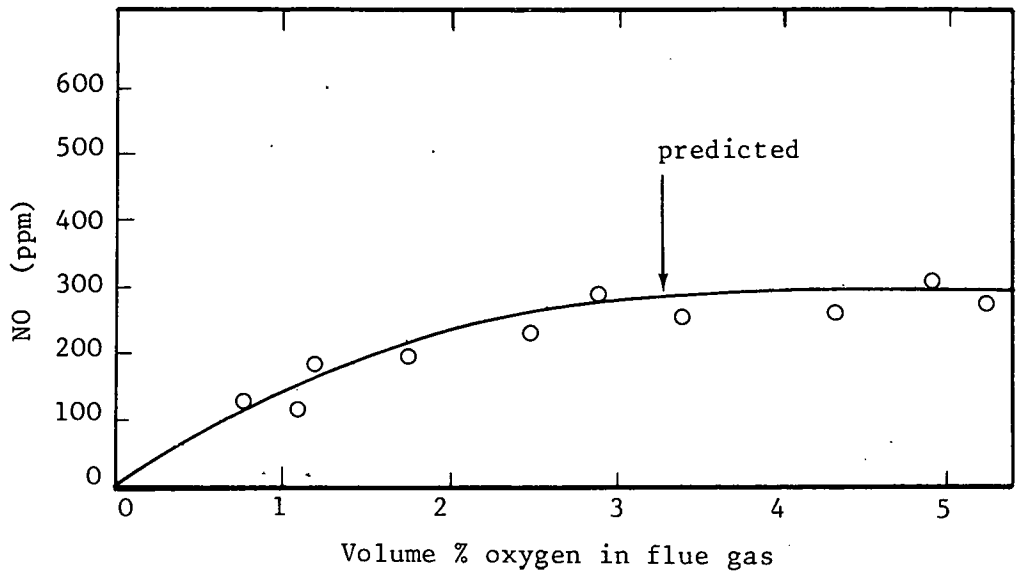

Figure 4. predicted and measured conversion of N_2 to NO at equilibrium in combustion flue gas for 950 Redwood second fuel oil.

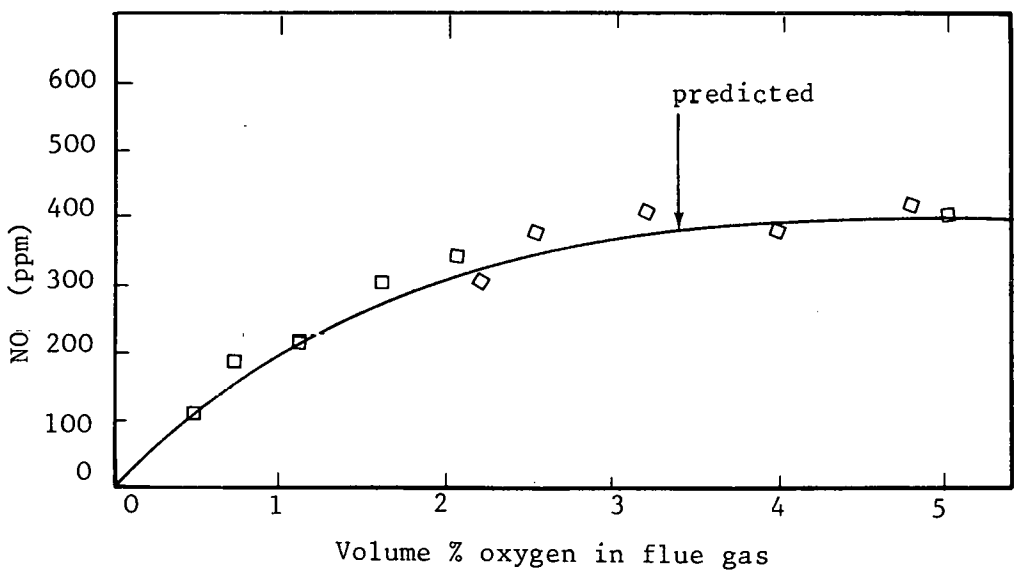

Figure 5. predicted and measured conversion of N_2 to NO at equilibrium in combustion flue gas for antracite low volatile coal-oil dispersion.

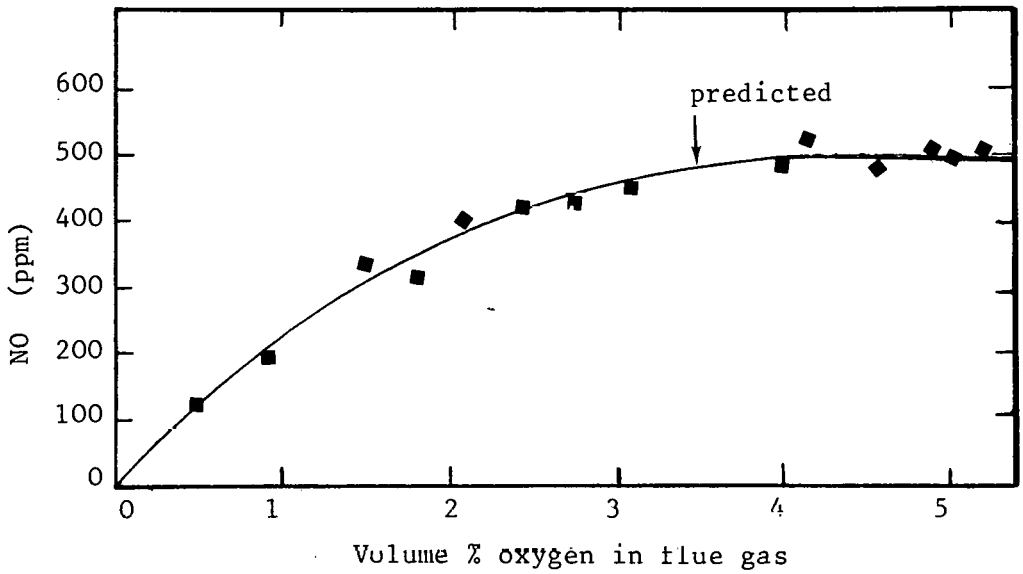

Figure 6. predicted and measured conversion of N_2 to NO at equilibrium in combustion flue gas for medium volatile coal-oil dispersion.

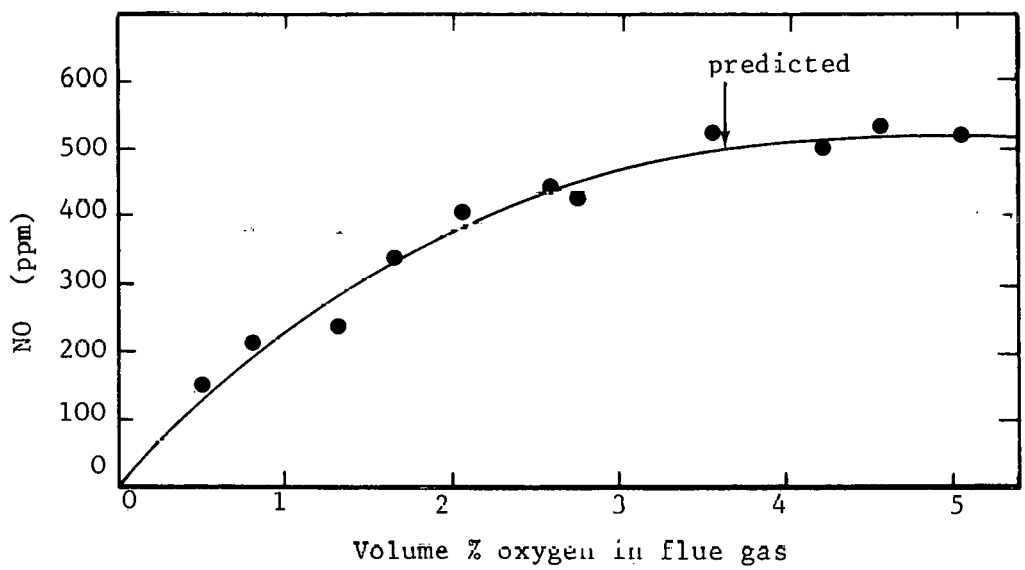

Figure 7. predicted and measured conversion of N_2 to NO at equilibrium in combustion flue gas for high volatile coal-oil dispersion.

these compounds will then react with oxygen and produce NO.

(ii) The combustion of char-nitrogen compounds occurs after the combustion of volatilized-nitrogen compounds. The remaining amount of the fuel-nitrogen is not easily released from the char matrix to which it is linked by much stronger bonds. However these amounts are released at higher temperatures when the tar ring bond is ruptured, (the C-N bond by the attack of oxygen). The released fuel-nitrogen will then react with oxygen and produce NO. The fuel-nitrogen compounds present in the char are mainly nitrile groups such as tolunitrile and benzonitrile. During the char combustion, some of the atmospheric nitrogen will react with carbon from the char and produce CN and HCN species which oxidise to prompt NO.

4. EMISSIONS OF SULPHUR DIOXIDE AND SULPHUR TRIOXIDE (SO_X)

The emissions of the oxides of sulphur play important roles both in atmospheric pollution and corrosion by flue gases. Sulphur dioxide (SO_2) and sulphur trioxide (SO_3) were measured during the combustion tests. During the combustion, the major part of the sulphur in the fuel is oxidised to SO_2, but a small proportion is further oxidised to SO_3. The percentage conversion of SO_2 to SO_3 was found to be dependent on the percentage of excess air. The level of SO_3 increased with available oxygen, and the SO_2/SO_3 ratio increased with increasing fuel sulphur content, and substantial reductions in the sulphur oxides (SO_X) emissions can be made by converting equipment from oil to coal-in-oil fuel burning.

4.1. Mechanism of SO_3 formation

Equilibrium considerations in combustion flue gases.

The following method predicts the theoretical percentage conversion of SO_2 to SO_3 in the combustion products of the fuel at equilibrium. This is compared with the measured percentage conversion of SO_2 to SO_3 (see Section 4.2).

Assuming equilibrium conditions in the flue gas at the sampling point:

$$SO_2 + \tfrac{1}{2} O_2 \rightleftarrows SO_3 \qquad (29)$$

$$K_p = \frac{[SO_3]}{[SO_2][O_2]^{\frac{1}{2}}} \qquad (30)$$

The free energy for the reaction (29) is given by Bodenstein and Pohl[11].

$$\Delta G^{\theta} = -22600 + 21.36T \qquad (31)$$

$$\log K_p = \frac{4939}{T} - 4.67 \qquad (32)$$

where $$K_p = \frac{P_{SO_3}}{P_{SO_2} \times P_{O_2}^{\frac{1}{2}}} \quad (33)$$

$$K_p \times P_{O_2}^{\frac{1}{2}} = \frac{P_{SO_3}}{P_{SO_2}} \quad (34)$$

$$\frac{P_{SO_3}}{P_{SO_2} + P_{SO_3}} = \frac{K_p \; P_{O_2}^{\frac{1}{2}}}{1 + (K_p \times P_{O_2}^{\frac{1}{2}})} \quad (35)$$

4.2. Comparison of measured percentage conversion of SO_2 to SO_3 with theoretical predictions

The measured SO_2/SO_3 concentrations which were obtained after sampling through a heated probe are compared with the theoretically calculated equilibrium concentrations at flue gas temperatures in Figures 8-11.

5. CONCLUSIONS

1. Flame burn-out time of various coal-oil dispersions is generally increased by the presence of coal in the oil, except in the case of low volatile, low reactivity coals.

2. Emissions of oxides of nitrogen are increased when burning coal-oil dispersions, and fuel nitrogen oxidation is the major source of NO emissions.

3. Increasing temperature increases the proportion of fuel nitrogen volatilized and decreases the proportion left in the char.

4. The nitrogen is more easily released with higher rank coals.

5. Equilibrium calculations are unreliable for calculating NO in the flue gas, but for the SO_2 to SO_3 reaction may produce satisfactory predictions.

6. NO_x emissions can be minimised by suitable burner design and operation, and the use of low nitrogen content fuels.

7. The substitution of coal-in-oil fuels for heavy fuel oils will result in lower SO_x emissions.

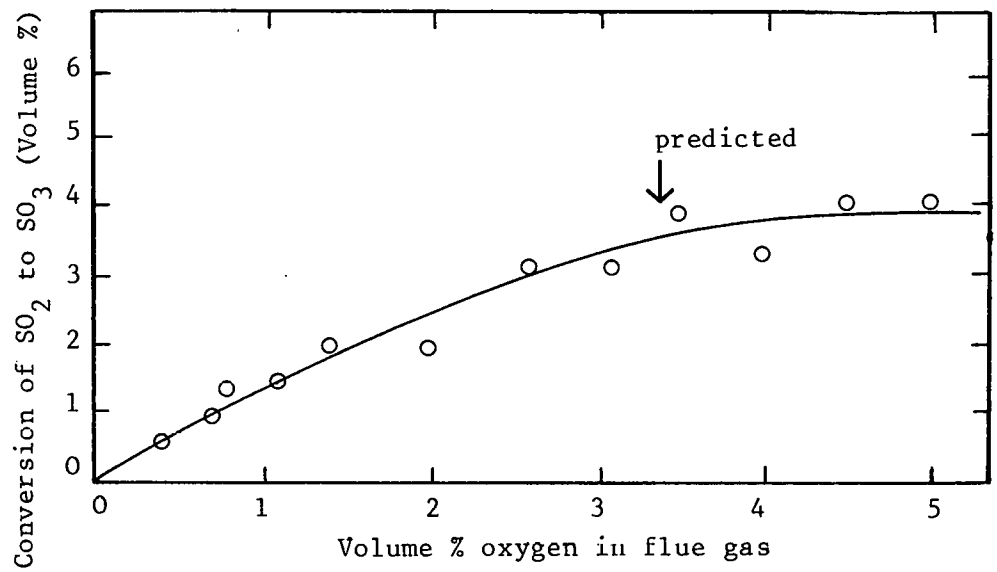

Figure 8. predicted and measured % conversion of SO_2 to SO_3 at equilibrium in combustion flue gas for 950 Redwood second fuel oil.

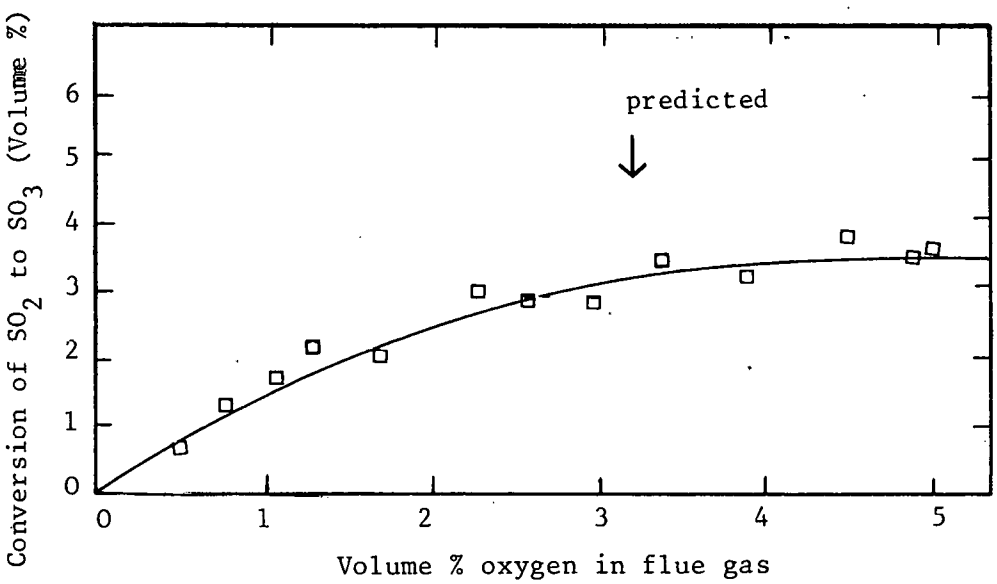

Figure 9. predicted and measured % conversion of SO_2 to SO_3 at equilibrium in combustion flue gas for antracite low volatile coal-oil dispersion.

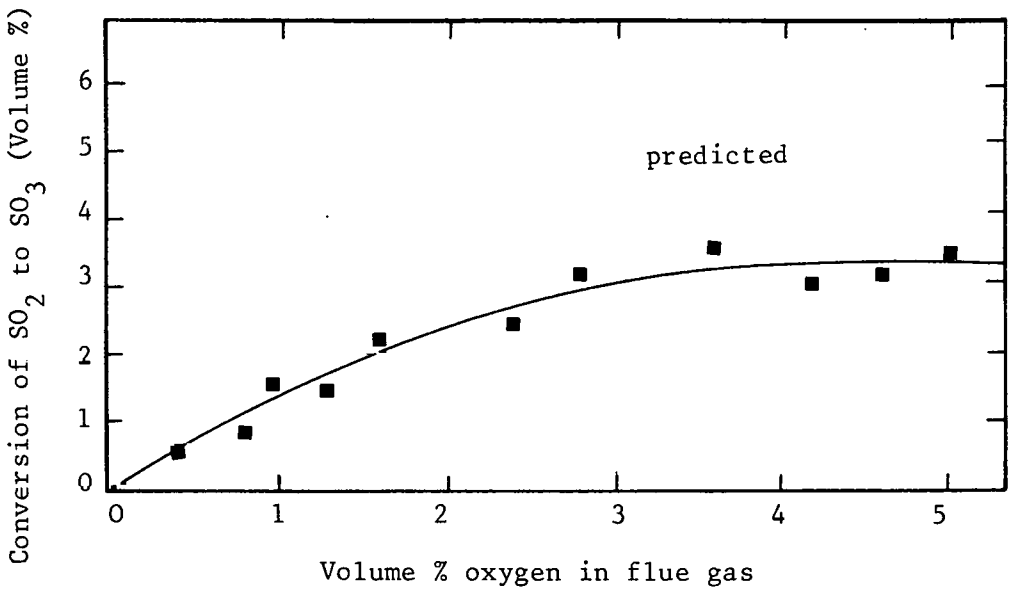

Figure 10. predicted and measured % conversion of SO_2 to SO_3 at equilibrium in combustion flue gas for medium volatile coal-oil dispersion.

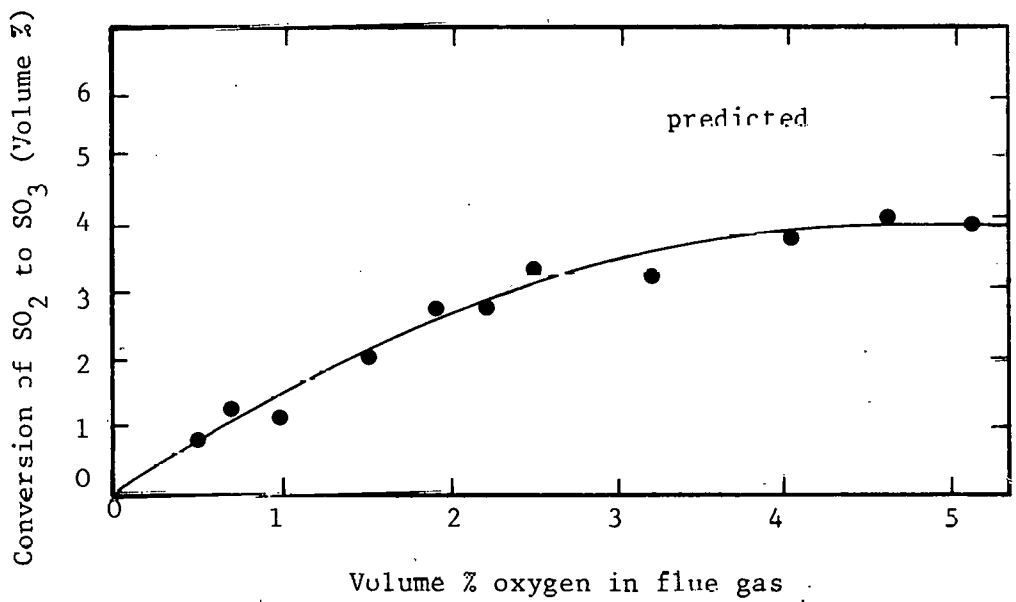

Figure 11. predicted and measured % conversion of SO_2 to SO_3 at equilibrium in combustion flue gas for high volatile coal-oil dispersion.

REFERENCES

1. ALABAF, J.S.

   Coal-in-oil fuels (dispersions and mixtures).

   4th International Symposium on coal-slurry combustion. U.S. Dept. of Energy, Orlando, Florida, U.S.A., 10-12 May, 1982.

2. ALABAF, J.S.

   Handling, combution and emissions from various coal-oil dispersions.

   4th International Symposium on coal-slurry combustion. U.S. Dept. of Energy, Orlando, Florida, U.S.A., 10-12 May 1982.

3. PRUCE, L.M.

   NO_x - reduction efforts for gas turbines continue in face of stiff regulations, fuel uncertainties.

   Power, 125, 66-68, 1981.

4. ZELDOVICH, J.

   The oxidation of nitrogen in combustion and explosions.

   Acta Physicochimica U.R.S.S. 21, 576-628, 1946.

5. FINE, D.H., SLATER, S.M., SAROFIM, A.F., and WILLIAMS, G.C.

   Nitrogen in coal as a source of nitrogen oxide emission from furnaces.

   Fuel, London. 53, 120-125, 1974.

6. NERNST, W.
   On the formation of nitric oxide at high temperatures.
   Anorg.Chem. 49, 213-228, 1906.

7. HOMER, J.B., JENKINS, D.R., and SUTTON, M.M.

   Kinetics of nitric oxide formation

   International Flame Research Foundation, Ijmuiden, 156-159, 11-12 May 1972.

8. BODENSTEIN, M., and KATAYAMA, M.

The dissociation of H_2SO_4 and of NO_2.

Zeit.Fur Elektrochemie, 15, 244-249, 1909.

9. BODENSTEIN, M., and KATAYAMA, M.

A satisfactory method of measuring steam densities dissociation of hydrated sulphuric acid and nitrogen dioxide.

Zeit.Physik.Chem. 69, 26-51, 1909.

10. RICHARDSON, A.

Action of heat on peroxide of nitrogen

Jnl.Chem.Soc. 51, 397-402, 1887.

11. BODENSTEIN, M. and POHL, W.

Equilibrium measurement of contact sulphuric acid

Zeit. Fur Elektrochemie, 11, 373-384, 1905.

ACKNOWLEDGEMENTS

The assistance of members of FERGUS is gratefully acknowledged.

Thanks are also due to British Petroleum Research Centre, Sunbury, England for the gift of the fuel.

TABLE A.1. Effect of temperature and NCB rank of coal on nitrogen remaining in char from various coal-oil dispersions.

Coal-Oil dispersions	Volatile matter content of coal in dispersion (wt %)	Nitrogen content in coal-oil dispersion (wt %)	Temperature (^{o}C)	Nitrogen volatilized from coal-oil dispersion (wt %)	Nitrogen remaining in char from coal-oil dispersion (wt %)
101/950	7.6	0.564	600	0.107	0.457
"	"	"	800	0.138	0.426
"	"	"	1000	0.262	0.302
"	"	"	1500	0.418	0.146
301/950	20.1	0.620	600	0.156	0.464
"	"	"	800	0.205	0.415
"	"	"	1000	0.286	0.334
"	"	"	1500	0.491	0.129
501/950	35	0.683	600	0.215	0.468
"	"	"	800	0.274	0.409
"	"	"	1000	0.445	0.238
"	"	"	1500	0.568	0.115

Table A.2. Chemical analysis of particulates emissions from the combustion of various coal-oil dispersions

Coal-Oil dispersions	% O_2 in flue gas	% Excess Air	Oil flow rate (l/hr)	Volatile matter content of coal in dispersion (wt %)	Nitrogen content in coal-oil dispersion (wt %)	Unburned nitrogen (wt %)
101/950	2.5	12.0	23	7.6	0.564	0.163
301/950	2.5	12.0	22	20.1	0.620	0.147
501/950	2.5	12.0	23	35	0.683	0.135

Table A.3. Structure of fuel-nitrogen compounds

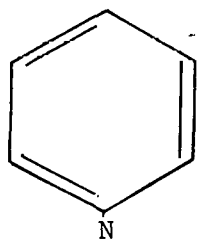

PYRIDINE

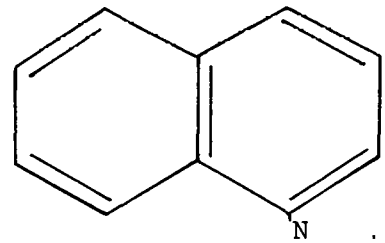

QUINOLINE

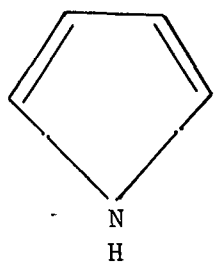

PYRROLE

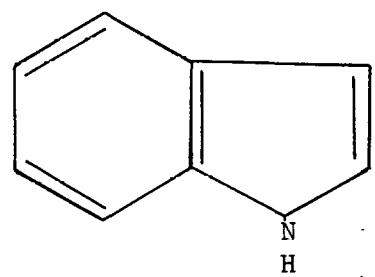

INDOLE

a. Structure of fuel-nitrogen constituents pyrroles and pyridines

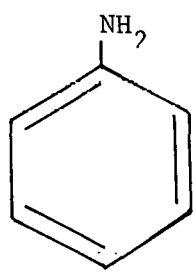

ANILINE

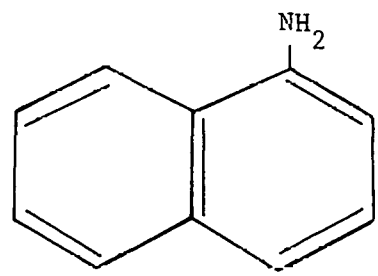

NAPHTHYLAMINE

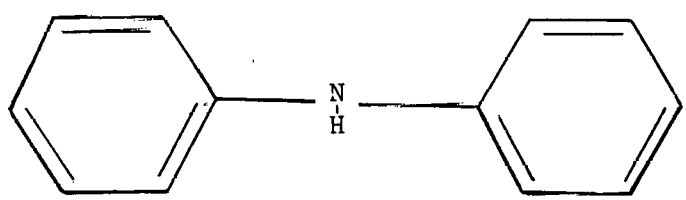

DIPHENYLAMINE

b. Structure of fuel-nitrogen constituents:

Amines (RNH_2, RRNH)

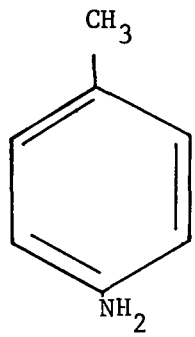

TOLUIDINE

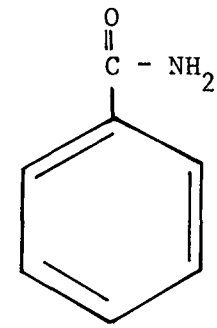

BENZAMIDE

c. Structure of fuel-nitrogen constituents

Amides ($RCO\ NH_2$)

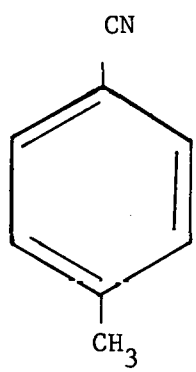

TOLUNITRILE

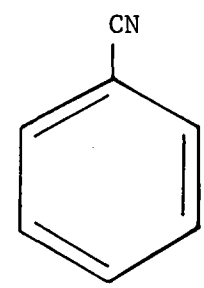

BENZONITRILE

d. Structure of fuel-nitrogen constituents

Nitriles (R CN)

SO_x AND SOLIDS BURDEN SAMPLING PROBES

by

J.S. ALABAF

UNIVERSITY OF SURREY

DEPARTMENT OF CHEMICAL ENGINEERING

GUILDFORD, SURREY, GU2 5XH, ENGLAND

1. SO_x sampling probes

A gas sampling probe must be designed to prevent the cooling of the gaseous mixture below the dew-point of sulphuric acid which is the first to condense. An electrically heated sampling probe with a stainless steel water-cooled jacket, as described below was found to operate satisfactorily[1].

1.1. Design of SO_x sampling probe

The electrically heated sampling probe is shown in Figure 1. Part A consists of an inner Heralux fused silica tube, which has greater heat resistance than a normal silica tube. This sampling probe is wound with nichrome wire. The winding is covered with alumina cement for insulation. A thermocouple made up with Ni-cr/NI-Al wire was inserted through a small hole drilled through the silica tube in a central position at the cooled end and was sealed with alumina cement, and its purpose was to ensure that the sample gas stream was always maintained above the acid dew-point temperature. This probe is inserted into another Heralux fused silica tube for good heat and electrical insulation.

The assembly is inserted into a water-cooled jacket as shown in Figure 1 part B consisting of stainless steel coaxial flow and return sections. The outer shell has an expansion joint.

The designed unit was tested for repeatability of results and was found to operate satisfactorily.

2. Solids burden sampling probe

The solids burden of the combustion chamber flue gases was measured for various coal-oil dispersions and constituent fuel oil over a range of excess air 2-30% using sintered bronze filters housed in a modified Land pyrometer water-cooled stainless steel probe[1]. Figure 2 shows a general assembly of the probe, with a modified solids burden sampling nozzle and sintered bronze filter in position. This proved to be the most reliable of all methods which are available for sampling from flue gases at elevated temperatures[2,3].

During the initial test it was found that the considerable moisture present in the sampling nozzle, filter and particulate samples, was due to condensation from flue gases. This resulted in poor solids hold-up in the filter making results inaccurate and made the inconvenient subsequent drying of the samples necessary.

2.1. Modification to Land solids burden probe

For isokinetic sampling, two alternative methods are available. The velocity in the sampling nozzle may be adjusted to match the gas velocity in the duct by varying the nozzle area at constant sampling

1. spherical joint
2. thermocouple
3. leads
4. heat insulation
5. alumina cement
6. Heralux fused silica tube
7. nichrome winding (0.47 dia.)

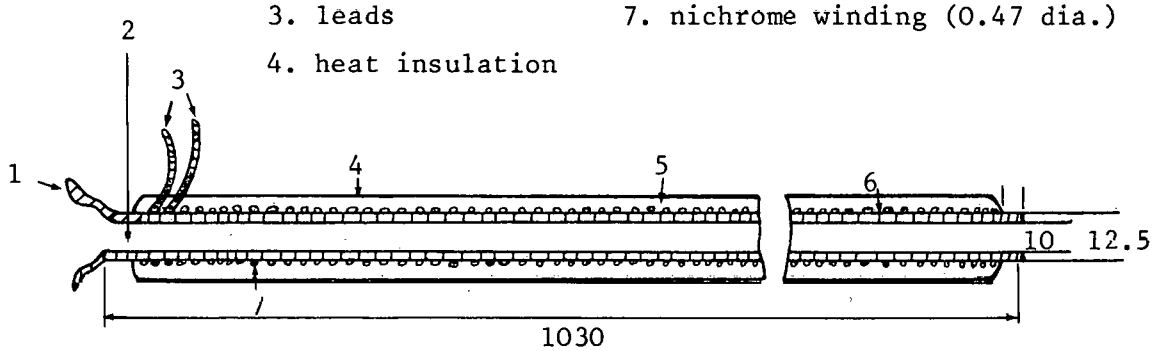

(A) Electrically heated SO_2, SO_3 sampling probe (in mm)

1. leads
2. Heralux fused silica tube (33 dia.) for heat insulation and electric
3. water connectors
4. rubber sleeve over expansion joint
5. hose clip
6. alumina cement
7. this end inserted in flue gas duct back end end furnace
8. thermocouple

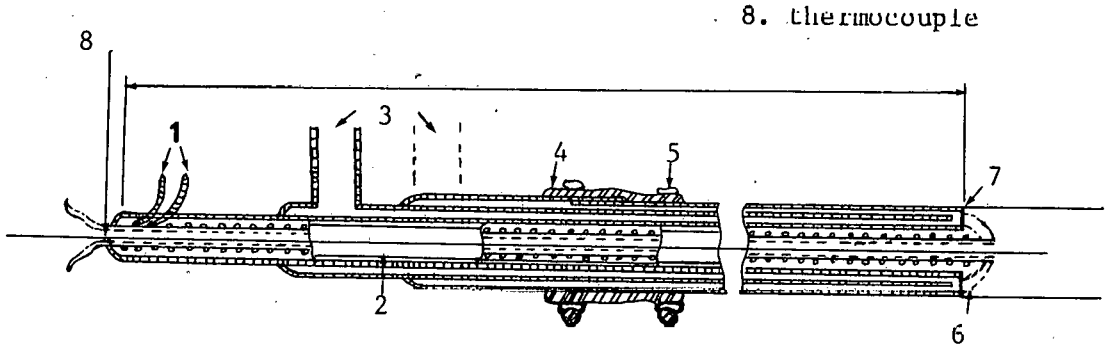

(B) Stainless steel water-cooled jacket on sampling probe

Figure 1 (A) and (B) electrically heated sampling probe with stainless steel water-cooled jacket for the determination of sulphur oxides (SO_2,SO_3) emissions (in mm).

rate for a fixed nozzle area. In the case of the Land solids burden probe the sampling rate was varied under combustion operation condition for a fixed nozzle area.

(i) Modified sampling nozzle

The modified sampling nozzle which was used is shown in Figure 3 and made of stainless steel with 12.5 mm O/D, 90° angle. The sampling nozzle stood proud from the probe head at a distance of 12.2 mm. Test results were very successful, with no condensation from combustion flue gases in the sampling nozzle, filter or particulates. This nozzle eliminated the need to dry filters and nozzle in the oven.

(ii) Cooling water flow rate adjustment

The solids sampling probe was modified by fitting a pressure gauge in the cooling water outlet line in order to assist in the control and adjustment of the cooling water flowrate. Condensation was eliminated by reducing the cooling water flowrate. This system was found to be entirely satisfactory.

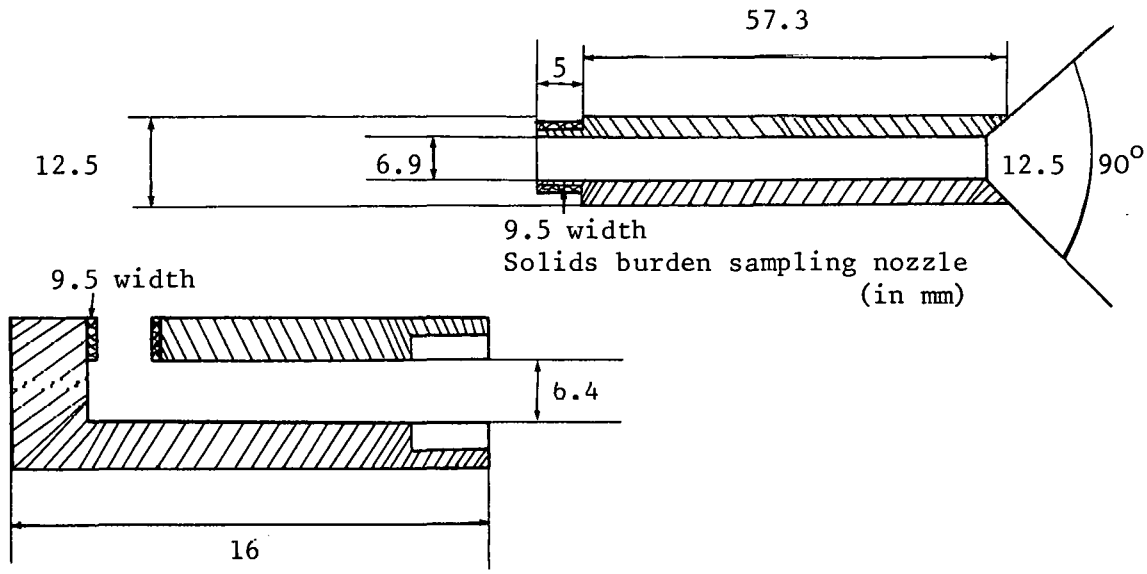

Filter guide (in mm)

1. sampling nozzle
2. sintered bronze filter
3. cooling water in
4. cooling water out

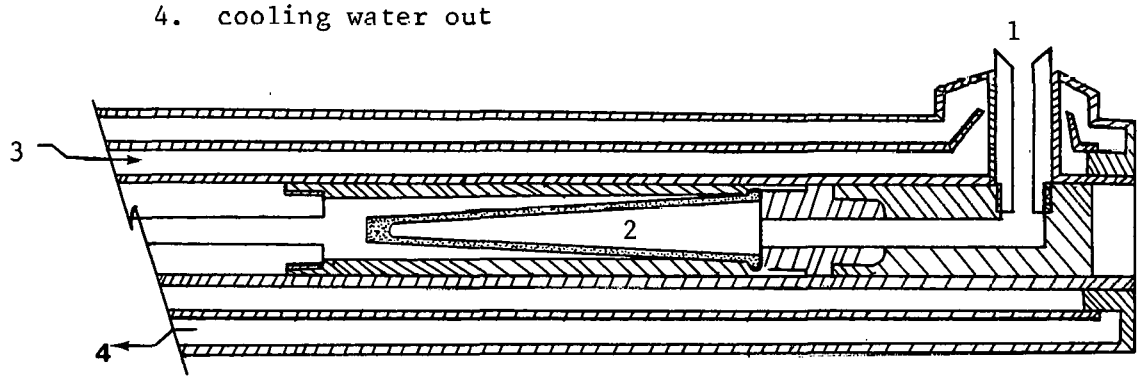

Figure 2. General assembly of water-cooled probe with solids burden sampling nozzle in position.

REFERENCES

1. ALABAF, J.S.

Handling, combustion and emissions from various coal-oil dispersions.

4th International Symposium on coal-slurry combustion.
U.S. Dept. of Energy, Orlando, Florida, U.S.A. 10-12 May 1982.

2. RENDLE, L.K.

Measurement of the flue gas solids burden from oil-fired installations using a silica wool filter. Jnl.Inst.Fuel, 37, 25-30, 1964.

3. HAWKSLEY, P.G.W., BADZIOCH, S. and BLACKETT, J.H.

Measurement of solids in flue gases, part 2.
B.C.U.R.A. Leatherhead, 1961.

The following manuscript was unavailable at time of publication:

A Procedure for the Evaluation of the Combustion Performance of Coal-Water Slurries

S. L. Chen, R. Payne, W. Richter and J. Wilborn
Energy and Environmental Research Corporation, Southern California Edison

DO NOT MICROFILM THIS PAGE

COAL SLURRY CHARACTERISTICS OF BITUMINOUS AND KOREAN ANTHRACITE

D.C.Kim, S.H. Cho, S.K. Kang and D.H. Shin

Korea Institute of Energy and Resources.

Introduction

In Korea, except for nuclear energy, almost all of the fuel consumption for electric power generation and industry is imported oil.

About 20 million ton of anthracite is produced annually from domestic sources. More than 80wt % of that is used for household fuel in a briquet type. Because the ash content is generally higher than 35 wt %, many difficult problems are encountered. Therefore it is expected that the anthracite, domestic fuel will be replaced with gas fuel, LNG or LPG in the near future, and the demand for domestic anthracite will be decreased remarkably. Then new methods to utilize the Korean anthracite will be urgently needed.

In order to study the utilization of domestic anthracite and reduction of the dependency on oil, research and development work for the application of imported bituminous coal and domestic anthracite as COM or CWM for industrial oil fired boilers and furnaces has been carried out in K.I.E.R. since 1981. Using anthracite with high ash content the deashing process development work was done in addition.

Research work included the following :

1) wet grinding for preparation of coal slurry
2) development of stabilizing agents for CWM and COM
3) additives for enhancing the coal contents in CWM
4) flow characteristics of the slurry
5) deashing of coal by spherical oil agglomeration
   - process improvement
   - experiments for finding optimum conditions depending on coal types
6) COM combustion test in tunnel furnace
7) economic analysis of COM in Korea
   - imported bituminous COM
   - deashed Korean anthracite COM

Experimental methods and Facilities

As raw coal,various samples of Korean anthracites and two of imported bituminous were used, and for the combustion test Hamtae coal as a Korea anthracite and South-african coal as an imported bituminous were selected. Their properties are listed in the Appendix 1.

Raw coals were ground into-3mm size particles with a hammer mill, then the crushed coal was charged into a continuous wet ball mill (420 mmID × 900 mmL, 30 Kg COM/hr production capacity) with heavy oil and additives for preparation of COM. The wet ball mill temperature was controlled at about 90°C by an electric heater attached on the shell. In the ball mill the coal particles were ground into 80% pass 200 mesh.

For the preparation of CWM the crushed coal and water were charged into the ball mill by leaving the temperature in an ambient condition.

In the case of using the high ash content Korean anthracite after the raw coal was ground into 80% pass 200 mesh and 50 wt % coal water slurry in the above ball mill, it was processed to remove the ash content. After the slurry was conditioned its water content was at about 25 wt %.
The slurry was then was transfered into a bench scale continuous deashing facility with the proper amount of bridging oil. The deashing process as a spherical oil agglomeration could treat 20 Kg of coal per hour continuously.
The deashed coal with heavy oil and additive was mixed with the high speed agitator and became COM at 90°C.
The
The prepared COM was stored at 70°C and the rod penetration method and the analysis method of the concentration were used for the slurry stability test. The slurry flow characteristics were investigated with the Brookfield viscometer RVT type.

For the combustion and atomizing test the oil fired steam jet burner with 5 Ton/hr steam production capacity was tried in a tunnel furnace (2.7m × 2.7m × 6.5m), in which the compressed air was applied as an atomizing medium. The COM was heated in a stirred tank with an electric heater before it was pumped to the burner. The burner nozzle was Y - jet type of hardened steel.

Results and Discussion

1. Flow Characteristics of COM

As the coal content is increased, the viscosity of the slurry increases. The viscosity of COM was plotted on the semi-log graph, Fig-1, by changing the coal concentration, and it showed the viscosity of COM was increased rapidly as the concentration was increased above 40-42 wt %. The data was correlated into the Thomas relation (1) by transforming the unit into volume concentration, but the erross were very severe.

$$um/uo = 1 + 2.5\phi + 10.05\phi^2 + A_1 \exp(A_2 \phi) \quad \text{--- (1)}$$

Where um : viscosity of mixture
uo : viscosity of liquid
ϕ : volumetric concentration
A_1, A_2 : constants

Thus,it seemed not to be applicable for this slurry. This result was, it is assumed, because equation (1) was Proposed for the system of Newtonian suspensions of uniform

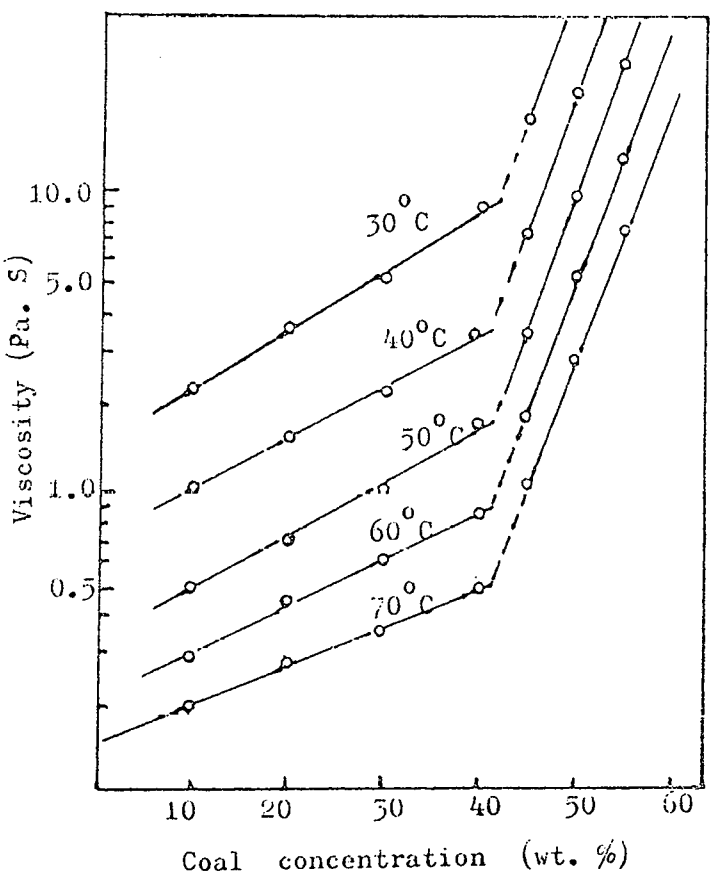

Fig. 1. COM viscosity vs coal concentration (without additive)

spherical particles, but the COM had different properties, that is, nonsphericity in its particle shape and non-Newtonian characteristics.

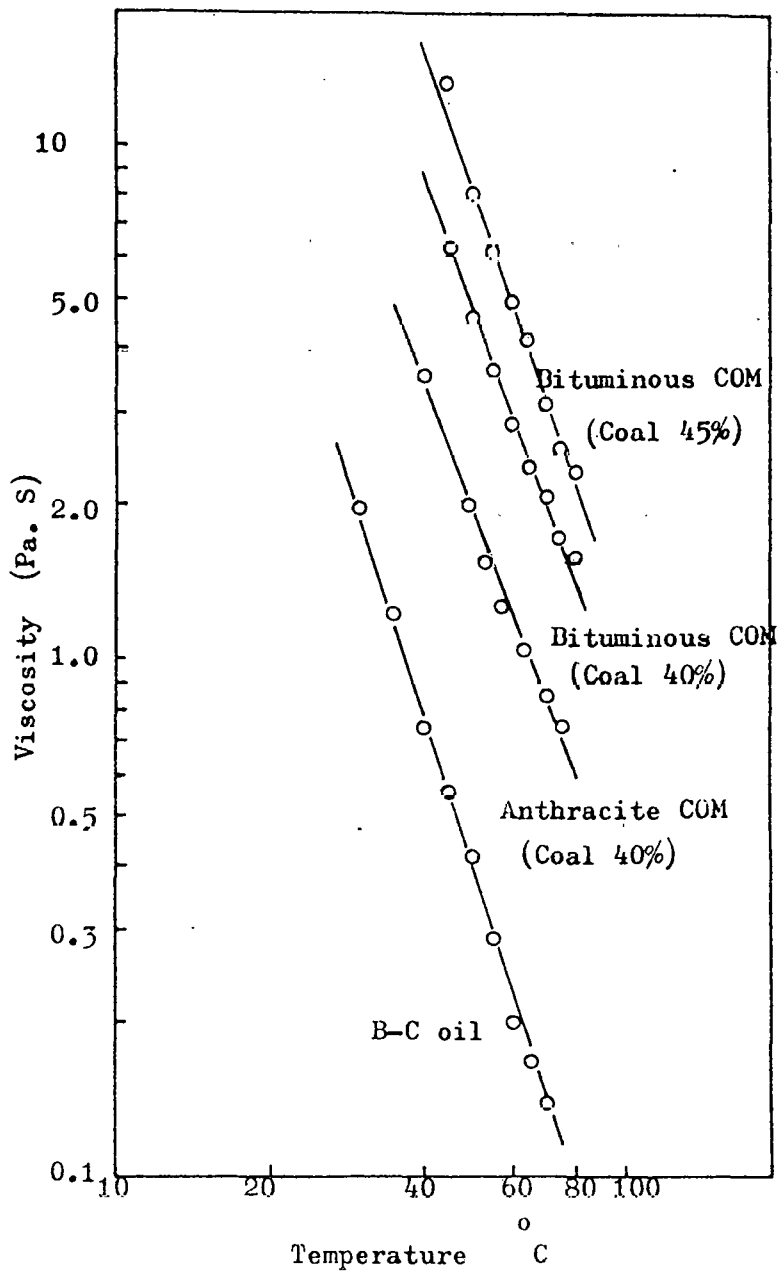

Fig. 2. COM Viscosity vs Temperature
(water 5% + additive 0.1%)

The COM viscosity was varied linearly on the log graph, Fig-2., by changing the temperature (in centigrade). So the correlation of the viscosity vs the temperature could be shown as (2).

$$um = C_1 t^{C2} \quad \text{---------- (2)}$$

where C_1, C_2 : constants

t : temperature in ^{o}C

The above relationship was assumed to apply as long as the temperature would not be high enough for the viscosity to increase by the coal particles swelling or hydrogenation.[2)]

On the other hand the viscosity of bituminous COM was about 2 times higher than that of anthracite under the same conditions.

The viscosity was increased also by increasing the water content in the slurry at the same coal concentration. For the 45 wt % coal COM the viscosity of 7% water was about 3 Pa. S higher than that of 5% at 50 ^{o}C, and about 1 Pa. S. higher at 75^{o}C.

In order to investigate the rheological properties of COM the shear stress was measured by changing the shear rate.

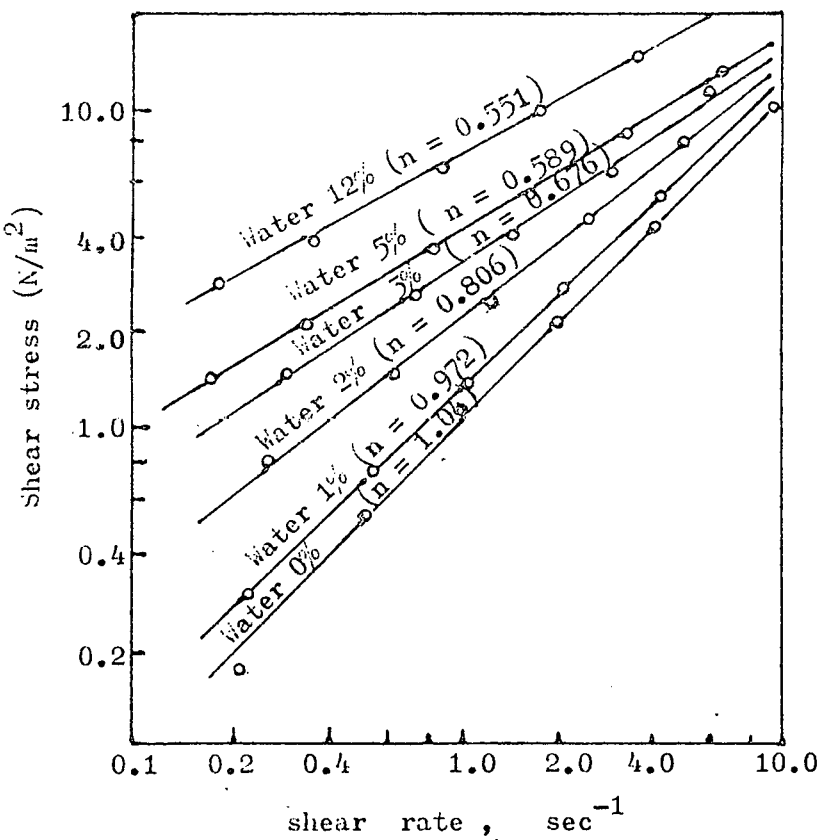

Fig. 3. Shear stress vs shear rate (40 % COM , 70^{o}C)

The plotted results showed an almost linear relationship on the log graph Fig. 3, and this indicated that the fluid properties would fit the power model. Since the slopes became smaller than 1 as the water contents were increased, the fluid was known to be a pseudoplastic and to approach non-Newtonian behavior gradually by increasing the water content. The flow index and flow consistency K are listed in Table 1.

Table-1. non-Newtonian Properties of COM (Additive 0.1% at 70°C)

Water.%	Flow Index. n.		Flow Consistency.K.	
	Coal 40% wt	Coal 45% wt	Coal 40% wt	Coal 45% wt
0	1.0402	0.9421	0.9371	1.8590
1	0.9717	0.8201	1.2143	2.4634
2	0.8060	0.8371	2.0559	3.2042
3	0.6762	0.7672	3.0574	4.0880
4	0.6085	0.7198	3.6282	5.2345
5	0.5895	0.7076	3.8503	5.6371
6	0.5742	0.7077	3.9208	7.2500
7	0.6074	0.7296	4.3442	7.2783
8	0.6441	0.5283	3.8453	11.1167

2. Enhancement of the coal content in CWM

For the preparation of high coal content CWM with good fluidity the vacant space among the coal particles should be minimized, and the hydrophobic coal surface should be made into hydrophilic one. To reduce the void the particle size distribution is the parameter to be controlled. Many theoretical particle size distributions to enhance the coal concentration in slurry can be suggested, but those are not easy to apply practically.

In order to broaden the particle size distribution two or three lots of ground solid particles of different fineness can be mixed into slurry with good fluidity. Fig-4, presents the viscosity of CWM which was made by blending a fine size coal and a coarse one. From the graph the fluidity is best when the blending ratio was about 1:2.

If the additive is applied for enhancing the fluidity of coal water slurries, another good effect can be acquired. The comparison of the viscosity of a CWM without additive with that of using additive (CWM 1002, 0.3% + electrolyte, 0.1%) is shown in Fig-5. This figure shows the possibility of increasing the coal concentration in CWM by about 10 wt %

by using an effective additive.

In addition to the effect of an additive, adjusting the particle size distribution allows a pumpable CWM with a coal concentration of more than 70 wt % to be prepared.

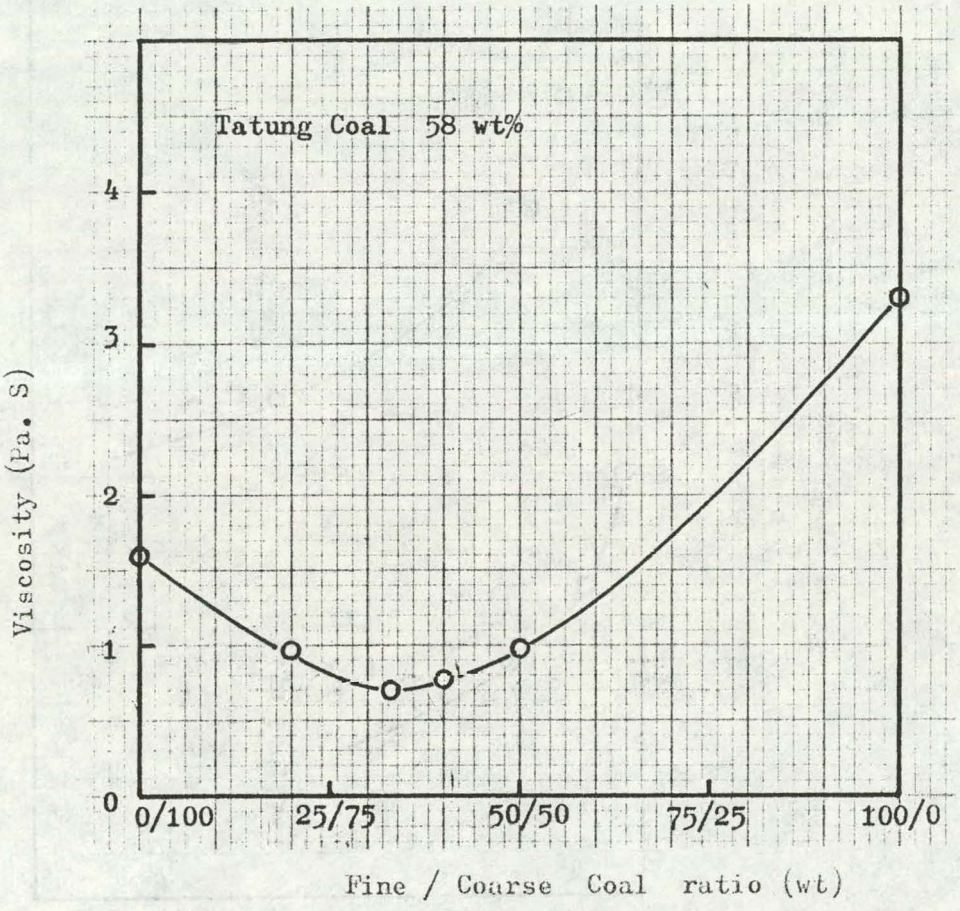

Fig - 4. CWM Fluidity vs Blending Ratio
(SP. No. 3. rpm. 10)

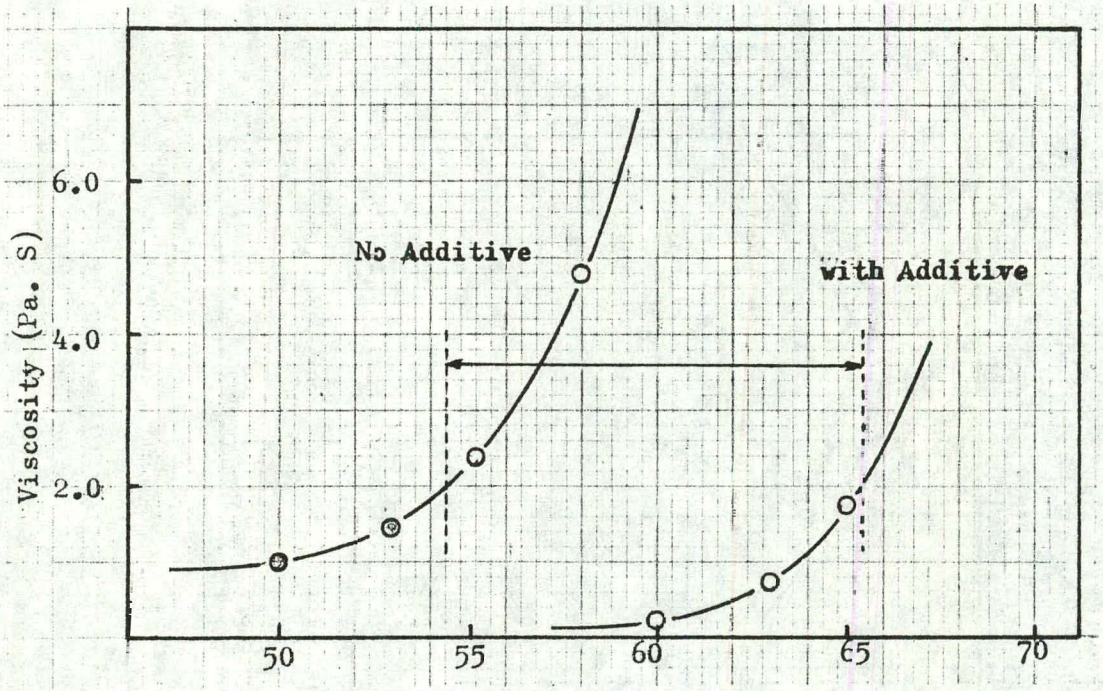

Fig. 5. Fluidity Ehancing Effect in CWM by using Additive

3. Coal deashing by spherical oil agglomeration process

The ash removal effect depends mainly on how the pure coal components are blended with the gangue in the mineralogical structure of raw coal.

Fig-6, shows the mineralogical structure of a Chansung anthracite sample, and good segregation of the coal components from the gangue seems to be made. The gangues are attached to the edge of the coal particles, so it seems possible to segregate the gangues from the coal particles easily if they are ground into fine particles of about 50 um.

But the coals like Chungnam anthracite, Fig-7, which has a bad segregation structure are supposed to be difficult to separate from the gangue even if they are ground into much finer particles.

Because the affinity of coal and oil depends on the rank of coal, in case of treating anthracite which has a high degree of maturation, the agglomeration was carried out easily and the ash removal ratio was high using light oil as a binding material.

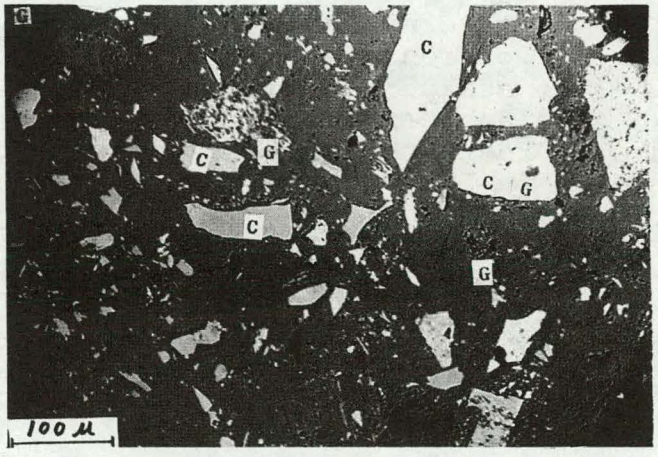

Fig-6. Microscopical structure of Changsung anthracite. (-200 mesh)

During this experiment the agglomerate size and strength, the ash removal ratio and carbon recovery was varied by changing the amount of oil and agitation speed.

Fig-7. Microscopical structure of Chungnam anthracite.(-325 mesh)

Optimum process variables can be considered by representing the process efficiency in (3).

$$Y = R\left(\frac{A_f - A_c}{A_f}\right) \qquad (3)$$

where Y is the efficiency of the agglomeration process,
R the percentage recovery of the coaly matter,
A_f the ash percentage in feed coal,
A_c rhe ash percentage in cleans.

Here Y is the product of R which represents the efficiency in amount, and $(A_f - A_c)/A_f$ which represents the efficiency in quality.

If Y is maximum, the efficiency of the process becomes maximum, and it is changed by variables, i.e., the amount and type of bridging oil, coal type, agitation speed, residence time and temperature. The results of deashing process acquired are listed in Table 2.

When the heavy oil was used as a bridging oil, the agglomeration was possible by heating the agglomeration tank to 60°C. However, by using deashing additives agglomeration was also possible at 35°C, and the residence time was reduced about a third under the same temperature.

As a subsequent effect to the ash removal the sulfate in raw coal was removed almost completely and half of the pyrite could be removed.

Table. 2. Results of Deashing Process

Coal		agglomeration Conditions					Ash Content		Carbon Recovery R.	Efficiency Y.
Class	Origine	Oil	Oil amount (%)	Agitation speed rpm	Retension time(min)	Temp. °C	Raw coal A_f.	Cleans A_c.		
Anthracite	EunSung	Diesel	15	1700	9.2	ambient	31.73	6.74	86.2	67.9
		Heavy oil	15	3000	30	60		9.77	87.1	60.3
"	ChangSung	Diesel	15	1800	10	ambient	37.87	9.71	89.0	66.2
		Heavy oil	15	3000	30	60		11.92	91.9	63.0
"	HamTae	Diesel	15	1600	9.3	ambient	27.16	10.93	89.0	53.2
		Heavy oil	15	3000	30	60		12.23	93.1	51.2
"	ChungNam	Diesel	12.5	1780	9.2	ambient	63.30	20.26	68.1	46.3
		Heavy oil	12.5	3000	30	60		23.32	42.4	26.8
Bituminous	Tatung	Diesel	35	1800	9.2	ambient	11.05	6.79	90.6	34.9
		Heavy oil	35	3000	30	60		8.41	96.4	23.1

4. Combustion Test

For the purpose of investigating the combustibility and atomizability of COM made from deashed Korean anthracite (Hamtae coal) and bituminous (South African coal), the combustion test was carried out during a week, and the results showed the both anthracite COM and bituminous COM could be atomized and burned in a furnace with an oil fired steam jet burner.

After the ignition of COM the condition was adjusted to make the flame stable and the flue gas smokeless. During the continuous operation the flue gas analysis was carried and the flame was observed through sight glasses.

Results shown in Table 3 indicate that the excess air ratio could be controlled at 7-10% by maintaining a good flame.

Table 3. Combustion Test Conditions

	fuel Temp. ^{o}C	fuel Pressure Kg/cm^2	Atomizing Air. Pressure Kg/cm^2	Combustion Air ratio m	Nozzle	CO_2 in flue gas
Anthracite COM	66	4.0	2.4	1.070	8 holes (1.4 mmφ) 70°	16.4%
Bituminous COM	68	3.0	2.4	1.069	6 holes (1.4 mmφ) 55°	15.0%
Bituminous COM	74	2.3	1.5	1.104	6 holes (1.4 mmφ) 55°	14.5%

Most of the combustion seemed to be carried out within 1.5m from the burner nozzle, and some unburned material was burnt after 1.5m. It was assumed to be similar to the results presented by Y.Q. Cao.[4)]

In the combustion and atomization, the anthracite COM was not remarkably different from the bituminous COM but the CO_2 content in flue gas was a litte higher in case of anthracite.

Generally COM was serviced to the burner at high temperature. However in this case the fuel was serviced at about 70°C and atomized and burned relatively well.

5. Economic Evaluation

In Korea oil supply depends entirely on import, so the heavy oil calorific price is relatively high. Therefore the economic evaluation in case of replacing the heavy oil with COM for industrial boiler showed that it would be feasible.

For the industrial oil fired boiler of 20 Ton steam production an hour, the rate of return on investment (R.O.I) was estimated to be 28.5% and the pay out period 2.4 years.

Even if the cheaper Korean anthracite is used for COM, the cost is about the same as using imported bituminous coal because of the added ash removal cost for the Korean anthracite.

Conclusion

For the development work of COM and CWM application to the reducing of energy supply dependency on imported oil, the developing of new utilization measures of Korean anthracite and the diminishing of energy cost of industry, bench scale experiments were carried out.

Through the work the flow characteristics of COM was acquired and it was possible to raise the coal concentration by 10 wt% higher than that without additives.

In the case of using Korean anthracites the appropriate deashing process conditions were induced respectively, and the result of combustion of the deashed anthracite COM showed that it could be atomized and burned as well as bituminous COM.

Since the heavy oil price is high in Korea it was shown that COM would be very attractive economically here in Korea.

Reference

1) D.G. Thomas, "Transport characteristics of suspensions part VIII, A note on the Viscosity of Newtonian Suspensions of Uniform Spherical Particles.", J. Colloid Sci. 20 (1965), P 267.

2) J.R. Thurgood, R.W. Hanks, G.E. Oswald and E.L. Young blood, "The Rheological Characterization of Coal Liquefaction Preheater Slurries", J. AIChE, Vol.28.P 111. (1982).

3) R.N. Bhattacharyya, A.K. Moza and G.G. Sarkar, "Role of Operating Variables in Oil-agglomeration of Coal" Agglomeration 77, Volume 2, 2nd International Symposium on Agglomeration, P 93 (1977).

4) Y.Q. Cao, Zhejiang University, "Experimental Stady of COM combustion Process in the Tunnel Furnace", 3rd International Symposium on Coal-Oil Mixture Combustion.

Appendix.1. Coal Properties.

		Hamtae Anthracite	South african bituminous
Proximate analysis			
Moisture	(%)	3.48	1.8
Ash	(")	27.16	14.7
Volatile	(")	3.94	25.8
Fixed Carbon	(")	65.96	57.7
Ultimate analysis			
C	(%)	66.72	68.40
H	(")	1.21	8.30
N	(")	0.09	0.20
O	(")	3.50	7.63
S	(")	0.67	0.56
Ash	(")	27.80	14.91
Heating Value (Kcal/Kg)		5480	6780
True density (g/cc)		1.966	1.48
HGI.		103	49
Ash fusion point (^{o}C)			
IDT		1400	1300
S T			1340
F T			1380

Appendix.2. Economic Analysis

A. Deashing Cost (unit : U$ 1000)

1.	Capital Investment	1964
2.	Deashing Cost	
	a. material	
	anthracite	13031
	Heavy oil	16747
	b. utility	1215
	c. maintenance	161
	d. Ash Disposal	971
	e. others	67
	Total	32195
3.	Unit cost	$ 108.4/Ton. of cleans including oil
4.	Calorific cost	$ 14,453/10^6 Kcal

*. Calculation basis

Capacity : Cleans Coal 30 Ton/hr (237,600Ton/Year)
Including Binding Oil : 297,000Ton/Year

Raw coal : $ 31.28/Ton
H.V : 4300 Kcal/Kg
Ash content : 43%

Heavy oil : $ 0.27/ℓ
20% of Cleans is required

Ash content in clean coal : 10%

Coaly matter Recovery : 90%

B. Deashed COM Producing Cost

1. Plant Capacity : 600,000 Ton/Year.

2. Product : Deashed Coal 40% included COM

3. Capital Investment (U$ 1000)

Deashing Plant :	1964
COM Preparation:	17333
Sub Total :	19297

4. Annual Cost

a. Direct materical

Clean coal + Binding oil :	32520
Heavy oil :	84587
additive (0.1%)	800
Sub Total	117907

b. Indirect Cost

General expence	4133
Interest (10%/Year)	1933
Depreciation	2761
Sub Total	8827

c. Profit 3853

Total 130587

5. Unit Cost

$ 217.6/Ton

$ 24.4/10^6 Kcal

C. Economic Evaluation in Case of retrofit Industrial Oil fired boiler with COM.

1. Basis

Steam generation capacity : 20 Ton/hr

Thermal Efficiency : 85% for oil firing

83% for COM firing

Operating load : 70%. 330 day/Year

Calorific price : $ 27.33/10^6Kcal for Heavy oil

$ 24.40/10^6Kcal for COM

2. Economic analysis (unit : U$ 1000)

Item.	Heavy oil	COM
1. Retrofit Cost		267
2. Annual Cost		
Fuel	2100	1920
Interest		27
Depreciation		37
Other expense		40
3. Evaluation		
Fuel saving		180
Net saving		76
Pay out period		2.4 year.
Return on investment		28.5%

Session VIII

PILOT TESTING

Wednesday, April 27, 1983

Chairman: Horace Whaley,
Canada Centre for Mineral and Energy Technology

THE SWEDISH STRAW-OIL-MIXTURE PROJECT (SOM PROJECT)

Author: Dr Allan Haag
Sponsor: The Swedish National Board for Energy Source Development (NE)
Administrative organization: The Scanian Farmers' Association Inc.
Skånska Lantmännen Ek.För.(SL)
von Troils v. 1
S-213 01 MALMÖ

1. Introduction

In Sweden about 6 million tons of straw are obtained when harvesting the crops. Approximately 3 million tons are available for fuel, whilst the remainder - 3 million tons - is used for animals.

So far the straw has mainly been ploughed back or burned on the fields, as the demand for straw for fuel has been practically non-existent.

The use of domestic fuel, straw for example, has increased rapidly in Sweden. The reason being that we import 30 million tons of oil products and have no domestic coal.

2. The chemical composition of straw

C = 45 % (50 %) Variations occur
O = 45 % (40 %) " "
H = 5.5 %
N = 0.4 %
S = 0.1 %
A = 4 % (ash in fuel)
Σ 100 %

3. Net caloric value of straw (dry straw)

According to STEUER the net caloric value of solid fuels can be calculated as follows:

$$W_c = [81(C - \frac{3}{8} \times O) + 57 \times \frac{3}{8} \times O + 345(H - \frac{O}{16}) + 25 \times S - 6(H_2O + 9\,H)] \times \frac{1}{860} \quad \text{(kWh/kg)}$$

This is regarded to be the formula that corresponds best with the actual measured values.

The thermal values of the straw during the analyses

C = 45 % and	50 %	respectively and
O = 45 % and	40 %	respectively

then become:

$$W_{e_{45}} = [81 \times (45 - \frac{3}{8} \times 45) + 57 \times \frac{3}{8} \times 45 + 345(5.5 - \frac{45}{16}) + 25 \times 0.1 - 6 \times 9 \times 5.5] \times \frac{1}{860} = \underline{4.50 \text{ kWh/kg}}$$

$$W_{e_{50}} = [81 \times (50 - \frac{3}{8} \times 40) + 57 \times \frac{3}{8} \times 40 + 345(5.5 - \frac{40}{16}) + 25 \times 0,1 - 6 \times 9 \times 5.5] \times \frac{1}{860} = \underline{5.15 \text{ kWh/kg}}$$

Note: It is practical to use a rounded - off value of 5 kWh/kg for straw fuel with a moisture content of 0 %.

4. Heavy fuel oil

Only heavy fuel oil, Bunker C, (1,500 Redwood 1 secs) has been used in the burning tests with SOM (about 25 tons) which have been carried out so far.

British Petroleum (BP) states the following specification:

BP: F 81 CIF Eo5LS - 1,500 SECS

Density at 20°C	max. 987 kg/m^3	(SIS 021411)
Flash-point (P.M.)	min. 66°C	(SIS 021812)
Lowest flow temperature	max. 42°C	(SIS 155109)
Viscosity at 50°C	max. 175 cSt	(calculated value)
" " 50°C	max. 23°E	(" ")
" " 37.8°C (100°F)	max. 1,500 Redwood 1 Secs	
Net caloric value	min. 11.28 kWh/kg	
" " "	min. 11.13 MWh/kg at 20°C	
Sulphur content	max. 1 %	(ASTM D 1552)
Water content	max. 0.75 %	(SIS 150208)
Sediment content	max. 0.1 %	(ASTM D 473)
Ash content	max. 0.1 %	(SIS 155106)
Vanadium content as V	max. 75 ppm	(ASTM D2788)
Sodium as Na	max. 50 ppm	(ASTM D2788)

This product meets the requirements in SIS 155404 Eo5LS. (SIS = The Swedish Standards Association)

5. Fuel prices

5.1 Straw

In Sweden baled straw with a natural water content (about 10 %) can be bought for 100-300 SEK/ton ex. supplier, alternately free delivered to the place

for shredding or grinding.

As no business activities have been started yet in Sweden, it is consequently difficult to state a valid market price for straw intended for conversion to fuel.

This report uses a value of 200 SEK/ton, free delivered to the place for fuel conversion.

The specific price for straw with a natural moisture content and a net caloric value of about 4.43 kWh/kg or 4.43 MWh/ton will then be:

$$k_{spec} = \frac{200}{4.43} \approx \underline{45 \text{ SEK/MWh}}$$

5.2 Heavy fuel oil

According to available statistics for November 1982 a heavy fuel oil - No Eo4LS, which is slightly lighter than Bunker C - free delivered to a tank in the Malmoe region costs 1,950 - 2,085 SEK/m^3. Bunker C is usually not much cheaper and the price can be estimated at approx. 1,850 SEK/m^3.

The specific price will then be approx.

$$k_{spec} = \frac{1,850}{11.13} \approx \underline{166 \text{ SEK/MWh}}$$

5.3 Dust coal from Poland or USA

Depending on the quantity the coal price in South Sweden is approx. 60 - 70 SEK/MWh (460 SEK/ton; 7.98 MWh/ton; 8 % Ash content) free unloaded in a coastal port. Some additions must be made for the handling of pulverized coal from the port to the pulverized-coal burner in, for example, a power station. Advanced flue-gas cleaning with electric precipitators must be included in the calculations. This should not be necessary when burning SOM,as the fine shredding means that the burn-up is very good and that small cyclone units can manage the separation demands of the ash.

6. The SOM price

Up to now and without the assistance of so called surface-active additives, a max. mixture ratio of 28% straw dust in the oil has been measured.

We believe that, with surface-acitve additives in the mixed fuel, we can achieve a mixture ratio of straw powder which corresponds to about 50 % (by weight).

In which case it seems probable that the SOM net price in South Sweden would be:

$W_{e\,straw}$ = (4.43 MWh/ton with a moisture content of 10 %)

W_e = 0.5 x 4.43 + 0.5 x 11.28 = 2.22 + 5.64 = 7.86 MWh/ton

K = 0.5 x 200 + 0.5 x $\frac{1850}{0.987}$ = 1,037 SEK/ton

$k_{spec} = \frac{1,037}{7.86} \approx$ 132 SEK/MWh

For the higher mixture ratio (50 %) there will consequently be 34 SEK/MWh available for the preparation of SOM.

If, as in Malmoe, a plant which has been fully depreciated, is used for the preparation of the powder, it can be presumed that SOM is cheaper than Bunker C. It is also possible to burn SOM in the same boilers as those for Bunker C. However, the capacity will be lower.

Note: Continued tests will show whether straw powder and oil can be supplied separately. Tests have already shown that straw powder can be supplied directly into the air fan and distributed to the mouth of the HOLEC burner, where it will be extremely good mixed together with the warm oil. An extended and transparent flame is obtained.

It is hardly necessary to point out that, if this procedure can be used on a larger scale, it would result in a lower fuel price for efficient MWh after a boiler and in the form of hot water or steam.

7. Use of oil in Sweden

Today the Swedish oil import is about 30 Mtons/year. Parliament and the Government have proclaimed that, before 1990, 9 Mtons/year must be replaced by coal and domestic fuels, such as biological fuels and peat. 3 Mtons per year must also be saved by using the fuels in a more sensible way.

According to the investigation "Transfer to solid fuels", SOU 1980:9, in 1979, Swedish industry used a total of 237 oil-fired boilers in the range 10-150 MW. The total power was 6,531 MW.

At the same time there were 275 oil-fired boilers, within the same power range, in district-heating plants. The total power was 9,980 MW.

Apart from this there were 18 boilers which were larger than 150 MW.

Consequently, in 1979, Sweden possessed 530 oil-fired boilers larger than 10 MW. The total installed power was 23,383 MW.

Assume that the average efficiency of all these boilers is 80 % during one year of operation, and that the full-load operating time is 4,000 h/year then the required amount of oil is:

$$\dot{G} \approx \frac{23{,}383 \times 4{,}000}{0.8 \times 11.3} \approx 10{,}350{,}000 \text{ tons/year} \Rightarrow \approx 10.5 \text{ Mtons per year}$$

It is consequently possible to save oil, if large investments are made. These must be made quickly if the target is to be reached by 1990. The chances of success appear to be few.

8. Field of application for SOM

SOM can in principle be used in all boilers mentioned in 7. SOM is probably not a suitable fuel in boilers below 2-3 MW. The reason being the required pre-heating and the necessary investments for the preparation of SOM.

Many of these boilers are also in areas where large amounts of straw are not available. The use of SOM must therefore be limited to four areas in Sweden. These are Skåne, Västergötland, Östergötland and Uppland. Södermanland may also be of interest.

Another limiting factor for the use of SOM in Sweden is probably the results obtained from collecting, drying and preparing other biological fuels than straw as well as the development of the coal price. The demands on flue-gas cleaning and the resulting dust discharge will also be important.

Regardless of how the development progresses during the 1980's, we in Sweden have to realise that all possible domestic fuels and coal must be used in order to reach the economic target where oil is concerned. Consequently there is a chance for SOM.

9. Description of a plant

9.1 Picture B 1

The picture shows a 25 MW hot-water boiler. It also shows how the HOLEC burner with fan and instrument panel has been installed. The position of the fuel pump (mono pump) and pressure gauge is shown. A centrifugal pump is also discernible. It is used when the oil is preheated and circulated for the heating of the total system, before mixing and starting.

The entire plant is controlled from the control panel. Mixer and powder silo can be seen above the panel.

The distance between the fuel tank and the burner is only 3 m and the fuelline after the pump is heated by district-heating water at a temperature of 90°C.

9.2 Picture B 2

This picture shows in detail how the powder is fed into the silo and how the sprinkler line has been connected according to the regulations of the Malmoe Fire Brigade.

9.3 Picture B 3

The picture shows the upper part of the mixer as well as the gas evacuation channel and the halogen extinguisher, which will start automatically if there is a fire during the mixing of oil/straw powder.

9.4 Picture B 4

The picture shows the dust filter and the exhaust pipe for the gas evacuation from the mixer.

9.5 Picture B 5

This picture shows the lower part of the silo and the feed screw with a variable speed drive. The screw has double helices and pulls the transported material towards the centre of the bottom of the silo, from where it falls into the mixer which stands on a weighing unit.

9.6 Picture B 6

The picture shows how the mixer stands on an accurate weighing unit which transmits the weight to the control panel. An accuracy of $\pm$ 0.5 kg is easily obtained when weighing both straw powder and oil.

It is consequently possible to determine the mixing accurately.

This picture also shows how SOM falls into the fuel tank, which is insulated and has electric immersion heaters with a total power of 24 kW. The tank holds 1 m^3. There is also a halogen fire extinguisher in accordance with the demands of the Fire Brigade.

9.7 Picture B 7

The picture clearly shows the operations which can be performed from the control panel. It also shows the installation of the speed controlled (frequency control) pump. The pipe connection for the straw powder feed pipe can be seen at the bottom left of the picture.

9.8 Picture B 8

The picture shows the front of the boiler with the recently installed HOLEC burner with ignition burner and flame guard.

Protective insulation has been fitted on the lower part of the burner as the temperature on the sheet-metal housing reaches 180°C.

9.9 Picture B 9

This picture shows the burner before the protective insulation. To the left is the mechanism for the operation of the lance and the automatic, quick-acting shut-off valve for fuel. It closes if the flame goes out or if there is no fuel in the tank.

9.10 Picture B 10

The picture shows the insulated fuel tank with the immersion heaters and the halogen extinguisher.

9.11 Picture B 11

The picture shows the agitator system in the fuel tank and the immersion heaters. The agitator system, driven by a variable speed drive operates as long as there is any fuel left in the tank.

9.12 Picture B 12

The picture shows part of the partly discontinued "Foderkorallen" with its silos. The transport vehicle is a standard means of transport for fodder. When time allows, straw powder is transported to the heating plant.

9.13 Pictures B 13 - B 14 - B 15

The pictures show the hammer mill used for grinding the straw. The mill has two motors. The mill feeding units can also be seen.

9.14 Picture B 16

The picture shows a screen with the dimensions used as well as a number of hammers.

9.15 Picture B 17

The picture shows the small shredder which was used in the first shredding/grinding experiments. It is fed manually and the capacity is low.

9.16 Picture B 18

This picture shows the large shredder, bought by SI for other purposes than the SOM project. The capacity is much higher than that of the shredder in B 17.

9.17 Picture B 19

The picture shows the rotating part of the shredder with the discs between which the hammers are fitted.

9.18 Picture B 20

The picture shows the dust meter which we built ourselves. It consists of a gas probe, a filter which can be weighed, a gas cooler, a gas meter, a vacuum pump and the necessary hoses. Accurate metering of dust is possible with this unit.

10. Burning tests

10.1 General

Some 25 tons SOM have been burned in the boiler since the plant was ready for tests. In the beginning the speed of the monopump was controlled manually. The appearance of the flue gas was also studied when it left the chimney stack at a height of about 65 m.

Different test batches with different straw/oil ratios have been mixed and burned. The SOM preheating temperature has also been varied in order to determine the change of viscosity in relation to the temperature of the mixture.

An electronic instrument for the determination of O_2; CO_2 and flue-gas temperature was used during the first tests. This instrument also indicated the efficiency on one scale for solid fuels and on another for fuel oils

The measuring equipment is being completed and a series of measured results will be presented during spring 1983.

The following Table with measurement results also shows efficiency values. The calculations are based on the known quantities of SOM (known quantity of straw and known quantity of oil) and the known amount of heat delivered. The latter was read on the heat volume indicator. The efficiencies seem to be high. However, at this initial stage it has not been possible to calibrate the electronic instrument in the flue-gas channel. On the other hand the weight of the straw and oil and the heat volume are correct and we must accept this efficiency for the time being.

10.2 Burning test Oct. 21st. 1982

Quantity SOM	= 500 kg
Quantity straw powder	= 21.7 %
SOM temperature before burner	= 78°C
Flue-gas temperature after boiler, mean value	= 135°C
Soot number (Bacharach)	= 4
Oxygen (O_2) in flue-gases, mean value	= 2.0 %
Carbondioxide (CO_2) in flue-gases, mean value	= 12.8 %
Efficiency was not determined in this case	---

10.3 Burning test Oct. 28th. 1982

Quantity SOM	= 1,536 kg
Quantity straw powder	= 22.4 %
SOM temperature before burner	= 78°C
Flue-gas temperature after boiler, mean value	= 121°C
Soot number (Bacharach)	= 3
Oxygen content in flue-gases, mean value	= 2.0 %
Carbondioxide content in flue-gases, mean value	= 14.1 %
Efficiency	= 92.5 %

10.4 Burning test Nov. 1st. 1982

Quantity SUM	-
Quantity straw powder, mean value	= 23.4 %
Flue-gas temperature after boiler	= 140°C
Oxygen content in flue-gases after boiler, mean value	= 4.5 %
Efficiency	= 87.6 %

This mixture was difficult to pump and burn.

10.5 Burning test Nov. 8th. 1982

Quantity SOM	= 455 kg
Quantity straw powder	= 22.1 %
Flue-gas temperature after boiler, mean value	= 135°C
Oxygen content in flue-gases, mean value	= 1.9 %
Efficiency	= 76 %

10.6 Burning test Nov. 12. 1982

Quantity SOM	-
Quantity straw powder	= 23 %
Flue-gas temperature after boiler	= 120°C
Oxygen content in flue gases, mean value	= 4.0 %
Pressure after monopump.	= 9.5 bar g

Note 1.: Max. continuous pressure = 8 bar g
2.: Oil temperature before mixing with straw powder was 102°C.

Output heat effect from boiler (The heat volume meter indicates MWh and timing states the time. Output heat effect is derived from this)	= 2.95 MW
Efficiency	= 90 %

10.7 Burning test Dec. 29th. 1982

10.7.1

Quantity SOM	= 430 kg
Quantity straw powder	= 20.6 %
Flue-gas temperature after boiler, mean value	= 140°C
Oxygen content in flue-gases, mean value	= 2.6 %
Efficiency	= 85 %

Note: Smoke from chimney stack was white and "thin". SOM temperature in tank dropped from 80°C to 73°C during the test.

Pressure in pipe between pump and burner was 6.5 - 7.0 bar g.

10.7.2

Quantity SOM	= 470 kg
Quantity straw powder	= 22.5 %
Oxygen content in flue-gases, mean value	= 1.4 %

Note: The mixture was thick and O_2 meter, controlling the pump speed, did not function well and therefore the pump-speed had to be controlled manu-

ally. Temperature in the tank was 78°C and pump pressure 7 bar g.

10.8 Burning test Jan. 21. 1983

A speed controlled conveyer screw has been installed between the powder silo and the fan. Straw powder can therefore be supplied directly into the fan and blown into the burner and outside the oil lance.

There is a strong turbulence of powder and oil and the burn-up in the ceramic nozzle is very good. The flame, which is filling the boiler well, can be watched through different observation holes in the boiler wall and in the back wall. The flame is bright.

We will measure the temperature in the flames with a pyrometer. This will be done with oil burning, SOM burning and burning powder/oil, individually. On the day in question we burned 96.5 kg Bunker C together with straw powder for 40 minutes. The quantity of straw powder could not be measured with the screw conveyer arrangement, but it was possible to measure the heat volume which was 3 MWh.

In the efficiency is estimated at 85 % and the net caloric value is 11.28 MWh/ton for oil and 4.43 MWh/ton for straw powder (10 % moisture content), the quantity of straw powder can be calculated as follows:

$$96.5 \times 11.18 + G_s \times 4.43 = \frac{3000}{0.85}$$

$$G_s = 551 \text{ kg}$$

The mixture ratio is then $= \frac{551}{551 + 96.5} \times 100 \approx 85\ \%$

Conclusion:

This is extremely good and increases our hopes of finding a satisfactory solution to the problem straw as fuel, regardless of whether surface-active additives are available or not.

The definite answer as to how the straw powder should be burned will be given sometime during 1983, when our burning tests have been evaluated.

Translations:

1 MW	=	1,000 kW
1 MWh	=	1,000 kWh
1 kWh	=	860 kcal
1 kWh	=	3,600 kJ (J = Joule; 1 J = Ws)
1 kcal	=	3.9679 Btu
1 bar	=	1.01972 kp/cm^2
1 kp/cm^2	=	14.2233 lbf/in^2 (psi)
1 kg	=	2.205 lbf
1 Mton	=	1 Million tons
1 $US	≈	7.5405 SEK (Jan. 23rd. 1983)
1 SEK	=	1 Swedish krona

THE SWEDISH SOM - PROJECT

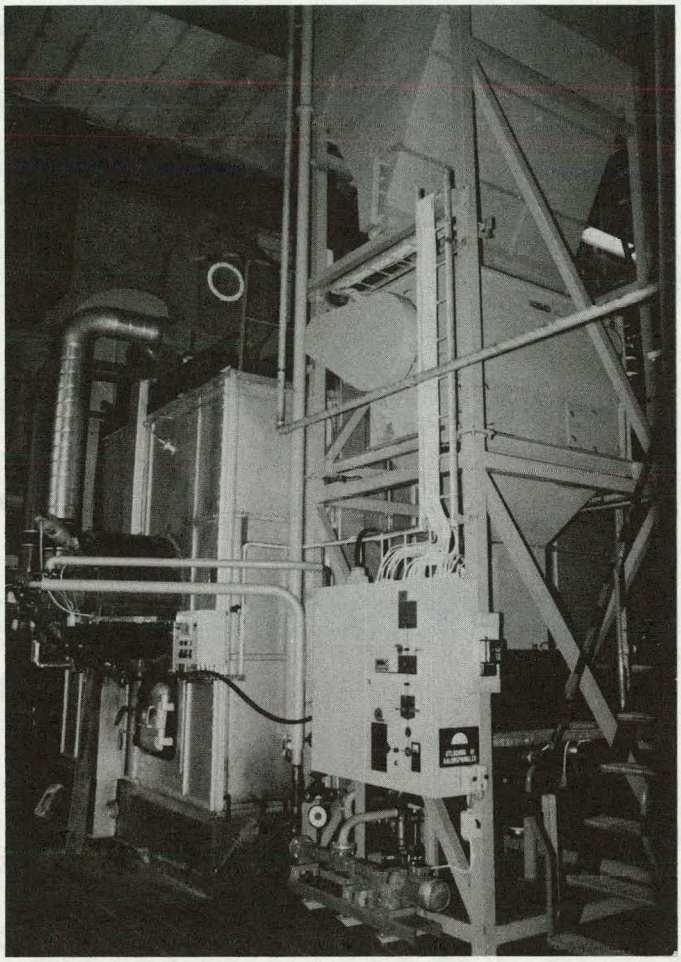

Photo of the total installation in the boiler house.

THE SWEDISH SOM - PROJECT

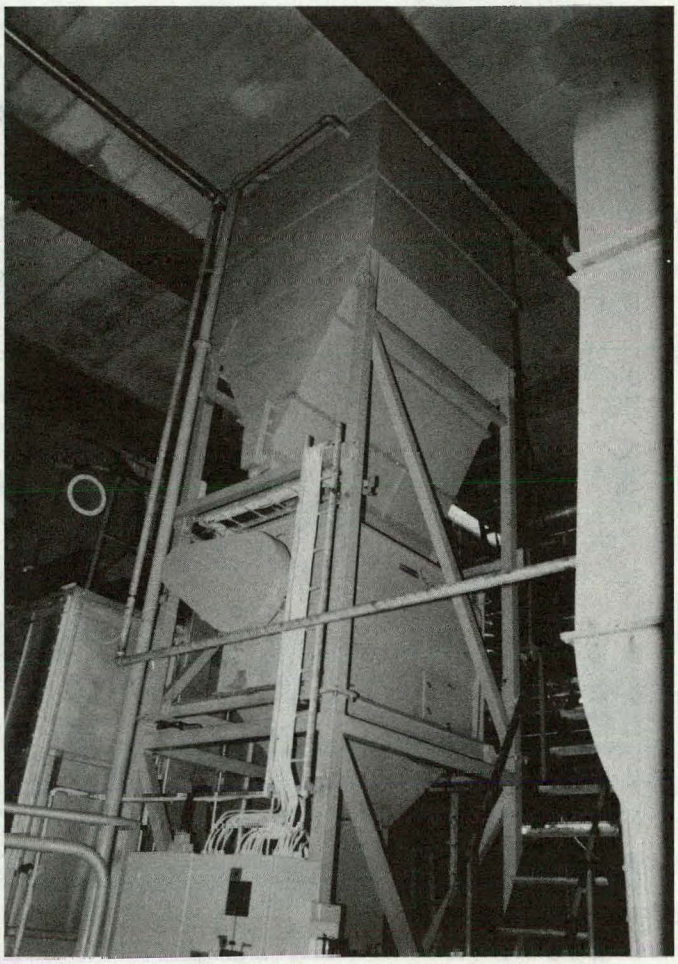

Photo of the silo and the mixer in the boiler house.

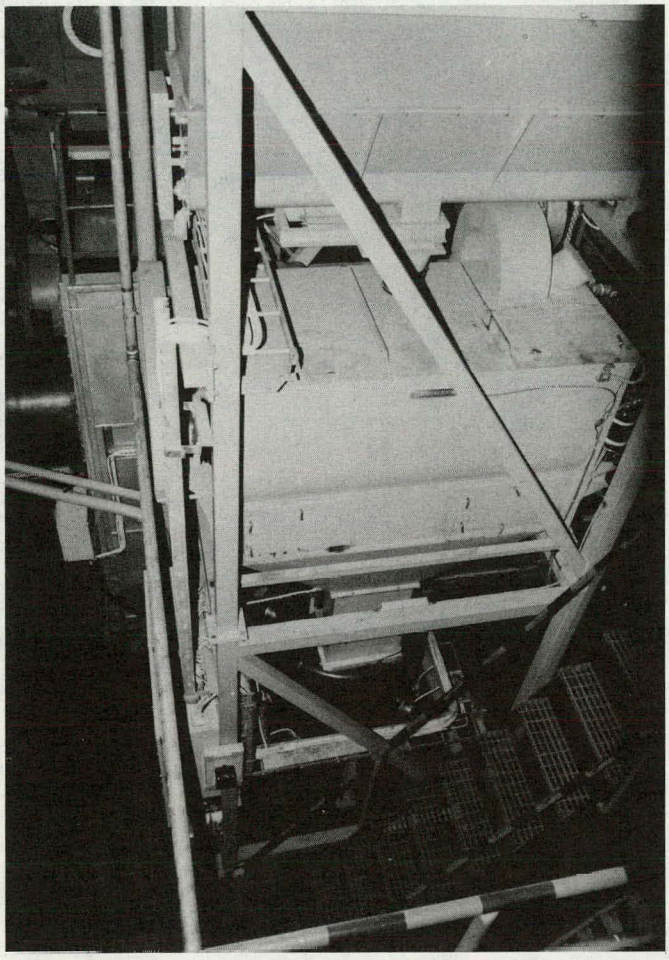

Photo of the top of the mixer, the suction outlet and the fire extinguisher for the mixer.

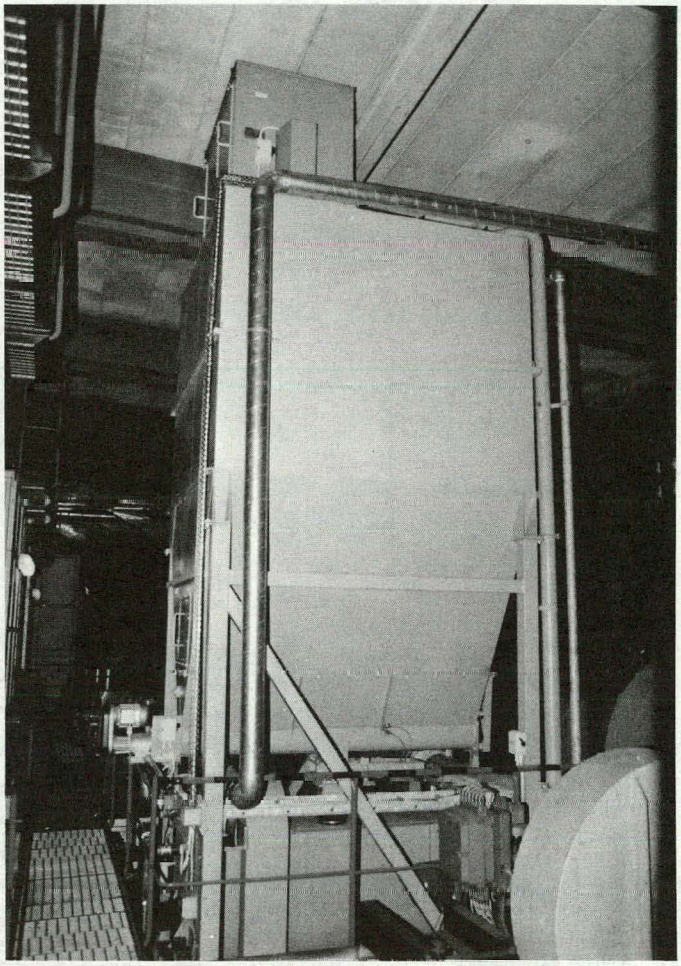

Photo of the dust collector at the top of the silo.

THE SWEDISH SOM - PROJECT

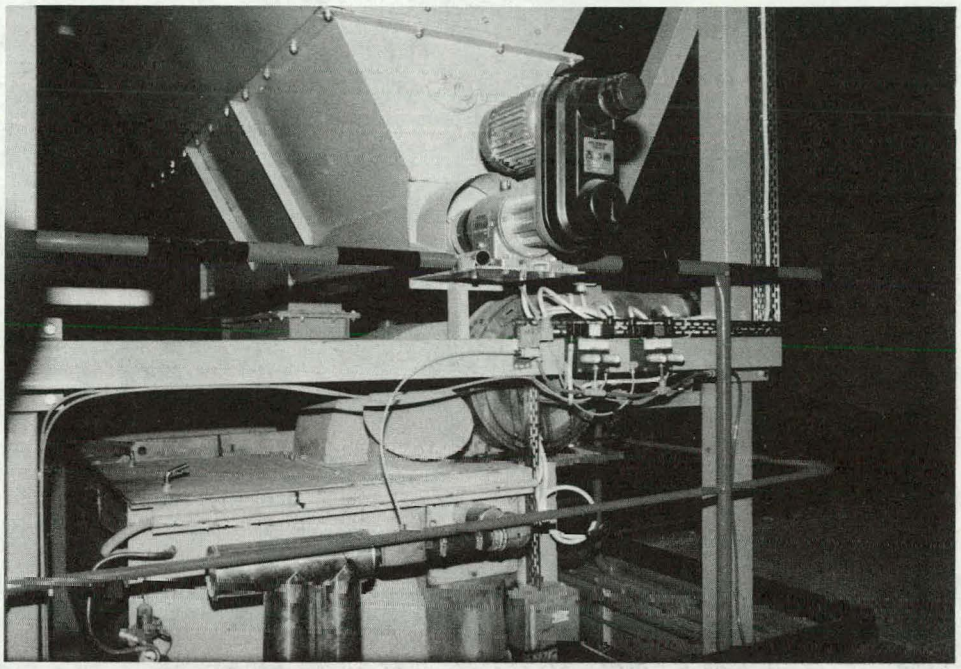

Photo of the feeding out device of powder from the silo bottom.

The double threaded screw is equipped with a variator for speed variation.

THE SWEDISH SOM - PROJECT

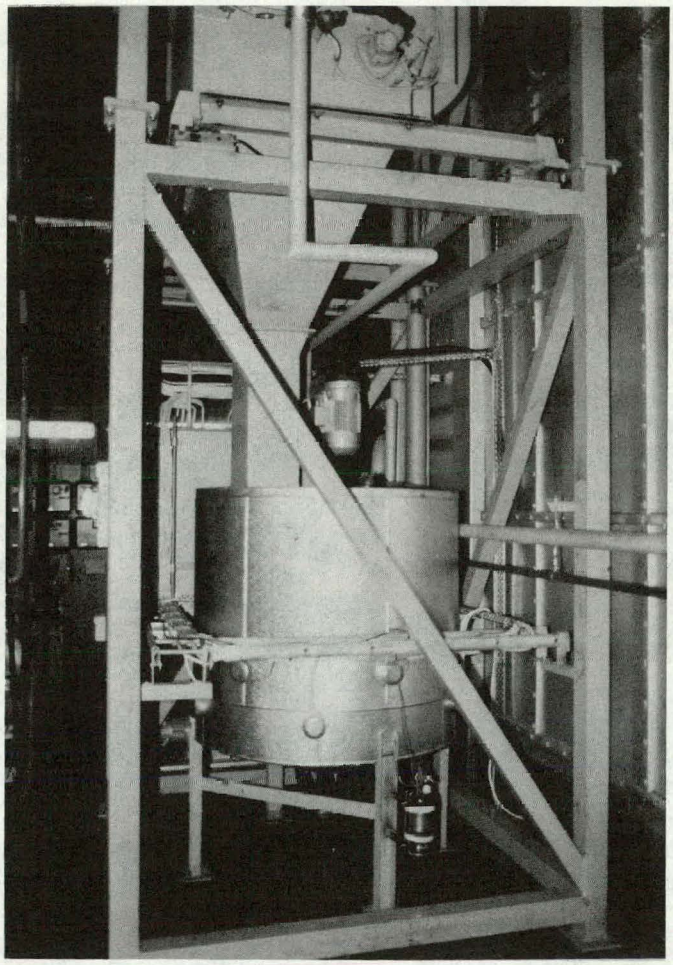

Photo of the fuel tank with the paddle-system.

At the top of the tank the driving system with the variator can be seen.

Down at the bottom of the tank is the fire extinguisher for the fuel tank erected (the red one at the right).

THE SWEDISH SOM - PROJECT

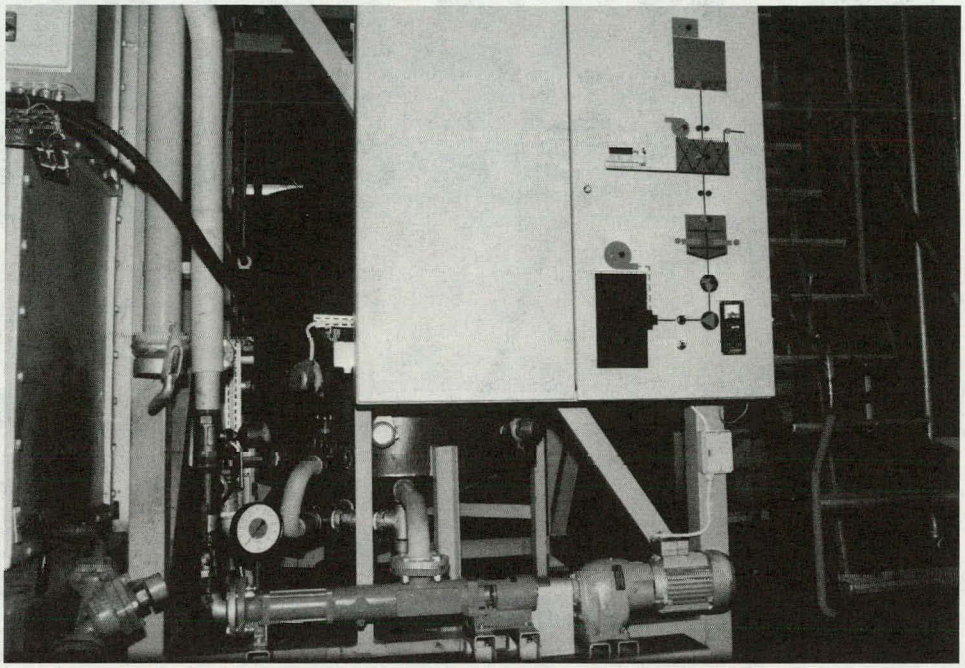

Photo of the plant control panel.

Underneath the mono-screw-pump can be seen as well as its manometer.

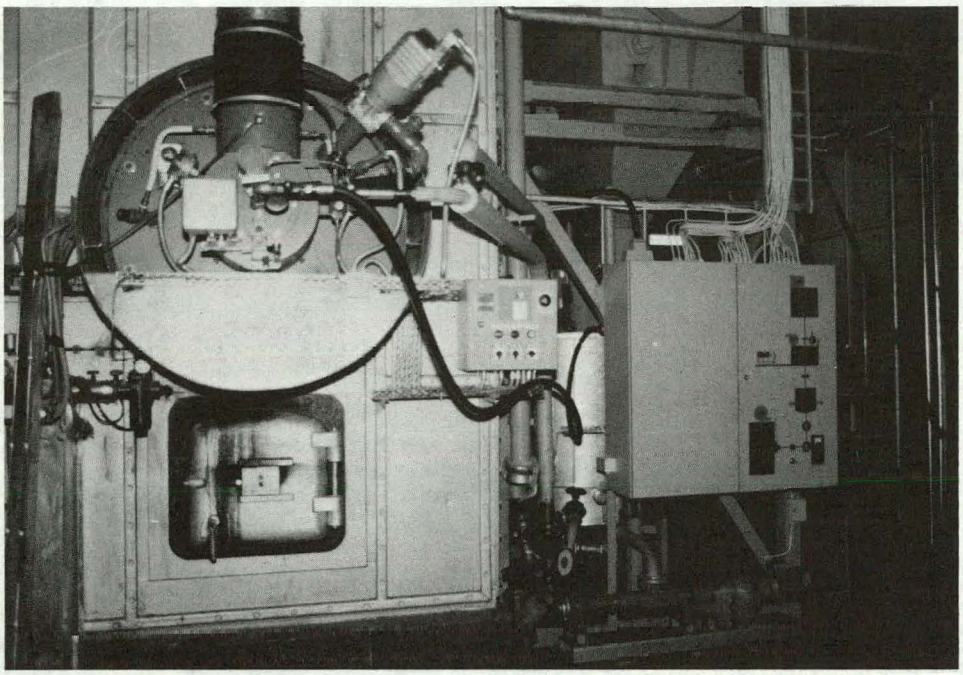

Photo of the screen protected burner and its own little control panel.

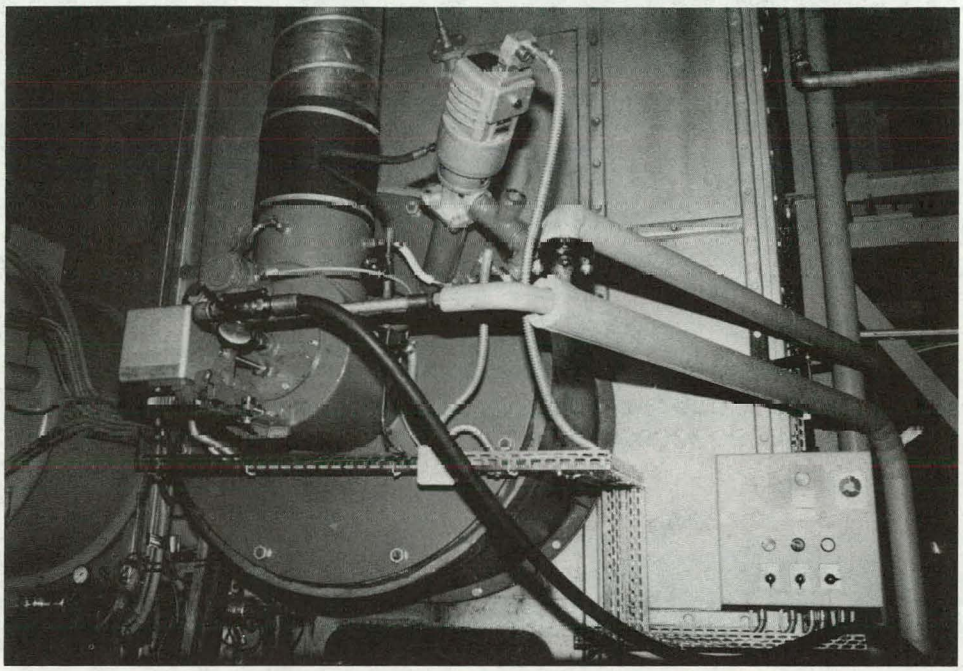

Photo of the pilot burner, the quick-shut-off valve and the recirculation system for fuel to be used when starting after heating of the ceramic.

THE SWEDISH SOM - PROJECT

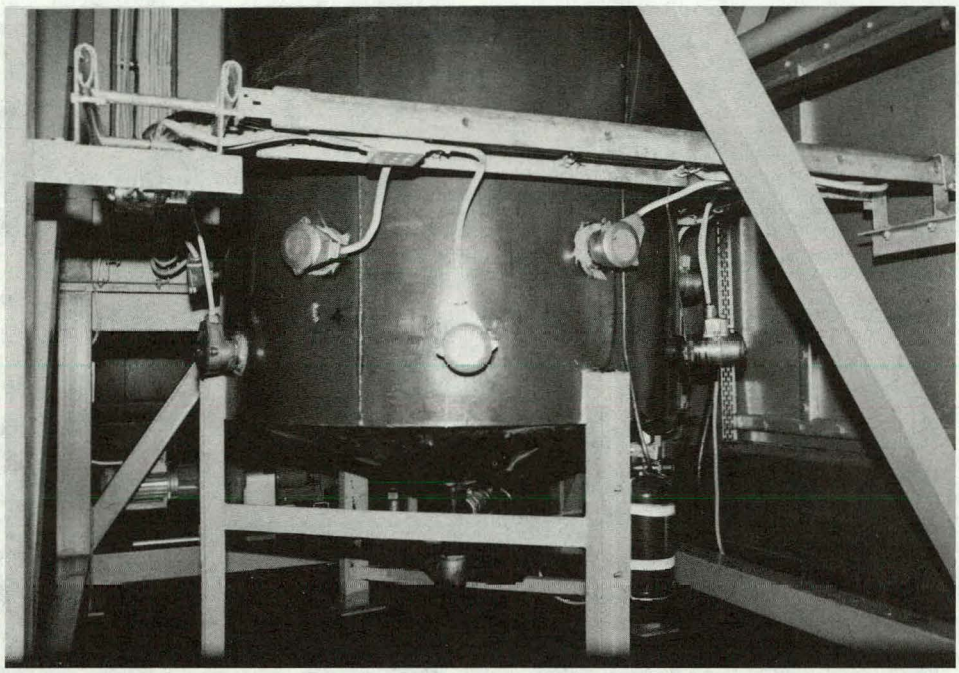

Photo of the non-insulated fuel tank with its heating system.

Underneath the red centrifugal pump can be seen. This pump is to be used when the total plant (fuel tank, mixer and pipings) shall be heated.

THE SWEDISH SOM - PROJECT

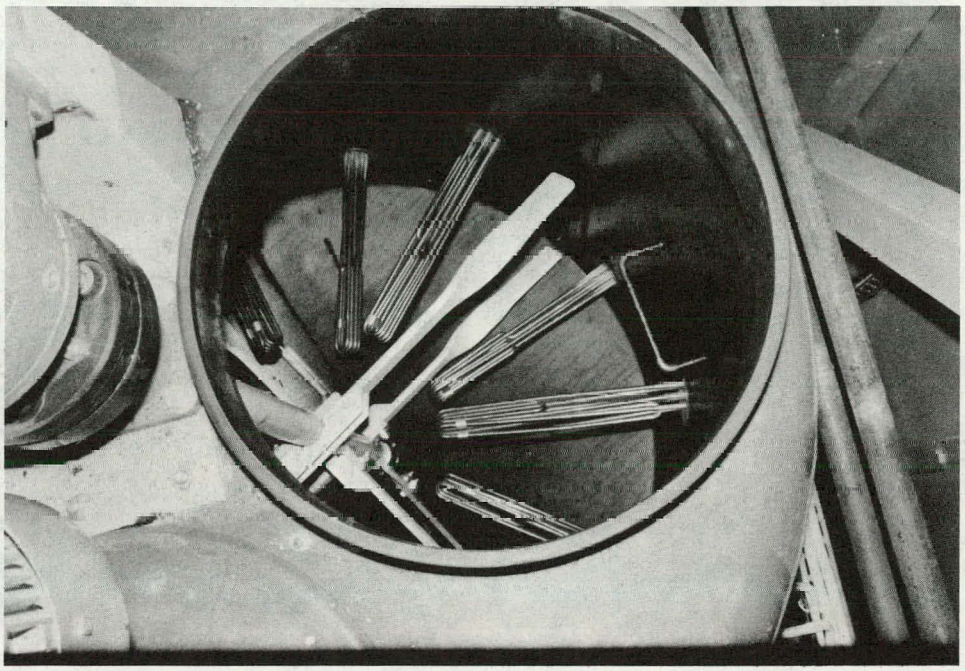

Photo of the paddles and the heating elements in the fuel tank.

THE SWEDISH SOM - PROJECT

Photo of the transport vehicle for powder from the reinforced concrete silos (in the harbour district in Malmoe) to the little silo in the boiler house.

The transport distance is about 7 kilometer.

THE SWEDISH SOM - PROJECT

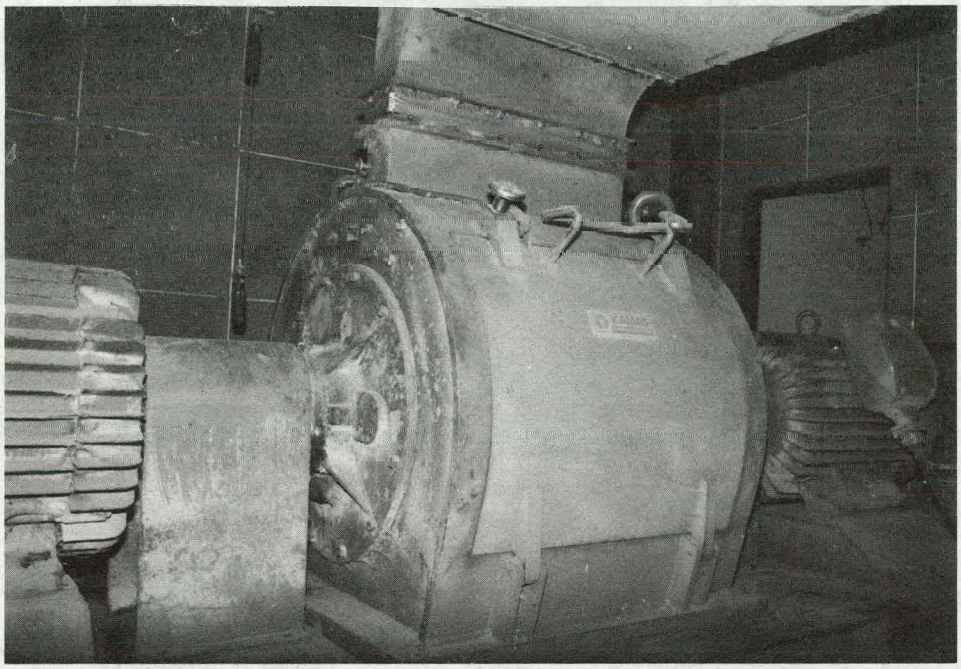

Photo of the hammermill with its two motors.

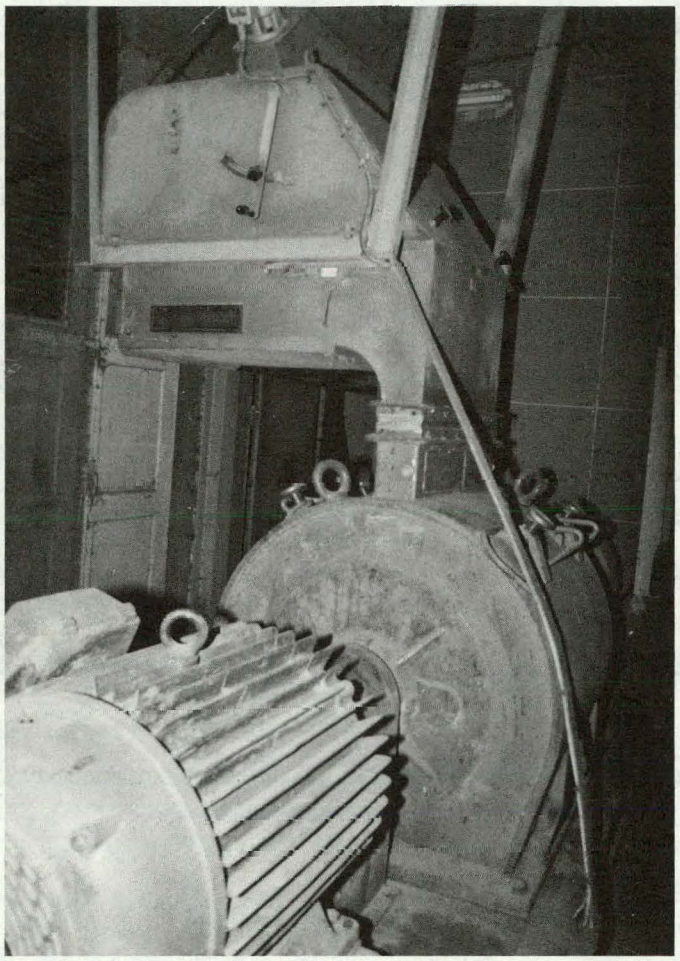

Photo of the feeder of the hammermill.

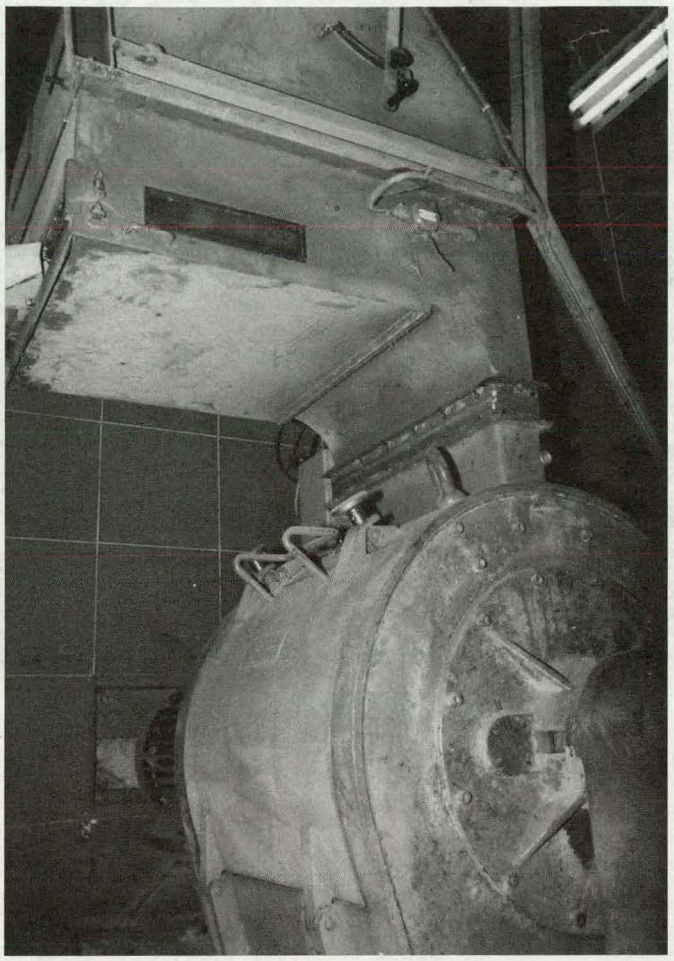

Photo of the feeder of the hammer mill (from underneath).

THE SWEDISH SOM - PROJECT

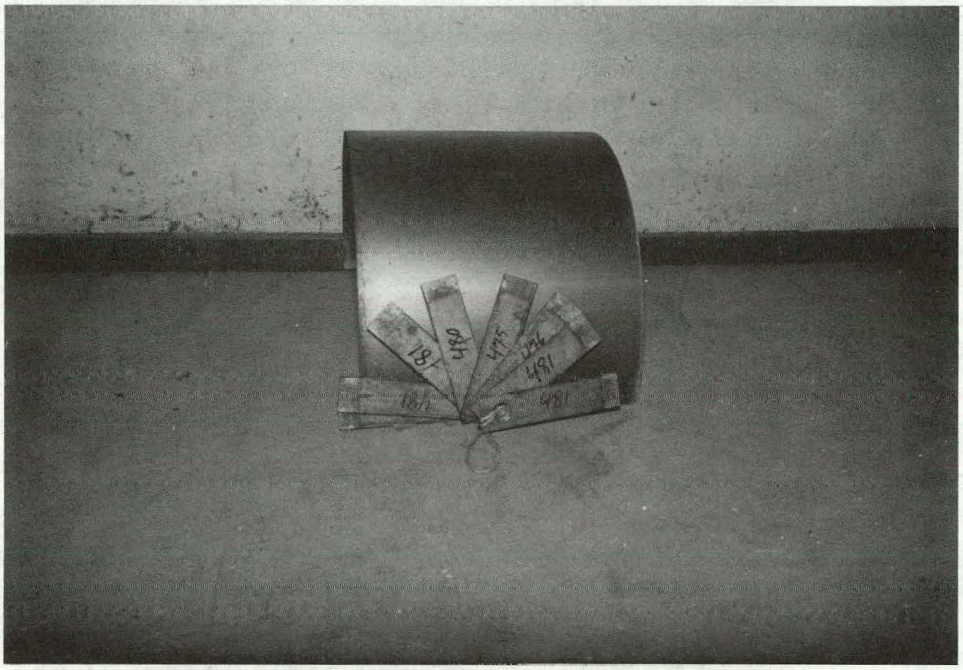

Photo of a sieve and some hammers.

THE SWEDISH SOM - PROJECT

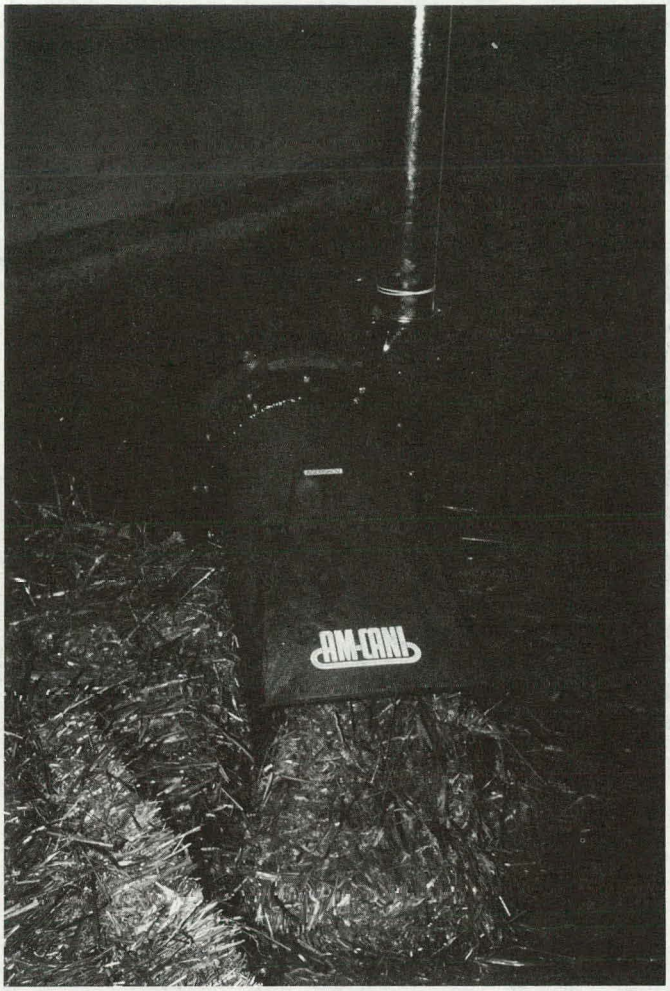

Photo of the little shredder for straw. This shredder was used at the beginning of the project.

THE SWEDISH SOM - PROJECT

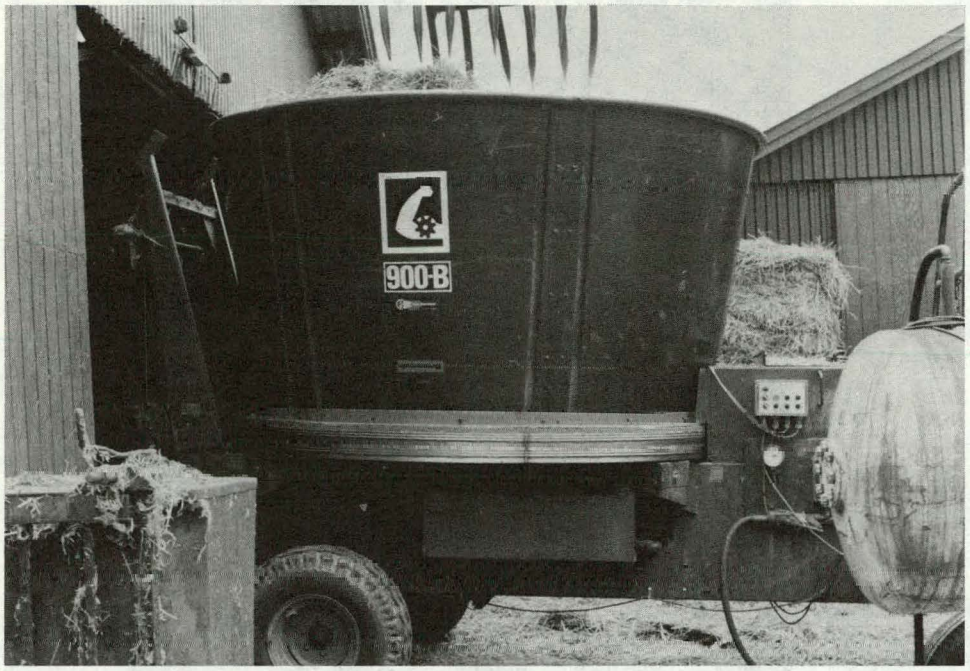

Photo of the big shredder. This shredder has a capacity of 4 - 6 ton/hour. Straw - moisture around 12 - 15 %.

THE SWEDISH SOM - PROJECT

Photo of the internal part of the shredder.

THE SWEDISH SOM - PROJECT

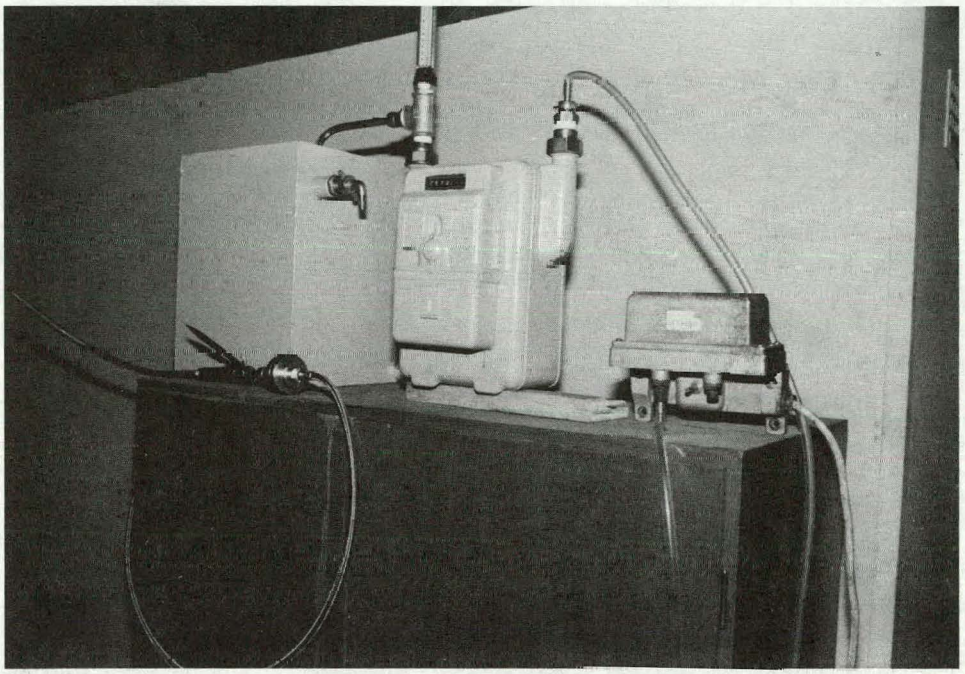

Photo of the dust-metering system which has been built by ourselves.

THE DEVELOPMENT OF COAL-WATER MIXTURE TECHNOLOGY FOR UTILITY BOILERS IN EASTERN CANADA

by

D.M. Rankin,[1] R.P. Nicholson,[2] H. Whaley,[3] and I.D. Covill[4]

ABSTRACT

Eastern Canada is the only region of the country where electricity is generated from oil and it is this region which is most dependent on imported oil. In addition, natural gas is not yet generally available local oil tends to be high in ash and sulphur and in need of upgrading. This scenario has prompted Energy, Mines and Resources Canada, in collaboration with the New Brunswick Electric Power Commission (NBEPC) and the Cape Breton Development Corporation (C.B.D.C.) to undertake a major collaborative initiative in Eastern Canada under the National Energy Program (NEP) to develop coal-water mixture technology for utility boiler application.

The current status of the following main activities of the project are described together with the future potential for CWM's in the Maritime Utility sector:

1) Process development for coal/water mixture fuel preparation.
2) Burner Development for front-wall and tangentially-fired utility boilers.
3) Pilot Plant construction for coal-water fuel preparation.
4) Demonstration trials in a small utility boiler of each configuration at Chatham, New Brunswick.

---

1) New Brunswick Electric Power Commission -
527 King Street, Fredericton, New Brunswick, Canada, E3B 4X1
2) Cape Breton Develoment Corporation -
P.O. Box 1330, Sydney, Nova Scotia, Canada B1P 6K3
3) Energy, Mines and Resources Canada -
CANMET, 555 Booth Street, Ottawa, Ontario, Canada K1A OG1
4) Nova Scotia Power Commission -
P.O. Box 910, Halifax, Nova Scotia, Canada B3J 2W5

INTRODUCTION

Coal-liquid mixtures could replace oil in many stationary combustors and possibly in some mobile uses provided that they can be burned reliably, cleanly, safely and economically. Canada is a net importer of some ten percent of its oil consumption and will become even more dependent on foreign oil unless new ways are found to substitute for the depletion of its limited conventional oil supplies. The chosen approach to reducing reliance on imported oil is a multifaceted one which includes conservation, upgrading of bitumens, heavy oils and residuums and replacement by other indigenous fuels, particulary natural gas and coal. Coal-liquid mixtures (CLM) offer a means of replacing oil by coal where direct substitution of a solid fuel is impossible or economic.

In central and western Canada, natural gas and coal are readily available and can be chosen as replacements for oil depending on price and convenience. However, in eastern Canada, the only part of the country where electricity is generated from oil, natural gas has not been generally available and local coal tends to be both expensive and high in sulfur. The need for oil substitution is thus most urgent where it is most difficult to find an economic substitute.

As the federal government agency responsible for formulating and implementing energy policy for Canada, the Department of Energy Mines and Resources (EMR) has been encouraging the substitution of coal for oil with special emphasis on the four maritime provinces, Newfoundland, Nova Scotia, Prince Edward Island and New Brunswick.

The Canadian National Energy Program (NEP) has established funds under the special Atlantic initiatives in order to accelerate the shift away from dependence on imported oil which is characteristic of the Atlantic region. These initiatives include a coal utilization program designed to identify, develop, demonstrate and then commercialize new technologies that would enhance the local use of indigenous coal under environmentally acceptable conditions. Through this activity, EMR Canada will assume a large share of the technical risk associated with the introduction of new technologies.

The emerging technology of coal-water mixtures (CWM) was identified early as showing special promise for the Cape Breton Coal Industry both to serve local markets and for export purposes. In Eastern Canada the potential for CWM fuel initially relates to oil substitution in utility boilers that are not designed for conventional pulverized coal combustion or cannot readily be converted to that technology.

BACKGROUND

Interest in CLM technology as potential oil replacement fuels has been continuing in Canada since the early seventies when an early research effort [1] led to three phases of a coal-oil mixture (COM) technology demonstration from 1977 to 1980 in a small generating station at Chatham, N.B.[2] It is not fortuitous that the demonstration aspects of the present project will also take place at Chatham later this year. The Chatham generating station is small, with two boilers of 12.5 and 22 MW(e) which are no longer required to supply power to the grid. Thus, it has the operational flexibility necessary for the CWM burner evaluation tests of the present project.

In April of 1982 EMR Canada, the New Brunswick Electric Power Commission (N.B.E.P.C.) and Cape Breton Development Corporation (C.B.D.C.) entered into a collaborative agreement to demonstrate the preparation of CWM and its utilization in utility boilers. In addition, CBDC has signed a licencing agreement with AB Carbogel of Sweden to manufacture and market CWM based on proprietary Carbogel technology with exclusive rights to eastern Canada. The agreement provided for the construction of a 4 tonne/hour CWM pilot plant to be located in Sydney, N.S. It also specified that burners should be developed and tested for the 12.5 MW(e) unit No. 1 front-wall fired boiler and the 22 MW(e) unit No. 2 tangentially-fired boiler at Chatham, N.B. The project was to be administered by a management committee comprising of representatives of EMR Canada, N.B.E.P.C., C.B.D.C., the Nova Scotia Power Commission (N.S.P.C.) and AB Carbogel. (see Figure 1) Technical input to the project is through a technical committee which in addition to management committee members, includes representatives of the National Research Council (NRC), Ontario Hydro, New Brunswick Research and Productivity Council and the Centre for Energy Studies of the Technical University of Nova Scotia.

The major objectives of the project were to build a pilot-plant to produce 6000 tonnes of CWM for burner evaluations to be undertaken in the Chatham units after the necessary preliminary testing had taken place at the manufacturer's test facilities. Since the agreement called for the burner development program to run concurrently with the CWM pilot plant design and construction, 550 tonnes of the CBDC coal were shipped to AB Carbogel in Sweden for design fuel manufacture. This fuel was to be used in burner testing prior to installation in the Chatham units.

CAPE BRETON DEVELOPMENT CORPORATION CWM PREPARATION FACILITY

CBDC is a federal Crown Corporation which was established in 1968 and is located in Sydney, Nova Scotia. At the time of its inception its mandate was two-fold; to phase out the mining operations of the former Dominion Coal Company in the face of declining coal markets; and to attract and establish a broader base of secondary industry in a predominantly steel and coal oriented community to off-set the effects of the unemployment created from mine closures.

Now, due to the dramatically altered position of coal in the world energy picture, CBDC's task now becomes the establishment of a viable coal

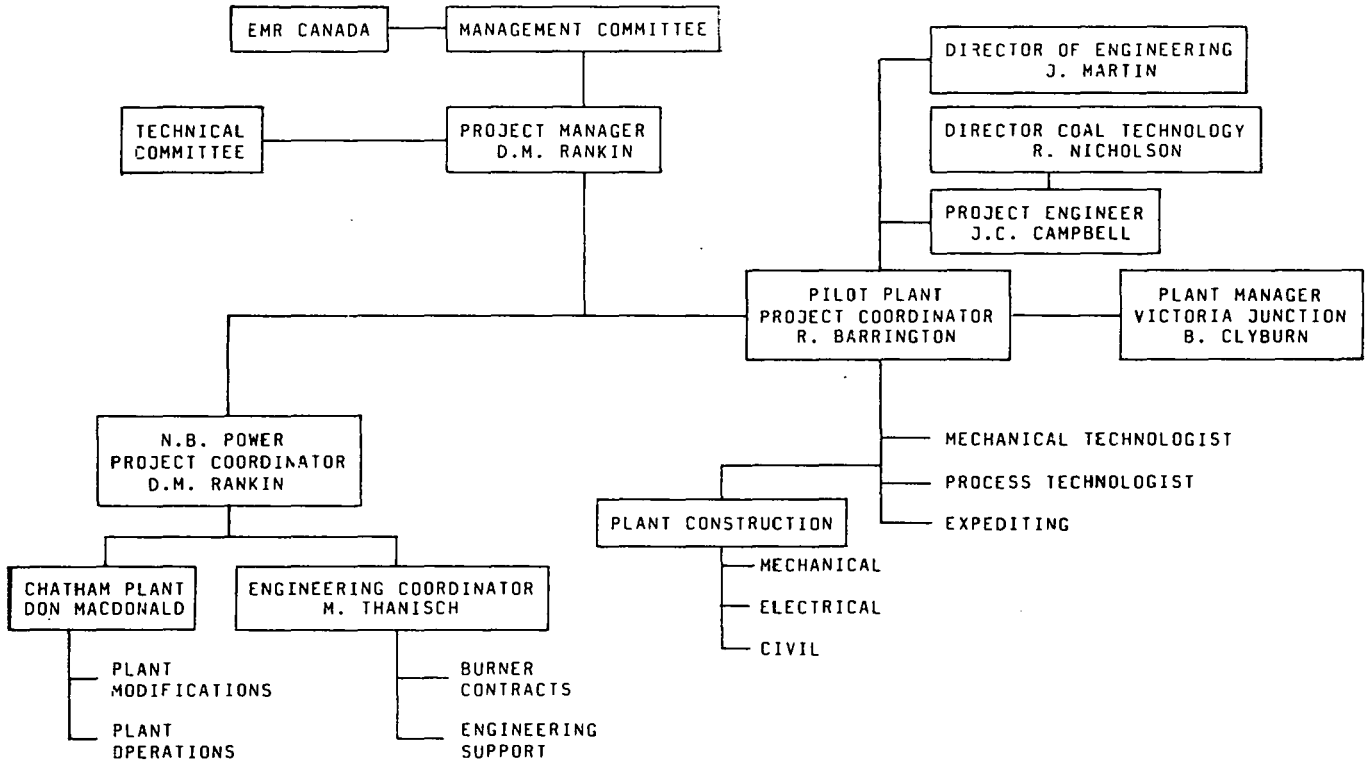

Figure 1 - CWM Project Organization

industry to meet rising domestic and export demands for high quality coal. The old Industrial Development Division still exists with the same mandate, that of broadening the regional industrial base. There are now three mines in operation, two of which are new, and the total production is about 3 million tonnes per year of which slightly more than half is thermal coal. CBDC has plans to develop three more mines and the anticipated annual coal production is expected to reach 10 million tonnes by the early 1990's.

The seams currently being mined or developed all extend out under the Atlantic ocean for several kilometers and the coal is mostly extracted by longwall mining techniques. The coals are mainly high volatile bituminous "A" ASTM ranking with smaller quantities of high volatile bituminous "B". Drill core samples indicate the deeper seams may contain some medium volatile coals. A layout of the Cape Breton coal fields in eastern Canada are shown in Figure 2.

Although the presently mined coals exhibit excellent combustion properties, one of the less favourable characteristics is the inherently high sulfur content typical of most eastern Canadian coals. Sulfur is present in organic and inorganic form; the organic content is fairly consistent throughout, but the inorganic, present mostly in the form of pyrite, varies quite widely. Much of the pyrite is finely disseminated throughout the coal, but can be partly removed after grinding by various fine washing techniques. Standard coal preparation methods do in fact effect some pyrite reduction. With increasing environmental regulatory pressures to limit sulfur emissions, and energy policies emphasizing the replacement of imported oil with indigenous coals, CBDC can obviously enhance its marketing position if it can both reduce the sulfur content of its coal, and offer the finely ground beneficiated coal in a marketable form. CWM's appear to be an ideal way to meet both of these requirements.

The agreement signed between the three parties in April 1982 provided for about 500 tonnes of CWM to be made by AB Carbogel in Sweden, which was to be used for preliminary burner tests and for 6000 tonnes of CWM to be made in a 4 tonne/hour pilot plant operated by CBDC. The agreement further provided for two designations of fuel: Design Fuel and Commercial Fuel. The fuel made in Sweden and the 6000 tonnes to be made in the pilot plant were classified as design fuel and were to be made from a mix of Harbour Seam coals (Lingan and No. 26 mines). These coals are normally beneficiated together to produce a metallurgical grade coal, with the middlings going to thermal coal, and are generally the highest quality coals produced by CBDC. Commercial Fuel was to be used for later phases of the program involving larger utility boiler tests and would probably be the fuel that CBDC would develop and sell on a commercial basis. Commercial Fuel will be made from Prince Mine coal (Hub Seam) which is currently sold as a thermal coal and is not beneficiated.

Typical analyses of Harbour and Hub Seam coals are given in Table 1.

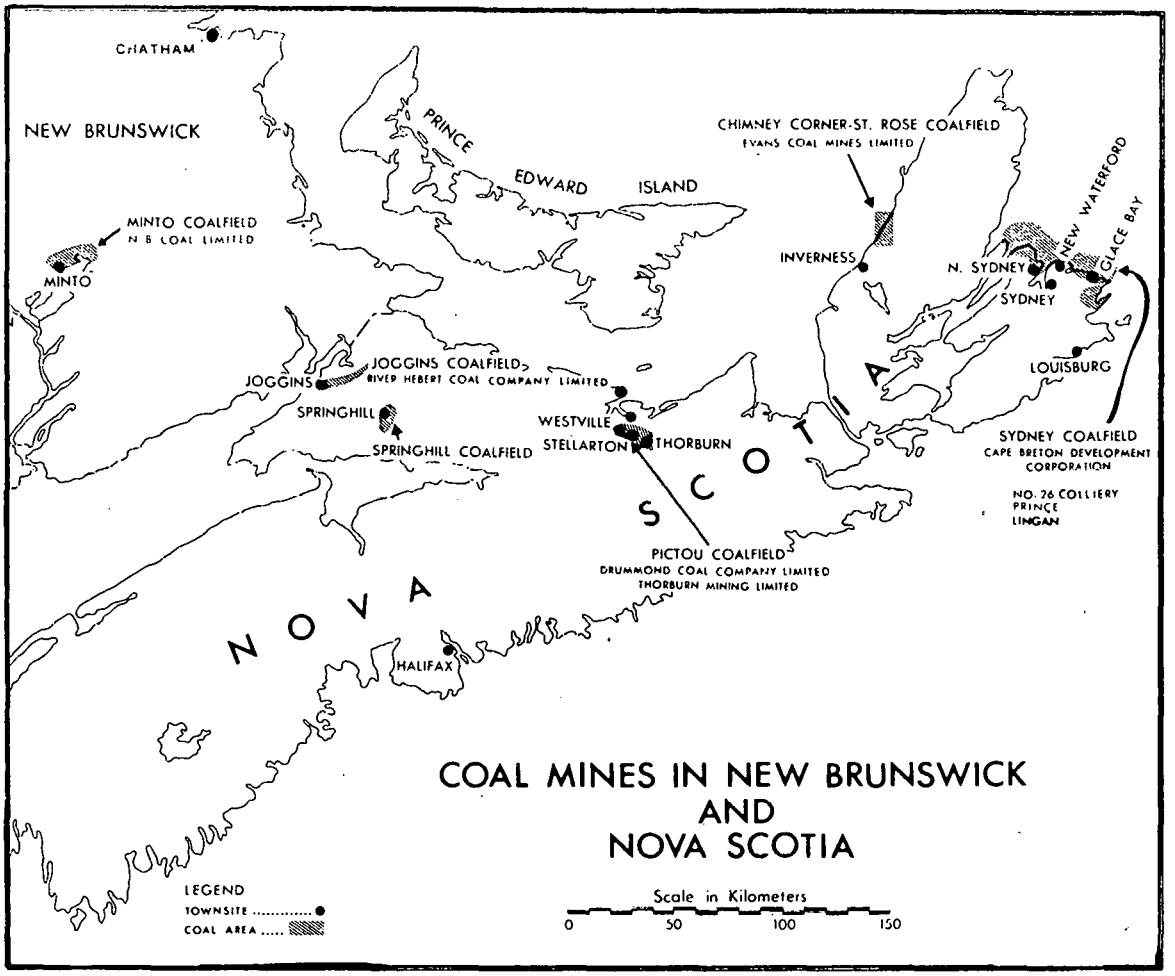

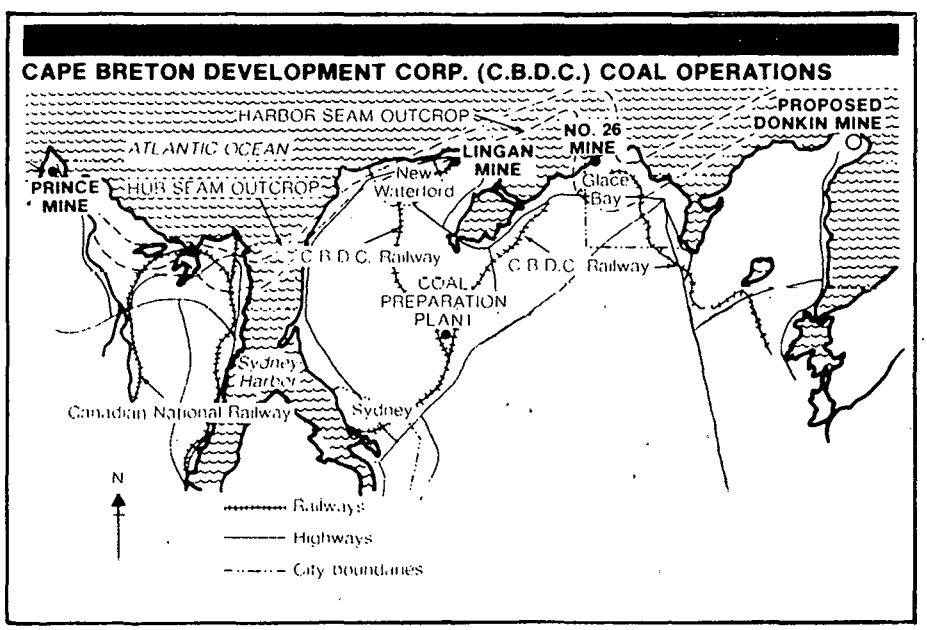

Figure 2 - Map of CBDC's Sydney NS Coal Fields

Table 1

	Harbour Seam			Hub Seam
(% dry basis)	As Mined	Beneficiated	CWM	As Mined
Ash	15.0*	2.8	1.7	16.0
Sulfur	1.8	1.2	0.9	4.5

* - Includes rock from mining operations; in-seam coal analyses show 5.0% ash.

The properties of the Hub Seam commercial CWM are still under investigation by AB Carbogel and the University of Minnesota and the final quality projections have yet to be made. It is expected that comparable reductions in ash and sulfur to that achieved with the Harbour Seam, will be obtained.

Upon signing of the agreement, a CBDC project team was formed from representatives of coal preparation operations, engineering, and coal technology. A basic process flow sheet and material balance was developed with Carbogel engineers, and basic equipment requirements determined with Carbogel and Boliden, a part-owner of A.B. Carbogel and a large mineral processing company in Sweden and internationally. Because it was impractical to locate the CWM plant in the existing Victoria Junction coal preparation facilities, a separate building was planned in an adjacent area. The site choice was logical since Victoria Junction is at the junction of rail lines serving the Lingan and Glace Bay mines, and the shipping docks at Sydney. Thus the plant has ready access to road, rail or water transportation as well as to the coal mines.

The CWM plant building of sectional prefabricated steel was erected in December 1982 with overall dimensions of 38m x 18m.

Initially, operation of the pilot plant was scheduled to be on a single shift a day, 5 days per week operation. However, growing concern about the time necessary to produce the 6000 tonnes for the NBEPC burner evaluations, and the subsequent effects on operating costs of spreading the tests over a long period, and the lack of capacity to meet a perceived demand for similar tests in other locations, led to a decision to increase the production capacity of the plant and also to increase the number of operating shifts. Consequently, in January 1983, it was decided to increase the capacity to 7 tonnes/hour and to operate on a 3 shift per day basis, effectively increasing the theoretical output from about 6000 tonnes per annum, at 80% availability, to about 38,000 tonnes per annum.

An examination of the flow sheet illustrated in Figure 3 and equipment capacities showed clearly that the limiting factor in the production rate was the vacuum filter. Most of the other items of equipment specified had excess capacity, but the filter was limited to the 4 tonnes/hour original design specification. Since there was sufficient space and floor support to install a second filter in parallel to the first, and

feed piping from the flotation unit could be split to feed both units simultaneously, the plant capacity could be increased by about 75%, for the relatively modest cost of the second vacuum filter.

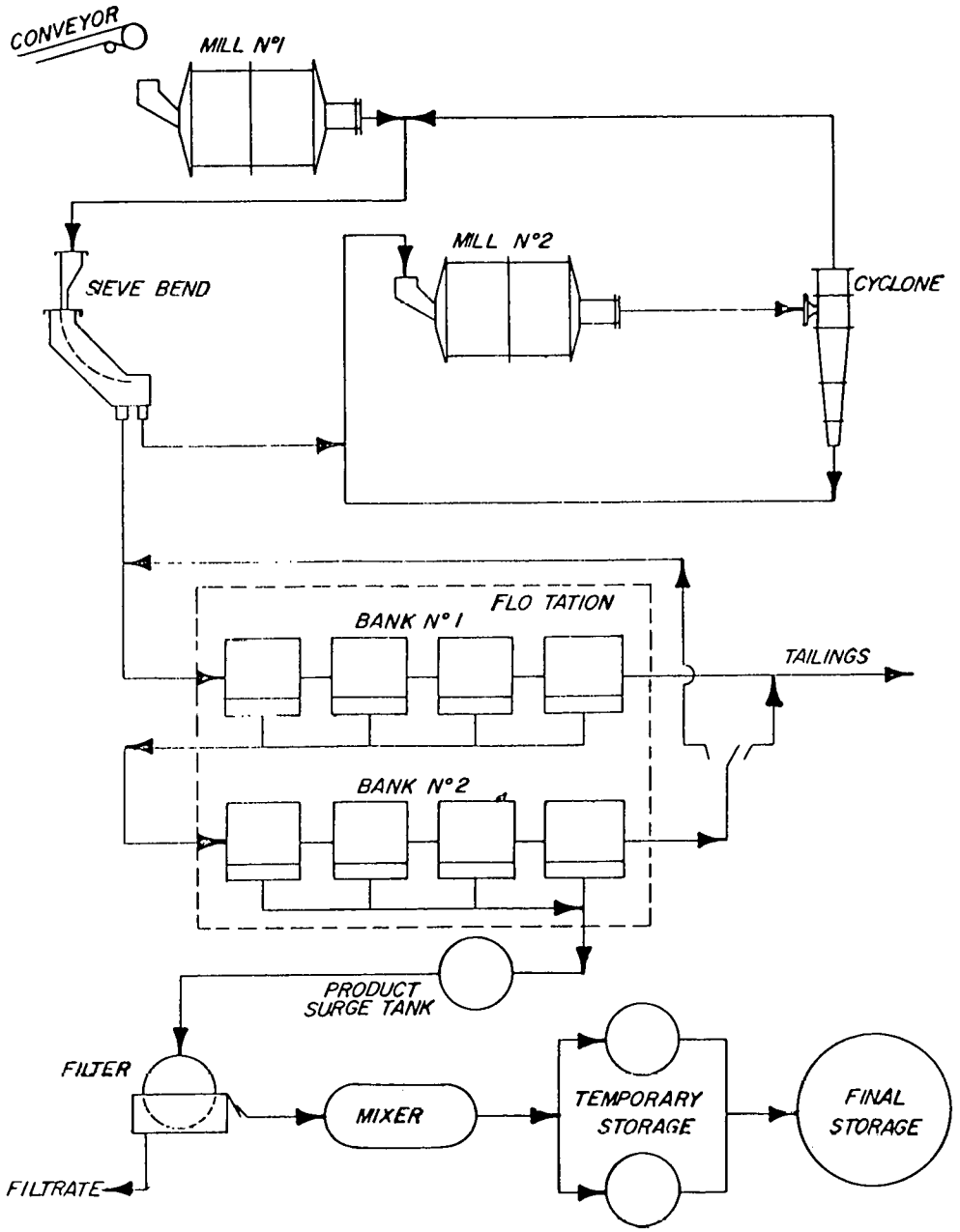

Figure 3 - Schematic Illustration of CWM Preparation Plant Flow Sheet

At the time of writing this paper the CWM plant is on schedule, see Figure 4. Equipment procurement is being monitored by expeditors and delivery schedules are being maintained. It is still anticipated that the first CWM fuel will be produced by the plant in June 1983.

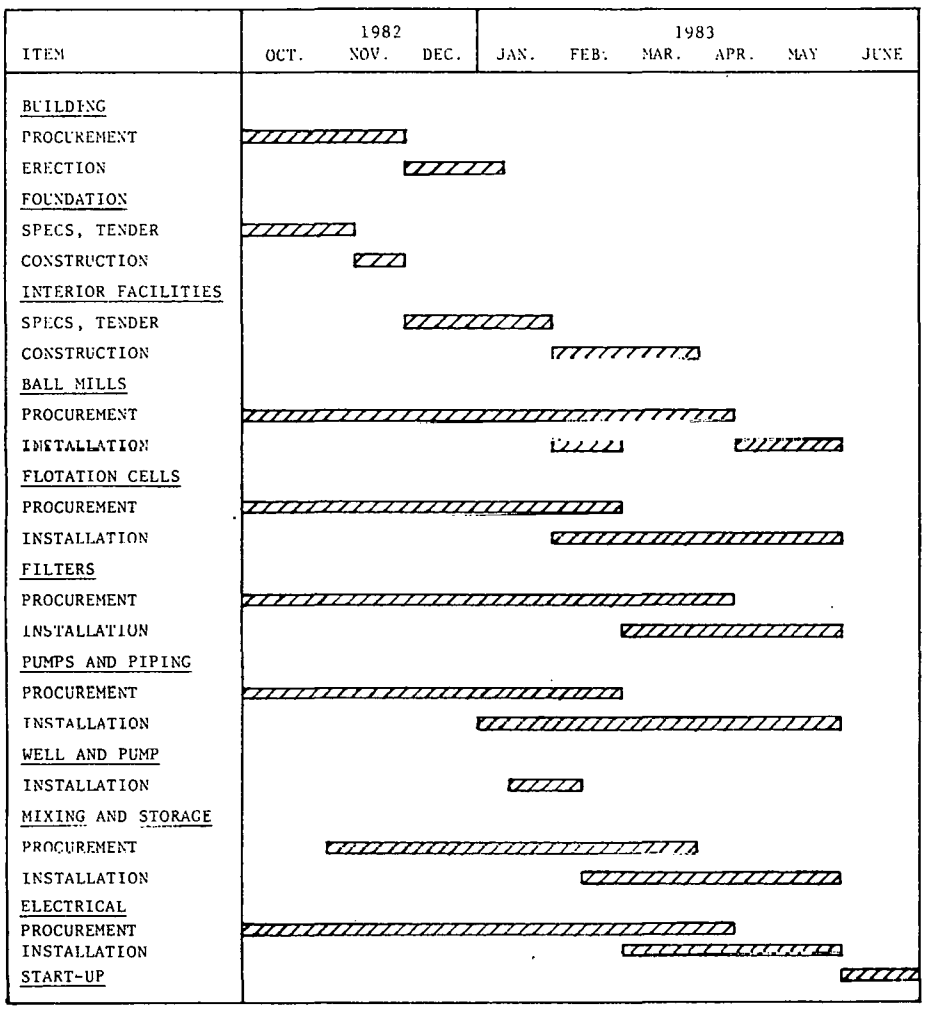

Figure 4 - Schedule for CBDC CWM Pilot Plant Combustion

CWM BURNER DEVELOPMENT

The tripartite agreement provided for the development and evaluation of CWM burners for the two units of the Chatham, N.B. generating station. Consequently, under the management of NBEPC two CWM burner development contracts have been awarded, one to Foster Wheeler Canada Ltd. for the development of burners for the front-fired boiler, unit No. 1, and one to Combustion Engineering Canada for the development of burners for the tangentially-fired boiler, unit No. 2. As mentioned earlier, about 500 tonnes of CWM design fuel have been produced in Sweden for these burner manufacturers to utilize in this stage of the burner development program. Specifically this stage consists of the design, testing and evaluation of a burner rated at approximately 30 GJ/h thermal input and of a type

suitable for CWM firing in a front-wall boiler. A parallel activity will address the tangentially-fired boiler. At the time of writing (February 1983), the burners for the front-wall fired unit No. 1 have been tested by Forney Engineering of Dallas and four burners are being manufactured ready for installation by July 1983. The tangentially-fired CWM burner has not yet been finalized and tested, but atomization tests have been conducted by CE. It is expected the burner test evaluation will take place in late February 1983. (see Figure 5). The second phase of the CWM burner development activity is the installation and testing of the burners in the boilers at Chatham, N.B.

Chatham unit No. 1 is a front-wall fired Foster Wheeler balanced draft boiler 12.5 MW(e) designed to burn coal but converted to burn No. 6 fuel oil. This boiler was used in earlier COM tests as noted previously[2]. The main specifications of the boiler are given in the Appendix.

Unit No. 2 is a tangentially-fired CE balanced draft boiler 22 MW(e) also designed to burn coal but converted to No. 6 fuel oil. The specifications of unit No. 2 are given in the appendix.

Figure 5 shows that burner evaluations are due to begin in June 1983 in unit No. 1 and September 1983 in unit No. 2, and progress to date is on time.

In addition, all engineering support services are on schedule. These are fuel transportation, pumping, storage and compressed air for atomization.

LONG RANGE STRATEGY

If the projects at Chatham and Sydney are successful, it is quite clear that there are significant implications both for the CWM supplier and for the maritime utilities. To put the former into perspective, there are about 10 GW of potentially convertible oil-fired generating capacity in New England and about 5 GW in eastern Canada, including Ontario and Quebec. All of the Canadian capacity is accessible by water without the need for expensive conventional coal docks as are over 75% of the U.S. stations. Taking utilization factors into account, this translates into a potential market for about six million tonnes of CWM fuel available by water routes and about one million tonnes requiring rail access. In addition, a preliminary view of the west European market has indicated sales potential for a further three million tonnes there. Since CWM fuel made at Sydney will be based on expensive coal from under the sea, it will only be able to compete with other coal-water fuels in markets where it can be delivered for the least expense. Thus transportation costs become extremely important and these will need to be investigated carefully.

The primary objective of the burner tests at Chatham is to develop burners that will provide satisfactory flame and combustion properties and withstand the abrasive action of CWM for a reasonable period of time. From the utility viewpoint, this period of time is considered to be about 2000 hours.

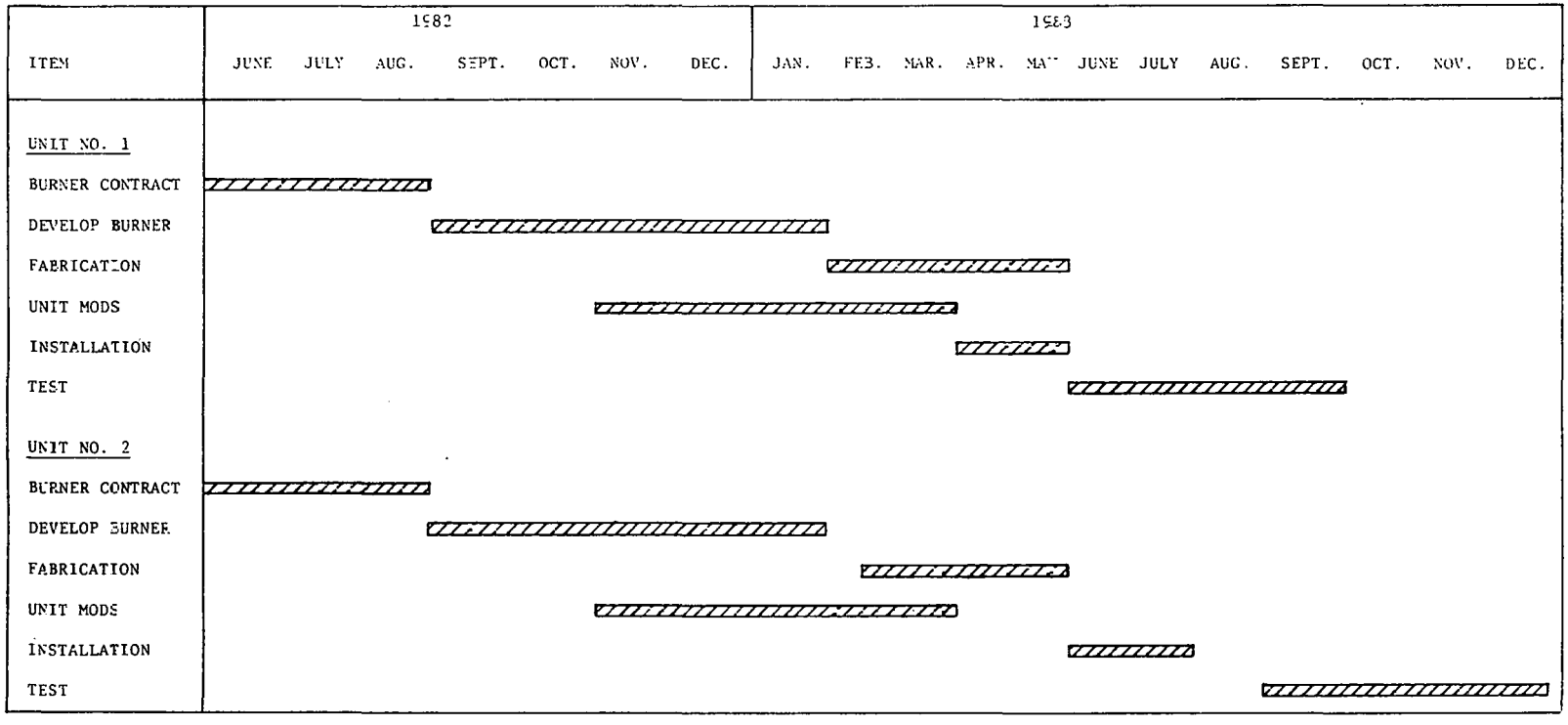

Figure 5 - Schedule for Burner Development and Testing: Chatham CWM Project

Other pertinent information required from the Chatham Project will be to establish operating data on the physical properties of CWM's, particularly in relation to long distance transportation, storage, pumping and recirculation, and atomization.

As both steam generators at Chatham are small and since both were originally designed to burn coal, financial inducements to the utilities will only occur in the Maritime provinces if expensive imported oil is displaced in larger furnaces now burning residual oil.

In the provinces of Newfoundland, New Brunswick and Nova Scotia, there are eight oil-designed steam generators in the range of 100 MW(e) to 150 MW(e), which may be suitable for conversion to CWM.

For such a conversion, a number of alternatives are open, namely:

1. Convert to CWM and derate the unit output as imposed by the characteristics of the CWM.
2. Convert to CWM and, consider boiler design changes that will enable full rating to be maintained.
3. Convert to CWM, but retain the capability for oil-firing. Hence full load may be achieved when firing oil and a derated output when firing CWM.
4. Convert to CWM, but retain capability to burn oil or CWM by boiler design changes, to achieve full load operation by either mode of firing.

The preferred alternative may vary for each utility, since the best engineering and economic choice may depend upon a number of "site specific" factors. There are many common engineering considerations of conversion, the major ones being fuel handling, ash disposal, furnace gas and air pass configuration.

FUEL HANDLING

Apart from establishing that CWM's do not destablize during the transportation, storage, pumping and recirculation processes, because of the severe winters in the Maritime provinces, CWM fuels must be protected from freezing. This may call for special fuel heating arrangements which will add to the conversion costs. Also, it must be ensured that existing oil tanks and transfer pipework and pumps are suitable for storing and transporting CWM with agitation, heating and heat tracing if necessary.

ASH DISPOSAL

Even with a beneficiated CWM, containing about 2% ash, a 150 MW(e), steam generator, will, at full load produce about a tonne of ash per hour. This quantity, especially in a furnace designed to burn residual oil, poses a number of problems, such as:

(a) Reduction of gas velocities to maintain tube erosion within acceptable limits. Average gas velocities usually in the range of 25-30 m/s when firing oil may be limited to 12-15 m/s when firing CWM.

(b) The gas temperature entering the close pitched first pass should be less than the initial deformation temperature of the ash, which may be below 1100°C with some eastern Canadian coals. Also, if slagging of the first pass heating surface is to be avoided, the ash fusion characteristics of all potential CWM coals should be known.

(c) A complete reassessment of water wall, superheater, reheater, economizer and air heater sootblowing requirements may be necessary.

(d) Installation of a new, or modifications to the existing, bottom ash removal system. Either option could involve excavating below grade level. Due to the steeper ash hopper slope required for coal firing, modifications may have to be made to the furnace bottom which would affect furnace heat release rates.

(e) Installation of new, or upgrading of existing, dust collection equipment to ensure that particulate emission rates comply with regulatory requirements. In units where there is a little room between the air heater gas outlet and the stack breaching, retrofitting of dust collecting equipment could prove expensive, if not impossible.

(f) The acquisition of suitable ash disposal areas including the most economic method of transportation if no other means of disposal is available.

(g) Increase in operating and maintenance costs in converting to CWM.

FURNACE GAS AND AIR PASSES

(a) The mass flow rate of combustion gases when firing coal in the form of CWM is typically 15%-20% greater than the equivalent oil-fired products of combustion at the same thermal input. Unless the oil-fired unit was designed for gas recirculation, gas velocities will increase through the various heat exchange surfaces. In addition to the impact on tube erosion as discussed earlier, this increase in mass flow rate will also affect heat absorption rates. This could affect superheater/reheater temperature control.

(b) Furnace Plan Heat-release rates (EPRS) for oil-designed furnaces are typically of the order 8.0×10^6 w/m^2. When firing coal this figure could be restricted to about 5.0×10^6 w/m^2. As a first approximation these figures are indicative of a reduced furnace height and, therefore, the reduced "residence" times of oil designed steam generators.

(c) Depending upon the extent of modifications to the boiler, a reassessment will have to be made of fan power requirements:

If the preferred choice is to modify the boiler gas and pressure components to meet full load requirements when burning CWM, it

would be necessary to establish whether the existing fans can meet the increased pressure and volume requirements.

Conversely, if derating is the preferred route, the fans will probably meet the requirements but will probably be operating less efficiently. Either option will add to the cost of CWM conversion.

(d) Since CWM's contain approximately 30% water, there will be a modest increase in wet flue gas losses.

(e) If major modifications are proposed to the boiler gas and pressure components then boiler support steel, including foundations will have to be thoroughly re-examined.

Of the eight steam generators in the Maritimes capable of being converted, some will be more amenable than others. Apart from the engineering aspects discussed in this section of the paper, other aspects such as age of unit, projected load factor, fuel transportation costs and existing furnace dimensions, particularly furnace heights, will influence the final selection.

The paper has attempted to emphasize that conversions to CWM's are site specific, for in addition to the engineering aspects which influence the economic choice, plant layout drawings are required to ensure that proposed modifications are feasible.

Any utility contemplating conversion to CWM will need to cooperate closely with the boiler manufacturers in order to obtain the best technical and financial data necessary to complete an accurate economic evaluation.

As the work at Chatham proceeds, it is hoped to establish which of the boilers in the 100 MW(e) - 150 MW (e) range in the Maritime provinces is the preferred engineering and economic choice.

REFERENCES

1) Canadian Combustion Research Laboratory
"Proceedings of the Coal in Oil Seminar",
May 17, 1972, FRC72-95-CCRL, 1972.

2) Whaley, H. Whalen, P.J. and Davies, F.W.
"Utilization of Beneficiated COM in a Small Utility Boiler",
Proceedings 6th Members Conference, International Flame
Research Foundation, Noordwijkerhout, The Netherlands, 1980.

APPENDIX

THE NEW BRUNSWICK ELECTRIC POWER COMMISSION

CHATHAM STATION UNIT NO. 1

No. 1 Boiler

Manufacturer	- Foster Wheeler
Steam Flow	- 63,500 kg/h
Operating Pressure	- 4170 kPa
Steam Temp	- 446°C
Reheat	- None
Feed Water Temp	- 177°C
Type of Boiler	- Balanced Draft
Fuel	- Original design New Brunswick Coal - Presently firing No. 6 Oil
Ignition	- No. 2 Oil
Burners	- 4 Front-Fired

No. 1 Turbine

Manufacturer	- Parsons
Output (Gross)	- 12,500 kw
Number of Cylinders	- One
Generator Cooling	- Air Cooler
Type of Turbine	- Condensing

CHATHAM STATION UNIT NO. 2

No. 2 Boiler

Manufacturer	- Combustion Engineering Superheater Ltd.
Steam Flow	- 95,500 kg/h
Operating Pressure	- 5930 kPa
Steam Temp	- 482°C
Reheat	- None
Feedwater Temp	- 179°C
Type of Boiler	- Balanced Draft
Fuel	- Original Design New Brunswick Coal - Presently firing No. 6 Oil
Ignition	- No. 2 Oil
Burners	- 4 Corner Fired - Oil Guns - 8 Corner Fired - Coal Burners

APPENDIX (Cont'd)

CHATHAM STATION UNIT NO. 2

No. 2 Turbine

Manufacturer	-	Brown Boveri
Output (Gross)	-	22,000 kw
Number of Cylinders	-	One
Generator Cooling	-	Hydrogen Cooler at 3.5 kPa
Type of Turbine	-	Condensing

MIXING TANK TESTS FOR ENLIGHTENED COAL SLURRIES

Robert R. Faddick
Colorado School of Mines, Golden, CO

INTRODUCTION

Enlightened coal slurries are a phenomenon first observed by the writer in 1973 during a pipeloop test with minus 3 mesh (7mm) metallurgical coal from West Virginia (1). This slurry exhibited the unusual characteristic of being pumpable at solids concentrations up to 74% by weight. Bench-scale mix tank tests with agitation showed that the solids stayed in suspension, even after a three-month duration. It was known that the coal had been cleaned by froth flotation so it was assumed that alcohol and/or oil reagents were responsible for these characteristics. Intuition suggested that small air bubbles were formed by the flotation reagents which in turn attached themselves to the coal particles and effectively reduced their density, hence the name, "enlightened slurry."

In a subsequent study in 1976 (2), five coals from both eastern and western U.S. locations and of steam and metallurgical grade were tested for enlightenment by the addition of air and chemicals in a bench-scale mixing apparatus. All the coals, including particle sizes up to 1/2-in became enlightened. The maximum concentration achieved was 75% by weight.

This apparent ease of suspendability immediately suggested several advantages - stability of the slurry through reduced settling, which in turn would reduce the specific power of pumping, and specific wear by erosion. All of these advantages would be attributed to the development of a more uniform solids-concentration profile rather than the usual asymmetric concentration profile associated with coarse coal slurries. Presumably the reason for this ease of suspendability was the effective reduced density of the coal due to bubble attachment, the phenomenon called enlightened slurry.

The obvious disadvantage would be that enlightened coarse coal particles might not be conducive to rapid settling and thus slurry dewatering would be difficult. On the other hand, the enlightened slurry, if sufficiently concentrated, perhaps could be marketed without dewatering, e.g., by direct combustion in a fossil-fired generating plant. Combustion characteristics of enlightened slurries were not part of this study. However combustion is not expected to be a problem due to the nature and low dosages of the reagents.

The two earlier studies were performed for the U.S. Department of Commerce, Maritime Administration by the Colorado School of Mines Research Institute (CSMRI) serving as subcontractor to Litton Industries and Marconaflo, respectively. The present study was performed for the U.S. Bureau of Mines with CSMRI as contractor.

The objective of this program was to perform bench-scale mixing tests to define the mechanisms by which enlightened slurries are formed. These tests were supplemented by microscopic examinations of the slurries to determine how enlightenment occurs. Pumping tests were then performed to demonstrate and evaluate the hydrotransport characteristics of an enlightened coarse coal slurry. Slurry samples taken from the pipeloop tests were examined microscopically. Due to the extensiveness of the program only the mixing and settling tests will be discussed here. The pumping tests and microscopy work are discussed elsewhere (3).

The present study differs from the previous mixing studies because:
a) More coals were used, including a wider spectrum of eastern and western steam and metallurgical coals,
b) coarser coals were used, 1/2 in and 1-in top size, along with coal mine refuse of higher density than coal,
c) pipeline tests and microscopy work supplemented the mixing tank studies,
d) many more tests were performed.

BENCH SCALE MIXING AND SETTLING TESTS

The objective of the test program was to examine the effect of particle size, reagents, and refuse loading, with the presence or absence of air on the suspendability and settling characteristics of four different coal slurries.
Four coals were selected of both steam and metallurgical grade from underground coal mines in the eastern and western United States. See Table 1.

TABLE 1. COALS TESTED

Location and Type	Specific Gravity, S
Pittsburgh Seam, PA (steam)	1.315
refuse	1.648
Pocahontas #3 Seam, VI (met.)	1.302
refuse	1.783
Hawk's Nest, CO (steam)	1.298
refuse	2.212
Snowmass, CO (metallurgical)	1.336
refuse	1.734

Particle Size Distribution

The particle size distributions of both the minus 1/2-in. coal and refuse samples were determined by screening. The results of the screen analyses for the minus 1/2-in. samples are shown in Figs. 1 and 2.

Reagents

Three common flotation reagents were used for the bench scale test. In order to enhance the hydrophobicity of the coals, fuel oil was used as a collector in all tests with reagents. The quantity of oily collector used in coal flotation applications is generally 0.025% to 0.150% (lb per 100 lb of coal). In these bench scale tests, fuel oil concentrations ranged from 0.105% to 0.178%.

Two different frothers were used in conjunction with the fuel oil. Methyl isobutyl carbinol (MIBC), is a short-chain alcohol that is commonly used in flotation applications. It is essentially not adsorbed by the coal and thus has no collecting properties. Concentrations of MIBC typically range from 0.005% to 0.025%. In these bench scale tests, MIBC concentrations ranged from 0.0033% to 0.0080%. The second frother used in the bench scale tests was Aerofroth 65, a product of the American Cyanamid Company of Tucson, Arizona. Aerofroth 65 is a water-soluble polyglycol that is generally used in the same concentrations as MIBC. Aerofroth 65 concentrations in these bench scale tests ranged from 0.0052% to 0.010%.

Air

Previous tests demonstrated the need for air to develop enlightened slurries. However, neither rate of ingestion nor total volume was quantified. In this series of tests the volume and time of inflow were measured but no evidence surfaced that the measurements were important. It appeared that there might be a minimum amount of air required to initiate enlightenment, but excessive air only generated more froth, which was more of a nuisance than a benefit. The opinion was formed that while air was a necessary ingredient, very little was required for the bench-scale mixing tank. During the pipe loop tests, no air was added save for what entered the pipeline system when coal was loaded by gravity into the pipeline mixing tank.

Test Apparatus

Based upon a study by Lavingia and Faddick, a bench-scale apparatus was modified to serve a a mixing tank, (4,5). Modifications included replacement of the glass tank with an acrylic tank, installation of a support system to stiffen the baffles, and fabrication of an air supply system complete with flowmeter, pressure gauge, and the necessary tubing and fittings. Specifications for the equipment shown

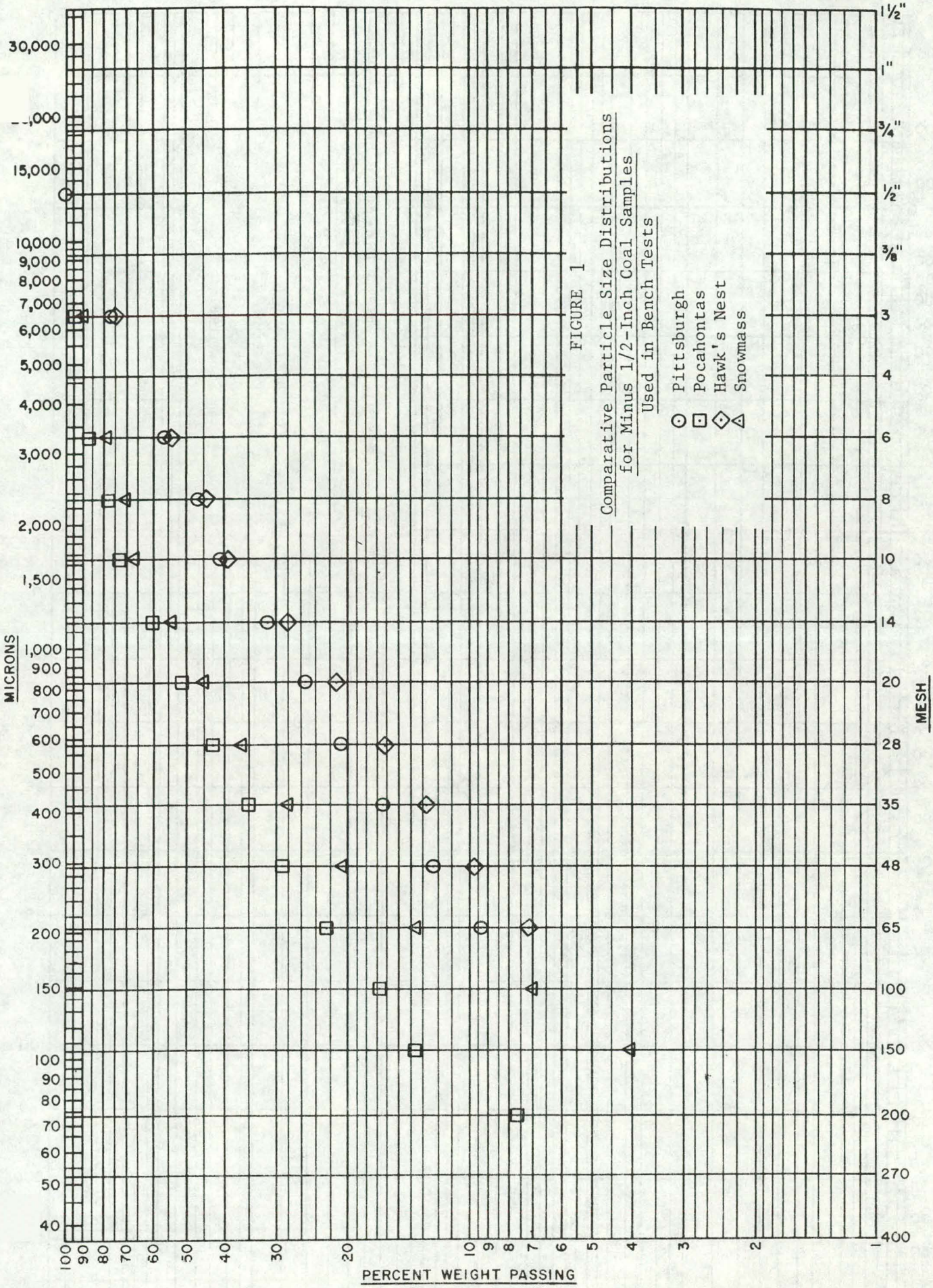

FIGURE 1

Comparative Particle Size Distributions
for Minus 1/2-Inch Coal Samples
Used in Bench Tests

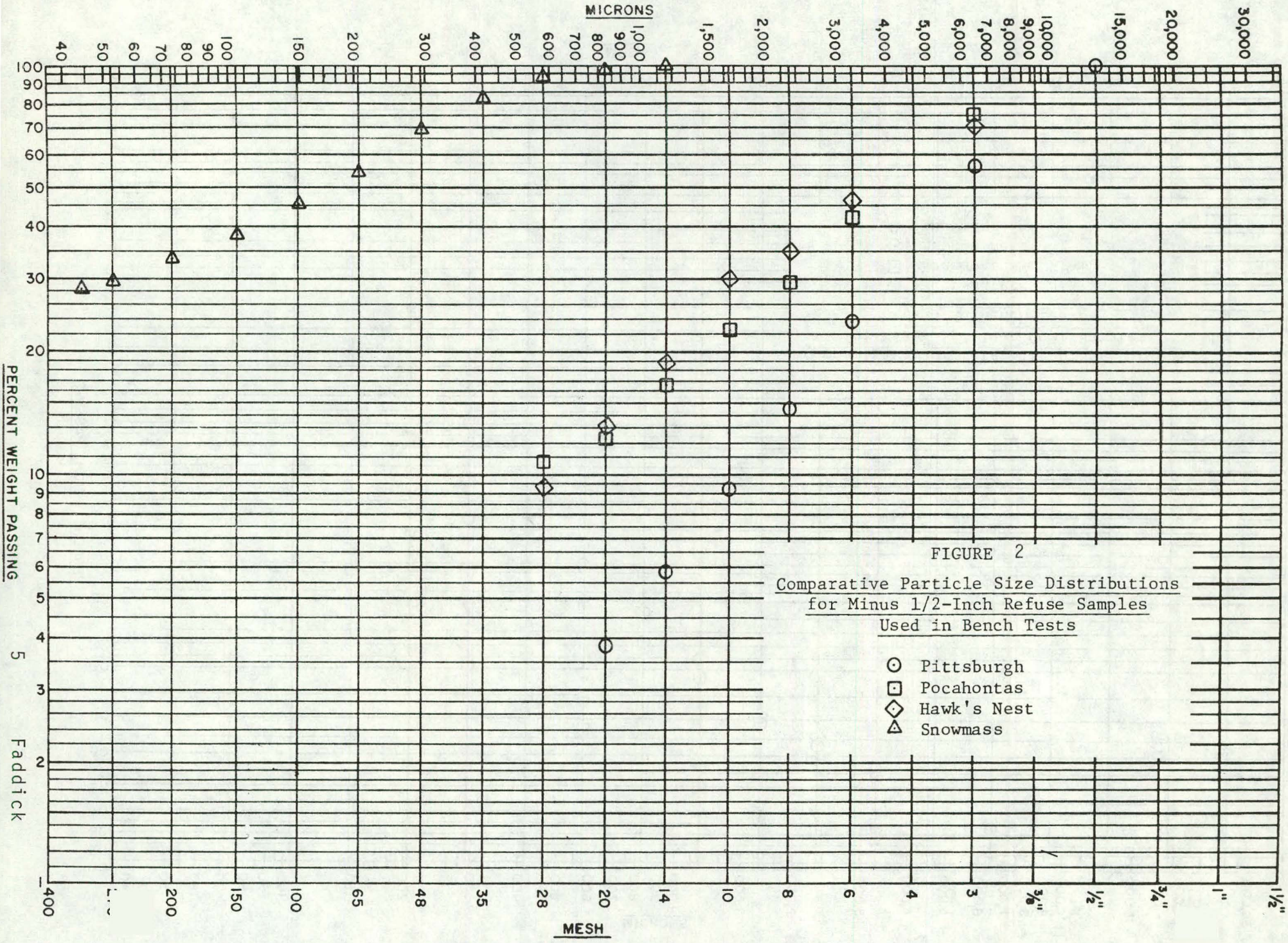

FIGURE 2

Comparative Particle Size Distributions for Minus 1/2-Inch Refuse Samples Used in Bench Tests

in Fig. 3 were as follows:

Equipment:	Agitator driven by 1/4-hp, totally enclosed, 115v, 60 Hz, single phase, variable speed motor with Ametek/Hunter Spring Model L-2 Dynamometer. Speed controlled by 1/4-hp, reversible Boston Ratiotrol and measured by a Type 1531-A Strobotac.
Impeller:	Speed range infinitely variable from 0 to 1,200 rpm. Six 4-in. diam. stainless steel blades pitched at 45 deg., 2-in. from bottom of tank.
Baffles:	Four at 90 deg. around tank perimeter, 1-in. by 18-in. set 1/2-in. from bottom of tank; held in position by 1/4-in. copper air tubing at base of tank.
Tank:	Acrylic, ID - 11.75 in.; depth of slurry - 11.75 in.; overall height - 18-in.; volume - 5.5 gal.
Force Gauge	Lever Arm: 10-in.
Air Supply:	Lab compressor at 100 psi. Pressure at mixing tank measured by Bourdon gauge in psi. Flow measured by Fisher & Porter rotameter in cm /mim. Between each baffle are several 1/32-in. diam. holes to discharge air into the tank.

The impeller was rotated to suspend the solids completely while the force on the dynamometer attached to the impeller was measured. In this manner, the power required to suspend the solids in each slurry was calculated. The ratio of power required to achieve complete suspension of the solids to the power required to mix clear water was used to rate the mixing or preparation characteristics of each slurry. The effects of air and reagents on the enlightenment of the slurries could be evaluated readily, accurately, and inexpensively.

Mixing Theory

The governing equations for mixing are as follows:

$$T = F \cdot r \tag{1}$$

$$P = T \cdot w \tag{2}$$

$$w = 2\pi N/60 \tag{3}$$

$$Re = VD\rho/\mu = RwD\rho/\mu = ND^2\rho/60\mu \tag{4}$$

$$Np = Tw/\rho N^3 D^5 = Pg/\gamma N^3 D^5 \tag{5}$$

where:

- T - torque, 1b(f)-ft
- F - force measured by dynamometer gauge, 1b(f)
- r - dynamometer lever arm, 10-in.
- P - power to achieve mixing, 1b(f)-ft/s
- w - angular velocity, radians/s
- N - rpm of impeller
- Re - Reynolds number of mixing, dimensionless
- Np - power number, dimensionless
- V - representative velocity, i.e. tangential velocity, ft/s, of impeller (V = Rw)

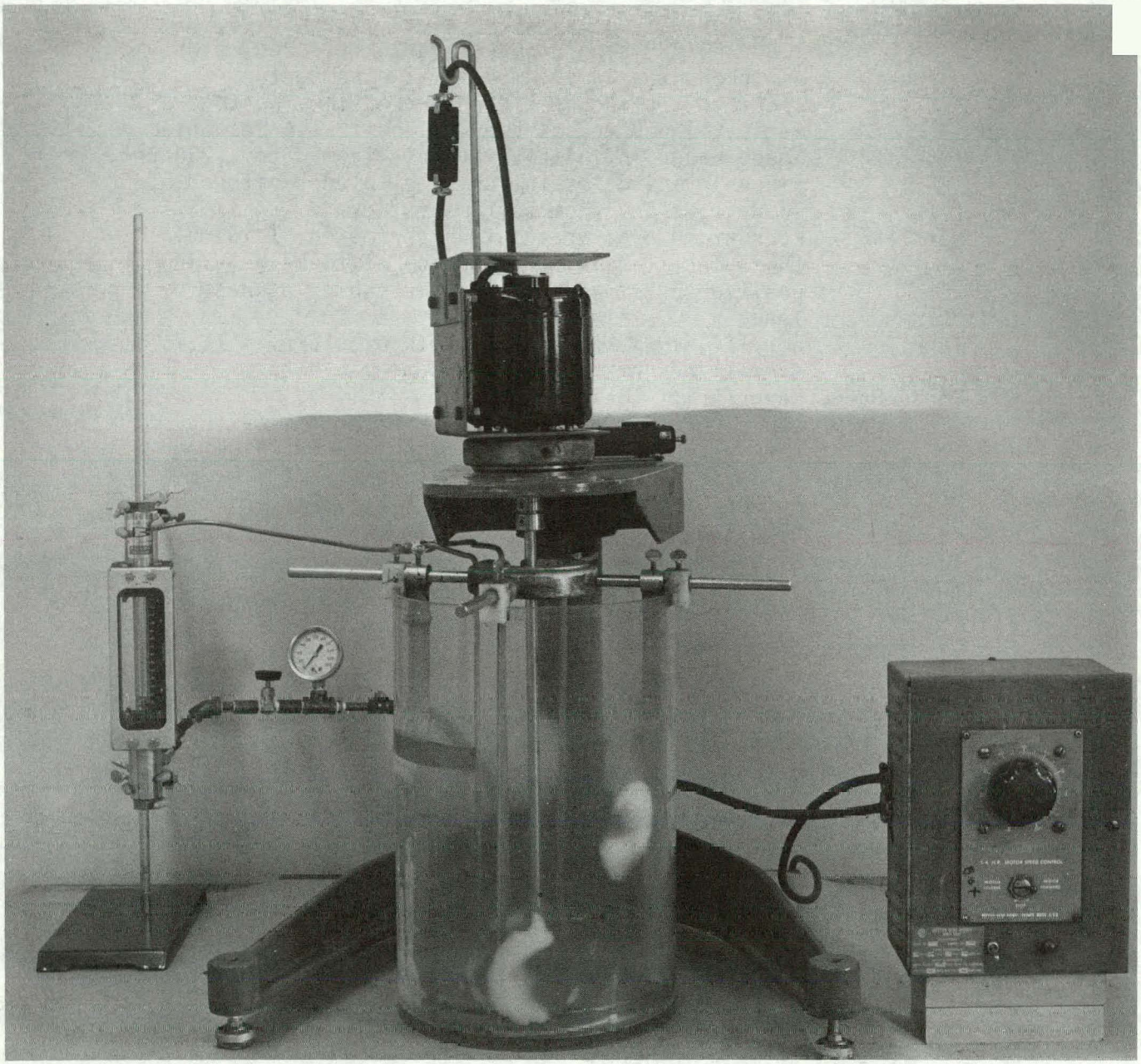

FIG. 3. MIXING AND SETTLING TANK

D - representative length, i.e. impeller diameter, ft
p - density of slurry, lb(m)/ft^3
u - dynamic viscosity of slurry, lb(f)-s/ft^2
R - radius of impeller, ft
γ - specific weight of slurry, lb(f)/ft^3
g - gravitational acceleration, ft/s^2

Plotting torque versus rpm produces a curve, the area under which is the power required to achieve mixing. Plotting Power number versus Reynolds number of mixing results in an essentially horizontal line with Np = 2.0. Then it can be seen from Eq. 5 that $T \propto N^2$ for clear water. For slurries, the exponent changes because the slurry density in Eq. 5 changes, yet Np still remains essentially constant. References 4 and 5 suggest that a correlation can be made between the Power number versus Reynolds number mixing relationship, and the pipe friction factor versus Reynolds number to determine pipeline flow relationships. This relationship was considered to be outside the scope of this work and was not investigated here.

Procedure

1. A water run was made before testing the coal slurries to check the system and calibrate the force gauge.
2. The four-inch diameter, six-bladed, 45 deg. pitched impeller was installed two inches from the bottom of the tank.
3. Air jets were checked to ensure free flow, and tank baffles were tightened to prevent vibration.
4. Coal was added to produce a solids concentration of 50 wt% (usually 30-50 lb). Slurry level was maintained equal to the tank inside diameter (11.75 in.).
5. If reagents were to be used, these were added to the slurry and mixed by the impeller.
6. Initial temperature and slurry properties were recorded.
7. The spotlights and impeller were turned on. The air was turned on as required to desired pressure and capacity.
8. The impeller was freed from the coal by hand and the impeller speed was increased to 300 rpm. Impeller speed was varied from 300 to 1,200 rpm then back to 300 rpm in increments of 100 rpm. As the impeller speed was increased, the force was measured, frothing was observed, wave paterns, if any, were noted, and settling and mixing of the coarse coal particles were observed. The air was turned off after enlightenment was achieved, usually after several minutes. When the air was turned off, the impeller speed usually dropped 50 to 60 rpm and the force reading increased by 0.1 lb(f). The rpm was noted at which all of the coal was in suspension. The maximum impeller speed was typically between 1,000 and 1,200 rpm, depending on the motor load and excessive surface wave patterns. When enlightenment was present, considerable froth could be generated, so the increase in slurry level was recorded. The test was repeated with descending rpm until deposition occurred and a layer of solids built up on the tank bottom.
9. At the end of each run, the force gauge zero setting was checked.

Impeller, lights, and air supply were turned off. Final slurry temperature was recorded.
10. If a settling test followed, the level of clear water measured from the surface was noted as a function of time in minutes after impeller shut-off.
11. The slurry sample was checked for solids concentration, solids specific gravity and screen analysis.
12. The tank was emptied and cleaned for next test.
13. Data were plotted as torque versus rpm and Power numer versus Reynolds number of mixing. Settling was analyzed by evaluating time of settling and increase of solids concentration.

RESULTS

A. Mixing Tests

Results of the mixing test are summarized in Tables 2 through 5. Some sixty mixng tests were made including about three with minus 1-in. coal. Due to the extensiveness of the data only two plots of torque versus impeller rpm and Power Number varsus Reynolds Number for one coal slurry are shown in Figs 4 and 5 as an example. Mixing torque for clear water is proportional to the square of the agitator speed, according to theory. The exponent on speed for clear water varied from 1.82 to 2.17, an error range of +9%. For coal slurries, the exponent ranged from 1.59 to 2.20.

The product of torque and speed is power, as shown in Eq. 2. By determining the ratio of coal slurry power to clear water power, a dimensionless power rating is obtained for ranking the effectiveness of enlightenment. The technique involves determining the area under the torque vs rpm curve from 400 to 1,000 rpm. Power ratios for each slurry were determined using the results of clear water tests performed at nearly the same temperature. The power ratios thus obtained are shown in Tables 2 through 5.

For the Pocahontas coal in the unenlightened state, the power rating was approximately 20% greater than that for clear water. The addition of reagents and air caused a marked decrease in the power rating, thereby demonstrating the effectiveness of enlightenment. The effect of adding refuse to the slurry is shown as a slight increase in the power rating.

For the Hawk's Nest coal in the unenlightened state, the power rating was approximately 60% greater than that for clear water. As with the Pocahontas coal, the addition of reagents and air caused a decrease in the power rating and the addition of up to 20% refuse caused an increase in the power rating. There was no significant difference between the results obtained with the two frothers, but with either frother, an increase in reagent concentration caused a slight increase in the power rating. With this coal then, the best enlightenment can be expected at reagent concentrations lower than 0.178% fuel oil and 0.0066% MIBC.

TABLE 2. MIXING/SETTLING DATA FOR 1/2-IN POCAHONTAS COAL

(Temp: 18-22 C; pH: 7; Solids Concentration - 50 wt %)

Test No.	Concentration in lb per 100 lb coal Fuel Oil	MIBC	Aerofroth 65	Refuse	Power Rating	Final Cw,%	HSRF	Air
P-1 *	-	-	-	-	1.00	-	-	No
POC-1	-	-	-	-	1.20	67.7	1.35	No
POC-2	-	-	-	-	0.95	66.2	1.76	Yes
POC-3	0.108	0.0034	-	-	1.06	58.9	0.62	No
POC-4	0.107	0.0033	-	-	0.93	50.0	-	Yes
POC-5	0.105	0.0033	-	9.02	0.95	60.6	0.34	No

TABLE 3. MIXING/SETTLING DATA FOR 1/2-IN HAWK'S NEST COAL

(Temp: 20-25 C; pH: 8-9; Solids Concentration - 50 wt %)

HN-6*	-	-	-	-	1.00	-	-	No
HN-7	-	-	-	-	1.59	64.6	I.S.	No
HN-8	0.108	0.0034	-	-	1.40	61.4	4.91	No
HN-9	0.107	0.0033	-	-	1.20	61.4	3.69	Yes
HN-10	0.178	0.0066	-	-	1.28	59.7	2.39	Yes
HN-11	0.178	0.0066	-	10.0	1.27	58.9	4.71	No
HN-12*	-	-	-	-	1.00	-	-	No
HN-13	-	-	-	-	1.63	64.6	I.S.	No
HN-14	0.108	-	0.0052	-	1.54	61.4	3.66	No
HN-15	0.107	-	0.0051	-	1.20	61.4	3.69	Yes
HN-16	0.178	-	0.010	-	1.24	56.6	4.53	Yes
HN-17	0.178	-	0.010	9.6	1.30	63.2	2.17	No
HN-18	0.178	-	0.010	20.1	1.35	67.2	0.70	No

I.S. - immediate settling

* - water run

TABLE 4. MIXING/SETTLING DATA FOR 1/2-IN PITTSBURGH COAL

(Temp: 18-24 C; pH: 6-7; Solids Concentration - 50 wt %)

Test No.	Concentration in lb per 100 lb coal Fuel Oil	MIBC	Aerofroth 65	Refuse	Power Rating	Final Cw,%	HSRF	Air
PS-19	-	-	-	-	1.56	68.3	4.10	No
PS-20	0.108	0.0040	-	-	1.37	60.6	4.85	No
PS-21	0.108	0.0040	-	-	1.11	58.1	2.79	Yes
PS-22	0.178	0.0080	-	-	1.08	58.1	2.79	Yes
PS-23	0.178	0.0080	-	10.0	1.18	58.9	2.02	No
PS-24	0.178	0.0080	-	21.0	1.19	58.1	2.79	No
PS-25	-	-	-	-	1.63	75.6	3.63	No
PS-26	0.108	-	0.0051	-	1.41	62.4	2.14	No
PS-27	0.108	-	0.0051	-	1.19	58.1	4.65	Yes
PS-28	0.178	-	0.010	-	1.07	55.9	1.68	Yes
PS-29	0.178	-	0.010	9.6	1.21	62.2	0.34	No
PS-30	0.178	-	0.010	20.1	1.22	61.2	1.05	No

TABLE 5. MIXING/SETTLING DATA FOR 1/2-IN SNOWMASS COAL

(Temp: 20-27 C; pH: 6-7; Solids Concentration - 50 wt %)

SM-32*	-	-	-	-	1.00	-	-	No
SM-33	-	-	-	-	1.23	66.0	5.28	No
SM-34	0.107	0.0040	-	-	1.19	61.9	7.42	No
SM-35	0.107	0.0040	-	-	1.09	61.6	2.46	Yes
SM-36	0.178	0.0080	-	-	1.07	60.2	6.02	Yes
SM-37	0.178	0.0080	-	10.0	1.02	58.6	1.76	No
SM-38	0.178	0.0080	-	21.0	1.01	58.6	1.41	No
SM-40*	-	-	-	-	1.00	-	-	No
SM-41	-	-	-	-	1.32	65.8	6.08	No
SM-42	0.108	-	0.0051	-	1.22	61.3	7.35	No
SM-43	0.108	-	0.0051	-	1.11	59.6	3.58	Yes
SM-44	0.178	-	0.010	-	1.02	61.0	2.44	Yes
SM-45	0.178	-	0.010	10.0	1.01	65.5	1.31	No
SM-46	0.178	-	0.010	21.0	1.03	64.3	1.19	No
SM-48*	-	-	-	-	1.00	-	-	No

* - water run

FIG. 4

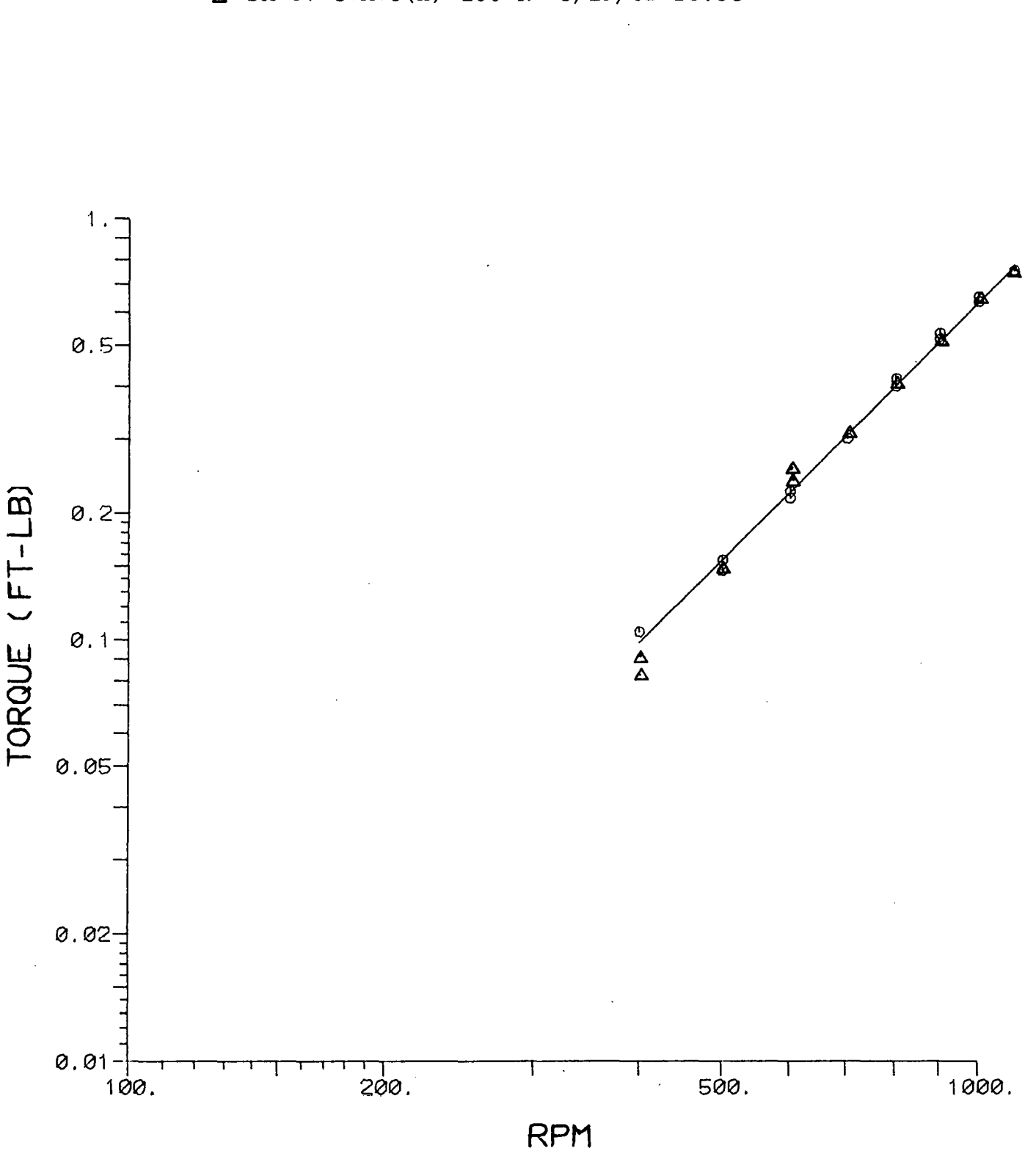
SM-32 WATER 3/16/82 20.5C
SM-37 C+M+O(H)+10% R 3/19/82 23.5C
TORQUE (FT-LB)
1.
0.5
0.2
0.1
0.05
0.02
0.01
100.
200.
500.
1000.
RPM

FIG. 5

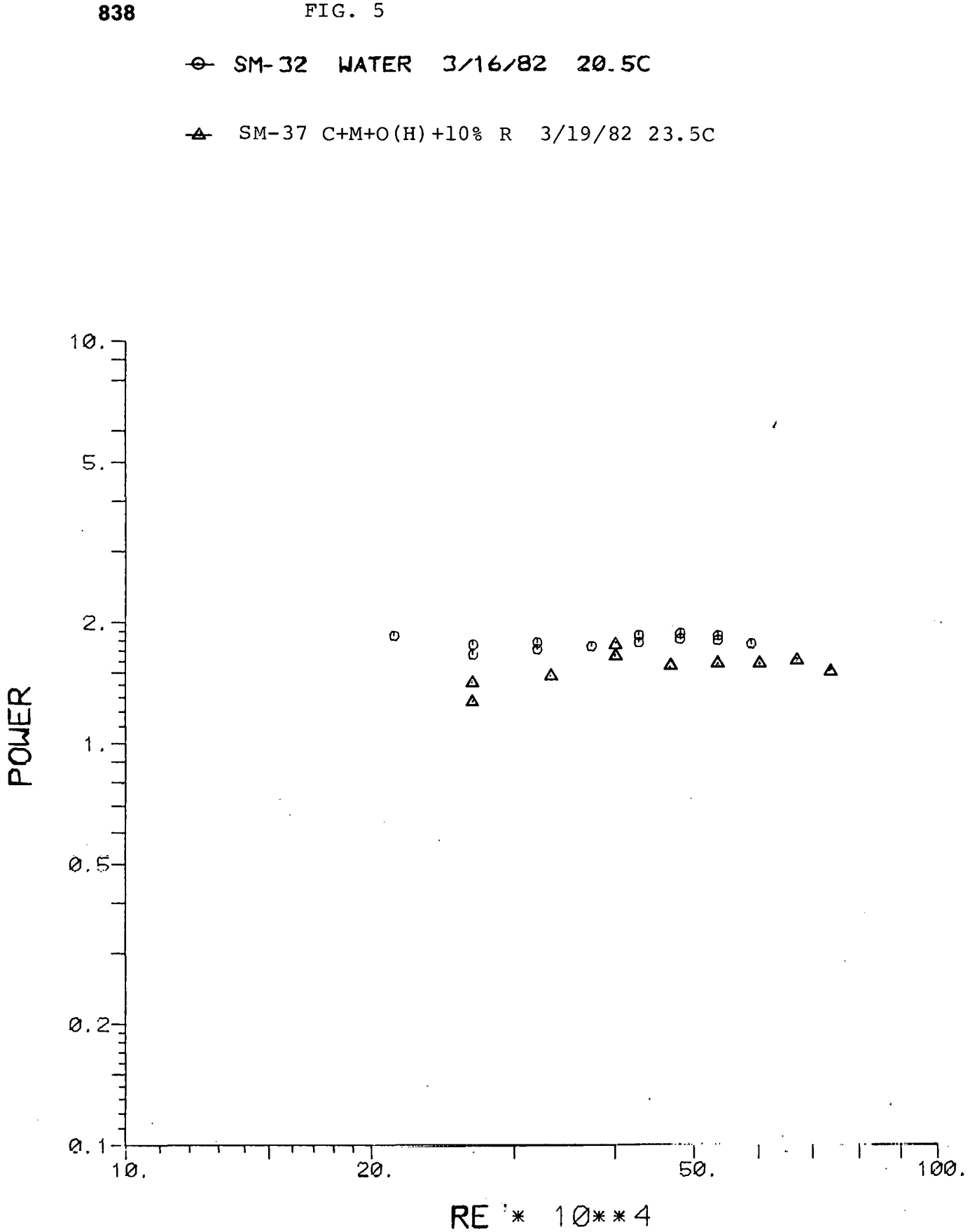
SM-32 WATER 3/16/82 20.5C
SM-37 C+M+O(H)+10% R 3/19/82 23.5C
10.
5.
2.
1.
0.5
0.2
0.1
POWER
10.
20.
50.
100.
RE * 10**4

For the Pittsburgh and Snowmass coals, the pattern of results was similar to those obtained with the Hawk's Nest coal with the exception that an increase in reagent concentration resulted in a decrease in the power rating.

The effects of particle size and distribution on the power rating also followed an expected pattern. As shown in Fig. 2, the coarsest of the four coal samples was the Hawk's Nest coal followed, in order, by the Pittsburgh, Snowmass, and Pocahontas coals. The power ratings of the unenlightened and enlightened slurries decreased in this same sequence.

B. Settling Tests

Results of the settling tests are summarized in Tables 2 through 5. The settling characteristics of each slurry have been rated according to an Hourly Settling Rank Factor (HSRF) defined as:

$$HSRF = Cw(final) \times 60 / (Cw(initial) \times t(final)) \qquad (6)$$

where concentrations are expressed as percentages and times are expressed in minutes. The initial solids concentration in each case was 50 wt %. A high value of HSRF means rapid settling with little effect from the enlightenment.

Tables 2 through 5 show that, for all coals, the addition of reagents and air resulted in a significant decrease in the HSRF. This result has three implications: first, the coal slurries were enlightened by the addition of reagents and air; second, slurries that are so enlightened should exhibit increased stability in a pipeline as a result of reduced settling characteristics induced by enlightenment; and third, enlightened slurries are not easily dewatered.

CONCLUSIONS

1. Bench-scale testing with a mixing tank is an adequate and successful procedure for testing the mixing and settling characteristics of slurries. Small slurry samples can be tested in a simple apparatus to rank slurries according to the power requirements for mixing and their rate of gravity settling.

2. Enlightened coal slurries are produced by the addition of flotation reagents, namely alcohol and oil in the presence of air to form aeroflocs of small bubbles, covered with coal dust and attached to coarse coal particles reducing the effective density of the coal. In the last decade, enlightenment has been achieved for nine different U.S. coals.

3. As shown by the mixing tests, the addition of refuse up to 20 % by weight of dry coal to an enlightened slurry without additional air, increased the power rating in eight cases out of twelve,

but not significantly.

4. As shown by the settling tests the addition of refuse up to 20% by weight of dry coal to an enlightened slurry without additional air, decreased the hourly settling rank factor in almost every case but not by a significant amount. In other words,the presence of a denser solids phase did not reduce the enlightenment effect significantly.

5. Enlightened coal slurries show potential in producing high-concentration slurries with reduced specific power requirements both for mixing and hydrotransport. When used in underground coal mines, two benefits should accrue from enlightened slurries-increased coal production and improved safety due to the lower specific power levels and containment of the haulage system for safety.

The combination of higher solids loading and combustible additives should provide an energy slurry for direct combustion without pollution or corrosion side effects.

Also, there is a strong possibility, although untested, that pulverized coal could be enlightened to increase the solids throughput of long-distance overland slurry pipelines for direct combustion of the slurry.

ACKNOWLEDGEMENTS

The study was performed by the Colorado School of Mines Research Institute under the sponsorship of the U.S. Bureau of Mines (BOM), Pittsburgh Research Center. The BOM Technical Project Officer was Richard C. Wang. The author expresses his thanks to him and to his colleague Anthony J. Miscoe, and also to Robert Griffis, Project Engineer at CSMRI for his assistance.

REFERENCES

1. "Bulk Commodities Form Changes and Alternative Transportation Modes," Final report prepared for U.S. Dept. of Commerce, Maritime Administration, Contract No. 2-36252 by Litton Industries, December 31, 1973.

2. "The Application of Slurry Technology to the Maritime Industry," Final report prepared for U.S. Dept. of Commerce, Maritime Administration, Contract No. 5-380 30 by Marconaflo, Inc., San Francisco, CA, May 31, 1976.

3. Faddick, R., "Enlightened Coal Slurries," Slurry Transport Assoc., 8th Annual Conf., San Francisco, CA, March 16, 1983.

4. Lavingia, N.J., and Faddick, R.R., "Mixing of Mineral Slurries," Proc. of Symposium on Polyphase Flow-The Fluid Mechanics of

Mixing in Multi-Component Flows, ASME, Georgia Tech, Atlanta, GA, June 20, 1973.

5. Lavingia, N.J., and Faddick, R.R., "Investigation of a Slurry Bench Test," Hydrotransport 3, Paper H2, Brit. Hydromech. Res. Assoc. (BHRA) and Colorado School of Mines, Golden, CO, May 16, 1974.

6. Faddick, R., "Mixing of Coarse Coal-Water Slurries," Proc. 2nd European Conf. on Mixing, BHRA, St. John's College, Cambridge, UK, March 30 - April 1, 1977.

RECENT STUDY ON HIGHLY LOADED COAL WATER SLURRY

Yasuyuki Nakabayashi
Electric Power Development Co., Ltd.

Noboru Sato
Kenichi Fujii
Shoichi Takao
Nitaro Suzuki
Kawasaki Heavy Industries, Ltd.

1. Introduction

In Japan, since 1980, research and development of Highly Loaded Coal Water Slurry (hereinafter referred to as Coal Water Mixture, abbreviated as CWM) has been tackled with Electric Power Development Co. acting as a promotor. In this research and development, several plant manufacturers including Kawasaki Heavy Industries, Ltd. as well as several additive makers, have been taking part as joint researchers.

Our research and development with reference to CWM is now at a stage developing from laboratory-level basic tests to a pilot plant test and we are now constructing a pilot plant.

For the purpose of obtaining data for designing this pilot plant, the tests for manufacturing CWM utilizing the existing pilot plant for fine COM were carried out twice. The results of the first test were already reported at the last session of the Symposium [3]. Therefore, this time, we will refer to the second manufacturing test and some knowledge obtained from the subsequent bench scale test.

Following, we will make a report of the results of a small-scale combustion test of CWM, which is the main content of this thesis.

This combustion test was carried out using the test material, CWM, which was manufactured from the second manufacturing test. What should be noted is that we fired pulverized coal of the same brand and the same lot as the raw material of this CWM, under the same combustion furnace conditions with the same volumetric heat release conditions, having compared CWM with pulverized coal.

2. Preparation of Highly Loaded Coal Water Slurry

2.1 Bench Scale Test

2.1.1 Experimental

(a) By two methods, namely, one-stage grinding method and two-stage grinding method shown in Fig. 2-1, CWMs were prepared. As test devices, two wet ball mills, namely, a wet ball mill (A) (317ϕ x 683 long) and a wet ball mill (B) (284ϕ x 603 long) were employed. In the case of the one-stage grinding method, the wet ball mill (A) was employed, and in the case of the two-stage grinding method, the wet ball mill (A) was employed at a first stage, and the wet ball mill (B) was employed at a second stage, wherein coal is pulverized in a wet state with additives to prepare CWM.

The coal was Tatung coal lot No. 5612, and two kinds of additives were used, anionic dispersant "A" and nonionic dispersant "N".

(b) As will be mentioned later, at a test on a pilot scale, despite the fact that the two coals were of the same brand, the upper limit concentrations being different, we conducted a comparative test of Tatung coal lot No. 5612 and Tatung coal lot No. 5707.

Namely, we analyzed the coal properties of the two lots of coal, at the same time. We mixed pulverized coals of the two lots with additives and water by a "Labo-Disperser" to prepare CWMs, and compared the two.

2.1.2 Results

(a) The test results of the one-stage grinding method and the two stage grinding method are shown in Fig. 2-2.

At a coal concentration of 67%, in the case of the one-stage grinding method, the viscosity of CWM was 1350 CP. By contrast, in the case of the two-stage grinding method, the viscosity of CWM was 750 CP, which means that by the two-stage grinding method, the fluidity of CWM could be sharply improved.

And as shown in Table 2-1, the productive capacity of CWM was 8.0 kg/h according to the one-stage grinding method, by contrast, according to the two-stage grinding method it was 16.0 kg/h, and when converted to per unit capacity of the mill, they became o.15 kg/h.1 and 0.17 kg/h.1, respectively. This means that the two-stage grinding method increased the productive capacity by about 13%. This is attributed to the high grinding efficiency at the first stage pulverization, wherein the additives dispersed more smoothly than in the case of the one-stage grinding method, resulting in mixing

CWM into a well dispersed state.

Upon comparing the additives, anionic dispersant "A" with the nonionic dispersant "N ","N" turned out to be excellent with respect to the concentration raising effect.

However, when "N" was used, foams occurred depending on the manufacturing conditions, stopping discharge of CWM from the wet ball mill. By contrast, when "A" was used a stable effect was brought about even if the manufacturing conditions were changed, "A" being suitable for the wet manufacturing method.

(b) The results of analysis of Tatung coal lot No. 5612 and Tatung coal lot No. 5707 are shown in Table 2-2.

Compared with lot No. 5612, lot No. 5707 became large in moisture, O/C atomic ratio and BET specific surface area, or the fuel ratio became lower.

With reference to these two kinds of Tatung coal, results of the CWM preparation test using "A" are shown in Fig. 2-3, while results of the same test, but using "N" are shown in Fig. 2-4.

In the case of using "A", influence of the coal properties was small and the difference in coal concentration at the same viscosity was about 2%. By contrast, when "N" was used, influence of the coal properties was large and the difference in coal concentration at the same viscosity was about 4%.

2.2 Test for Pilot Plant Design

Utilizing the Nagasaki Fine COM Pilot Plant, tests for preparing CWM were carried out in December 1981 and again in July 1982.

A report will be made below with reference to the test carried out in 1982.

2.2.1 Experimental

The flow diagram of a plant for preparing CWM is shown in Fig. 2-5.

Because only one wet ball mill had to be used in applying the two-stage grinding method, the test for preparing CWM was carried out by a batch method as mentioned below.

(a) First stage grinding method

Coal is pulverized in advance to an extent of 3mm under 90% by a pulverizer and supplied to a pulverized coal hopper.

The given amount of coal is fed to the wet ball mill (1200ϕ x 2400 long) from the pulverized coal hopper by a constant feed weigher. At the same time, the specified amounts of water and additive are fed by a pump to the wet ball mill so as to make the coal concentration to a given value and the coal grinding the conducted to prepare slurry. The prepared slurry is supplied to a mixing tank. When the mixing tank is filled, the first stage grinding method is finished.

(b) Second stage grinding method

Similar to the first stage grinding process, the given amount of coal is fed to the wet ball mill from the pulverized coal hopper by the constant feed weigher. At the same time, in order to bring about the given coal concentration, the first stage slurry is fed to the wet ball mill from the mixing tank by a pump to prepare CWM.

The coal employed in the tests was Tatung coal lot No. 5707 which was the same coal as used in the bench scale test.

The same additives used in the bench scale test, "A" and "N" were also used.

2.2.2 Results

The various comparisons between the first and second tests are also shown in Table 2-3, 2-4 and Figs. 2-6, 2-7.

In Table 2-3, one example of the operation conditions and operating data of CWM is shown. The results of chemical analysis of CWM obtained thereby are shown in Table 2-4 and the particle size distributions of slurry prepared in different conditions are shown in Fig. 2-6 and Fig. 2-7.

Upon comparing CWM prepared in 1981 using Tatung coal lot No. 5612 with CWM prepared in 1982 using Tatung coal lot No. 5707, the difference of about 3% is shown in the coal concentration of CWM, despite the use of the same additive "A" and the viscosities of the same extent.

Also, the discharge characteristic of CWM from the mill does not correspond to the measured value of viscosity by a B-type viscometer; when "A" was used, even though CWM having a viscosity of more than 1000 cP was discharged well from the mill, whereas, in the case of using "N ",CWM having a viscosity of about 300 cP was not discharged well from the mill.

2.3 Conclusions

It was revealed that properties of CWMs, especially the upper limit values of coal concentration, are significantly effected by the difference of lots, even though they are prepared from coals of the same brand.

This difference is considered attributable to the difference in coal properties.

In both tests, Tatung coals were used, but differences could be found in analytical values. Especially, the differences were noticeable in moisture, volatile matter and calorific value.

From these results, the properties of CWM seem to depend greatly on the properties of the coal from which it is prepared, especially the degree of coalification. It is necessary to conduct a study in this respect.

Judging from the fact that the discharge characteristic of CWM from the mill is not determined by viscosity only, it is necessary to conduct a further study on this.

3. Combustion Test

3.1 Approach

As it is seen in the summary of Essenhigh [1], research items that are required with reference to the combustion of CWM cover a diversified range including slurry characterization, atomization, evaporation, ignition, combustion, flame characteristics, ash properties and NOx emission characteristics. Of these, what is acquiring special importance in Japan, where environmental restrictions are severe, is the technology of controlling NOx and unburned carbon in flyash. (hereinafter referred to as C%).

McHale and Sheffee et al, [4]-[6], have studied the influence of coal brand and fineness on combustion efficiency, through the basic research on CWM combustion. However, under the restriction of a small scale furnace with high volumetric heat release rate combustion, the emission of CO is on the level of several hundred ppm, combustion efficiency is 80-90%, that is to say that the unburned carbon in flyash exceeds 50%. These experimental results are far removed from the requirement of unburned carbon in flyash in a power boiler in Japan, which is less than 5%.

Judging from the fuel composition of a mixture of pulverized coal and water, combustion of CWM is considered basically similar to combustion of pulverized coal (hereinafter referred to as PC). As the emissions of NOx and C% depend strongly on coal brand and combustion conditions [2], it is desirable to perform a comparative combustion test of CWM and PC under the same combustion conditions using the same parent coal. However, in the previous researches, a comparative combustion test has not been conducted, and also there has been no published data on the reduction of NOx in CWM firing [1].

In view of this situation, the authors et al performed a comparative combustion test of CWM and PC prepared from the same parent coal, under close conditions of NOx reduction countermeasure, furnace temperature and volumetric heat release rate in a furnace that substituted for the real boiler, for the purpose of obtaining comparative test data of NOx and C% in CWM firing and PC firing.

As a result, it has become clear that CWM firing shows the following characteristics compared with PC-firing.

(a) The Combustion temperature inside the furnace is lower by about 100°C.

(b) Emissions of NOx and CO are somewhat smaller.

(c) Although the combustion temperature decreases to some extent, the emission level of unburned carbon in flyash remains as large as in PC firing due to the combustion promotion effect.

(d) Adoption of two-stage combustion makes it possible to reduce NOx certainly, but an increase of C% in conjunction with the reduction of NOx is unavoidable.

3.2 Experimental

CWM obtained in the aforementioned test, and PC prepared from parent coal of the same brand and the same lot were burned under conditions of the same furnace and the same volumetric heat release rate to compare the emission characteristics of NOx, CO and C%.

3.2.1 Furnace

The combustion tests of CWM and PC were carried out using a small scale furnace shown in Fig. 3-1. The furnace was a water-cooled cylindrical type having an internal diameter of 800 mm, a length of 4900 mm and an effective furnace capacity of 2.0 m^3. The internal wall of the furnace is lined with refractory material to maintain the furnace temperature as is expected in the real boiler at the normal volumetric heat release rate in the furnace (193 kW/m^3). On No. 1 - 8 ports on the side of the furnace, PR thermocouples were fitted for the continuous measurement of the average temperature of the respective cross sections. The flame condition was observed through an observation port.

Atomizing air at room temperature and primary air preheated to 80°C was used for the combustion of CWM and PC, respectively. Secondary air and two-stage air were both preheated to about 300°C and then supplied to the furnace. Two-stage combustion air was injected into the furnace from one of the two-stage combustion ports in the drawing (T3P: TS_4 - TS_6). Ash sampling for measuring the unburned carbon was carried out at the furnace end, while gas sampling was carried out in the flue at a low temperature.

3.2.2 Burner

For the combustion test of CWM, dual-fluid air atomizing burners of various types were specially designed, and after a series of selection tests, an intermediate mixing burner tip, shown in Fig. 3-2, was selected as the optimum one. Due to the physical restriction that CWM (which contains coal particles) has to be burned with a small capacity burner (70 kg/h) in a small scale furnace, the fuel nozzle has a single hole and the spray angle becomes narrow (20 - 25°). As a result, plugging of CWM in the burner tip and impingement of spray onto the inner wall of the furnace were avoided. On the other hand, in PC firing, a small-scale model of a real burner [2]

was used. Swirl of combustion air was added by a swirl type flame holder in CWM firing and by a register vane in PC firing.

3.2.3 Fuel Feed

Supplying of fuel to the burner was carried out by a simplified method, as shown in Fig. 3-1, because the test was small in scale. In the CWM system, CWM obtained in the preparation test was at first pretreated in a pot mixer, and then CWM stored in the compressed type slurry tank was forwarded by air pressure. In the piping system, a 10 mesh auto-strainer was installed to remove coarse particles. On the other hand, pulverized coal stored in the hopper was cut away by a constant feeder, and conveyed to the burner by primary air.

3.2.4 Coal Properties

It is well known that the combustibility of coal depends on coal properties, and particularly C% varies greatly according to the coal brand [2]. In this research, CWM and PC were prepared using the same parent coal and subjected to the combustion test. The results of analysis of the parent coal subjected to the test are shown in Table 2-2 at lot No. 5707. The fuel analyses of CWM and PC subjected to the combustion test are shown in Table 3-1. The values are somewhat different from those at the time of the preparation test, the main reasons for this are (a) addition of small quantities of water (0 - 2%) at the time of the combustion test, to adjust the viscosity, (b) aging for only 3 months at the longest since it was prepared. The coal concentration was about 64%, the viscosity was greater than the range 401 - 2000 CP and the particle size was 200 mesh under 65-79%. On the other hand, the particle size of PC was 200 mesh under 85%, meaning that PC was finer than CWM in particle size.

3.3 Results

3.3.1 Flame characteristics

Although the flame for PC firing is a stable one attached to the flame holder, according to observations from the observation port at the end of the furnace, numerous small particles floating inside the furnace make the interior of the furnace opaque. On the other hand, the flame for CWM firing is a lifted one formed at positions several tens of centimeters away from the flame holder, due to the small spray angle and a large amount of water. In addition, the interior of the furnace is quite transparent compared to PC firing. A luminous flame of the burning volatile matter is barely observed, being similar to the flame of PC firing with gas mixing. Therefore, in the case of CWM firing, formation of soot derived from the volatile matter seems to be restricted due to the fact that (a) combustion proceeds in an atomized state, (b) a lifted flame is formed, and (c) a large amount of water is contained.

3.3.2 Effect of Furnace Temperature

It is known [2] that C% and NOx in PC firing depend on the combustion temperature, the same could be said of CWM firing. Since the combustion temperature depends on the degree of insulation of the furnace, the steady furnace temperature in the specified test furnace has no universal significance. Because of that, experiments in the preheating process of the furnace were conducted for the purpose of clarifying the relation between the combustion temperature and the combustion products.

Fig. 3-3 shows the variation of the furnace temperature and the combustion products. The furnace temperature is represented by the measured temperatures T_5, T_8 at the measuring points Nos. 5, 8. Fig. 3-3 (a) relates to the case wherein no NOx reduction techniques are taken, and as time elapses, the furnace temperature rises, NOx rises, CO decreases and C% decreases suddenly. On the other hand, Fig. 3-3 (b) relates to the case wherein $TS_5\%=30$, 30% of the total combustion air flow is injected from two-stage combustion air port No. 5, and as time elapses, the NOx level tends to be roughly constant, CO tends to decrease and C% tends to decrease remarkably.

Fig. 3-4 shows the results of PC firing, that are similar to those of CWM firing, but the NOx level in the case of $TS_5\%=30$, is somewhat higher and NOx increases as time elapses.

In the meantime, judging from the temperatures (T_5, T_8) at a time considered close to the steady furnace temperature (180 - 230 minutes), the temperature in the case of CWM firing decreases by about 100°C than that of PC firing.

In Figs. 3-5, 3-6, are shown the emissions of NOx and C% obtained during the preheating process of the furnace, as a function of the furnace temperature T_5. It has no particular significance that the measured values of NOx in the cases of CWM firing and PC firing under $TS\%=0$ happen to coincide with each other. However, it should be noted that the NOx levels of the two firing forms are close to each other and that NOx emission increases as the temperature increases. When $TS_5\%=30$, CWM firing is lower in NOx emission and the temperature dependence is smaller.

On the other hand, as shown in Fig 3-6, C% (or combustion efficiency) depends largely on the furnace temperature regardless of the firing form of CWM firing or PC firing. Upon comparing the data at the same temperature of the shaded symbol of PC firing (●, ◆) with the open symbol of CWM firing (○, ◇), C% of CWM firing is half of PC firing, and this trend is observable regardless of whether combustion is in two-stage or not.

Additionally, the solid curve and broken curve represent predicted values of PC firing and CWM firing, respectively, the comparison of which with experimental values will be discussed in the subsequent paragraph 3.4.

3.3.3 Effect of O_2

Figure 3-7 shows the effect of the percentage of O_2 in flue gas on the emissions of NOx,CO and C% under the steady furnace temperature. Results of 5 cases combining TSP and TS% are summarized. The trends of data of CWM firing and PC firing are similar as a whole. As O_2 increases, NOx increases and C% decreases. And the sequence of the NOx emission of the 5 cases is precisely in the reverse relation to the sequence of C%, suggesting that the simultanuous reduction of them is considerably difficult. Within the range where O_2 does not become extremely low, CO emission is about 10 ppm in CWM firing and about 20 ppm in PC firing.

3.3.4 Effect of TS% and TSP

Two-stage combustion is a well known technique to reduce NOx emission. In Fig. 3-8 is shown the effects of the primary parameters of TSP and TS% on emission characteristics. In both of the fuels, NOx decreases and C% increases with increasing TS%, or moving TSP to the down-stream direction. On the other hand, the effect of reducing NOx in conjunction with an increase of TS%, becomes larger in the case of CWM firing, being somewhat different from the case of PC firing.

3.3.5 Effect of GM

Exhaust gas mixing (GM) is broadly adopted as a method of reducing NOx of a gaseous fuel and a liquid fuel. However in the case of CWM, though it is also a liquid fuel, it contains large amounts of bonded nitrogen in the fuel, accordingly, as shown in Fig. 3-9, a gas mixing technique increases NOx emission to some extent, and also remarkably, increases C%. From the fact that these results are also in accord with much of the data from PC firing, it can be concluded that GM cannot become a method of reducing NOx in coal firing.

3.3.6 Effect of CWM Properties

Figure 3-10 shows the effect of CWM properties on NOx and C%. As shown in Table 3-1, these four kinds are about the same in coal concentration, and with respect to particle sizes, No. 5713A and No. 5714 are the smallest in particle diameter, followed by No. 5715 and No. 5717, and C% increases roughly in that sequence. However, in the case of No. 5715, perhaps because it is high in viscosity and poor in atomization, C% in the case of TS%=0 becomes large. Therefore, for reducing C%, increase of fineness and advancement of the atomization performance may be the most important factors.

On the other hand, in the emission level of NOx, the meaning difference due to the properties of CWM can not be recognized.

3.4 Discussion

Having confirmed that NOx, CO and C% are the main environmental pollutants resulting from the combustion of coal, CWM firing is inferior to PC firing only in C%. We will, therefore, examine C% based on the kinetic theory of coal combustion.

The authors et al have reported that prediction of C% of PC firing is possible to some extent by numerical analysis of the combustion process in the furnace. As regards the details of that method of calculation, please refer to reference (2). In that method, a shrinking particle model is basically adopted on the assumption that a group of pulverized coal particles burn through a surface reaction with oxygen in the furnace of one dimensional flow having temperature and air ratio distributions. Results of that calculation are shown by the solid curve in Fig. 3-6, that are in good agreement with the experimental results of the corresponding PC firing.

On the other hand, with reference to CWM firing, the assumption was made that CWM separates to inert water vapor and pulverized coal having the particle size distribution of CWM (No. 5717) immediately after atomization. Predicted results are shown by the broken curve in Fig. 3-6. Namely, in the case of CWM firing, (a) the diameter of the particle is large, (b) the amount of primary air is small, and (c) due to added water vapor, the residence time of coal particles in the furnace is shorten and the O_2 concentration on a wet base is decreased. Due to the combined effects of these, increase of C% is unavoidable. The dominant factor amongst these elements is (a). The results of the calculation are considerably larger than the experimental data of the corresponding CWM firing.

Judging from the basis that the calculated value and experimental value of PC firing are roughly in accord with not only those of this case, but also with those of other many kinds of coal, CWM firing is considered to have combustion promotion effects compared with PC firing. As to the reasons for this, various reasons are conceivable, such as the gasification reaction by water vapor and the swelling of the char particles, however they have not yet been clarified.

3.5 Conclusions

The comparative combustion test of CWM and PC was carried out using a small scale combustion furnace. The following conclusions have been obtained with reference to the emission characteristics of NOx and unburned carbon in flyash.

(a) Characteristics common to both CWM firing and PC firing

(i) As the furnace temperature rises, NOx rises and C% decreases suddenly.

(ii) For reducing NOx, anyone of (1) low O_2 operation, (2) adoption of a two-stage combustion port at the down stream side of the furnace, or (3) increase of the two-stage combustion ratio, is effective, however, C% increases definitely in each case.

(iii) Adoption of recirculation of the exhaust gas not only has very little effect on the reduction of NOx, but also remarkably increases C%.

(b) Characteristics of CWM firing compared to PC firing

(i) NOx is generally lower, and the NOx reducing effect by two-stage combustion is larger.

(ii) C% is remarkably lower under the same furnace temperature.

(iii) Under the steady conditions, although the furnace temperature is about 100°C lower, C% remains as large as in PC firing, due to the combustion promotion effect.

(iv) The emission of CO is lower.

(v) The flame appears clear-cut and the amount of soot formed from the volatile matter appears to become smaller.

(c) Effect of CWM properties

(i) Significant differences were not recognized among the four fuels prepared from the same parent coal.

(ii) The unburned carbon in flyash is large under the coarse particles and the high viscosity slurry.

(d) Comparison of experimental C% with the predicted one

(i) Concerning C% of PC firing, the experimental data is in good agreement with the predicted values, which endorses the validity of the prediction.

(ii) Concerning C% of CWM firing, the experimental data is far lower than the predicted values (on the assumption of separating CWM to pulverized coal and water), which suggests the combustion promotion effect of CWM firing.

4. Outlook

We are at present proceeding with construction of a pilot plant exclusively for CWM at the Wakamatsu Power Station of Electric Power Development Co.. The said pilot plant will manufacture CWM at a rate of 1.5 t/h, besides we will jointly construct test equipment for the transport and storage of CWM. By performing the test from fiscal 1983 using this plant and equipment, we are scheduled to not only manufacture CWM, but also to accumulate data concerning handling of CWM.

On the other hand, by testing CWM manufactured at the pilot plant in a large scale combustion test furnace and accumulating data, we should like to make it possible to apply CWM to a real boiler.

References

(1) Essenhigh, R.; "chairman's summaries", Proceedings of the Coal-Water Fuel Technology Workshop, (March 1981), 146.

(2) Kato, K. et al, "Studies on the Unburned Carbon in Flyash with Pulverized Coal Combustion, 1st Report and 2nd Report", Bulletin of the Japan Society of Mechanical Engineers, Ser.B in Japanese, 49-437, (Jan. 1983).

(3) Kamao, M., et al, "Preliminary Test of High-Concentration Coal-Water Slurry", 4th International Symposium on Coal Slurry Combustion, (May 1982).

(4) McHale, E.T. et al, "Combustion of Coal-Water Slurry", Combustion and Flame 45, (1982), 121.

(5) Scheffee, R.S. et al, "Coal-Water Slurry as Utility Boiler Fuel", EPRI CS-2287, Final Report, (March 1982).

(6) Scheffee, R.S. et al, "Further Development and Evaluation of Coal-Water Mixture Technology", 4th International Symposium on Coal Slurry Combustion, (May 1982).

Table 2-1 Operating condition and test results of wet preparation (Bench Scale)

Run No.	1	2		3	
Preparation method	1 stage grinding method	2 stage grinding method		2 stage grinding method	
Coal brand	Tatung Lot No.5612	Tatung Lot No.5612		Tatung Lot No.5612	
Parameters		1st stage	2nd stage	1st stage	2nd stage
Additive brand	"A"	"A"	"A"	"N"	"N"
Additive feed rate kg/H	0.038	0.074	0	0.062	0.062
	Total 0.7% vsC		Total 0.7% vsC		Total 1.0% vsC
Coal feed rate (wet base) kg/H	6.0	8.0	3.4	10.7	2.7
Slurry preparation rate kg/H	8.0	12.6	16.0	15.0	17.7
Results					
Coal concentration (dry base) wt%	66.9	56.3	67.8	66.2	69.6
Viscosity cp	1350	210	1070	540	1520
Flow value	50	57	53	53	39
Tan α in a Rosin Rammler chart	0.87	0.82	0.70	1.09	0.75
Size distribution					
>48 mesh wt %	1.2	0.1	3.5	0.1	1.5
48 ~ 145 mesh wt %	13.3	3.9	14.3	7.1	15.6
145 ~ 200 mesh wt %	10.5	5.4	7.3	11.2	12.0
200 ~ 350 mesh wt %	16.0	12.8	12.0	21.6	9.5
<350 mesh wt %	59.0	77.8	62.9	60.0	61.4
<200 mesh wt %	75.0	90.6	74.9	81.6	70.9

Table 2-2 Analysis of Tatung Coal

		Lot No.5612	Lot No.5707
Proximate analysis ;			
Moisture	%	5.3	6.1
Ash	%	7.9	8.5
Volatile matter	%	26.8	28.0
Fixed carbon	%	60.0	57.4
Fuel ratio	-	2.24	2.05
Ultimate analysis ;			
Carbon	%	76.5	74.3
Hydrogen	%	4.5	4.7
Nitrogen	%	0.84	0.87
Oxygen	%	9.2	10.5
Sulphur	%	0.71	0.61
Calorific value	Kcal/kg	6940	6650
Specific gravity		1.45	1.51
BET Specific surface area	m^2/g	9.7	14.6

Table 2-3 Operation Condition and Operating Data(Pilot scale)

Test Period	1981		1982		
Coal	Tatung coal lot No. 5612		Tatung coal lot No. 5707		
Run No.	211-1	211-2	5704	5713A-1	5713A-2
Grinding Stage	1st	2nd	1st	1st	2nd
Set Value:					
Production rate(T/H)	1.0	1.4	1.2	1.0	1.4
Coal/Water ratio	60/40	68/32	65/35	57/43	65/35
Coal feed rate(Kg/H)	662	320	877	704	467
Water feed rate (Kg/H)	293	-	267	271	-
Slurry feed rate (Kg/H)	-	1080	-	-	933
Additive	"A"	-	"N"	"A"	-
Additive feed rate (Kg/H)	44.6	-	55.2	25.1	-
Operating Data:					
Pulverized coal temp. (°C)	30	30	25	26	27
Water temp (°C)	16	16	26	25	25
Slurry temp. (°C)	33	46	42	53	56
Mill power consumption (KW)	30	30	28.8	29.4	28.0

Table 2-4 CWM Characteristics (Pilot Scale)

Test Period	1981		1982		
Coal	Tatung coal lot No. 5612		Tatung coal lot No. 5707		
Run No.	211-1	211-2	5704	5713A-1	5713A-2
Grinding Stage	1st	2nd	1st	1st	2nd
Coal Concentration(%)	59.9	68.5	65.7	57.6	65.6
Specific Gravity/(°C)	1.17 (27)	1.20 (43)	1.22 (42)	1.19 (42)	1.22 (47)
Viscosity (cP)/(°C)	615 (27)	1560 (43)	336 (42)	270 (40)	1220 (40)
Size Distribution					
<200 mesh	82.06	81.34	75.40	85.55	82.51
> 48 mesh	0.0	0.29	0.71	0.0	1.00
48 ∿ 100 mesh	2.71	4.08	5.69	1.48	4.00
100 ∿ 200 mesh	15.23	14.29	18.20	12.97	12.49
200 ∿ 250 mesh	5.08	4.66	7.96	5.56	6.50
250 ∿ 350 mesh	13.20	10.50	10.34	12.59	10.49
<350 mesh	63.78	66.18	57.10	67.40	65.52

Table 3-1 Analyses of Coal-Water Mixture and Pulverized Coal used for Combustion Test

Fuel	Coal - Water Mixture				Pulverized
	5713A	5714	5715	5717	Coal
Coal concentration [%]	63.8	64.3	64.1	63.4	——
Specific gravity [-]	1.24	1.24	1.23	1.23	——
Viscosity 60rpm [cp]	>2000	834	>2000	401	——
(30 °C) 30rpm [cp]	3300	1025	2847	480	——
Size distribution					
200 mesh pass [%]	78.6	78.4	72.9	64.6	85.0
Rosin const. n [-]	0.89	0.94	0.92	0.88	1.19

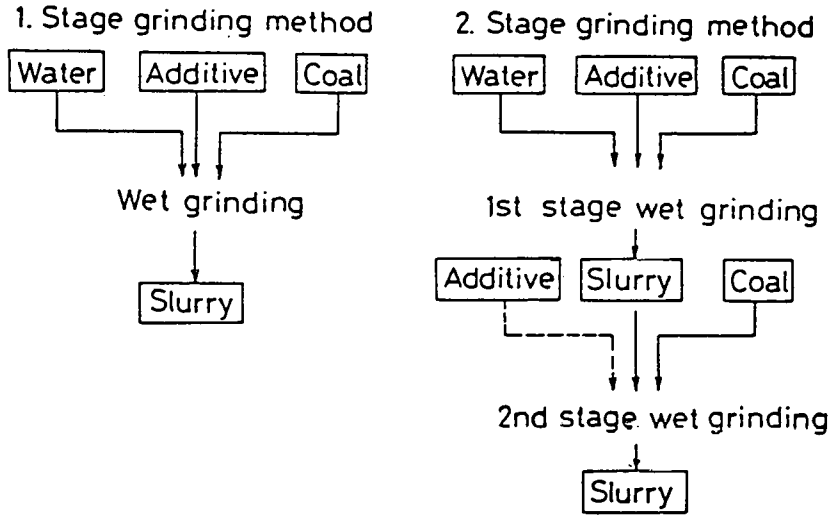

Figure 2-1 Wet preparation process of slurry

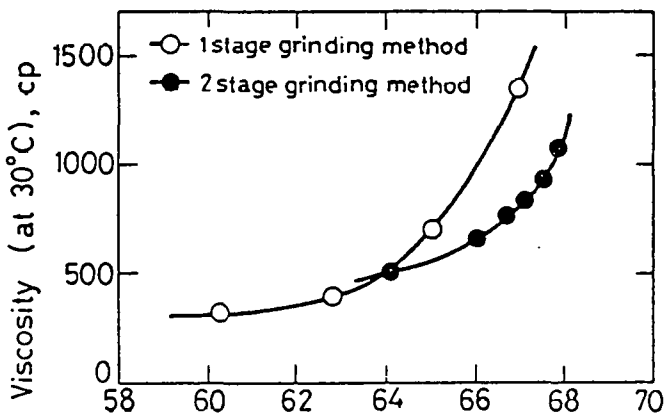

Coal : Tatung Lot No.5612
Additive : "A" 0.7wt%, dry coal base

Figure 2-2 Comparison of 2 stage grinding method with 1 stage grinding method

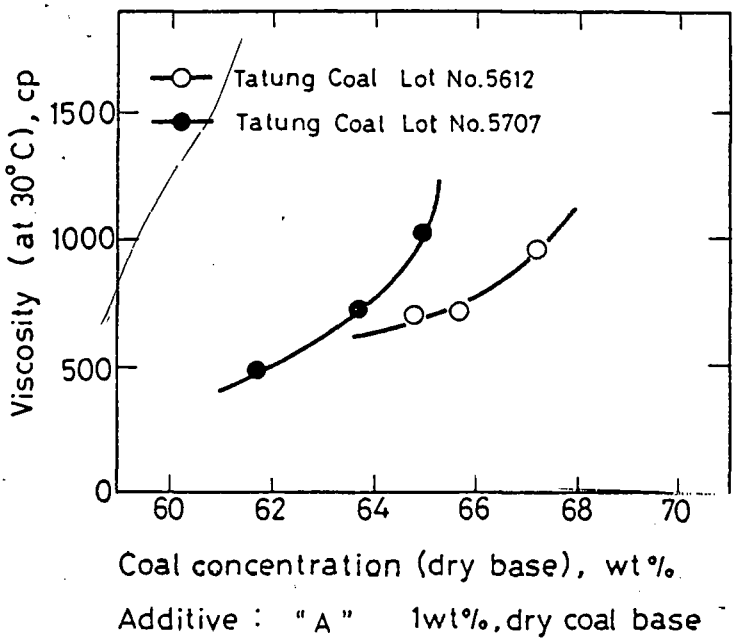

Figure 2-3 Effect of coal properties (1)

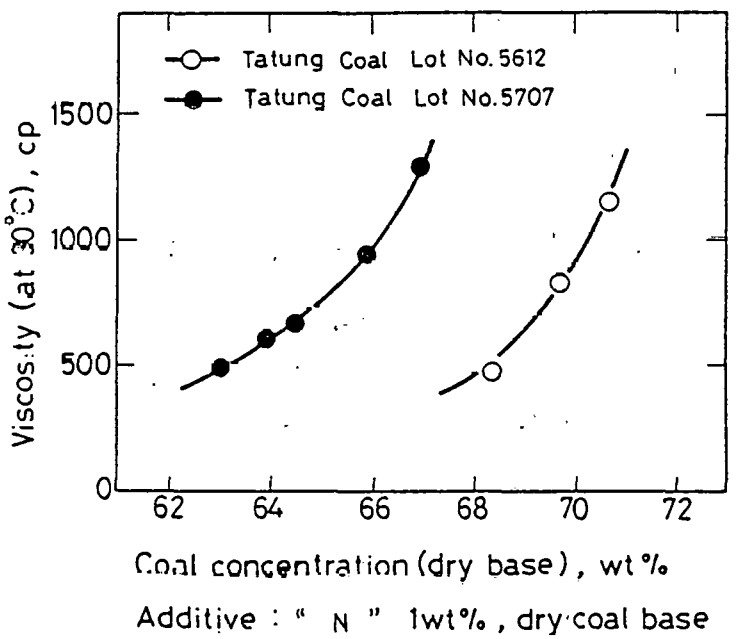

Figure 2-4 Effect of coal properties (2)

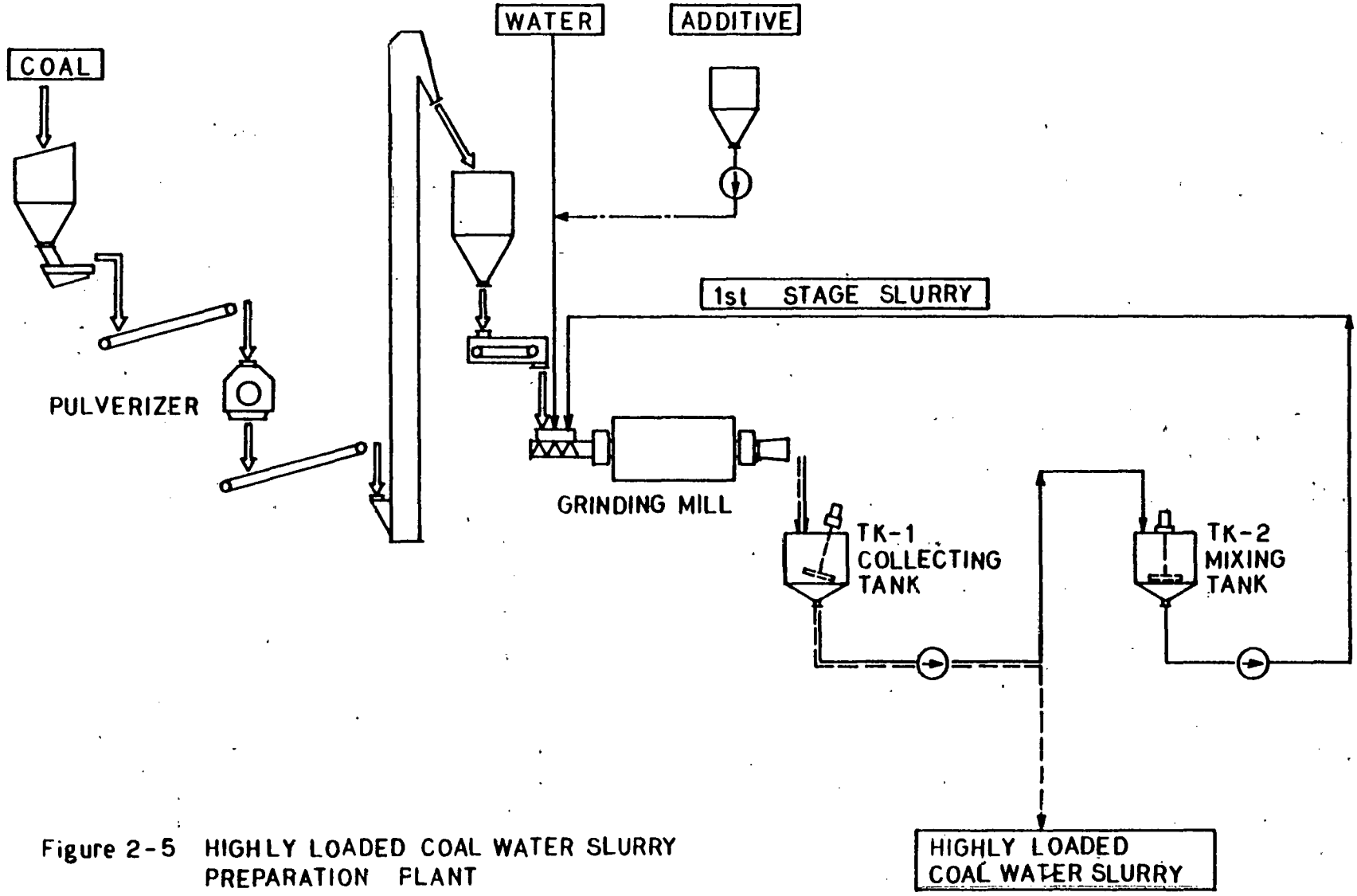

Figure 2-5 HIGHLY LOADED COAL WATER SLURRY PREPARATION PLANT

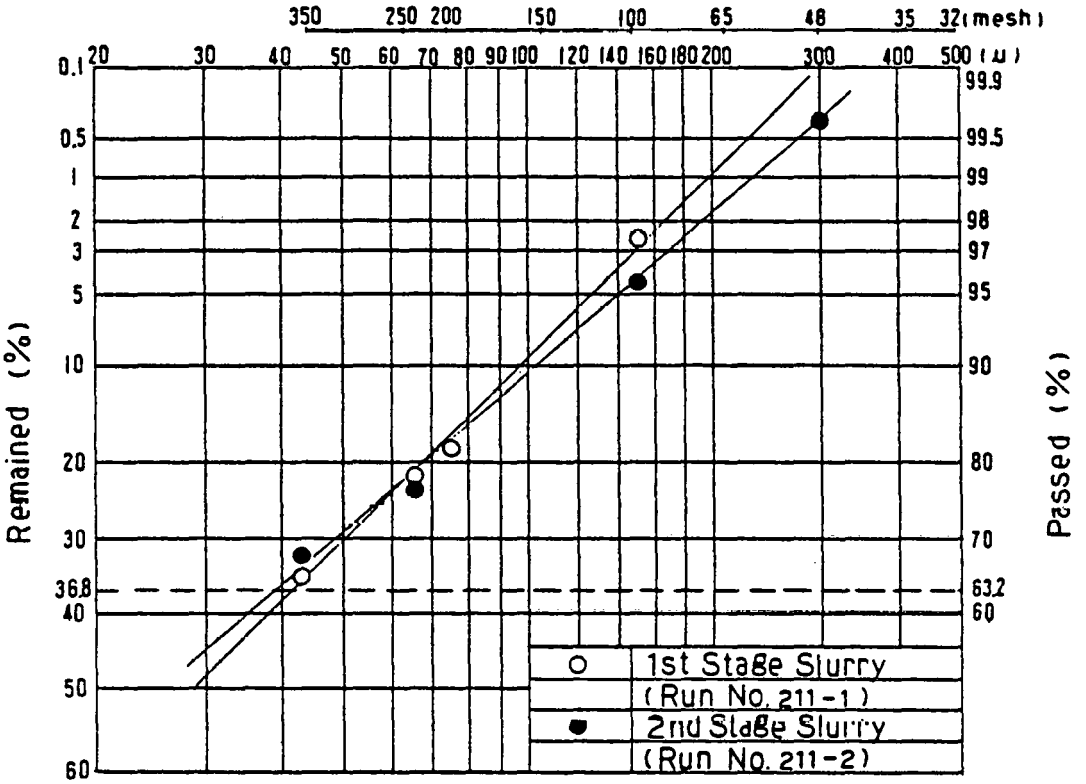

Figure 2-6 Size Distribution of Slurry (1)

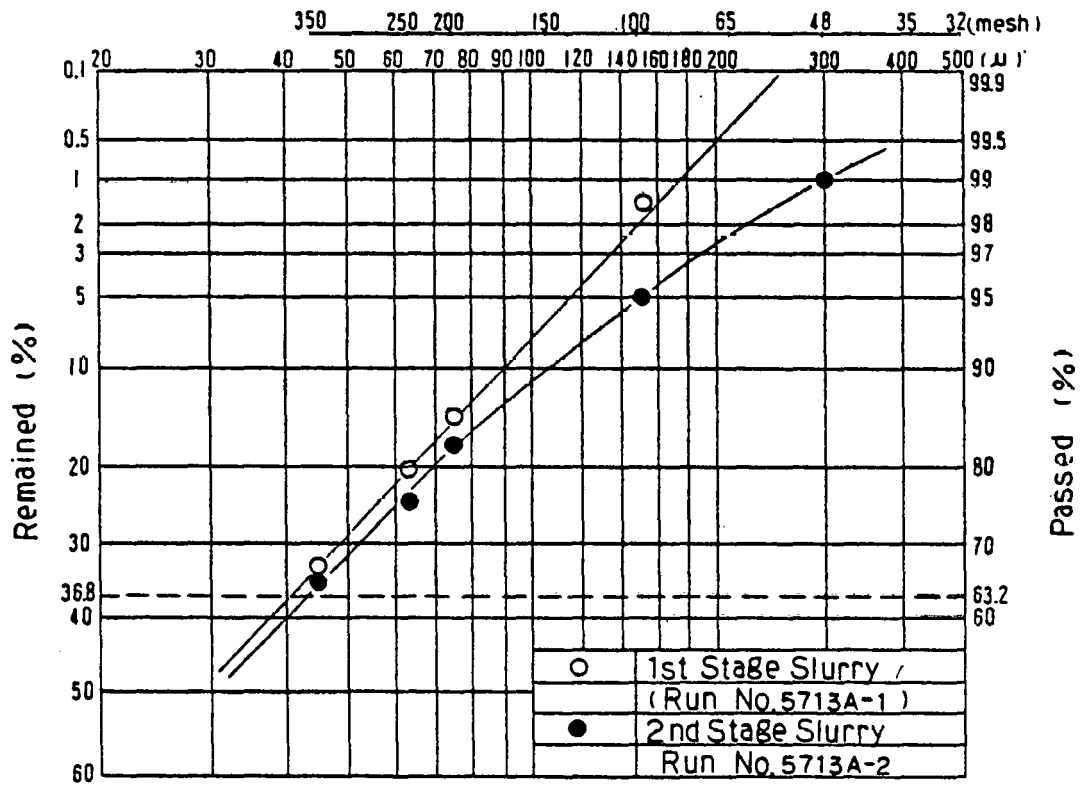

Figure 2-7 Size Distribution of Slurry (2)

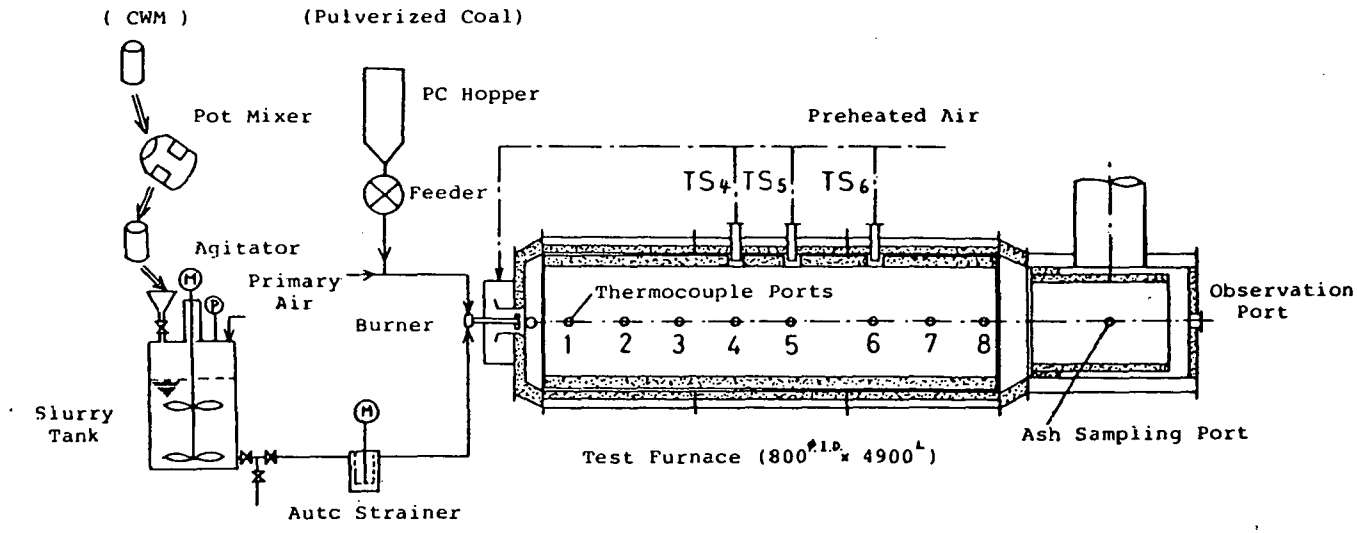

Figure 3-1 Schematic diagram of experimental furnace facility

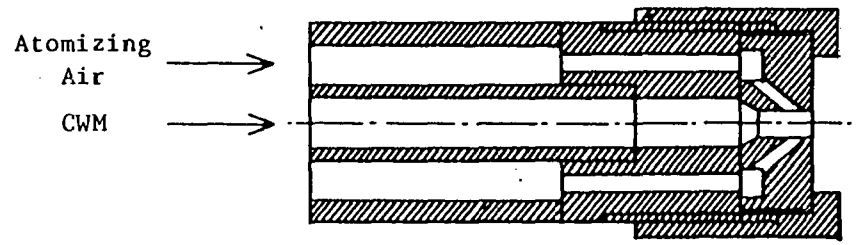

Figure 3-2 Atomizer for Coal-Water Mixture

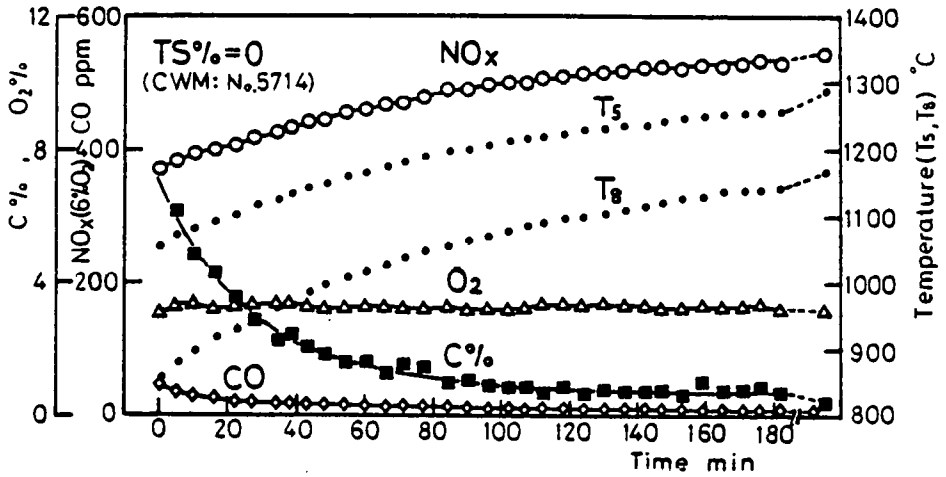

(a) TS%=0

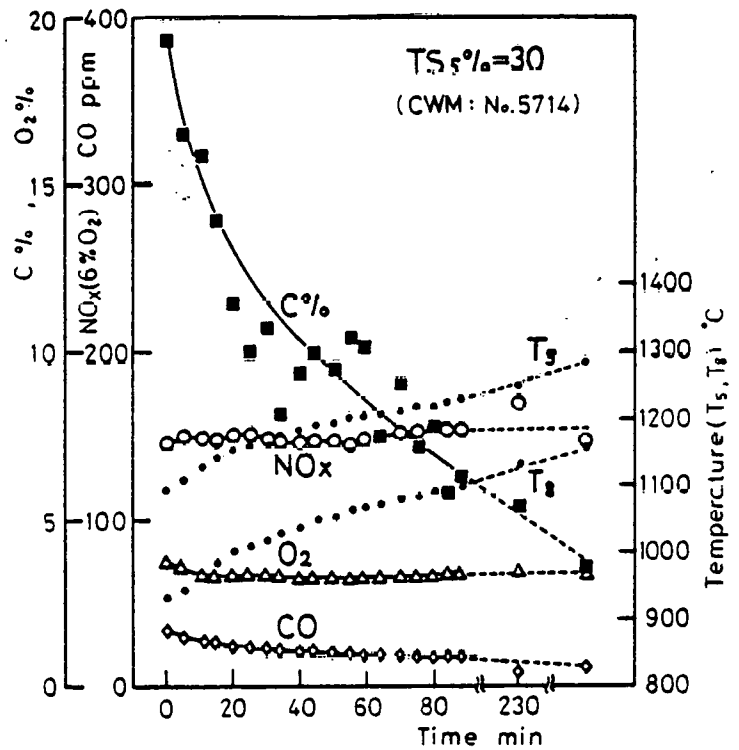

(b) TS_5%=30

Figure 3-3 Variation of furnace temperature and combustion products with CWM firing

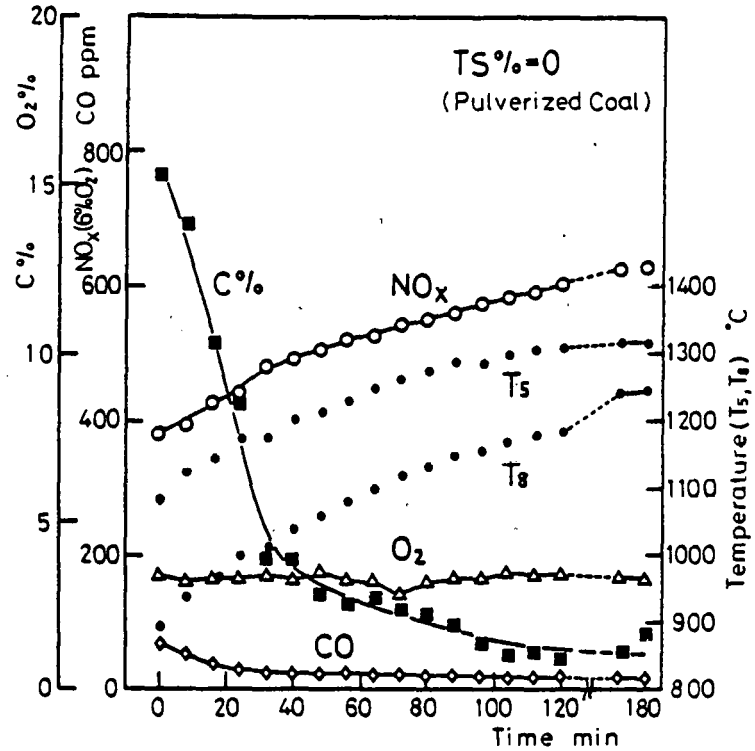

(a) TS%=0

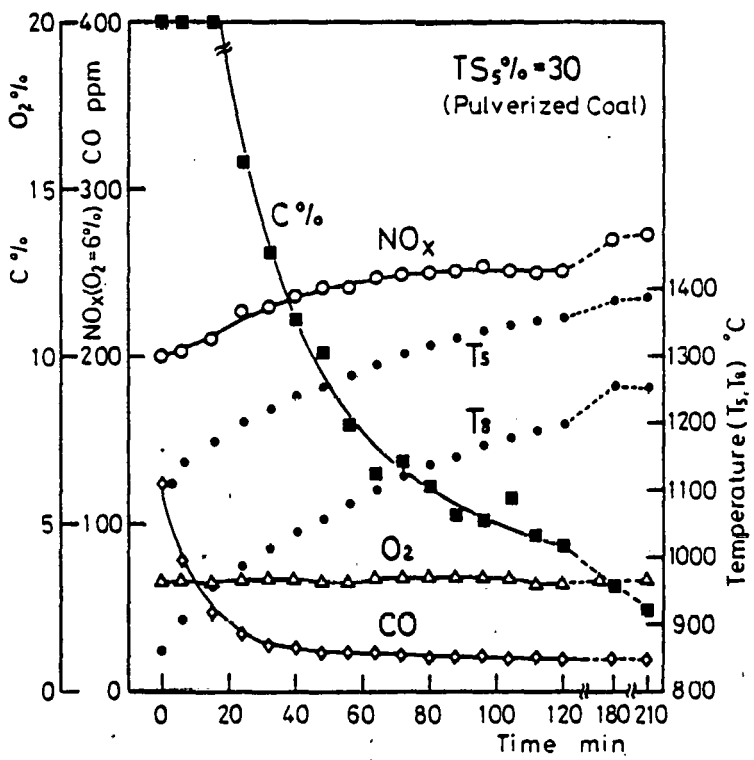

(b) TS_5%=30

Figure 3-4 Variation of furnace temperature and combustion products with PC firing

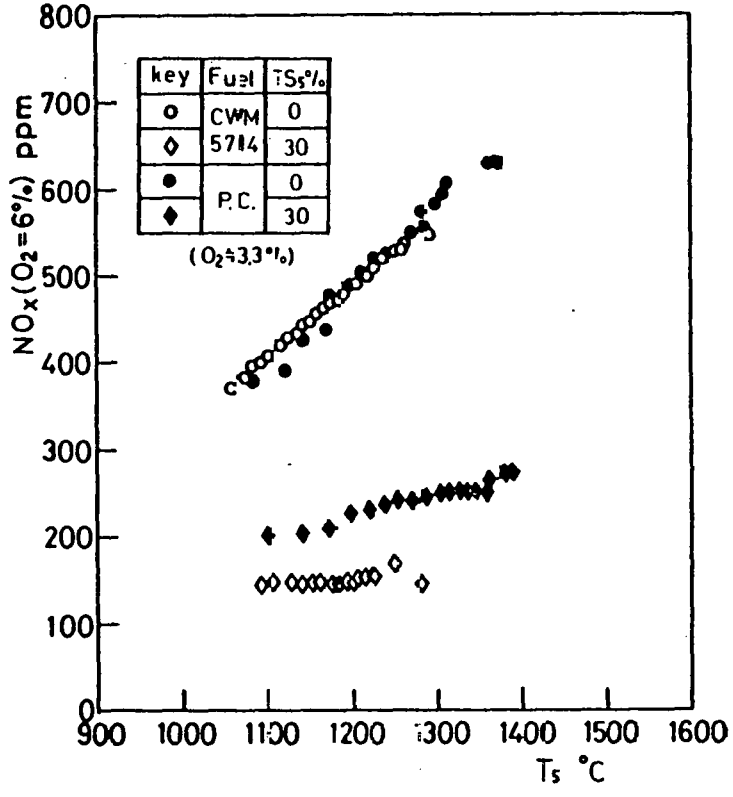

Figure 3-5 Effect of furnace temperature on the NO_x emission

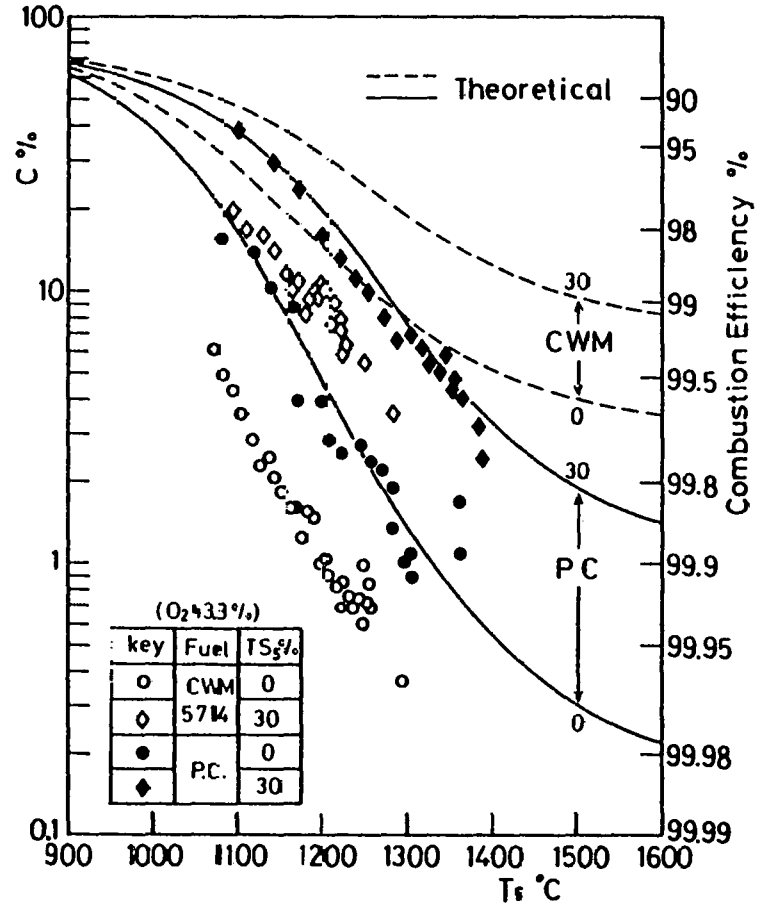

Figure 3-6 Effect of furnace temperature on the unburned carbon in flyash

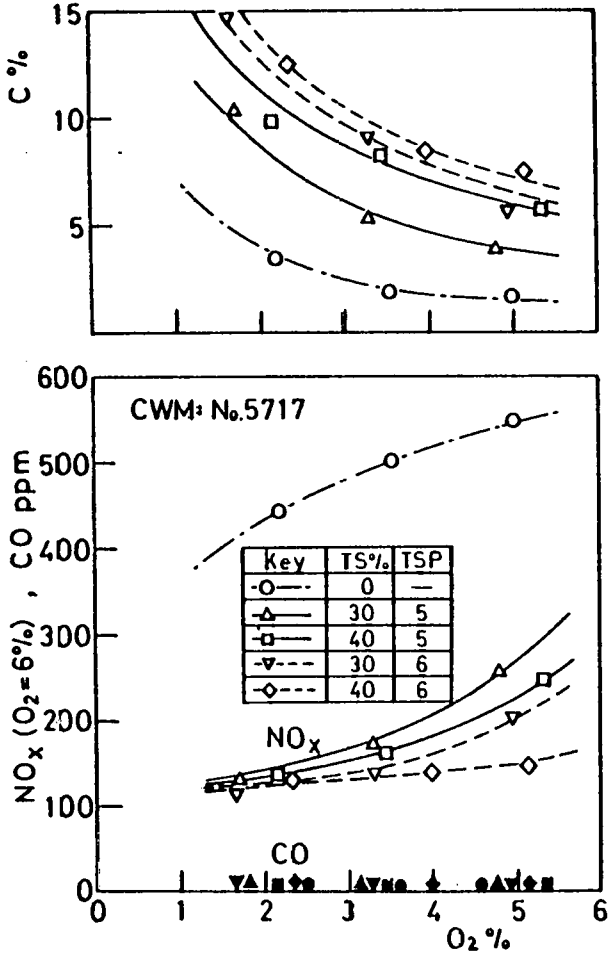

(a) Coal-Water Mixture

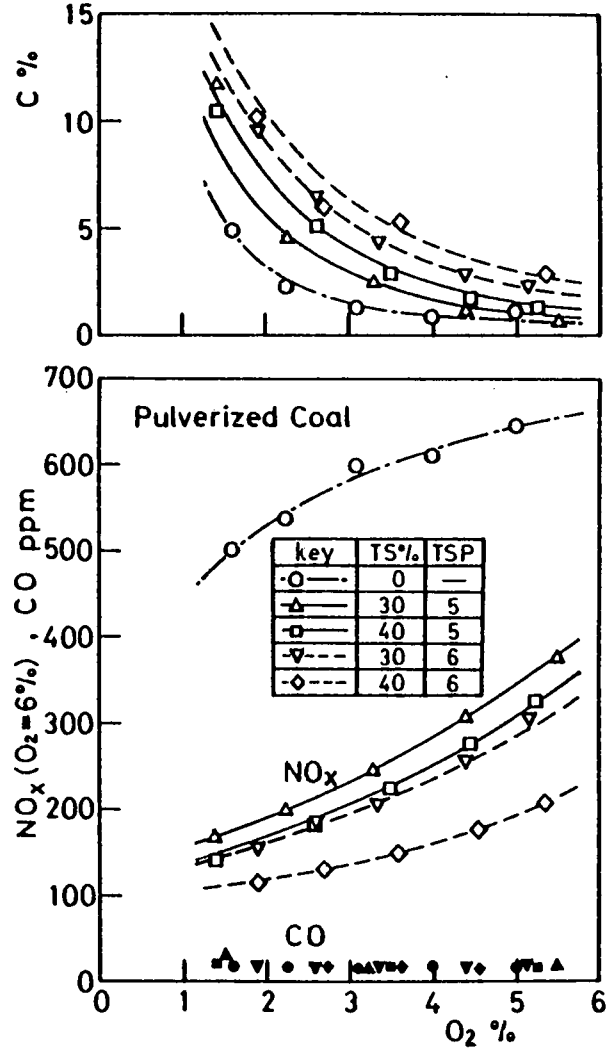

(b) Pulverized Coal

Figure 3-7 Effect of percent O_2 in flue gas on NO_x, CO and C%

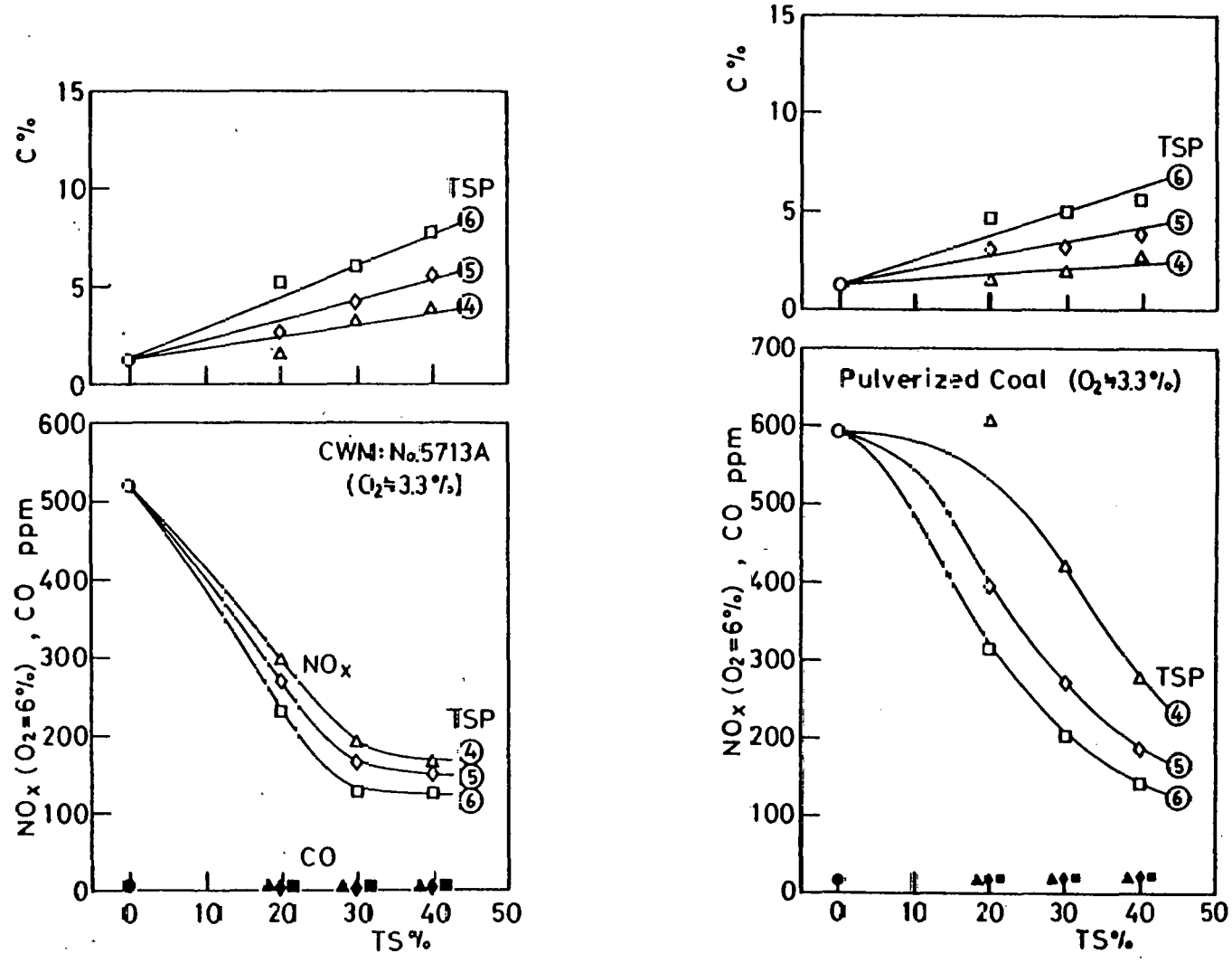

(a) Coal-Water Mixture

(b) Pulverized Coal

Figure 3-8 Effect of TS% and TSP on NO_X, CO and C%

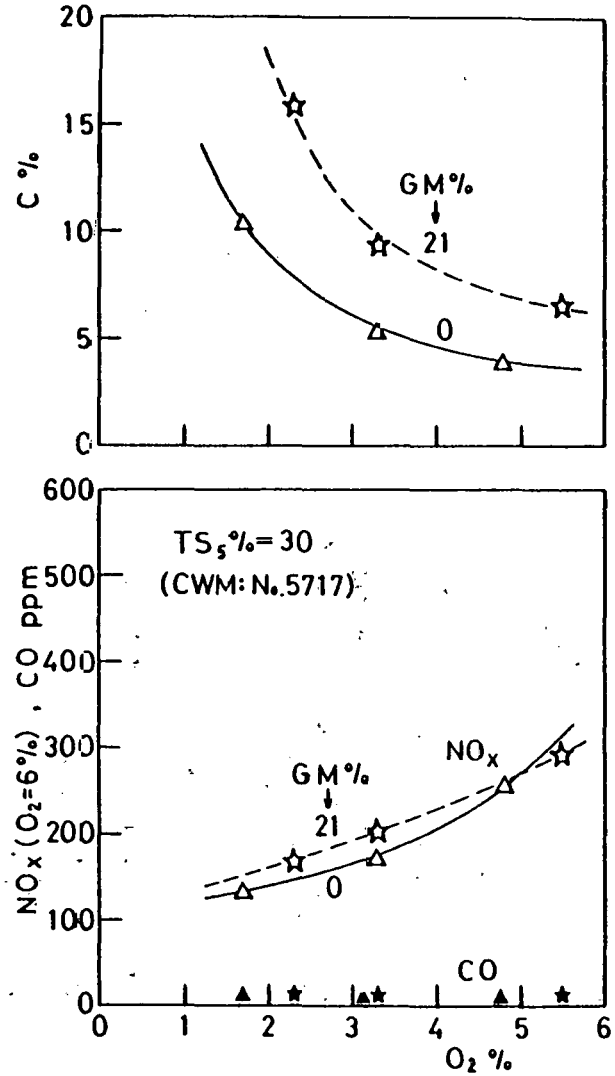

Figure 3-9 Effect of gas mixing on NO_x, CO and C%

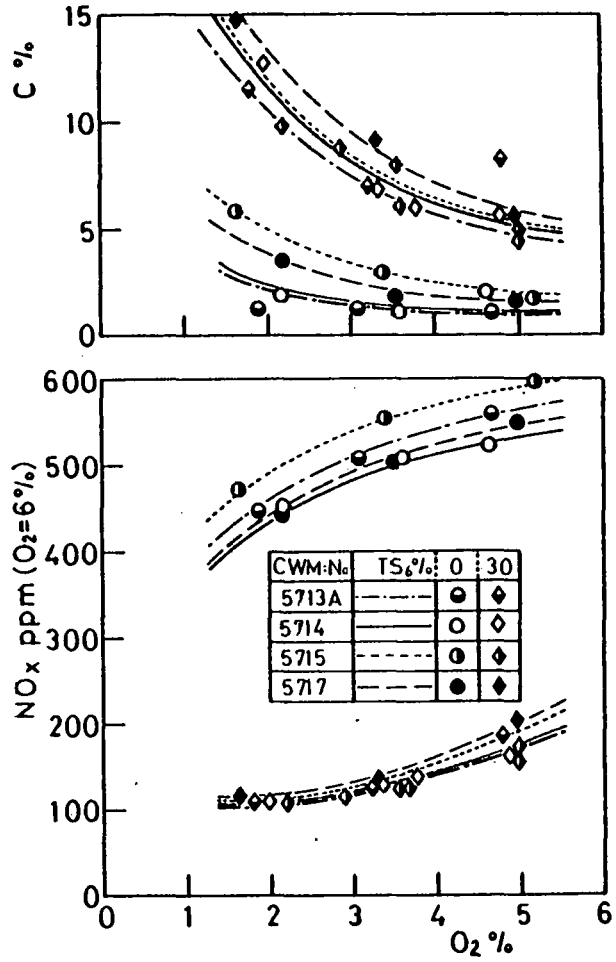

Figure 3-10 Effect of CWM properties on NO_x and C%

COAL SLURRY FUELS: MOVING TOWARD COMMERCIAL UTILIZATION

BY

GARY A. MAIER*, RICHARD E. BARRETT**,
BRUCE W. RISING**, and ROBERT D. GIAMMAR**

* FLORIDA POWER AND LIGHT COMPANY
P. O. Box 14000
Juno Beach, FL 33408

** BATTELLE COLUMBUS LABORATORIES
505 King Avenue
Columbus, OH 43201

CONTENTS

I. Introduction

II. Review of the FPL COM Demonstration

III. Coal-Water Mixture (CWM)

IV. Commercialization of CWM Fuel

V. FPL CWM Research

VI. Battelle Small Scale Combustion Tests

- A. Description of Combustion Test Facility
- B. Data Collection and Analysis
- C. Slurry Fuels Fired
- D. Test Conditions
- E. Results
- F. Conclusions

VII. Areas Requiring Additional Work

- A. Coal Cleaning
- B. Burners
- C. Particulate Control
- D. CWM Compatibility

VIII. Summary

COAL SLURRY FUELS: MOVING TOWARD COMMERCIAL UTILIZATION

BY

GARY A. MAIER*, RICHARD E. BARRETT**,
BRUCE W. RISING**, and ROBERT D. GIAMMAR**

* FLORIDA POWER AND LIGHT COMPANY
** BATTELLE'S COLUMBUS LABORATORIES

INTRODUCTION

Oil price increases and supply manipulations during the past decade have caused large users of fuel oil to search for alternative fuels to fire in existing oil-designed steam generators. In the United States, approximately one-quarter of the fuel oil and natural gas consumed is used for power production in utility and industrial boilers, and for industrial process heat needs.(1)

Florida Power and Light Company (FPL) is one of the largest utility consumers of fuel oil in the United States (40 million barrels in 1981), and consequently, has set a major R&D objective for the 1980's to identify and develop economically and technically sound fuel alternatives. FPL has nine 400 MW and four 800 MW oil designed units which are candidates for conversion to an alternative fuel. Many possibilities have been examined, or are still in the process of being evaluated, including pulverized coal, peat, synthetic gas from coal, synthetic liquids from coal, alcohol mixtures, petroleum coke, coal-oil mixtures (COM), coal-oil-water mixtures (COWM), and coal-water mixtures (CWM).

Coal, which is an abundant domestic fossil fuel, is likely to be the fuel choice for new generating capacity installed during the next several decades. If coal could be successfully burned in existing oil designed boilers, the resultant fuel cost savings might significantly help hold down the cost of generating electricity.

Unfortunately, conversion to pulverized coal (or any other solid fuel) would require major capital expenditures. The liquid fuel feed systems would have to be replaced by solids handling systems. Pulverizers would have to be installed. Storage facilities for large quantities of solid fuel would be required, as well as ash handling equipment, emission control systems, and an infra-structure to transport fuel to generating stations. The additional land which would be required may be difficult to obtain at some candidate conversion sites. Engineering studies have shown that conversion to pulverized coal is not financially attractive at this time.

Many of the above problems would be eliminated if coal could be burned and handled in a liquid form. However, research and development still has a long way to go before synthetic liquids from coal can be made commercially competitive with petroleum fuels.

COAL SLURRY FUELS: MOVING TOWARD COMMERCIAL UTILIZATION

The technology for suspending finely-ground coal particles in a liquid, to produce a stable and pumpable slurry fuel, has been developing rapidly. Such a slurry can be handled, transported, and stored much like conventional liquid fuels, thus requiring less modification of currently used equipment. Slurry fuels can also be commercialized in the near term, because no significant advances in hardware technology are needed to produce utility quantities of fuel.

REVIEW OF THE FPL COM DEMONSTRATION

In a major effort to prove the feasibility of firing coal-oil mixture (COM) in a utility boiler originally designed to burn oil, Florida Power and Light conducted a full-scale demonstration at the Sanford #4 power station from April 1980 to April 1981. The Sanford #4 unit is a 400 MW, Foster Wheeler designed steam generator, fired through 18 burners in a common windbox. The burners are located on the front wall. Soot blowers and wall blowers were installed for the demonstration. A bottom ash removal system was also installed.(4)

The demonstration was a success (4-8). Full load was obtainable while firing COM with coal concentrations up to 42% by weight. FPL is convinced that COM is a technologically feasible alternative to No. 6 fuel oil; however, at present, the fuel cost differential between oil and coal does not appear sufficient to justify the facility investment and extra operating cost necessary to continue COM firing on a regular basis. Future use of the COM alternative is an economic and/or strategic decision to be made at FPL's top management level.

COAL WATER MIXTURE (CWM)

Coal-water mixtures are now being evaluated as an alternative to No. 6 fuel oil in oil-designed utility boilers. The fuel is prepared by suspending finely ground coal in water and adding various chemical additives to improve stability and viscosity. A typical CWM fuel consists of 70% coal, 29% water, and 1% chemical additives. Coal particle size control can also be used to increase solids loadings and reduce viscosity. CWM boiler fuel should not be confused with coal-water slurry for pipeline transportation, which generally consists of coarsely ground coal, not more than 50% solids by weight. The high solids loading of CWM boiler fuel produces viscosities one or more orders of magnitude greater than those of dilute transportation slurries. Pipeline transportation of CWM fuel for more than a few miles would be economically unattractive.(2)

Preliminary economics comparing CWM with COM for oil backout have shown CWM to be more attractive(3). On an energy basis, $/MM BTU, coal is presently a cheaper fuel than No. 6 fuel oil, and therefore, should be utilized to the greatest extent possible in any fuel mixture. A relatively simple calculation will show that in a COM fuel with 50% coal by weight only about 40% of the total energy is supplied by the coal. With CWM fuel, 100% of the energy is supplied by the coal. In addition, the energy penalty due to the presence of water in the fuel is surprisingly small, somewhere between 3 and 5% depending on solids loading and energy content of the coal.

CWM also appears to have some technical advantages over COM. For example, the lower flame temperature obtained due to the presence of water in the fuel helps to reduce formation of NO_x (1 and 9). The lower temperature also helps to reduce slagging. In addition, CWM may benefit from a reduced slagging potential when compared with COM because some suspected detrimental synergistic effects of combining oil ash and coal ash are avoided.

For the above reasons, CWM has now become the primary focus for fuels research at Florida Power and Light.

COMMERCIALIZATION OF CWM FUEL

At present, CWM fuel is not available to utilities in commercial quantities. Pilot production facilities have been built which are capable of producing industrial scale quantities. It is conceivable that enough fuel could be accumulated over time to run some utility tests, however, they would necessarily be short tests.

The commercialization of CWM presents a dilemma to both utilities and potential fuel suppliers. Large utility users are not readily willing to sign a long term fuel agreement until all technical and economic issues have been resolved by a full scale utility demonstration. Conversely, a potential CWM supplier is not readily willing to build a utility scale fuel preparation facility without the security of a long term contract. FPL believes that a solution to the quandary can be found, and will require an equitable distribution of risks and rewards among all parties.

FPL CWM RESEARCH

Florida Power and Light has been following the development of CWM fuel for a number of years, and has been directly active in CWM research work since mid-1981. In an important program sponsored by FPL, Battelle Columbus Laboratories has recently completed laboratory scale (700,000 BTU/HR) combustion tests of five CWM fuels. These tests are described in more detail below.

FPL has co-sponsored work at the Massachusetts Institute of Technology to conduct an in-depth evaluation of CWM combustion. These tests are designed to facilitate detailed measurements of flame properties while acquiring accurate combustion and heat transfer data.

FPL is active on the advisory committee for the Adelphi University loop testing program. The objective of this program is to test CWM fuels under extreme pumping conditions, and also to obtain erosion and corrosion data. Some burner pump wear was experienced during FPL's COM demonstration, and it is expected that pump wear with CWM will be worse due to the relatively higher abrasive characteristics of the fuel.

BATTELLE SMALL SCALE COMBUSTION TESTS

The goal of the fuel evaluation trials performed by Battelle was to identify potential problems related to the use of CWM fuels in conventional utility boilers. To accomplish this goal, Battelle conducted combustion tests in a refractory-lined furnace designed to fire solid, liquid, and gaseous fuels and solid-liquid dispersions. The furnace and downstream ducting were designed to simulate the furnace and convection regions of a utility boiler.

Description of Small-Scale Combustion Facility

The tests were conducted in Battelle's Multifuel Furnace. Figure 1 is a schematic drawing showing the arrangement of components for this facility.

Furnace. The Multifuel Furnace is a refractory-lined, cylindrical, horizontal furnace. The internal dimensions of the unit are 24 inches diameter and 60 inches long. The furnace is designed to give a residence time of about 1.0 second when fired at 60 lb/hr; at these conditions the furnace outlet temperature is about 2100° F. The outer construction of the furnace consists of a water-cooled steel shell. The furnace is equipped with 8 viewing ports.

Fuel is fed into the furnace through a two-fluid external atomizing nozzle inserted through the burner. Combustion air is supplied to the furnace through the water-cooled burner. Movable vanes are incorporated such that various degrees of swirl may be induced to the combustion air. Atomization and combustion air are supplied to the furnace from a compressed air system; combustion air can be preheated to 500° F using an electric heater.

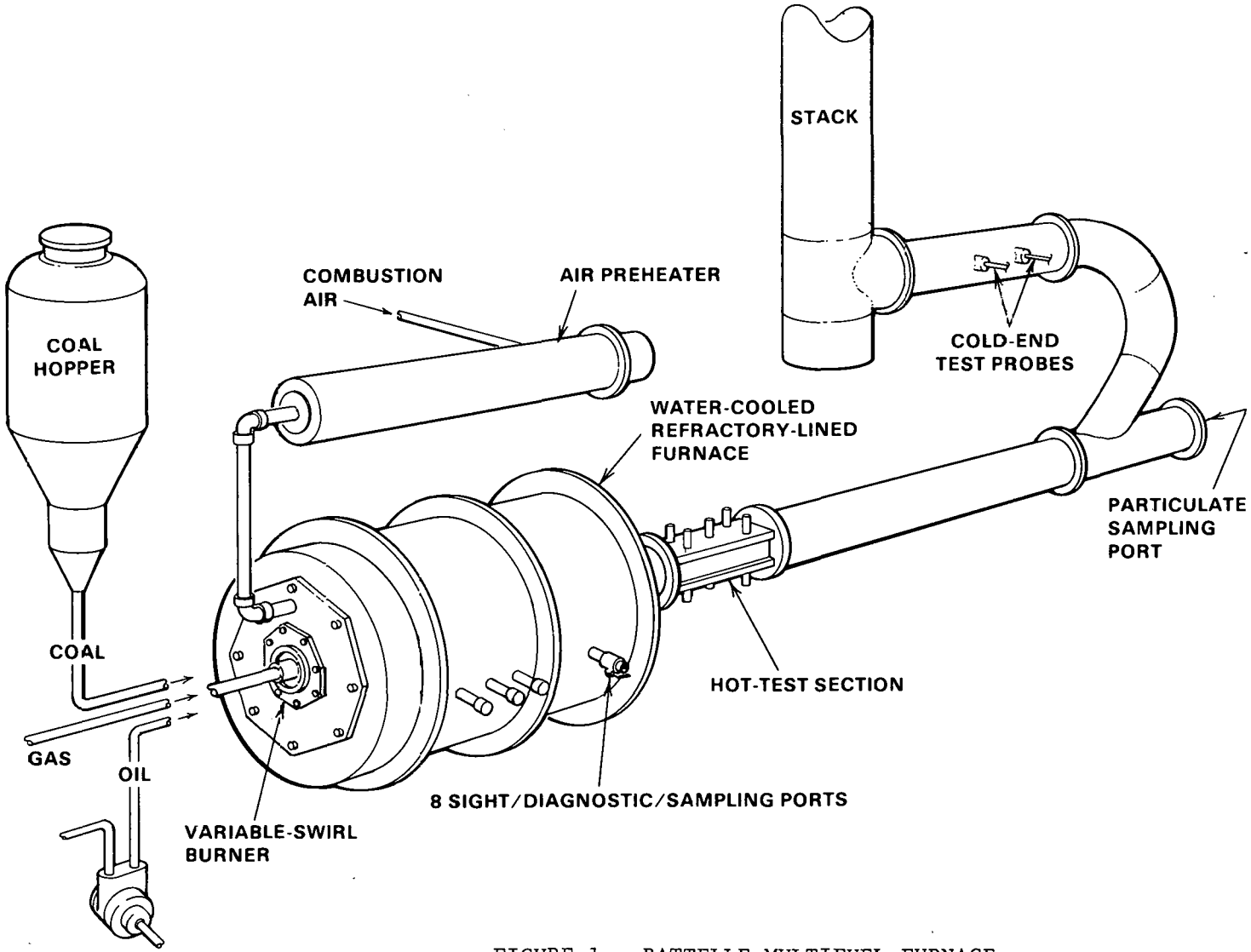

FIGURE 1. BATTELLE MULTIFUEL FURNACE

Fuel Feed System. Pumping slurry fuels presented some difficulties. Initial efforts to use a gear pump and a progressive cavity pump were unsuccessful. Replacement of these pumps with a different model of progressive cavity pump with a larger stator cavity permitted the slurries to be fed to the Multifuel Furnace without difficulty. The COM was preheated to 180° F for firing while the CWM fuels were fired at room temperature.

Care was taken to eliminate sharp bends from the fuel feed lines as such bends increase flow resistance.

Deposit Probes. During fuel evaluation tests, probes were maintained at sites that were intended to be representative of heat-exchanger surfaces within a utility boiler. The probe locations and their boiler analogs are:

Laboratory Furnace	Utility Analog
In-furnace probe	Wall tubes
High-temperature test section	Superheater tubes
Low-temperature test section	Air preheater surface

The probes were maintained at selected temperatures by air cooling.

The in-furnace probe was inserted transversely across the furnace and maintained at approximately 750° F. This probe was intended to collect deposits representative of those that might form on the wall tubes in a utility boiler. The in-furnace probe was a 1-inch diameter tube 4 feet long.

Five simulated superheater test probes were placed in a test section located immediately downstream of the furnace exit. The gas temperatures and velocities in this test section were selected to simulate conditions found in the superheater region of a boiler. The five probes were vertically oriented and were located in 3 rows, 8 inches apart. The tubes were maintained at the following temperatures:

Tube Row	Metal Temperature, F
1	1100°
2	1000°
3	900°

During a test, the metal temperatures fluctuated about 50 to 100 degrees F because of changes in fuel and air feed rates. (For example, the fuel feed rate could change if the nozzle became momentarily plugged.) The probes located in this test section usually collected the largest quantity of deposits.

A low-temperature probe was located in the stack where gas temperatures were less than 600° F.

The stainless steel tube was maintained at a metal temperature between 300°F and 450°F. This probe was intended to simulate the heat-exchanger surface found in the air preheater section of a boiler.

Data Collection and Analysis

A large volume of recorded data and samples was collected during an average six hour test. Much of the data was collected electronically, stored on magnetic tapes, and processed on a minicomputer. These data included:

- o O_2 (vol percent); paramagnetic analyzer
- o CO_2 (vol percent); nondispersive infrared (NDIR) analyzer
- o SO_2 (vol ppm); electrochemical cell or NDIR analyzer
- o NO/NO_x (vol ppm); chemiluminescent analyzer
- o Air preheat temperature
- o Furnace exit gas temperature
- o Probe temperatures

In addition to the above, the following data was taken manually to monitor combustion conditions:

- o Air feed rate
- o Fuel feed rate
- o Atomizing air pressure
- o Burner swirl setting.

Non-quantitative assessments of furnace operating conditions were also made during and after each test. Observations included:

- o General flame characteristics
- o Presence or absence of combustion chamber sparklers
- o Ease of fluid handling
- o Appearance of deposits on furnace walls.

Probe Analysis. After the probes were removed from their ports at the conclusion of a test, they were photographed. Ash samples were taken from the probes and the furnace walls for chemical analysis.

Fly Ash Samples. Fly ash samples were collected using EPA Method-5 procedures and were analyzed gravimetrically to determine total particulate emissions factors. Samples were also chemically analyzed to determine the carbon content of the particulate material and to permit calculation of combustion efficiency.

Slurry Fuels Fired

One coal-oil mixture, one coal-oil-water mixture, and five coal-water mixtures were test fired. The COM was a duplicate of the fuel burned during FPL's demonstration at Sanford; it was used as a baseline fuel due to the previous experience of firing it in a large boiler.

Table 1 gives the analyses of the COM and the CWM's fired in this project.

Some CWM's exhibited problems related to fuel preparation, such as:

- o Fuel inconsistent from drum to drum
- o Some oversize particles (approaching 1/8 inch) in the fuel
- o Settling of particles.

The first two problems relate to quality control in CWM production. It is envisioned that these problems can be eliminated with modest efforts.

Regarding settling, most of the slurries tended to suffer from particle settling after standing for any length of time. On standing for short periods, say, one month or less, the settled particles could be redistributed by stirring. On standing for longer periods, some CWM fuels tended to form a hard layer of solid at the bottom of the drum; these hard accumulations of solids could not be redistributed with reasonable stirring efforts.

Test Conditions

During a test, the furnace operating conditions were chosen to produce flame temperatures and flue gas compositions similar to conditions encountered in normal utility operations. Table 2 lists the combustion test conditions for the firing of each fuel ie.firing rate, O_2 and CO_2 in flue gas, and furnace exit temperatures. The firing rates varied from 612,000 to 747,000 BTU/hr. Excess air was maintained at about 25 to 30 percent, while furnace exit gas temperatures were maintained at 2100° F $\pm$ 100° F.

Results

Quantitative results were obtained for

- o Fly ash emissions
- o Carbon in fly ash
- o Combustion efficiency
- o Gaseous emissions

Qualitative results were obtained for

- o Fuel stability
- o Fuel handling and pumping
- o Atomization
- o Flame stability
- o Ash deposition.

Table 2 summarizes the emissions data.

COAL SLURRY FUELS: MOVING TOWARD COMMERCIAL UTILIZATION

TABLE I. ANALYSES OF SLURRY FUELS

	COM[a]	CWM-A	CWM-B	CWM-C	CWM-D	CWM-E
Proximate Analysis, wt. percent						
Moisture	3.00	29.95	31.46	32.34	30.08	31.01
Ash	3.23	4.64	5.71	1.34	1.46	4.17
Volatile	--	20.54	23.65	26.93	25.43	22.95
Fixed Carbon	--	44.87	39.1	39.38	44.04	41.87
Ultimate Analysis, wt. percent						
Moisture	3.00	29.95	31.46	32.34	30.08	31.01
Carbon	79.86	57.37	51.99	56.23	60.03	56.43
Hydrogen	7.46	3.56	3.58	3.86	3.91	3.64
Nitrogen	1.38	1.09	0.92	1.06	1.13	1.01
Chlorine	0.06[b]	0.05	0.13	0.10	0.10	0.16
Sulfur	1.25	0.53	0.56	0.76	0.67	0.58
Ash	3.23	4.64	5.71	1.35	1.46	4.17
Oxygen	3.82	2.81	5.63	4.30	3.63	3.00
Ash Analysis, wt. percent[c]						
SiO_2	47.30	52.64	58.90	39.49	35.05	47.73
Al_2O_3	31.53	27.14	26.01	26.25	18.32	33.26
TiO_2	1.39	1.40	1.50	1.60	1.41	2.32
Fe_2O_3	8.66	10.04	8.58	20.18	36.47	7.99
CaO	2.70	1.87	1.72	3.92	1.59	3.13
MgO	1.48	1.21	0.84	0.88	0.99	0.86
K_2O	2.28	2.01	2.10	1.25	1.19	1.32
Na_2O	0.83	1.27	0.32	1.19	1.20	0.43
Heating Volume, Btu/lb	16,351	10,203	9,465	10,106	10,820	10,133
Slagging Index	0.25	0.15	0.13	0.46	0.71	0.14
Fouling Index	0.17	0.25	0.05	0.49	0.91	0.08
Free Swelling Index	--	8	3	6.5	8.5	8.0
Fusion Temperature, F						
Oxidizing						
IT	2800+	2320	2635	2300	2070	2700+
ST	2800+	2700+	2700+	2540	2620	2700+
HT	2800+	2700+	2700+	2590	2670	2700+
FT	2800+	2700+	2700+	2700+	2700+	2700+
Reducing						
IT	2660	2270	2592	2250	1910	2700+
ST	2800+	2650	2700+	2400	2150	2700+
HT	2800+	2700	2700+	2440	2200	2700+
FT	2800+	2700+	2700+	2540	2520	2700+

(a) Oil in COM contained 200 ppm vanadium.
(b) Chlorine analysis calculated from coal value (0.14 percent).
(c) Ash analysis for COM is for coal only, not the COM.

TABLE 2. COMBUSTION CONDITIONS AND EMISSIONS FOR SLURRY TESTS

Fuel	COM[(a)]	CWM-A	CWM-B	CWM-C	CWM-D	CWM-E
Firing Rate, Btu/hr	624,000	612,000	650,000	698,500	747,000	715,000
Mean Furnace Exit Gas Temperature, F	2150	2150	2140	2070	2070	2030
Flue Gas Conditions,						
O_2, percent	5.3	4.3	4.1	4.8	4.8	4.9
CO_2, percent	12.6	14.8	15.6	14.7	14.9	13.9
Excess Air, percent	32	25	24	29	29	29
Mean Gaseous Emissions, ppm[(b)]						
CO	34	67	69	245	153	115
SO_2	804	193	511	689	481	487
NO_x	476	501	582	732	620	567
Gaseous Emissions, lb/10^6 Btu						
SO_2	0.49	0.45	0.47	0.53	0.53	0.45
NO_x	1.75	--	0.88	1.2	0.89	0.82
Particulate Emissions						
Grains/dscf at 3% O_2	1.0	1.1	0.42	0.47	0.73	1.2
lb/10^6 Btu	1.6	1.5	0.54	0.58	0.99	1.5
Carbon Content of Fly Ash, percent	--	23	6	30	37	39

(a) Fired with fuel preheated to 140 F. (b)Corrected to 3 percent O_2.

Gaseous Emissions. Emissions of SO_2 (corrected to 3 percent O_2) for CWM firing ranged from 193 to 689 ppm. Most tests gave values for SO_2 emissions corresponding to 74 to 88 percent conversion of fuel sulfur to SO_2. For one test, the SO_2 emission was significantly below the theoretical SO_2 emission value calculated from fuel sulfur. The reason for this low SO_2 emission value is not known, although an instrument problem is a possibility.

Emissions of NO_x (corrected to 3 percent O_2) for the CWM tests ranged from 501 to 732 ppm. Comparing the measured NO_x emission values to the fuel nitrogen, and ignoring thermal NO_x, it was determined that the NO_x represented conversion of 22 to 33 percent of the fuel nitrogen. Nitrogen conversion values in this range are typical of such values for coal-fired power plants.

Carbon monoxide emission values generally were low for the five CWM's tested. Average CO emissions ranged from 50 ppm to 225 ppm. Although normal CO emissions were low during CWM firing, there were brief periods of higher values (500 to 2000 ppm) for most fuels; these peaks were often associated with disruptions in fuel flow, such as momentary nozzle plugging.

Particulate Emissions. Particulate emission values are somewhat difficult to evaluate when conducting small-scale combustion studies. One reason for this is that all parameters cannot be modeled when designing a small-scale combustor to simulate large boilers. Generally the practice is to model temperatures and residence times and to sacrifice on gas velocity, reducing real gas velocities in the test combustor to about 5 feet per second versus 50 feet per second for large boilers. Unfortunately, reducing gas velocities in test rigs permits ash particles to settle out of the flue gas before exiting the furnace.

Secondly, and maybe more importantly, the high surface to volume ratio of small combustors permits a much greater loss of particulate on furnace walls, especially if the ash has a low ash-softening temperature. Typically, small pulverized coal combustors retain 40 to 60 percent of the coal ash in the combustor.

The particulate emission values measured during the fuel tests (measured downstream of the high-temperature deposit test section) ranged from 0.5 to 1.5 $lb/10^6$ BTU. These emissons are equivalent to 9 to 73 percent of the ash in the fuel, with three tests giving fly ash emissions of 38 ± 6 percent of the fuel ash. Some of the fly ash emission samples contain appreciable carbon. Reducing the particulate values for their carbon contents, the ash emission values were 0.5 to 0.9 $lb/10^6$ BTU, which represents 8 to 46 percent of the ash in the fuel.

Combustion Efficiency. Combustion efficiency was determined by analyzing fly ash collected in particulate samples for carbon content, and comparing the carbon particulate to the quantity of carbon fired. Combustion efficiency values determined in this way ranged from 98.9 to 99.9 percent. These values compared well to values for pulverized coal fired power plants, which range

from 99.0 to 99.9, with most values between 99.3 and 99.9 percent. Thus, the CWM fuels fired in these tests gave good combustion efficiencies and the presence of 30 percent water was not detrimental to carbon burnout.

Although combustion efficiency is acceptable from consideration of its impact on boiler efficiency, other factors need to be considered. Because the ash contents of the fuels are low, firing with even high combustion efficiency can produce a fly ash with 30 percent carbon or more. For example, three fly ash samples collected in this program contained 30 to 40 percent carbon. High carbon fly ashes can be difficult to collect in electrostatic precipitators due to low resistivities. Also, accumulations of deposits containing 30 percent carbon downstream of the furnace (e.g., in economizer hoppers, air preheaters, particulate control devices, etc.) could represent a significant fire safety problem for power plants.

Fuel Stability. One of the major factors in CWM fuel formulation is the selection of stabilizing additives. The problem of creating stable slurries is compounded by the fact that additives that increase stability are also likely to increase fuel viscosity, making the fuel difficult to pump and atomize. Also, the additive may be a significant part of the fuel cost and, hence, there is interest in minimizing the quantity of additive used.

Most CWM's evaluated in the laboratory trials showed evidence of coal particle settling, frequently within a few days. Major particle settling was observed after a few months with all but one. However, a major observed difference between the fuels was whether the settled particles could be reentrained by physical mixing (stirring) or whether a hard, concrete-like deposit formed at the bottom of the drums. The best fuels could be stored for two to three months with only moderate settling and the settled particles could be dispersed by stirring.

A one to two month stability for CWM fuel is likely to be satisfactory for most utility operations. However, in unusual circumstances (e.g., a strike by those delivering the fuel, or failure of a major plant component causing a long-term outage) this stability might not be adequate. It might be necessary to consider using minimum amounts of additives on a routine basis and using more additives when necessitated by other events.

Fuel Handling/Pumping. Pumping CWM presented some difficulty. Gear pumps, which were adequate for feeding No. 6 fuel oils to the laboratory furnace, could not be used. A progressive cavity pump successfully handled COM, but could not pump CWM. Finally, a progressive cavity pump with a larger stator cavity successfully pumped each of the CWM fuels. Stator and rotor wear was not evident after several hundred hours of pumping. However, seal and bearing wear was significant, requiring replacement every 75 hours.

The various CWM fuels exhibited significantly different flow resistance in the fuel feed lines and nozzle. One slurry could be fed to the furnace and

atomized at a fuel pressure of 50 psi, while another fuel required 215 psi to feed at the same rate. Diluting the slurries to lower solids contents reduced fuel feed pressures somewhat (e.g., 215 psi at 70 percent solids and 180 psi at 67 percent solids).

Atomization. Atomization was somewhat of a problem, complicated by the small scale at which the work was done. The nature of the fuels, having entrained particles and higher viscosities than conventional liquid fuels, made them somewhat difficult to atomize. Also, FPL's experience with COM suggested that nozzle wear can be a significant problem. Hence, a two-fluid, external mixing nozzle was designed for use on this program. The nozzle produced reasonably good atomization, however, a significant number of large agglomerates were present in the fuel sprays. Observation of agglomerates by spraying onto a target and by viewing droplet impacts on the furnace walls (where large fuel droplets appeared as momentary black spots against the bright refractory background) showed that droplets of 1/8 inch diameter, or larger, formed for some fuels. The number and size of the agglomerates was a function of fuel properties with the less viscous fuels producing fewer and smaller agglomerates. Better atomization probably could have been achieved with a greater effort on atomizer development, however, atomizer development was not a major objective of this project.

Flame Stability. Flame stability is inherent when firing into a furnace having a refractory lining that reaches high temperatures (1600 ^{o} F). The refractory surface temperature is sufficient to promote ignition and flame stability, and will even cause reignition if the flame is lost due to a brief interruption in fuel flow. However, even within such a furnace some inferences can be made of flame stability by observing the stability of the flame front near the burner and by observing the flame for pulsations or other signs of instability. Observation of flames showed that the flame front was located farther from the burner for CWM firing, than for pulverized coal. This suggests an ignition delay, which is likely due to the time required for water evaporation from the fuel droplets. The ignition delay caused no problem in the refractory lined laboratory furnace, but may warn of problems in cold wall units, especially at low loads. Other observations suggested that flame stability was good.

Ash Deposits. Figures 2 through 7 are photographs of ash deposits formed in the simulated superheater test section as a result of six hour firing tests. Figure 2 shows deposits from firing a COM similar to that fired in FPL's 120-day test at the Sanford plant. Figures 3 through 7 are from firing of CWM fuels.

The COM test produced deposits about 0.25 inch thick, with all tubes accumulating about equal deposit quantities.

Deposits formed from firing CWM fuels ranged from negligible (Figure 6) to up to 2 inches thick. The thickness of the deposit can be a function of several factors, the most important of which are the ash content of the coal and

the ash properties. The effect of coal ash properties on deposits may not be simple. Coals with low ash fusion temperatures are more likely to form high temperature tube deposits than are coals with high ash fusion temperatures. However, the low ash fusion coals may also form molten or plastic deposits on the furnace wall, thereby retaining a higher fraction of the ash within the furnace and not providing as much material for deposition on downstream probes.

In general, the extent of deposits for these tests (determined by measuring the maximum depth of deposits) correlated with the quantity of ash being introduced into the furnace. For one pair of tests with two fuels having similar ash contents, but with different ash properties, the coal with the higher ash softening temperature unexpectedly produced the greater deposit.

None of the deposits formed on simulated superheater tubes represented slagging or molten deposits; rather, they represented sintered deposits of varying strengths. Generally the deposits were not tightly bonded to the simulated superheater tubes.

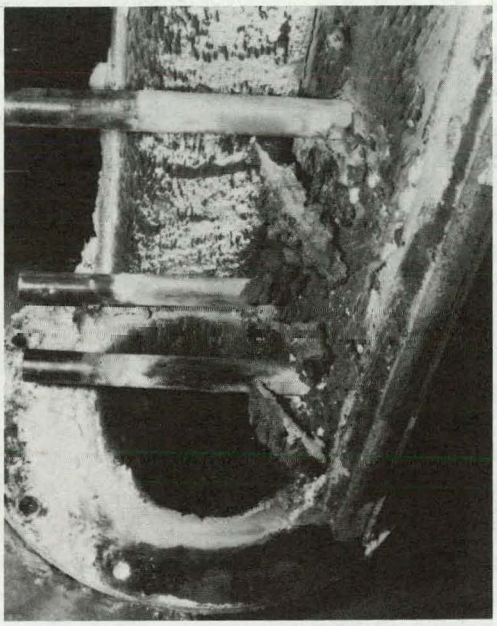

FIGURE 3
DEPOSITS FROM FIRING CWM-A

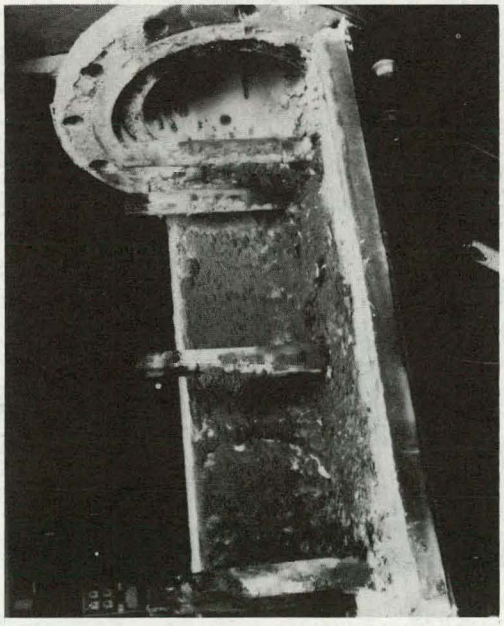

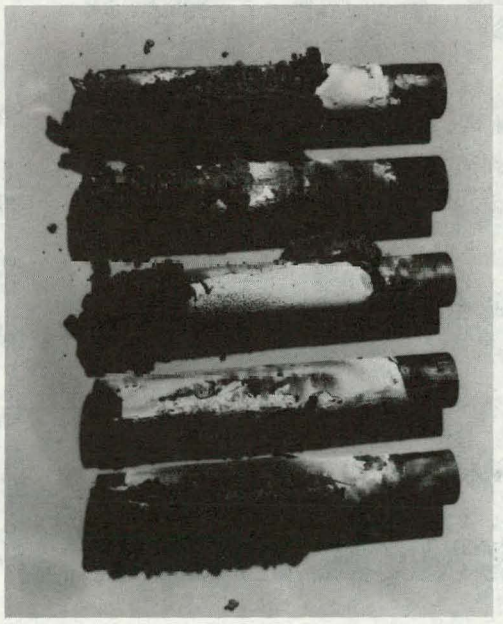

FIGURE 2
DEPOSITS FROM FIRING COM

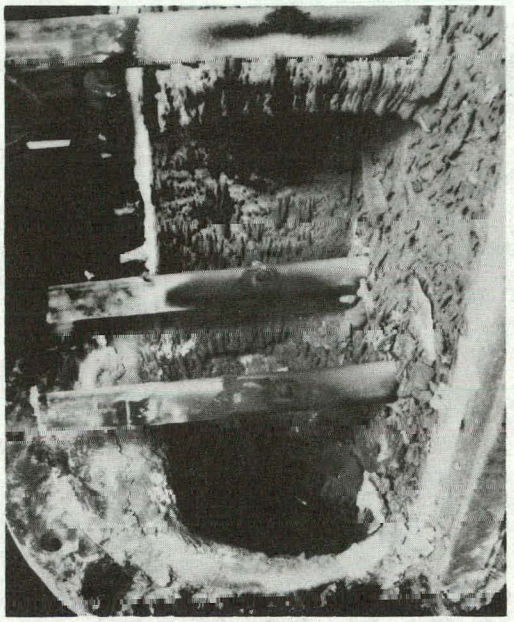

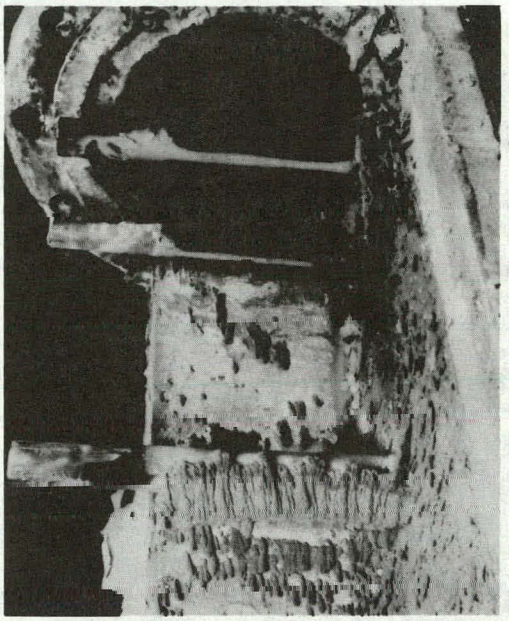

FIGURE 5
DEPOSITS FROM FIRING CWM-C

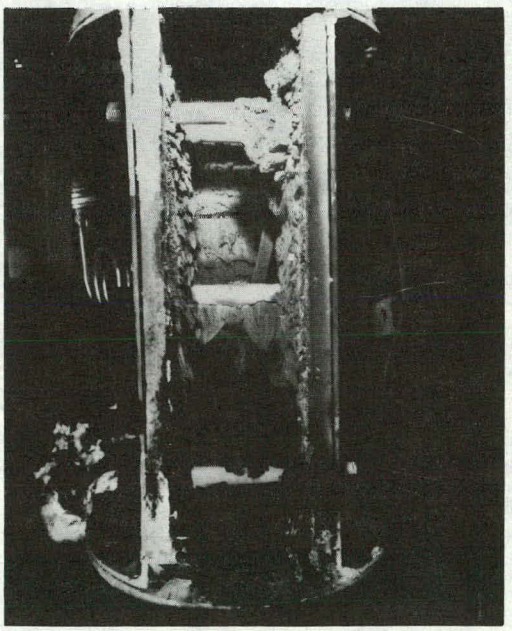

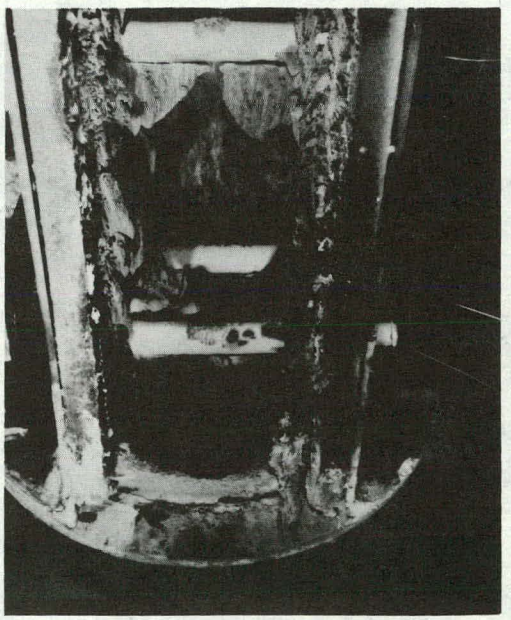

FIGURE 4
DEPOSITS FROM FIRING CWM-B

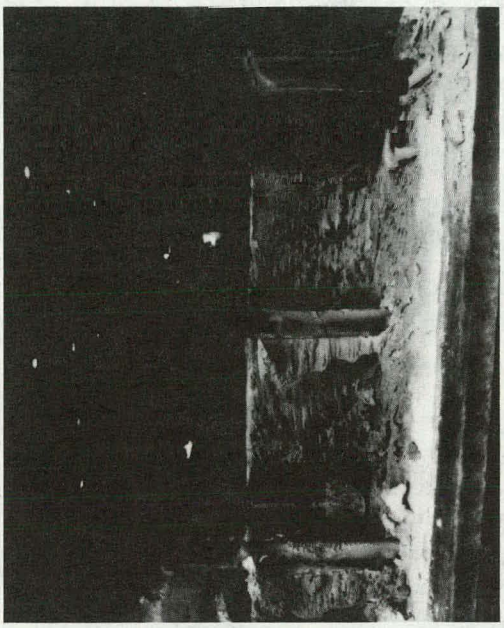

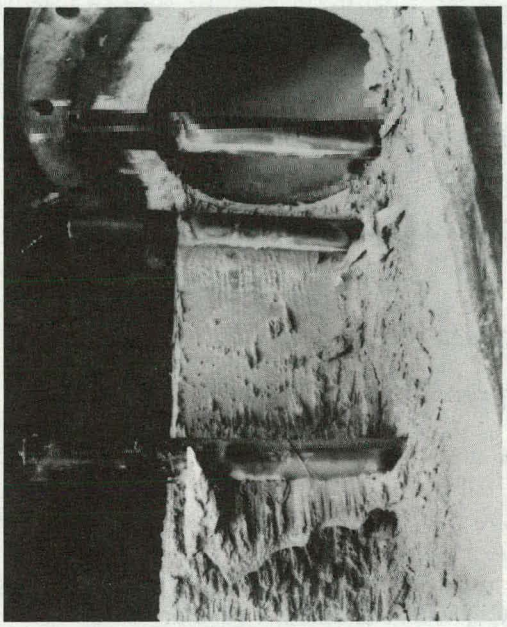

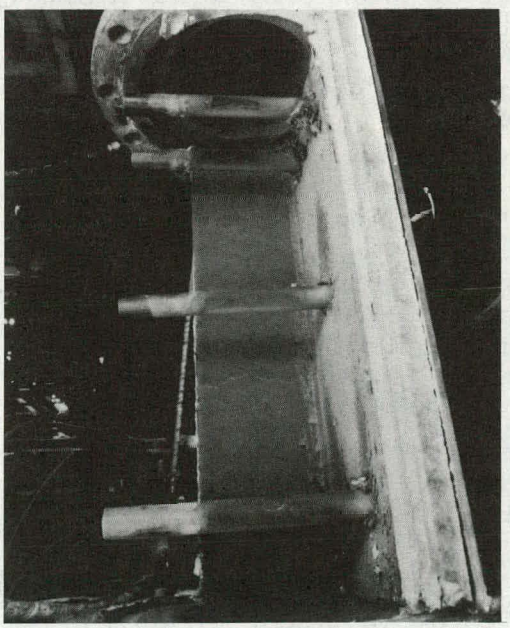

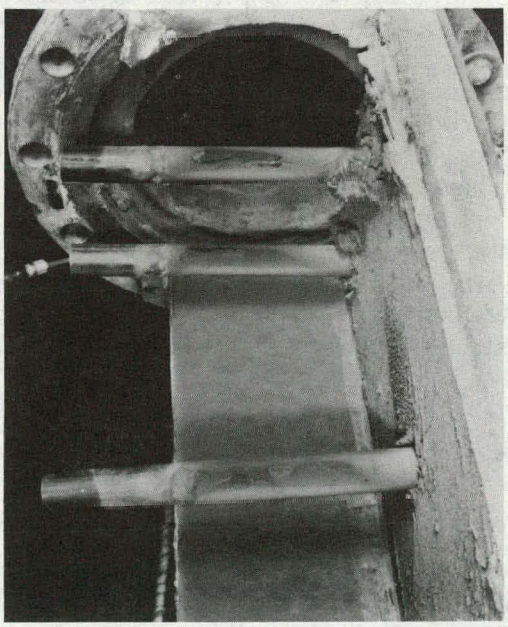

In some of the deposit photographs, it can be seen that significant deposits accumulated on the refractory blanket used to insulate the test section. This refractory blanket was uncooled and, therefore, operated at higher temperatures than the cooled tubes. Bonding of ash deposits to this hot surface is not surprising, nor is it an indication that the fuel will generate deposit problems in boilers.

No significant quantity of deposits was observed on the in-furnace probe at any point in the tests.

Only light powder dustings of deposits were found on the cold-end probe for all tests with CWM.

Conclusions of Laboratory Trials

As a result of Battelle's fuel trials, it was concluded that:

1. CWM fuels could be successfully fired in a small laboratory unit at 70 lb/hr.
2. Quality control can be a problem when producing CWM fuels.
3. Achieving good atomization of CWM fuels is difficult; further atomizer development is necessary.
4. CWM fuels could be burned with high combustion efficiencies, e.g., 99 to 99.9 percent.
5. Fly ash may contain 30 to 40 percent carbon, even with high combustion efficiency, due to the low ash content of some of the fuels; this could make particulate collection in ESP's difficult and could pose a fire hazard in operating plants.
6. Gaseous emissions (SO_2 and NO_x) were consistent with fuel properties.
7. Carbon monoxide emissions generally were low (100 ppm), but were as high as 2000 ppm for brief periods (frequently as a result of momentary upsets in fuel feed).
8. Simulated superheater deposits generally were proportional in thickness to the ash content of the fuel.
9. Although significant deposits accumulated on simulated superheater tubes (2 inches in 6-hour tests), the deposits were not strong and were not strongly bonded to the tubes. (This would be a function of coal properties.)

AREAS REQUIRING ADDITIONAL WORK

Now that it has been demonstrated that CWM fuel can be readily burned, some thought must be given to the entire CWM fuel scenario, including issues such as transportation, solid waste disposal, sensitivities of the various slurry processes to varying coal sources, effects of fuel additives on the boiler, and the applicability of conventional emission control systems to CWM firing. Economics for both fuel preparation and coal cleaning need to be further refined.

COAL SLURRY FUELS: MOVING TOWARD COMMERCIAL UTILIZATION

Coal Cleaning

The economical integration of a coal cleaning process (to reduce coal ash) with a slurry preparation process is highly desirable from FPL's point of view, due to the higher expected boiler availability, higher capacity, reduced transportation cost, reduced slagging and fouling, and reduced emission control requirements. FPL has examined both conventional and advanced coal cleaning techniques, and has reached the conclusion that the only processes which are likely to be economically feasible in the near term are those which rely on physical separation techniques, such as froth flotation, selective flocculation, or agglomeration.

CWM fuel technology appears to be developing at a faster rate than advanced coal cleaning technology, therefore, it is expected that there will be several generations of CWM fuel. The first generation fuel will most likely be prepared using conventional cleaning techniques. It is hoped that the 3% ash level will be economically achievable. The first generation fuel will be most successful in very generously designed oil boilers or coal designed boilers which have been converted to oil.

FPL also anticipates the development of second generation fuels with ash contents as low as 1%. It is possible that this second generation fuel will be the only coal alternative for the more tightly designed 800 MW boilers which FPL currently operates on oil. Basic research sponsored by FPL is intended to accelerate the development of advanced cleaning techniques and second generation CWM fuels.

Burners

FPL has been actively following the development of CWM burners. Atomizer erosion was a problem during the Sanford COM demonstration, and extensive redesign was necessary to achieve acceptable atomizer life. CWM, being even more abrasive than COM, will likely present further problems.

Before a full-scale utility demonstration of CWM fuel takes place, a full size burner demonstration (200 MM BTU/HR) is desirable. A demonstration of this size has not yet occurred. Fortunately, several burner manufacturers are pursuing the development of CWM burners, and a resolution appears likely. FPL is looking forward to reviewing the results from the following tests.

1. Tobacco Co., in Malmo, Sweden, single burner at $15X10^6$ BTU/HR.

2. EPRI sponsored demonstration tentatively scheduled at DuPont. 5 burners, each rated at approximately $15X10^6$ BTU/HR.

3. Energy, Mines, and Resources Canada sponsored demonstration with New Brunswick Electrical Power Commission.

   a. 12.5 MW_e Foster Wheeler coal designed unit, 4 burners each rated at approximately $40X10^6$ BTU/HR.

   b. 20 MW_e Combustion Engineering coal designed unit, 4 burners each rated at approximately $70X10^6$ BTU/HR.

4. City of Lund (Sweden), three 50 MW_e units, with burners rated at $85X10^6$ BTU/HR.

Particulate Control

Electrostatic precipitation is the most commonly used method of particulate control in the power industry. Adequate design of an electrostatic precipitator requires that the chemical and physical properties of the fuel and ash be well known. (The alternative in the absence of this knowledge is to grossly over design the unit.) This presents a problem as the formulations of CWM fuels are still going through an evolutionary process. Researchers are using different solids loadings, different particle size distributions, and different proprietary chemical additives. Some are employing a cleaning step prior to slurrying. The anticipation of a second generation CWM fuel adds even more variables to the problem.

To determine the sensitivity of electrostatic precipitators to the above mentioned CWM fuel variables, FPL has undertaken an in-house computer modeling study of electrostatic precipitation. The primary tool for this study is the mathematical model of electrostatic precipitation developed over the past decade by Southern Research Institute. Gaps between the available laboratory data and the SRI model are being filled by some additional computer models developed by Research Triangle Institute. Preliminary data from this effort indicates significant differences between slurries prepared via different processes. The choice of fuel additives can alter ash resistivities by orders of magnitude.

Baghouses are gaining utility acceptance for use while firing low sulfur western coal. EPRI is currently sponsoring tests, in the Florida panhandle, utilizing a baghouse on a boiler burning high sulfur eastern coal. Baghouses are more tolerant to variations in fly ash resistivity and flue gas composition than electrostatic precipitators. For this reason alone, a baghouse may be the best choice when firing a fuel which is going through an evolutionary process in itself.

Accelerated fabric life testing methods have been devised and can be carried out with relatively small quantities of fuels. It may be desirable to conduct such tests after CWM and coal fuel choices have been narrowed down.

FPL is also following the development of several emerging technologies for particulate control such as electrified filter beds, venturi systems, and charged fabric filters.

CWM Compatibility

CWM fuel compatibility is an issue which has not yet been addressed. It may be premature to worry about fuel compatibility, however, if CWM is successfully commercialized and becomes available from several sources, compatibility may become important. What will happen if Fuel A is mixed with Fuel B in a large storage tank? Each fuel may have a different particle size distribution and a different choice of chemical additives. Early testing has shown some CWM fuels to be incompatible. Viscosities of fuel blends can be more than an order of magnitude greater than either of the original CWM fuels (10). It is possible that some industry standards for CWM fuel compatibility may be required at some point in the future.

COAL SLURRY FUELS: MOVING TOWARD COMMERCIAL UTILIZATION

SUMMARY

In summary, FPL has drawn the following conclusions from experience to date.

1) CWM fuels are readily combustible.
2) Fuels can be produced which exhibit acceptable handling and storage properties.
3) Preliminary economics appear attractive, however, more refinement is needed.
4) No significant advances in hardware technology are needed to produce CWM on a utility scale.
5) Advanced coal cleaning concepts may take longer to commercialize than CWM fuel, therefore, CWM will likely go through several generations of evolution.
6) A large scale demonstration of CWM fuel in an oil-design utility boiler is needed to resolve all technical and economic issues.

The FPL staff is optimistic about the potential of CWM as a near term alternative to No. 6 fuel oil, and plans to continue a thorough investigation of the remaining technical and economic issues. However, some questions can only be answered by a full scale utility demonstration.

FPL is currently exploring the possibility of conducting a full scale, 400 MW demonstration, most likely at the Sanford plant. The costs and technical requirements of such a demonstration are being scoped. Data from this study is required before decisions regarding a demonstration can be made. Should a full scale demonstration prove successful, and the economics of CWM firing continue to look attractive, FPL would adapt CWM as a commercial alternative fuel for appropriate units.

REFERENCES

1. R. G. Donnelly, "Formulation, Handling & Combustion Characteristics of Coal-Water Mixtures", Proceedings of the 5th International Coal Utilization Exhibition & Conference, (1982).

2. L. Green, Jr., "Rail Transportation of Coal-Water Slurry Fuels", Proceedings of the 5th International Coal Utilization Exhibition & Conference, (1982).

3. R. C. Furman, "Power Plant Conversions to Coal, Coal-Oil Mixtures, and Coal-Water Slurries", Proceedings of the 4th International Symposium on Coal Slurry Combustion, (1982).

4. A. D. Schmidt(FPL); "Full Scale Tests Firing Coal-Oil Mixtures in a 400 MW Steam Generator", Proceedings of the 3rd International Symposium on Coal-Oil Mixture Combustion, (1981).

5. L. D. Slepow(FPL) and A. S. Mendelssohn(FPL), "FPL's Sanford COM Demonstration Project", Proceedings of the 3rd International Symposium on Coal-Oil Mixture Combustion,(1981).

6. A. J. Kasprik(FPL), H. Causilla, and P. Kartzke, "Design Considerations and Operating Experience of the Sanford COM Test Facility", Proceedings of the 3rd International Symposium on Coal-Oil Mixture Combustion, (1981).

7. W. R. Lane, R. J. Burgess(FPL), and N. E. Takvoryzn, "Pilot Electrostatic Precipitator Test Results Sanford COM Project Florida Power and Light Company", Proceedings of the 3rd International Symposium on Coal-Oil Mixture Combustion,(1981).

8. K. F. Kosky, A. M. Schumacher, and R. N. Allen(FPL), "Environmental Licensing of Coal/Oil Mixtures", Proceedings of the 3rd International Symposium on Coal-Oil Mixture Combustion, (1981).

9. EPRI CS-2286, Project 1895-2, "Combustion Tests of Coal-Water Slurry", March 1982.

10. Private conversations, J. Dooher and B. Gilmarten, Adelphi University.

ACKNOWLEDGMENTS

FPL and Battelle would like to thank the fuel companies and researchers whose generous cooperation made this program possible.

Advanced Fuels Technology (Gulf and Western)
Atlantic Research Corporation
Carboqel
Coaliquid, Inc.
Columbia Fluidized Coal Energy, Inc.
Development Energy Group
Island Creek Coal Company
Occidental Research Corporation
United Coal Company

Also, thanks to J. Kuhns for her patience while typing this manuscript.

COMPARISON OF COAL CONVERSION ALTERNATIVES*

By: E. Kimel
Burns and Roe, Inc.
Oradell, NJ 07649

&

R. Kurtzrock
DOE Pittsburgh Energy Technology Center
Bruceton, PA 15236

1.0 INTRODUCTION

The present high costs of oil and gas, likelihood of future price increases, and potential supply problems continue as strong incentives for the conversion of oil-fired power plants to coal.

Recent developments in preparation and combustion of pumpable, stable coal-water mixtures (CWM) containing about 70% coal have advanced this technology from laboratory to pilot scale installations. It is hoped that the current extensive research and development work will advance CWM technology to commercial applicability for industrial and utility installations within a few years.

A proven option is retrofitting the oil-fired boiler to pulverized coal (PC) firing. This may be accomplished by modifying some boiler components and adding coal firing equipment, preferably retaining the existing means of firing oil.

Under the auspices of the U.S. Department of Energy, Pittsburgh Energy Technology Center, a study was performed on three large utility installations to assess the technical feasibility and economics of converting the boilers from oil to either pulverized coal (PC) or to CWM firing. The three boilers selected for the study consist of a B&W Universal pressure boiler at Jacksonville Electric Authority's (JEA) Northside Unit 1 rated 275 MW, a CE tangential fixed boiler at United Illuminating Co.'s New Haven Harbor Unit 1 rated 460 MW and a Riley Stoker box type boiler at JEA's Northside Unit 3 rated 518 MW.

The results of the study for Northside Unit 3 are discussed in this paper. The study was performed by Burns and Roe, Inc. with assistance from Riley Stoker on boiler performance evaluation.

*Work was performed under the auspices of the U.S. Department of Energy Contract No. DE-AC22-80PC30283.

2.0 PLANT MODIFICATIONS

2.1 STEAM GENERATOR MODIFICATIONS AND PERFORMANCE FOR PC FIRING

Unit 3 has a Riley Stoker subcritical drum-type reheat steam generator of box type configuration, designed and constructed for oil firing. The unit first entered service in 1977. Boiler performance parameters on oil are presented on Table 1.

The performance of the existing boiler with minimal modifications to accommodate PC firing was evaluated at a number of different loads. It was found that the flue gas velocity in the convection passes limits boiler capacity to about 73% BMCR. At this load, the main steam temperature was only 970°F and the reheat steam was 950°F (Table 2). Both temperatures are below the 1005°F required for efficient turbine operation. It was felt that 73% BMCR, without making steam temperature, was unacceptable for a conversion.

To overcome the limitation on coal performance imposed by the boiler convection passes, the following modifications were developed to permit the boiler to achieve 100% load.

Convection Pass

The depth of the convection pass will be increased by moving both the rear furnace wall and the rear convection pass wall outward. The upper rear furnace wall will be moved 8 feet outward to increase the depth of the ascending (flue gas side) convection pass. The rear convection pass wall will be moved 10 feet outward to increase the depth of the descending convection pass by 2 feet. The new furnace upper rear wall will be formed by dividing the existing tubes into two sections. Every third tube will remain in its original location, and together these tubes will form the 2 inch OD, 9 inch pitch waterwall stringers that support the high temperature superheater, high temperature primary superheater, and reheater. The remaining tubes will branch off vertically and flow into the 3 inch OD, 4-1/2 inch pitch tubes that form the new rear wall of the ascending convection pass.

Due to the increased depth of the convection pass, the secondary superheaters and the reheater will be replaced in order to meet the heat transfer and dimensional requirements.

The new high temperature superheater (HTSH) will consist of 1-3/4 inch OD tubes with 27 inch spacing, which is considered adequate for firing the design coal. The new high temperature reheater (HTRH) will consist of 2-1/4 inch OD tubes with 9 inch spacing. Waterwall stringers from the furnace rear wall will be used to support the HTSH, HT primary superheater, and the HTRH. Capped stubs on the inlet and outlet headers of the HTSH and HTRH will accommodate addition of tubes to provide 10% more surface area if required.

The primary or low temperature superheater (LTSH) will consist of a horizontal assembly of 2 inch OD tubes with 4-1/2 inch spacing and a pendant assembly of 2-1/4 inch OD tubes with 9 inch spacing. Since the

LTSH will be in a region of relatively low gas temperatures, the resulting lateral clear tube spacing will be adequate.

The downcomers will be rerouted to accommodate the extended rear wall.

Casing, insulation and lagging at the furnace bottom, penthouse, and convection passes will be replaced.

Convection tube penetration seals will be replaced. The new seals will be a sliding type, which should be satisfactory for balanced draft PC operation.

The header enclosure pressurizing fan will be used to ensure that no gas leakage occurs.

A cross-section of the existing oil-fired steam generator is shown on Figure 1. A similar section of the steam generator retrofitted to coal is shown on Figure 2.

Burners and Windbox

The boiler is currently equipped with 24 oil burners mounted on the front wall and arranged on three levels with 8 burners on each level. They will be replaced with 24 Controlled Combustion Venturi Low NO_x Burners in the same positions. The new burners were selected to provide the maximum required heat input of approximately 193×10^6 Btu/hr per burner when firing PC. The register, 15 inch coal nozzle, igniter and burner front plate will be supplied as part of the new burner.

The existing furnace depth of 40 feet will be satisfactory for PC firing with the new burners. The vertical distance from the centerline of the upper row of burners to the lowest superheater tube will be 38 feet, 6 inches, and the distance from the centerline of the lower row of burners to the hopper tangent will be 9 feet. These distances will be suitable for PC firing.

Furnace Hopper

The existing hopper has a 40^o slope and a 3 foot opening for ash removal. To provide adequate slope and clearance for ash removal, the hopper will be replaced, including waterwall tubes, side waterwall headers, hopper headers, and feeders. The new hopper will have a 55^o slope on the front wall, a 50^o slope on the rear wall, and a 4 foot opening. The hopper opening is offset towards the front wall so that the burner elevation need not be changed.

Flue Gas Recirculation

The existing flue gas recirculation system takes flue gas from the outlet of the economizer, introduces it into the hot air duct, and passes it through the burners. When firing PC, such recirculated gas would result in unacceptably high pressure drops and high air velocities at the burners because of the increased air requirements, the nature of the proposed burners, and the register settings required to maintain stable flame conditions.

The modified system will introduce the recirculated gas into the furnace through the furnace hopper. Furnace tubes on the rear wall will be offset near the header to allow for gas entry. To prevent fan erosion, two mechanical dust separators will be installed upstream of the two gas recirculation fans. The modified system will include double isolation dampers and hot and cold seal air systems.

Wall and Sootblowers

Two dual-purpose, retractable sootblowers (one per side), with coverage of about 30 feet, will be added to clean the sloping section of the rear waterwall. Additional sootblowers will be provided in the furnace and economizer hoppers. Four retractable sootblowers (two per side), with coverage of about 30 feet, will be added near the HTSH. Since major convection surface changes will take place, most of the existing full and half retractable sootblowers will be relocated, along with their piping systems and access platforms.

Performance

Table 3 presents the performance of the modified boiler at 100% BMCR when firing PC. It shows that the modified boiler is able to meet the BMCR requirements on main steam flow and temperature, reheat steam flow and temperature, and total heat transfer to steam. The boiler efficiency was calculated to be 89.92%.

Most of the furnace heat release rates are within the guidelines established for coal conversion. The volumetric heat release rate, 21,543 Btu/cu ft/hr, is slightly above the limit established for standard fineness coal. However, to reduce the required residence time of the coal particles in the furnace, the pulverizers have been sized to produce coal at 80% through a 200 mesh. This will make the volumetric heat release rate at 100% BMCR acceptable.

The EPRS heat release rate, 115,540 Btu/sq ft/hr, is within the limits for PC firing, as is the plan area heat release rate, 2,030,000 Btu/sq ft/hr.

The burner zone heat release rate, 665,000 Btu/sq ft/hr is slightly above the recommended limit, but investigation has shown that the heat flux in the burner zone will be within acceptable limits.

The gas temperature leaving the furnace and the spacing of the convection surfaces are such that excessive fouling and bridging of the convection sections will not occur. The limit of 75 fps on flue gas velocity is not exceeded at any point. Figure 3 shows the flue gas temperatures and velocities throughout the boiler.

Since the boiler can produce full BMCR steam flows and temperatures when firing PC, oil will only be used during coal supply emergencies. The modifications were designed for optimum boiler performance on PC firing. As a result, full BMCR steam flows and superheat temperature can be achieved on oil firing, but reheat temperature cannot. Full reheat steam temperature could be achieved through gas recirculation, but the

fan motors would have to be replaced with motors of higher capacity. Since flue gas velocity for oil firing is limited chiefly by power considerations, gas recirculation could be increased without violating the conversion principles. The modified boiler performance on oil firing is presented on Table 4.

The existing oil-fired unit meets the NO_x emission requirements by using over-fire air and flue gas recirculation through the burners. However, as part of the conversion to PC firing, the recirculated flue gas will enter the furnace through the furnace hopper. This modification will slightly increase NO_x emissions.

2.2 STEAM GENERATOR MODIFICATIONS AND PERFORMANCE FOR CWM FIRING

Performance of the existing boiler was evaluated for CWM firing, and again flue gas velocities were found to limit boiler capacity. The boiler was modified to permit achievement of 100% BMCR steam flows within the parameters established for CWM conversion. The modifications are similar to those required for PC firing, but additional heat transfer surface had to be added to achieve the superheat and reheat design temperatures. Figure 4 presents a tabulation of flue gas temperatures and velocities throughout the boiler. Boiler efficiency on CWM was calculated to be 87.12%. Performance of the retrofited boiler on CWM is summarized on Table 5.

The heat release rates and gas velocities are within acceptable limits for CWM firing.

2.3 PLANT MODIFICATIONS AND ADDITIONS FOR COAL FIRING

Coal Handling System

Northside Unit 3 receives fuel oil barged to an unloading pier on the St. John's River about 3,000 feet southeast of the plant. Rail delivery is considered the most practical and economical means of coal supply to the site. A spur with storage tracks will be constructed from the main railroad line. (See Figure 5 for coal handling system layout.) The coal will be off-loaded from bottom dump hopper cars to an underground hopper system capable of unloading two cars simultaneously. At maximum capacity on coal, Unit 3 will consume approximately 170 tons per hour of coal, or 28,600 tons per week. This will require delivery of 290 carloads per week.

The unloading hoppers will feed a stock-out conveyor system will consist of car shakers, feeders, conveyors, integrating and recording scales, "as received" sampling equipment, dust collection and disposal system, fire detection and protection systems, and controls.

The coal reclaim system rated will include underground reclaim hoppers, feeders, conveyors, magnetic separators, coal scales, crushers, "as-fired" sampling equipment, dust collection equipment, fire detection/protection systems, and controls.

A travelling tripper conveyor will deposit the coal in the day silos located above the mills.

There will be four vertical spindle pulverizers, each capable of feeding 45 tons of coal per hour and sized to provide 80% through 200 mesh with 10% margin for wear. The coal grind will be finer than that normally used in a boiler designed for PC. This will provide a shortened flame and enhanced combustion efficiency necessary because of limited furnace retention time. Each of six burners will be connected to its respective pulverizer by an 18 inch diameter coal pipe. The pattern of burners served by each mill will be arranged to minimize the effects of a mill shutdown on the symmetry of the flame pattern, while taking advantage of furnace height variations for flue gas temperature control at start-up and low loads.

Draft System

The existing air preheaters are adequate for the new service conditions. The existing forced draft and induced draft fans will require upgrading. The induced draft fans will be modified to handle the abrasive ash associated with PC firing by adding wear resistant surfaces and new seals. They will also be relocated so that they can be connected to the electrostatic precipitator outlet and discharge into the existing stack breeching.

A mechanical ash separator will be installed upstream of the gas recirculation fans to reduce the amount of abrasive ash going through the fans during PC firing.

Two primary air booster fans will supply heated air to the pulverizers. Hot air will be drawn from the air heater air outlet and tempered as required with cold air drawn from the forced draft fan discharge will be supplied to the pulverizers to maintain the air/fuel mixture to the burners at 175^{o}F.

Flue Gas Particulates Removal

All particulates from oil firing are discharged to the atmosphere. When firing coal, approximately 9 tons per hour of fly ash will be generated; therefore, an efficient particulate removal system is necessary.

An electrostatic precipitator (ESP) will be provided for a minimum specific collecting area of 400 sq ft per 1000 ACFM of flue gas flow. This size was estimated based on a predicted ash resistivity of $3x10^{11}$ ohm centimeters. The ESP will provide the collection efficiency in excess of 99.3% required to meet an expected emission requirement of 0.03 lb/MBtu.

The ESP will be installed downstream of the boiler air preheater as shown on Figure 6. New ductwork will be required from the air preheater to the ESP, from the ESP to the two induced draft fans, and from the latter to the existing stack.

Weighted wire and rigid frame ESP designs were considered. The rigid frame design was chosen since it has proven most effective with low sulfur, high resistivity coals where ash buildup on the discharge electrode and collecting plate is a problem. The rigid frame design lends itself to the higher rapping forces needed to minimize this build-up and generally has lower operating and maintenance costs.

Ash Handling System

Approximately 91 tons of bottom ash (including mill rejects) and 199 tons of fly ash can be generated each day. The ash handling system was designed to provide separate short-term on-site storage of bottom ash and fly ash in silos. Ultimate disposal is assumed to be off-site, with removal by truck or railcar, as the site space limitations and proximity to natural bodies of water are assumed to preclude economical on-site ponding or landfill.

The sizing of the bottom ash handling system was based on an hourly bottom ash production of 4.3 tons per hour at 100% BMCR, including pyrites and design margins. The modified furnace hopper provides a clearance of 4 feet from the hopper bottom to the boiler area floor. This restricted headroom will require excavation below the furnace hopper. The requirements to minimize this excavation and for dry storage and disposal of the ash appear to make a scraper conveyor the most practical method for bottom ash collection and removal. The moist (approximately 15% water) bottom ash is reduced in size by a clinker grinder, and transferred via a belt conveyor system to a storage silo.

The fly ash handling system must collect, transport, and store (for periods of up to 5 days) the ash deposited in the economizer, air heater, and ESP hoppers. Including design margins, the system is sized for fly ash production of 8.8 tons per hour at 100% BMCR. A vacuum-pneumatic conveyor system will be used.

Instrumentation and Controls

Existing plant controls will be retained where safety and operability are not compromised. In general, controls required for start-up, operation, and shutdown of the plant will be provided in the control room. Logic circuitry for these systems will be located in the relay room. Auxiliary systems not directly associated with power generation will be operated locally, with essential monitoring instruments and alarms located in the control room.

The burner management system will be replaced with new controls suitable for both oil and coal firing. A main control room insert will be provided for burner indications and controls. Local burner monitoring equipment will also be installed.

New ignitors and flame scanners will be provided for coal firing. The existing scanners will be retained for oil and ignitor flame monitoring.

The combustion control system will be modified to include controls for coal feed rate, air/fuel ratio, and associated parameters, along with controls and indicators for primary air fans and dampers, all of which will be mounted on a new board section in the main control room.

Coal receiving and unloading will be controlled by local stations near the car dump station.

The ESP controls will be located on a remote panel near the ESP. Critical alarms and damper position indications will be provided in the control room.

Bottom ash and fly ash controls will be automatic after manual initiation. Controls and logic circuitry will be mounted in free standing weatherproof panels near the equipment. System trouble alarms and status indicators will be provided in the main control room.

Emission monitoring systems will be upgraded to meet all applicable regulations for coal firing, including NO_x and opacity monitors.

Electrical

The estimated net increase in peak auxiliary power requirements when firing PC after conversion is 4.5 MW at BMCR. The large size of the existing auxiliary transformer, 50 MVA, can accommodate the additional load.

Additional 4 kV metal clad switchgear extensions will be provided to supply the ESP, primary air fans, pulverizers, and new unit substations near the ash handling systems and the coal handling area. Low-voltage services will be furnished from these substations and, where practical, from existing sources.

Civil/Structural

New foundations will be required for the railcar coal unloader, coal conveyors, transfer towers, tripper house, reclaim tunnel, bottom ash scraper conveyor and transfer conveyors, bottom ash and fly ash silos, pulverizers, ESPs and ductwork, primary air fans, and control houses. Relocation of the induced draft fans to accommodate the ESPs will also require new foundations.

A pit measuring 98 by 31 feet by 10 feet deep will be excavated under the furnace hopper to permit access for maintenance. This work will require hand excavation, as the area is too restrictive for use of large equipment.

The boiler suspension steel structure will be altered to accommodate the modified boiler. The boiler column locations will be unaffected, but some buckstays, platforms, etc., will require reinforcement to accommodate the ash and slag accumulations, new heat transfer and waterwall surfaces, and additional equipment.

2.4 PLANT MOFIFICATIONS AND ADDITIONS FOR CWM FIRING

CWM Handling System

CWM will be shipped by barge to the station and unloaded at the existing oil barge pier equipped with a separate unloading arm and piping system for CWM. The pier arrangement and general site layout are shown in Figure 7.

The CWM barge unloading arm will be connected by a pipe to six unloading pumps arranged in parallel. The general CWM unloading, piping, storage, and flushing system is shown on Figure 8. Each unloading pump will be a progressive cavity, constant speed unit with a maximum capacity of 600 gallons per minute. With all six pumps operating at full capacity, a 3000 ton barge will be unloaded in about 4 hours. At full load on CWM, the unit will consume 5,553 tons of CWM per day.

From the unloading pumps, the CWM will pass through sonic and mechanical flow meters into five storage tanks arranged in parallel. The sonic device will record bulk deliveries; the mechanical meter will be used to calibrate the sonic meter.

The five 60,000 barrel storage tanks will give about 10 days of fuel reserve at full load. Each tank will be equipped with agitators to assure homogeneity from freezing, a suction heater to raise the CWM temperature, if required, test ports for fuel sampling, level transmitters, and temperature probes.

Three pumps will be provided for transferring the CWM from the storage tanks to a day tank of 1000 barrel capacity, sufficient for 1 hour at full CWM boiler load. The day tank will have an agitator and internal baffling to keep the CWM homogeneous.

Three feed pumps arranged in parallel will pump the CWM from the day tank to the burners. Each pump will be a 450 gallon per minute, variable speed, progressive cavity unit sized for 50% of maximum fuel flow to the burners. Two pumps will operate, with the third held as a spare. The burner feed pumps will be located close to the burner front.

Draft System

The draft system for CWM firing includes the forced draft fans, induced draft fans, and gas recirculation fans. The modifications for CWM firing are the same as those required for PC firing.

Flue Gas Particulates Removal

When firing CWM, approximatley 9 tons per hour of fly ash will be generated. Therefore, an efficient particulate removal system will be necessary. CWM does not require as high a specific collection area as PC because the added moisture in CWM lowers ash resistivity, making it easier to collect. Thus, in spite of the increased gas flow associated with firing CWM at the same boiler load as PC, the ESP recommended for PC can be used for CWM.

Ash Handling

The ash handling system for CWM will be identical with that required for PC firing.

Instrumentation and Controls

Conversion to CWM firing will, in general, involve the same changes to control systems as required for PC firing. Systems such as those for coal handling and preparation will not be needed, but new controls will be needed for CWM receipt, storage and handling.

CWM receiving and unloading will be controlled from a local panel at the unloading pier. Interlocks for line heating, filling, CWM pumping, flowpath verification and flushing will be included to minimize the possibility of operator error. Flow measurement and recording will be provided primarily by ultrasonic devices, but with frequent calibration by a positive displacement device which can be easily isolated and removed for maintenance. A sample collection system will be provided for "as-received" analysis.

The storage tanks will be provided with automated controls to maintain the CWM in a homogeneous mixture at the proper temperature. Critical alarms and level indication will be provided locally in the main control room, and at the barge unloading pier.

The fuel transfer and burner feed systems will be fully automatic, with appropriate status indications, day tank levels, and critical alarms displayed in the main control room. Line filling temperature maintenance, and flushing systems will be fully automatic. CWM burner pressure will be monitored by variable speed pump controls and a modulated "V-notch" ball valve recirculation system.

Electrical

The net increase in peak auxiliary loads while firing CWM is estimated at only 0.7 MW. Accordingly, the existing auxiliary transformer will be adequate. Additional 4 kV metal clad switchgear extension will be required to supply power to the ESP and new unit substations for the ash handling system and the CWM unloading and transfer pumps. Low-voltage services will be supplied from these substations and, where practical, from existing sources.

Civil/Structural

New foundations will be required for the CWM pumps, pipelines, storage and flushing tanks, bottom ash scraper conveyor and transfer conveyor, bottom and fly ash silos, ESPs, ductwork and relocated induced draft fans.

The CWM marine unloading arm can be installed on the existing unloading pier with minimal modifications. The CWM day tank and burner feed pumps will be mounted on existing boiler steel, with some reinforcement.

The CWM storage and flush tanks will be supported on concrete ring foundations.

3.0 CONVERSION COSTS AND ECONOMICS

3.1 CAPITAL COSTS

The cost of converting Northside Unit 3 to PC firing is estimated at $163,700,000 ($316/kW), while conversion to CWM is estimated at $112,600,000 ($217/kW). A new coal-fired boiler with FGD would cost about $541,300,000 ($1,045/kW). The breakdown of costs by major items is shown on Table 6.

The cost estimates are based on a project start date of January 1983 and completion of the conversions to PC or CWM by January 1987, or to the new boiler by January 1989. The estimates assume indirect costs to be 20% of directs, a contingency of 15%, escalation at 8% per year, and interest during construction at 12% per year.

Conversions to PC and CWM are based on the use of low sulfur coal which will not exceed present SO_2 emission limitations of 1.98 lb SO_2 per million Btu, and it is assumed that a flue gas desulfurization[2] (FGD) system will not be required. It is believed that a new boiler will have to meet the New Source Performance Standards and therefore will be provided with an FGD system and fired by cheaper high sulfur coal.

3.2 OPERATING AND MAINTENANCE (O&M) COSTS

When converted to coal, the unit will incur a higher annual O&M expenditure than for oil firing. The incremental O&M costs in mid 1982 dollars are $3.6 million for CWM, $4.7 million for PC, and $9 million for a new boiler with FGD. O&M costs are assumed to escalate at 8% per year.

3.3 ECONOMIC EVALUATIONS

The economic evaluations are based on a remaining plant operating life of 15 years at an annual average capacity factor of 65%.

The present prices for fuel delivered to the site are $28/barrel ($4.44/million Btu) for oil, $69/ton ($2.60/million Btu) for low sulfur coal, and $57/ton ($2.40/million Btu) for high sulfur coal. CWM is assumed to cost $3.50/million Btu. All fuel prices are assumed to escalate at 8% per year.

The results of the economic evaluation are shown on Figure 9. Conversion to either PC or CWM yields considerable economic benefits when compared with oil firing or addition of a new coal-fired boiler.

ACKNOWLEDGEMENTS

The authors wish to thank P. Kemeny, G. Fontana and C. Meara of Burns and Roe, and D. Dunphy of Riley Stoker for their constributions to the study work. They also wish to express appreciation to C. McCann of PETC for his valuable comments during the course of the work.

Table 1

PERFORMANCE OF EXISTING BOILER - OIL FIRING

Percent BMCR	75	100
Steam Evaporation - lbs/hr	2,661,000	3,548,000
Reheat Steam Flow - lbs/hr	2,330,000	3,139,000
Furnace Exit Gas Temperature - ^{o}F	2,315	2,520
Excess Air at Economizer Exit - %	15	15
Temp. of Air Entering Air Heater - ^{o}F	167	167
Temp. of Gas Leaving Air Heater - ^{o}F (Uncorr.)	263	275
Final Superheat Steam Temperature - ^{o}F	1,005	1,005
Final Reheat Steam Temperature - ^{o}F	1,005	1,005
Superheat Steam Pressure - PSIG	2,475	2,500
Reheat Outlet Steam Pressure - PSIG	409	556
Fuel Fired - lbs/hr	186,100	241,400
Combustion Air to Furnace - lbs/hr	3,046,000	3,950,000
Total Gas Air Heater Inlet - lbs/hr	3,230,000	4,189,000
Recirculated Gas - lbs/hr	700,000	640,000
Volumetric Heat Release - Btu/ft^3	18,260	23,680
EPRS Heat Release - Btu/ft^2 hr	83,640	108,500
Plan Area Heat Release - Btu/ft^2 hr	1,469,000	1,905,000
Burner Zone Heat Release - Btu/ft^2 hr	481,400	624,400
Boiler Efficiency - %	90.80	90.25
Gross Heat Input - Btu x 10^6/hr	3554.5	4610.7

Table 2

PERFORMANCE OF EXISTING BOILER WITH MINIMAL MODIFICATIONS

PULVERIZED COAL FIRING

Percent BMCR	73
Steam Evaporation - lbs/hr	2,590,000
Reheat Steam Flow - lbs/hr	2,238,600
Furnace Exit Gas Temperature - ^{o}F	1,965
Excess Air at Economizer Exit - %	40
Temp. of Air Entering Air Heater - ^{o}F	80
Temp. of Gas Leaving Air Heater - ^{o}F (Uncorr.)	-
Final Superheat Steam Temperature - ^{o}F	970
Final Reheat Steam Temperature - ^{o}F	950
Superheat Steam Pressure - PSIG	2475
Reheat Outlet Steam Pressure - PSIG	409
Fuel Fired - lbs/hr	249,500
Combustion Air to Furnace - lbs/hr	3,534,000
Total Gas Air Heater Inlet - lbs/hr	3,767,000
Recirculated Gas - lbs/hr	0
Volumetric Heat Release - Btu/ft^3 hr	16,000
EPRS Heat Release - Btu/ft^2 hr	107,250
Plan Area Heat Release - Btu/ft^2 hr	1,594,000
Burner Zone Heat Release - Btu/ft^2 hr	492,000
Boiler Efficiency - %	90.3
Gross Heat Input - Btu x 10^6/hr	3374.2

Table 3

PERFORMANCE OF MAJOR MODIFIED BOILER - PULVERIZED COAL

Percent BMCR	100
Steam Evaporation - lbs/hr	3,548,000
Reheat Steam Flow - lbs/hr	3,139,000
Furnace Exit Gas Temperature - ^{o}F	2,250
Excess Air at Economizer Exit - %	20
Temp. of Air Entering Air Heater - ^{o}F	80
Temp. of Gas Leaving Air Heater - ^{o}F (Uncorr.)	243
Final Superheat Steam Temperature - ^{o}F	1,005
Final Reheat Steam Temperature - ^{o}F	1,005
Superheat Steam Pressure - PSIG	2,500
Reheat Outlet Steam Pressure - PSIG	556
Fuel Fired - lbs/hr	341,60
Combustion Air to Furnace - lbs/hr	4,074,000
Total Wet Gas Air Heater Inlet - lbs/hr	4,387,500
Recirculated Gas - lbs/hr	500,000
Volumetric Heat Release - Btu/ft^3 hr	21,540
EPRS Heat Release - Btu/ft^2 hr	115,540
Plan Area Heat Release - Btu/ft^2 hr	2,029,000
Burner Zone Heat Release - Btu/ft^2 hr	665,000
Boiler Efficiency - %	89.92
Total Heat to Steam - Btu x 10^6/hr	4149.9
Gross Heat Input - Btu x 10^6/hr	4615.1

Table 4

PERFORMANCE OF MAJOR MODIFIED BOILER - OIL FIRING

Percent BMCR	100
Steam Evaporation - lbs/hr	3,548,000
Reheat Steam Flow - lbs/hr	3,139,000
Furnace Exit Gas Temperature - ^{o}F	2,110
Excess Air at Economizer Exit - %	15
Temp. of Air Entering Air Heater - ^{o}F	122
Temp. of Gas Leaving Air Heater - ^{o}F (Uncorr.)	258
Final Superheat Steam Temperature - ^{o}F	1,005
Final Reheat Steam Temperature - ^{o}F	982
Superheat Steam Pressure - PSIG	2,500
Reheat Outlet Steam Pressure - PSIG	556
Fuel Fired - lbs/hr	248,000
Combustion Air to Furnace - lbs/hr	3,922,600
Total Wet Gas Air Heater Inlet - lbs/hr	4,166,500
Recirculated Gas - lbs/hr	1,000,000
Volumetric Heat Release - Btu/ft^3 hr	21,375
EPRS Heat Release - Btu/ft^2 hr	112,750
Plan Area Heat Release - Btu/ft^2 hr	1,980,000
Burner Zone Heat Release - Btu/ft^2 hr	649,000
Boiler Efficiency - %	90.16
Total Heat to Steam - Btu x 10^6/hr	4105.4
Gross Heat Input - Btu x 10^6/hr	4584.3

Table 5

PERFORMANCE OF MODIFIED BOILER - COAL-WATER MIXTURE FIRING

Percent BMCR	100
Steam Evaporation - lbs/hr	3,548,000
Reheat Steam Flow - lbs/hr	3,139,000
Furnace Exit Gas Temperature - ^{o}F	2,110
Excess Air at Economizer Exit - %	20
Temp. of Air Entering Air Heater - ^{o}F	80
Temp. of Gas Leaving Air Heater - ^{o}F (Uncorr.)	241
Final Superheat Steam Temperature - ^{o}F	1,005
Final Reheat Steam Temperature - ^{o}F	1,005
Superheat Steam Pressure - PSIG	2,500
Reheat Outlet Steam Pressure - PSIG	556
Fuel Fired - lbs/hr	473,310
Combustion Air to Furnace - lbs/hr	4,239,900
Total Wet Gas Air Heater Inlet - lbs/hr	4,713,200
Recirculated Gas - lbs/hr	268,200
Volumetric Heat Release - Btu/ft^3 hr	22,235
EPRS Heat Release - Btu/ft^2 hr	112,080
Plan Area Heat Release - Btu/ft^2 hr	1,968,340
Burner Zone Heat Release - Btu/ft^2 hr	645,100
Boiler Efficiency - %	87.12
Total Heat to Steam - Btu x 10^6/hr	4146
Gross Heat Input - Btu x 10^6/hr	4763

Table 6

CAPTAL COST ESTIMATES
(NOMINAL 518 MW)

Item	Description	Conversion to Pulv. Coal	Conversion to CWM	New Coal Fired Boiler
1	Fuel Receiving and Handling	19,769,000	6,858,000	21,646,000
2	Steam Generator and Auxiliaries	36,000,000	27,000,000	80,960,000
3	High Pressure Piping System	-	-	2,161,000
4	Ash Handling and Storage	3,736,000	3,736,000	4,380,000
5	Particulate Controls	13,500,000	13,500,000	15,320,000
6	Flue Gas Desulfurization System	-	-	77,200,000
7	Chimney	-		4,500,000
8	Electrical	1,187,000	1,014,000	2,400,000
9	Civil/Structural	6,562,000	2,934,000	12,382,000
10	Instruments and Controls	960,000	1,002,000	3,675,000
11	Misc. Plant Systems	750,000	750,000	1,000,000
12	SUBTOTAL DIRECT COSTS	82,500,000	56,800,000	225,700,000
13	Engineering, Construction Management and Owner's Costs	16,500,000	11,400,000	45,100,000
14	Contingency	14,900,000	10,200,000	40,600,000
15	TOTAL PLANT COST	113,900,000	78,400,000	311,400,000
16	Escalation	24,200,000	16,600,000	96,200,000
17	Interest During Construction	25,600,000	17,600,000	133,700,000
18	TOTAL PLANT INVESTMENT	163,700,000	112,600,000	541,300,000

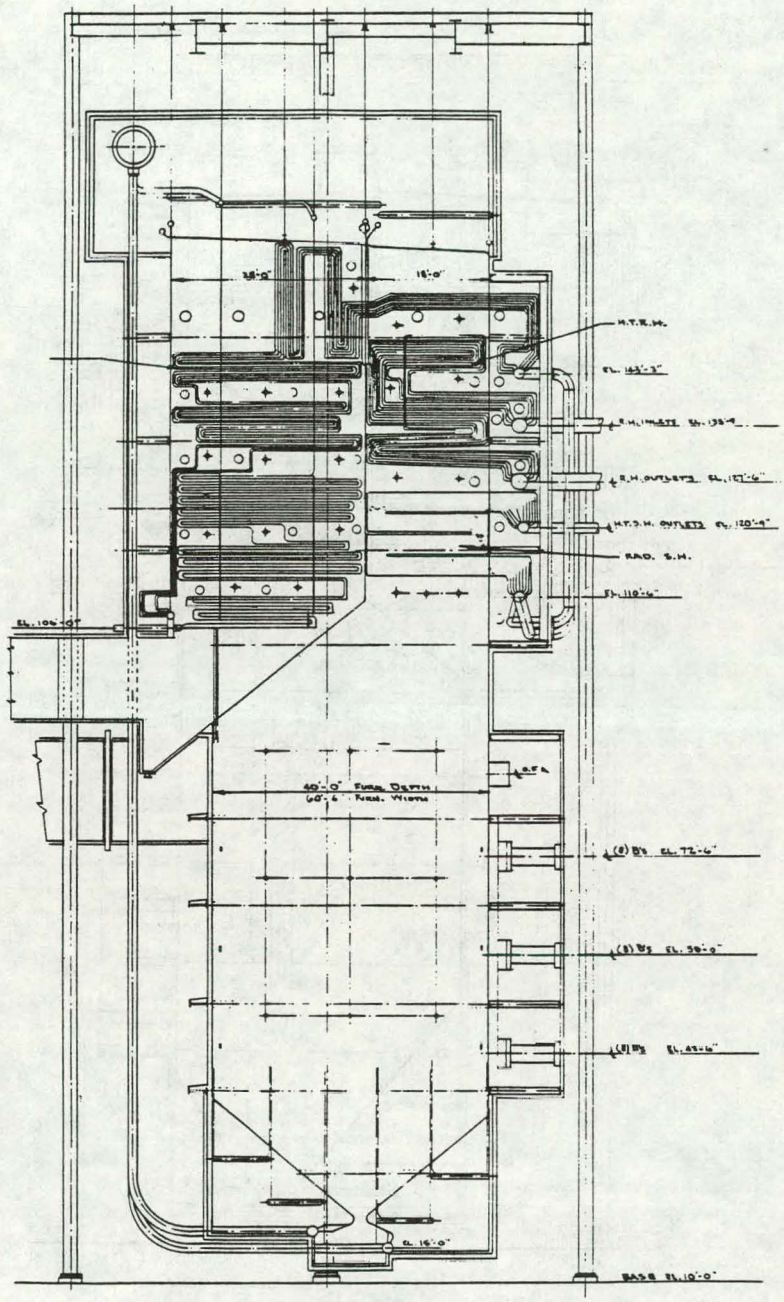

Figure 1
EXISTING OIL-FIRED BOILER

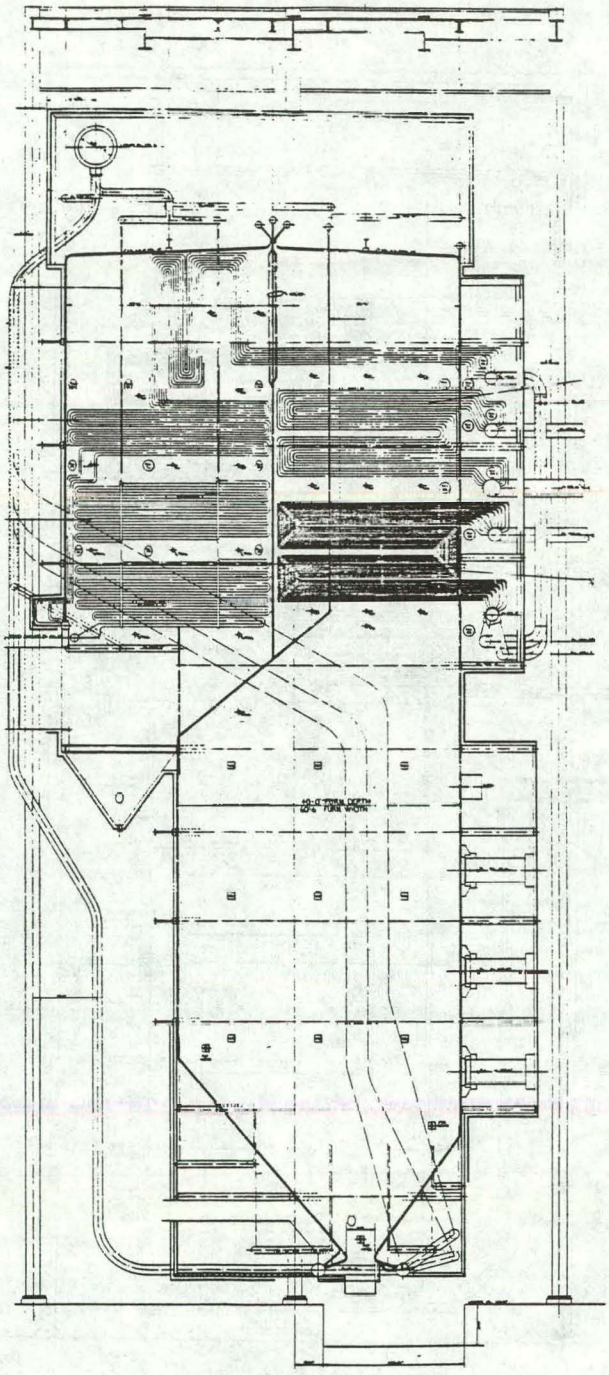

Figure 2
MODIFIED BOILER FOR PC OR CWM FIRING

Figure 3
FLUE GAS TEMPERATURES AND VELOCITIES
PULVERIZED COAL FIRING

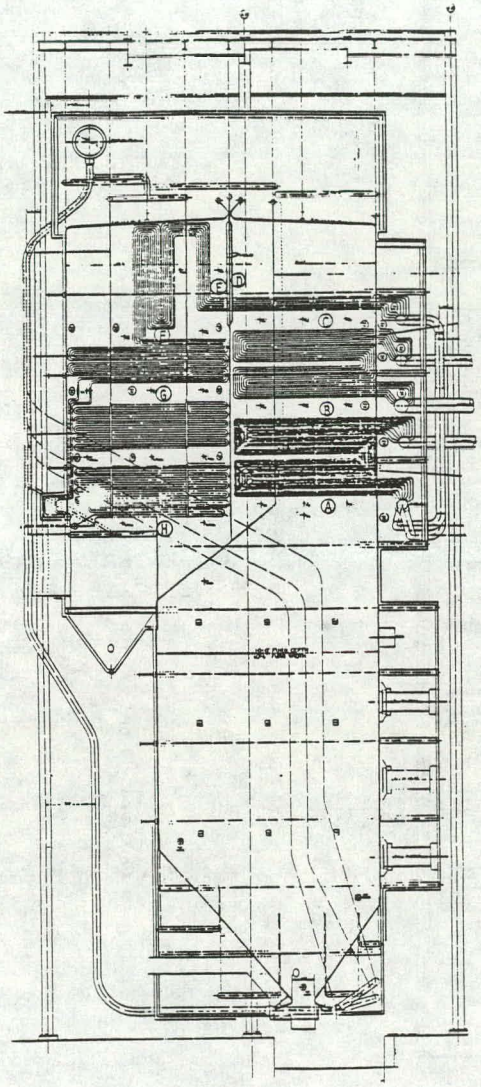

FLUE GAS TEMP., °F	
LOCATION	LOAD BMCR
A	2455
B	2250
C	1835
D	1790
E	1755
F	1420
G	1150
H	732

ENTERING GAS VELOCITY, FT/SEC	
LOCATION	LOAD BMCR
A	65
B	73
C	62
D	74
E	68
F	69
G	67

Figure 4
FLUE GAS TEMPERATURES AND VELOCITIES
COAL-WATER MIXTURE FIRING

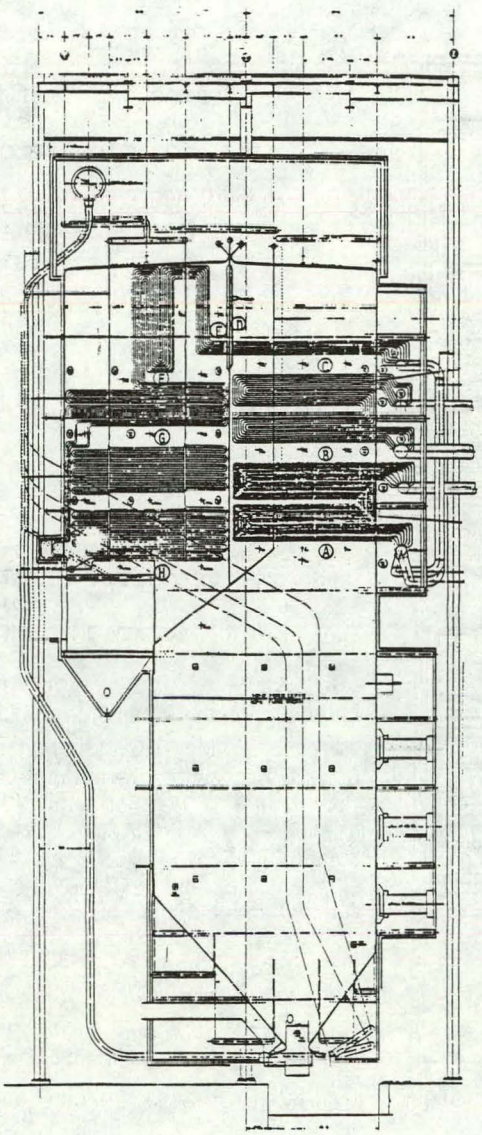

FLUE GAS TEMP., °F	
LOCATION	LOAD BMCR
A	2340
B	2110
C	1745
D	1700
E	1675
F	1355
G	1105
H	725

ENTERING GAS VELOCITY, FT/SEC	
LOCATION	LOAD BMCR
A	66
B	74
C	63
D	75
E	70
F	71
G	69

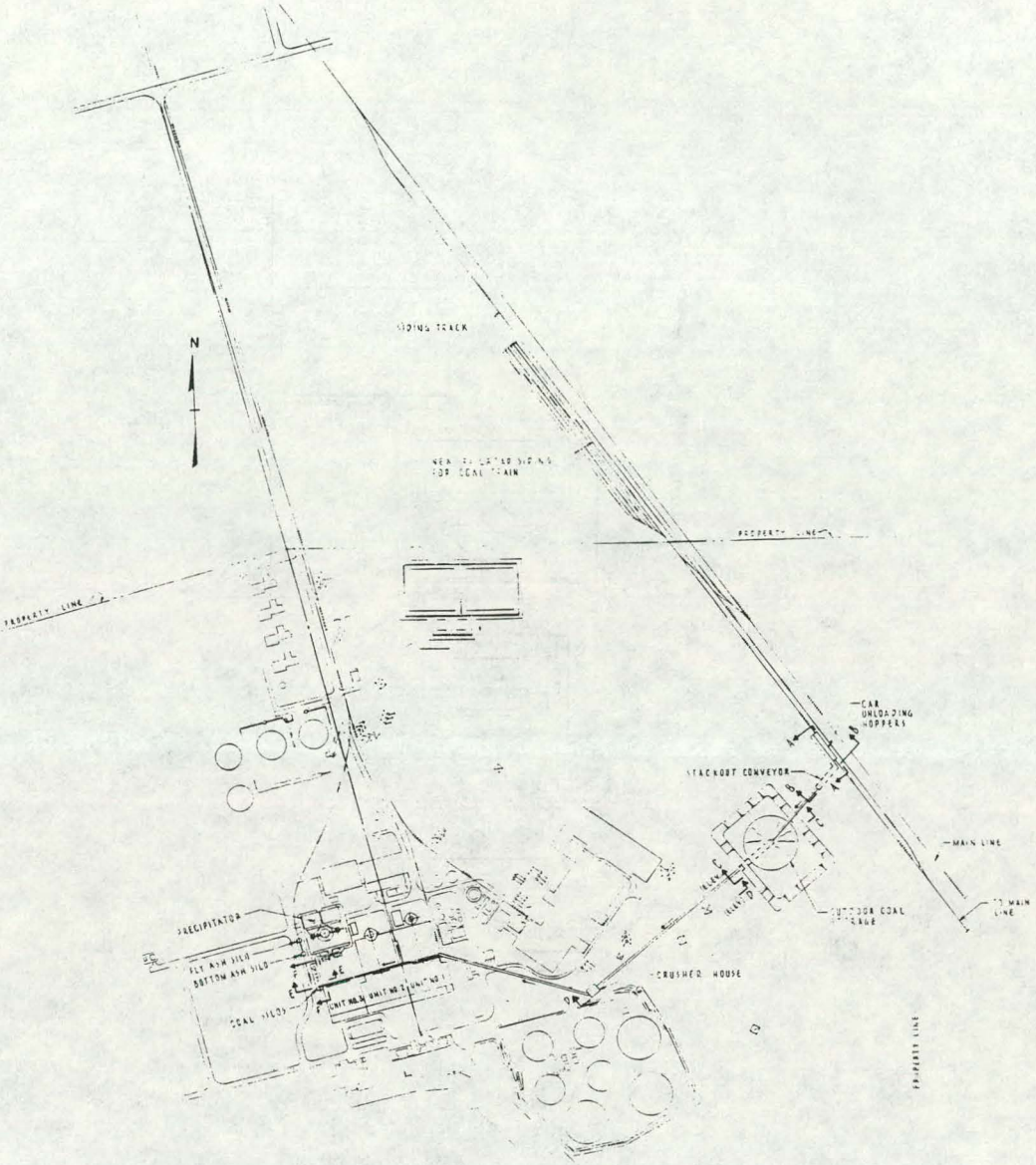

Figure 5
COAL HANDLING SYSTEM

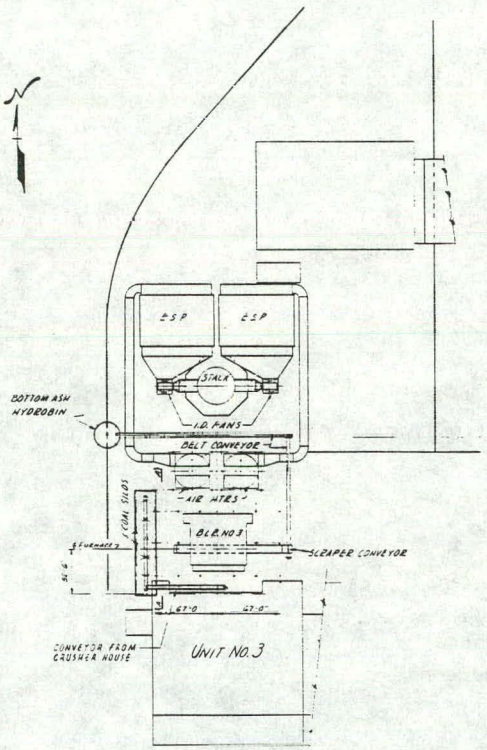

PLOT PLAN
SCALE 1" = 50'-0"

Figure 6

PLAN VIEW OF MODIFIED PLANT FOR PC FIRING

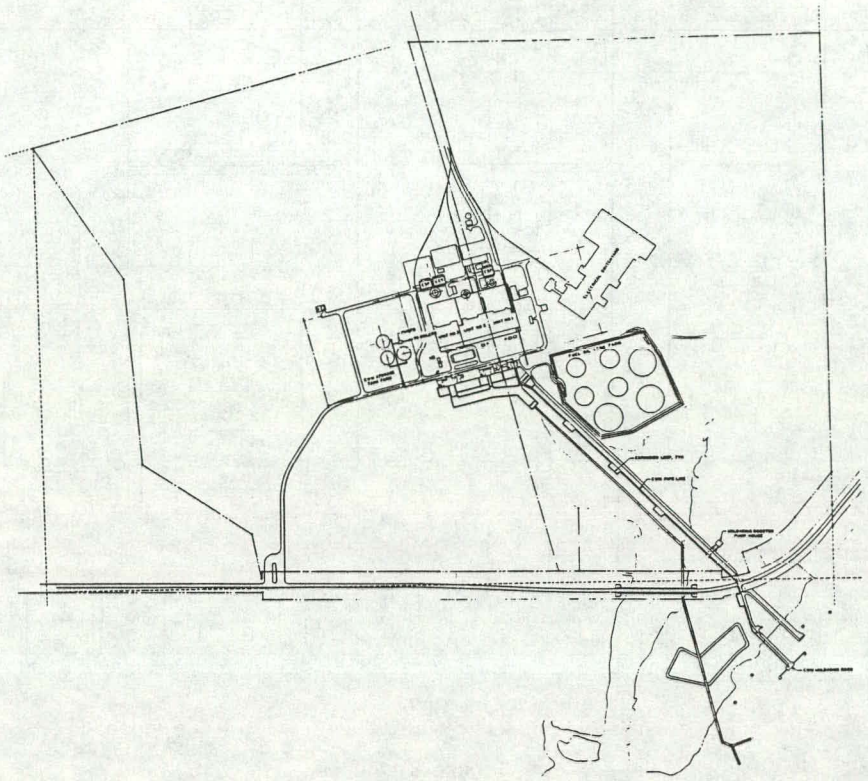

Figure 7
CWM SYSTEM

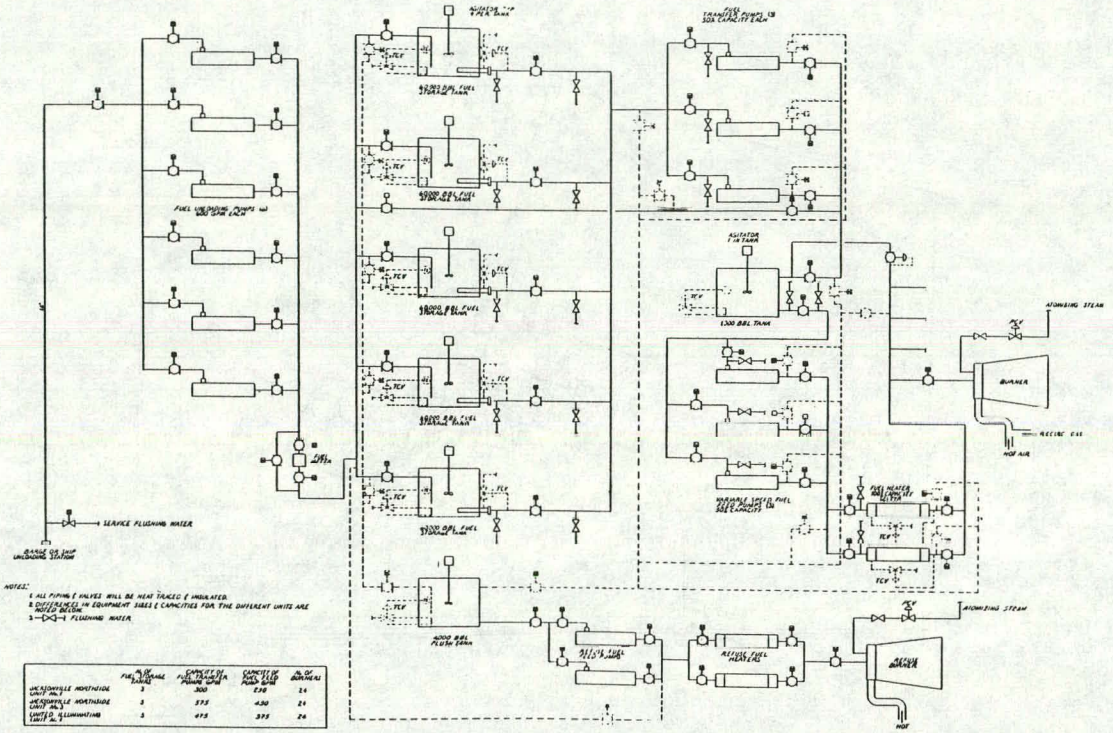

Figure 8

FLOW DIAGRAM CWM SYSTEM

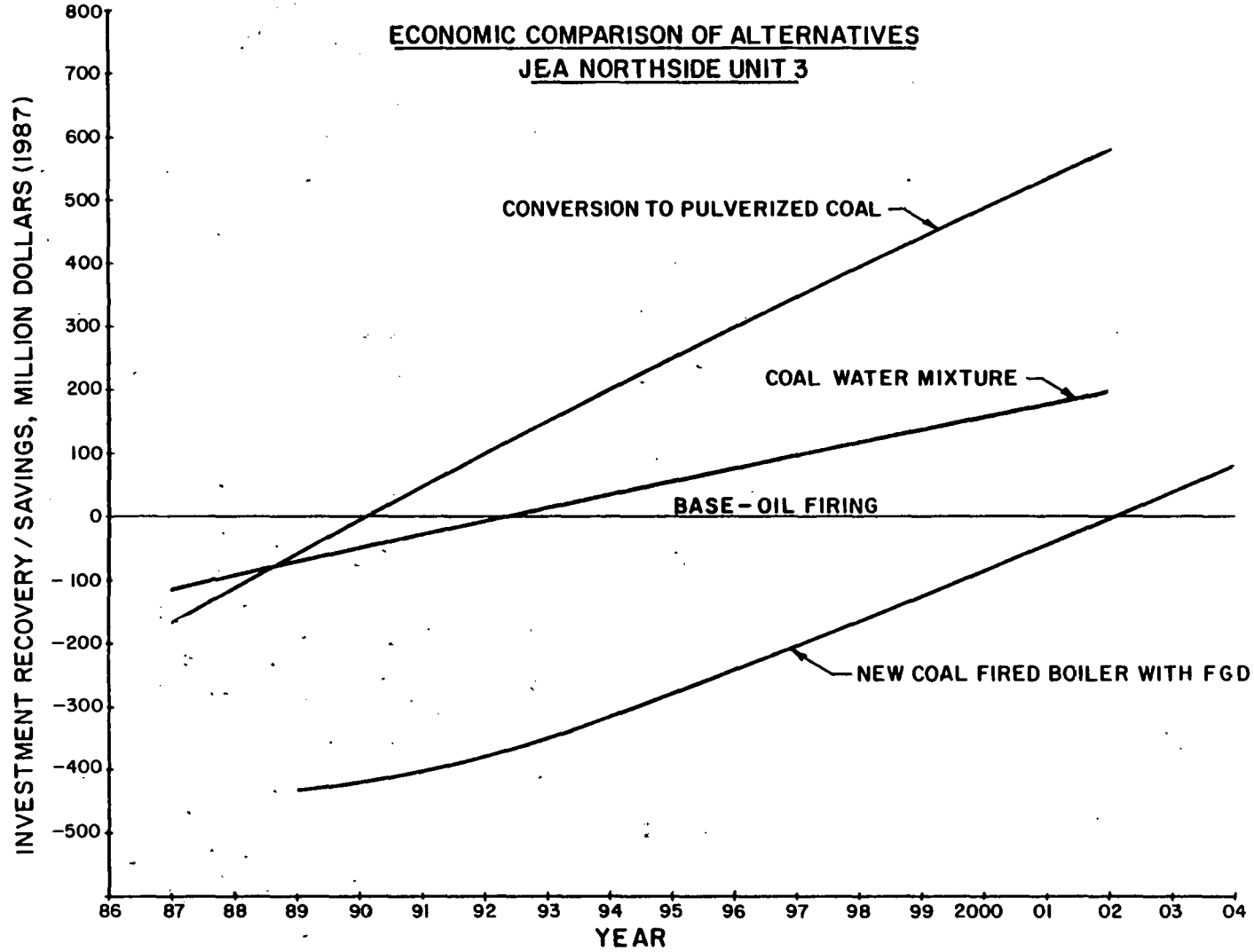
ECONOMIC COMPARISON OF ALTERNATIVES
JEA NORTHSIDE UNIT 3
INVESTMENT RECOVERY / SAVINGS, MILLION DOLLARS (1987)
800
700
600
500
400
300
200
100
0
-100
-200
-300
-400
-500
CONVERSION TO PULVERIZED COAL
COAL WATER MIXTURE
BASE - OIL FIRING
NEW COAL FIRED BOILER WITH FGD
86
87
88
89
90
91
92
93
94
95
96
97
98
99
2000
01
02
03
04
YEAR

FIGURE 9

AN EXAMINATION OF THE BEHAVIOUR AND STRUCTURE OF SINGLE DROPLETS OF COAL-OIL FUELS DURING COMBUSTION

by

K.J. Lapwood
Fuels and Energy Research Group, University of Surrey, England

P.J. Street
Marchwood Engineering Laboratories
Central Electricity Generating Board, England

F.D. Moles
Fuels and Energy Research Group, University of Surrey, England

1. INTRODUCTION

The idea of improving both the combustion and handling characteristics of coal by mixing it with oil is by no means a new one, the original patent on the subject[1] dating back just over 100 years. In fact, it is quite possible that some unknown contemporary of Sir Walter Raleigh ground up sea-cole in a pestle and mortar in order to mix it in with whale oil, thereby increasing the light emitted by his oil lamps. Equally likely he gave up his experiments in response to complaints from his wife about the mess! It was, of course, the 1973 Oil Crisis which triggered off the explosion of commercial interest, in coal-oil-water mixtures as substitute fuels, of which this present work forms a small part.

Research into the handling and combustion of coal-oil dispersions began at the University of Surrey in 1977. A series of BP sponsored pilot plant trials, already reported at an earlier DOE Symposium[2], demonstrated that coal rank was the significant factor affecting coal-oil fuel heat release patterns in furnaces and boilers. Jenkins et al[3] analysed these results and proposed the theory that the rank of the coal used in manufacturing the dispersion affected the physical mechanisms whereby individual coal-oil droplets devolatilised and then burned. A further study of this phenomenon was therefore undertaken, mostly with the same BP fuels but using a well tried, single particle, laboratory technique instead of, the far more expensive, pilot plant. This laboratory technique had been developed nearly 20 years ago by one of the present authors[4] at the U.K.'s Central Electricity Generating Board. Captive single droplets of coal-oil and coal-oil-water fuels can be rapidly heated and photographic records made of their combustion histories. Such experiments have been carried out by many previous workers, for instance at Sheffield University, on coal particles by Essenhigh[5] and oil drops by Masdin[6]. The results must be regarded with caution, because, in actual combustors, the particles/droplets occur in clouds and consist, mainly, of much smaller sized spheres. Nevertheless these isolated single particle methods are now well established as a quantitative tool which can usually shed some light on the likely behaviour of solid or liquid fuels in large combustion chambers.

2. INVESTIGATIVE TECHNIQUE

2.1 EQUIPMENT

The apparatus (Figure 1) has been described previously[4,7]. Essentially, it consists of a heating enclosure at the centre of which is suspended a single droplet of fuel. Radiation from two 1000 W tungsten filament projector lamps is focussed onto the droplet from two adjacent sides of this chamber through two collimating lenses. Concave mirrors are

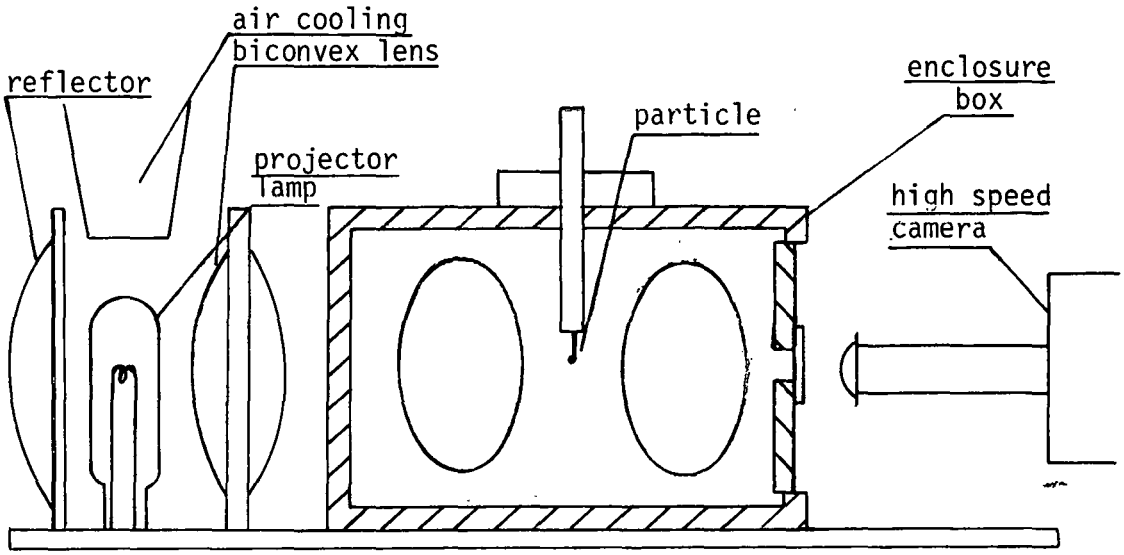

Fig. (1) Schematic diagram of the equipment

mounted directly opposite each lens so that radiation which bypasses the droplet is reflected back, thus ensuring that the sample is evenly heated from four sides. Thin brass shields protect the droplet from premature exposure to the radiation and the removal of these shields marks the beginning of the heating period.

The droplets which were typically 400-800μm in diameter, were mounted on quartz filaments 40-60μm in diameter. A small gas flame was then inserted about 10 mm above the sample to provide an ignition source for any flammable vapours involved.

The combustion history of each sample was photographed through an observation window in the corner of the heating enclosure using a 16 mm WF14(T) Fastex camera. The camera was nominally operated at 1000 frames per second; however, the actual framing speed was determined from a 1000 Hz spark imaged onto the film. Droplets of fuel are fully exposed to heating rates typical of those found in large boilers, a maximum about 10^4 ^{o}C sec^{-1} within 6 milliseconds. Records of the combustion history of each of the fuels investigated were obtained on black and white film, and later analysed using a motion analysis projector.

2.2 FUELS USED

A number of coal-oil dispersions, containing coals from high to low rank, were investigated. These were supplied by the British Petroleum Company (the coal particles being ground to a size distribution which ensured the stability of the resultant fuel). They included medium and low rank coals in 3500 second oil, petroleum coke dispersions, and dispersions doped with kaolin to simulate a high ash content coal. Two other dispersions were also prepared in the laboratory by the authors by grinding 101 and 301a NCB rank coals in 950 seconds fuel oil until a stable mixture was obtained.

Coal-oil mixtures were prepared by mixing samples of coal ground to normal p.f. distribution with 950 second fuel oil. These lacked inherent stability and were used soon after preparation. The effect of coal particle size was further investigated by mixing specific size cuts of coal, in the ranges 45-53μm, 53-63μm, 63-75μm and 75-125μm, with fuel oil. The concentration of coal in all of the coal-oil fuels was, typically, 35% by weight.

Finally, up to 20% by weight water was added to certain coal-oil mixtures using a laboratory homogeniser. This produced an emulsion of approximately 2μmdiameter water droplets in the oil phase.

3. RESULTS

The combustion of each droplet consisted of three main stages: initial heating, ebullition and combustion of the residual carbonaceous char (Plate 1). The first evolution of volatile matter occurred during the initial heating period. A gaseous shell was formed around the droplet by diffusing volatiles. This stage continued until the droplet reached its boiling point, which was marked by the commencement of vigorous surface bubbling. Dense clouds of volatiles were produced by explosive bursts at the surface and the diameter of the droplet fluctuated rapidly. Ignition of the volatile matter was often observed during this period, causing a thin flame front to surround the droplet. As the droplet continued to boil it became increasingly more viscous causing surface craters and blowholes to appear at the points where explosions had taken place. Eventually surface bubbling ceased completely and a solid residue remained on the filament. The combustion of the residual char, which was the final and longest stage, continued until an ash residue was formed.

The diameter of each droplet was measured at several points throughout the combustion period and subsequently plotted against time (Figures 3-10). These diameter histories were based on an equivalent spherical diameter, in order to account for the distortion of the droplet on the filament. Several differences, within the three stages of the combustion sequence, were observed in the behaviour of different types of fuel. These quantitative observations were supported by the diameter history plots.

3.1 EFFECT OF COAL RANK

The rank of coal used in the fuel was a very significant factor in the combustion mechanism of the residual char. Different char structures were formed by different coals, and two extremes of structure were identified. Low and high rank coals formed loosely agglomerated chars which comprised of many lightly fused, discrete particles (Plate 4c). Such chars had a granular surface, through which the filament was often visible. Mid-rank coals formed hollow chars with homogenous, completely fused surfaces which were pitted with blowholes (Plate 3). Coal rank also affected the size of the char formed. Mid-rank coals formed chars which were larger than the original droplets, whereas low and high rank coals of the same coal concentration formed chars which were about the same size as the original droplet (Figure 2). The swelling of mid-rank coal chars takes place at the end of the ebullition stage.

The initial structure of the char strongly affected the subsequent burnout characteristics. The loosely agglomerated chars eventually disintegrated into small clusters of individual particles (Plate 4d), whereas the well fused chars lost some mass by erosion around the surface blowholes but effectively stayed as single particles of approximately constant diameter until only an ash residue remained (Plates 1 and 3).

3.2 EFFECT OF THE FUEL OIL

All of the oils which were used in the manufacture of the coal-oil fuels were subjected to single droplet combustion analysis without the addition of coal or water (Plate 2). The combustion of fuel oil droplets is similarly a three stage process comprising of initial heating, ebullition and residual char combustion. The size of the carbonaceous char formed depended on the type of oil but was always smaller than chars formed from coal-oil fuels. The initial chars of coal-oil mixtures and dispersions had a shiny appearance which gave way to a dull surface as the droplet diameter rapidly decreased (Figures 3-7).This effect was apparent to some extent for all coal-oil fuels but was much more noticeable in fuels containing heavier oils. These observations suggest that the initial chars consist of an inner core of fused, or partially fused, coal particles surrounded by a layer of oil coke (Plate 1d).

During initial heating and ebullition the oil component of the droplet became increasingly more viscous as the volatile matter was evolved. Explosive bursts of volatiles were observed in all fuel droplets, which sometimes resulted in the formation of satellite droplets and blowholes on the surface of the solid carbonaceous residue. Fuels containing heavier oils, however, tended to experience more surface disruption than fuels containing lighter oils.

3.3 EFFECT OF COAL PARTICLE SIZE

Studies of fuels made with different size distributions of 301a NCB rank coal did not reveal any significant differences in the combustion

1a_Droplet

(20 msec)

⊢ 510μ

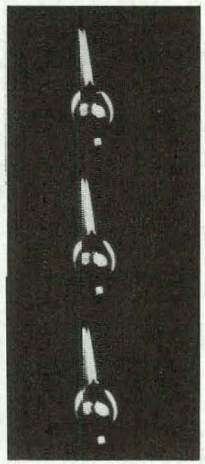

1b_Initial heating

(80 msec.)

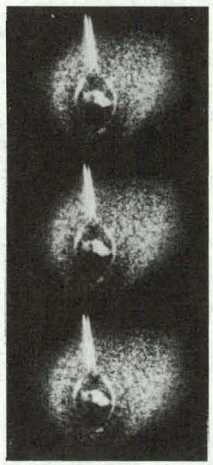

1c_Ebullition

(310 msec.)

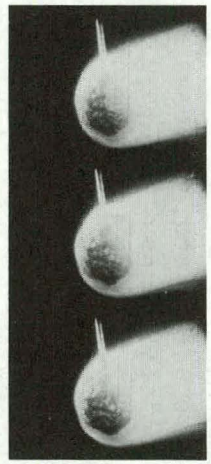

1d_Initial char

(530 msec.)

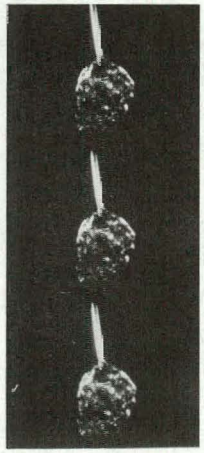

1e_Fragment-ation

(1350msec.)

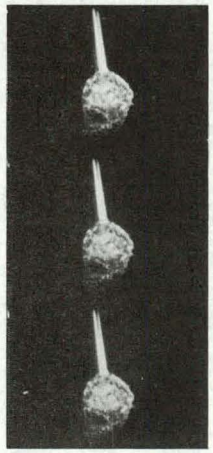

1f_Ash residue

(1870 msec.)

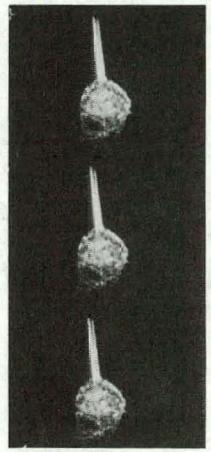

Plate 1– 35% Coal-Oil Mixture [301a NCB Rank(75-90μ) and 950 Second Oil]

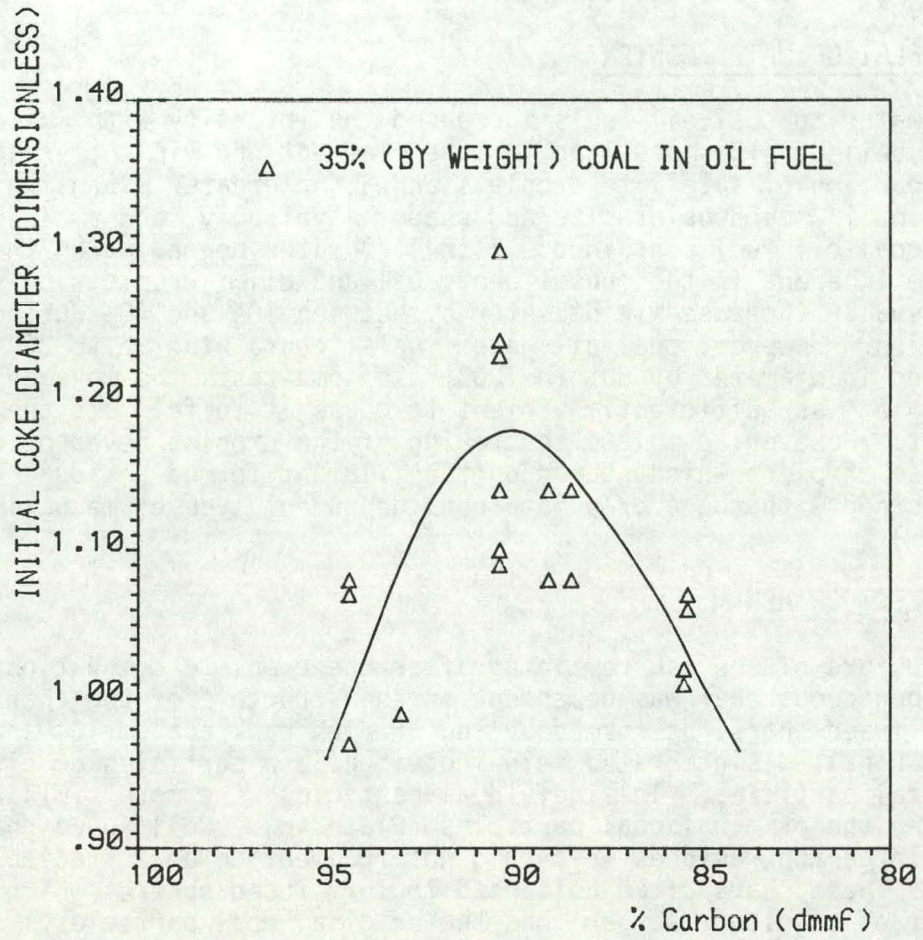

FIG(2)-Carbon Content of Coal vs Initial Coke Diam.

mechanism. This was also true of the comparison of a 101 NCB rank dispersion and a 101 mixture made with coal of typical p.f. distribution. Larger coal particles caused slightly larger carbonaceous residues to be formed, if the coal was prone to swelling but the burnout mechanism was not altered.

3.4 EFFECT OF WATER CONTENT

Adding water to coal-oil fuels increased the intensity with which the droplet boiled. This resulted in more frequent and violent explosions, the production of satellite droplets and a far greater expansion and distortion in the droplet size and shape. Typically, a normal 35% by weight coal-oil fuel contained 0.7 to 1.7% water depending on the moisture inherent in the constituent coal and oil. Droplets of such fuels usually increased in diameter by between 10% and 40% during ebullition. However, coal-oil-water fuels, containing up to 20% water, increased in diameter by 80% to 100%. In some tests the movement of the droplet was sufficiently violent to cause it to fall off the filament. However, complete shattering of the droplet never occurred and those droplets which stayed on the filament formed residual chars which burned with the appropriate coal dependent type of mechanism (Plate 5).

3.5 EFFECT OF ASH

The structure of the ash remaining after the complete combustion of the carbonaceous char was dependent on the structure of the char. Lightly fused chars, as formed by low or high rank coals (101 and 802 NCB rank), disintegrated into individual ash particles or clusters of several particles. The individual particles were more similar in size than the original coal particles (Plate 4d). Well fused chars formed large ash residues which did not fragment to an appreciable extent. These chars often collapsed to form fused spheres which were an order of magnitude larger than the original coal particles. This shape was termed an ash 'blackberry' (Plate 3c). Well fused chars which did not collapse formed hollow, lacy ash particles which were similar in diameter to the original fuel droplet (Plate 1f).

Ash fusion temperature did not affect the type of ash residue formed to the same extent as char structure. Anthracite (101 NCB rank) coal ash had a comparatively low deformation temperature of 1220°C. This, however, broke up into small ash particles. Grimethorpe (602 NCB rank) coal ash, with an initial deformation temperature of 1245°C fused to form a 'blackberry' shaped ash residue.

4. DISCUSSION OF THE RESULTS

4.1 FORMATION AND STRUCTURE OF COAL-OIL CHARS

In all combustion equipment char structure and burnout mechanisms have significant effects on flame characteristics. The combustion of coal or oil residues takes far longer than the evolution and subsequent combustion of the associated volatile matter. Consequently, char combustion affects flame length, heat release rates, particulate

2a - Droplet

(35 msec.)

⟝ 450μ

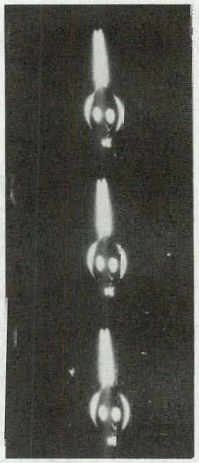

2b - Ebullition

(420 msec.)

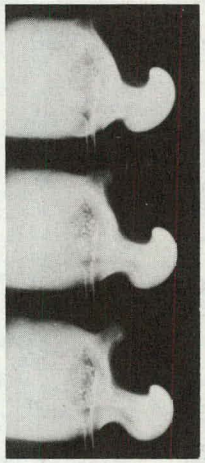

2c - Initial char

(600 msec.)

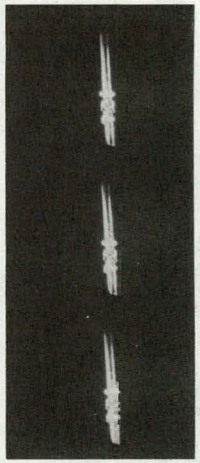

Plate 2 - 950 Redwood Second Fuel Oil

3a - Initial char

(620 msec.)

⟝ 770μ

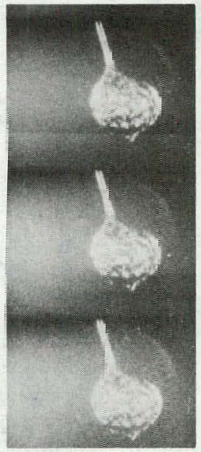

3b - Burning char

(1530 msec.)

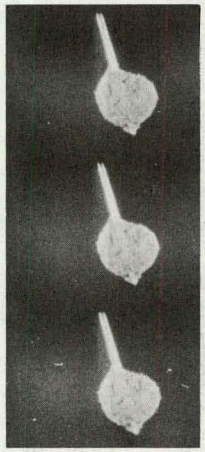

3c - Ash residue

(1970 msec.)

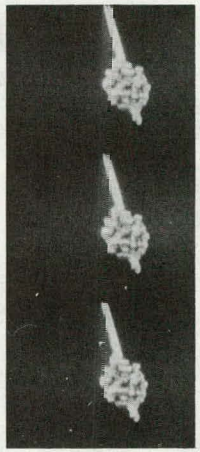

Plate 3 - 34.2% Coal-Oil Dispersion [602 NCB Rank and F80 Oil]

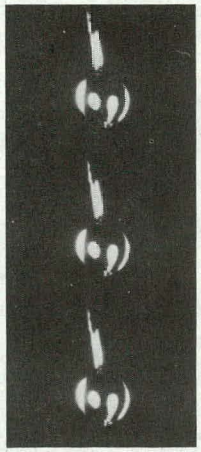

4a
Droplet
(10 msec.)
⟷ 680μ

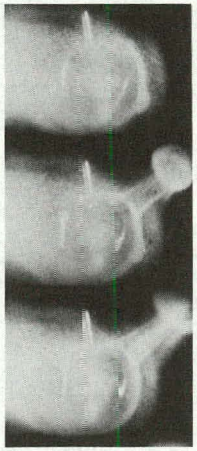

4b
Ebullition
(330 msec.)

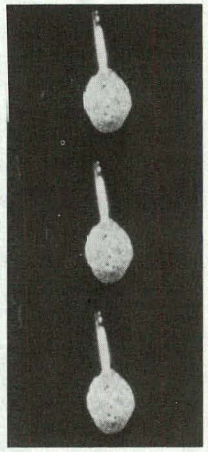

4c
Burning char
(1250 msec.)

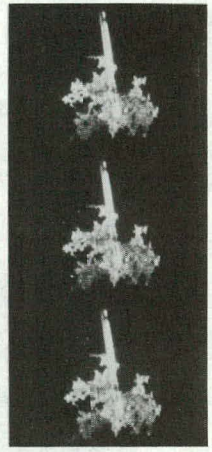

4d
Ash residue
(2010 msec.)

Plate 4–35% Coal-Oil Mixture [101 NCB Rank and 950 Second Oil]

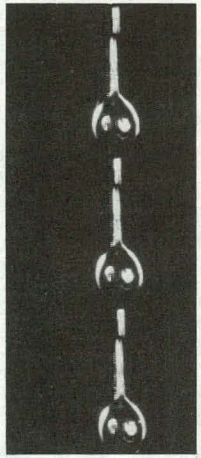

5a
Droplet
(30 msec.)
⟷ 630μ

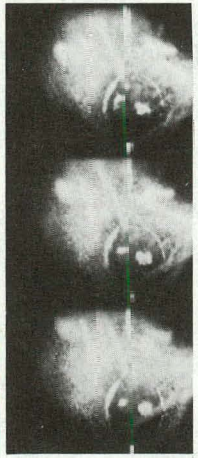

5b
Ebullition
(130 msec.)

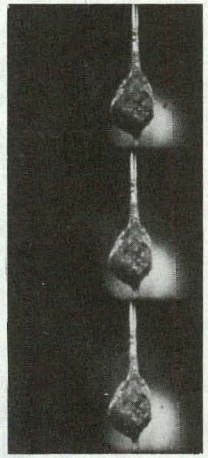

5c
Initial char
(790 msec.)

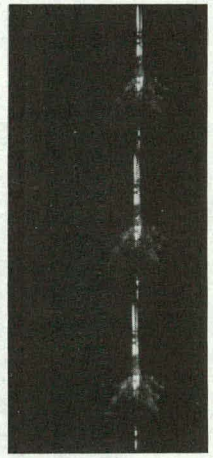

5d
Ash residue
(2300 msec.)

Plate 5—Coal-Oil-Water Mixture [29% 101 NCB Rank, 51% 950 Sec. Oil, 20% Water]

emissions and ash structure. It is, therefore, useful to discuss the formation and structure of coal slurry chars before considering the practical aspects of this work.

The principal finding of this study has been the dependence of char structure and burnout mechanism on coal rank. The swelling of coal-oil slurry chars has been reported by other workers in both single particle [8] and furnace trials [2]. In both cases a similar degree of swelling has been observed for coals of equivalent rank. It is evident that the char swelling ratio is less than would be given by the British Standard Swelling Test for constituent coals. This is consistent with the reported swelling ratios of coal particles in p.f. flames [9].

The agglomeration of coal particles within coal-oil droplets has been attributed to the effects of rapid internal recirculation in the drop [10]. It has also been shown that recirculatory motion within a multicomponent droplet allows the more volatile components to be preferentially vaporised [11]. The oil component of a coal-oil fuel would, therefore, be gradually distilled off leaving a core of agglomerated coal particles. Conversely, a lack of recirculation would result in the formation of gas pockets within the droplet and subsequent surface bubbling or explosions. The present results support the view that most of the oil is vaporised during initial heating and ebullition stages, leaving an inner core of coal particles surrounded by a thin layer of oil coke. However, violent bubbling of droplets during devolatilisation suggests that very little internal recirculation occurs.

Coking and swelling of mid-rank coals is due to their behaviour in the heating range 400-550°C. Within this range structural changes at a molecular level cause the coal to soften or liquefy [12]. The primary degasification of all ranks of coal occurs in this region, but marked softening occurs exclusively in a limited range of rank (about 85-92% carbon). Recent workers have explained this phenomenon using molecular, space-filling, models for coals of different ranks [13,14]. The temperature range is interesting with regard to the lifetime of coal-oil droplets since it corresponds to the middle or upper end of the distillation range for the constituent oils.

Lightman and Street [15] have measured the surface temperature of heavy fuel oil droplets during combustion and found that temperatures during their ebullition stage are typically in the range 300-800°C. It is therefore likely that disruptive boiling and devolatilisation of the oil occurs simultaneously with softening, fusion and primary devolatilisation of the coal. Under these circumstances a lack of internal recirculation is of little consequence except that the escape of trapped gases from within the droplet causes hollow, blowholed chars to be formed. Differential thermal analysis of coal has shown that secondary degasification occurs in coals of medium to low rank at between 600°C-700°C [16]. This explains the appearance of a second separate cloud of volatiles at the beginning of the char combustion period for some coal-oil fuels.

4.2 PARTICULATE EMISSIONS

High levels of unburnt carbon at the combustion chamber exit, due to

incomplete char burnout, represent wasted fuel and environmental problems.

Char burnout times between 55% and 85% of the total droplet lifetimes have been recorded in this investigation. This is particularly relevant if coal slurry fuels are to be burnt in conventional oil-fired equipment since the particle residence time here will be low. Possible options available for reducing the amount of solid residue left unburnt include reducing the concentration of coal in the fuel, improving atomisation and using a high pressure combustion system. The present study suggests that coal rank may also be an important factor, quite apart from any influence it may have on the inherent chemical reactivity of the fuels. Both high and low rank coals form loosely agglomerated structures with a relatively high available surface-to-mass ratio which break up during combustion. Mid rank coals, on the other hand, burn at nearly constant diameter having formed well-fused particles which, despite being swollen, have relatively less available surface since oxidant gas has to enter the surface blowholes and diffuse through the internal spaces to react. It is relevant to note that examination of the cine record revealed that wastage occurred preferentially around the blowholes of these spheres indicating that the oxygen concentration was being depleted even before the gas could penetrate the inside. It is also worth recording that a mathematical model for coal-oil dispersions involving a non-fused char mechanism for anthracite combustion and a completely fused structure for mid-rank coals[3] - assumptions which the present study have substantiated - has given good agreement with the results obtained from a pilot-scale furnace, which were reported to the Third Symposium in the present Series[2].

Finally, char burdens can in theory be reduced if the droplet shatters during evaporation. The result is again one of increased surface-to-mass ratio. Several workers[17] have advanced this mechanism in explanation for the significant decrease in unburnt carbon which has been reported during the firing of oil-water emulsions. However, furnace trials have not always revealed any significant decrease in the size distributions of the particulates collected[18]. The present work tends to support this finding: no significant mass loss occurred by shattering although small satellite droplets were formed due to the increased intensity of surface boiling. It is planned to investigate further the influence of water additions to coal-oil mixtures in future rig trials.

4.3 HEAT TRANSFER

In practice the rate at which heat is transferred from a flame is controlled primarily by radiative exchange in the combustion chamber. The factors which affect this process are the temperature, emissivity and geometry of the system[19]. The mechanism of char burnout is of significance here as it does not only affect the surface area for heat exchange with the surroundings, but also the rate of reaction and hence the temperature of the particles, as well as the pattern of heat transfer in the furnace.

4.4 ASH

The additional ash which coal-oil mixtures and dispersions possess may present difficulties when these fuels are burnt in conventional oil-fired burners. Fouling and slagging of the heat exchanger surfaces and flue gas cleaning are likely to be particular problem areas.

As noted previously, the structure and size of the ash would appear to be determined less by the chemical nature of the original mineral matter than by the fusion behaviour of the char particles themselves. By influencing combustion rates and heat loss to the surroundings, this will determine particle temperature but perhaps more importantly it will control whether or not the minerals are brought into contact with one another during droplet evaporation.

As a broad generalisation, well-fused chars (i.e. those from mid rank coals) will tend to form well fused and larger ash particles than lightly-fused chars. Thus they are more likely to result in a reduction in heat transfer efficiency by the formation of slagged and soot-blower resistant deposits[20] than the fine, fluffy ash resulting from the combustion of low and high rank coals. Conversely they are less likely to give problems in gas cleaning, the efficiency of which is universely related to the size of the solids carried forward.

5. CONCLUSIONS

The size and shape of the chars resulting from the combustion of coal-oil fuels is influenced by the rank of the coal present. Two extremes of structures have been identified: loosely agglomerated (partially fused) chars formed from high and low rank coals and similar in size to the original droplets; and swollen, well-fused spheres formed from mid-rank coals.

The structures produced influence the rate and mechanism of burnout. The partially fused type possesses a relatively high available surface-to-mass ratio and fragments during combustion. The well-fused type has a lower available surface since oxidant gas has to diffuse through the internal spaces of the particles to react internally. This burns at near-constant diameter.

Any advantages in short burnout times which might have been expected from fine grinding are largely negated by particle fusion. The chars from low rank coal-oil fuels (801-902) have the highest rates of reaction.

The structure and size of the ash produced is dependent less on chemical composition than on the fusion behaviour (and hence the rank) of the coal present. Broadly speaking, well-fused chars tend to form large well-fused ash particles which may give rise to furnace slagging problems although they should be amenable to conventional flue gas cleaning measures.

The present study does not encourage the belief that addition of water to a coal-oil fuel will result in drop shattering.

6. REFERENCES

1. SMITH, H.R. and MUNSELL, H.M.
   Liquid Fuel
   U.S. Patent 219, 181, 24 February (1879).

2. ALABAF, J.S., PATTERSON, M.C. and MOLES, F.D.
   "Handling, Combustion and Emissions from Coal-oil Dispersions When Fired through an LPA Burner"
   pp. 1081-1100, 3rd Int. Symp. on Coal-Oil Mixture Combustion, Orlando, 1-3 April (1981).

3. JENKINS, B.G., ALABAF, J.S., PATTERSON, M.C. and MOLES, F.D.
   "The Effect of Coal Rank on the Heat Release from Coal-Oil Dispersions"
   Proceedings 64 Canadian Inst. of Chemists Coal Symposium, Ottawa, October (1982).

4. ANSON, D., MOLES, F.D. and STREET, P.J.
   "Structure and Surface Area of Pulverised Coal During Combustion"
   Combustion and Flame, 16, pp 265-274 (1971).

5. ESSENHIGH, R.H. and THRING, M.W.
   "Measurement and Burning Times of Single Coal Particles"
   pp. D21-D27, Conference on Science in the Use of Coal, Sheffield, 15-17 April (1958) Inst. Fuel London.

6. MASDIN, E.G.
   "The Combustion of Droplets of Liquid Fuel"
   Univ. of Sheffield, Fuel Soc., Jul. 12, 17-28 (1961).

7. STREET, P.J.
   "Physical Changes Occurring in Pulverised Coal Particles During Combustion"
   Ph.D. Thesis, University of Surrey (1969).

8. BRAIDE, K.M.
   "The Combustion of Coal-Oil Mixture Droplets"
   Ph.D. Thesis, University of Leeds (1980).

9. LIGHTMAN, P. and STREET, P.J.
   "Microscopical Examination of Heat Treated Pulverised Coal Particles"
   Fuel (London), 47 (1968).

10. MIYASAKA, K. and LAW, C.K.
    "Combustion and Agglomeration of Coal-Oil Mixtures in Furnace Environments"
    Combustion Science and Technology, 24, pp. 71-82 (1980)

11. LAW, C.K.
    "Multicomponent Droplet Combustion with Rapid Internal Mixing"
    Combustion and Flame, 26, pp. 219-233 (1976).

12. VAN KREVELEN, D.W. and SCHUYER, J.
    "Coal Science"

Elsevier (1957).

13. SPIRO, C.L.
"Space Filling Models for Coal: a Molecular Description of Plasticity"
Fuel, 60, pp. 1121-1126, Dec. (1981)

14. SPIRO, C.L. and KOSKY, P.G.
"Space Filling Models for Coal 2. Extemsion to coals of Various Ranks"
Fuel, 61, pp. 1080-1084, Nov. (1982).

15. LIGHTMAN, P. and STREET, P.J.
"Single Drop Heating Experiments on Residual Fuel Oils and Fuel Oil Fractions"
Jnl. Inst. Energy, March (1983).

16. GLASS, H.D.
"Differential Thermal Analysis of Coking Coals"
Fuel, 34, pp. 253-268 (1955).

17. JORDAN, J.B. and WILLIAMS, A.
"Fuel Oil-Water Emulsions"
Institute of Energy Symposium, Portsmouth Polytechnic, Portsmouth, Nov. (1981).

18. Private communication
P.J. Street, July (1982).

19. FIELD, M.A., GILL, D.W., MORGAN, B.B. and HAWKSLEY, P.G.W.
"Combustion of Pulverised Coal"
Br. Coal Util. Res. Assoc. (1967).

20. G.W. HIMUS
"Fuel Testing"
Leonard Hill Ltd, London (1954).

ACKNOWLEDGEMENTS

One of us, K.J. Lapwood, would like to thank the U.K. Central Electricity Generating Board for their financial support.

The authors gratefully acknowledge the contributions of Dr. B.G. Jenkins and Dr. M.C. Patterson to this work, and the assistance of Mr. C.L. Norman during the experimental studies.

Permission to publish this work has kindly been granted by the British Petroleum PLC and the U.K. Central Electricity Generating Board.

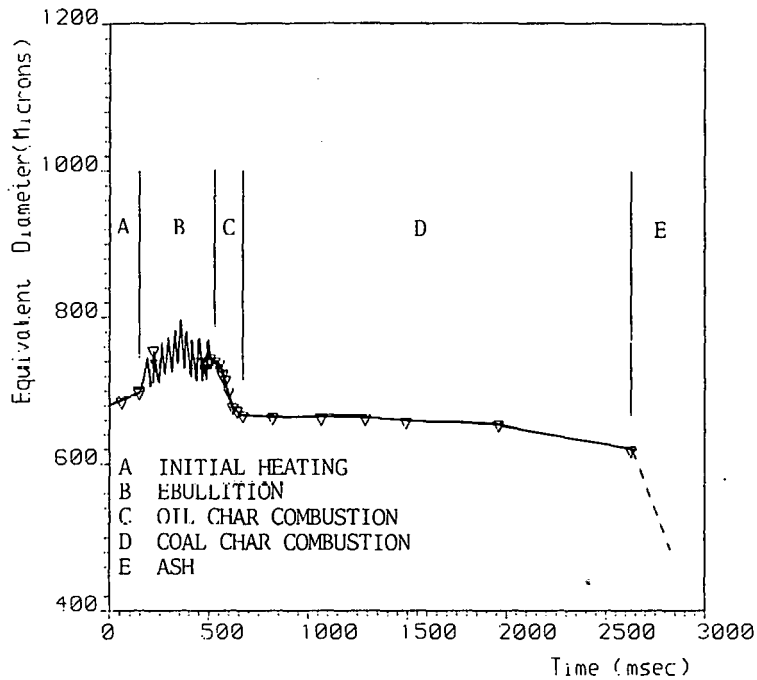

FIG(3)-35% Anthracite [NCB Rank 101] Dispersion

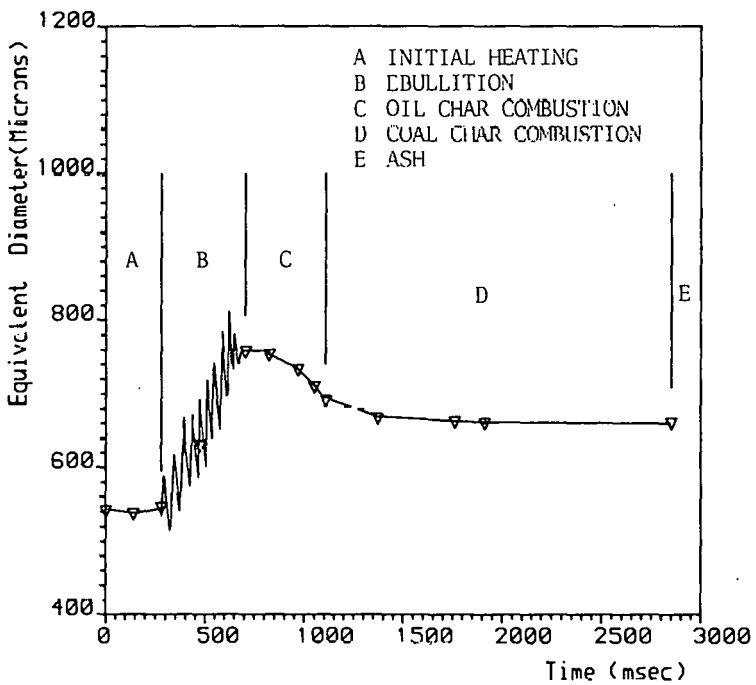

FIG(4)-NCB Rank 301a (75-90) & 950 Second Oil Mixture

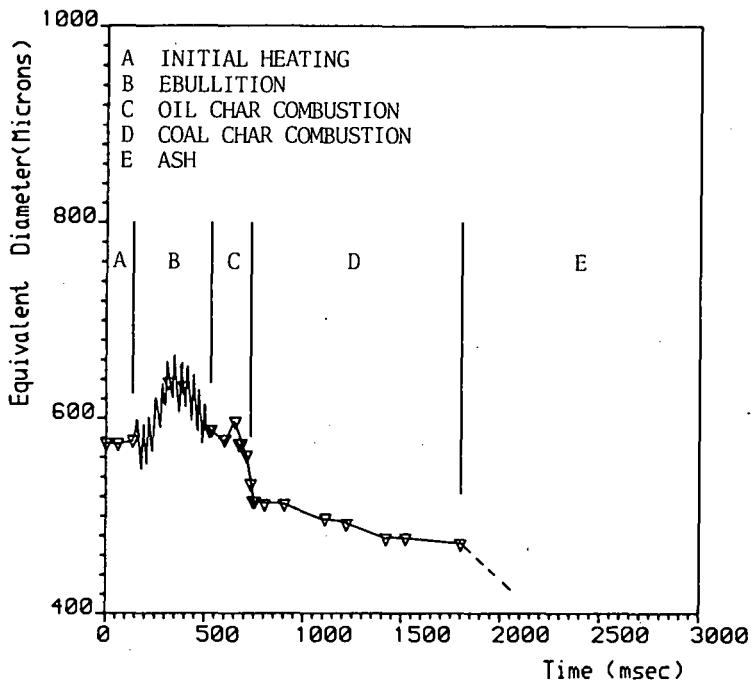

FIG(5)-34% Butterwell [NCB Rank 802] Dispersion

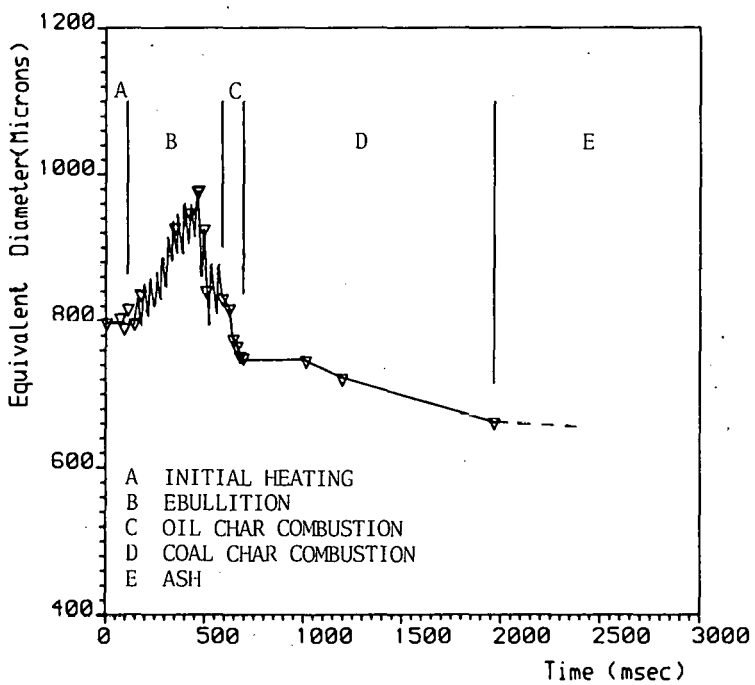

FIG(6)-33% Grimethorpe [NCB Rank 602] Dispersion

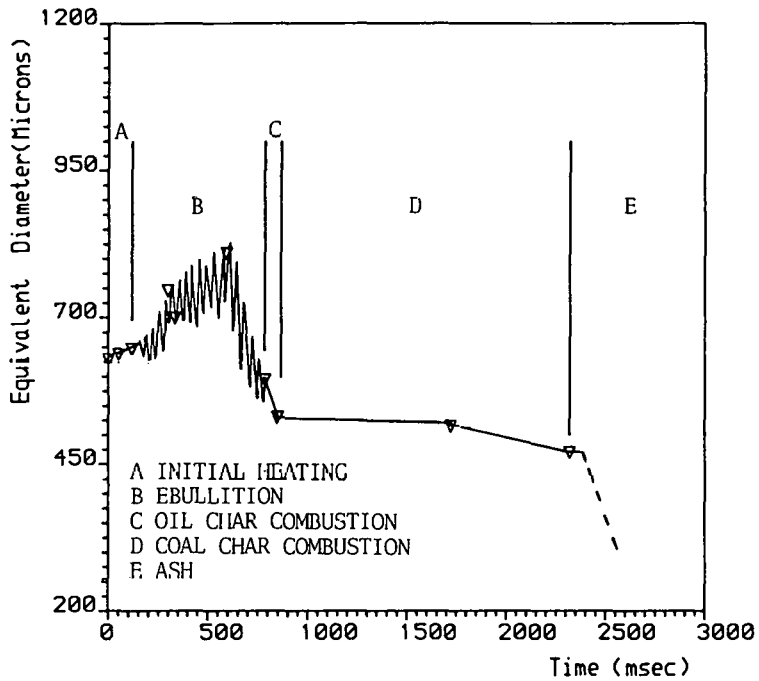

Fig(7) 32% Anthracite,21%Water & 47% 950 Second Oil

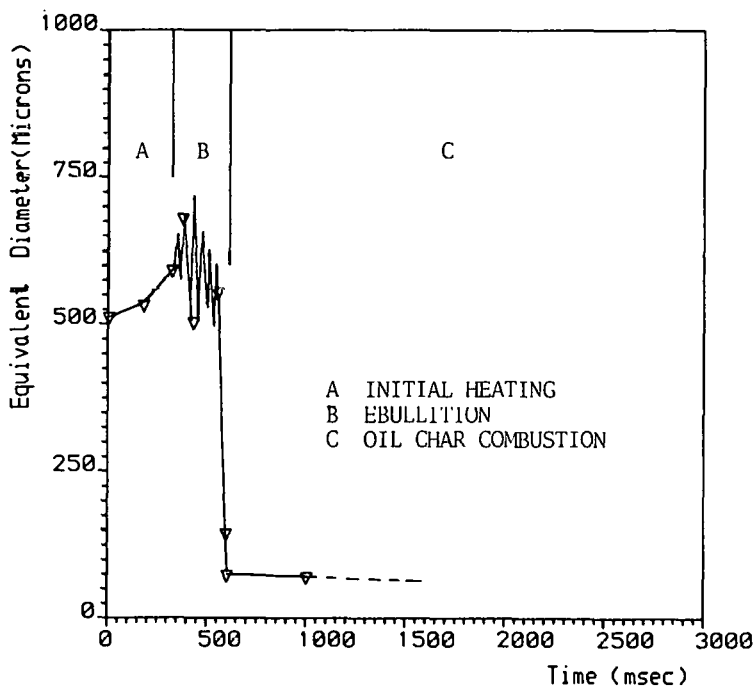

Fig.(8) 950 Second Fuel Oil

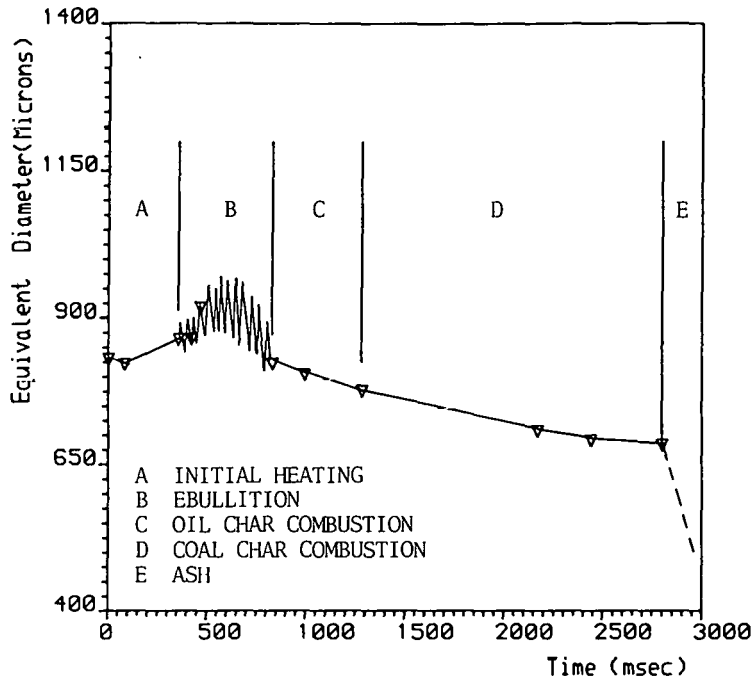

Fig.(9) 36% Petroleum Coke Dispersion

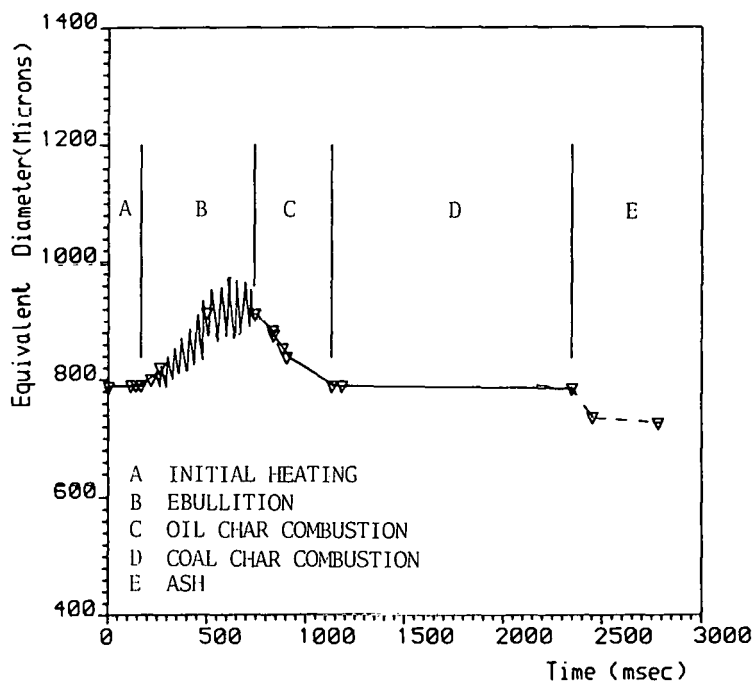

Fig.(10) Ashington [NCB Rank 702] & Kaolin Dispersion

APPENDICES

Analysis of Fuels

Table (A1) SUMMARY OF COAL SLURRY FUELS TESTED

TABLE (A2) ANALYSIS OF COALS USED IN COAL-OIL FUELS

TABLE (A3) FUEL OILS USED FOR COAL-OIL FUELS

FUEL	NCB RANK	OIL*	COAL CONCENTRATION (% wt)	WATER CONCENTRATION (% wt)	COAL PARTICLE SIZE
Anthracite dispersion	101	950	35.0	0	Note (1)
Anthracite mixture	101	950	36.1	0	98.4% < 125 μm
Cwm dispersion	301a	950	34.7	0	Note (1)
Cwm mixture	301a	950	35.2	0	45-63 μm
Cwm mixture	301a	950	34.6	0	53-63 μm
Cwm mixture	301a	950	35.2	0	63-75 μm
Cwm mixture	301a	950	34.9	0	75-90 μm
Herrington dispersion	301b	F80	40.5	0	Note (1)
Grimethorpe dispersion	602	F80	33.1-33.7	0	Note (1)
Pleasley dispersion	602-701	F80		0	Note (1)
Ashington & Kaolin dispersion	702	F80	29.0 coal 6.3 kaolin	0	Note (1)
Butterwell dispersion	802-902	F80	33.4-35.8	0	Note (1)
Coal-oil-water 1	101	950	31.7	20.7	98.4% < 125 μm
Coal-oil-water 2	101	950	27.1	17.9	98.4% < 125 μm
Petroleum coke dispersion	-	F35	36.1	0	Note (1)

Note (1) - Coal particle ground until stability of fuel is assured.
* - Refer to Table (A3)

TABLE (A1) - SUMMARY OF COAL SLURRY FUELS TESTED

COAL	NCB RANK	CHEMICAL ANALYSIS (% wt.)					ASH CONTENT	ASH FUSION TEMP. °C			MOISTURE
		C	H	N	O	S	(% wt)	D.T.	H.T.	F.T.	(% wt)
Anthracite	101	82.04	3.06	1.20	2.03	0.97	5.9	1220	1280	>1500	1.7
Cwm	301a	84.59	4.44	1.30	3.91	0.76	8.0	1290	>1500	>1500	1.4
Herrington	301b	†	†	†	†	†	6.5	1500	>1500	>1500	†
Grimethorpe	602	53.6	3.31	1.10	4.35	1.69	34.7	1245	1390	>1500	1.6
Pleasley	602-701*	72.8	-	1.95	-	1.25	10.6	1150	1210	1330	2.2
Ashington	702	50.1	3.75	1.15	7.25	1.14	23.2	1385	1455	1495	3.2
Butterwell	802-902*	72.6	4.18	1.55	7.15	1.38	9.0	1270	1385	1430	4.5
Petroleum Coke	-	89.1	3.68	1.05	1.80	3.40	0.4	-	-	-	0.9

* - Dependent on seam † - Analysis not available

TABLE (A2) - ANALYSIS OF COALS USED IN COAL-OIL FUELS

OIL	SPECIFIC GRAVITY ($d15.5^{o}C/15.5^{o}C$)	VISCOSITY (mm^2/sec)			CARBON RESIDUE (% wt)	ASH (% wt.)	MOISTURE (% wt)
		$60^{o}C$	$80^{o}C$	$100^{o}C$			
950 Redwood Second	0.9510	70.0	33.4	18.3	†	0.019	0.2
F80	0.9830	213.0	74.5	36.4	13.0	0.043	0.2
F35	0.9857	77.8	33.3	17.1	14.5	0.05	NIL

† - not available

TABLE (A3) - FUEL OILS USED FOR COAL-OIL FUELS

Session IX

COMBUSTION

Wednesday, April 27, 1983

Chairman: Roy C. Kurtzrock,
Pittsburgh Energy Technology Center, DOE

SIZE DISTRIBUTION, DENSITY AND YIELD OF CARBON PARTICLES GENERATED IN COAL-OIL SLURRY FLAMES

by Robert P. Cossee* and Alan B. Hedley‡

Abstract

This paper reports on measurements of the quantity of unburnt carbon and the size distribution and density of char particles produced after devolatilisation and partial combustion of coal-oil slurry sprays. In a previous publication by the authors the above parameters were shown to be important considerations when attempting to predict the carbon burn-out rates of slurry-type fuels.

Char particles were collected from coal-oil slurry flames at a pre-determined point in the furnace where essentially no further oxidation of solid carbon occurred, and size distributions and densities of the extracted char particles were subsequently measured using a technique based on the forward scattering of a parallel beam of monochromatic light.

Measurements were done for several atomising and combustion air flow rates, fuel temperatures and fuel types. It was observed that reductions in atomising air flow rate caused a progressively significant increase in the size of the char particles produced, accompanied by a decrease in particle density; it was apparent that particle agglomeration was increased, with a simultaneous increase in the degree of swelling. Fuel composition and combustion air-fuel ratio also had an effect, however, no significant change was observed when fuel temperature was slightly reduced. The theoretical burn-out of some experimentally determined char size distributions was calculated to illustrate the potential effect of a change in atomising air flow rate on combustion efficiency.

* Research Worker.

‡ Director,
SHELL/NCB Coal Technology Research Group,
Department of Chemical Engineering and Fuel Technology,
University of Sheffield, Mappin Street,
Sheffield S1 3JD, United Kingdom.

SIZE DISTRIBUTION, DENSITY AND YIELD OF CARBON PARTICLES GENERATED IN COAL-OIL SLURRY FLAMES

by Robert P. Cossee (Research Worker) and
Alan B. Hedley (Director)

SHELL/NCB Coal Technology Research Group,
Department of Chemical Engineering and Fuel Technology,
University of Sheffield,
Mappin Street,
Sheffield S1 3JD, United Kingdom.

1. Introduction

The possible substitution of oil or gas with a coal-slurry fuel in any industrial application involves a consideration of many factors, one of these being the effect it has on carbon conversion efficiency. The rate of burn-out of carbon in coal-liquid mixture flames depends on a considerable number of parameters ranging from excess air levels and air preheat to the quality of atomisation, however, additional factors such as the reactivity of the carbon particles (or chars) that are formed, and the extent to which agglomeration occurs also need to be considered.

This work forms part of a current study which is specifically concerned with an investigation of carbon burn-out rates of coal-oil slurries using a Controlled Mixing History (CMH) furnace. In the primary zone of this furnace char particles are generated by allowing a fuel (spray or particle suspension) to undergo devolatilisation and partial combustion with a proportion of the stoichiometric combustion air. In the secondary zone of the furnace the remainder of the combustion air is added, thus initiating the burn-out of these particles. In a previous paper[1], which also described the CMH furnace, it was shown that the yield of unburnt carbon and the size distribution and density of the char particles produced in the primary zone would be parameters essential to the study mentioned above. This paper is primarily a report of measurements of these parameters, which were obtained during a series of coal-oil mixture combustion trials. In addition to forming part of a data base required for the combustion rate calculations, the results can be used separately to show how the various atomising, combustion and fuel parameters affect the nature of the particles that are formed as the droplets undergo devolatilisation, and can provide an insight into the degree of particle agglomeration and swelling that can take place during this process.

2. Experimental Apparatus and Procedure

The primary zone of the furnace is shown in fig. 1. The principle objective was to allow ignition, devolatilisation and partial combustion of a coal-oil fuel spray to take place in such a manner that

an evenly distributed mixture of furnace gas and devolatilised char particles was produced with a minimum amount of recirculation or deposition. Only a proportion of the stoichiometric combustion air (46-67%) was mixed with the fuel spray. The burner which was developed to suit these requirements is shown in fig. 2. A twin-fluid, internal-mixing atomiser (fig. 3) was used, with high pressure air as the atomising fluid. Fuel flow rate was accurately controlled using a variable-speed positive displacement pump and fuel temperature was measured with a thermocouple situated at the fuel inlet of the atomiser body. The atomising air was set to the desired flow rate, rather than pressure. Fuel and air pressures ranged from 1 to 2 and 1.5 to 2.5 bar, respectively.

Sampling from the flame was done with a water-cooled sampling probe as close to iso-kinetic conditions as practically possible and solids were collected in sintered bronze filters. An on-line infra-red analyser was used for the immediate measurement of CO_2 concentration, and additional furnace gas samples were collected in gas bottles for subsequent analysis of N_2, O_2, CO_2, CO, H_2 and CH_4 concentrations using gas chromatography. Fig. 4 is a schematic diagram of the sampling train.

Char particles were extracted from the flame axis at the end of the primary zone (port 4). To ensure that the furnace gas was uniformly mixed during all the experimental runs, CO_2 concentrations were measured across the furnace diameter using the i.r. analyser, and the CO_2 profile was found to be flat within the accuracy of the instrument ($\pm$ 0.05% CO_2) in each case. To check that the oxidation of solid carbon had essentially ceased, a series of gas samples were taken at ports 3 and 4, and the corresponding degree of carbon burn-out was calculated by means of a carbon balance. The calculations showed that an insignificant amount (< 1%) of the fuel carbon was consumed as the gases passed from port 3 to port 4, which was estimated to take 0.16 seconds in this case. An additional check showed that, for a constant overall air-fuel ratio, the amount of unburnt carbon was not significantly affected by a reduction in fuel and air flowrates of more than 20%, which corresponded to an increase in residence time in the primary zone of approximately 30%.

3. Particle Size Distribution and Density Measurement

The technique used for measuring the size distribution of the extracted particles was developed at Sheffield University[2] and is now available commercially*. The principle, which is described in detail in the literature[3], is based on the forward scattering of a parallel, monochromatic beam of light, where the angle of diffraction is a function of particle size (see fig. 5). The size distribution of a spray or particle suspension is calculated by microprocessor from the composite diffracted light energy distribution, as shown in fig. 6. Early versions calculated parameters of model size distributions such as Rosin-Rammler or Log-Normal. More recently, it has been possible to reliably determine model-independent size distributions, owing to two

* Malvern Instruments Limited, U.K.

factors; a) improved optics giving higher signal to noise ratios, and b) the incorporation of better algorithms in the software. The use of the model-independent facility proved essential to the present work, as conventional particle size distribution equations were found to give poor fits when applied to the char samples.

The instrument was set up to measure particle diameters in the range 5.8 to 564.0 μm. The char particles were wetted with a strong aqueous solution of surfactant* and subsequently suspended in water. The presence of soot caused considerable obscuration of the laser beam and gave rise to erroneous results. This was overcome by wet screening the sample at 5 μm. Since most samples were found to have no char particles below 10 μm, it was concluded that removal of the -5 μm cut would not affect the char size distribution. The suspension, which had a typical concentration of 0.3 (mg/ml), was processed in batches of approximately 15 ml and the overall size distribution and density of the particles was determined from the averaged light energy data. The volume concentration of the sample was calculated from[4]

$$C_v = \frac{-\ln(I/I_o)}{3 \cdot L \cdot \sum_{i=1}^{15} (V_i/d_i)} \quad (m^3/m^3) \qquad .....(1)$$

where

C_v = volume fraction occupied by the particles in the suspending liquid (m^3/m^3),

I/I_o = attenuation of the laser beam due to the particles,

L = path length of the laser beam in sample cell = 14.3×10^{-3} (m),

V_i = volume fraction of the ith particle size band,

d_i = average diameter of the ith size band,

i = number of the size band in the particle size analyser (15 in total),

which was used to calculate the average particle density, ρ:

$$\rho = \frac{W}{C_v \cdot V_s} \quad (kg/m^3) \qquad .....(2)$$

where

W = weight of char sample (kg),

V_s = volume of suspending liquid (m^3).

* Nonidet

For reasons which will become clear in the next section, an expression was derived for the specific external surface area, A_E, that is the external area per unit weight of the particles. Consider the external surface area per unit volume of char sample

$$A'_E = \sum_{i=1}^{15} \left(\frac{6}{d_i} \cdot V_i \right) \qquad (m^2/m^3) \qquad .....(3)$$

where

$\frac{6}{d_i}$ = external surface area per unit volume of a sphere of diameter d_i,

then the specific external surface area, A_E is given by

$$A_E = \frac{A'_E}{\rho} = \frac{6}{\rho} \cdot \sum_{i=1}^{15} \left(\frac{V_i}{d_i} \right) \qquad (m^2/kg) \qquad .....(4)$$

substituting equations (1) and (2) into (4) gives

$$A_E = \frac{-2 \cdot V_s \cdot \ln (I/I_o)}{L \cdot W} \qquad (m^2/kg) \qquad .....(5)$$

Although A_E is a function of particle density and size distribution it can be obtained from the raw input data without calculating the size distribution first. This follows directly from the fact that the ratio of the external area to the average projected area of any convex body with random orientation is constant irrespective of size or shape[5].

The size distributions were corrected for errors due to non-isokinetic sampling, using a method outlined by Badzioch[6,7].

4. Experimental Results and Discussion

The experimental runs illustrated the effect of various parameters on the unburnt carbon yield, and the size distribution, density and specific external area of the char particles. These parameters were the atomising air flow rate, the fuel temperature, the type of coal and oil in the fuel and the combustion air-fuel ratio. Because only a limited quantity of fuel was available for the measurements, a full parametric study was not possible. The experimental conditions are summarised in table 1.

The slurry fuels were made up with one of three different types of bituminous coal (see table II) and a 1000 or 2000 second Redwood 1 fuel oil. The desired oil viscosities were obtained by mixing gas oil with 3500s fuel oil. Prior to being mixed with the oil, the coal was dried in air at 30°C to remove any free moisture. The water concentrations given in table II refer to the total moisture content of the slurries, determined according to BS 1016; Part 1 (1973), using petroleum spirit (boiling range 100-120°C) instead of toluene.

For each condition the unburnt carbon yield was calculated from fuel and gas analyses and input variables such as air and fuel flowrates. At least two char samples were taken at each condition, except for run 1, and for each sample the size distribution, density and specific external area was determined. All results have been tabulated (tables III-IX) and some size distributions presented in graphical form (figs. 7-10). A Student-t test was applied in several cases to estimate the significance of differences between mean values. It should be borne in mind that sample numbers were very small and that variables may not have been normally distributed about the mean, however, the test provided a useful method for comparison.

The graphs of the char size distributions from various runs also include the size distribution of the coal in the respective slurry, determined by screening down to 63 μm and using the Coulter Counter for the -63 μm cut. There is some uncertainty about the accuracy of the largest particle size fractions as some fines tended to cake together during the extraction of the oil.

4.1 Effect of changing the atomising air flowrate

The influence of a change in atomising air flowrate on the char particles produced was determined for three flowrates, 160, 132 and 107 l/min (0°C, 1 atm) with appropriate adjustments to the combustion air to maintain approximately the same overall combustion air-fuel ratio (run 3).

The data are presented in table III and fig. 7. Results of the corresponding Student-t tests are given in table IV, where underlined values denote differences which were significant to a confidence level of 95% or better. The differences between size distributions were based on the percentages (by volume) from the cumulative curve, not on those of each size band. It is apparent that a drop in atomising air from 160 to 132 l/min caused only a marginal change in size distribution, but that a drop from 132 to 107 l/min had a considerably greater effect. A comparison of the size distributions for 160 and 107 l/min conditions shows that there was a significant increase in char size over the approximate range 30-110 μm. It would appear from the data that above a certain atomising air flow rate, the value of which probably depends on other conditions, there is little change in the char size distribution, but that below this value the char size becomes progressively greater as the atomising air is reduced. Below 30 μm, the effect of a change in atomising air was negligible; above 110 μm there was indeed a difference in the size distributions, however, it was not statistically significant due to the increased scatter in the data. This was thought to be due mainly to two factors; a) the small number of large particles in the sample, and b) the particle sizer having a lower signal to background ratio for larger particles. A change from 160 to 107 l/min also brought about a significant decrease in the average particle density, together with a less significant increase in specific external surface area.

During this particular experiment the combustor wall temperature increased by 40-50 K because the furnace had not reached thermal

equilibrium. The increase, which reflected a similar increase in gas temperature, was thought to be insufficient to explain the observed changes. Other conditions such as air-fuel ratio and unburnt carbon yield were essentially constant (see table I). We concluded therefore that differences in char size distribution, density and area (A_E) were likely to be a direct result of a change in the original slurry droplet size, which implied that a certain amount of agglomeration was occurring during devolatilisation. If agglomeration was the only mechanism involved we would have measured a slight decrease in both density and specific external area, however, the small increase in area suggests that some particle swelling was also taking place.

An estimate of the relative proportions of these two phenomena can be obtained by comparing the changes in size, density and area, A_E. Consider the hypothetical case where all particles have the same density and swell uniformly irrespective of size and without agglomeration; the changes in density and A_E are then given according to:

$$\frac{\rho_2}{\rho_1} = \left(\frac{d_1}{d_2}\right)^3 \qquad \ldots\ldots(6)$$

and

$$\frac{A_{E_2}}{A_{E_1}} = \left(\frac{d_2}{d_1}\right)^2 \qquad \ldots\ldots(7)$$

A decrease in atomising air from 160 to 107 l/min caused an increase in (volume) mean size of approximately 8%, a decrease in density of 12.4% and an increase in A_E of 7.0%. If we assume uniform swelling using equations (6) and (7) it can be shown that to produce these changes in density and area, an increase in size of approximately 4% would have been due to agglomeration and a further 4% due to swelling. It must be remembered that, due to the assumptions made above and the small number of data on which the calculations are based, these proportions are only rough indications.

4.2 Effect of changing fuel atomising temperature

The effect of changing fuel temperature was studied for 103°C and 119°C at an atomising air flow rate of 164 l/min (run 4). The results are shown in table V and figure 8. Using the statistical treatment mentioned previously, it was apparent that the lower temperature caused a slight increase in particle size. This result could not be regarded as significant however, as confidence levels were well below 60% owing to the relatively wide scatter of the data. Similarly, the small decrease in particle density and increase in area A_E were not significant, although confidence levels were somewhat higher. In all, there are indications that fuel temperature had a marginal effect, but that the difference was well within experimental error. The insensitivity to changes in fuel temperature was against expectations

and was thought to be partly due to the high atomising air flow rate, and partly to the thinner oil; it is possible that a similar increase in the fuel temperature would have had a more pronounced effect at lower atomising shear rates or if a 2000s (RI) oil had been used (see next section).

4.3 The effect of using a different coal and oil type

Atomising and combustion conditions in runs 2b, 3a, 4a, 5 and 6 were essentially the same, although the fuels had slightly varying water concentration (0.2 - 1.4%), coal concentration (45 - 51%) and coal size distribution.

The inclusion of water has been shown to have a potentially dramatic effect on the devolatilisation mechanism of slurry droplets[8] and hence on the type of char particles that are formed. In our case, however, the water content was relatively low and the majority of this was likely to originate from within the coal substrate, rather than be present either as free moisture on the coal surface or in the form of an emulsion with the oil. The small variations in water content were, therefore, assumed to have a negligible effect. Since the spray was likely to be influenced by the coal size distribution[9] a direct comparison of the char size distributions (and therefore the specific external surface areas) between one run and another was not possible. Only the char density and unburnt carbon yield could be used as indicators.

The char density in run 5 (table VI), using a 2000 sec. Redwood I oil, was significantly lower than that in run 4a, in which a 1000 sec. oil was used (424 kg/m^3 compared to 660 kg/m^3). Although it is not possible to draw conclusions on the basis of a change in char density alone, the lower density may have been the result of an increased amount of agglomeration and/or swelling. This in turn could have been caused by a coarser spray or a change in devolatilising behaviour due to the oil. The unburnt carbon, however, remained essentially unchanged.

A similar comparison was made between runs 6 (table VII) and 3a, run 2b (table VIII) and run 5 in which, respectively, coals A, B and C were used. The results, summarised in table IX, show that the fuels containing coal A consistently produced higher density chars. The difference between the densities from fuels containing coals B and C was not significant due to the greater spread of the data. The unburnt carbon for runs 6 and 3a were also considerably higher, which was attributed to the lower volatile matter content of coal A. These observed differences were probably due to the devolatilising behaviour of the coals, because coal type would not be expected to alter the atomisation process.

Thus, the results have indicated that both coal and oil can influence the devolatilisation of coal-oil slurries, which supports the findings of other investigators[10]. However, more extensive tests need to be done to determine to what extent atomisation quality and agglomerating tendency of the fuel are responsible, and which particulars of the

coals and oils determine such behaviour (e.g. asphaltene content of the oil and maceral types in the coal).

4.4 The effect of changing combustion air-fuel ratio

The effect of a change in the proportion of combustion air in the devolatilisation zone (run 2) on size distribution, density and area (A_E) is given in table VIII and fig. 9. There were insufficient samples for a statistical analysis, however, it was evident that, when more combustion air was added, the unburnt carbon was reduced considerably and the size distribution had shifted toward larger sizes. Coinciding with a higher air-fuel ratio in run 2b were slightly lower fuel and atomising air flow rates. Recent cold atomisation tests using a mineral oil have shown that a decrease in fuel flow rate tended to produce a finer spray[11] for a given atomising air flowrate. Assuming that the slight decrease in atomising air made little difference to the drop size distribution, the atomising conditions in run 2b might have given rise to smaller particles, which is contrary to that actually observed. The conclusion is therefore that the lower carbon yield and the increase in the average size were caused primarily by the larger proportion of the combustion air. A likely explanation for this is that the extra oxygen available consumed a greater proportion of the smaller particles.

4.5 Further remarks

An additional point emerging from the results is that the smallest char particles obtained from the flame were always considerably larger than the smallest coal particles in the slurry. One explanation for this is that all particles below a given size were consumed by oxygen, although inspection of fig. 9 suggests that some small particles would still have been present even when more oxygen was available. Another explanation is that the smallest char particles present were determined by a minimum droplet size containing several coal particles. The difference in the char size distributions obtained in runs 1 and 2a (fig. 10 and table VIII) would favour the latter case; the difference between the coal size distributions was comparatively small and the combustion conditions were effectively the same, only the atomising conditions were considerably different.

The combined effects of a higher fuel flowrate and a lower fuel temperature and atomising air flowrate in run 1 were apparently responsible for a larger minimum droplet size compared to run 2a. A further comparison between these runs revealed that the char sample with a larger mean size had a higher average particle density, which was the reverse of that observed in run 3. Further work is required to explain these matters.

The poor reproducibility of results in some experiments was primarily due to the low char sample weights obtained (< 20 mg). The accuracy of A_E was dependent principally on the sample weight, whereas that of the char density depended both on sample weight and the calculated size distribution.

Furthermore, the largest char particles observed were approaching the upper limit of the particle size analyser (in this case 564 μm). Since the sensitivity of the analyser to large particles is low and material above the upper limit is largely ignored, any real changes in the char size distribution would have appeared to be less if a significant fraction above this limit was involved. Consequently, some changes in size distribution may actually have been greater than those observed.

It must be emphasised that the results presented in this paper are likely to be highly specific to the type of fuel and probably the type of atomiser used. More work in this field will be necessary before we can predict the various properties of char particles produced in coal-oil slurry flames. We have shown, however, that both operating conditions and the type of fuel can influence the various parameters required for the combustion rate studies referred to earlier, and hence can affect the carbon conversion efficiency.

To illustrate the significance of some of the data, we calculated the burn-out achieved after one second by the two char size distributions determined experimentally for atomising air flow rates of 160 and 107 l/min. The model used for this purpose was essentially that described in reference 1, but with minor modifications to allow for the ash content in the chars[11]. The calculations showed that an increase in the atomising air flowrate from 107 to 160 l/min improved the theoretical combustion efficiency from 98.8% to 99.4% under hypothetical combustion conditions.

5. Conclusions

1. By allowing coal-oil slurry sprays to undergo devolatilisation and partial combustion, char particles have been generated of which the density, size distribution and yield were determined, thus providing data required for the study of carbon burn-out rates of these slurries using a Controlled Mixing History furnace.

2. The measurements obtained for various fuels and operating conditions have indicated that agglomeration and swelling takes place during devolatilisation of coal-oil slurry sprays, and have shown that various atomising and fuel parameters determine the extent to which this occurs.

6. Acknowledgement

The authors wish to thank SHELL Coal International and the National Coal Board for their financial support.

7. References

1. COSSEE, R.P. and HEDLEY, A.B.; "Combustion Rates of Coal-Oil Slurries", Proc. 4th International Symp. on Coal Slurry Combustion, Session VI, Vol. 3, May 10-12, 1982, Orlando, Florida, U.S.A.

2. SWITHENBANK, J., BEER, J.M., TAYLOR, D.S., ABBOT, D. and McCREATH, C.G.; "A Laser Diagnostic for the Measurement of Droplet and Particle Size Distribution", in "Experimental Diagnostics in Gas Phase Combustion Systems", Progress in Astronautics and Aeronautics, Vol. 53, pp. 421-447, 1977.

3. FELTON, P.G.; "Measurement of Particle/Droplet Size Distributions by a Laser Diffraction Technique", in Particle Technology - Nuerenberg, 2nd European Symposium on Particle Characterisation, Aug. 24-26, 1979, Nuerenberg, pp. 662-680.

4. DYSART, S.; "Crystal Nucleation and Growth using Laser Diffraction", Internal Report on SERC Research Studentship B81 300263, Sheffield University, Sheffield, U.K.

5. van de HULST, H.C.; "Light Scattering by Small Particles", J. Wiley & Sons, Inc., New York, and Chapman & Hall Ltd., London, 1957, pp. 110.

6. BADZIOCH, S.; "Collection of Gas-borne Dust Particles by means of an Aspirated Sampling Nozzle", British J. of Appl. Phys., Vol. 10 (Jan.), pp. 26-32, 1959.

7. BADZIOCH, S.; "Correction for Anisokinetic Sampling of Gas-borne Dust Particles", J. Inst. Fuel, Vol. 33 (Mar.), pp. 106-110, 1960.

8. KANG, C-F., REN, Y-Z., ZHAO, X. and CHEN, Y-S.; "Experimental Study of Combustion Process of Single COM Droplet and COM Spray", Proc. 4th Intl. Symp. on Coal Slurry Combustion, Session VI, Vol. 3, May 10-12, 1982, Orlando, Florida, U.S.A.

9. PETELA, R. and ZAJDEL, A.; "Atomisation of Coal-Liquid Mixtures", Fuel, Vol. 59 (July), pp. 495-498, 1980.

10. BRAIDE, K.M., ISLES, G.L., JORDAN, J.B. and WILLIAMS, A.; "The Combustion of Single Droplets of Some Fuel Oils and Alternative Liquid Fuel Combinations", J. Inst. Fuel, Vol. 52 (Sept.), pp. 115-124, 1979.

11. COSSEE, R.P.; Ph.D. Thesis, Sheffield University, to be submitted.

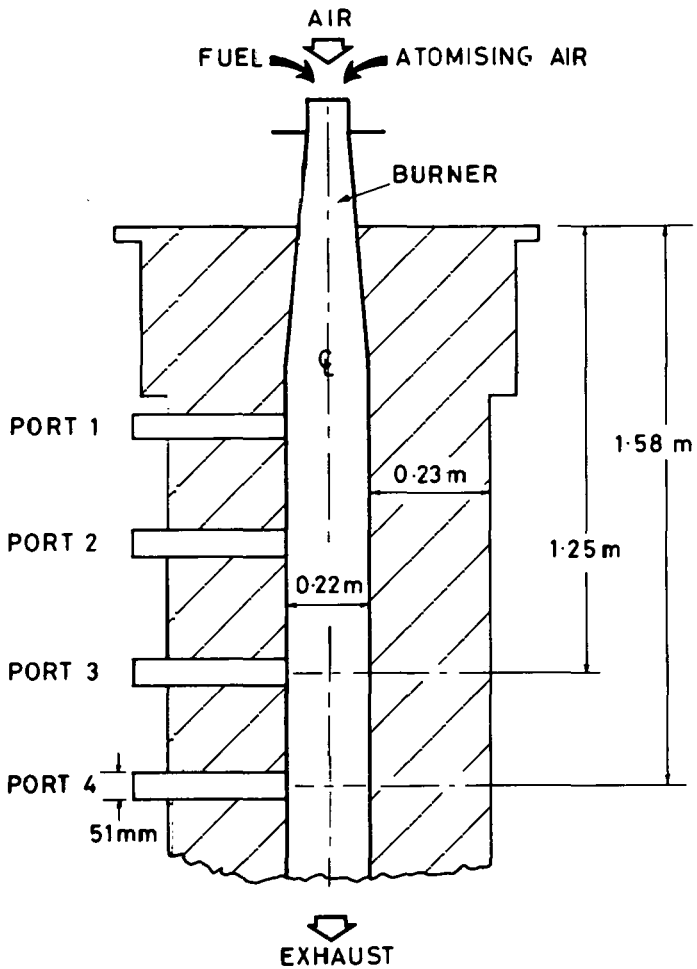

Fig. 1 Primary zone of CMH furnace.

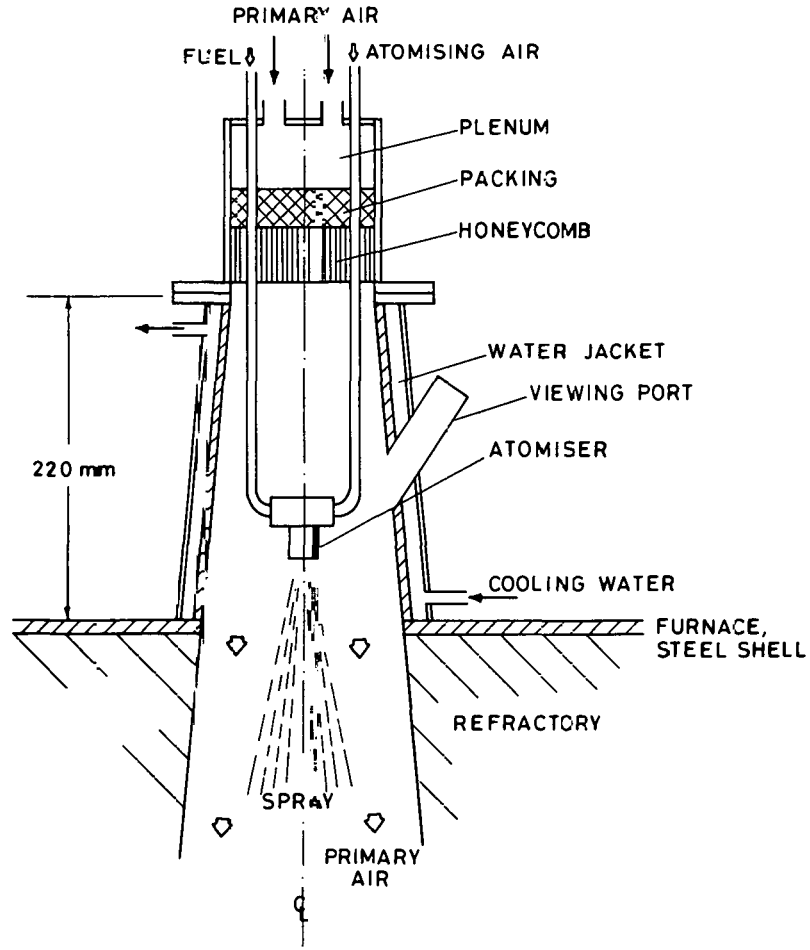

Fig. 2 Liquid and slurry fuel burner for CMH furnace.

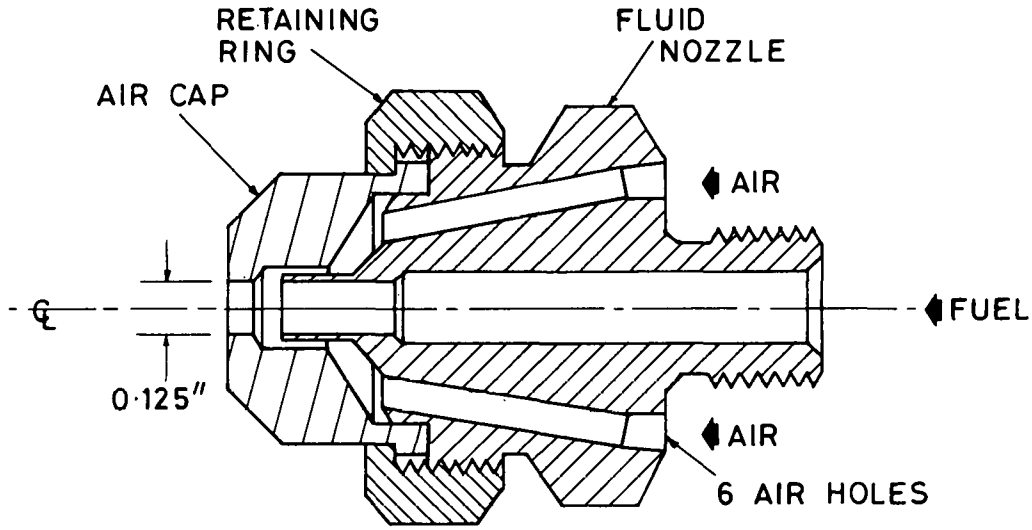

Fig. 3 Twin-fluid atomiser (Courtesy of C.T. (London) Ltd.) drawn to scale.

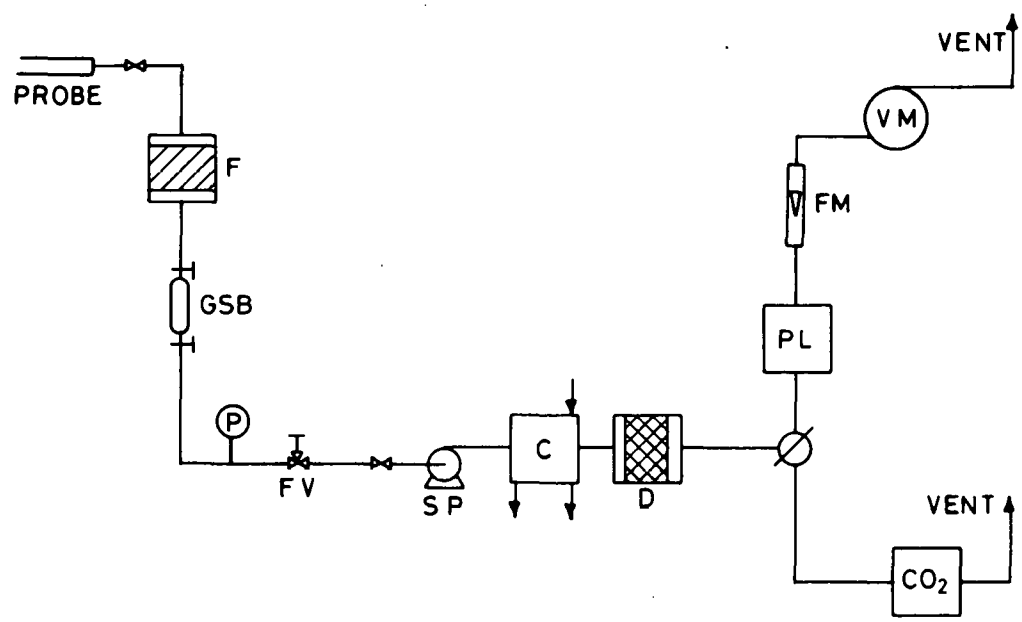

Fig. 4 Sampling train (F = filter, GSB = gasbottle, P = suction pressure gauge, FV = flow valve, SP = suction pump, C = condenser, D = Calcium Chloride drier, PL = plenum, FM = flow meter, VM = volume meter, CO_2 = CO_2 analyser.)

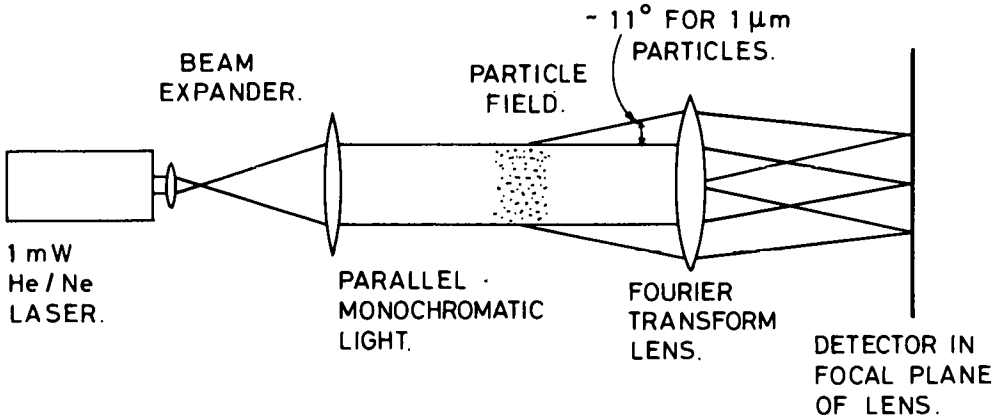

Fig. 5 Optical arrangement of particle sizer.

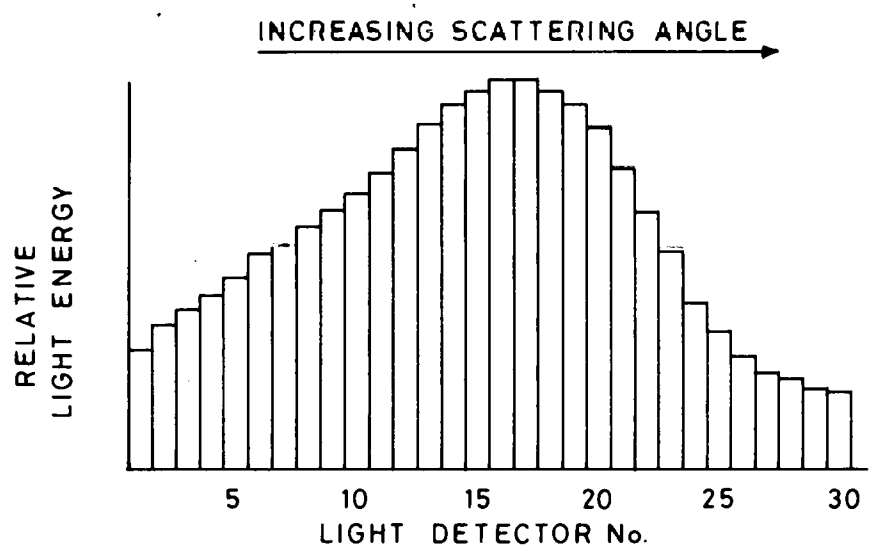

Fig. 6a Typical light energy distribution.

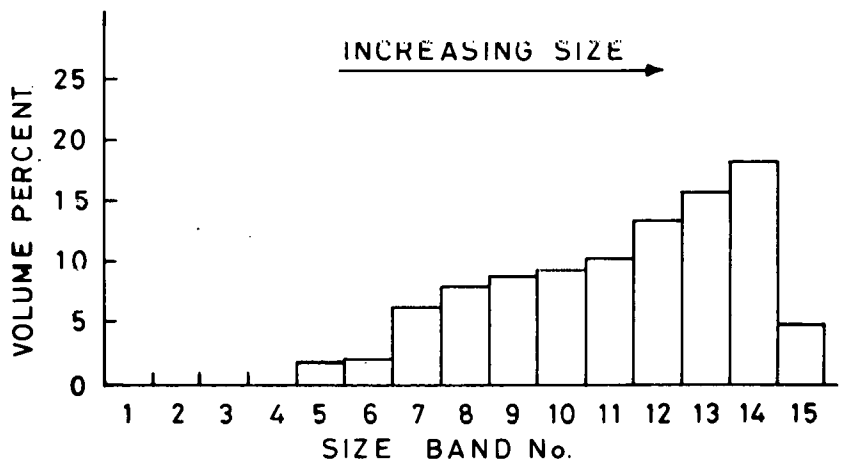

Fig. 6b Size distribution calculated from light energy distribution given in fig. 6a (size bands also given in Table III).

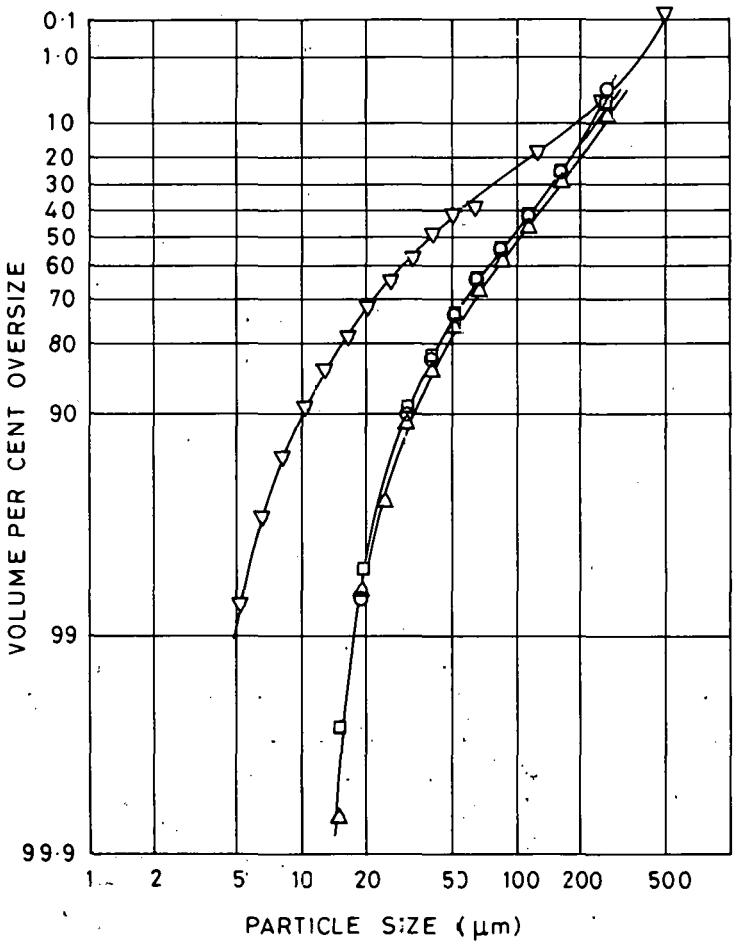

Fig. 7 Coal and char size distributions of run 3;

atomising air = 107 l/min (△), 132 l/min (□), 160 l/min (○), coal size distribution in slurry =▽ .

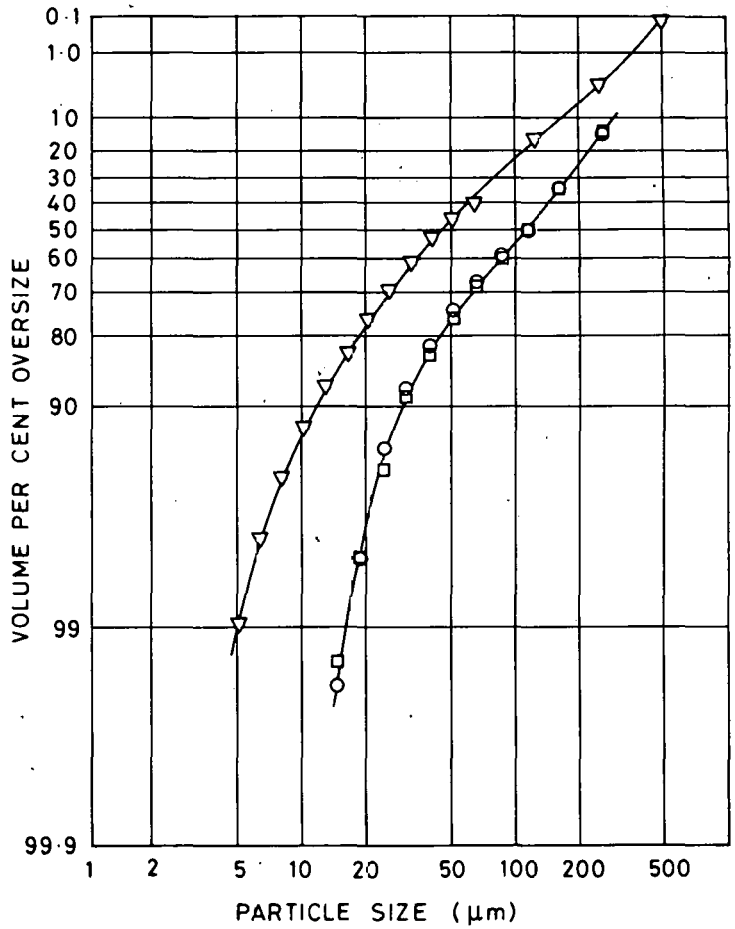

Fig. 8 Coal and char size distributions of run 4;

fuel temperature = 103°C (□), 119°C (○), coal size distribution in slurry = ▽ .

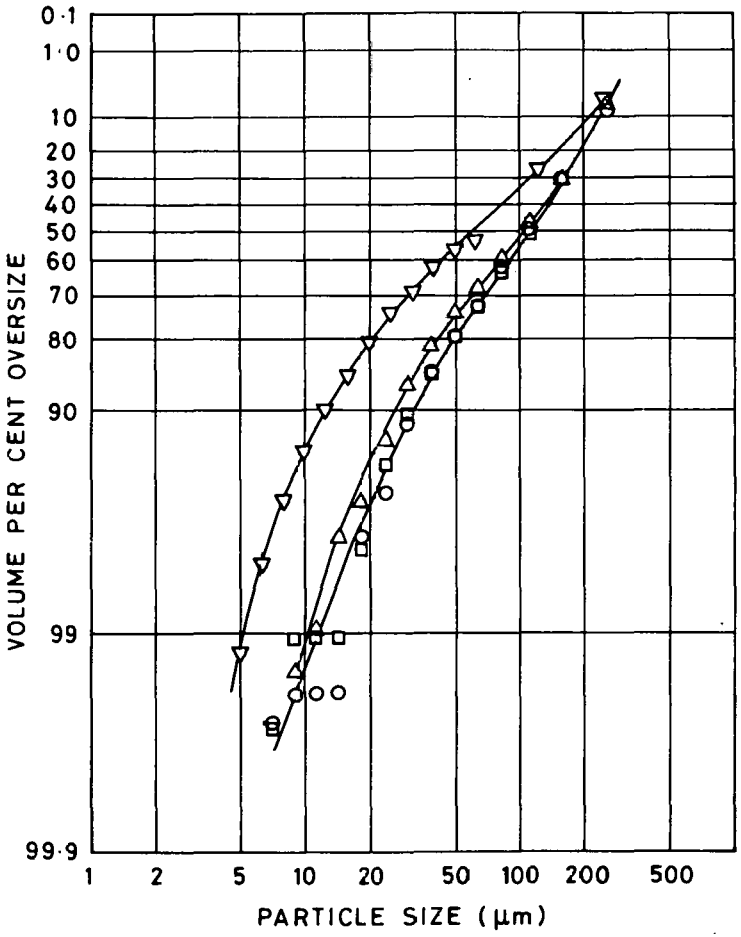

Fig. 9 Coal and char size distributions of run 2;
total air in primary zone = 48% (△) of stoich. requirement,
& 65% (○&□) of stoich. reqt.,
Coal size distribution in slurry = ▽.

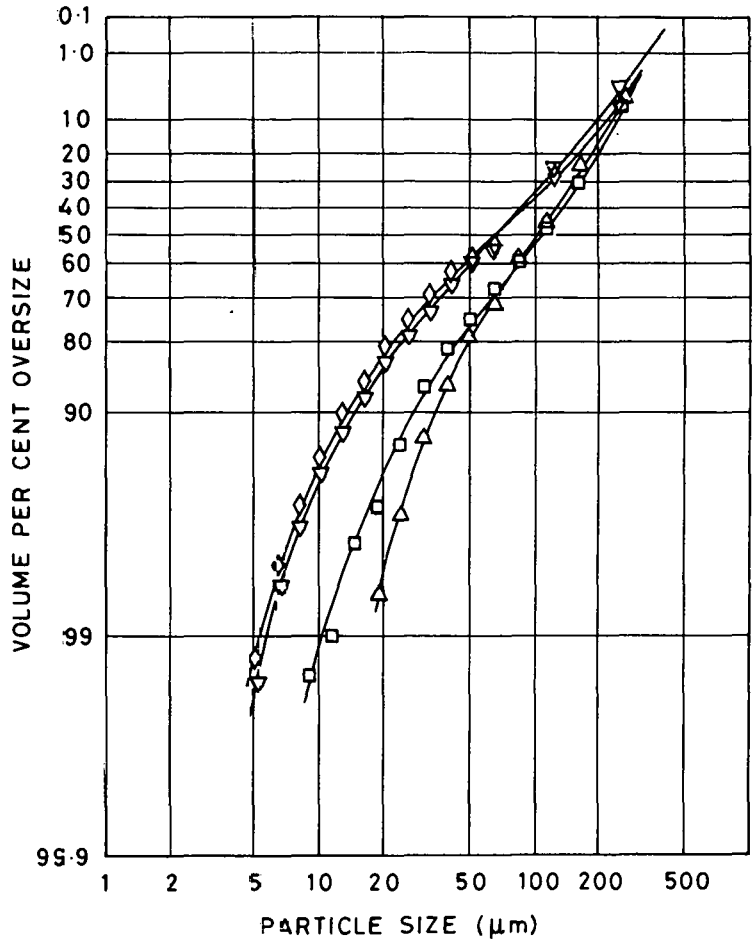

Fig. 10 Coal and char size distributions of run 1 and 2a;
run 1: ▽ = coal, △ = char (fuel = 17.3 kg/hr, air = 127 l/min, fuel = 92°C)
run 2a: ◇ = coal, □ = char (fuel = 12.3 kg/hr, air = 179 l/min, fuel = 105°C)

Run No.		fuel make-up (weight %)	fuel flow (kg/hr)	fuel temp (°C)	atom. air* (l/min)	prim. air* (l/min)	total air* (l/min)	air proportion (% stoich)	unburnt carbon field (%)	midway wall temp (°K)	char samples number	char samples weight (mg)	Table No.
1		44.3% coal B 51.4% 2000** oil 1.3% water	17.3	92	127	1104	1231	46	35	1565	1	26	VIII
2	a	45.0% coal B 53.6% 2000 oil 1.4% water	12.5	105	179	766	945	48	33	1465	1	33	VIII
	b		9.9	105	161	849	1010	65	15	1575	2	13,17	
3	a	46.6% coal A 53.2% 2000 oil 0.2% water	10.6	103	160	844	1004	65	23	1530	3	61,64,62	III & IV
	b		10.3	103	132	853	985	65	22	1560	2	64,60	
	c		10.3	103	107	887	994	66	23	1575	2	57, 59	
4	a	48-9% coal C 50.8% 1000 oil 0.3% water	9.8	103	164	861	1025	67	12	1545	3	17,19,18	V
	b		9.8	119	164	861	1025	67	11	1570	2	18,19	
5		48.3% coal C 50.5% 2000 oil 1.2% water	9.8	106	164	818	982	65	13	1585	2	10,16	VI
6		51.1% coal A 48.7% 2000 oil 0.2% water	10.4	103	161	849	1010	64	22	1575	2	37,40	VII

Table I Experimental conditions

*flowrates of air at 0°C and 1 atm.

**oil viscosities in seconds Redwood I at 38°C(100°F).

Coal	Moisture	Volatile Matter	Ash	Free Swelling Index
A	2.2	19.5	15.1	½
B	2.1	37.6	8.92	1½
C	4.7	35.1	3.34	2

Table II Proximate analyses of air dried coals prior to coal-oil slurry manufacture.

size (μm)	Volume % Undersize									
	atomising air = 160(1/min)			average	a.a. = 132(1/min)		average	a.a. = 107(1/min)		average
564.0	100	100	100	100	100	100	100	100	100	100
261.6	95.60	97.30	93.83	95.58	94.96	92.80	93.88	94.24	88.44	91.34
160.4	75.95	76.12	73.01	75.03	74.87	73.26	74.04	73.21	67.94	70.58
112.8	59.91	59.05	57.09	58.68	57.74	56.84	57.29	54.99	51.77	53.38
84.3	46.24	45.54	44.10	45.29	45.53	43.78	44.66	41.89	39.85	40.87
64.6	36.16	35.13	34.14	35.14	35.81	34.30	35.06	32.84	31.04	31.94
50.2	27.72	26.36	25.45	26.51	27.45	25.43	26.44	24.10	21.53	22.82
39.0	17.85	17.67	17.01	17.51	19.16	16.82	17.99	16.00	14.29	15.15
30.3	11.20	10.04	9.64	10.29	12.01	9.36	10.69	9.49	8.54	9.02
23.7	4.66	4.41	3.48	4.18	5.63	3.39	4.51	4.19	3.81	4.00
18.5	1.21	1.69	1.56	1.49	2.49	1.46	1.98	1.64	1.54	1.59
14.5	0.19	0.09	-	0.09	0.74	-	0.37	0.09	0.18	0.14
11.4	-	0.09	-	0.03	-	-	-	0.09	-	0.05
9.1	-	-	-	-	-	-	-	-	-	-
7.2	-	-	-	-	-	-	-	-	-	-
5.1	-	-	-	-	-	-	-	-	-	-
Density (kg/m^3)	547	558	566	557	486	542	514	490	486	488
A_E (m^2/kg)	176	170	163	170	204	169	187	186	177	182

Table III Char analyses of run 3.

	Change in Atomising Air		
Volume % undersize	160 → 132 l/min	132 → 107 l/min	160 → 107 l/min
261.6	0.870	0.580	1.231
160.4	0.532	0.896	1.390
112.8	0.994	1.654	2.467
84.3	0.470	1.992	3.018
64.6	0.072	1.875	2.421
50.2	0.052	1.568	2.162
39.0	-0.370	1.388	2.395
30.3	-0.248	0.839	1.431
Density	1.397	0.655	7.701
A_E	0.869	-0.196	1.557
Degrees of freedom	3	2	3
Confidence			
95%	2.353	2.920	2.353
90%	1.638	1.886	1.638

Table IV Results of Student-t tests for differences between char analyses of run 3 (underlined values denote significance levels exceeding 95%).

size (μm)	volume % undersize						
	fuel temperature = 103°C			average	f.t. = 119°C		average
564.0	100	100	100	100	100	100	100
261.6	86.44	89.21	84.36	86.67	86.13	85.70	85.92
160.4	66.47	67.69	61.56	65.24	65.98	66.28	66.13
112.8	51.74	53.38	46.91	50.68	49.47	51.48	50.48
84.3	40.29	41.71	36.62	39.54	39.10	43.26	41.18
64.6	30.21	32.95	28.46	30.54	30.37	34.60	32.49
50.2	22.23	24.94	21.01	22.73	23.83	27.13	25.48
39.0	15.59	17.67	15.41	16.22	16.99	19.39	18.19
30.3	9.81	11.52	9.84	10.39	11.45	12.51	11.98
23.7	4.67	5.57	5.52	5.25	6.58	6.47	6.53
18.5	2.15	2.52	1.64	2.10	2.16	2.04	2.10
14.5	0.63	0.78	0.69	0.70	0.90	0.18	0.54
11.4	-	-	-	-	-	-	-
9.1	-	-	-	-	-	-	-
7.2	-	-	-	-	-	-	-
5.1	-	-	-	-	-	-	-
Density $\left(\frac{kg}{m^3}\right)$	588	739	654	660	741	746	744
S_E $\left(\frac{m^2}{kg}\right)$	152	131	135	139	124	130	127

Table V Results of char analyses for run 4.

size (μm)	volume % undersize		average
564.0	100	100	100
261.6	100	95.29	97.65
160.4	78.31	73.82	76.07
112.8	55.07	51.86	53.47
84.3	36.40	39.84	38.12
64.6	24.89	28.43	26.66
50.2	17.41	21.18	19.30
39.0	11.11	14.54	12.83
30.3	7.40	9.50	8.45
23.7	2.84	5.56	4.20
18.5	2.84	3.37	3.11
14.5	0.28	0.46	0.37
11.4	0.28	0.46	0.37
9.1	0.28	0.46	0.37
7.2	0.28	-	0.14
5.1	-	-	-
Density (kg/m^3)	363	484	424
A_E (m^2/kg)	236	194	215

Table VI Results of char analyses for run 5.

size (μm)	volume % undersize		average
564.0	100	100	100
261.6	100	100	100
160.4	81.81	79.93	80.87
112.8	63.65	63.89	63.78
84.3	51.62	52.72	52.17
64.6	40.67	41.71	41.19
50.2	31.80	33.92	32.86
39.0	22.76	24.56	23.66
30.3	15.05	16.28	15.67
23.7	7.47	8.31	7.89
18.5	2.46	2.89	2.68
14.5	1.55	0.45	1.00
11.4	-	-	-
9.1	-	-	-
7.2	-	-	-
5.1	-	-	-
Density (kg/m^3)	483	543	513
A_E (m^2/kg)	231	211	221

Table VII Results of char analyses for run 6.

size (μm)	volume % undersize				
	Run 1	Run 2a	Run 2b		average
564.0	100	100	100	100	100
261.6	94.67	93.44	94.07	91.27	92.67
160.4	77.00	69.90	69.93	69.21	69.57
112.8	56.51	52.98	48.08	50.07	49.08
84.3	43.04	41.09	35.58	36.80	36.19
64.6	29.57	32.52	26.43	27.52	26.98
50.5	21.78	25.35	20.19	20.09	20.14
39.0	13.64	18.69	13.97	14.34	14.16
30.3	7.88	13.07	9.18	8.63	8.91
23.7	3.68	7.37	5.71	4.26	4.99
18.5	1.58	3.92	2.43	2.75	2.59
14.5	-	2.70	0.94	0.53	0.74
11.4	-	1.03	0.94	0.53	0.74
9.1	-	0.65	0.94	0.53	0.74
7.2	-	-	0.37	-	0.19
5.7	-	-	-	-	-
Density (kg/m^3)	453	290	287	385	336
A_E (m^2/kg)	222	357	317	231	274
air (% stoich)	123.(1/min) (46%)	945(1/min) (48%)	1010(1/min) (65%)		
fuel flowrate (kg/hr)	17.3	12.5	9.9		
fuel temperature	92 °C	105 °C	105 °C		

Table VIII Results of char analyses for runs 1 and 2.

coal type	coal conc	run no	measured densities	average density	unburnt carbon (%)
A	51.1	6	483,543	513	22
	46.5	3a	547,558,566	557	23
B	45.0	2b	287,385	336	15
C	48.3	5	363,484	424	13

Table IX Effect of coal type on char density.

The following manuscript was unavailable at time of publication:

Coal-Methanol Mixture Combustion Tests with Coals of Different Ranks

Y. S. Pan, G. T. Bellas, R. B. Snedden and J. I. Joubert
Pittsburgh Energy Technology Center

DO NOT MICROFILM THIS PAGE

COAL-WATER MIXTURE LABORATORY COMBUSTION STUDIES

Geoffrey J. Germane, L. Douglas Smoot, Stephen P. Diehl,
Kurt H. Richardson, and Douglas C. Rawlins
Combustion Laboratory
Brigham Young University
Provo, Utah 84602

Introduction

Coal-water mixtures (CWM) have significant economic potential to be used as a substitute for premium liquid and gaseous fuels in utility and industrial boilers, as well as in gas turbines. However, there are several technical issues which must be addressed. In addition to the preparation and handling of a solid fuel slurry for use in a system designed for liquid or gas, possible erosion and corrosion of handling equipment and boiler plugging, and nitrogen and sulfur pollutant formation and control techniques, fuel atomization and efficient burning. Combustion processes must be studied in detail to understand the effect of key variables on combustion efficiency and pollutant formation.

Background

The 4th International Symposium on Coal Slurry Combustion (1) presented a good review of the status of coal-water mixture technology. Of the 93 papers presented, approximately one-quarter dealt with coal-water mixtures with about 13 of these on slurry formation and handling, one on atomization, six on combustion and three on systems evaluation. Not all of the papers report experimental results. For example, only two papers on combustion (PETC, ARC) reported combustion data for pulverized coal-water mixtures.

About one-half dozen commercial organizations (e.g., Atlantic Research Corporation, Gulf and Western) are developing CWM for possible commercial use. Several have developed methods and equipment (pilot plants) for CWM slurries in 75-120 tpd capacity range. Present technology suggests optimum mixtures of about 70% coal/30% moisture, often with blended particles of small and large size. The use of small percentages (1-2%) of additives for control of viscosity and settling is common. Claims are made that mixtures are stable for significant periods of time, with little settling up to one month. Independent research (e.g., Eckmann, PETC (3)) has also been conducted on rheological properties of CWM.

Research in atomization of water and dispersion of coal in CWM has not been extensively studied. Only one specific paper on this subject (from BNL) was presented at the 4th International Symposium on Coal

Slurry Combustion and this was for coal loading levels well below the practical level. DOE/PETC has initiated sponsored resarch in this area (e.g., Carnigie-Mellon). Efficiency of coal burnout, fouling, and NO_x pollutant formation are all related to droplet atomization and particle dispersion. Atomization studies, and associated CWM nozzle design have also been conducted (but not emphasized) by those engaged in CWM combustion such as PETC and ARC. Commercially available nozzles have frequently been used in these early combustion studies.

Early investigators of the combustion characteristics of pulverized CWM include ARC (2), PETC (4) and EPRI/B&W (5). Tables 1 and 2 summarize selected combustion results for CWM. From these results, it is clear the pulverized coal can be burned with high percentages of water. Coal burnout levels of up to 98% have been reported and CWMs with up to 70% coal in CWM have been tested. PETC tests were conducted in 100 hp and 700 hp water tube boilers with up to 63% coal in the CWM. In the smaller unit, carbon conversion was up to 85% while in the larger unit, carbon conversion of up to 96% was obtained with maximum secondary air.

ARC (2) investigated CWM with coal percentages up to 65% in a small laboratory furnace (10^6 BTU/hr). Carbon conversion levels of up to 90% were reported. More recent tests (6) have shown up to 95% combustion efficiencies with 70% CWM in the small-scale furnace.

More recent investigations of CWM combustion are also underway at MIT and BYU, which will provide more details on the flame. Larger scale testing of CWM in a utility boiler have also been outlined by EPRI and by DOE(PETC)/CE.

Detailed CWM combustion and pollutant formation studies require the capability for steady, regulated slurry feed and atomization, the control of combustion air mass flow, flow pattern and temperature, and sampling and analytical equipment for flame and flue gas measurements. Some of the important quantities to be measured include the degree of carbon conversion, heat release rate, flame temperature and pollutant concentrations, both locally and for the overall process. The combustion of CWM can be characterized in detail by determining the effects on combustion efficiency of solids loading and coal characteristics, stoichiometry, combustion air temperature and swirl and reactor wall heat flux and wall temperature.

The combustion efficiency of CWM may be determined from the measurement of fuel heat input and energy release and from the indirect method by flue gas analysis. The CWM mass flow and combustion air flow are carefully measured for close control of combustion stoichiometry and for heat and mass input rates for combustion efficiency calculations. The reactor is sufficiently instrumented to fully describe heat losses to the walls as well as to the stack gases. In addition, combustion products, constituents of unburned and partially burned coal, and temperatures can be measured. Laboratory scale results can be compared to predictive computations from the two-dimensional computer code which has the capability to model swirling, particle-laden reacting flow.

This paper presents results of laboratory scale CWM combustion tests conducted in the BYU Combustion Laboratory. Combustion products were sampled from within the reactor for various conditions of combustion air swirl and stoichiometric ratio for a single coal-water slurry. Wall temperature profiles are also presented as an indication of heat release patterns. Planned slurry combustion tests will provide detailed local measurements of coal burnout and pollutant formation to gain further understanding of CWM combustion processes.

CWM Combustor Facility

The coal-water mixture (CWM) reactor is a vertical cylindrical combustor, 2.2 meters long, with slurry and combustion air inlet parts at the top of the reactor (7,8). Cooling water jackets are attached for wall temperature control under steady-state conditions. The reactor, shown in Figure 1, is designed for combustion profile mapping of coal burnout and pollutant formation from space-resolved measurements within the reactor. Slotted windows are located along the full reactor height for sampling probe and optical access to the combustion chamber. An induced draft fan with a controlled bypass enables slightly sub-atmospheric pressure testing to simulate industrial conditions and to allow removal of the sampling probe and replacement at a different location during tests without interrupting the combustion process.

Combustion air is supplied by a high pressure storage facility located outside the reactor building. The secondary air flow is throttled with an automatic control valve and the rate is measured by a Micro-Motion mass flow transducer. It passes through a Chromalax 75 KW electric heater prior to entering the swirl block plenum on top of the reactor. The swirl generator can create flows with a theoretical swirl number from 0 to 9.6. Atomizing air is supplied by the low pressure building supply with a separate control valve and electric heater, and is measured with a rotometer. Methane is used for reactor preheating, and ignition is achieved using a spark-ignited hydrogen/air jet. The methane flow is measured with a rotometer and enters the reactor through a circumferential burner surrounding the quarl section, to which the swirl block and nozzle are attached.

Coal slurry feed is achieved using a Moyno progressive nine cavity positive displacement pump. The pump is driven hydraulically with capability for infinitely variable speed. Feed rate is measured at steady state using an elapsed timer and an electronic weigh scale, with pump speed-slurry flow correlation used as a backup indicator. Slurry quantities sufficient for combustion tests of several hours duration are contained in a small holding tank on the scale. Typical tests consume about 13 kg coal per hour (18 kg/hr CWM).

Reactor Sections

The CWM reactor consists of seven cylindrical sections stacked vertically to eliminate asymmetric buoyancy effects. Each section is 30 cm high and is encased in a water jacket for heat flux control. A

ceramic insulation layer 5 cm thick is cast to the inside of the cooling jacket. A cast ceramic cylindrical combustion chamber fits within the ceramic insulation layer with a concentric 1 cm gap which provides space for wall heaters and/or selected insulation materials to help control heat flux through the walls. Figures 2(a) and 2(b) show the ceramic combustion chamber inserts and outer casing for reactor section. The combustion chamber sections are 35 cm in diameter for a total reactor volume, with seven sections, of 202 ℓ. Each section has a 1.3 cm wide vertical slot nearly the full height of the section to allow optical or sampling probe access at any axial location along the assembled reactor height. The sections are also instrumented with thermocouples to measure wall temperature profiles and water jacket thermocouples to monitor the temperature of the cooling water.

Burner and Swirl Generator

A CWM nozzle and atomizer was developed at the Combustion Laboratory to accommodate the relatively low slurry flow rates utilized in the combustion tests. The nozzle, shown in Figure 3, employs an atomizer similar to an oil nozzle used successfully by PETC with coal slurries in demonstration burning tests (4). Atomization was accomplished with 6.8 kg/hr of low pressure atomizing air at ambient temperature. The atomizing air flows radially into the slurry stream at a 60° angle through an adjustable gap. A fan spray pattern is caused by the radial shearing action of the air on the mixture as it exits the nozzle tip.

Preheated secondary air enters the reactor through a swirl generator, shown in Figure 4. The generator has the capacity to produce theoretical swirl numbers from 0 (no swirl) to 9.6. A valve is used to divert all or a portion of the secondary air through tangential ports and the balance through radial ports. The swirling and recirculation zones created with swirl enhances mixing of the atomized slurry and combustion air, recirculates hot combustion gases for potentially increased flame stability, and increases the residence time of the burning coal particles in the reactor.

Sample Probe and Sampling System

Samples may be collected from within the reactor, isokinetically with the average gas flow velocity, using a water cooled probe at various radial and axial positions to study particle burnout and pollutant formation within the flame. Figure 5 is a schematic diagram of the sampling probe. Analyses are conducted on the collected solid, liquid and gaseous samples for coal burnout, sulfur and nitrogen pollutants, and other gaseous products including oxygen, carbon dioxide and carbon monoxide. The sampling system, the operation of which was described previously (9), is shown in Figure 6.

Combustion Tests

The slurry used for the combustion tests was obtained from Atlantic Research Corporation (ARC) in Alexandria, Virginia. The slurry, based

on Montana bituminous coal with a particle size distribution of 87% through 200 mesh, contained about 70% solids including additivies. Table 3 contains the coal analysis and selected mixture properties (10). The heating value of the as-received coal is relatively high (33,888 kJ/kg) which results in a coal slurry with a heating value of about 23,675 kJ/kg, a reduction of about 10,213 kJ (30%) per kilogram of fuel. An additional 696 kJ per kilogram of slurry is required to vaporize the water during combustion, resulting in a net reduction in fuel heating value of about 32%. The stoichiometric air/fuel ratio for the coal is 11.1:1 and 7.77:1 for the slurry.

Coal-Water Mixture Tests

Table 4 summarizes the test matrix for the series of combustion runs to identify conditions for best coal burnout. For tests 1 through 12, swirl number was varied from 9.6 to 0. At each of the four swirl numbers used, three settings of the stoichiometric ratio (SR) were used. Coal feedrate was constant at approximately 12.7 kg per hour (18.2 kg slurry per hour). The flow of preheated secondary air was varied to achieve the range in stoichiometric ratios. Stoichiometric ratio (SR) is defined as the ratio of the test air on a mass basis to the air required for complete combustion of the coal. Atomizing air was fixed at 6.8 kg/hr and the nozzle was located at a fixed depth into the quarl section. The combustion air included 10.2 kg/hr of combustion air used for methane preheating, as well as the atomizing air. Reactor pressure was relatively constant at -0.174 kPa (-0.7 in H_2O).

The combustion sampling probe was located in the end section about 2 meters from the nozzle tip at a radial position halfway between the reactor centerline and the combustion chamber wall. Samples of the solid and gas combustion products were collected for each test and wall temperatures were measured for each reactor section. Figure 1 shows the location of the sampling probe and wall thermocouples on a schematic of the reactor.

For tests 13-17, the swirl number was fixed at 9.6, and the SR was 1.01 while the probe was moved radially to sample five zones of equal annular area to determine particle flux and mass weighted overall coal burnout.

The coal burnout, defined as the mass percent of solid combustible matter that is consumed, was determined from elemental analysis of the collected particles, and by completing the particle combustion in an ashing oven. The Perkin-Elmer Model 240 Elemental Analyzer, which requires only about 10 mg of solid for accurate analysis, subjects the particles to higher temperatures than the ashing oven, which requires 1 gram of sample. The Perkin-Elmer analysis indicated coal burnouts which were within 1% of those obtained from the ashing oven, and are the results which are reported here.

Results

Stable slurry combustion without methane support was achieved for all combustion conditions. Slurry feed was held constant and secondary air was adjusted. The flame was never quite attached to the nozzle, and moved away from the nozzle as the swirl number was decreased. At the highest swirl number, the flame was located approximately 15 cm from the nozzle. As swirl number was set to zero, the onset of the combustion zone moved down the reactor to about 45 cm from the nozzle, and the flame appeared to fluctuate above and below this location. The flame was also observed to move farther down the reactor for higher stoichiometric ratios and for lower combustor pressures.

Calculations of the residence time of the particles for the coal and air feed rates used show that the particles were in the reactor between about 0.8 and 1.5 seconds, depending on the average temperature of the combustion products and the stoichiometric ratio. The residence time with swirl may have been higher due to large-scale recirculation zones which may have developed within the combustor.

The coal burnout values for all tests are shown in Table 5. The coal burnout levels ranged from 84% to 99% and increased with increasing swirl number. Figure 7 shows the variation of burnout with secondary air swirl number for the three stoichiometric ratios. Test 16 and test 2 had essentially identical conditions, including sampling probe radial location. The similarity of the measured coal burnout values indicates good reproducibility of the tests. The unusually high burnout (97.2%) measured at high swirl number for an SR of 0.75 was due to the location of the sample probe. This may be explained by Figure 8, which shows the near-exit plane coal burnout and particle mass flux radial profiles for a swirl number of 9.6 and an SR of 1.01. The effect of swirl number on the particle mass flux is shown. Table 6 lists the radial sampling positions near the reactor exit plane. The measured burnout decreases slightly at positions near the wall.

Tests of the atomizer (11) showed an included slurry spray angle of nearly 40° which would also tend to concentrate the particles near the wall, even when no swirl was used in the secondary air. The combustion of an injected CWM which is not premixed with air occurs with diffusion flames which are locally stoichiometric. This, coupled with the reduced particle concentration near the centerline due to the slurry spray angle, could account for the relatively high burnout achieved at an SR of 0.75 with no swirl.

The measured wall temperature profiles provide some insight into the effects of both swirl and stoichiometric ratio on the combustion heat release within the reactor for fixed values of slurry feed rate, atomizer position and secondary air temperature. Figure 9 shows the wall temperatures for various axial locations down the combustor for a stoichiometric ratio of 0.74 and with four different swirl numbers. The positions of the wall thermocouples are shown on the figure as the ratio of the thermocouple axial distance, X, from the top of the reactor to the total reactor length, L. The wall temperature

thermocouple locations are also shown in Figure 1. The location of the seven thermocouples corresponded to X/L values of 0.07, 0.2, 0.33, 0.47, 0.6, 0.73 and 0.87. The temperature data are throught to be erroneous at X/L = 0.33 because of the depth of the thermocouple placement in section 3 of the reactor. The data are shown on the figure but are not included in the analysis. It appears that with swirl, the axial distance to near maximum temperature ranges from X/L = 0 to about X/L = 0.2. In all cases the first wall temperature is greater than the combustion air temperature. Some reaction occurs as the water vaporizes and the coal devolatilizes. Peak recorded temperatures with swirl occur, at X/L = 0.2, corresponding to the highest heat release rate. Combustion is nearly completed by X/L = 0.7 as the temperature profiles flatten out. While the initial recorded reactor temperatures seem to be higher with increasing swirl number, the exit temperatures were higher with decreasing swirl number. The profile with no swirl shows that the maximum temperature occured further down the reactor at about X/L = 0.5, indicating an extended mixing period. Reaction was still occurring near the end of the reactor (X/L = 0.75). The reactor exit temperature is also highest with no swirl.

Figure 10 shows the wall temperature profiles for the case of excess combustion air (stoichiometric ratio of 1.23). The peak temperatures occur farther down the reactor compared to those for lower SR values, except for the largest swirl numbers. Peak and overall average temperatures for all swirl conditions were also lower than in Figure 9, due to the presence of excess air. The mixing and combustion regions are similar for the three profiles corresponding to no swirl, and swirl numbers of 0.72 and 5.1. For these conditions, the combustion is nearly complete near the end of the reactor as evidenced by the flattening temperature profile.

The effect of stoichiometric ratio on reactor wall temperatures is shown in Figures 11 and 12 for no swirl, and a swirl numbr of 0.72, respectively. Peak temperatures are similar for both swirl conditions. With no swirl, the heat release patterns are similar for all stoichiometric ratios, but a large reduction in profile average temperature and peak temperature occurs with 23% excess air (SR = 1.23). When swirl is introduced, the location of peak temperature moves up the reactor as mixing is enhanced. Excess air caused a spatial delay in the location of the maximum temperature to X/L = 6, similar to the no swirl case. This delay is largely due to increased gas flow velocities as airflow increases, reducing the particle residence time.

The reactor conditions for maximum burnout were found at the highest swirl number with SR values of 1 or higher. Quite high coal burnout was measured near the exit plane for the small-scale laboratory reactor for theoretical swirl numbers as low as 0.72. Figure 13 compares CWM carbon conversion data from these tests with other CWM combustion results. Several other combustion system variables including atomizer and nozzle design and operation, slurry pre-heating, wall temperature control and combustion aerodynamics, can be optimized to provide enhanced mixing and increased coal burnout, while

minimizing the required swirl level, excess air and pollutant formation for successful industrial application of CWM.

Test Plans

Reactor conditions for maximum burnout have been identified in terms of swirl number, stoichiometric ratio and atomizing air for a fixed nozzle type and position, reactor operating conditions, and slurry type. At these optimal burnout conditions, a space-resolved map of the combustor will be constructed, detailing pollutant concentrations (NO_x, SO_x, CO, HCN, etc.) and coal burnout for selected axial and radial sampling probe positions. Characteristic reactor combustion profiles for CWM (temperature, NO_x, burnout) will be used to compare to similar tests with pulverized coal.

Acknowledgement

This research was supported by the Pittsburgh Energy Technology Center of the U.S. Department of Energy under contract DE-FG22-80PC-30306, for which James D. Hickerson is the PETC technical officer. The support of the Brigham Young University Research Division is also appreciated. Acknowledgement is given to Robbins & Myers which supplied the Moyno slurry pump used in the test program, and to Atlantic Research Corporation which provided the coal-water mixtures. The authors also express gratitude to research colleagues in the BYU Combustion Labortory for their cooperation and support during the combustion testing and analysis, including Dr. P.O. Hedman, D. Sloan, J.A. Johnson, R.M. LaFollette and J. Glassett.

References

1. Fourth International Symposium on Coal Slurry Combustion, sponsored by PETC, Orlando, Florida (May 1982).

2. McHale, E.T., Scheffee, R.S., Rossmeissel, N.P., Comb. Flame 45, 121 (1982).

3. Eckmann, J.H., "Transport and Handling Characteristics of Coal Water Mixtures," 4th International Symposium on Coal-Water Mixtures, Orlando, Flordia (May 1982).

4. Pan, Y.S., et al., "Exploratory Coal-Water and Coal-Methanol Mixture Tests in Oil-Designed Bilers," 4th International Symposium on Coal Slurry Combustion, Orlando, Florida (May 1982).

5. EPRI Report of Joint B&W/EPRI study.

6. Scheffee, R.S., et al., "Further Development and Evaluation of Coal-Water Mixture Technology," 4th International Symposium on Coal-Water Mixtures," Orlando, Florida (May 1982).

7. Germane, G.J. and Smoot, L.D., "Basic Combustion and Pollutant Formation Processes for Pulverized Fuels," Quarterly Technical Progress Report No. 6, U.S. DOE, Grant No. DE-FG22-80PC-30306,

Brigham Young University, Provo, Utah (April, 1982).

8. Germane, G.J. and Smoot, L.D., "Basic Combustion and Pollutant Formation Processes for Pulverized Fuels," Quarterly Technical Progress Report NO. 9, U.S. DOE, Grant No. DE-FG22-80PC-30306, Brigham Young University, Provo, Utah (January, 1983).

9. Germane, G.J., et al., "Coal-Water Mixture Combustion Studies in a Laboratory Cylindrical Combustor," 4th International Symposium on Coal Slurry Combustion, Orlando, Florida (May, 1982).

10. Germane, G.J., private communication with Edward T. McHale, Manager of Combustion and Physical Science Department, Atlantic Research Corporation, Alexandria, Virginia (Janury, 1983).

11. Peterson, S.N., "Development of a Swirl-Air Generator and a Coal-Water Mixture Atomizer," Master of Engineering Project Report, Mechanical Engineering Department, Brigham Young University, Provo, Utah (April, 1982).

TABLE 1

COMBUSTOR AND SLURRY CHARACTERISTICS
FOR CWM LABORATORY COMBUSTION TESTS

Company	Scale Combustor (MMBTU/hr)	Coal	Slurry Coal/water%	Add. %
ARC	1	a) MV bit.	65/34	1
		b) HV bit.	62/38	1
PETC	a) 2-5	HV bit.	6C.6/38.9	0.5
	b) 20-60			
B & W	4	HV bit.	66/33	1
BYU	0.5	HV bit.	70/30*	1

* from ARC

TABLE 2

CWM TEST CHARACTERISTICS AND RESULTS

Investigator/ Company	Slurry Flow lb/hr	Burnout Method	Burnout Range %	No. Tests	Sec. Air Temp °F
ARC	57-126	C in ash	46-92	20	350-600
PETC	a) 251-672 b) 3029	C in ash	a) 81-93 b) 94	7	300-585
B & W	430-500	gas-analysis	89-93	5	600
BYU	50	ash & gas	90	4	600

TABLE 3

MONTANA BITUMINOUS COAL ANALYSIS AND SELECTED ARC COAL-WATER MIXTURE PROPERTIES (5)

Coal Analysis	As-Received	Dry Basis
Proximate, %		
Moisture	1.45	---
Ash	4.68	4.75
Volatile Matter	31.84	32.31
Fixed Carbon	62.03	62.94
Heating Value (kJ/kg)	33,888	34,383
Ultimate, % (dry basis)		
Carbon		83.57
Hydrogen		5.18
Nitrogen		1.87
Chlorine		0.14
Sulfur		0.90
Ash		4.75
Oxygen		3.59
Slurry Analysis		
Solids Loading	70.4%	
Particle Size	87%-200 mesh	
Viscosity (25°C)	1150 cp at 88 sec^{-1}	
Stabilizer/additives	1%	

TABLE 4

CWM TEST MATRIX FOR BURNOUT AND PROFILE TESTS

Test No.	Theoretical Swirl No.	Coal/Air Stoichiometric Ratio	Radial Probe Position (cm)**
1	9.6	0.75	8.75
2	9.6	1.00	8.75
3	9.6	1.23	8.75
4	5.1	0.74	8.75
5	5.1	1.01	8.75
6	5.1	1.24	8.75
7	0.72	0.72	8.75
8	0.72	1.01	8.75
9	0.72	1.24	8.75
10	0	0.72	8.75
11	0	1.01	8.75
12	0	1.24	8.75
13	9.6	1.01	16.58
14	9.6	1.01	14.60
15	9.6	1.01	12.32
16	9.6	1.01	9.45
17	9.6	1.01	0

**Distance off reactor centerline, with axial location of probe near combustor exit.

TABLE 5

SUMMARY OF CWM COMBUSTION TESTS FOR VARIOUS SWIRL NUMBERS AND STOICHIOMETRIC RATIOS

Test	Coal Feed kg/hr (dry basis)	Combustion Air Flow Rate Kg/hr*	Stoichiometric Ratio	Swirl No.	Coal Burnout Mass % (daf)	Combustion Chamber Wall Temperature, °C						
						Sec. 1***	Sec. 2	Sec. 3	Sec. 4	Sec. 5	Sec. 6	Sec. 7
1	12.1	101	0.75	9.6	97.2	818	1101	1012	1026	1001	790	800
2	12.9	143	1.0	9.6	99.3	746	1030	990	978	955	692	685
3	12.8	175	1.23	9.6	99.2	847	1044	1024	1020	984	817	786
4	12.3	101	0.74	5.1	95.5	836	1071	1027	1028	1018	814	811
5	12.7	143	1.01	5.1	96.5	739	995	955	973	968	788	782
6	12.7	175	1.24	5.1	96.5	619	891	928	966	961	822	786
7	12.7	101	0.72	0.72	88.0	658	1105	972	1062	1049	859	857
8	12.7	143	1.01	0.72	96.6	678	1008	904	944	947	763	787
9	12.7	175	1.23	0.72	96.4	546	798	857	921	943	845	820
10	12.7	101	0.72	0	84.0	680	1079	976	1096	1087	917	890
11	12.7	143	1.01	0	92.6	744	1052	970	1083	1071	952	891
12	12.7	175	1.23	0	96.4	546	911	798	938	964	789	809
13	12.7	143	1.01	9.6	98.4	788	1086	1000	1052	1008	802	815
14	12.7	143	1.01	9.6	97.9	786	1103	1018	1064	1009	828	842
15	12.7	143	1.01	9.6	99.4	788	1104	1018	1066	1007	831	848
16	12.7	143	1.01	9.6	99.2	780	1100	1025	1064	1010	843	852
17	12.7	143	1.01	9.6	**							

*Secondary air temperature maintained at 316°C (600°F) for all tests.
**Insufficient sample collected for analysis and steady wall temperatures not achieved.
***Section 1 is at top of reactor; section 7 contained sample probe at exit plane.

TABLE 6

RADIAL PARTICLE FLUX AND BURNOUT PROFILE FOR
REACTOR EXIT PLANE (SWIRL NUMBER = 0.6; SR = 1.01)

Test	Probe Radial Distance From Centerline, cm	Particle Flux mg/min	Local Coal Burnout Mass % (daf)
13	16.6	86.8	96.4
14	14.6	61.8	98.4
15	12.3	38.6	97.9
16	9.5	30.0	99.4
17	0	*	*
			98.7[a]

* Insufficient sample collected for analysis.

[a]sampling plane average.

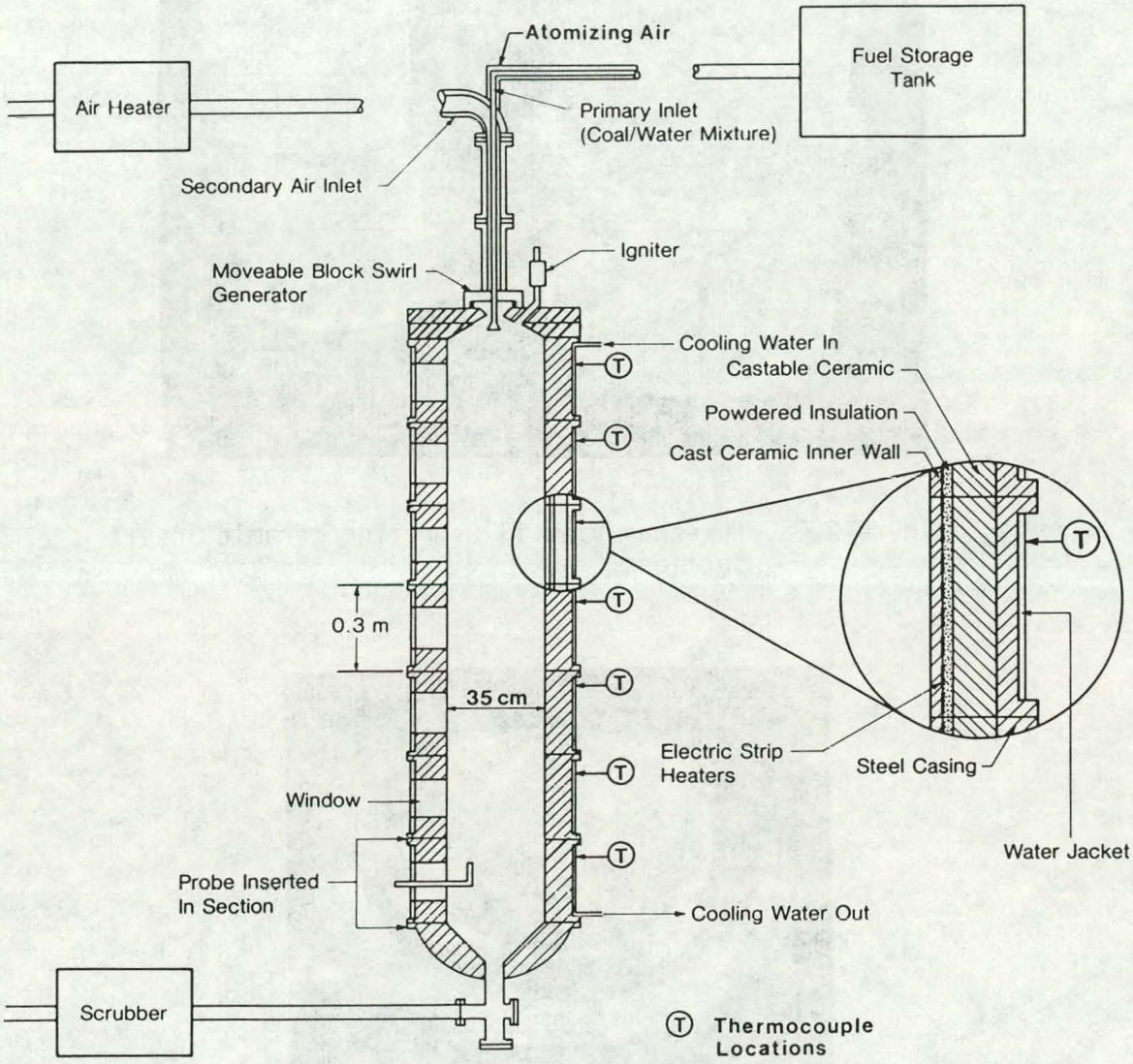

Figure 1. Reactor schematic showing major support facilities.

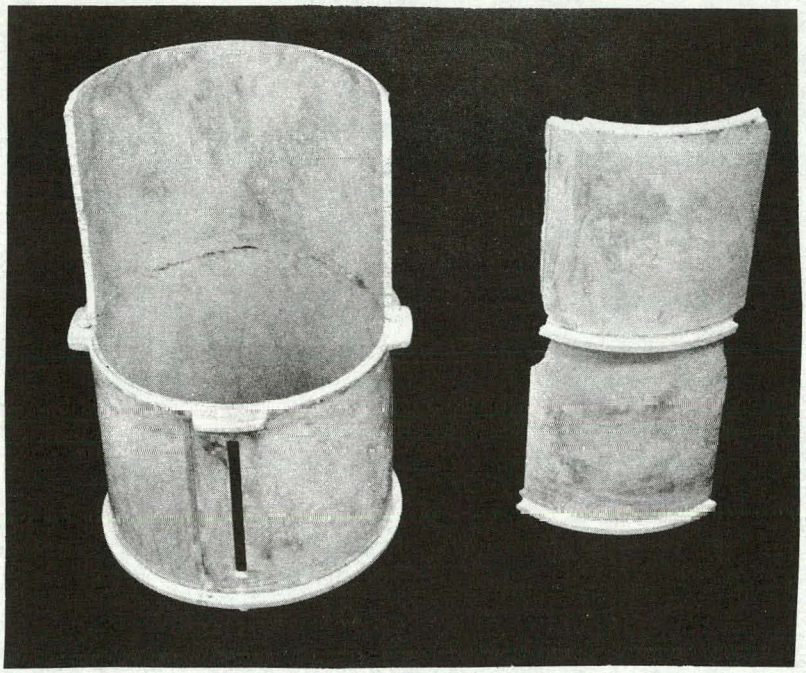

Figure 2. a. Cut-away view illustrating ceramic insert sections.

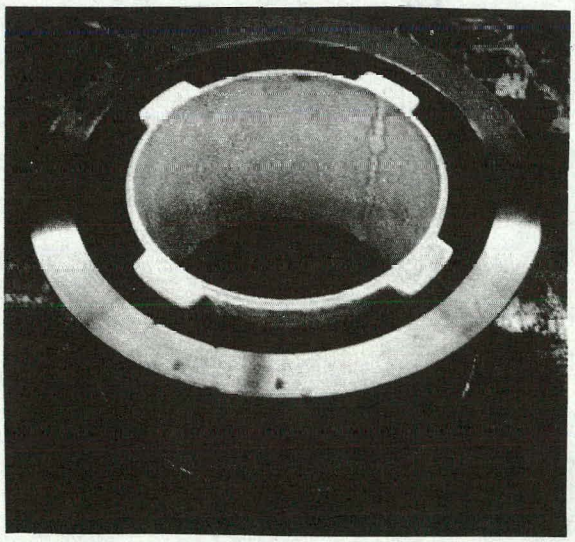

Figure 2. b. Ceramic insert inside steel section (without outer ceramic insulation layer).

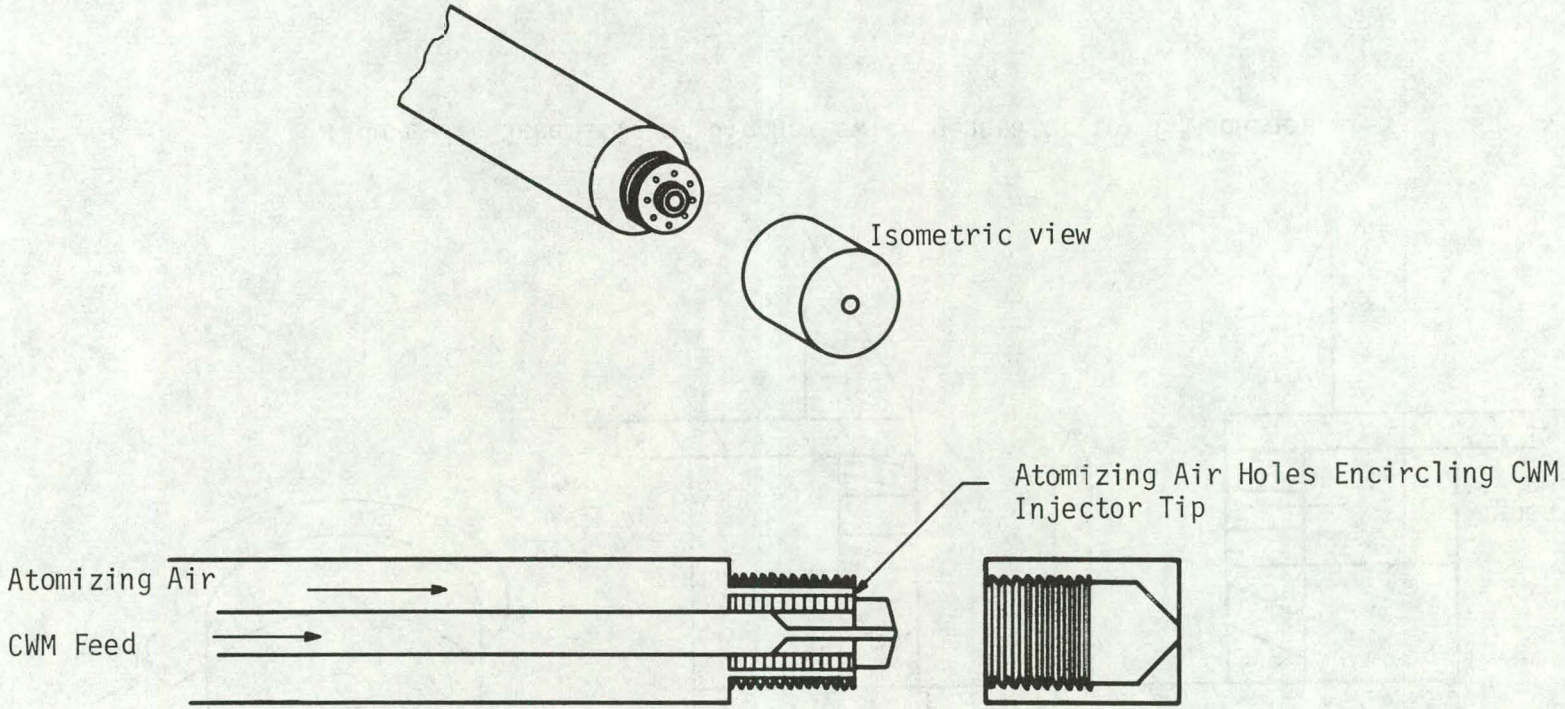

Figure 3. CWM nozzle used in combustion tests.

066

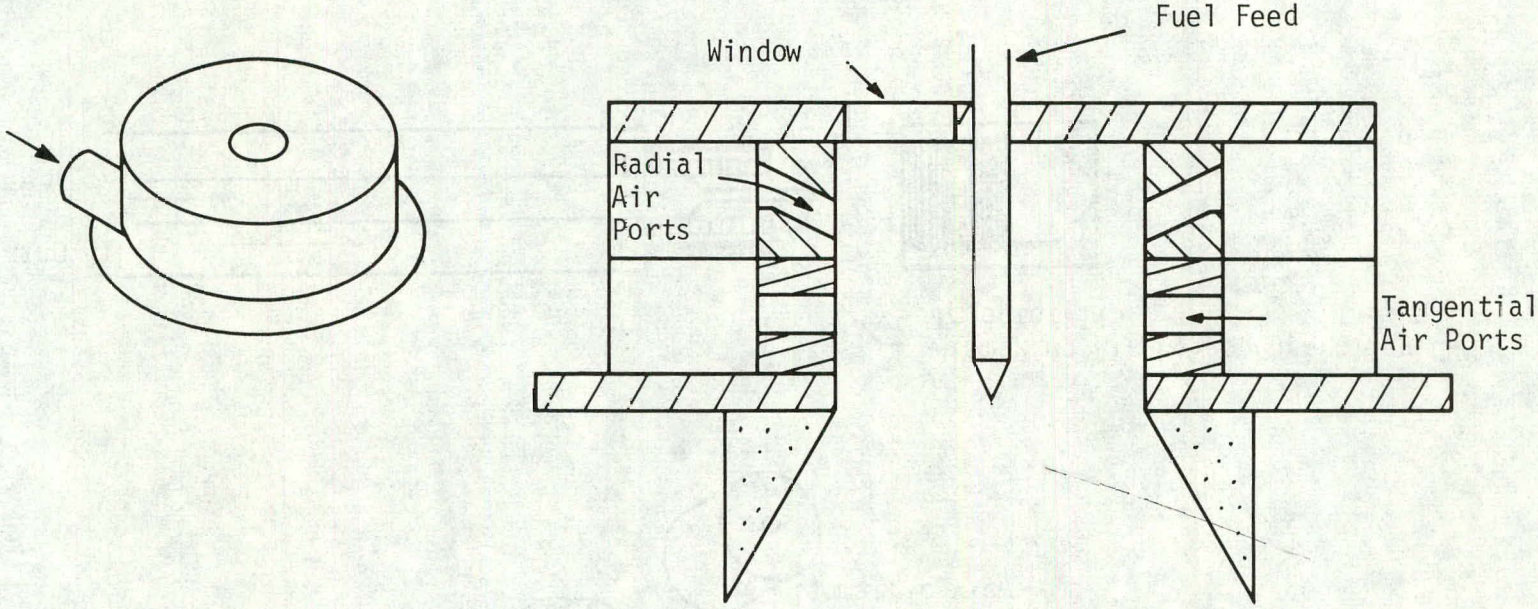

Figure 4. Schematic of air jet swirl generator for CWM burner.

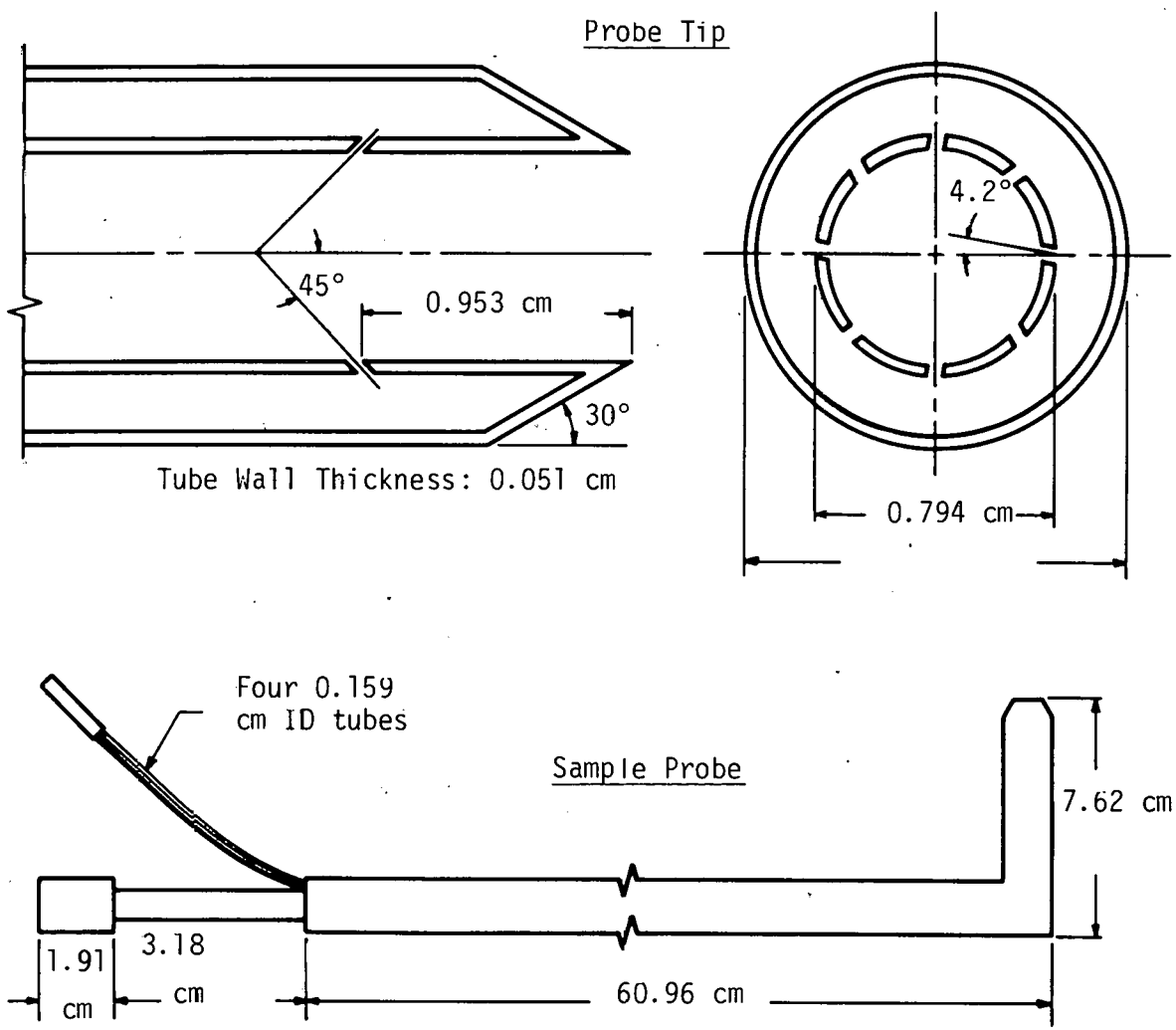

Figure 5. Schematic diagram of sample probe and probe tip. Tubing is stainless steel.

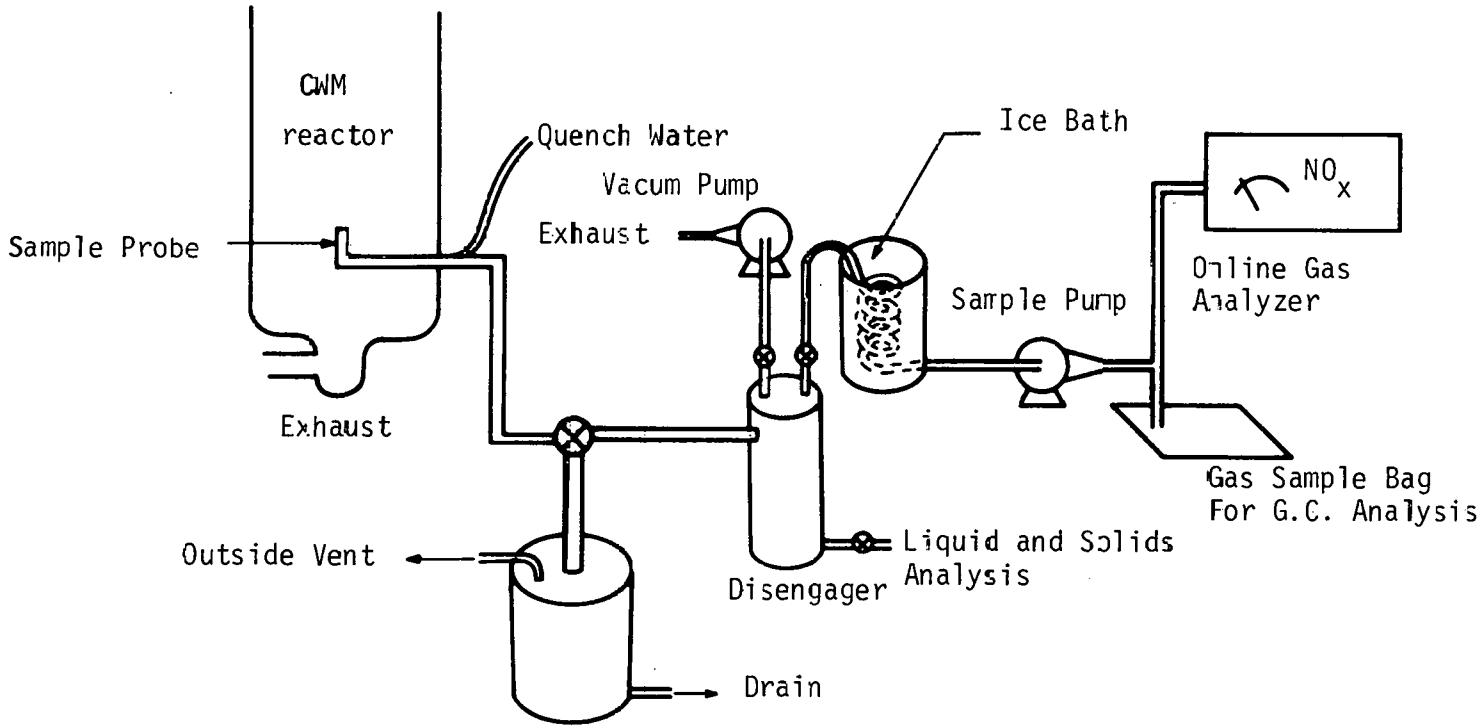

Figure 6. CWM sampling system.

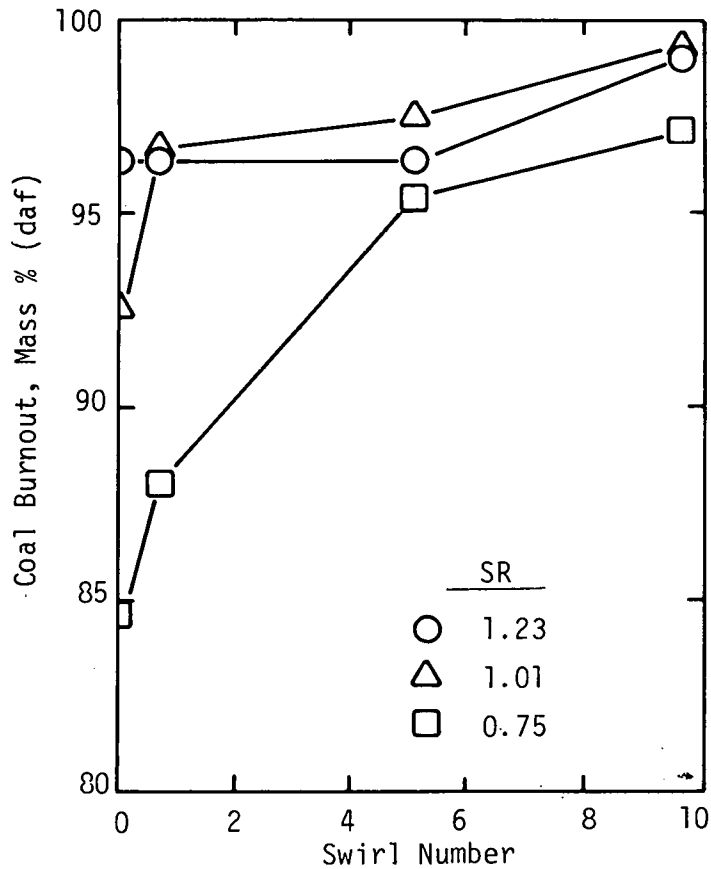

Figure 7. Effect of swirl number and stoichiometric ratio on burnout of coal in CWM.

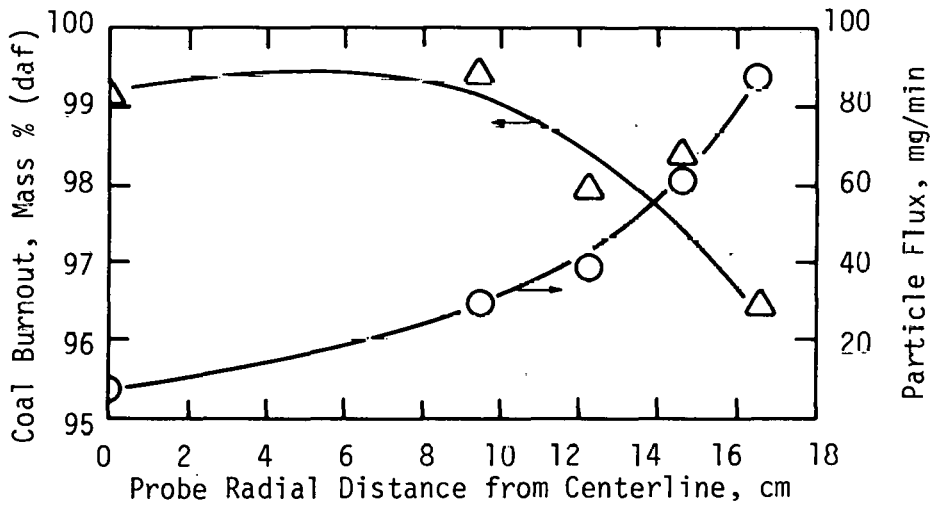

Figure 8. Near exit plane coal burnout and particle flux profiles for swirl number = 9.6 and SR = 1.01.

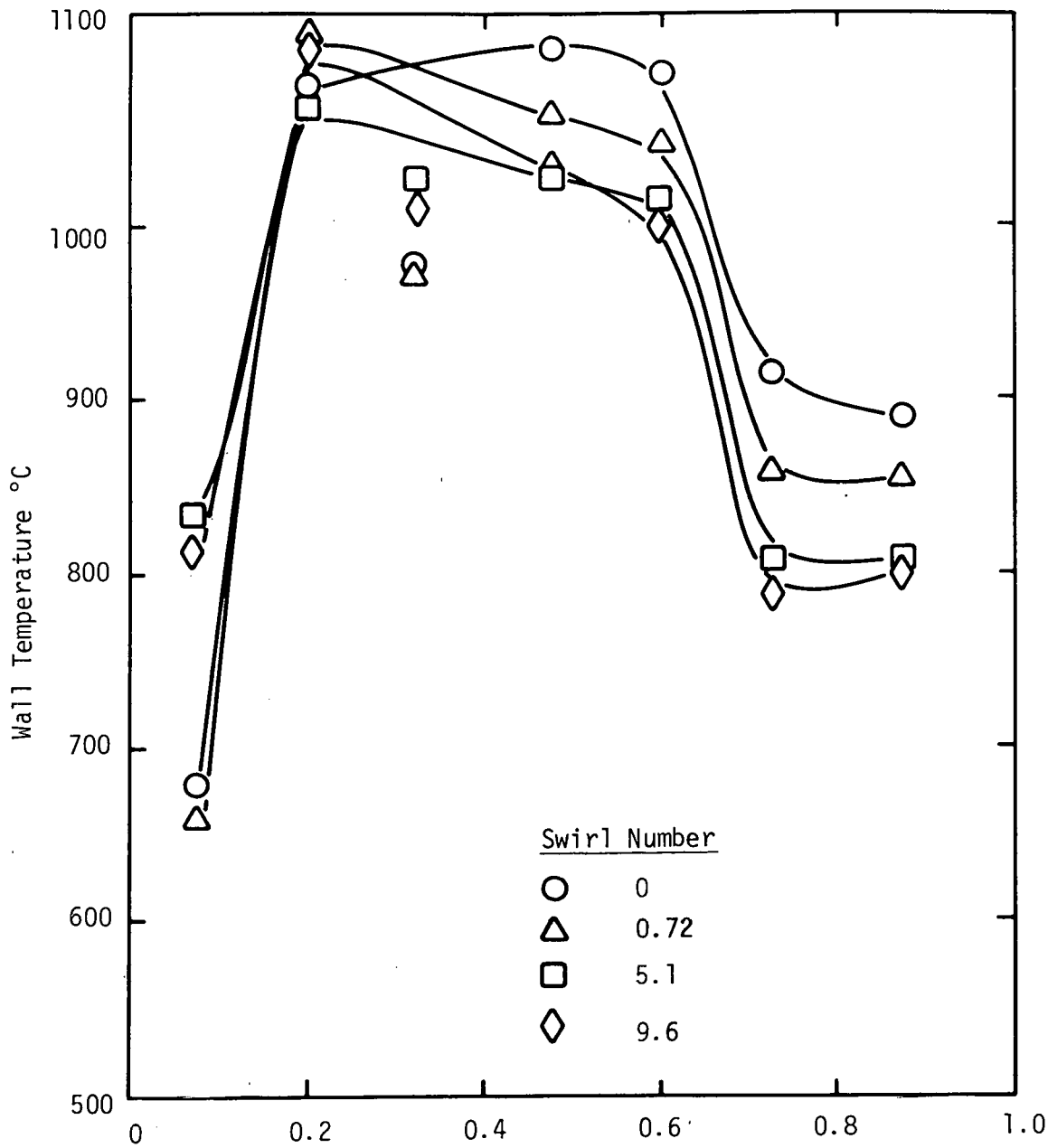

Figure 9. Reactor wall temperature profiles for various theoretical swirl numbers with a stoichiometric ratio of 0.74.

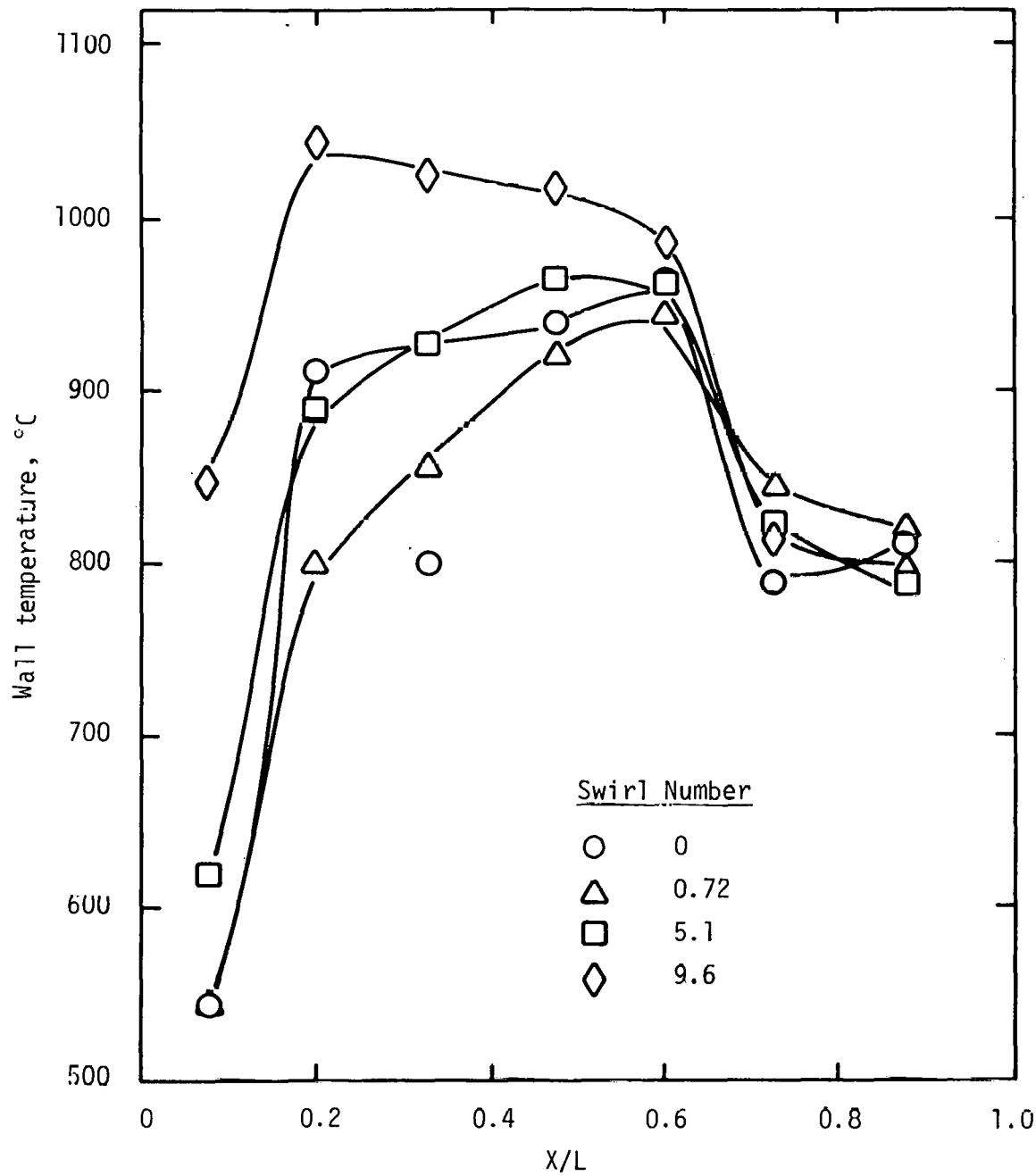

Figure 10. Reactor wall temperature profiles for various swirl numbers with a stoichiometric ratio of 1.23.

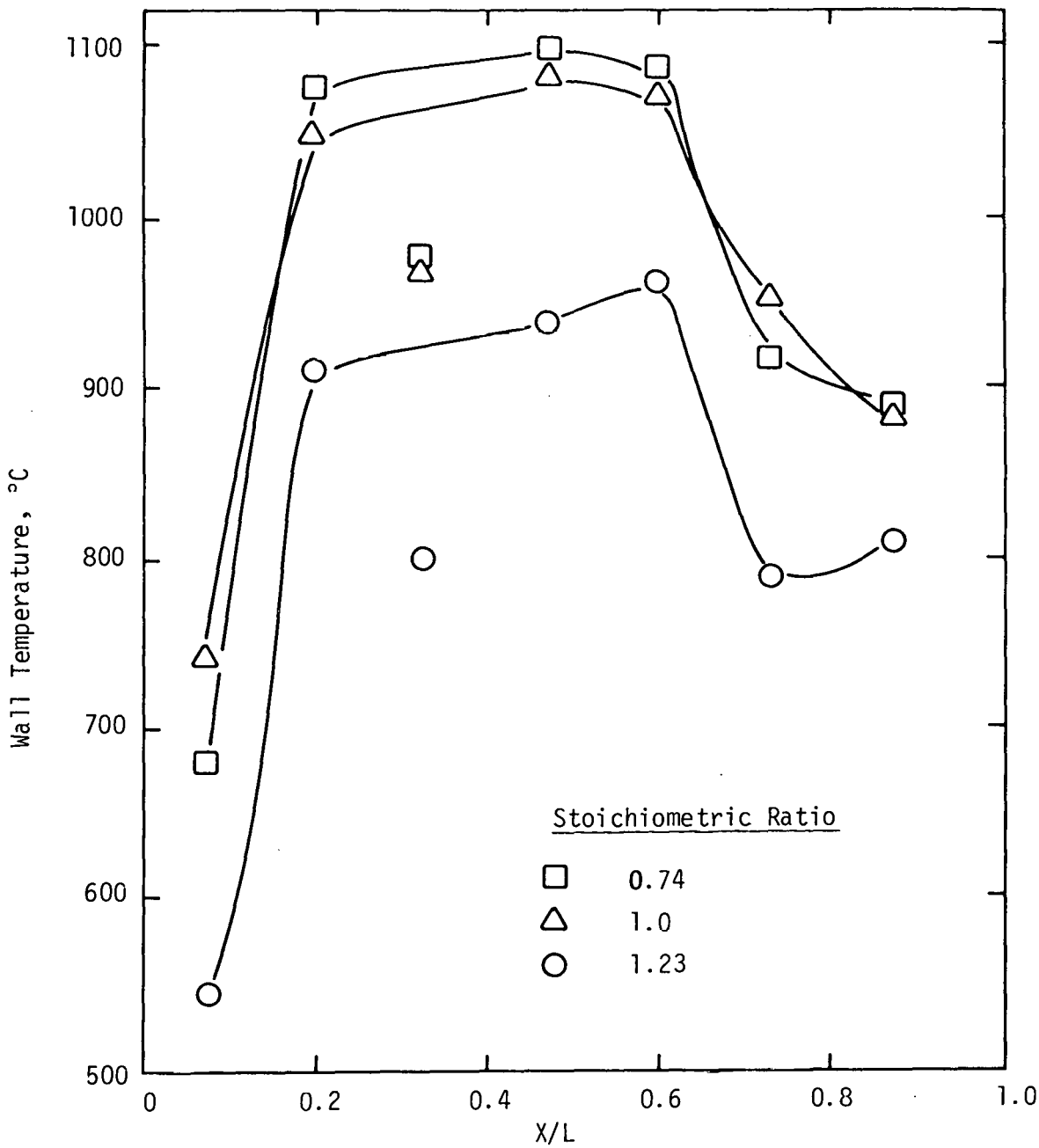

Figure 11. Effect of SR on axial wall temperature profiles in the absence of swirling flow.

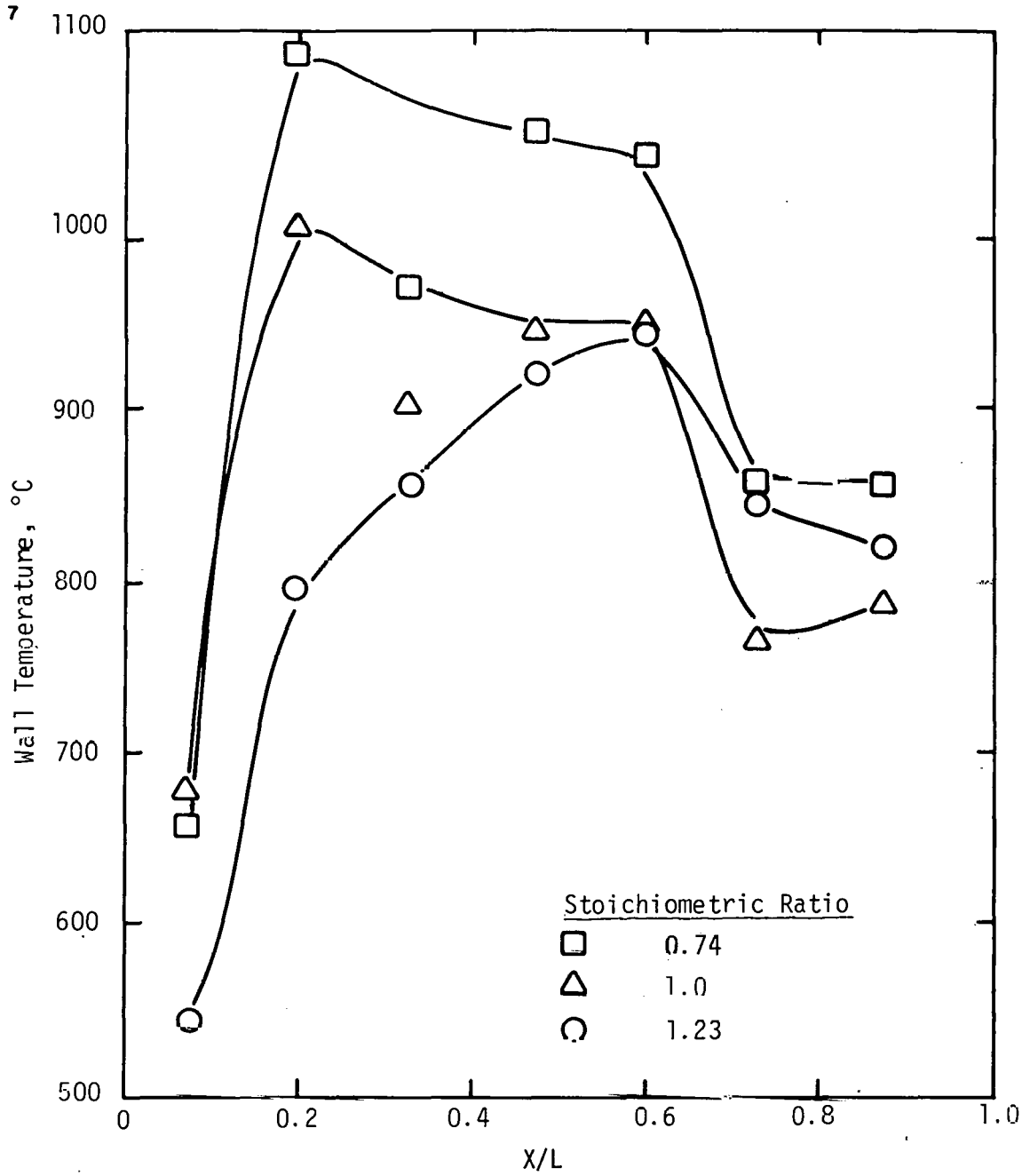

Figure 12. Effect of SR on axial wall temperature profiles for a swirl number of 0.72.

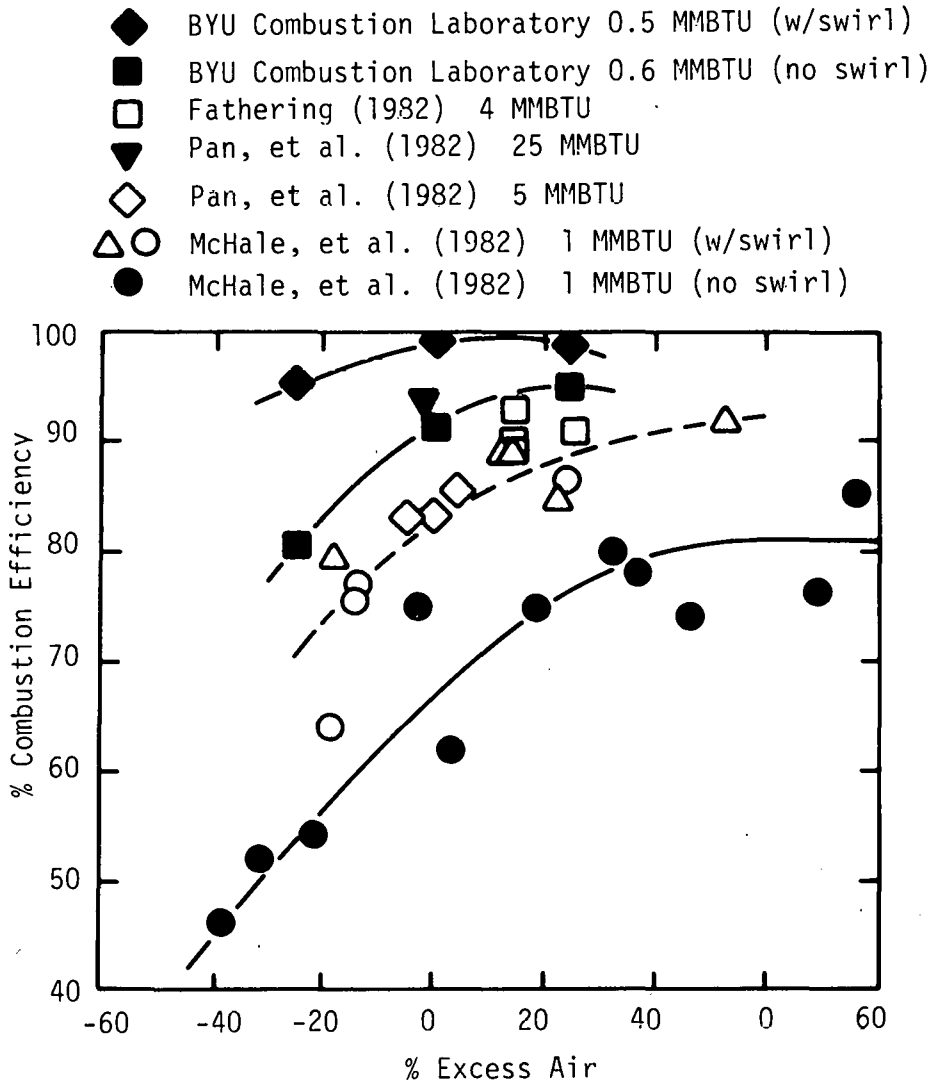

Figure 13. Carbon Conversion Data for CWM.

SOME ASPECTS ON PREPARATION TECHNIQUE OF COAL WATER SLURRY AND ITS COMBUSTION PERFORMANCE

Huang Zhaoxiang Wu Yifeng Wang Yizhen Li Zhangjie
(Institute of Engineering Thermophysics, Academia Sinica)

Zhai Wenhui
(Institute of Chemistry, Academia Sinica)
(Beijing, the People's Republic of China)

ABSTRACT

Theoretical computation and experimental investigation of porosities and its saturated water content within rigid ball piles with equal dia. or more than one groups of dia. have been carried out in order to simulate the coal powder slurry properties, and acceptable accuracy can be obtained from its results. The optimum particle dia. ratio and the corresponding optimum mass ratio calculated by our theory have been verified in the slurry preparation process at our laboratory. It can be predicted also that the minimum water content of coal-water slurry will be 25% as 2 groups of coal powder with 2 kinds of dia. are used.

The combustion performance of slurry droplets by using a precise analytical thermobalance has been carried out in our laboratory; the microstructure of slurry has also been recorded by an electronic microscope.

NOMENCLUTURE

B flow parameter
C volume percentage occupied by large particle
d particle diameter

g_c force-mass conversion factor
G shear rate
R radius of cylinder
W weight percentage of water

Greek Letters
δ equivalent dia.
ε porosity
ζ dia. ratio (d/d_V)
η suspension viscosity
η_o viscosity parameter at low shear rate
η_∞ viscosity parameter at high shear rate
θ shear stress necessary to overcome particle-particle contact
μ liquid vehicle viscosity
ξ shape factor defined as the ratio of the surface area of a sphere of equivalent volume to the surface area of the particle
ρ_p suspension density
σ_g geometric standard deviation for particle dia.
τ_{rz} shear stress in axial direction
τ_y suspension yield stress
ϕ volume fraction of coal powder
ϕ_m max. value of volume fraction for coal powder

Subscript
e experimental artificial filling
i inside
l large
o optimum; outside
p practical stirring
s small
v vessel

INTRODUCTION

Coal-water slurry(CWM) is often used now in boilers and industrial furnaces to replace the oil fuel although derating will result from the evaporating of its water content. Reduction of the slurry viscosity is necessary in order to give a fine atomization by which the more complete combustion can be obtained. Beside, reduction of pipe transportation cost can be resulted by low viscosity slurry. The slurry viscosity can be reduced either by additives or by particle size selection while its water content keeps unchanged.

Gay and etc[1] suggested the following formulas to describe the relationships between the shear stress and the shear rate of thick suspensions

$$\tau_{rz} - \tau_y = \frac{\eta_\infty}{g_c} G + \theta \tag{1}$$

$$\theta = \frac{(\eta_o - \eta_\infty)/g_c}{1+G(\eta_o - \eta_\infty)/g_c B} G \tag{2}$$

$$\tau_y = 200\left(\frac{d}{\Phi_m - \Phi}\right)\left(\frac{\Phi_m}{1-\Phi_m}\right)^2\left(\frac{1}{\xi^{1.5}\sigma_g^2}\right) \tag{3}$$

$$\eta_\infty = \mu \exp\left\{\left[2.5+\left(\frac{\Phi}{\Phi_m-\Phi}\right)^{0.48}\right]\frac{\Phi}{\Phi_m}\right\} \tag{4}$$

$$\frac{B}{\tau_y} = 0.066\left(\frac{\Phi_m^2}{\Phi_m-\Phi}\right)\left(\frac{\mu^2}{d^2 \rho_p \tau_y}\right)^{0.21} \tag{5}$$

Landel[2] gave:

$$\eta_o = \mu\left(\frac{\Phi_m}{\Phi_m-\Phi}\right)^{2.5} \tag{6}$$

In the above equations we have:

$$\varepsilon = 1 - \Phi_m \tag{7}$$

The reduction of natural porosity for rigid ball piles has been investigated both theoretically and experimentally by the present authors. The optimum particle size

ratio, the influence of slurry preparation technology upon its rheology characteristic and its combustion performance can be obtained. It can be shown also that the minimum viscosity can be resulted at constant water content, or minimum water content can be obtained at constant viscosity level by proper particle size selection.

INVESTIGATION OF NATURAL POROSITY

The natural porosities of rigid ball piles for equal dia. balls predicted by our analysis in appendix is 37.7%, which agree to the experimental results satisfactorily; it can be shown also that the minimum porosity obtained from the most compact ball pile is 26%. The natural porosity can be further reduced by filling the gap space with small rigid balls, the smaller balls with dia. $d_s < 0.11 d_l$ can flow into the gap formed by the larger balls easily in our experiments. It can be shown also that the porosity of equal dia. ball pile filled within a finite spherical space is strongly influenced by $\zeta = d/d_v$ as shown in fig.(1).

Φ_m decreases as ε increases, and this results the increase of η_∞ according to equ.(4). Hence the viscosity of flowing slurry in large dia. pipe is different from that flowing through narrow channels, the viscosity of the later is generally larger than the former due to the decrease of Φ_m as the slurry flows through a narrow channel. The ratio of particle dia. to the channel dimension should be kept beyond 0.1 in order to approach an accurate viscosity.

The natural porosity is severely influenced by the shape factor of particles; for spherical particle, for instance, $\varepsilon = 0.37$. ε is larger for equal dia. particles if ξ is much less than 1. As to bitumionous coal:

$$\varepsilon = 0.50(\delta_o/\delta)^{0.060} \qquad (8)$$

for anthracite:

$$\varepsilon = 0.50(\delta_o/\delta)^{0.11} \tag{9}$$

in which δ_o=0.5mm, $\delta \leq 0.5$mm. We can find $\varepsilon \cong 0.50$ when $\delta > 0.5$mm as illustrated in fig. (2) and (3).

The porosity of coal particle pile with a wide particle size distribution is generally a little bit smaller than the porosity of coal particle pile with some equal dia. particle sizes. The theory developed by the present authors using only two particle dia. can be used to predicte the characteristics of coal-water slurry with two peak coal powder sizes.

We can find from fig.(4) that ε_o is an optimum value when a certain optimum value of C has been given as d_s/d_l was fixed, in this figure the relationship between the natural pile porosity ε and the volume percentage occupied by the larger balls C is illustrated. There existed two $\varepsilon_o$values in fig.(4) and (5) as $d_s/d_l < 0.11$, namelyε_{oe} and ε_{op}, $\varepsilon_{op} > \varepsilon_{oe}$ with corresponding C_{oe}, C_{op}, in which C_{op} is a little smaller than C_{oe}. ε_{oe} can be obtained as the smaller balls flowed into the gap formed by larger balls; while ε_{op} can result from evenly mixed by stirring. The larger balls can not contact each other closely in the later case; but they can contact each other very closely in the former case, hence it has only theoretical significance.

If $d_s/d_l \to 0$, then

$$\varepsilon_{oe} \to \varepsilon_l \cdot \varepsilon_s \tag{10}$$

We have

$$Coe \to \frac{1}{1+\frac{1-\varepsilon_s}{1-\varepsilon_l}\varepsilon_l} \tag{11}$$

When $C > Coe$, $d_s/d_1 \to 0$, we have

$$\varepsilon \longrightarrow \varepsilon_1 - (1-\varepsilon_1)\left(\frac{1}{C}-1\right) \tag{12}$$

when $C < Coe$, $d_s/d_1 \to 0$, we have

$$\varepsilon \longrightarrow \frac{1-C}{1-C\,\varepsilon_s}\,\varepsilon_s \tag{13}$$

The accuracy is satisfactory by using equations(10), (11), (12), (13) when d_s/d_1 is sufficiently small, for example, 0.035, as illustrated in fig. (6) which has been verified by our experiments.

When $0.6 < d_s/d_1 < 1$, the pile porosity of rigid balls with two sizes is very similar to the porosity of equal dia. ball pile; but when $d_s/d_1 \leq 0.6$, we have

$$\varepsilon_{op} = \varepsilon_1 \varepsilon_s + 0.34(d_s/d_1)^{0.628} \tag{14}$$

as shown in fig. (7).

The equations (10)-(13) are still valid if the particles were irregular in form when d was replaced by δ .
When $\delta_s/\delta_1 \to 0$
we have

$$\varepsilon_{oe} \longrightarrow \varepsilon_1 \cdot \varepsilon_s \tag{15}$$

$$C_{oe} \longrightarrow \frac{1}{1+\frac{1-\varepsilon_s}{1-\varepsilon_1}\,\varepsilon_1} \tag{16}$$

if $C > C_{oe}$, $\delta_s/\delta_1 \to 0$, we have:

$$\varepsilon \longrightarrow \varepsilon_1 - (1-\varepsilon_1)\left(\frac{1}{C}-1\right) \tag{17}$$

and as $C < C_{oe}$, $\delta_s/\delta_1 \to 0$, we have:

$$\varepsilon \longrightarrow \frac{1-C}{1-C\,\varepsilon_s}\,\varepsilon_s \tag{18}$$

Equation (14) is still valid for irregular and relatively smooth particles as verified by the experimental results by Qing Hua Univ.[4], hence we have:

$$\varepsilon_{op} = \varepsilon_1 \varepsilon_s + 0.34(\sigma_s / \delta_1)^{0.628} \qquad (19)$$

as illustrated in fig. (7). The following equation can be used satisfactorily for fine coal particles with very rough surface which has been derived from experiments for $\delta_s / \delta_1 \leq 0.5$.

$$\varepsilon_{op} = \varepsilon_1 \varepsilon_s + m(\delta_o / \delta_1)^n \qquad (20)$$

in which m=0.38, n=0.56 as illustrated in fig. (7). The above two equations are similar in form but with different values of m and n, and valid for irregular smooth particles or coal powder with rough surface respectively.

The natural pile porosity for coal particles with equal dia. decreases as particle size decreases, hence the general expression of equations (8) and (9) can be shown as follows:

$$\varepsilon = 0.50(\delta_o / \delta)^a \qquad (21)$$

in which $\delta_o = 0.50mm$, $\delta \leq 0.50mm$, $a > 0$. Then we have:

$$\varepsilon_s = 0.50(\delta_o / \delta_s)^a \qquad (22)$$

$$\varepsilon_1 = 0.50(\delta_o / \delta_1)^a \qquad (23)$$

The following expression can be obtained by substituting equations (20) and (23) into (20):

$$\varepsilon_{op} = 0.25(\delta_o)^{2a} \cdot \delta_1^{-a} \cdot \delta_s^{-a} + m\delta_1^{-n} \cdot \delta_s^{n} \qquad (24)$$

The size of larger particles should be choosen to meet the requirements of slurry preparation technology, then

the size of smaller particles can be selected reasonablly in order to obtain the minimum natural porosity. From:

$$\frac{\partial \varepsilon_{op}}{\partial \delta_s} = 0 \qquad (25)$$

we have:

$$\delta_s = \left(\frac{0.25a \cdot \delta_0^{2a} \cdot \delta_1^{n-a}}{n \cdot m}\right) \frac{1}{n+a} \qquad (26)$$

in which $\delta_0 = 0.50$mm, $\delta_1 \leq 0.50$mm. For example, the value of δ_s could be 8 μ for anthracite (a=0.11), and 2 μ for bituminous coal (a=0.06) if 0.1mm dia. has been choosen for the larger particles so that the minimum natural porosity can be obtained.

The coal-water slurry with 25% water content has been prepared succeededly in our laboratory predicted by our theory. The sizes of coarse and fine particles within the coal-water slurry can be seen clearly on the electronic microstructure pictures shown in fig. (8); the fine particle size magnified by 1500 times can be seen also in fig.(9).

SLURRY VISCOSITY

The relationship between the shear stress and shear rate of coal-water slurry without any additives by using the cylindrical viscosimeter with $(R_o - R_i) >> 10d_1$ is illustrated in fig. (10) and (11). Cen[3] concluded that the viscosity measured by cylindrical viscosimeter is identical with the viscosity measured in a pipe. The yield stress for thick slurry can be observed from these figures, the rigidity of non-Newtonian fluid at static condition is sufficient to resist the stress below the yield stress, hence only beyond the yield stress the slurry begins to flow. The slope of τ-G performance curve (viscosity)

decreases when the shear rate increases, and it remains a constant value η_∞ at high shear rate finally as illustrated in these figures. The value of η begins to remain constant as G is greater than 15 s^{-1} for the coal-water slurry commonly used. For slurry A in Fig. (10), $\phi_m = 0.532$ and ϕ varies from 0.353 to 0.526; for slurry B in fig. (11), $\phi_m = 0.609$ and ϕ varies from 0.526 to 0.553. It can be observed easily that η_∞ increases as ϕ increases, and η_∞ increases severely as ϕ approaches to ϕ_m. It can also be found that $\eta_{\infty B} < \eta_{\infty A}$ from fig. (11) due to $\phi_{mB} > \phi_{mA}$ although $\phi_B > \phi_A$.

The additives are very important for the stability and rheology properties of coal-water slurry as shown in fig. (10), it can be observed that the slurry viscosity decreases from 20,000~30,000 centi-poise down to 1,000 centi-poise, as ϕ is 2-3% less than ϕ_m with additive; the slurry viscosity will go back to 20,000 ~ 30,000 centi-poise again, because the water will separate from slurry after a short duration if there is no additive in the slurry at all.

COMBUSTION PERFORMANCE

The performance curves of TG (Thermogravimeter) and DTA (Differencial Thermal Analysis) taken from a precise analytical thermobalance are shown in fig. (12) to (18), the samples were heated up at the speed of 10°C/min from room temperature. The coal content in each slurry sample are all 20 mg; the average dia. of coal particle, the slurry porosity and the environment temperature are illustrated in the following table:

	Average dia. μm	Porosity %	Furnace temperature at ignition T°C
Slurry No.1	77	47	431
Coal powder No.1	77	47	416
Lump coal	2900	0	460
Slurry No.2	20	58	392
Slurry No.3 with additive	50	39	416
Slurry No.4	113	56	424

The ignition temperatures are determined from the intersection points of the dotted lines in fig.(12) to (17).

The coal particle dia. of Slurry No. 1 is exactly same with coal powder No.1, some heat must be spent on the pre-evaporating process before ignition and combustion after the escape of its volatile matter. The ignition temperature of slurry No. 1 is 431°C which is a little bit larger than that (416°C) for coal powder.

There are two peaks on the DTA performance curve of slurry No.2, the first peak was caused by the pre-oxidization process of its volatile matter. The first peak of DTA curve for slurry No.4 is comparatively lower due to its larger particle size; the first peak for lump coal can not be seen at all, hence the combustion rate for smaller particles is higher than larger particles due to its larger surface area and the higher oxidizing rate of its volatile matter content. It's obvious that the ignition temperatures for both slurry and coal powder with higher porosity is rather lower, this is the results, we believe, of the higher volatilizing rate and its higher combustion rate due to its higher porosity

the slope of DTA curves for slurry, coal powder and lump coal are the same in value as shown in fig. (12) to (18),

because the controlling factor of its combustion rate is the diffusion rate only which is nearly the same for different samples.

The influence of additive upon the combustion rate of slurry is very weak as shown by the experiment for slurry No.3, but the evaporating rate for slurry with additive is only slightly slower than other samples.

CONCLUSIONS

(1) The minimum porosity for slurry must be kept in order to obtain the minimum water content and the minimum viscosity.

(2) The method of reducing slurry porosity and the calculation formulas have been verified to be very satisfactory by the present authors.

(3) The ignition temperature and the combustion rate of coal-water slurry are nearly equal to that for powder coal combustion.

ACKNOWLEDGEMENT

Thanks to Mr. Li Duanyi for electronic microstructure picture preparation, and also to Mrs. Xia Luhua for photo picture preparation. Thanks to Mrs. Qi Zongmin for her helpful discussion on slurry preparation technology. Much thanks to Mr. Wang Chenhai for the printing of graphical illustrations.

REFERENCE

(1) Gay, E. C., Nelson. P. A. and Armstrong, W. P.: Flow Properties of Suspensions with High Solids Concentration.

AIChE Journal, Vol. 15, No.6, PP.815, 1969.
(2) Landel, R. R., Moser, B. G. and Bauman, A. J. : Proc. Intern. Congr. Rheol. 4th, PP.663, New York, 1965.
(3) Cen Kefa and etc. : The Theoretical and Experimental Investigations of COM. Zhejiang Univ., China. 1981.
(4) Heat Energy Engineering Dept., Qing Hua Univ. : The Fluid Bed Combustion Boiler, Scientific Press, China. 1980.

APPENDIX

3kinds of typical arrangements for rigid ball piles with equal dia. balls are described as follos:

(1) The most compact pile : The centers of each balls are located at the apex of a tetrahedron as shown in fig. (19). Let d be the ball dia., n be the total number of balls within a unit volume, be the porosity of ball pile, and d_{max} be the dia. of the max. ball which can be filled into the gap space between balls. Then

$$n = \sqrt{2}/d^3 \qquad (d << 1)$$

$$\varepsilon = 1-n\pi d^3/6 = 0.260$$

$$d_{max} = 0.114d$$

(2) The medium compact pile : The balls keep the most compact form on X-Y plane, but just contact each other on Z plane. The center of each ball located at the apex of a rhombohedron as shown in fig. (20).
Then

$$n = 2/\sqrt{3}d^3$$

$$= 1-n\pi d^3/6 = 0.395$$

$$d_{max} = (\sqrt{2}-1)\, d = 0.414d$$

(3) The most loose pile : The center of each ball located at the apex of a cube as shown in fig. (21). Then

$$n = 1/d^3$$

$$\varepsilon = 1-n\pi d^3/6 = 0.476$$

$$d_{max} = (\sqrt{3} - 1)\, d = 0.732d$$

The average value of the above 3 kinds of ball piles is the natural porosity appeared in industry. Hence

$$\varepsilon = \frac{0.476 + 0.395 + 0.260}{3} = 37.7\%$$

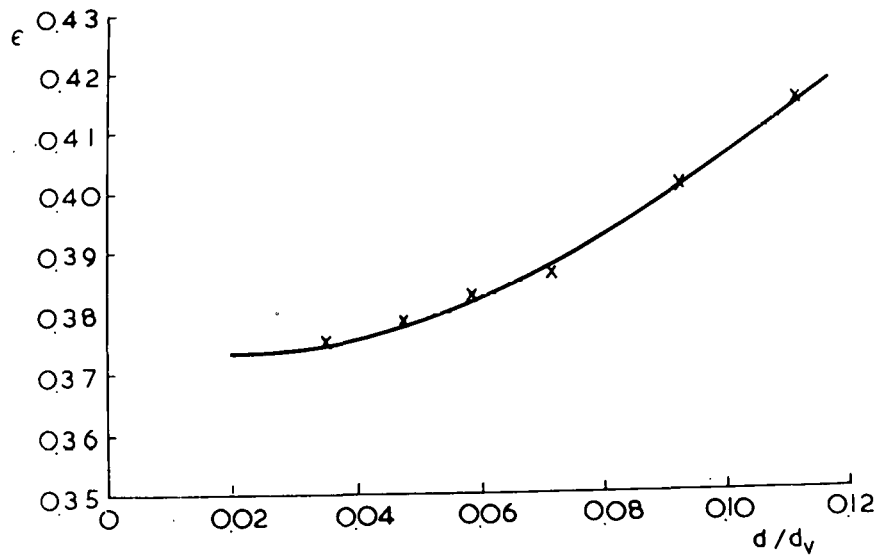

Fig (1) Porosity Vs. Vessel Dimension

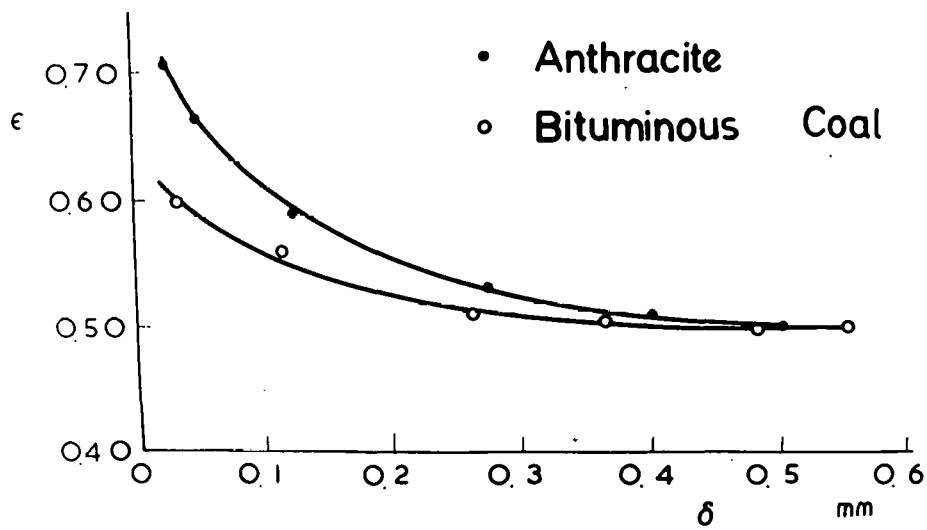

Fig (2) Porosity Vs. Coal Particle Size

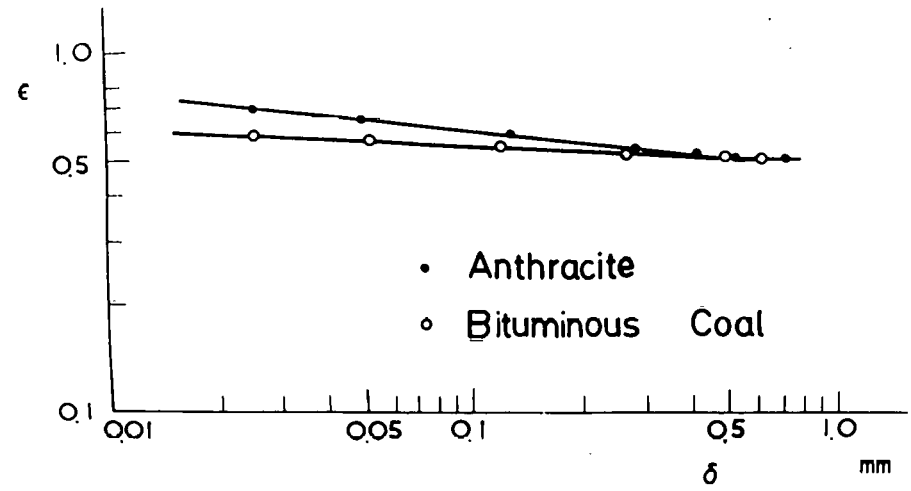

Fig. (3) Porosity Vs. Coal Particle Size

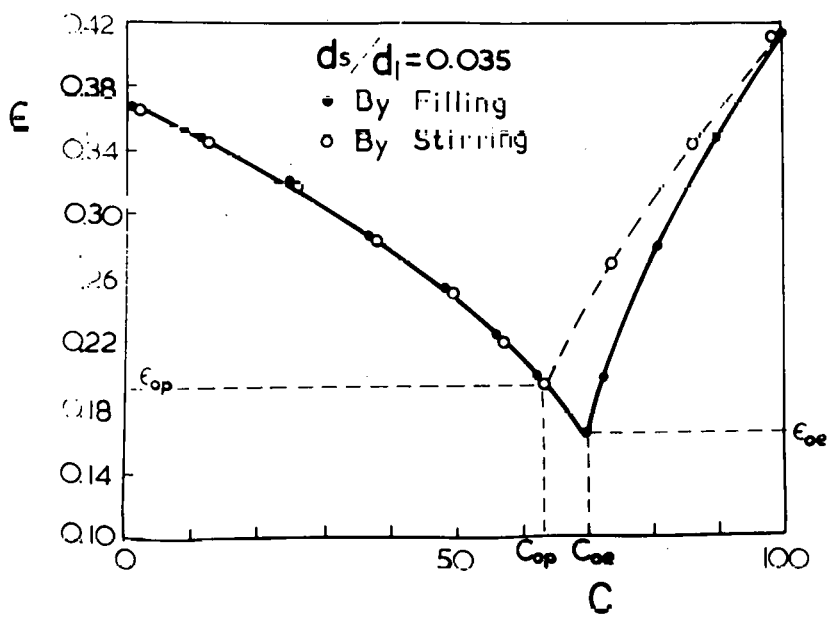

Fig (4) Porosity Vs. Concentration of Large Particles

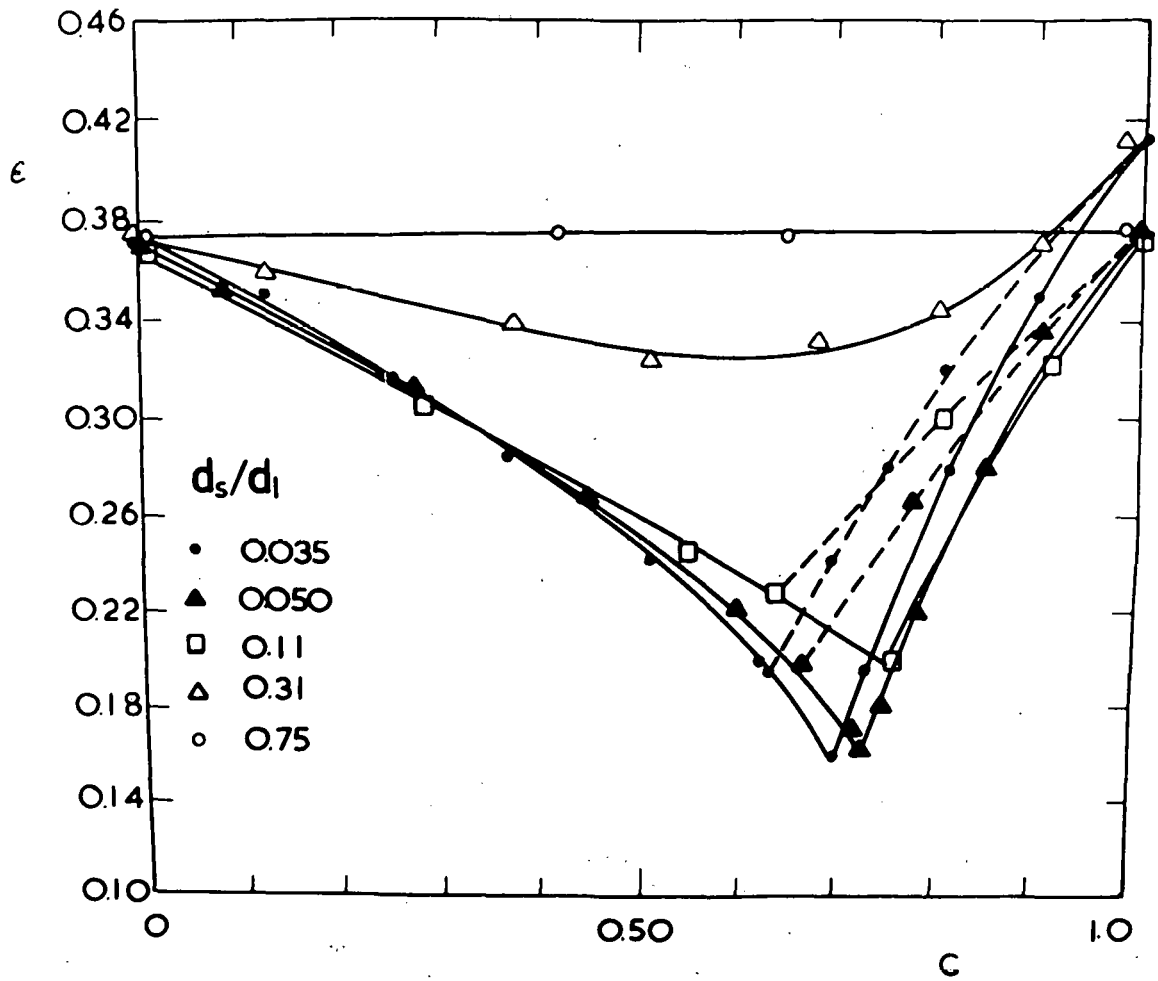

Fig. (5) Porosity Vs. Concentration of Large Particles for different d_s/d_l

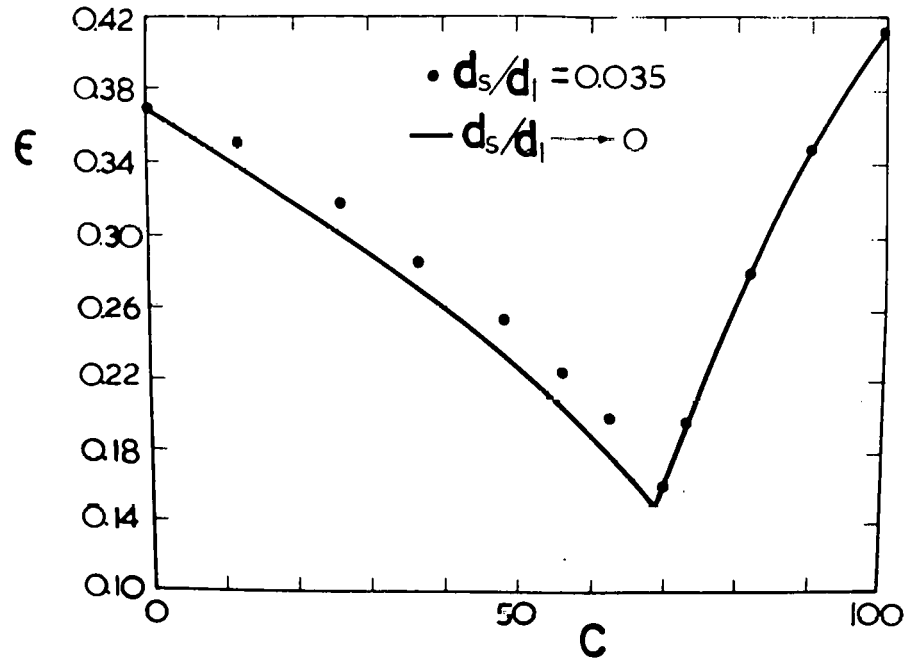

Fig (6) Theoretical Porosity Vs. Concentration of Large Particle for very Small d_s/d_l

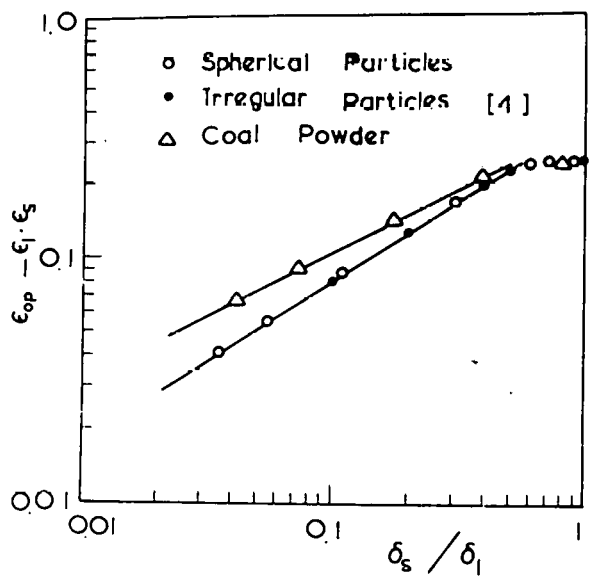

Fig (7) Porsoty Vs. Particle Size Ratio

1 CM

Fig (8) Large Particle Surrounded by Small Particles in Slurry (X 300)

Fig (9) Small Particle in Slurry (X 1500)

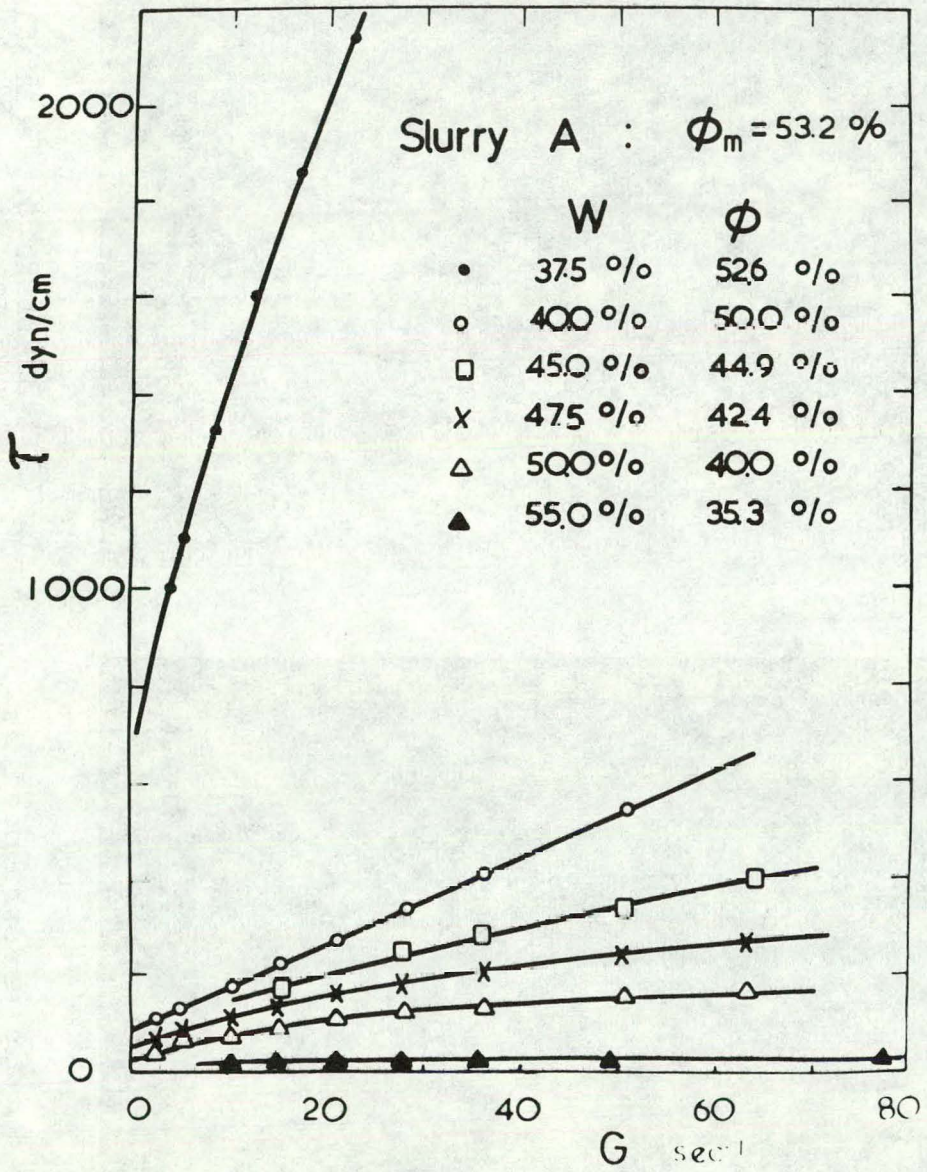

Fig (10) Shear Stree Vs. Shear Rate of Slurry

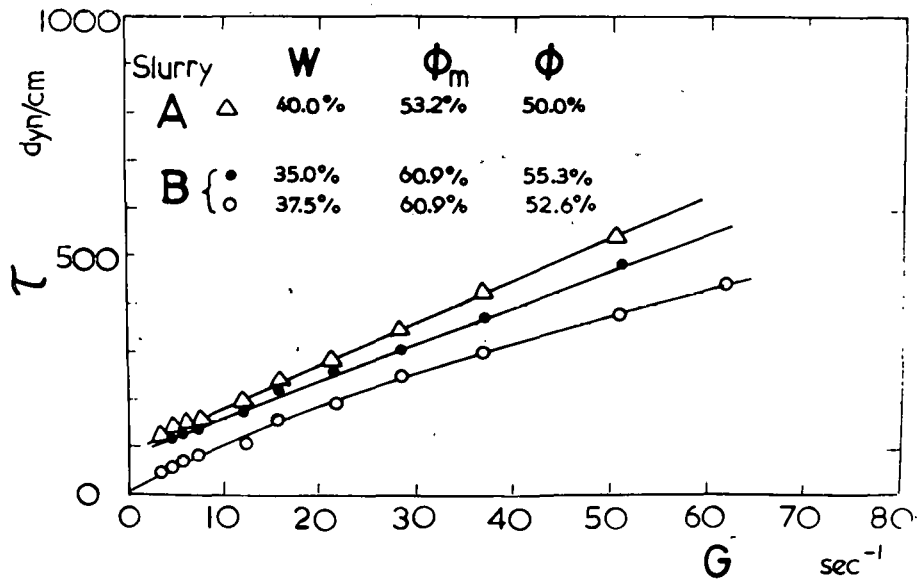

Fig (11) Shear Stress Vs. Shear Rate of Slurry

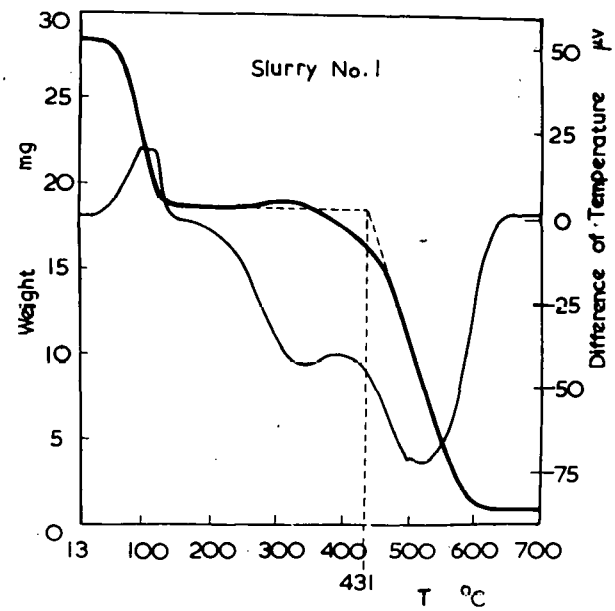

Fig (12) Combustion Performance of Coal-Water Slurry No.1
——— TG Curve, —— DTA Curve.

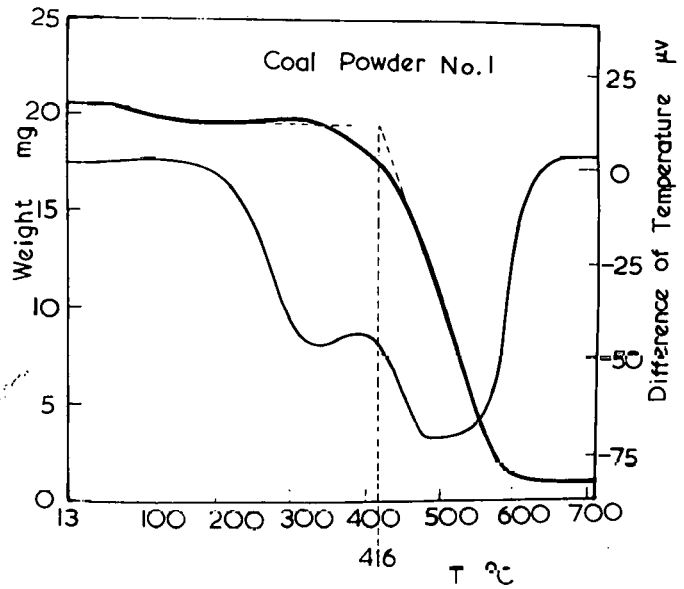

Fig (13) Combustion Performance of Coal Powder

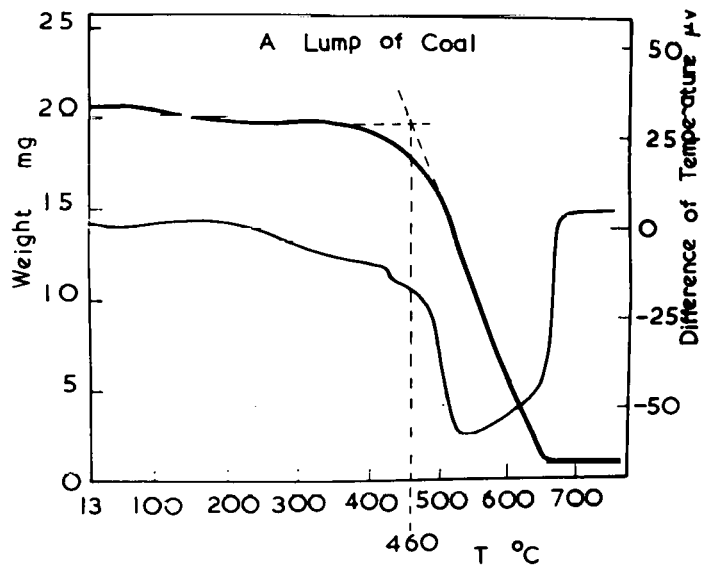

Fig (14) Combustion Performance of Lump Coal

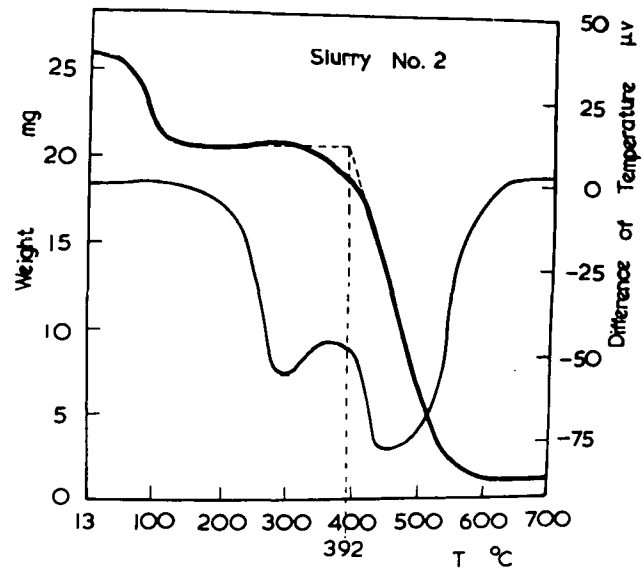

Fig (15) Combustion Performance of Coal-Water Slurry No.2

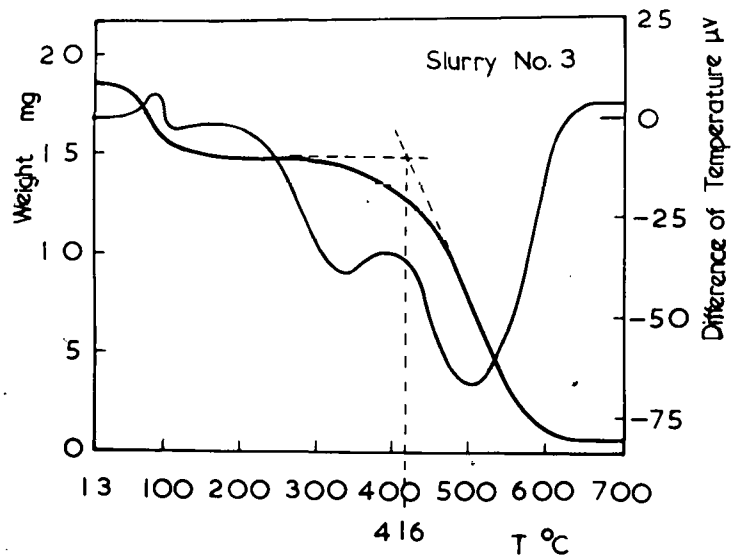

Fig (16) Combustion Performance of Coal-Water Slurry No.3

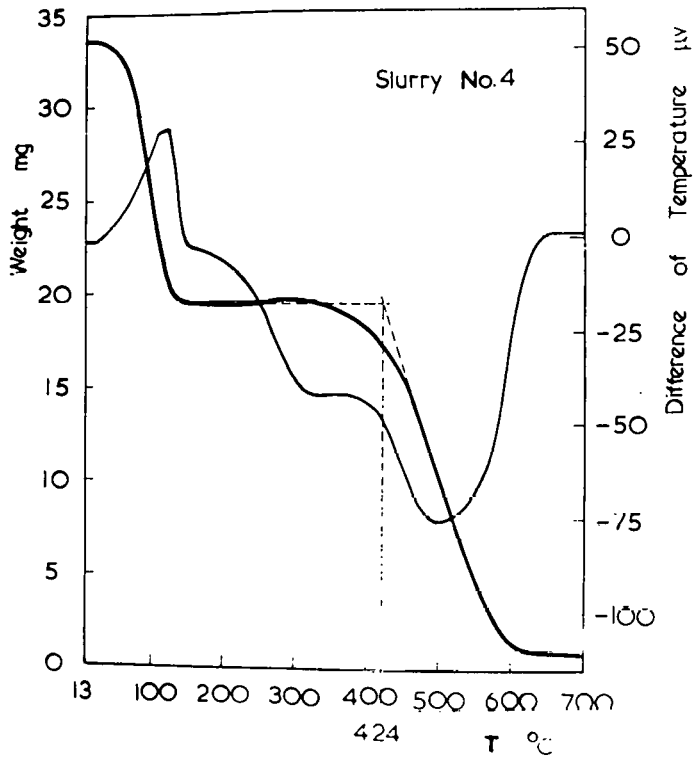

Fig (17) Combustion Performance of Coal-Water Slurry No.4

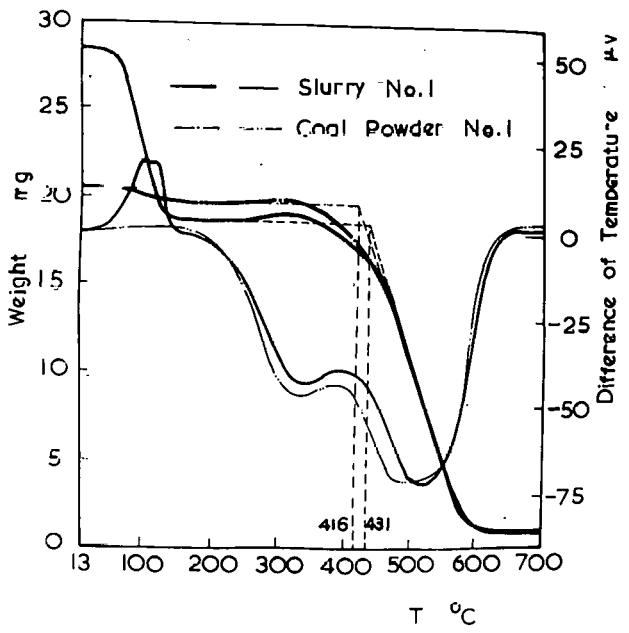

Fig (18) Combustion Performance of CWS No.1 and Coal Powder No.1.

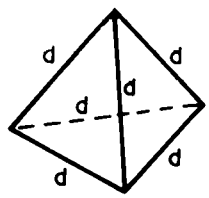

Fig (19) Tetrahedron Model

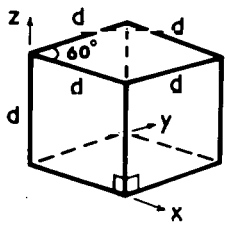

Fig (20) Rhombohedron Model

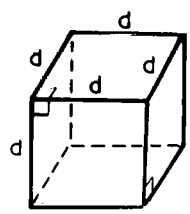

Fig (21) Cube Model

COMBUSTION AND FUEL CHARACTERIZATION OF COAL-WATER MIXTURES

M. J. HARGROVE
A. A. LEVASSEUR
COMBUSTION ENGINEERING, INC.
WINDSOR, CONNECTICUT

B. E. DAVIS
GULF RESEARCH AND DEVELOPMENT COMPANY
HARMARVILLE, PENNSYLVANIA

ABSTRACT

A three year research project for the Department of Energy on coal-water mixtures has as its overall objective to provide sufficient data on coal-water mixture (CWM) chemical, physical, and combustion properties to assess the potential for commercial use in furnaces designed for oil firing. Combustion Engineering (C-E) and its sub-contractor Gulf Research and Development Company (GRDC) are under contract to the DOE's Pittsburgh Energy Technology Center (PETC) to develop the required data.

The test program concentrates on two major areas of CWM utilization: combustion behavior/burner modification; and performance characteristics/ unit derating and availability. The program has been separated into six subtasks:

1) CWM Selection and Preparation
   a) Coal Acquisition and Screening Tests
   b) Test Coal Beneficiation
   c) Slurries Preparation
2) Bench-Scale Characterization and Screening Tests
3) CWM Preparation and Test Slurry Supply
4) Combustion Evaluation/Atomization and Burner Testing
5) Ash Deposition Performance Testing
6) Commercial Application and Performance Predictions

The program has been structured in a sequence so that each task will use knowledge gained during the preceeding task. It is believed that the use of beneficiation will be critical to the successful development of CWMs. During the CWM selection and preparation, an in-depth evaluation of the washing characteristics of selected coals will be conducted to provide the required data for technical and economic assessment of the fuel's potential for CWM use. Tasks 1 and 2 will address the selection of CWMs to be studied during the large-scale combustion and performance testing. Bench-scale, pilot-scale and full-scale laboratory testing will be conducted. Combustion evaluations and performance testing (Tasks 4 and 5) will be performed separately and conducted in parallel. Most of the testing will be completed within three years.

To develop a wide technological base that covers the key characteristics that may have significant impact on steam generator and process heater performance, a representative cross-section of CWMs will be evaluated. The performance of oil-designed units firing CWMs will be predicted, and retrofit economics will be determined. The units to be studied include three utility steam generators, two industrial steam generators, and two process heaters.

INTRODUCTION

Combustion Engineering, Inc. (C-E) has been awarded a contract by the U.S. Department of Energy's Pittsburgh Energy Technology Center (PETC) to research the combustion and fuel characteristics of coal-water mixtures. C-E has teamed with Gulf Research and Development Company (GRDC), a major subcontractor, to conduct the studies. The research project is designed to develop the basic information needed for industry to assess the commercial potential of burning coal-water mixture (CWM) in steam generators and process heaters.

The project is divided into two major segments. In the first tasks, GRDC will select the coals to be studied. Small samples of specified CWMs will be obtained from commercial suppliers and the characteristics of these fuels will be determined by C-E and GRDC. CWM typically consists of 70 percent dry coal and 30 percent water by weight. Mixture stability, viscosity and the effects of beneficiation will be studied as the coal and slurry preparation are varied. GRDC will then obtain larger samples of mixtures for the second project segment, which will be conducted by C-E.

The combustion of different CWM's will be analyzed in the C-E laboratory. Ignition stability, carbon burnout and atomization quality will be evaluated, as the fuel source, coal source, and burner used are varied. Ash deposition will also be studied. Each selected CWM will be beneficiated to two levels of residual ash. Based on the results of the ash deposition tests, C-E will predict the performance of selected commercial steam generators and furnaces firing CWM's. The economics of CWM retrofits will then be evaluated.

The project is expected to take approximately three years, as outlined in Figure 1. The inter-relationship of subtasks is illustrated in Figure 2. Each successive subtask employs the results of preceding substasks. Each of the subtasks are described below.

Project results will be available from the Pittsburgh Energy Technology Center. Mr. Roy Kurtzrock is the PETC Project Manager for DOE's overall program. Mr. Michael Hargrove is the Project Manager for the C-E/GRDC team.

SELECTION OF TEST FUELS

The fuels tested will be CWM's having formulations representative of those that are expected to become available commercially. The selected CWM's will be made from four coal sources, two levels of beneficiation, and at least three commercial suppliers.

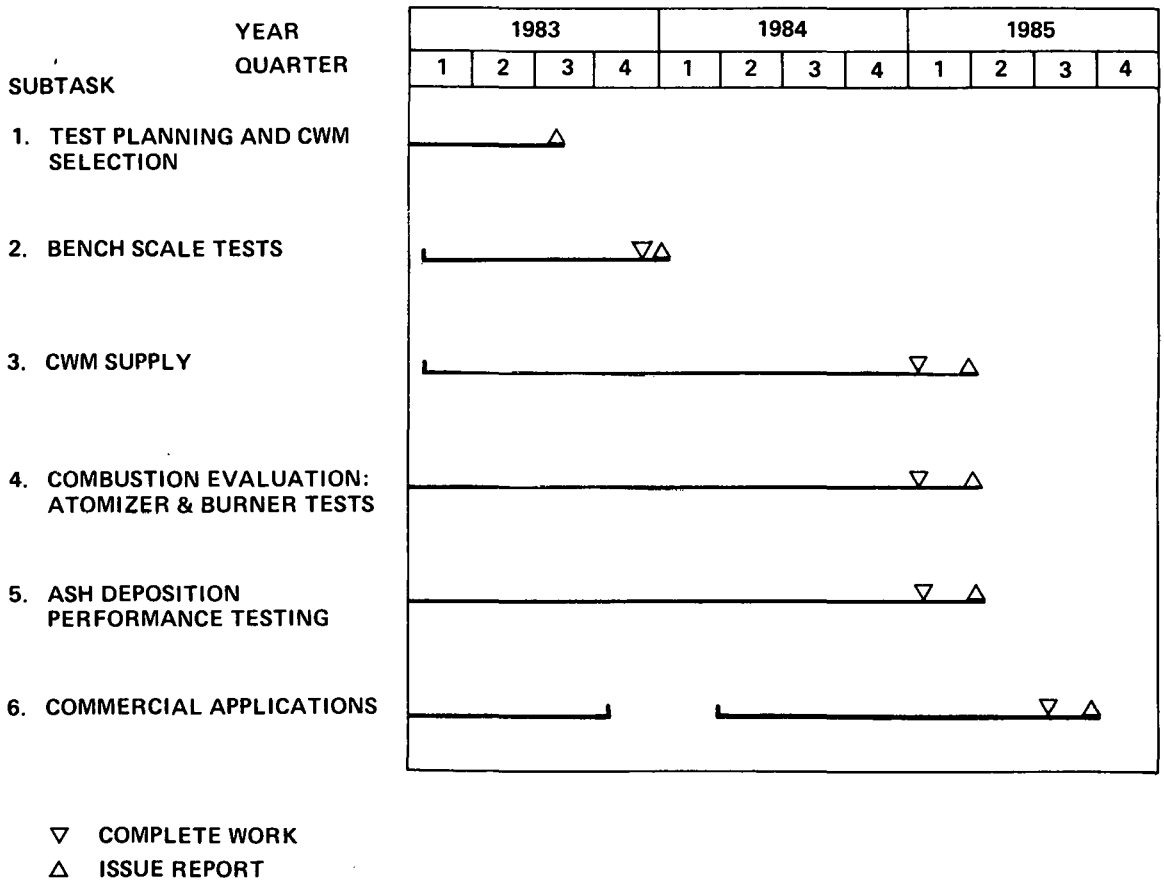

Figure 1: DOE CWM Project Schedule

Initially 20 coals from the Eastern United States will be selected. The coals will then be surveyed for commercial significance, beneficiation potential, ash content and quality, sulfur content, volatile matter content, and char reactivity. Since coal beneficiation is expected to play a major role in the commercial use of CWM's, selection of the candidate coals will consider the anticipated characteristics of the coal after beneficiation. The twenty selected coals will be subjected to a series of first level screening tests. These tests will consist of gravity separation (14 mesh x 0 at 1.3 specific gravity), and subsequent analysis of the two density fractions plus the raw coal.

Using the results of the first level screening tests, eight coals will be selected for second level screening tests. These tests will consist of detailed "washability" analyses and detailed fuel analyses.

The results of the second level screening tests will be used to make an assessment of the potential use of these coals for coal-water mixtures, and four coals will be selected for preparation of test CWM's. These selected coals will have a variety of fuel characteristics;

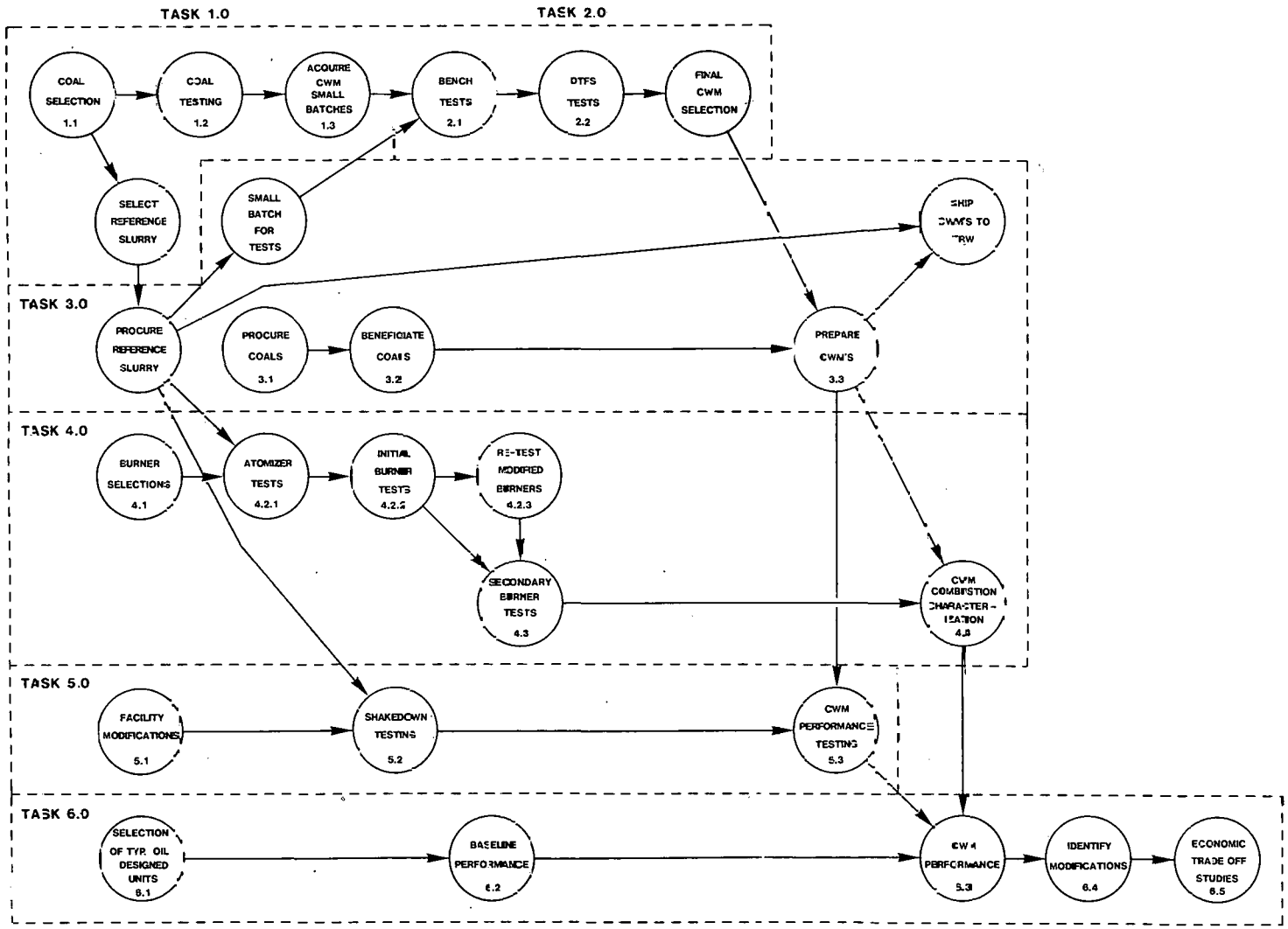

Figure 2: Project activity network

for example: varying volatiles, ash fusion temperature, etc., in order to develop sets of comparative data. It is anticipated that the atomization and combustion characteristics will be affected significantly by the coal rank and by the slurrying process itself. Conversely, equipment performance (which is affected by ash deposition, for example) will depend more on the quantity and quality of mineral matter in the CWM and the level of beneficiation.

BENCH SCALE TESTS

The bench scale tests will characterize the properties of a cross-section of slurries and provide the bases for CWM selection for large scale testing.

The test matrix will include eighteen CWMs, using four coals, two levels of beneficiation and three slurry suppliers. The fuel properties to be evaluated will include ignition stability, char reactivity, furnace slagging, convection pass fouling, atomization, slurry stability, emissions, corrosion, and flyash erosion. Representative five-gallon samples of the eighteen candidate CWM's will be prepared and evaluated. Each CWM will be subjected to the tests listed in Table I.

TABLE I
BENCH-SCALE TESTS FOR CWM CHARACTERISTICS

Total moisture
Percent solids
Slurry density
Particle size distribution
Effect of temperature changes
Proximate analysis
Ultimate analysis
Higher heating value
Viscosity vs. temperature
Viscosity vs. shear rate
Settling rate
Slurry pH
Halogens (Cl, F)
Thermogravimetic analysis
Flammability tests
Probe surface area (coal and char)
True particle density (coal and char)
Apparent density (coal and char)
Ash composition
Ash fusibility temperatures
Sulfur forms
Gravity fractionation analysis
Acetic acid leaching analysis
SEM analysis
Trace elements (X-ray)
Corrosion index
Abrasiveness
Agglomeration
Aging effects

Based on the test results, 12 CWM's will be selected for the ash deposition tests and 6 CWM's will be selected for the burner evaluations.

One CWM for burner and deposition testing will be selected early in 1983. This will allow for procuring one test fuel soon enough to start burner and deposition tests by June, 1983.

In addition, a brief fundamental study will be conducted using a bench-scale Drop Tube Furnace System (DTFS) to assess the effect of moisture level on particle fracturing during rapid heating. Testing will consist of six test runs, using two selected coals, each prepared to three different moisture levels with the same slurry time-lapse history. The particle size of the coal feed will be controlled (200 x 400 mesh cut). The tests will all be conducted at relatively high furnace temperatures (approximately 2500 F), under an inert atmosphere (N_2 carrier gas), and at a specific residence time (approximately 0.2 seconds). Char samples will be collected and analyzed after exposure to the furnace. The particle size distribution of both the parent coal feed and char samples will be determined by appropriate analysis.

CWM PREPARATION AND TEST SLURRY SUPPLY

Representative samples of CWM's will be required for the test program. Activities will consist of the coordination and supply of the appropriate slurries, in the required quantities, in the proper time frames. This work is divided into four parts:

1. Coal Acquisition

This activity will include the acquisition and beneficiation of parent coals in the quantities required for evaluations and tests, which include that required for the 18 candidate slurries selected for bench-scale testing, the coal required for the 6 slurries to be tested during the combustion evaluation, and the coal required for the 12 slurries to be evaluated during the performance testing.

2. Beneficiation of Test Coals

The clean coals for preparing the CWM for the large-scale combustion tests will be produced from the beneficiation of the selected raw coals at coal cleaning plants.

3. CWM Preparation

Clean coal will be shipped to the selected slurry manufacturers who shall prepare CWM in the required quantities for the tests.

For CWM screening tests, a total of 18 different 5-gallon CWM samples will be prepared covering a range of coal properties, slurry properties, and manufacturers (formulations).

In general, slurries for large-scale burner tests will be prepared from beneficiated coal supplied to the CWM manufacturer. However, some manufacturers of CWM have integrated beneficiation and CWM preparation facilities; in these cases, samples will be obtained by their processing techniques, maintaining the identified beneficiation levels.

COMBUSTION EVALUATION/ATOMIZATION AND BURNER TESTS

Potential CWM burners and fuels will be tested and evaluated in large scale test facilities. These tests will show the reliability of firing CWM's in commercially available burners. CWM characteristics that affect burner performance will be identified.

The test program will be divided into four parts:

1. Commercial Burner Selection: Six burners will be selected for testing based on "commerciality" of design, availability in capacities from 20 to 50 million Btu per hour, number of burners in service, and CWM experience. Two burners designed by C-E and four burners from other suppliers will be selected and procured. Performance criteria to be used in both the selection and the performance evaluations will include ignition requirements, turndown limits, carbon burnout, atomization quality, and atomizer tip wear.

2. Initial Burner Evaluation: Each burner will be tested at approximately 25 million Btu per hour firing rate. First the atomizer will be installed in the Atomizer Test Facility (ATF) for cold flow testing (Figure 3).

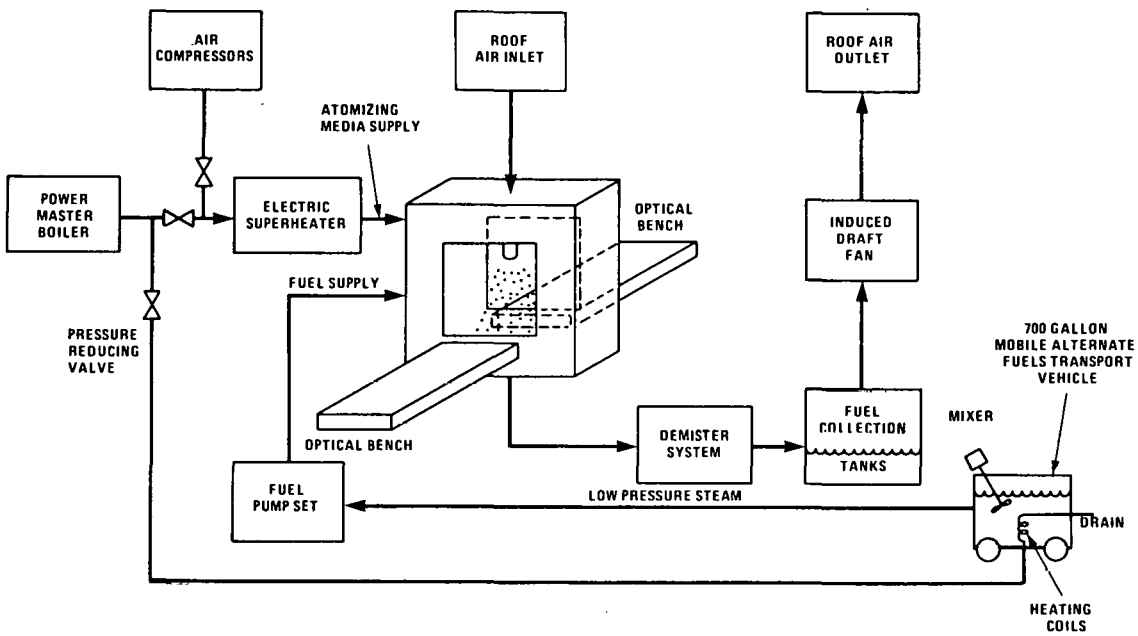

Figure 3: Atomizer test facility

The atomizer spray droplet size distribution will be measured using a laser diffraction technique (Figure 4). Spray droplet velocities and trajectories will be measured by the double spark photography technique (Figure 5). The data will be analyzed to determine which operating parameters are optimum for CWM atomization at each fuel mass flow rate. Erosion of critical atomizer dimensions will result in degradation of the quality of atomization. Therefore, atomizer erosion will be monitored and documented, and any deviations from the original orifice dimensions will be recorded. Test duration may be of sufficient length to establish approximate estimates of atomizer life.

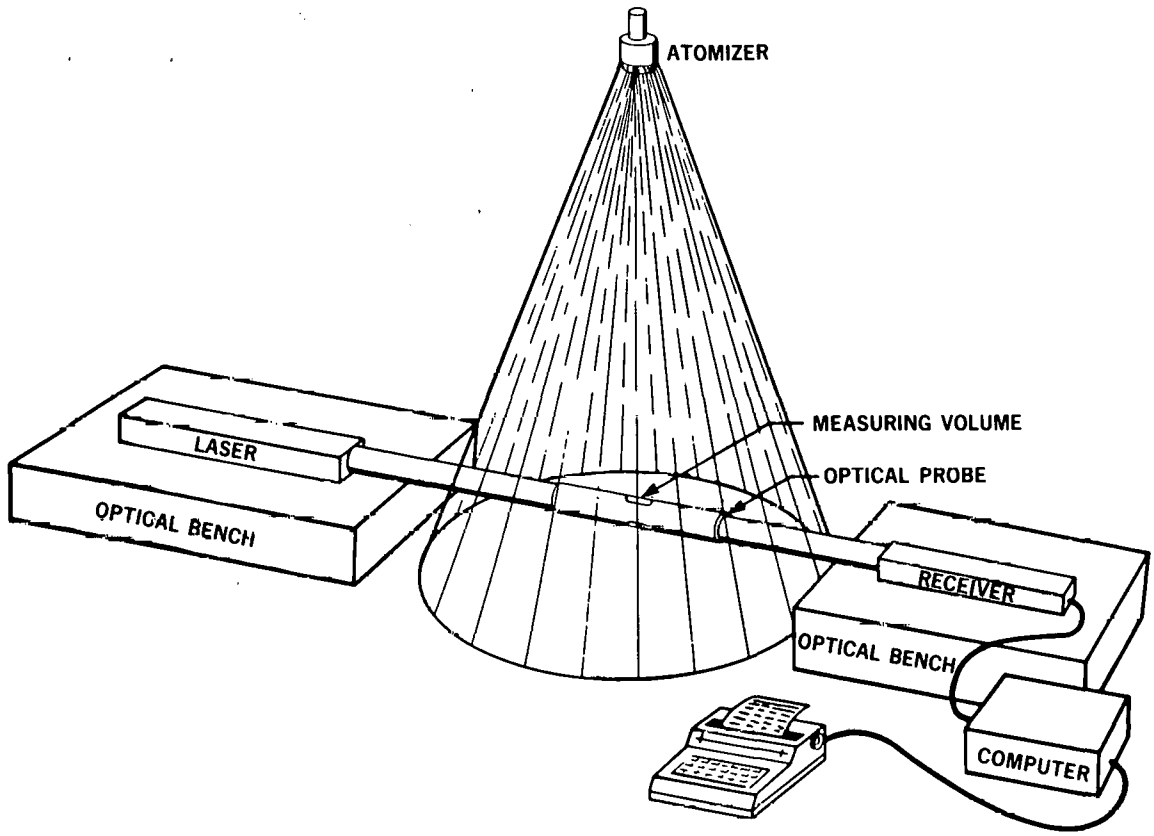

Figure 4: Laser diffraction measurement in dense sprays

The atomizer and burner register will then be installed in the Subscale Burner Facility (SSBF) for combustion pretesting. (The SSBF and its slurry handling and firing system are shown in Figure 6). These tests will concentrate on assessing burner operating requirements and identifying deficiencies in ignition, turndown, and carbon burnout.

The gaseous combustion products will be continuously analyzed. Flame quality will be documented with photographs and/or videotape. The combustion efficiency calculation will be based on a comparison of the carbon input (derived from an ultimate fuel analysis and the fuel mass flow rate) and a measurement of the gaseous and solid products of combustion.

Based on the pretest results, every burner will be evaluated according to the minimum performance criteria. If a burner fails to meet the minimum requirements, the manufacturer may modify the burner and subject it again to the same pretest procedures.

Any burner that fails a second time to meet the minimum requirements will be eliminated from further testing. Burners that pass the requirements the first time will not be pretested a second time in

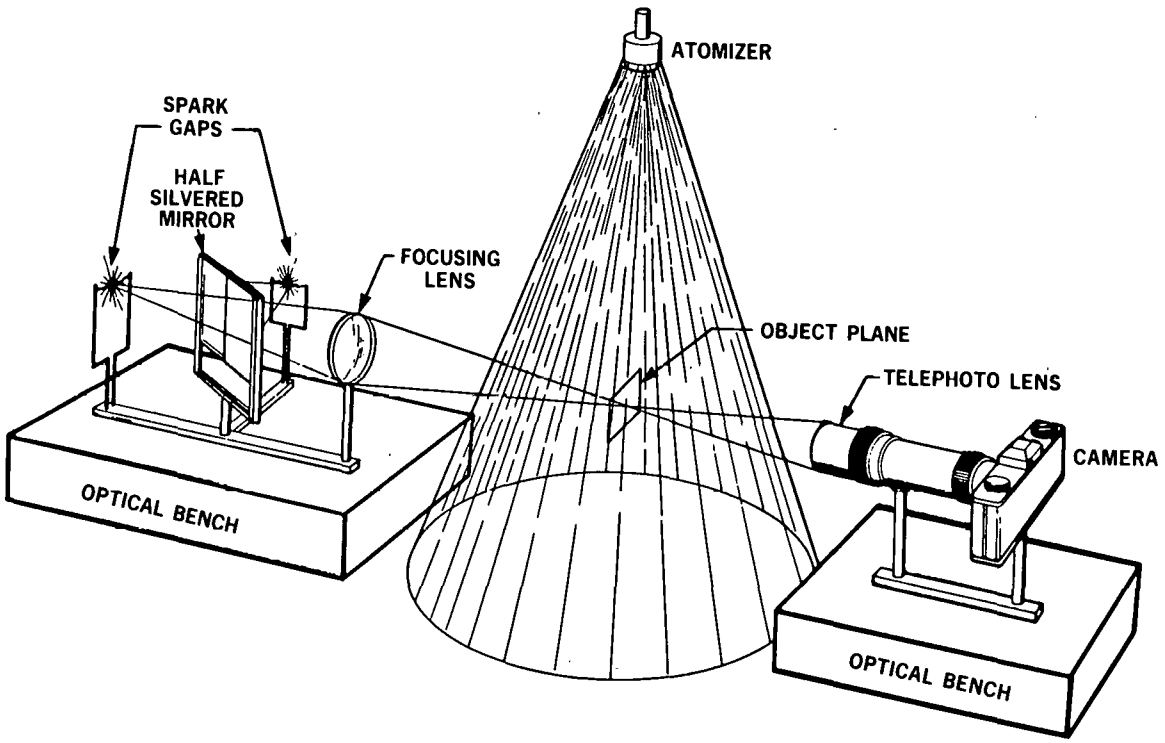

Figure 5: Double spark photographic measurements

either the ATF or SSBF. All burners that pass either the first or second round of pretests will be tested in the Secondary Burner Evaluation.

3. Secondary Burner Evaluation: The next evaluation will concentrate on developing the bulk of the information necessary for commercial CWM burner application decisions. Each of the 20-25 x 10^6 Btu/hr burners will be reinstalled in the SSBF. Optimized atomizer and burner register operating parameters determined during the Initial Burner Evaluation will be used for these tests. The following areas shall be studied as a function of excess air, combustion air temperature, and firing rate: optimized ignition requirements and turndown limits, carbon burnout, gaseous and particulate emissions, stack opacity, atomization quality, and atomizer life.

Solids loading samples, carbon burnout measurements, and furnace heat flux readings will be taken, in addition to the gaseous combustion products measurements, during some of the tests. The solids loading will be sampled isokinetically. The samples drawn will be analyzed for carbon burnout. Heat flux measurements will be taken with a network of heat flux meters located along the roof of the SSBF normal to the direction of flow. Flame stability will be documented with videotape and photographic records, as was done in the pretesting.

A comparative evaluation of all burners will be made on the basis of the minimum performance criteria. A 50 x 10^6 Btu/hr version of the best CWM burner design will be used as a "test bed" for the combustion

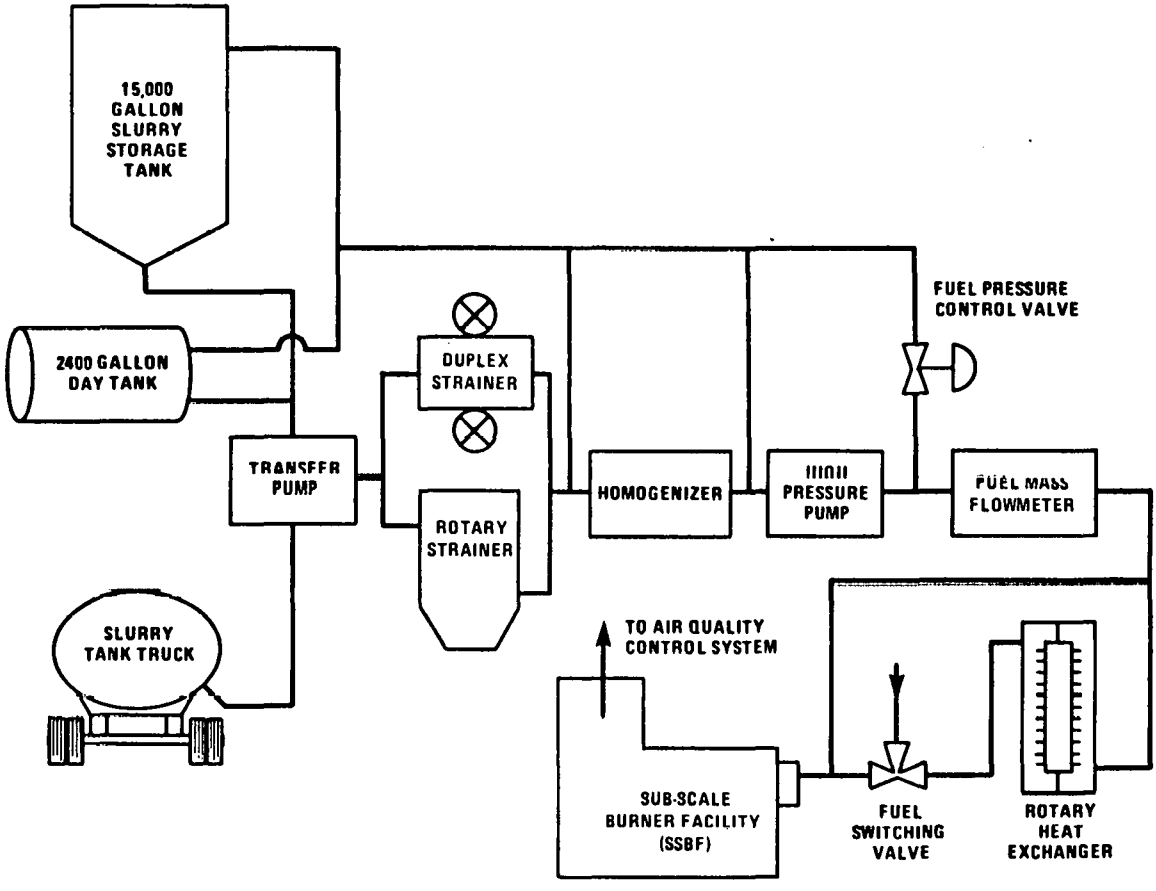

Figure 6: Sub-scale burner facility and CWM Handling and firing system schematic

characterization of five different CWM's.

4. CWM Combustion Characterization: Six different CWM's will be fired, compared, and characterized. Slurries from three producers using three parent coals at two beneficiation levels will be tested for atomization quality and for combustion performance in one 50×10^6 Btu/hr burner. The effect of CWM rheology, beneficiation, and slurry manufacturing processes on burner combustion performance will each be addressed separately. Results will be a compilation of data on the firing of the six CWMs.

ASH DEPOSITION/PERFORMANCE TESTING

Four major areas of CWM performance will be addressed under this task:

1. Furnace slagging
2. Convection pass fouling.
3. Fly ash erosion
4. Emissions

Testing will be run in the Fireside Performance Test Facility (FPTF) (Figure 7). The test facility will fire CWM's at rates up to 4 million Btu per hour simulating the design/operating conditions

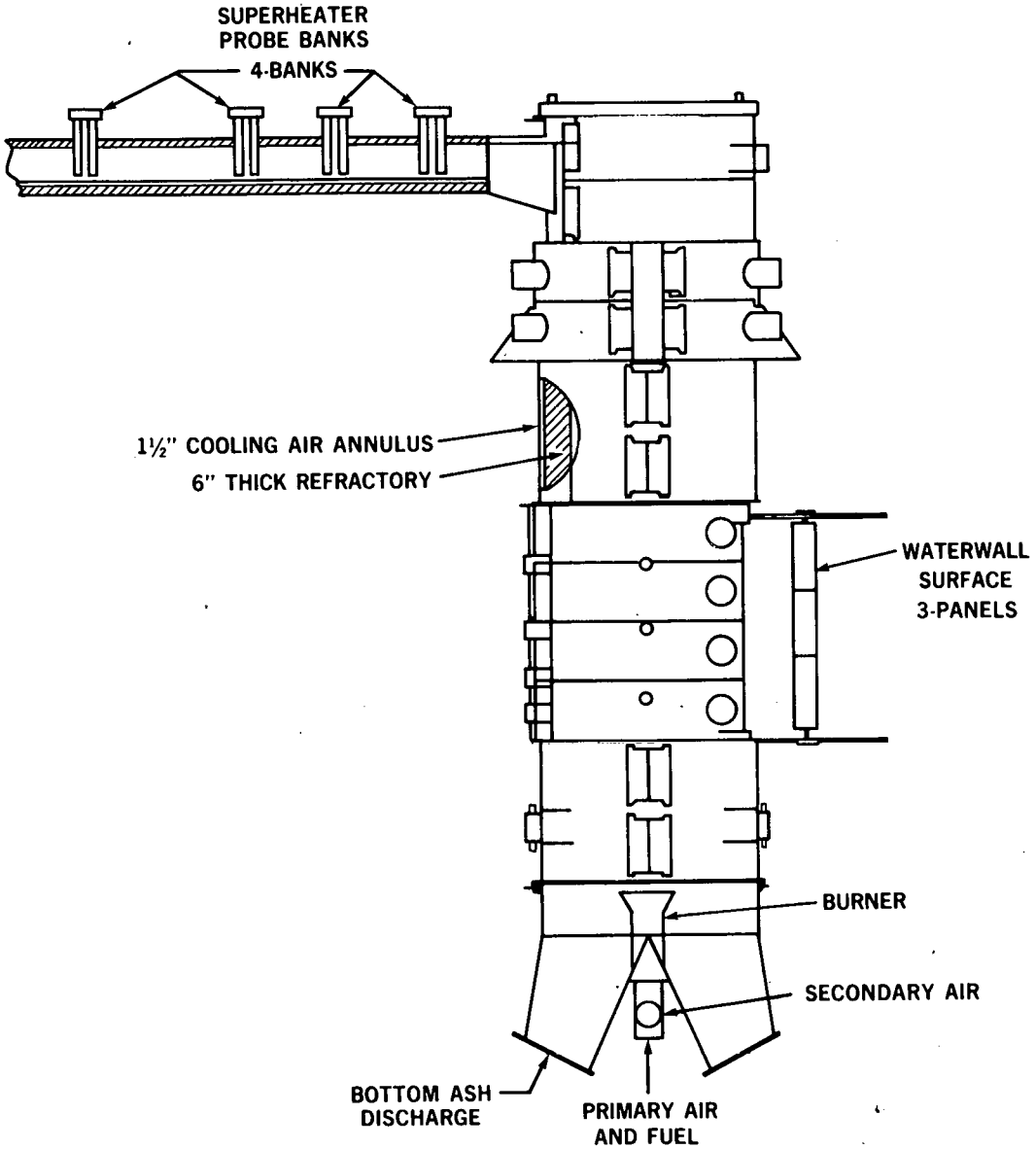

Figure 7: Fireside performance test furnace

representative of commercial CWM firing. The furnace section and the convection tube banks will model the geometry and temperatures in oil-designed units.

A special radiant section will be designed and installed in the test furnace to simulate the tube/wall configuration and conditions in process heaters. This section will be instrumented to measure the effects of deposition upon heat transfer, and to study the nature of deposits under process heater conditions.

Shakedown runs will be conducted with 100 percent oil to check out the fuel transport and firing system. After satisfactory results have been achieved, testing will be conducted to establish baseline conditions and comparative data when firing 100 percent oil. The primary data

obtained during these tests will be gas temperature distributions in respective radiant and convection test sections of the furnace, and the corresponding baseline (clean) waterwall and superheater heat absorption data. Tests will be conducted at three heat input rates, in order to bracket the gas temperature and velocity matrix to be run in the comprehensive CWM performance evaluations.

Twelve different slurries will then be extensively evaluated to provide a data base covering a range of key CWM performance-related variables. Testing will focus on ash slagging and fouling behavior, fly ash erosion characteristics, and gaseous and solid emissions characteristics of the selected CWM's. The effects of firing rate (gas temperature, gas velocity, heat release rates, ash loading, etc.) upon both radiant (furnace) and convection pass ash deposition will be examined. Some of the slurries will be evaluated in this respect by tests conducted at two different firing rates. The thermal input for the high and low firing rates will be determined from the baseline oil tests.

The program will address three different CWM variables: coal/mineral matter type, level of beneficiation, and slurry processing. The test slurries will be prepared from four different coal sources with different mineral matter characteristics. The effect of beneficiation will be assessed on all four coal types identified above. Each coal will be beneficiated to two different levels (7 percent and 2 percent residual ash).

The effect of slurry processing will be evaluated for one coal type at two levels of beneficiation. A total of six slurries (from the same coal and at two levels of beneficiation), which are prepared by three different manufacturers or processed in different manners, will be tested. The variations between these slurries could involve particle size distribution, percent solids, and/or surfactants and stabilizers.

In addition to the slurry performance tests, one clean coal (at a selected level of beneficiation which will be tested as a CWM) will be test-fired conventionally (pulverized state) in the FPTF, as a base case to assess the overall effects of slurrying on coal combustion/ash deposition performance.

This test will be a frame of reference to reflect any changes in mineral matter behavior after slurrying, and will provide data on gas temperature profiles, absorption rates, burnout rates, and emissions.

During each run, superheater (convection pass) deposit build-up rate will be measured by two methods: pressure drop tests and build-up tests. Pressure drop tests quantify the relative frequency of soot blowing in the FPTF. The frequency of soot blowing is a measure of the rate of deposit build-up (volume of deposit growth). At the end of each soot blowing cycle (before deposits are blown), in situ deposit-to-tube bonding strength measurements will be taken. After a specific "standard" test period, the furnace will be shut down, and the amount of deposit accumulated on each probe bank collected and weighed. Deposits will be carefully sampled for subsequent analysis.

Waterwall panel heat fluxes will be determined by monitoring coolant inlet and outlet temperatures, along with coolant flow rates to each set of waterwall panels, thus establishing the combined effects (emissivity, conductivity, etc.) of those deposits upon heat transfer. The "cleanability" of deposits will be assessed by operation of a deslagger.

The physical state of panel deposits and the approximate extent of coverage and thickness will be observed and documented throughout the testing. In addition, on-line measurements of waterwall deposits surface temperatures will be taken at 8-hour intervals, using both a special thermocouple probe and an optical pyrometer. Waterwall deposits will be sampled and analyzed.

Flyash erosion characteristics will be evaluated in the special high velocity section, using probes machined from a soft metal (such as brass). Probe erosion will be measured by determining weight loss, and microscopic evaluation of specimen surface. Although data will be obtained over short exposure times (80 hours), the soft probe metal and high gas velocities will accelerate wear and provide relative ratings of the erosion characteristics tested.

Isokinetic dust loadings will also be taken during each test run. Flyash particle size distribution, chemical composition and resistivity will be measured.

Gas temperature profiles in the convection sections and the furnace will be taken periodically, with high velocity suction pyrometers (at least once/8 hr shift). Flue gas composition and furnace operations data will be recorded. Deposit appearance will be recorded with on-line photographs.

COMMERCIAL APPLICATION AND PERFORMANCE PREDICTION

Seven oil-designed units, representing three generic classes of oil-fired equipment, will be selected:

- 3 utility steam generators
- 2 industrial steam generators
- 2 process heaters

Selection criteria for the utility and industrial steam generators will be defined to insure the greatest possible coverage of the subject clases of existing oil-fired equipment. The criteria include age, location, configuration, and environmental limits. The selected units for process heating shall center around two design configurations. These heater types represent a potentially large market for CWM.

Based on the fireside performance data, C-E will calculate predicted performance for the seven study units firing four different CWM fuels. The four fuels will be selected such that the effect on performance of beneficiation level, ash fusibility temperatures, and slurry type will be determined. This analysis will define the load capability of each particular unit for each CWM. The analytical procedure will examine several potential load-limiting factors, and determine which

is the critical load-limiting factor requiring the unit to be derated. The following list shows some of the potential load-limiting factors:

- Furnace slagging
- Convection pass fouling
- Inadequate furnace residence time for complete combustion
- Erosion in the convection sections
- Tube metal overheating
- Inside tube film temperature (process heaters only)
- Working fluid overheating
- Control flow limits

The performance analysis will be sensitive to both the quantity and quality of the ash contained in the various CWM's. If the load limit defined by one factor is significantly lower than the others, analysis of possible improvement methods will be studied. Economics will be the deciding factor as to whether the proposed change is effective. The performance analysis will also include an estimate of SO_x, NO_x, and particulate emission.

The use of the CWM fuel will require several changes to the existing units. The extent of these changes will be a function of the CWM characteristics and the predicted performance for the specific fuel.

The types of modifications anticipated include convection pass soot blowers, furnace wall deslaggers, dust collection hoppers, modified furnace bottoms, emission control equipment, fuel supply and storage system equipment, and burner system changes. Tube bank modification will be considered if, for example, load is severely limited due to a local high velocity area, such as in the screen tubes or crossover tube area.

Other possible pressure part modifications will be the replacement of spiral-finned economizer tubes with bare tubes.

Primary and secondary airflows and total combustion air will be changed, as required, to maintain satisfactory furnace performance. FD and ID fan additions or replacements will be considered, if necessary, to improve unit load capability.

A set of economic criteria will be defined for each of the three equipment types. Operating and maintenance costs will be estimated, based on using the established economic criteria, retrofit equipment costs, maximum load capability, maintenance costs, and fuel costs. Battery limits for the study will be the inlet to the induced draft fan and outlet of forced draft fan. Orientation economics will be developed for CWM production, based on a range of CWM's identified in the test program as being technically feasible. The estimates will be in terms of dollars per million Btu delivered to the ultimate user. Cost projections for commercial quantities of CWM will be obtained from the vendors of the slurries used in the program, and will be used as the basis for the orientation economics. Costs of CWM preparation obtained from the manufacturers will be integrated, as necessary, with the projected cost of coal beneficiation, as can be extrapolated from the state-of-the-art. Operating costs will be calculated for each

slurry and also for oil as a base case.

Operating costs will be the sum of the capital fixed charge, operating labor cost, maintenance material cost, and fuel cost. Total costs will be determined for using each of four CWM's having different qualities. An economic trade-off analysis will be made for each unit, comparing the plant costs (inversely proportional to CWM quality) to fuel costs (directly proportional to CWM quality). This will indicate the most economical fuel for each unit and will provide a basis for developing an optimum CWM fuel specification. This type of analysis will be done for each of the seven study units.

CONCLUSIONS

The three-year project described above will develop extensive and necessary CWM data to meet the following objectives:

1. Characterization of a commercially significant number of CWMs to establish a range of properties and provide a data base for the use of by industry.
2. Performance evaluation of commercial burners firing CWMs.
3. Ash deposition assessment of a significant number of CWMs.
4. Evaluation of flyash erosion.
5. Assessment of environmental impacts.
6. Determination of the advantages of coal beneficiation.
7. Evaluation of the performance of several oil-designed commercial units when firing various CWMs.
8. Assessment of the economics of retrofits for CWMs prepared from different coals at two levels of beneficiation.

ACKNOWLEDGEMENT

The authors gratefully acknowledge the contributions of G. F. Lexa, G. N. Liljedahl and P. Lindley to the project plan on which this paper is based.

A THERMODYNAMIC ANALYSIS OF THE GAS TURBINE/STEAM TURBINE COMBINED CYCLE WITH COAL-WATER SLURRY AS FUEL

Wang Ying-shi, Gao Li-jun, Zhang Ya-nan
(Institute of Engineering Thermophysics, Academia Sinica)
(Beijing, the People's Republic of China)

1. Introduction

Though coal deposits in China are abundant, how to improve thermal efficiencies of power plants remains to be an important technical problem in the course of saving the energy resources. The use of gas turbine/steam turbine combined cycle is an effective way to raise the overall thermal efficiencies of electric power generation plants. If coal could be used as the fuel of the combined cycle, even more could be explored that seem very attractive to us. Since the properties of coal-water slurries are more or less like those of common fluids, they might be used in gas turbine as alternative to fuel oil in the future. Gas turbine burning coal-water slurry combined steam turine may lead to very efficient and rational utilization at coal energy. When the slurry is used as the fuel, the water content in airflow through the gas turbine is so small that it can be ignored and its presence does not noticeably effect the efficiency of the combined cycle. However the increase of the output is significant. On the other hand, when the coal-water slurry is used in the steam generator, the heat loss due to the increment of the moisture in the flue gas must be taken into account lowering the efficiency as

well as the output of the simple steam turbine cycle. In this paper a detailed thermodynamic analysis is made to demonstrate the advantages of using gas turbine/steam turbine combined cycle fuelled with coal-water slurry.

2. Gas turbines/steam turbine combined cycle

Fig. 1 is a schematic diagram for a gas turbine/steam turbine combined cycle with the heat recovery boiler as the exhaust part of the gas turbine, which generates steam to supply the steam turbine. Its T-S diagram is shown in Fig. 2, where 1-2-3-4 represents the working processes of the gas turbine set, 6-7-8-9-10 those of the steam turbine set, 4-5 gas turbine exhaust passing through the recovery boiler and 6-9 the steam generating and superheating processes. The other processes are easily understood.

The parameters used in the thermodynamic calculation of the combined cycle are shown in Table 1. Such parameters are selected within the realm of current power plant practice in China. Such that they are of practical significance and, to some extent, typical.

Table 1. Parameters used in the thermodynamic calculation

Gas turbine set:			
Airflow rate	M_1		23.849 kg/sec
Compression ratio	R_{12}		7.548
Compressor efficiency	η_{12}		0.843
LHV of coal	Q_{LHV}	Datong coal	6735 kcal/kg
		Xuangang coal	5265 kcal/kg
Combustion efficiency	η_{23}		0.97
Inlet temperature of gas	T_3		1300°K
Turbine efficiency	η_{34}		0.86
Outlet temperature of exhaust gas from the recovery boiler	T_{be}		473°K

Efficiency of the recovery boiler	η_b	0.9
Steam turbine set:		
Selected from the specifications of medium-capacity sets existing in China		
Inlet stagnation temperature of steam	T_{st}	708°K
Inlet pressure of steam	P_{st}	35kg/cm²
outlet pressure of steam	P_o	0.08 kg/cm²
Enthalpy drop of flue gas in recovery boiler	ΔH_s	748.9 kcal/kg
Thermal effciency of steam turbine cycle	η_{st}	0.2956

In the thermodynamic calculation, variable specific heats are considered but not gas dissociation. For evaluation the effects of parameters a computer program was set up to speed the computation, in which not only the parameters of the cycle but also the data of the fuel can be changed. Since the water content in the slurry is only a small fraction of the weight of the flue gas, the efficiencies of the component parts of the cycle can be considered as constant and is not affected by the water content in the slurry.

As a rule, the smaller the temperature difference between the GT exhaust gas and the superheated steam and the lower is the temperature of the flue gas of the recovery boiler, the higher is the thermal efficiency of the combined cycle. But this also means more structural material is needed to build the recovery boiler. For present cases, 150°C is selected as the temperature difference between GT exhaust gas and the superheated steam.

For exemplification, two kinds of coal are assumed alternatively to be the constituent of coal-water slurry. One kind is Datong coal which has lower ash content and higher heating values.(HHV:7011 kcal/kg; LHV: 6735 kcal/kg.)

The other is Xuangang coal, widely used in power plant in China, has higher ash content and medium heating values (HHV:5484 kcal/kg; LHV:5265 kcal/kg). These are the two kinds of potential coals for making the coal-water slurry in China. Undoubtedly we are much interested in Datong coal because of its relatively high heat content and softer ashes, suitable for gas turbine and, in addition, the production cost of slurry per unit heating value of coal is lower. The ultimate analysis of the above two kinds of coal is shown in Table 2.

Table 2. Ultimate analysis of coal

Element	Datong coal	Xuangang coal
C (%)	73.24	56.81
H (%)	4.20	3.59
N (%)	0.73	1.09
O (%)	8.26	7.65
S (%)	1.20	1.02
Ash (%)	8.98	28.75
H_2O(%)	3.39	1.09

3. Some considerations in the computer program

(i) Calculation of thermodynamic properties of combustion products

According to reference [1][2], assume the composition of the fuel to be $(C_xH_yO_zN'_u\ S_v)_n$. The theoretical air required for complete combustion of one mole of fuel is:

$$L_o = 4.7737\ (x+y/4 - z/2 +v)$$

The reaction equation of combustion of β moles of fuel and L_o moles of air is:

$$\beta(C_xH_yO_zN'_u\ S_v)+(x+y/4-z/2+v)(O_2+3.7737N'_2) +\beta(x_A+x_B)H_2O(\text{liquid})+\beta wA \longrightarrow \beta[xCO+(y/2)H_2O+vSO_2+3.7737 +3.7737(x+y/4-z/2+v)N'_2+(u/2)N'_2] +(1-\beta)(x+y/4-z/2+v) (O_2+3.7737N'_2)+\beta(x_A+x_B)H_2O(\text{gas})+\beta wA \qquad (1)$$

where x_A —— moles of water content in one kilogram of fuel;

x_B —— moles of additional water for making one kilogram of coal-water slurry;

w —— moles of ash in one kilogram of fuel.

After simplification, we obtain

$$\beta(C_xH_yO_zN_u^!\ S_v)+L_o(Air)+\beta(x_A+x_B)H_2O(liquid)+\beta wA \longrightarrow$$
$$\beta(L_o+{}^y/_4+{}^z/_2+{}^u/_2+x_A+x_B+w)(Gas)_{\beta=1}+L\ (1-\beta)(Air) \qquad (2)$$

where $(Gas)_{\beta=1}$ represents one mole of combustion gas with $\beta = 1$; $(Gas)_{\beta=0}$ or(Air) represent one mole of air. The above equation shows that after combustion there will be $\beta({}^y/_4+{}^z/_2+{}^u/_2+x_A+x_B)+L_o$ moles of gas when fuel coefficient is β. This amount can be considered as a combination of $N_{\beta=0}$ moles of (Air) and $N_{\beta=1}$ moles of $(Gas)_{\beta=1}$, where

$$N_{\beta=0} = L_o(1-\beta) \qquad (3)$$

$$N_{\beta=1} = \beta(L_o+{}^y/_4+{}^z/_2+{}^u/_2+x_A+x_B+w) \qquad (4)$$

and $N_{\beta=0}$ and $N_{\beta=1}$ represent the fractions of $(Gas)_{\beta=0}$ and $(Gas)_{\beta=1}$ in one mole of $(Gas)_\beta$ respectively,i.e.

$$N_{\beta=0} = \frac{L_o(1-\beta)}{L_o+\beta({}^y/_4+{}^z/_2+{}^u/_2+x_A+x_B+w)} \qquad (5)$$

$$N_{\beta=1} = \frac{\beta(L_o+{}^y/_4+{}^z/_2+{}^u/_2+x_A+x_B+w)}{L_o+\beta({}^y/_4+{}^z/_2+{}^u/_2+x_A+x_B+w)} \qquad (6)$$

If E represents any thermodynamic property; and $E_{\beta=0}$ and $E_{\beta=1}$ are the values corresponding to $(Gas)_{\beta=0}$ and $(Gas)_{\beta=1}$ respectively, we can determine E_β which is the value of that thermodynamic property of the combustion gas when fuel coefficient is equal to β by Datton's law:

$$E_\beta = N_{\beta=0}\ E_{\beta=0} + N_{\beta=1}\ E_{\beta=1}$$

For Datong coal

X =0.06103, y =0.04200, Z =0.005163, u =0.0005214,

v =0.0003750, w =0.001497

For Xuangang coal

x=0.04734, y=0.03590, Z=0.004781, u=0.0007790,

v=0.0003190, w=0.004792

Now we discuss how to calculate $E_{\beta=1}$ and $E_{\beta=0}$.

Neglecting the effect of pressure, the thermodynamic properties $E_{\beta=1}$ and $E_{\beta=0}$ are functions of the temperature, usually expressed in polynomials of absolute temperature T. The enthalpy, the specific heat, the ratio of specific heats and the relative pressure may approximately be represented as follows[2]:

Enthalpy $$I=B_0+B_1T+B_2T^2+B_3T^3+B_4T^4+B_5T^5 \quad (7)$$

Constant pressure specific heat $$C_p=B_1+2B_2T+3B_3T^2+4B_4T^3+5B_5T^4 \quad (8)$$

Constant volume specific heat $$C_v=B_1-1.98726+2B_2T+3B_3T^2+4B_4T^3+5B_5T^4 \quad (9)$$

Ratio of specific heats $$K=C_p/C_v \quad (10)$$

Logrithm of relative pressure

$$\log_{10}\pi^\circ = \frac{1}{2.302585\times1.98726}\int C_p \frac{dT}{T}$$

$$= \frac{1}{4.575835}\left(B_1\log_e T+2B_2T+\tfrac{3}{2}B_3T^2 +\tfrac{4}{3}B_4T^3+\tfrac{5}{4}B_5T^4+B_6\right) \quad (11)$$

The coefficients in Eq.(7)-(11) can be determined from available data in existing gas tables by fitting method. In general the coefficionts for $(Gas)_{\beta=1}$ can not be readily obtained, but it can be calculated from those for gases CO_2, N_2, H_2O (gas), SO_2 which constitute $(Gas)_{\beta=1}$, for example:

$$B_{\beta=1,J}=N_{CO_2}B_{CO_2,J}+N_{N_2'}B_{N_2',J}+N_{H_2O}B_{H_2O,J}+N_{SO_2}B_{SO_2,J} \quad (12)$$

In general the value of w is very small and especially during the preparation of the coal-water slurry, a part of the ash which consists in the coal can be washed away, so the effect of the ash on the calculation of the thermodynamic properties of the combustion products can be neglected.

(ii) Calculation of cycle efficiencies

Airflow rate, compression ratio, inlet temperature of GT,

recovery coefficients of stagnation pressure and efficiencies of component parts are all assumed to be constant. In the estimation of the influence of water content in slurry on the efficiencies and outputs of gas turbine, steam turbine and combined cycles, it must be noticed that to maintain constant gas temperature at the combustor exit, the flow rate of the slurry supplied to the combustor are not constant.

(a) Calculation of the parameters of the isentropic flow process with variable specific heats

We use the following equations

$h^*=h+\frac{W}{2gJ}$

$p^*/p=\pi^{o*}/\pi^o$ where relative pressure $\pi^o=e^{\frac{g}{R}\int_{T_o}^{T}\frac{c_p}{T}dT}$ [3]

$W=Ma\sqrt{kgRT}$

$\Lambda=RT/pW$

(b) Calculation of the compression process in the compressor

Stagnation pressure after compression $p_2^*=R_{12}p_1^*$

Stagnation temperature after isentropic compression T_{2S}^* can be determined with the following equation

$\pi^o(T_{2S}^*)=R_{12}(T_1^*)$

Actual compression work $L_c=\frac{1}{\eta_c}h^*(T_{2S}^*)-h^*(T_1^*)$, in which η_c is the compressor efficiency.

Outlet stagnation enthalpy $h^*(T_2^*)=h^*(T_1^*)+L_c$

(c) Calculation of the expansion process in the gas turbine.

Expansion work $L_T=h^*(T_3^*)-h^*(T_4^*)$. It consists of two parts, i.e., the work for compressing air $(=L_c\frac{L_o y_c}{(L_o+\beta x_A+\beta x_B+W)y_t}\cdot\frac{1}{\eta_o})$ and that for generating power.

In the expression of work for compressing air,

y_c — airflow rate passing through the compressor;

y_t — gas flow rate passing through the gas turbine;

η_o — mechanical efficiency of the compressor.

Stagnation outlet enthalpy after expansion $h^*(T_4^*)=h^*(T_3^*)-L_T$, from which stagnation outlet temperature T_4^* can be determined.

Stagnation outlet enthalpy after isentropic expansion $h^*(T^*_{4s}) = h^*(T^*_3) - L_T/\eta_t$ in which η_t is the efficiency of the gas turbine.

Stagnation pressure after expansion $p^*_4 = p^*_3 \pi^\circ(T^*_{4s})/\pi^\circ(T^*_3)$.

(d) Calculation of the combustion process

When the composition and LHV of the fuel, the efficiency of the combustion and the temperature of the gas at the combustor exit are known, the fuel coefficient β can be obtained from:

$$\beta = \frac{L_0[(I_{\beta=0})_{T_p^*} - (I_{\beta=0})_{T_a^*}] + Q_r}{Q_{LHV} + L_0[(I_{\beta=0})_{T_p^*} - (I_{\beta=0})_{T'}] - (L_0 + y/4 + z/2 + u/2 + x_A + x_B + w)[(I_{\beta=1})_{T_p^*} - (I_{\beta=1})_{T'}]}$$

where T^*_p —— stagnation temperature of gas at combustor exit;

T^*_a —— stagnation temperature of gas at combastor inlet;

T' —— reference temperature;

Q_r —— latent heat of water;

Q_{LHV} —— low heating value per mole of fuel.

Average mdecular weight and gas constant of one mole of the combustion gas can be determined from the following equations:

$$M = \frac{28.97L_0 + \beta(12.011x + 1.008y + 16z + 14.008u + 32.066v + 18x_A + 18x_B + 60w)}{L_0 + \beta(y/4 + z/2 + u/2 + x_A + x_B + w)}$$

$$R = \frac{847.83}{M}$$

4. Results and discussion

The computational results comprising thermal efficiencies and outputs of a gas turbine/steam turbine combined cycle with coal-water slurry as fuel are shown in Fig. 3, 4 and 5. The slurry has varying water contents and Datong coal and Xuangang coal are alternatively the constituent.

(i) From Fig. 3 and 4, it is seen that the species of coal has little effect on the thermal efficiency of the

combined cycle. While the thermal efficiency decreases with the increase of water content in the slurry, the output increases markedly. If the coal with higher heating values is used for making the slurry, we can obtain the thermal efficiency a little higher than that of the coal with lower heating values. On the other hand, use of coal with lower heating values, such as Xuangeng coal, is more advantageous for improving the output.
From the view-point of energy-saving, the efficiency of combined cycle is most important, so higher heating value coals, eg. Datong coal, are preferred.

Aside from the thermodynamic consideration, to reduce the erosion of the turbine blades also requires the use of coals with higher heating values, eg. Datong coal, which have softer ash and lower ash content.

(ii) It is shown in Fig. 5 that the higher the water content in the slurry, the greater is the decreasing rate of the combined cycle efficiency. Thus, while preparing the slurry, low water content is desirable. However, it is impractical to unduly reduce the water content so as to deplete the fluidity of the slurry.

(iii) From the above figures, the trend of the change of efficiency and output of the combined cycle may roughly be estimated for a particular kind of coal used.

5. Conclusion and perspective

According to the above analysis, there exist broad prospects for using coal of higher heating values as the fuel of the combined cycle. This paper puts forward some suggestions based upon thermodynamic analysis. It is aimed at drawing more power engineers' attention to this

problem. For coal-water slurry much research works are yet to be done, such as the combustion performance of the slurry in gas turbine combustor, the recovery of the fly ash in the flue gas, the influence of fly ash on the blade erosion etc. These problems must be solved satisfactorily beforehand.

6. References

[1] Wu Chung-Hua, Tables of Thermodynamic Properties of Combustion Products, Second Edition, Science Press, Beijing, China 1959.

[2] Zhang Shi-Zheng, Polynomial Expressions of Thermodynamic Properties of the Products of Combustion of Fuel with Air, Chinese Journal of Engineering Thermophysics, Feb.1980.

[3] Keenan J.H. and Kaye J., Gas Tables, 1949.

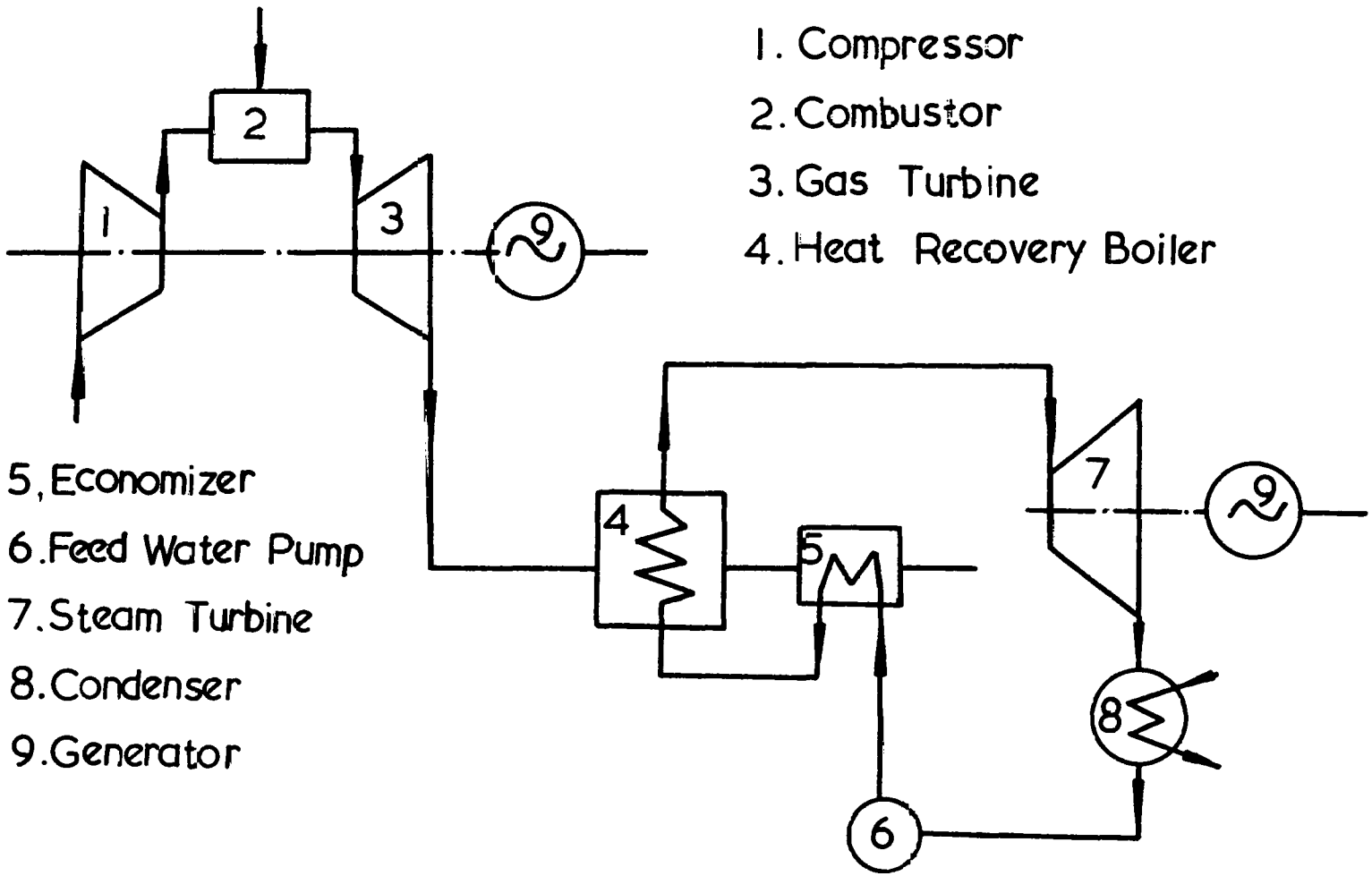
1. Compressor
2. Combustor
3. Gas Turbine
4. Heat Recovery Boiler
5, Economizer
6. Feed Water Pump
7. Steam Turbine
8. Condenser
9. Generator
1
2
3
4
5
6
7
8
9

FIG · 1

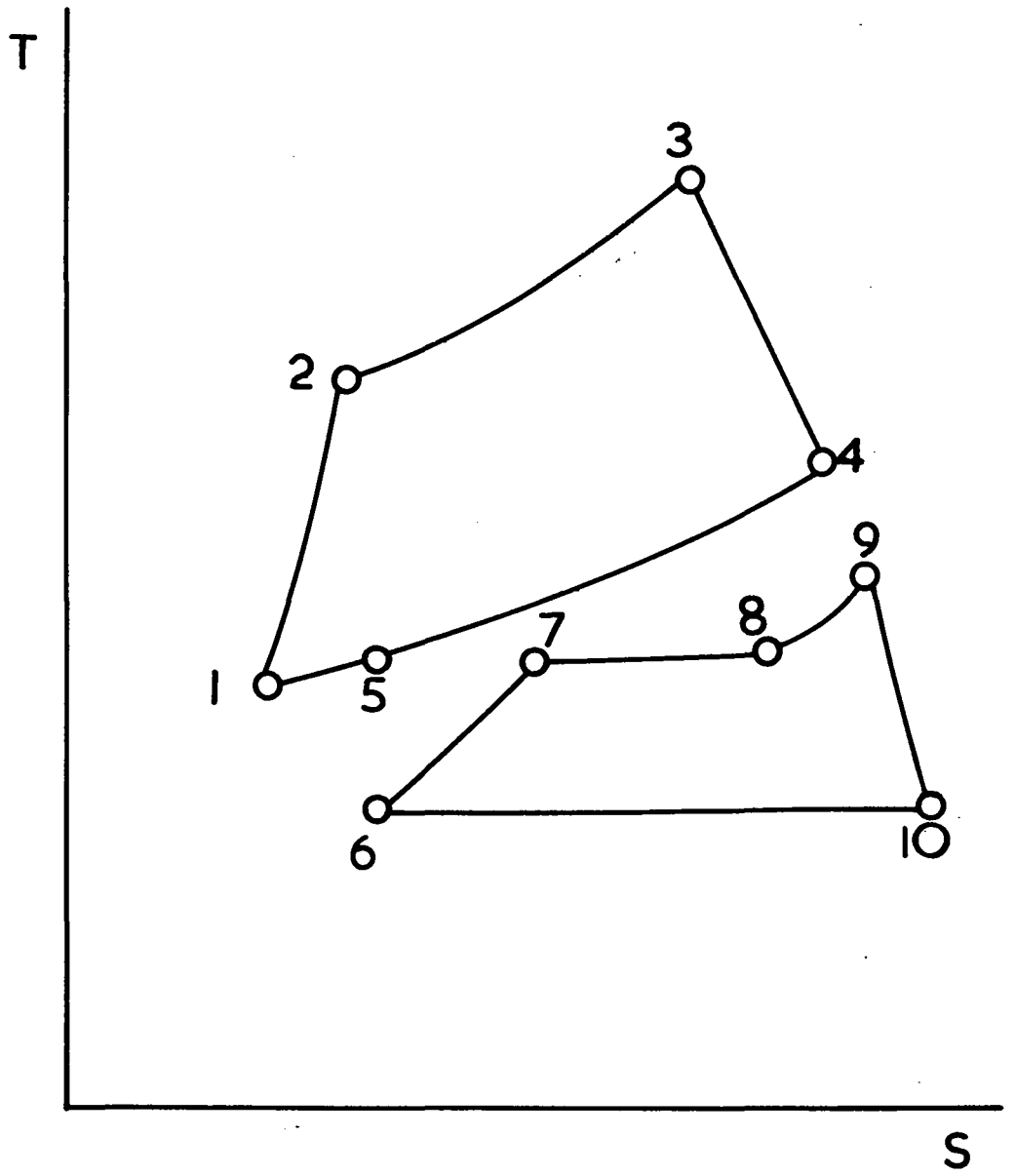

FIG . 2

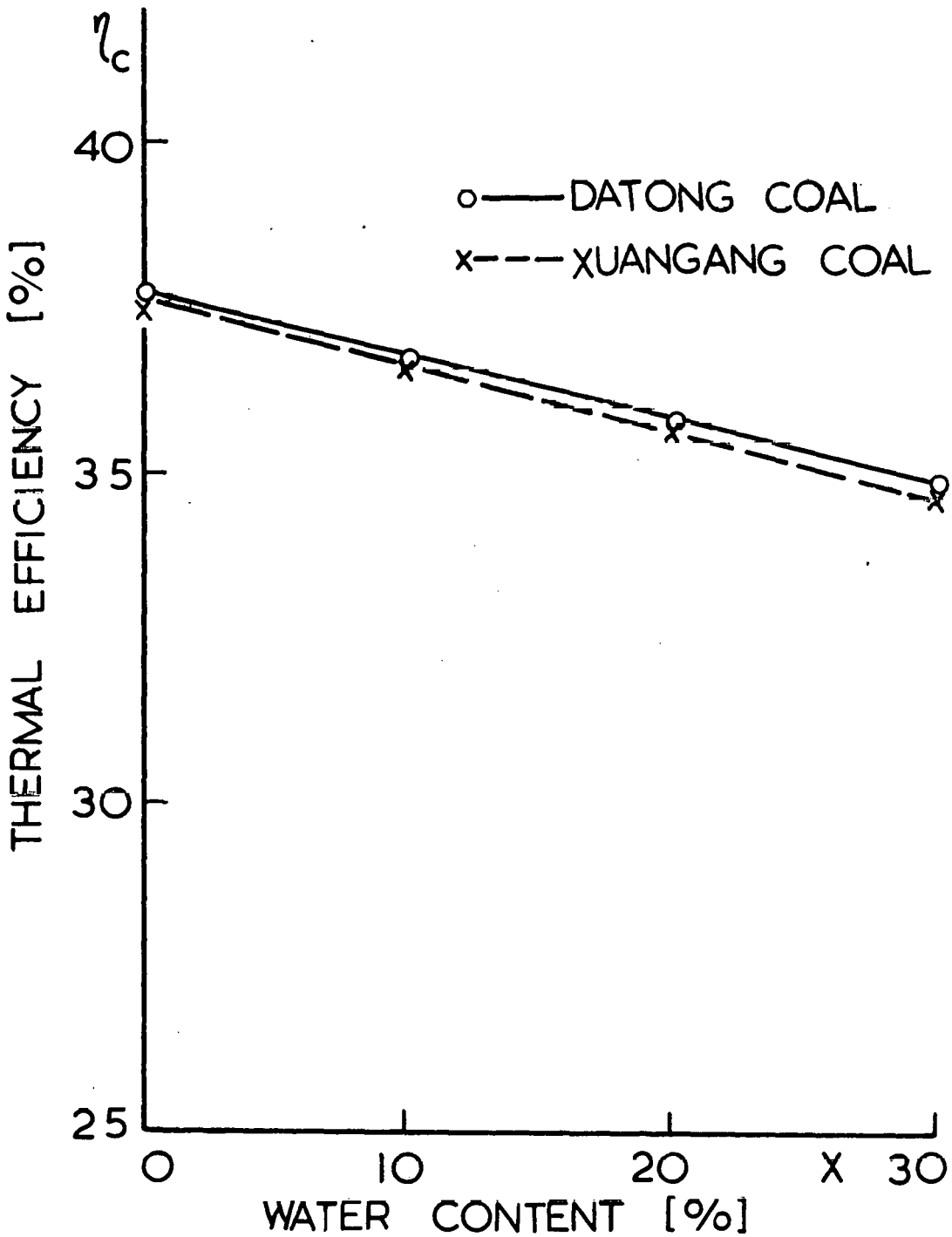
η_c
40
35
30
25
THERMAL EFFICIENCY [%]
o——DATONG COAL
x---XUANGANG COAL
0
10
20
X 30
WATER CONTENT [%]

FIG. 3

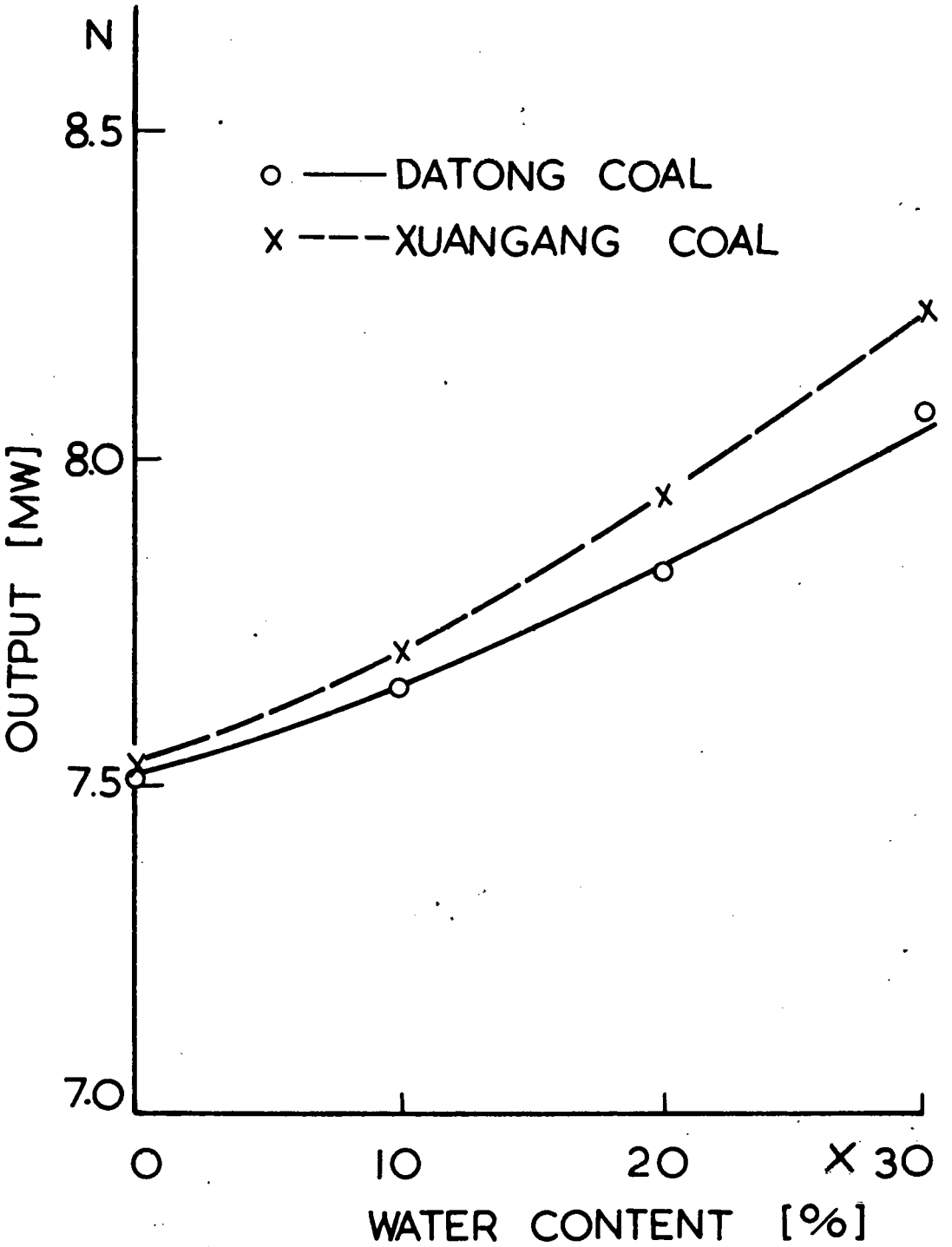
N
8.5
8.0
7.5
7.0
OUTPUT [MW]
o —— DATONG COAL
x --- XUANGANG COAL
0
10
20
X 30
WATER CONTENT [%]

FIG. 4

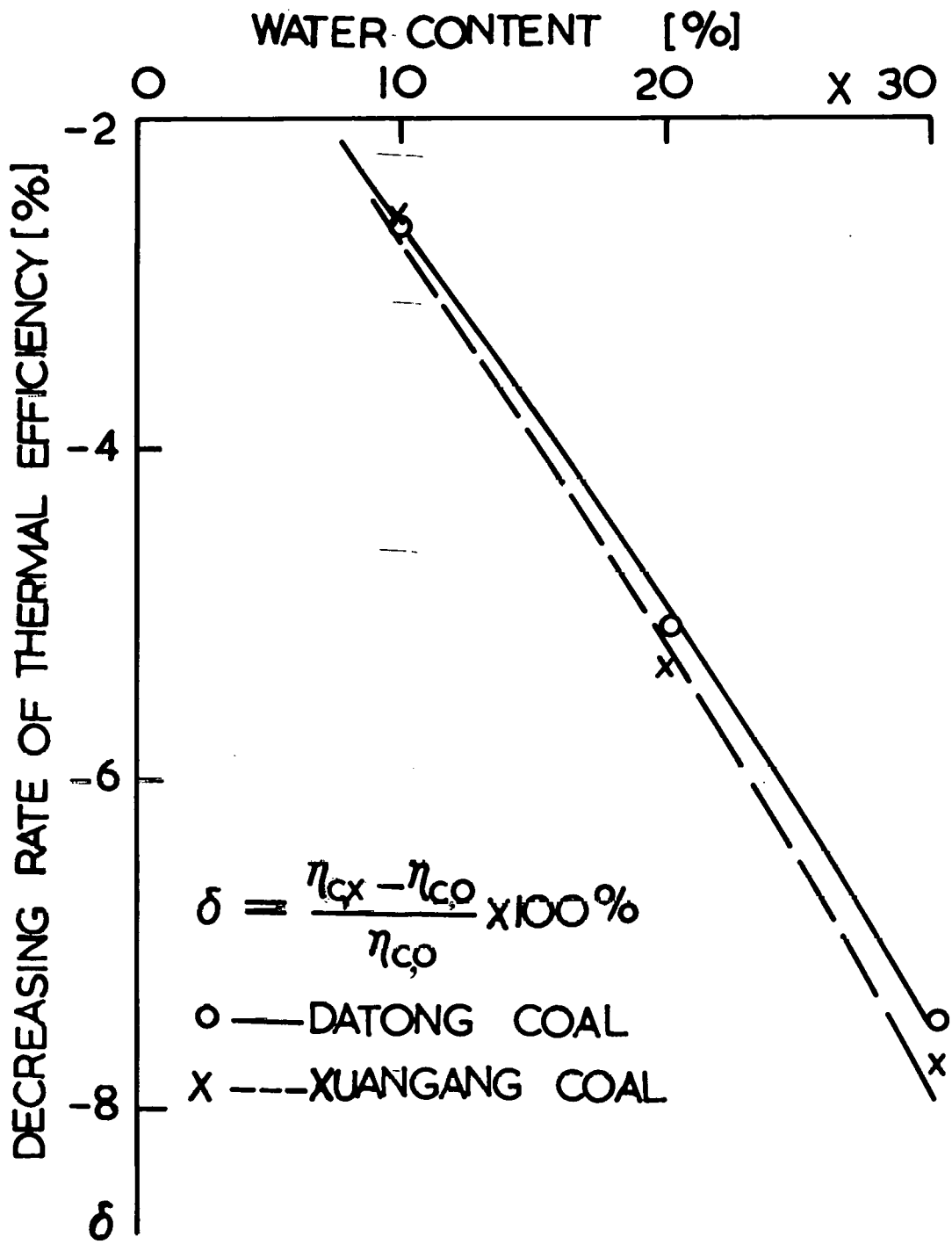
WATER CONTENT [%]
0
10
20
X 30
-2
-4
-6
-8
δ
DECREASING RATE OF THERMAL EFFICIENCY [%]
$\delta = \frac{\eta_{cx} - \eta_{co}}{\eta_{co}} \times 100\%$
o —— DATONG COAL
X --- XUANGANG COAL

FIG. 5

LARGE SCALE CWS FIRING TESTS AT THE S. BARBARA POWER STATION

G. De Michele (^), M. Graziadio (^), S. Ligasacchi (^), G. Saccenti (^)
G. Salvi (^^)

(^) - Enel-CRTN Pisa

(^^) - SNAMPROGETTI

At the S. Barbara Power Station, a series of firing tests was performed by Enel - CRTN on a range of CWSs processed by Snamprogetti.

5÷18 MW_t flames were established in two conventional or slightly modified HFO burners by using CWSs whose coal weight concentration range was between 68 and 72%.

Three types of coals with the following volatile percentage were used, a high (32%), a medium (23%) and a low (17%), as the CWS parent coal.

Internal mixing, Y-jet and ultrasonic atomizers were employed unsuccessfully during the CWS firing tests.

A new atomizer geometry, named y-mixing, was developed. This allowed stable and luminous flames to be set up with CWSs produced both with the high and medium volatile coal.

Work accepted for the presentation at the Fifth International Symposium on Coal Slurry Combustion and Technology - Tampa, Florida, April 1983.

2. OBJECTIVE OF THE STUDY

In the field of CWS combustion the first problem to be investigated concerns flame ignition and stability.

Some investigators have already studied this subject operating on pilot plants. J. Barsin , for example, by setting-up flames with different types of CWS in a 1.2 MWt experimental boiler, found that parameters such as the relative paret coal volatile content, the combustion air and CWS preheating level, played a major role on flame stabilization /1, 2/. He pointed out too that the burner aerodynamics were strongly affecting the flame ignition phenomena and a better combustion air distribution, along with a proper swirl effect, could broaden the operating limits of CWS combustion systems /2/.

The approach adopeted during the ENEL-Snamprogetti demostration work was rather different.

The main objective of the work was, in fact, to demonstrate that a combustion system originally designed for HFO and for pulverized coal firing, could be switched to CWS firing after a few modifications of the burner geometry.

Two existing HFO burners (each rated at 1,500 kg/h oil mass flow i.e. 14÷15 MWt) were employed during the CWS firing tests, after the introduction of minor modifications. They belonged to a group of HFO burners originally designed for supporting lignite combustion in the two 125 MWe boiler units of the S. Barbara power station.

These tests investigated the influence of the following parameters on flame ignition and stability performance: burner geometry, CWS quality and operating conditions, such as air combustion temperature, slurry preheating and the type of atomizing medium.

It is obvious that only qualitative results were to be achieved during this large scale experimental work.

Observation of flame, photography and high speed cinematography were used.

1. INTRODUCTION

The role of coal in the Italian energy programme in the short and medium term, is growing. The main area of coal utilization is that of electricity generation. The energy programme in this area takes into account two stages, the first concerning the use of coal in those power stations which were originally designed both for oil and coal firing but which are actually operated only with oil, the second stage involving the commissioning of new coal fired stations.

The total load of the italian power stations designed only for oil firing amounts to about 18,000 MWe on the global figure of about of 25,000 MWe. This data alone explains the interest in converting some of these plants to coal. On the other hand the difficulties and the costs of this conversion are well known and, for several of these plants, conversion is strongly impeded by the lack of coal storage, preparation and handling areas. For these plants alternative fuels like COM and CWS could be a viable solution.

Against this background two italian companies, ENEL (the Italian Electricity Generating Board) and Snamprogetti (an engineering company belonging to the ENI group) have been involved in the last few years in R & D programmes in the field of CWS.

The interest of ENEL lays in the utilization of CWS and, therefore, in setting up a proper CWS combustion technology. The fields of CWS processing and transportation via pipeline were explored by Snamprogetti.

In 1982 ENEL and Snamprogetti joined their efforts and set up a common demostration programme concerning direct firing of CWS in a large scale burner at the S. Barbara power station. The tasks of this programme were subdivided between the two Companies so that ENEL was busy with the development of a proper combustion system, and Snamprogetti attended to the development and the production of CWS in its own pilot plant at Fano.

3. CWS CHARACTERISTICS

The CWSs employed during the tests were produced by Snamprogetti at Fano. Table I provides data on the composition of the parent coals and in table II the main characteristics of the corresponding CWSs are reported.

Suitable CWSs stability and fluidity were obtained by doping the mixtures with proper additives.

The coal particle size distribution was generally consistent with the specification of p.f. for utility boilers (~80% passing through 200 mesh sieves).

It is noteworthy that all types of CWSs employed during the tests were characterized by the same coal particle size distribution.

4. EXPERIMENTAL APPARATUS

4.1 Combustion chamber

The two 125 MWe boiler units of the S. Barbara power station had been designed and constructed by Deutsche Babcock & Wilcox in 1958. They could be operated both with lignite and oil.

The combustion chamber of the two boiler units is of dodecagonal cross-section and the lignite and the HFO burners are arranged at different levels. Fig. 1 describes schematically the cross section and the configuration of the boiler unit selected for the CWS firing tests. The position of the two burners operated with CWS is illustrated. During the CWS firing tests, some of the remaining burners of the boiler unit were operated only with oil, thus producing about 60% of the nominal load of the unit. In this latter set up, the visibility in the combustion chamber was excellent and, as such, convenient observation, photographing and filming of the CWS flames was possible.

4.2 Burners

The two burners operated in turn with CWS are described in fig. 2. The first one, named "Burner A" and illustrated in fig. 2a, corresponded to the original B & W design. It was equipped with a support gas burner.

The second one, named "Burned B" and reported in fig. 2b, was obtained from the former after modification of the air register and the substitution of the original impeller for a 45° vane angle swirler. It was always operated without the support of gas burner /3/.

In fig. 3 the swirl number (Ns), generated by the air register, is plotted against the register modification.

In total, 14 different tip versions were tested with Burners A and B during the experimental work /3, 4/ and four different types of atomizing systems were tested:

- internal mixing atomizer
- Y-jet atomizer
- a new design named Y-mixing atomizer
- ultrasonic atomizer.

The internal mixing and Y-jet atomizers were of a rather conventional design but of a size suitable for high viscosity fluids.

The new, so called Y-mixing atomizing tip, developed during these tests is schematically represented in fig. 4. In practice this consisted of a two stage atomizer: in the first stage, a high energy exchange between CWS and the atomizing medium was achieved in a sort of Y-jet configuration; in the second stage, the CWS atomization was completed in a larger chamber, similar to that of an internal mixing atomizer. At last, the CWS-atomizing medium mixture was injected into the combustion chamber through holes with a proper jet angle. The design of this atomizer was patented.

For all of these atomizers, inner and outer holes and different spray angles were tested.

4.3 CWS feeding system

In fig. 5 the flow diagram of the CWS storage and feeding system is represented. CWS pumping was conveniently arranged with a volumetric pump of the Moyno type (~ 25 bar available head). An on-line electrical heat exchanger allowed CWS preheating levels of up to 120°C to be reached. The CWS volume flow rate measurements were made by calibrating the pump moto-variator.

The whole feeding system was equipped with several joints for a proper flushing with water during the start-up and shut-down operations.

5. EXPERIMENTAL RESULTS

5.1 Burner inputs and operating conditions

During the overall series of the CWS firing tests, the burner inputs and operating conditions were varied in the following range:

		Range
- load	(MWt)	5 ÷ 18
- CWS mass flow rate	(kg/h)	900 ÷ 3500
- CWS temperature	(°C)	25 ÷ 110
- secondary air temperature	(°C)	160 ÷ 230
- atomizing air temperature	(°C)	25 ÷ 120

As regards the secondary air temperature range, the close limits indicated above depended on the ordinary operational set-up of the boiler. The CWS firing tests described later were carried out piecemeal and totalled about 25 h of continuous firing and 20 tons of CWSs were fired. However they can be divided schematically into three phases.

PHASE I: Here emphasis was laid on the burner performance and, in particular, on the atomizing system.

The B&W HFO burner in its original configuration (indicated as

burner A in fig. 2a) was lighted with CWS 1 (see tab. II) under the most favourable operating conditions allowed by the combustion system:

- CWS temperature: 110°C
- atomizing air temperature: 120°C
- secondary air temperature: 230°C

With this burner, and using always the same fuel CWS 1, both the internal mixing and the Y-jet atomizers did not lead to any satisfactory flame. No appreciable improvement of the burner performance was obtained by varying the tip spray angle (in the 50°÷90° range) and the exit port size.

On the contrary, when the newly designed y-mixing atomizing type was used, a flame was immediately established.

Flames of up to 18 MW thermal load could be set up even under more difficult operating conditions, i.e.:

- CWS temperature: 20°C
- atomizing air temperature: 25°C
- combustion air temperature: 180°C
- support gas burner: off.

PHASE II: Here the aim was to investigate the influence of burner aerodynamics on CWS flame ignition and stabilization.

For this reason, in the second phase of the CWS firing tests the burner B, characterized by a higher overall swirl number was employed. The same CWS type (CWS 1) was fired during the tests. With this burner and slurry both the Y-jet and the internal mixing atomizers could not lead yet to any appreciable flame. Even the resort to an ultrasonic air atomized tip revealed to be unsuccessfull.

On the contrary, the introduction into burner B of the Y-mixing atomizer (above all in the 50° and 60° spray angle versions) gave

rise to the best CWS 1 flames even under the rather difficult operating conditions described above.

PHASE III: With the optimized Y-mixing tip assembled on burner B the experimental study was extended to the whole series of CWSs.

As described in table II, the six CWSs used were different because the parent coal type (see also table I) and the coal concentration (Cw) were different.

During these series of the CWS firing tests, the attention was focused firstly on the study of the combustion performances of CWS 1, CWS 3 and CWS 5 which differed only in the volatile content of their parent coals.

The tests showed a light worsening of flame stability and general structure, when one passed from CWS 1 (high volatile coal) to CWS 3 (medium volatile coal), and a poor flame performance when one passed to CWS 5 (low volatile coal).

In the case of the latter slurry, the ignition was difficult and flames were only occasionally stabilized.

The influence of coal concentration was subsequently investigated and CWS 2, CWS 4, CWS 6 were fed to the burner.

The improvement was really impressive: all CWSs were ignited and good flames were stabilized (see fig. 6), especially when high and medium volatile coal was employed.

The use of steam was also tested in place of air as an atomizing medium, with some selected favorable flame inputs. In all these cases the resort to atomimizing steam introduced a clear deterioration of the CWS flame ignition phenomena by moving the flame ignition front away from the burner quarl. This result applied both to the high coal concentration CWS 1 and CWS 3 and to the diluted CWS 2 and CWS 4.

During this undoubtedly short period no erosion of the atomizer tips was experienced. In any case the erosion problem is presently being studie

in the ENEL laboratories.

6. CONCLUSIONS

The CWS firing tests carried out by ENEL and Snamprogetti at the S. Barbara power station could provide useful, though only qualitative, information on the novel CWS combustion technology.

The following series of conclusions might be drawn from this study:

- The use of the conventional internal mixing and Y-jet atomizer types, together with an ultrasonic atomizer, did not produce satisfactory flame, even if burner operating conditions were favourable.
- The design of a proper atomizer geometry (named Y-mixing) and the introduction of minor modifications to the swirl generation equipment of a conventional HFO burner, led to the establishment of boiler flames of CWSs derived from a high volatile (32%) coal, a medium volatile (23%) coal and a low volatile coal (17%).
- The less concentrated slurry (68%) produced more impressive flames with all types of CWSs.
- The concentrated CWS (Cw = 72%) produced a worsening in the flame ignition stability performance, especially when low volatile coal was used.
- Preheating of atomizing air and CWS did not apparently have any influence on flame ignition performance, but it could have some effect on combustion efficiency. Additional confirmation of this is needed, however.
- The resort to steam as an atomizing medium produced a clear worsening of the flame ignition pattern, by moving the flame ignition front away from the burner quarl.

The results of this tests need to be investigated further. Some of this work will take place in a specific research planned by ENEL on a fully instrumented industrial boiler at Livorno power station in 1983.

ACKNOWLEDGEMENT

This work has been possible for the support of S. Barbara power station staff. The authors thank especially Mr. D'Alessandro for his help and suggestions during the tests.

BIDLIOGRAPHY

/1/ Barsin, J. "Investigation of Coal-Water Mixtures". Presented at "Coal Phoenix of the '80s" (June, 1981).

/2/ Barsin, J.; Sommer, T.M. "Commercialization of Coal-Water Slurries" Presented to "4th Annual Symposium Industrial Coal Utilization" (April, 1982).

/3/ ENEL-CRTN/Snamprogetti "Prove di combustione di miscele acqua-carbone dense" - Doc. T1-01-83 (January, 1983).

/4/ ENEL-CRTN/Snamprogetti "Prove di combustione di miscele acqua-carbone dense" - Doc. T1-02-82 (October, 1982).

COAL TYPE	A	B	C
VOLATILE MATTER	32	23	17
CFIX , %	56	62	66
ASH , %	12	15	17
Hv , KCAL/kg	6350	6550	7043

TAB. 1- COMPOSITION DATA ON CWS PARENT COALS

CWS	1	2	3	4	5	6
PARENT COAL	A	A	B	B	C	C
Cw , %	72	68	72	68	72	68
μ , poise	14.2	4.80	12.63	4.70	11.0	4.20
Hv, KCAL/kg	4570	4318	4716	4454	5071	4789

TAB. 2 - SOME OF THE PROPERTIES OF THE CWSs FIRED AT THE S. BARBARA POWER STATION

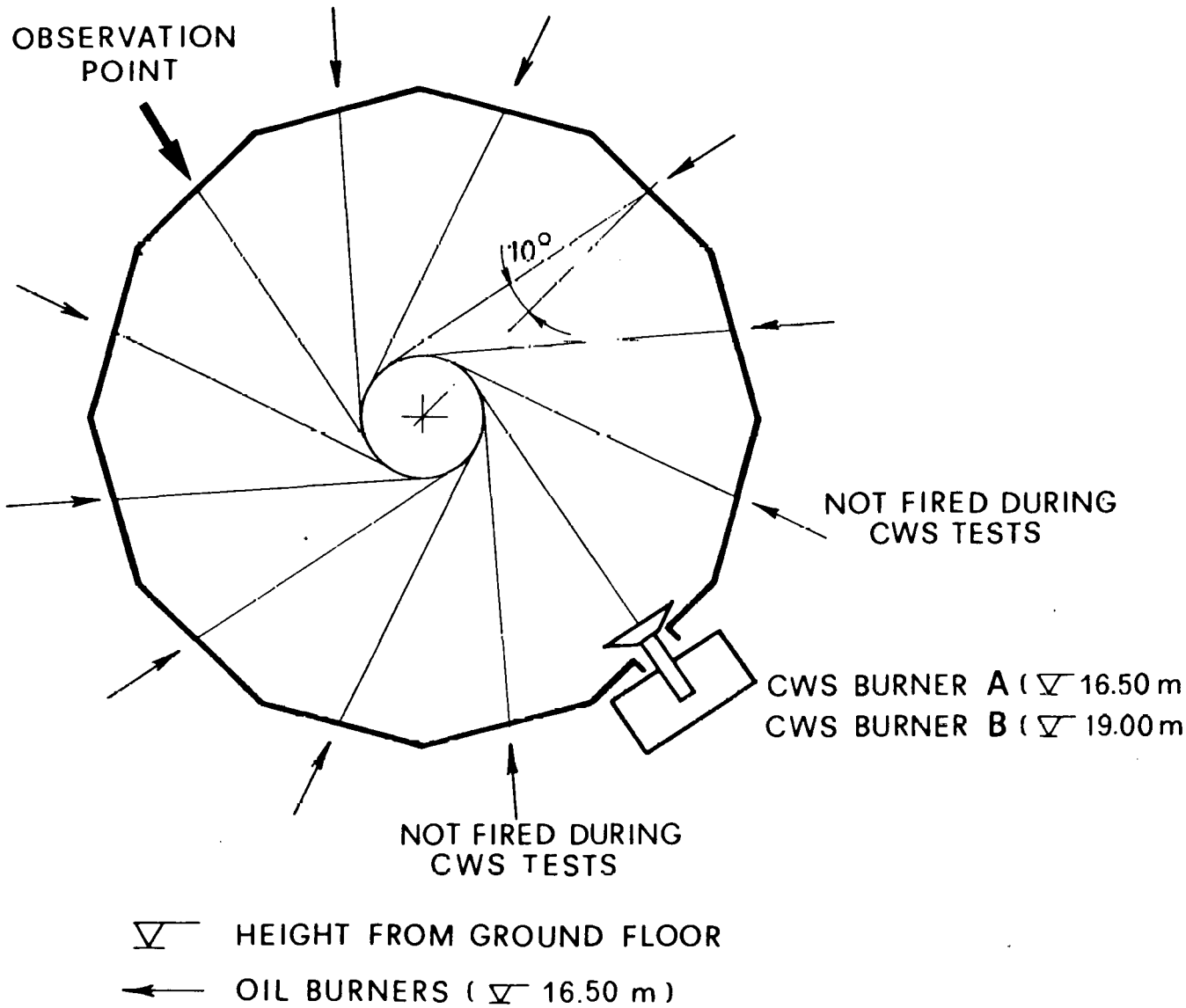

FIG. 1 - CROSS SECTION OF THE BOILER

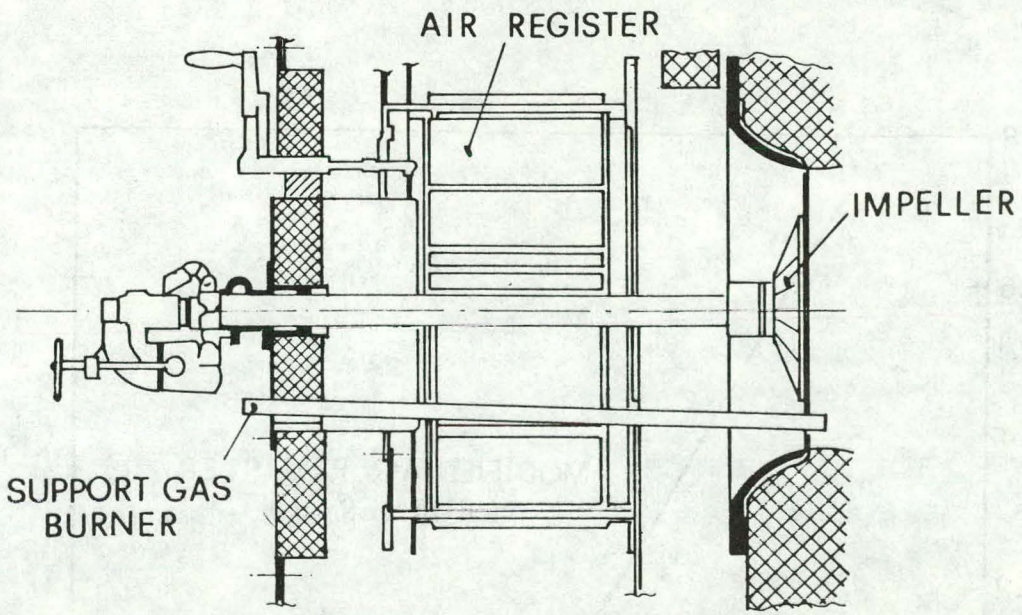

a) - Original B & W burner (BURNER A)

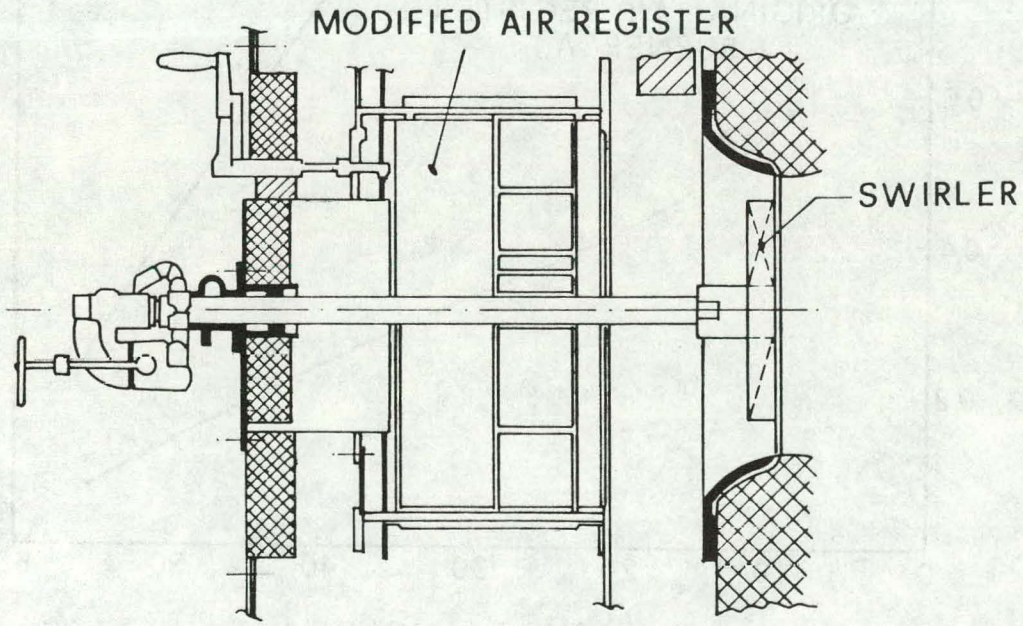

b)- Improved burner (BURNER B)

FIG. 2 - SCHEMATIC SECTION OF THE TWO BURNERS EMPLOYED FOR CWS FIRING

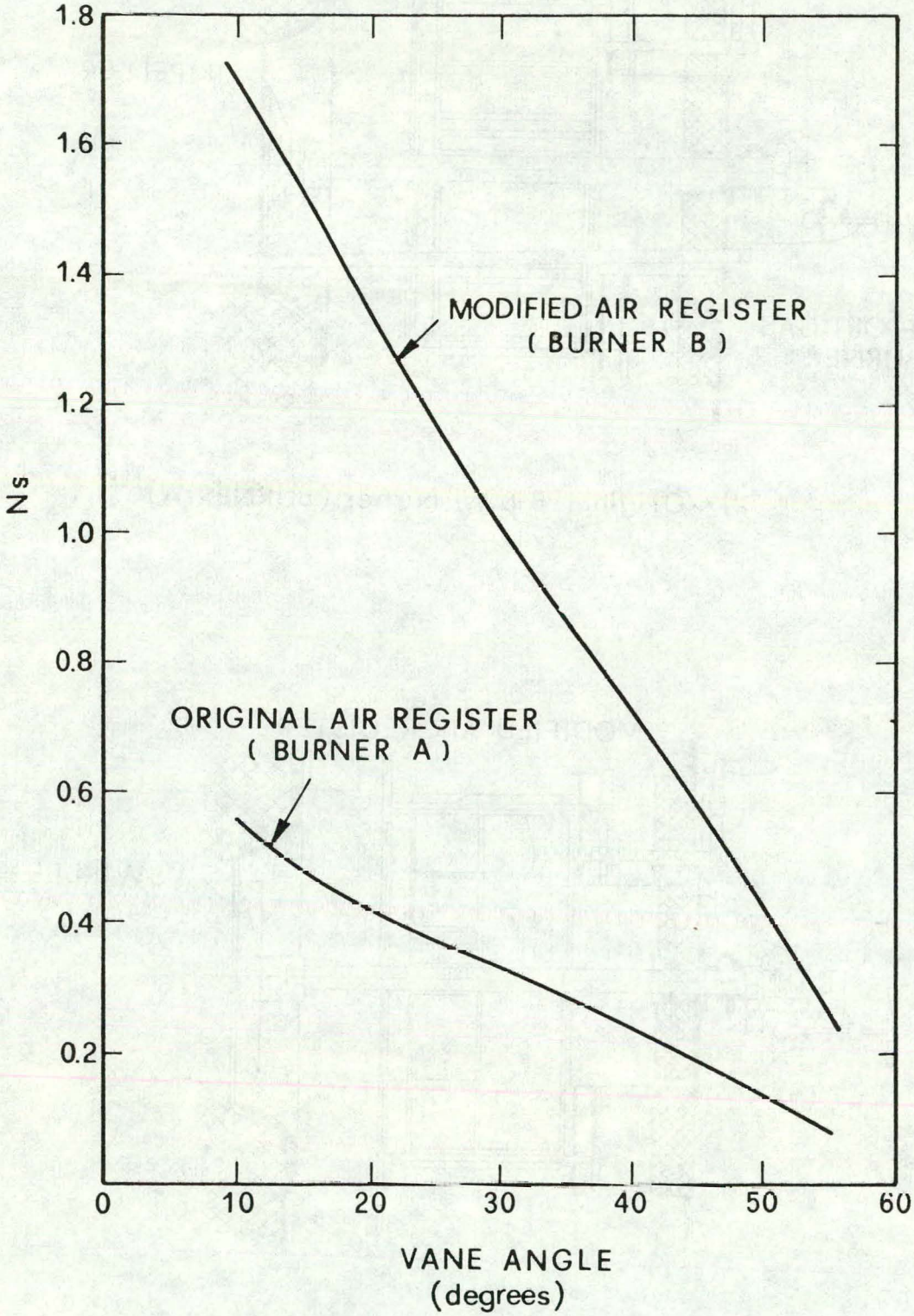

FIG.3 - VARIATION OF CALCULATED SWIRL NUMBER (Ns) WITH AIR REGISTER VANE ANGLE FOR THE ORIGINAL AND MODIFIED REGISTER

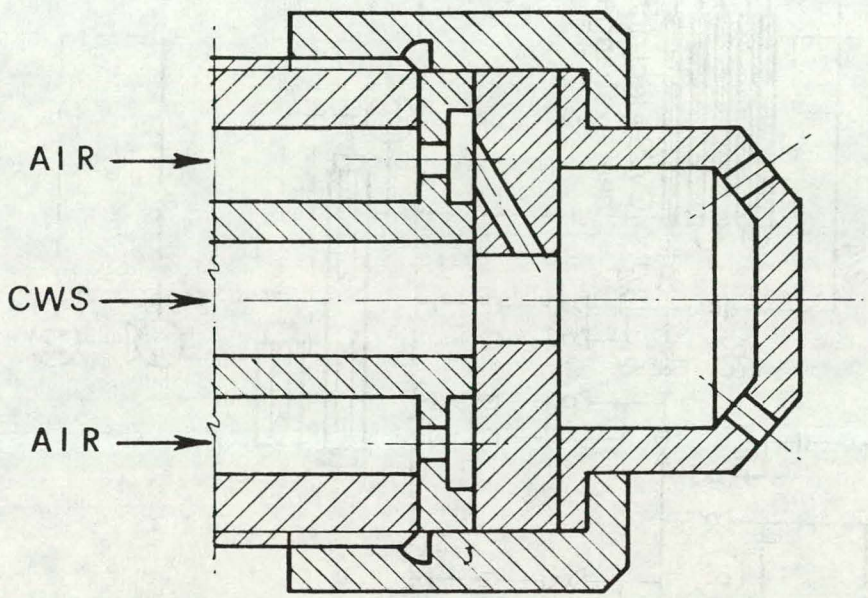

FIG. 4 SCHEMATIC SECTION OF Y-MIXING ATOMIZER

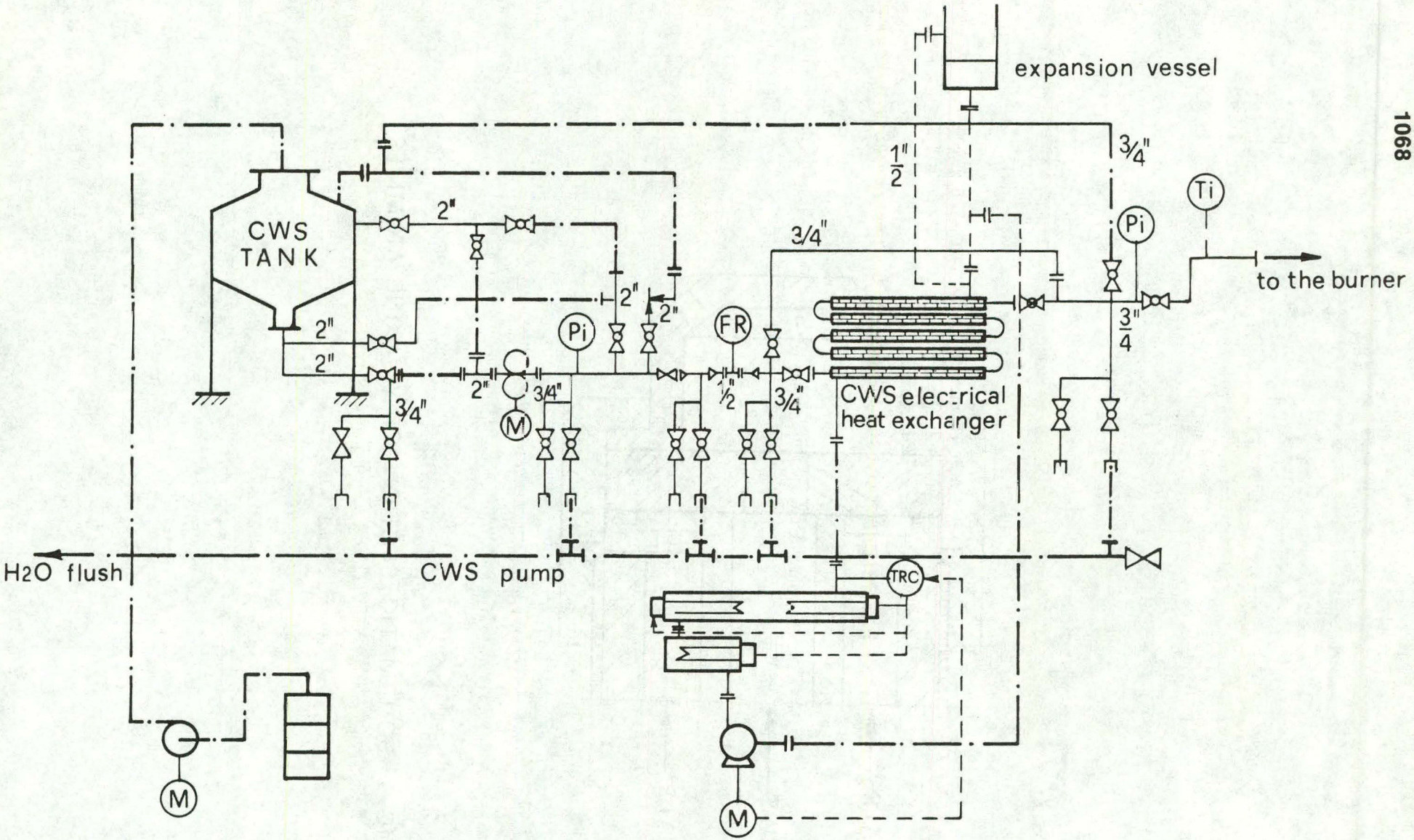

FIG. 5 - FLOW DIAGRAM OF THE CWS STORAGE AND FEEDING SYSTEM

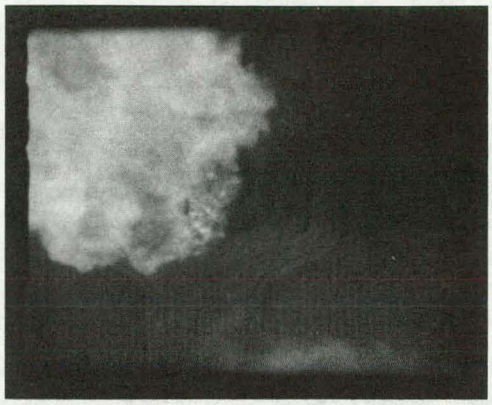

CWS 2 FLAME

CWS 4 FLAME

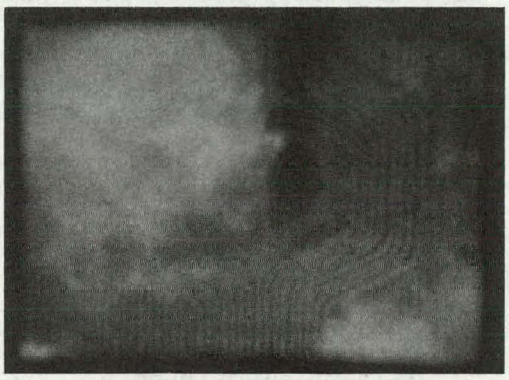

CWS 6 FLAME

FIG. 6 FLAMES OBTAINED WITH DIFFERENT PARENT COAL CWSs

ON THE IGNITION CHARACTERISTICS OF COAL/WATER SLURRIES

K. C. Adiga, V. R. Pai Verneker‡, G. Gettinger,

B. M. Moudgil*, and D. O. Shah

Departments of Chemical Engineering and Anesthesiology

Department of Materials Science and Engineering*

University of Florida

Gainesville, Florida 32611

ABSTRACT

Ignition characteristics of coal/water slurries have been investigated under dynamic heating conditions by employing Differential Thermal Analysis technique. It is seen that the ignition temperatures of coal water slurries are lower than coal powder and critical mass for ignition of slurry is far lower than coal.

Kinetic parameters of ignition of coal and coal/water slurries have been evaluated by appropriate heat balance equations, applicable to DTA sample environment. Using the kinetic parameters evaluated and physical properties of coal, critical diameters and critical mass have been predicted by thermal ignition theory. The relative increase in effective surface area of coal, after evaporation of water from the slurry appears to be responsible for the increased reactivity of slurry towards heterogeneous coal-O_2 reaction. This factor was

---

‡United Nations Development Program Visiting Scholar from the Indian Institute of Science, Bangalore, India.

experimentally confirmed and has been incorporated in the theory. Kinetic analysis also indicated the higher reactivity of coal dried from slurry. As a result, the mechanism of ignition of slurry and coal appears to be essentially the same and only apparent rates are higher for coal slurries, suggested to be due to larger surface area and porosity of coal surface.

INTRODUCTION

Coal/water mixtures are presently viewed as an attractive alternative fuel for power generation. Coal/water slurries provide the following advantages: decreasing dependence upon foreign oil, stretching existing domestic petroleum reserves, taking advantage of cheaper and available coal, minimum expenditure for modification of oil fired installations. Feasibility of coal/water slurries as boiler fuels has been shown recently as evidenced by the previous (Fourth) International Symposium on Coal Slurry Combustion meeting.

Combustion and ignition characteristics of coal/water slurries have been evaluated at laboratory scale and also in test firings in modified oil fired burners.[1,2] It is evident that the ignition and combustion characteristics require further studies to evaluate the effect of water on ignition time, ignition temperature, combustion rate and completeness of combustion and emission.

The mechanism of the ignition and the combustion of coal-water mixture (CWM) has been the subject of discussion of several of the papers presented at the Fourth International Symposium on Coal Slurry Combustion.[2] Thus, for instance, Scheffe et al.[3] point out that the burning is probably a mass transfer process rather than a kinetically controlled process, indicating that increased turbulence rather than increased temperature should promote combustion rates. Cen Ke-fa et al.[4], elaborating on the mechanism, suggest that the combustion process of CWM can be divided into three overlapped stages (1) evaporation of water (2) devolatilization and combustion of volatiles and (3) combustion of coke. They add that (a) the ignition temperature of CWM is much lower than that of dry coal and (b) once

the droplet of CWM is ignited, its combustion rate is not lower than that of pulverized coal. Germane et al.[5], on the other hand, point out that introduction of water into the combustion zone causes ignition delay which get reduced by high solids loading. The increasing moisture acts as a heat sink and retards ignition and reduces peak temperatures but not significantly. Hao Lin[6] carefully draws attention to the fact that in thermogravimetry (TG) and differential thermal analysis (DTA) experiments in CWM, nearly all the water in CWM was evolved at a temperature around 100-150°C. Thereafter, CWM behaved like coal as judged by the results from TG and DTA. It is quite evident from the above cited references that the mechanism of ignition and combustion of CWM is far from clear. In fact, even the observations are not consistent, i.e., "The ignition temperature of CWM is much lower than that of dry coal (vf. Cen Ke-fa et al.[4]" vis-a-vis "introduction of water into the combustion zone causes ignition delay (Germane et al.[5])". In view of this we have initiated a progam to understand the mechanism of ignition and combustion of CWM. Some preliminary results on ignition of CWM, coal and coal dried from CWM as studied by DSC are presented here. Both conventional DSC runs using different heating rates as well as isothermal DSC runs giving the ignition times are reported.

OBJECTIVES

- Determine ignition temperatures of coal/water slurries and coal powder as a function of mass and heating rate.
- Determine the critical mass of coal/water slurries under identical experimental conditions.

- Evaluate the detailed kinetic parameters and quantitatively relate the parameters to critical conditions.
- Compare the ignition characteristics of coal and coal/water slurries based on experimental results and evaluated kinetic parameters.

EXPERIMENTAL

Coal used in the present investigation was obtained from Florida Power and Light Company, Florida. The coal used as such or in CWM had a particle size of 80% of minus 200 mesh and 20% of minus 325 mesh. The CWM had a 50:50 composition of coal/water. In a typical experiment dealing with the determination of the ignition temperature, coal or the CWM weighing 1-20 milligrams was taken in an aluminum cup and was placed in an atmosphere of oxygen flowing at the rate of 2 cubic feet/hour. The DSC assembly was then heated at a predetermined rate. When study was made of the effect of the rate of heating on ignition, the mass and the particle size were kept constant. Similarly when the effect of other variables like mass, particle size was studied, the other two variables were kept constant.

RESULTS AND DISCUSSION

A thermal reaction of coal can result either in thermal decomposition or ignition followed by combustion depending on whether the heating is carried out in an inert-atmosphere or in an atmosphere of oxygen. The thermal ignition theory, however, predicts that ignition-combustion can peter out into decomposition if a critical mass and a critical heating rate are not employed during the thermal reaction. Thus, Pai Verneker and Maycock[7] have shown that the

explosivity of lead azide is governed by the mass of the sample and the rate at which the sample is heated. An interplay of these factors can influence the reaction either in favor of an explosion or decomposition. The thermal behavior of coal or CWM in an atmosphere of oxygen is very much akin to that of lead azide and is in tune with the predictions of the thermal ignition theory (table 1). It can be seen that under the conditions of the experiments (the rate of flow of oxygen, the shape and size of the DSC cup and hence the packing density of the sample) twenty milligrams of coal ignite and burn at 330°C (exhibited by a very sharp exotherm) when heated at a rate of 100°/min. Ten milligrams, however, ignite only partially at 330°C, finally decomposing at 500°C. A three milligram sample decomposes in two stages, one at 390°C and another at 530°C. Similarly, a twenty milligram coal sample which ignites at 330 when heated at 100°/min shows partial ignition at 325°C followed by decomposition at 460 on being heated at a rate of 15°/min. Also ten and six milligrams of CWM, ignites at 360° and 370°C, respectively, when heated at the rate of 100°/min, while a three milligram sample of CWM under the same heating rate, decomposes in two stages, one exotherm at 360° and the second exotherm at 500°C. Similarly, a 20 milligram sample of CWM ignites at 310°C with a heating rate of 100°/min whereas 20 milligram sample of CWM at the heating rate of 15°/min decomposes at 310°C and ignites at 470°C.

The very first step occurring when a CWM sample is heated at a rate of 100°/min or 15°/min is the evaporation of water at around 100°C (Fig. 1). If the heating is stopped at 150°C and the sample weighed it is clear that the residue consists of coal only. In 50:50

CWM, 50% weight loss is observed. The ignition and decomposition takes place much later when the temperature is over 300°C. Therefore, if all the water had evaporated from the sample of CWM, the residue, consisting of only coal, would be expected to behave just like coal which has never been in contact with water. The results of the present investigation point out that the ignition temperature of CWM is lower than that of coal (table 1) and the critical mass required for ignition is also much lower in the case of CWM than in the case of coal. Together with the fact that water has evaporated from CWM at assured 100°C, the coal resulted from drying of the slurry appears to have different surface characteristics. This was further confirmed by measuring the density of dried coal by an independent experiment and considerable increase in volume was observed. Hence, in the typical heterogeneous reaction of coal-oxygen, the increase in reactivity appears to be quantitatively related to surface area and porosity of coal.

Before one discusses the relevance of the DSC results to the actual ignition and combustion of coal and CWM in practical boilers, it may be appropriate to compare the results of the present investigation with those of other investigations discussed earlier. In a broader sense the technique used in the present investigation is akin to the DTA technique employed by Hao Lin[6], except that the DuPont Thermoanalyzer (DSC) is sensitive and quantitative. There is agreement on the fact that around 100-150°C all the water from the CWM is lost. Whereas, Hao Lin reports that coal water slurry (covered in the investigation as coal water mixture CWM) behaves like coal as indicated by TG and DTA, the results of the present investigation

clearly reveal that CWM requires a much less critical mass for ignition than coal, and has a lower ignition temperature than coal. This difference could have arisen due to the following facts: (a) Hao Lin has used very low heating rates whereas the present investigation predominantly used 100°/min. This low heating rate could leave coal from CWM dried up for a much longer time. Therefore, CWM was heated up to 200°C, removed from the DSC assembly for several hours (up to 5 hours) and a DSC scan was rerun. The behavior was reproducible and akin to the DSC scan of CWM. (b) In the present investigation when comparisons are made between coal and CWM, the mass, the heating rate, the particle size are kept constant, Hao Lin (1982) does not mention the heating rate or the particle size. He emphasizes the fact that different weights were taken to compensate for the heating values of the different systems.

Theory and Kinetic Parameters

The evaluation of the kinetic parameters of coal particles ignition is an important problem in combustion. According to Semenov's[8] thermal ignition theory, the ignition of coal particles is determined by the interaction of heat liberated due to chemical reaction and heat gain of loss due to emission and radiative heat exchanges. The essential conditions to be fulfilled are: (1) heat loss to surroundings is equal to heat generated due to chemical reaction, (2) heat loss curve is tangential to the heat generation profile.

Gross and Amster[9] have proposed a simplified approach to evaluate the kinetic parameters for self heating explosives and propellants. In the present approach for quantitative data, DSC assembly was

employed with a linear heating rate. Therefore, the heat balance equation was modified suitably.

Thus, writing the heat balance around the coal sample in a rising-temperature environment gives the following relation for heat fluxes,

$$Q_s = QZe^{-E/RT_s} - \frac{k}{d}(T_s - T_w) \tag{1}$$

where Q_s is the rate of heat generation at the coal sample, cal/sec

QZ is the preexponential factor and Q heat of reaction, cal/gsec

E, activation energy of ignition, cal/mole

T_s, sample temperature, °K

T_w is the reference furnace temperature, °K

d, distance between the thermocouples T_s and T_w

k, thermal conductivity of sample block, cal/(sec) (cm^2)(°K/cm)

Modifying this relation to the present experimental conditions and also writing as derivative of temperature/time history of the sample,

$$mcp\frac{dT_s}{dt} = mcp\frac{dT_w}{dt} + mQZe^{-E/RT_s} - \frac{k}{d}(T_s - T_w) \tag{2}$$

where, $\frac{dT_w}{dt}$ is linear and predetermined, heating rate, Hr

m is the mass of sample.

Also $T_w = T_0 + Hrt$

where T_0 is ambient temperature.

cp, heat capacity of coal, cal/g.°K.

Rearranging the terms and expressing in terms of rate of surface temperature rise yields

$$\frac{dT_s}{dt} - Hr = \frac{QZ}{c\rho} e^{-E/RT_s} - \frac{k}{d \cdot cpm} (T_s - T_w) \qquad (3)$$

By examining the various terms in the above heat balance equation, it is seen that, with initial condition t = 0, T = T_0. If (1) $\frac{QZ}{c\rho} e^{-E/RT_s} = 0$ following $T_s = T_w$, indicates that the sample temperature rise is determined only by the heating rate Hr. Further, for ignition, by equating the heat gain due to chemical reaction to heat loss.

(2) critical ignition occurs at

$$\frac{QZ}{c\rho} e^{-E/RT_s} + Hr = \frac{k}{dcpm} (T_s - T_w) \qquad (4)$$

For evaluating the parameters QZ and E, equation (3) can be written as

$$\ln\left(\frac{dT_s}{dt} - Hr + Q_L\right) = \ln\left(\frac{QZ}{cp}\right) - \frac{E}{RT_s} \qquad (5)$$

where Q_L is the heat loss term in equation (1) given by $\frac{k}{dcpm} (T_s - T_w)$. A linear plot of the right hand side of the above equation versus $\frac{1}{T_s}$ yields QZ and E by intercept and value of heat capacity of coal.

Figure 3 shows the plots of $\ln\left(\frac{dT_s}{dt} - Hr + Q_L\right)$ versus $\frac{1}{T_s}$ for coal and coal water slurries with varying sample size but identical particle size distribution. It is seen that the plots are indeed linear and correlation coefficients are 0.98 or above. From these plots, kinetic parameters such as QZ and E are evaluated for

coal and coal water slurries and are shown in table 2. The QZ parameter was not further evaluated for Q and Z separately. It was further used for predicting the critical diameters for ignition.

Consider now the case of finite sample of coal igniting in a constant temperature atmosphere. The thermal ignition theory yields[10]

$$c\rho\,(dT/dt) = Q\rho\,(dn/dt) + k\,[d^2T/dx^2 + (n/x)(dT/dx)] \qquad (6)$$

$$dn/dt = f\,(T,n)\,A\,\exp(-E/RT) \qquad (7)$$

where $A = QZ$ as before.

With appropriate boundary conditions, approximate solutions have been obtained by Frank-Kameneskii[11] and Chambre[12]. The solutions yield values of sample size (radius, if sphere) as a function of surface temperature, if exceeded will ignite. In their solution, critical conditions are expressed in terms of dimensionless parameter.

$$\delta = \left(\frac{n_s}{\theta_s}\right)^2 \exp\,(-1/\theta_s) \qquad (8)$$

where

$$n_s = \left(\frac{\rho QZR}{kE}\right)^{1/2} \gamma$$

where ρ is the density of coal, R is the universal gas constant, and γ is the radius or half thickness and k_s, thermal conductivity of coal.

$$\theta_s = \frac{RT_s}{E}$$

For $\theta_s \to 0$, the limiting values of δ_c are $S_{slab} = 0.88$

$S_{cylinder} = 2.00$

$S_{sphere} = 3.32.$

The final equation for γ_c (critical radius) in terms of critical parameters can be written as

$$r_c^2 = \frac{\delta}{n_s/\theta^2 \cdot \exp(1-1/\theta_s)} \tag{8}$$

where γ_c is the critical radius of coal for ignition.

The critical radius of coal/water slurries and coal, calculated using the above theory are shown in table 3.

From the table 2 it is seen that the activation energies of various coal and coal slurries are similar but the preexponential functions which also involve Q (heat of reaction) and rate parameters differ. For example, coal powder exhibits the highest QZ factor and coal powder obtained by drying from slurry has the lowest. Critical mass predicted from theory, as shown in table 3, interestingly indicate that below 300°C slurries are more reactive and have lower critical mass than coal. At higher temperatures, coal is more reactive than slurries. The experimental critical mass ratio and predicted from theory are similar. It is further suggested that such analysis of ignition behavior could be carried out on highly loaded coal/water slurries (80-85% wt coal) such as those proposed by Ren[13]. The analysis provides further information on ignition and combustion characteristics of highly loaded coal/water slurries.

CONCLUSIONS

1. Coal slurries exhibit higher preignition temperatures than coal powder.
2. Coal slurries have lower critical mass than coal powder under similar experimental conditions.
3. Activation energy of ignition of coal and coal/water slurries are similar but the apparent rates widely differ. The porosity and increased surface area of coal resulted after preheating may be responsible for the accelerated heterogeneous reactions of coal-oxygen.
4. The critical masses of coal/water slurries and coal, predicted from thermal ignition theory using the kinetic parameters evaluated from DSC runs indicate that critical mass of slurry and coal are strongly temperature dependent. Further, coal slurries exhibit higher reactivity than coal at lower temperatures and coal ignites faster at higher temperatures.
5. The modified heat balance equation for DSC can be employed to evaluate the kinetic parameters of coal and thermal or ignition characteries can be predicted.

ACKNOWLEDGMENTS

The authors acknowledge the financial assistance of the EIES, UF College of Engineering (Grant Nos. 124516189 and 124516102) and Florida Power and Light Company, Florida. One of the authors (Pai Verneker) also acknowledges the United Nations Development Program for financial support.

Table 1

Effect of mass and heating rates on the ignition characteristics of coal and coal/water slurries

Mass (mgs)	Dynamic DSC Peak Temperatures, °C		Heating Rate °C/min
	Coal Powder		
20	330°C (i) 325 (pi)	460 (de)+	100 15
10	330 (pi)	500 (de)	100
3	390 (de)	530 (de)	100
	Coal/Water Slurry		
20(10)*	310°C (i) 320 (de)	470 (de)	100 15
10(5)*	360 (i)		100
6(3)*	370 (i)		100
3(1.5)*	360 (de)	500 (de)	100

( )*refers to the weight of coal in the slurry.

(i) and (pi) indicate ignition and partial ignition, respectively.

(de) indicates decomposition.

Table 2

Kinetic parameters of ignition of coal and coal/water slurries

Fuel Specification	Temperature Range °C	QZ cal/g.sec•10^9	E cal/mole•10^3
coal powder 20 mg.	250 - 350	57.25	22.72
coal/water slurry 20 mg.	250 - 320	3.41	19.16
coal/water slurry 10 mg.	250 - 400	10.01	20.80
coal/water slurry 6 mg.	250 - 410	7.81	20.61
coal powder dried from slurry 10 mg.	250 - 360	1.03	17.30

Table 3

Critical mass of coal and coal water slurries for ignition

Surface Temperature °C	Critical mass mg		$\frac{M_{coal}}{M_{c\ slurry}} = M_c^*$	
	Coal	Coal/water slurry	Predicted	Experimental
200	19.01	6.69	2.85	3.30
220	4.90	2.20	2.22	
240	1.46	0.79	1.84	
280	0.16	0.13	1.23	
300	0.06	0.05	1.20	
320	0.01	0.02	0.50	

$^*M_c = \frac{\text{critical mass for ignition of coal}}{\text{critical mass for ignition of slurry}}$

REFERENCES

1. McHale, E. T., Scheffee, R. S., and Rossmeissl, N. P. (1982) Combustion and Flame 45, 121.

2. Fourth International Symposium on Coal Slurry Combustion, May 10-12, (1982), Proceedings, Vol. 1-4, held at Orlando, Florida.

3. Scheffee, R. S., Skolnik, E. G., Rossmeissl, N. P., Heaton, H. L., and McHale, E. T., "Further Development and Evaluation of Coal-Water Mixture Technology," Proceedings of Fourth International Symposium on Coal Slurry Combustion, May 10-12, (1982), Vol. 3, Orlando, Florida.

4. Ke-fa, Cen, Xin-yu, Cao, Ji-yu, Hong, Shui-yuan, Kong, Ming-Jiang, Ni, and Yun-Sien, Chen, "Experimental Study on Combustion of Coal-Water Slurry," Proceedings of Fourth International Symposium on Coal Slurry Combustion, May 10-12, (1982), Vol. 3, Orlando, Florida.

5. Germane, G. J., Smoot, L. D., Diel, S. P., Richardson, K. H., and Peterson, S. N., "Coal-Water Mixture Studies in a Laboratory Cylindrical Combustor," Proceedings of Fourth International Symposium on Coal Slurry Combustion, May 10-12, (1982), Vol. 2, Orlando, Florida.

6. Lin, Hao, "The Combustion Characteristics of Coal-Oil Mixtures and Coal-Water Slurry Under Low Heating Rate," Proceedings of Fourth International Symposium on Coal Slurry Combustion, May 10-12, (1982), Vol. 2, Orlando, Florida.

7. Pai Verneker, V. R. and Maycock, J. N. (1969) Anal. Chem. 40, 1325.

8. Semenov, N. N., Cited in the 'Physics of Combustion and Explosion,' (by L. N. Khitrin), Oldbroune Press, London (1965), p. 434.

9. Gross, D. and Amster, A. B., Eighth Symposium (Int.) on Combustion, p. 728 (1962) Williams and Wilkins: Baltimore.

10. Merzhanov, A. G. (1967) Combustion and Flame 11, 201.

11. Frank-Kamenetskii, D. A. (1965) Acta Phys. Chem. (USSR) 10, 365.

12. Chambre, P. L. (1952) J. Chem. Phys. 20, 1795.

13. Ren, Tsu Yi, "Ren's Liquidized Pulverized Coal," International Surfuel, Inc., January 1982.

FIGURE CAPTION

1. DSC curves of (A) coal/water slurry 50:50 weight %, 20 mg, (B) slurry heated up to 200°C, 20 mg, (C) the residue after heating up to 200°C, 10 mg and (D) coal powder, 10 mg.
2. Arrhenius plot of temperature-time data for coal and coal/water slurries.

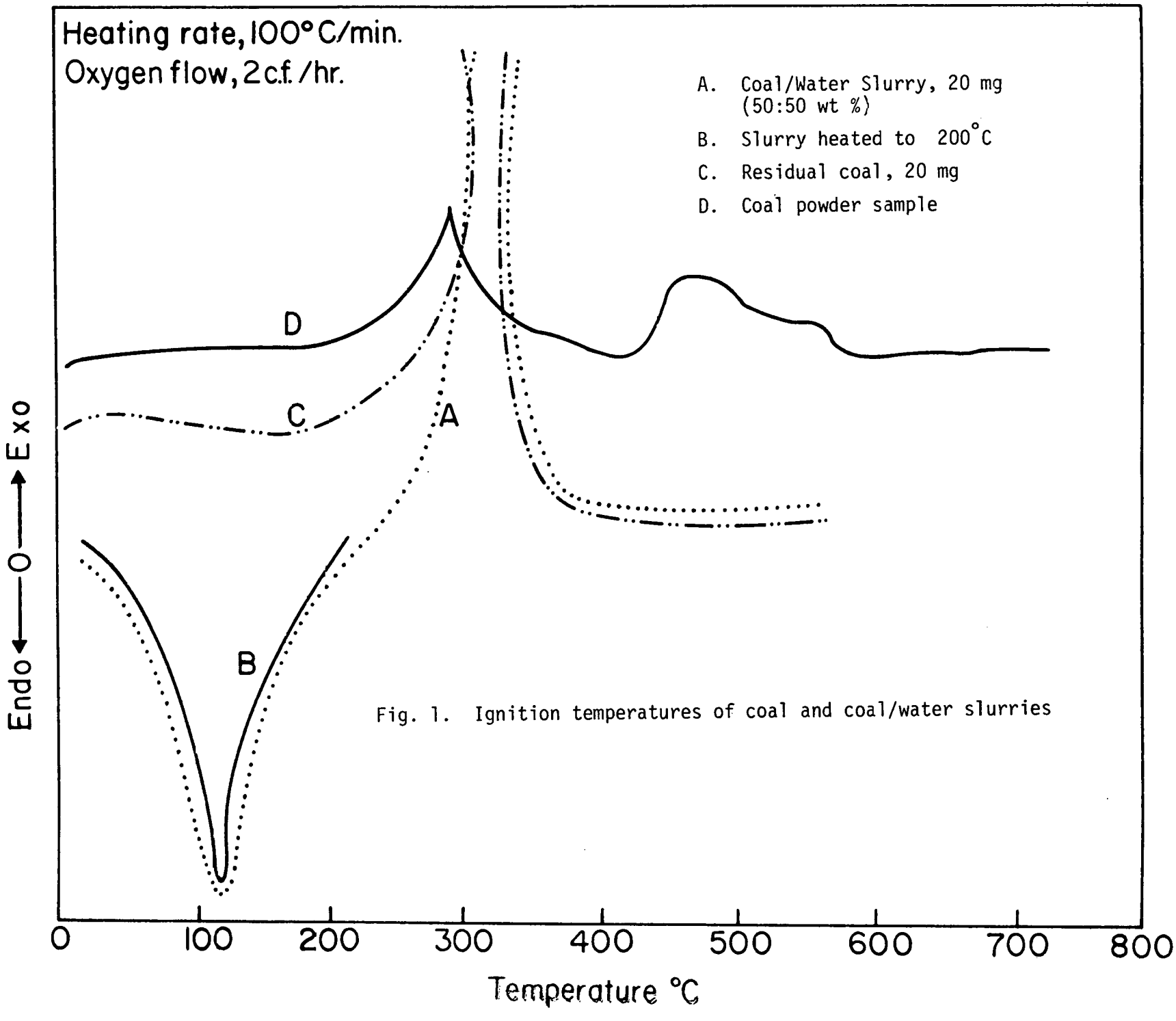

Fig. 1. Ignition temperatures of coal and coal/water slurries

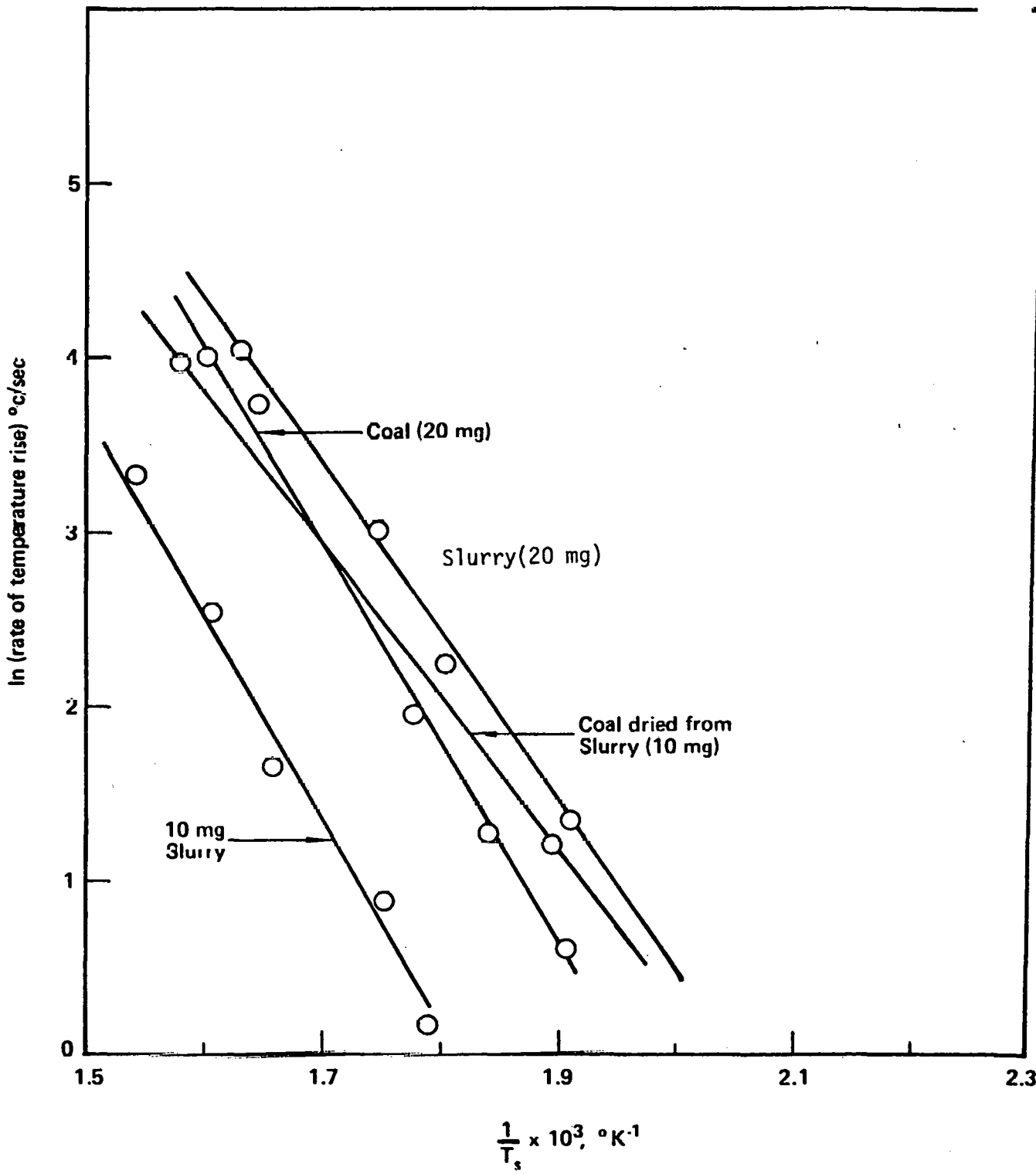

Fig. 2 Arrhenius Plot for Coal and Coal/Water Slurries

The following manuscript was unavailable at time of publication:

Co-Firing of CWS With Natural Gas

J. Dooher, T. Kanabrocki and D. Wright
Adelphi University

Experimental Study on Vaporization, Agglomeration and Combustion of Coal/Water Slurry Droplets

Cen Kefa Xie Minghu Ni Mingjiang Cao Xinyu
Yuan Zhenfu Huang Guoquan Lu Chongqing
Lu Deshou Chen Yunsien
Deparment of Thermophysical Engineering
Zhejiang University Hangzhou China

Introduction

In the previous paper of the authors[1] some experimental results about combustion properties of coal-water slurry (CWS) were reported. It was pointed out that under high environmental temperature the CWS droplets made of caking coal would form porous agglomerates, of which the burning process could be divided into three a little overlapping stages, i.e. water evaporation, devolatilization and residue coke combustion. In this paper some detailed information about these stages will first be reported. Then a brief discussion on the technological method of burning CWS in the fluidized bed combustor will be given.

Experiments and Analyses about Burning Process of CWS Droplets

1. Evaporation of Water

CWS is characterized by its high water content so the first thing we are interested in is the evaporating process of water and its influence on burning process.

According to D.B.Spalding,[2] evaporating rate and evaporating equilibrium temperature of a water droplet can be

expressed by

$$R_w = \frac{\lambda_m Nu}{2 C_{pm} \gamma_p} \ln\left[1 + \frac{C_{pm}(t_g - t_k)}{L - Q_r/4\pi\gamma_p^2 R_w}\right] \quad (1)$$

$$T_k = T_g - \left(\frac{L}{C_{pm}} - \frac{Q_r}{4\pi C_{pm} \gamma_p^2 R_w}\right)\left[\left(\frac{1 - C^{\infty}_{H_2O}}{1 - C^{s}_{H_2O}}\right) - 1\right] \quad (2)$$

Some experimental data about water evaporation of CWS droplets are compared with Eq·1 and Eq·2 in Fig1. Coal concentration of CWS used is 60% by wt. and diameters of droplets are about 2mm. The good agreement between experimental data and computed curves implies that for CWS droplets of which the size is not very big the influence of coal powder on evaporation of water is negligible and theoretical formulas like Eq·1 and Eq·2 can be used to estimate water evaporation of CWS directly.

Because the experiments have shown that diameter of CWS droplet does not change remarkably during water evaporation, we can simply use the following equation to compute evaporating time of CWS.

$$\tau = W G_0 / 4\pi\gamma_p^2 R_w \quad (3)$$

The computed curve is given in Fig2 along with some experimental results. We can see that Eq·3 predicts water evaporating time of CWS acceptably especially at high environmental temperature.

The Eq·1, Eq·2 and Eq·3 have been used to estimate water evaporating time of CWS droplets and results indicate that the evaporating time of a 100um droplet is 0.0074 sec. under 1400°C or 0.006 sec under 1600°C which is about 1.2-1.4% of the whole burning time of the droplet in the

furnace. Therefore with some measures to intensify ignition the flame length of CWS will not increase seriously.

As for the fluidized bed combustion, the water evaporating time is only about 0.05%–0.1% of the staying time of fuel in the bed. In addition the fluidized bed has great heat capacity. So the time occupied by water evaporation is not a problem at all.

2. The Release of the Volatile

After the evaporating of water in the CWS droplets, the temperature of droplets increase rapidly and the release process of volatile starts. Assuming that the release rate of all components in the volatile may be described as the form of the Arrhenius Law

$$\frac{dV_i}{d\tau} = K_{V0i} \exp\left(-\frac{E_{Vi}}{RT}\right)\left(V_i^f - V_i\right) \qquad (4)$$

then the total release rate is

$$\sum_i \frac{dV_i}{d\tau} = \sum_i K_{V0i} \exp\left(-E_{Vi}/RT\right)\left(V_i^f - V_i\right) \qquad (5)$$

By now the rule of release of various components has not been recognized, hence a synthesis expression for the reaction rate is adopted as follow

$$\frac{dV}{d\tau} = R_V = K_{V0} \exp\left[-E_V/RT\right]\left(V^f - V\right) \qquad (6)$$

Here, K_{V0} is the synthesis frequence factor, E_V represents the activation energy and V^f is the ultimate release amount,

Experiments show that the ultimate release amount greatly depends on the temperature. The relation between them is given in Table 1.

Table 1

tg °C		300	400	500	600	700	800	900	1000
V^{f*}	a	3.7	11.3	16.7	19.0	20.3	21.0	22.7	24.0
	b	6.7	10.0	25.3	27.0	28.3	29.7	30.3	30.8

* V^f (dried basis)

a Pindinsan coal

b Datong coal

The synthesis frequence factor K_{VO} and activation energy E_V of volatile are experimently determined for the CWS made of Chinese Pingdingsan bituminous.

$$K_{V0} = 12000 \quad 1/s$$

$$E_V = 17000 \quad kcal/mol$$

In general, the release process depands on not only the temperature but also some other physical factors such as the resistance as volatile flowing off. Therefore, a large deviation would arise if the release rate of volatile is estimated only by Eq·6. But, for CWS, the effect produced by such physical factors as flow resistance is not very remarkble, because many passages for volatile's flowing off have been formed during evaporation of water. The calculated data by Eq·6 is compared with some experimental results which is illustrated in Figure 3. It is clear that such formula as Eq·6 is approximately available for the release process of volatile of CWS.

3. Combustion of Coke

The reaction rate of coke is generally expressed by

$$R_c = \phi \rho_{O_2} k_c C_{O_2 S}^n \qquad (7)$$

where

$$k_c = k_{c0} \exp[-E_c/kT] \qquad (8)$$

For convenient we assume that the reaction order n=1. Then the reaction dynamic data for the CWS made of Pingdingsan bituminous coal is experimently determined (Fig 4), and the apparent reaction activation energy E_C=28000 Kcal/mol the apparent frequency factor K_{CO}=84000 m/s. The apparent activation energy of coke formed from CWS is 20% lower than that formed from the same coal. The reason is that the porous constitution is formed as water evaporating and then the inner reaction surface is enlarged.

Experiments also show that the ash layer on the outside of CWS coke influences the combustion rate of coke quitely. Suppose the ash layer is fairly well-distributed around the surface of coke, by the diffusion formula in sphere coordinate, we get

$$C_{O_2}^{S} = \frac{C_{O_2}^{\infty}}{1 + \frac{K_c}{\beta}\left(\frac{r_i}{r_p}\right)^2 + \frac{K_c (r_p - r_i)}{D_i} \frac{r_i}{r_p}} \qquad (9)$$

Here the diffusion coeffiecient D_i for oxygen diffusing through ash layer is highly related with the constitution of ash layer and simply expressed by

$$D_i = K_i D_0 \qquad (10)$$

where K_i is an index correction and equal to 0.15-0.18 for CWS made of Pingdingsan bituminous, and the value is higher than that of the raw coal, although both of them have the same kind of cosl. Obviously it is caused by the larger porousity of the ash layer of CWS.

4. The Dimeter Variation of CWS Droplets in the Combustion Process

When the CWS droplets are hung and burnt in air flow, its diameter variation is shown in Fig 5. It is shown that in the process of evaporation of water, its diameter expands slightly and the expansion is less 2%, while in the pro-

cess of the devolatilization and at the begining of coke combustion process its diameter contracts about 20%, then during the entire residue combustion process its diameter remains constant approximately. Therefore, for CWS flame, the coke combustion simply obeys

$$\gamma_p = \gamma_{p_0} \tag{11}$$

$$\rho_p = \rho_{p_0} (G_T/G_0) \tag{12}$$

But the diameter variation is very different when CWS droplets are burnt in F.B.C. Experiments show that for the CWS made of such coal of medium ash content as Chinese Pingdingsan bituminous, there is only a thin ash layer around the surface of coke during its combustion, due to the violent motion of bed materials and the scouring of air current. Therefore, the combustion process may be described with "the shrink Model". The diameter variation of CWS agglomerates burning in F.B.C. in various conditions is illustrated in Fig 6 and approxiamately obeys

$$d/d_0 = (G_T/G_{T_0})^{1/3} \tag{13}$$

in other words its density remains constant in the combustion process.

5. The Mathmatic Model for Combustion of CWS Droplets

Just as analysed above, we can make the following differential equations as the calculating model for the evaporation, devolatilization and combustion of CWS droplets.

$$\frac{dG_W}{d\tau} = -4\pi r_p^2 R_W \tag{14}$$

$$\frac{dG_V}{d\tau} = -R_V G_0 \tag{15}$$

$$\frac{dG_c}{d\tau} = -\frac{4\ r_{in}^2 R_c}{1-A} \tag{16}$$

$$\frac{dT_p}{d\tau} = \frac{3}{\rho_p C_p r_p}\left[R_c Q_c - h(T_p - T_g) - Q_r - L\ R_w\right] \tag{17}$$

the initial conditions

$$G_w|_{\tau=0} = G_{wo} \tag{18}$$

$$G_v|_{\tau=0} = G_{vo} \tag{19}$$

$$G_c|_{\tau=0} = G_{co} \tag{20}$$

$$T_p|_{\tau=0} = T_{po} \tag{21}$$

In Eq 14, the evaporation rate of water may simply discribed as Eq·22 istead of Eq·1, since the heat transfer condition is fixed in Eq·17.

$$R_w = \rho_{H_2O}\ \beta_{H_2O}\ (C^s_{H_2O} - C^\infty_{H_2O}) \tag{22}$$

Assuming that the surface of CWS droplets is in a equilibrium state of gas with liquid, with an appropriate gas-liquid equilibrium equation, we can relate the concentration of vapour at the surface with the temperature of droplets and combine with Eq·17 to get the solution of evaporation of water.

R_v in Eq·15 may be obtained from Eq·6.

R_c in Eq·16 may be determined according to Eq·7 and Eq·9.

The absorption amount of radiant heat is determined by different methods according to different combustion ways. In suspension combustion, the conduction and radiation heat transfer of volatile or CO flame to fuel should be considered, while in F.B.C., since the scouring of the bed materials is so violent that the flame around the fuel is not complete, only the radiation heat transfer is

assumed to be existed between fuel with bed, as the initial approxiamate.

Finally, we discuss the calculating of the convection heat transfer and mass transfer, Ranz-Marshall equation is used for suspension combustion, but it is not suitable for F.B.C. The authors' investigation on single particle heat transfer in fluidized bed shows that the practice convection heat transfer coefficient is much larger than that determined from the Ranz-Marshall equation. In this model the convection heat transfer and mass transfer coefficient are calculated according to the following equations

$$Nu = 18 + 126.3\, Re_p^{0.98}\, Pr^{0.33}\, (\gamma_p/\gamma_m)^{-1.47} \tag{22}$$

$$Sh = 18 + 126.3\, Re_p^{0.98}\, Sc^{0.33}\, (\gamma_p/\gamma_m)^{-1.47} \tag{23}$$

$$Nu = \frac{2 h \gamma_p}{\lambda_g (1-\varepsilon_b)} \tag{24}$$

$$Sh = \frac{2 \beta \gamma_p}{D_{ge}(1-\varepsilon_b)} \tag{25}$$

Considering the effect of bed materials to the mass transfer, we use the effective diffusion coefficient D_{ge} to estimate the sh number.

Owing to the limited experimental conditions, authors do not believe that Eq·22 and Eq·23 coule be used in the situation largely different from those experimental conditions, and the more perfect formula is been carrying out.

Upon the basic data obtained from the electric oven and the calculated results by this model, the curves of weight

loss and temperature variation of single CWS droplet burning in fludized bed together with experimental data are illustrated in Fig 7.

Discussion on Fluidized Bed Combustion of CWS

The operation stability is the main difficulty problem when CWS made of caking coal burns in F.B.C. In this case the diameter of bed material would increase and the big agglomerate would sediment constantly in the bed, and then disturb the fluidizing condition, and finally lead to the destruction of the fluidized condition. To resolve this problem some scholars suggest a method limitting the maxium diameter of droplet to decrease the formation of over large agglomerate. But it usually leads to larger elustration loss of combustible so that the combustion efficiency is decreased. Therefore the problem is not resolved still.

By analysis and comparation, authors suggest a techniqual process, i.e.operating with high density bed material and with no overflow. In this way, the fluidized bed composed of high density bed material has larger apparent density and appeares "the water static buoyancy" to the agglomerate of CWS so that the agglomerate would not sedimentate in the bed even if they enlarge to several ten millimeters. Upon it the larger diameter of droplets of feed may be used so that the advantage of agglomeration of CWS is more obvious and only a small amount of fine particles would be formed, therefore the elutriation loss of combustible is decteased remarkably and higher combustion efficiency is gained.

The operation way with no overflow is aimed at keeping the stability in character of bed materials. In usual

practice, the high density bed material will be gradu substituted by ash if the height of bed is remained by overflow while the bed material is not supplemented. But the operation way with no overflow does not lead to the increase of bed material limitedly. Experiments show that most of the ash of agglomerate of CWS is loose and they certainly would be worne by the scouring of bed material in volent motion and brought out of fluidized bed provided there is enough residence time. Moreover the high density bed material is not easy to be worne and will stay in the bed throughout. Thus the height and character of bed material rial can be kept in stability. Experiments prove that by this technological method high combustion efficiency ($>96\%$) and stable operation can be gained.

1. For CWS droplets with not too much big diameter, the effect of coal powder may be neglected while the known formula for evaporate rate of water may be adopted in the process determing the evaporation rate of water.

2. Since the passage, which is formed during the evaporation of water, is favorable for devolatilization, as the initial approximate, the release process of volatile may be estimated in the view of thermo decomposition dynamics but the physical factor may be neglected.

3. Owing to the porousity of coke of CWS, its apparent activation energy is higher than that of raw coal, although both of them have the same kind of coal. Thus the combustion process may be accelerated.

4. By the operating way with high density bed material and with no overflow for CWS burning in F.B.C., we can get

higher combustion efficiency and satisfactive operation stability.

Nomenclature

A ash content of coke

$C^{s}_{H_2O}$ water vapour concentration at surface

$C^{\infty}_{H_2O}$ water vapour concentration of surroundings

$C^{s}_{O_2}$ O_2 concentration at surface

$C^{\infty}_{O_2}$ O_2 concentration of surroundings

C_p specific heat capicity of droplet or particle

C_{pm} specific heat capicity of surroundings gas

D_{ge} effective diffusion coefficient in the bed

D_i diffusion coefficient in ash layer

D_o diffusion coefficient in gas

E_c activation energy of coke

E_v activation energy for devolatilization

E_{vi} E_v for i component

G total weight of droplet or particle

G_c coke weight in the particle

K_i corrective factor

K_{vo} frequence factor for devolatilization

K_{voi} frequence factor for devolatilization of i component

L latent heat

Q_c heating value of coke

Q_r heat transfered by radiation

R_c reaction rate of coke

r_i inner radius of ash layer

r_m radius of bed material

r_p radius of CWS particle release

R_v release rate of volatile

R_w evaporating rate of water

T_g temperature of gas

T_k equilibrium evaporating temperature

T_p temperature of particle

V release amount of volatile

V^f ullimate release amount of volatile

V_i release amount of i component

G_o initial weight of the particle

G_v volatile weight of the particle

G_w water weight of the particle

K_c reacting rate constant

β mass transfor coefficient

ε_b voidage of fluidized bed

ρ_p density of particle

τ time

V_i^f ultimate release amount of i component

W water content of CWS

h coefficient of convective heat transfer

K_{co} frequence factor of coke

β_{H_2O} mass transfor coefficient for H_2O

ρ_{H_2O} density of H_2O

ρ_{O_2} density of O_2

ϕ converting factor

Reference

(1) Cen Kefa et. al. "Experimental Study on Combustion Property of CWS" 4th Inter. Symp. on Coal Slurry Combustion Vol III.

(2) Spalding, D.B "Convective Mass Transfer" 1963.

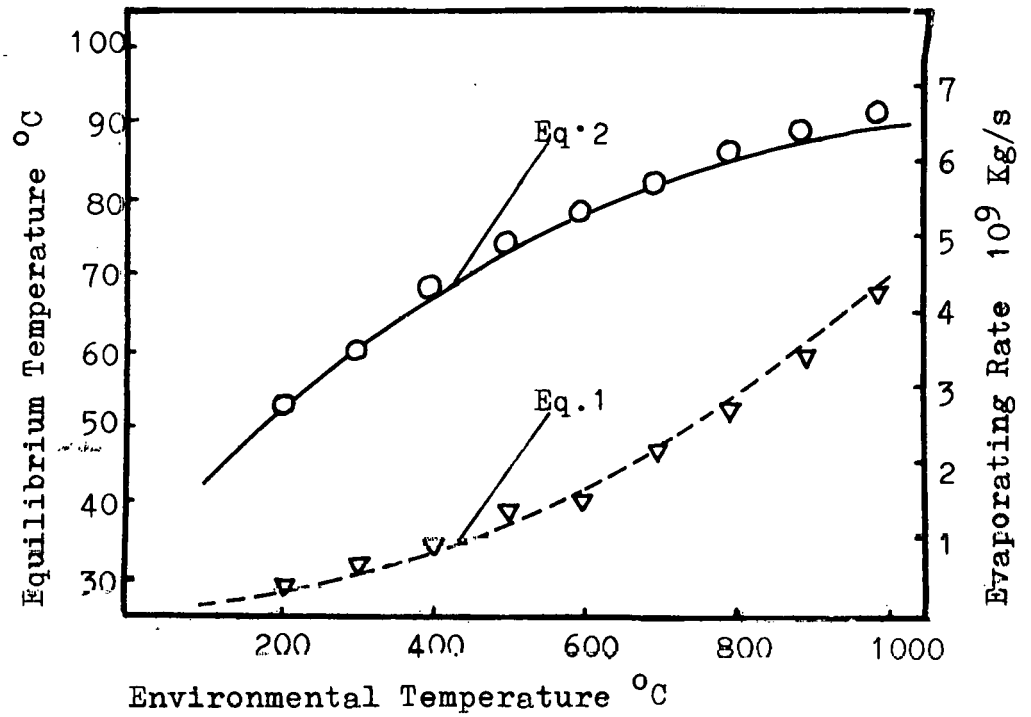

Fig.1 Water Evaporating Rate and Evaporating Equilibrium Temperature of CWS under Various Environmental Temperature

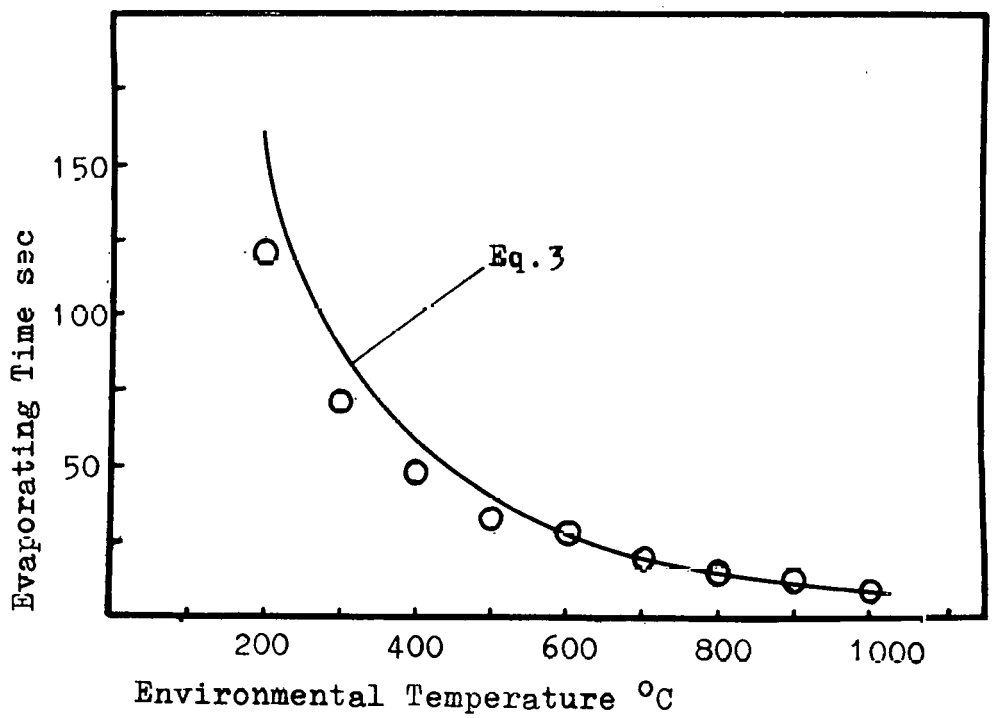

Fig.2 Water Evaporating Time of CWS under Various Environmental Temperature

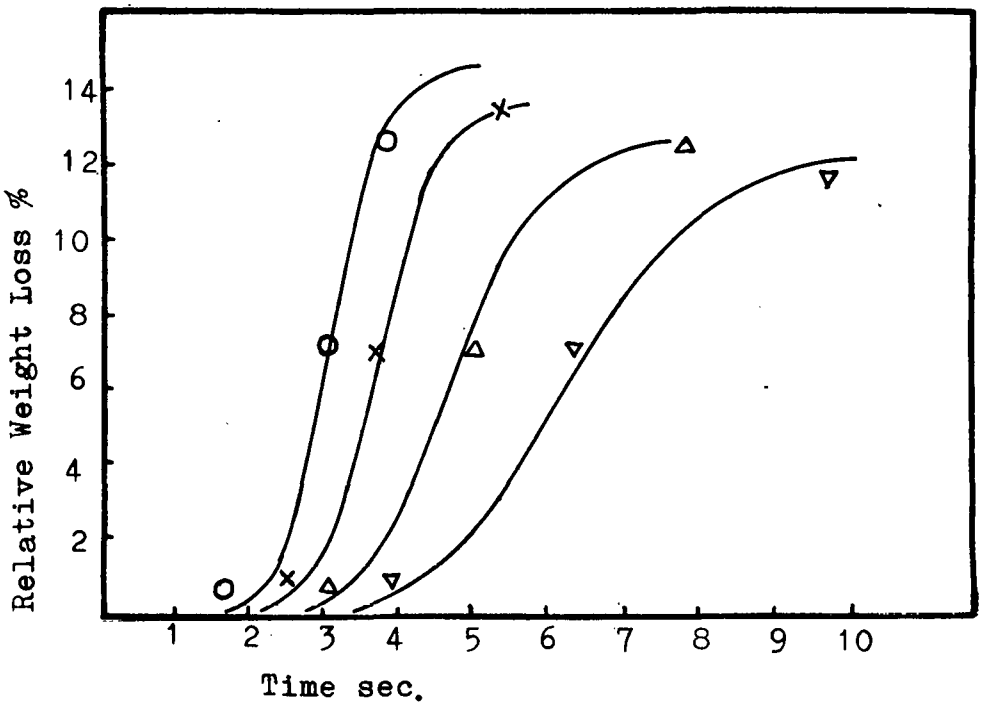

Fig.3 Devolatilizing Process under Various Environmental Temperature

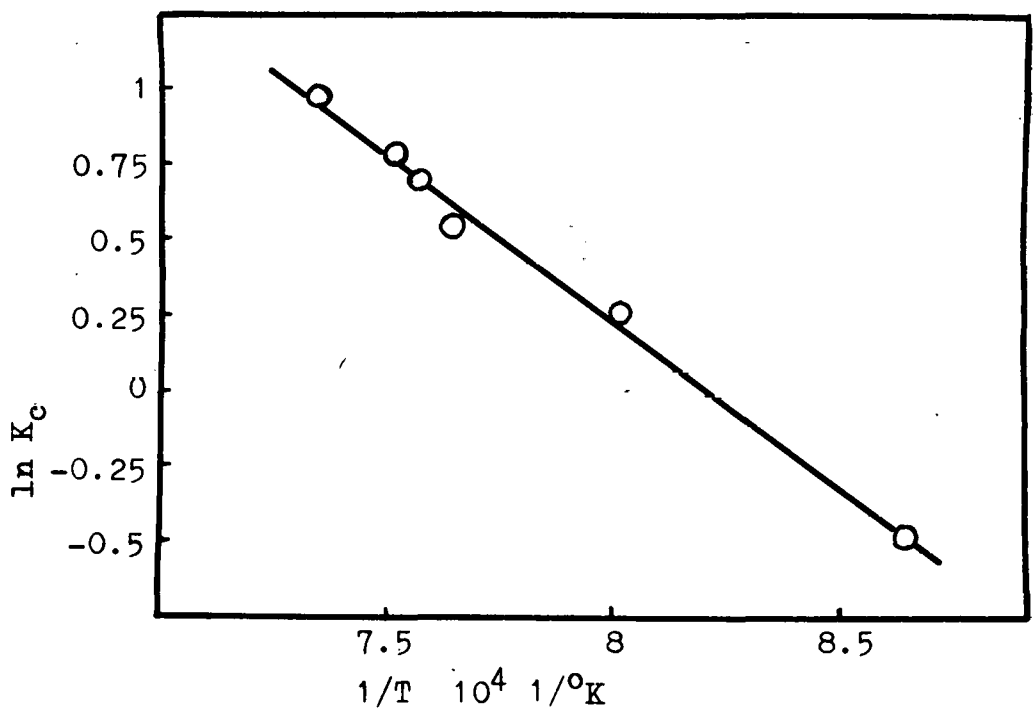

Fig.4 Determination of E_c & K_{co}

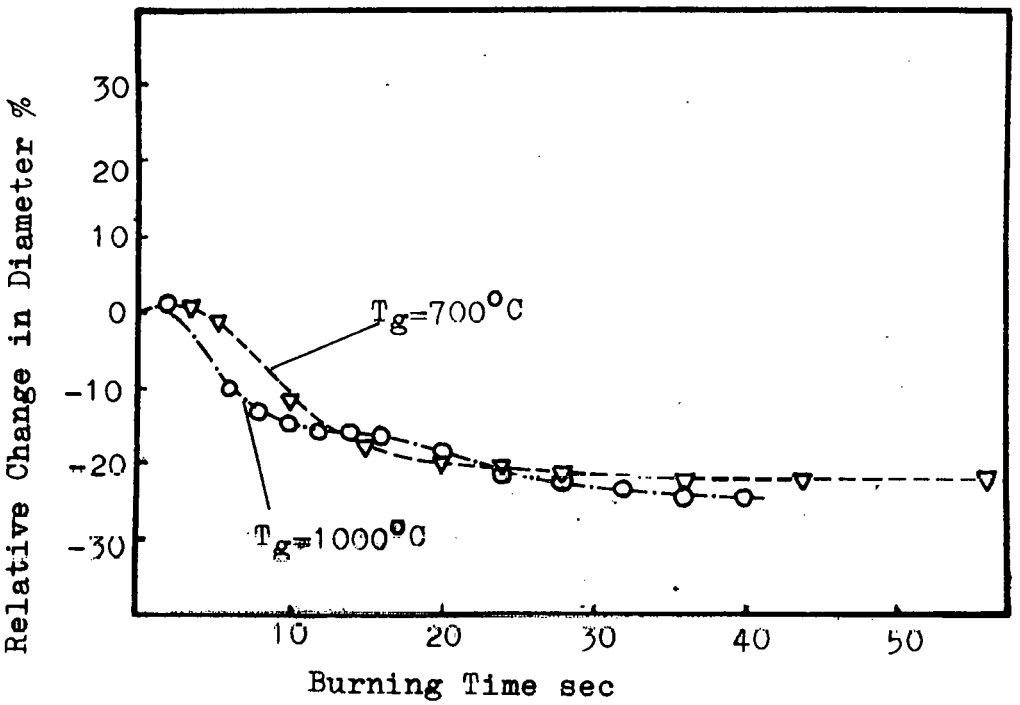

Fig.5 Variation of Droplet Diameter with Burning Time

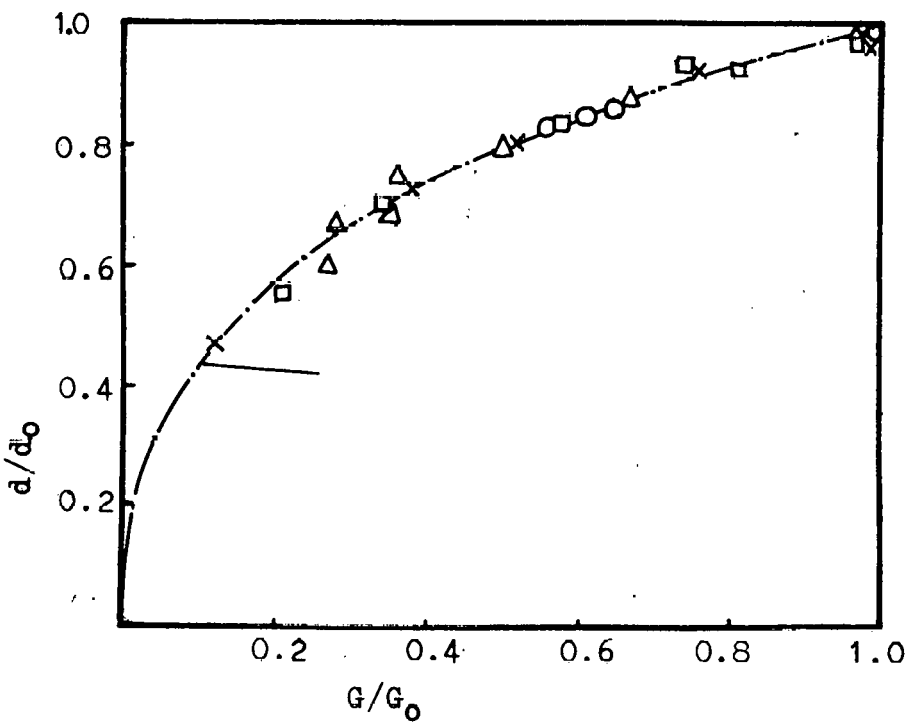

Fig.6 Relation Between (d/d_o) and (G/G_o) in the burning process

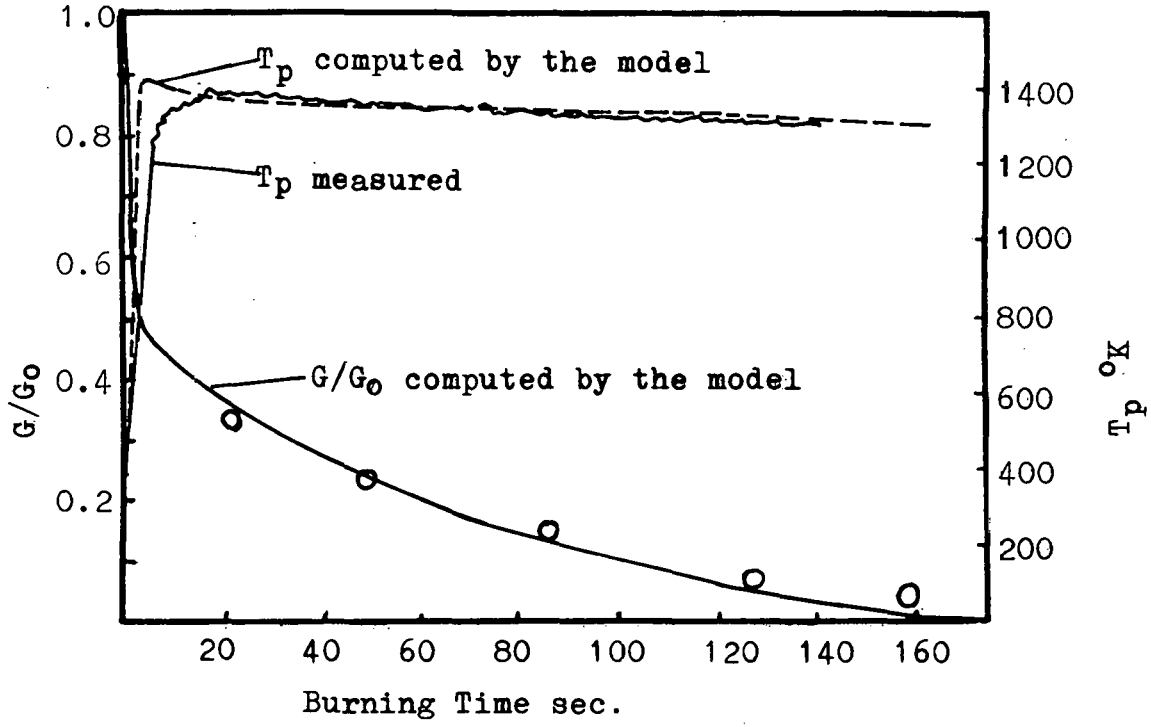

Fig. 7 Variation of T_p and G with Time
(G_o=20mg, T_b=1273°K)

Session X

RHEOLOGY AND CHARACTERIZATION

Wednesday, April 27, 1983

Chairman: Geoffrey Parfitt,
Carnegie-Mellon University

THE SPECIFIC VOLUME OF COAL SLURRIES IN AQUEOUS AND NON-AQUEOUS MEDIA

by

Robert L. Rowell
Department of Chemistry
University of Massachusetts
Amherst, Massachusetts 01003

Introduction

A thermodynamic approach to the determination of partial properties of binary mixtures is presented. We obtain the partial mass volume and the partial volume mass and derive the general relationship between volume fraction and mass fraction. Non-ideal mixtures with either or both components contributing to the non-ideal behavior are considered. The general application to coal slurries is discussed in order to illustrate the theory and to show how the theory may be used to examine kinetic effects, mixing effects and non-equilibrium effects in general.

Partial mass volume

In complete generality we may consider the volume to be a state function of mass and write

$$V = V(m_1, m_2) \qquad [1]$$

where m_1 and m_2 are the masses of components 1 and 2 that give a mixture of volume V. The mixture may be a true solution (uniphase), a two-phase system or even some more complicated state. We require only that the state properties be independent of time.

Since V is a function of two state variables we may write the total differential dV as

$$dV = \nu_1 dm_1 + \nu_2 dm_2 \qquad [2]$$

where ν_1 and ν_2 are the partial mass volume properties of components 1 and 2. The total differential may be integrated to obtain an expression for the relationship implied by equation [1].

$$\int_0^V dV = \int_0^{m_1} \nu_1 dm_1 + \int_0^{m_2} \nu_2 dm_2 \qquad [3]$$

If the integration is carried out at constant composition, then ν_1 and ν_2 are constants giving

$$V = \nu_1 m_1 + \nu_2 m_2 \qquad [4]$$

but, in general, ν_1 and ν_2 may depend on composition.

The total volume V is an extensive property which may be replaced by a more convenient intensive property such as the volume per unit mass of material or the mass-average volume defined by

$$v_{12} = V/(m_1 + m_2). \qquad [5]$$

In this way we obtain

$$v_{12} = \nu_1 x_1 + \nu_2 x_2 \qquad [6]$$

where x_1 and x_2 are the mass fractions of components 1 and 2.

By the law of conservation of mass x_2 and x_1 will always add up to 1 so that

$$v_{12} = \nu_1 + (\nu_2 - \nu_1)x_2. \qquad [7]$$

At constant composition, equation [7] gives a straight line so that a graph showing $v_{12}(x_2)$ possesses a tangent at the constant composition chosen with intercepts at 0 and 1 giving ν_1 and ν_2 respectively.

If ν_1 and ν_2 are constants, i.e. independent of composition at constant temperature, we may replace them by v_1 and v_2 which are the specific volumes of components 1 and 2. In this case, equation [4] reduces to

$$V = v_1 m_1 + v_2 m_2 \qquad [8]$$

which is a statement of volume additivity. We shall take the property of volume additivity as an essential property of an ideal mixture.

The foregoing concepts may be simply summarized in the schematic graph of Figure 1.

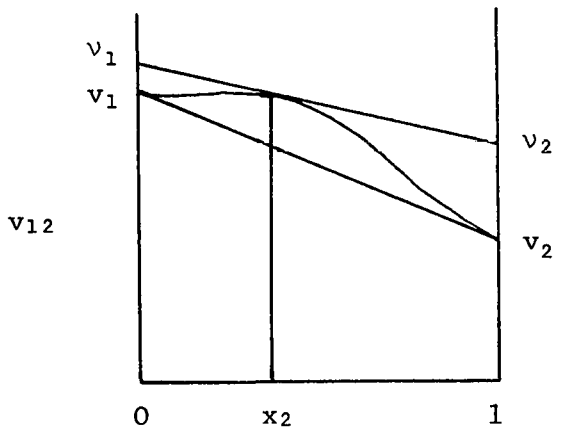

Fig. 1. Dependence of the mass-average volume v_{12} on mass fraction x_2 for ideal mixtures with specific volumes v_1 and v_2, and for non-ideal mixtures showing partial mass volumes ν_1 and ν_2.

Partial volume mass

Again, in general, we may consider the mass of a system to be a state function of the volumes V_1 and V_2 of components 1 and 2.

$$m = m(V_1, V_2) \qquad [9]$$

Writing the expression for the total differential in the form

$$dm = \rho_1 dV_1 + \rho_2 dV_2 \qquad [10]$$

introduces the partial differential coefficients ρ_1 and ρ_2 so that $\rho_1 = \partial m/\partial V_1$ is the partial volume mass of component 1 and ρ_2 is the similarly defined partial volume mass of component 2. In general ρ_1 and ρ_2 may be functions of the composition of the system.

The total differential may be integrated to give the explicit state function

$$\int_0^m dm = \int_0^{V_1} \rho_1 dV_1 + \int_0^{V_2} \rho_2 dV_2. \qquad [11]$$

Consider the special case at constant composition where ρ_1 and ρ_2 are

constants to obtain

$$m = \rho_1 V_1 + \rho_2 V_2 \qquad [12]$$

Now V_1 and V_2 are extensive state variables which may be replaced by the more convenient intensive state variables ϕ_1 and ϕ_2, the respective volume fractions i.e. $\phi_1 = V_1/V$. Note that the volume fractions may be defined solely with respect to the total volume V which is independent of any statement about the additivity or non-additivity of volumes. In this way, [12] becomes

$$\rho_{12} = \rho_1\phi_1 + \rho_2\phi_2 \qquad [13]$$

where $\rho_{12} = m/V$ is the volume-average mass or density of the mixture. Clearly, the density of the mixture may be regarded as the volume average mass whether or not the property of volume-additivity holds.

Since the whole is equal to the sum of its parts, $\phi_1 + \phi_2 = 1$ and [13] may be rewritten as

$$\rho_{12} = \rho_1 + (\rho_2 - \rho_1)\phi_2 \qquad [14]$$

If the whole is the sum of its parts and the volume of the whole is independent of composition then we have volume additivity and the partial volume masses ρ_1 and ρ_2 become the densities of the separate components d_1 and d_2, i.e.

$$d_{12} = d_1 + (d_2 - d_1)\phi_2 \qquad [15]$$

We conclude that the system density is a linear function of the volume fraction for ideal mixtures as given by [15] and the partial densities or partial volume mass properties ρ_1 and ρ_2 may be determined from the tangent drawn at constant composition in a plot of $\rho_{12}(\phi_2)$ as shown by [14].

The foregoing concepts are illustrated in Figure 2.

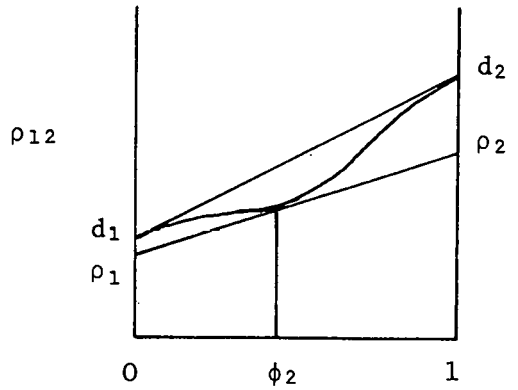

Fig. 2. Dependence of density ρ_{12} on volume fraction ϕ_2 for ideal mixtures with densities d_1 and d_2 and for non-ideal mixtures with partial densities or partial volume masses ρ_1 and ρ_2.

Relationship between volume fraction and mass fraction

We have shown that in ideal mixtures the density is a linear function of volume fraction while the specific volume of the mixture is a linear function of mass fraction. We have also shown that in any mixture at a single constant composition the partial densities and partial specific volumes (partial volume masses and partial mass volumes) can be obtained from straight lines, i.e. tangents. It is also clear that if v_{12} (x_2) shows a positive deviation, then ρ_{12} (ϕ_2) will show a negative deviation and vice versa. It is of interest to obtain a general relation between ϕ_2 and x_2 which is valid for both ideal and non-ideal systems.

We begin by obtaining x_2 from [7]

$$x_2 = (v_{12}-v_1)/(v_2-v_1). \qquad [16]$$

Since $v_{12} = 1/\rho_{12}$, $v_1 = 1/\rho_1$ and $v_2 = 1/\rho_2$, independent of composition we may substitute and obtain

$$x_2 = [(\rho_{12}-\rho_1)/(\rho_2-\rho_1)][\rho_2/\rho_{12}] \qquad [17]$$

Then from [14] we obtain an expression for ϕ_2

$$\phi_2 = (\rho_{12}-\rho_1)/(\rho_2-\rho_1) \qquad [18]$$

which turns out to be the first factor in [17] so that the general relation becomes

$$\phi_2/x_2 = \rho_{12}/\rho_2 \qquad [19]$$

It is clear that the calculation of ϕ_2 at a known x_2 requires the mixture density ρ_{12} and the partial density or partial volume mass of component 2 at the mass composition x_2.

If components 1 and 2 form an ideal mixture then ρ_{12} is independent of composition and reduces to d_{12} while ρ_2 becomes constant and equal to d_2 giving

$$\phi_2/x_2 = d_{12}/d_2 \qquad [20]$$

It is easy to show that alternative forms of [19] may be written in terms of the partial properties of the components as

$$\phi_2 = 1/(1+x_1\rho_2/x_2\rho_1) \qquad [21]$$

and

$$\phi_2 = 1/(1+x_1\nu_1/x_2\nu_2) \qquad [22]$$

Binary mixtures with one ideal component

The preceding formal arguments constitute a general approach but it is important to point out the nature of the analysis required when one component is ideal. We assume that component 1 is ideal and that all deviations from ideality occur by reason of changes involving component 2. For this case, equations [7] and [14] reduce to [23] and [24] respectively.

$$v_{12} = v_1 + (\nu_2-v_1)x_2 \qquad [23]$$

$$\rho_{12} = d_1 + (\rho_2-d_1)\phi_2 \qquad [24]$$

The results are also straight lines as shown in Figures 3 and 4 for v_{12} and ρ_{12} respectively. In this case, we note the important point that the straight lines are not tangents to the experimental non-ideal curves but are always drawn through a point on the curve and through the ideal intercept, either v_1 or d_1.

In this way, an experimental knowledge of v_1, and v_{i2} at x_2 allows determination of ν_2 from [23], as illustrated in Figure 3. Furthermore, ϕ_1 can be computed from ρ_{12} and ρ_1 at x_1 from the same data, using the component-1 counterpart of [19]. With ϕ_1 known, one can obtain ϕ_2 from $\phi_2 = 1-\phi_1$ which holds at x_2 independent of volume

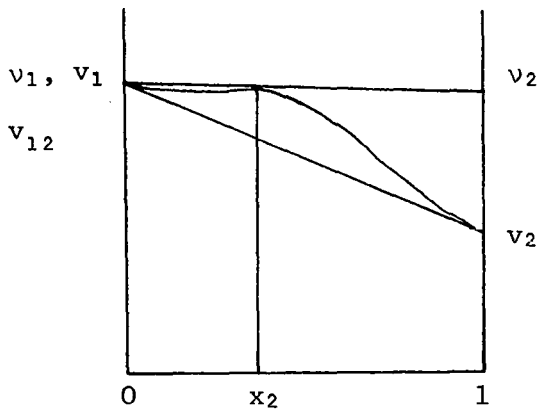

Fig. 3. Dependence of the mass-average volume v_{12} on mass fraction x_2 for ideal mixtures, straight line from v_1 to v_2, and for non-ideal mixtures with component 1 ideal, straight line from v_1 to ν_2.

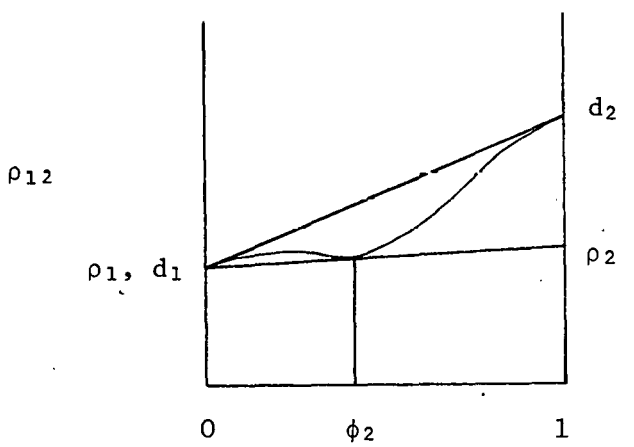

Fig. 4. Dependence of the density ρ_{12} on volume fraction ϕ_2 for ideal mixtures, straight line from d_1 to d_2 and for non-ideal mixtures with component 1 ideal, straight line from d_1 to ρ_2.

additivity. Since $\rho_{12} = 1/v_{12}$ and ϕ_2 has been obtained, one can compute ρ_2 from [24] which, of course, must be equal to $1/v_2$.

Application to coal slurries

The theory is of general application to binary mixtures at constant temperature so that coal-oil mixtures and coal-water slurries are merely particular applications.

The theory is offered as a general framework for the study of binary mixtures which may include other components in amounts sufficiently small that the expressions [1] or [9] may be used within the degree of approximation acceptable.

It is suggested that the partial mass properties obtained from v_{12} (x_2) be regarded as the more fundamental since x_2 is unambiguously measurable. It has been shown how ρ_{12} (ϕ_2) can be computed from v_{12} (x_2).

The theory may be applied to non-ideal mixtures in which either or both components contribute to the non-ideality. We have shown the treatment required when one of the components is ideal and the other component is non-ideal. In order to test and determine if one component is ideal, one needs an independent measurement of the activity of that component such as might be obtained by measurement of a characteristic intrinsic property such as the vapor pressure.

The time dependence of v_1 and v_2 can be measured to check for kinetic effects, mixing effects etc. It is clear that non-equilibrium effects can be measured and identified as a prelude to understanding.

Acknowledgement

The subject of coal slurry fuels has been supported in our laboratory for several years, initially by the New England Power Service Company, then by the Electric Power Research Institute and currently by the Atlantic Research Corporation. Partial support has also come from Gimret and AB Carbogel. The major part of the theory presented above has come to fruition largely through the support of the Atlantic Research Corporation (ARC) and the many stimulating discussions held with my own students and with the ARC research group.

RHEOLOGY AND PUMPING CHARACTERISTICS OF COAL-WATER SLURRY FUELS PREPARED IN A COLUMBIA CHASE INTEGRATOR

Sushil K. Batra
Robert B. Kenney
GIMRET International, Inc.
415 Boston Turnpike Road
Shrewsbury, MA 01545

Austin O'Toole
Columbia Chase Corporation
Holbrook, MA 02343

ABSTRACT

Coal-water slurry (CWS) are potential fuels for replacement of fuel oil in oil fired boilers. These fuels offer several advantages over the use of solid coal in these boilers as CWS fuel can be transported, stored and burned similar to heavy fuel oil and requires minimum modifications and space. CWS fuels containing 65-70% (by weight) coal offer considerable cost savings over oil with substantially reduced conversion cost.

For designing storage and pumping systems for CWS fuels, it is most important to evaluate the characteristics of these fuels. The paper presents the results of test program and reviews the characteristics of CWS fuels prepared with various coal particle size distribution utilizing a Columbia Chase Integrator. A mixture of coal, chemical additive and water prepared externally is passed through the Integrator to enable thorough mixing and enhance stability of the mixture. Stability and rheology characteristics observed will be reported with varying coal concentrations. Also, the CWS prepared in a pilot plant was pumped through a test loop at varying flow-rate and temperature. The pumping characteristics of the CWS fuel are also reported in the paper.

INTRODUCTION

Due to the recent push to cut down the dependency on imported oil, interest in the use of coal and coal derived fuels has been increasing. Both industrial users and utilities are working towards substituting oil with a plentiful and less expensive boiler fuel-coal. At some plants, however, conversion to burn solid coal may not be practicable due to the short operating life of the equipment, lack of space for coal storage and handling facilities or high capital cost of conversion. In view of these factors, there has been great enthusiasm for the development of coal-water slurry (CWS) fuel. Use of CWS in oil-fired design boilers provides an opportunity to burn coal with minimum requirements of space at the user's site and minimum boiler modifications.

One of the attractive features of the use of CWS fuels for industrial applications is that the use of oil is completely eliminated. CWS fuel can be prepared off-site and transported to and stored at the user's site like fuel foil. The additional space and equipment required at the plant site is therefore minimal. CWS fuels can be pumped and burned like liquid fuels with minimum expense for retrofitting the existing installation.

In order to have reliable operation of the plant with the CWS fuel, it is most essential to understand the characteristics of the fuel with respect to storage, handling and combustion. The paper reviews the results of a test program to investigate the physical characteristics of the CWS fuels. The various factors affecting the stability and rheological characteristics of the CWS fuels are presented and the data obtained in the test program is given.

TEST PROGRAM

The characteristics of CWS fuel vary with the type of coal, coal particle size distribution, and the chemical additives used in the preparation of the fuel. The test program included three types of coal wity varying particle size distribution and chemical additives. The characteristics of the various CWS fuel samples prepared in a Columbia Chase Integrator (C.C.I.) were evaluated. The coal concentration in the CWS fuel was varied to study the effect of coal concentration on the stability and pumpability of the CWS fuel. Also, selected samples of CWS fuels were prepared and tested in a pumping test loop in order to determine the effect of pumping on the CWS characteristics. The coal particle size distribution of the various samples was determined. Also, the CWS fuels were characterized through testing the viscosity at varying shear rates and

determining their stability with respect to settling of coal particles. Various concentration and classes of chemical additives, found successful in a laboratory test program, were used in the preparation of the CWS fuel test samples in the pilot plant.

CWS fuel for the test program was prepared in a pilot plant utilizing the C.C.I. and the chemical additives identified in an extensive laboratory test program for providing stability and pumping characteristics. Figure 1 shows the flow diagram of the CWS fuel preparation pilot plant facility. Coal is ground in a ball and race pulverizer with nominal 85 wt.% coal passing through 200 mesh (75 microns) and mixed with the coal having size distribution plus 100 micron, in various proportions, as necessary. The chemical additive package is dispersed in water maintained at 80°F-90°F, depending upon the nature of the chemical additives used. The pre-dispersion is then mixed by means of a variable speed Lightnin Mixer installed in the mixing tank. After thorough mixing of the chemical additives, the coal is added gradually in the mixing tank. The coal-water slurry is mixed thoroughly, first by mixing with the mixer, and then supplementing with circulation of the slurry through the C.C.I. The C.C.I. mixing process imparts a uniform consistency to the CWS fuel and creates an effective dispersion.

COAL ANALYSIS

Table 1 shows the Proximate Analysis of three types of coal tested in the test program. These coals contained varying amount of Volatile Matter and Fixed Carbon and were obtained from Pittsburgh Seam and West Virginia. These coals were selected on the basis of a laboratory test program in which it was observed that for highly loaded coal water slurries, with coal concentration of 70 weight percent or higher, Bituminous coals were most suitable.

CHEMICAL ADDITIVES

The characteristics of the CWS fuels are greatly affected by the chemical additives used in their preparation. These chemical additives help reduce aggregation of coal particles and impart fluidity for a given coal and the particle size distribution. The various chemical additives tested in the laboratory prior to preparation of the CWS fuels in the pilot plant are given in Table 2. Based on the laboratory tests, both the anionic and non-ionic class of chemical additives were studied in detail in a pilot plant. Besides certain non-ionic chemical additives, combination of two additives, a deflocculant and a non-ionic polymer, which

build a gel structure, provided desirable characteristics of CWS fuels.

COAL PARTICLE SIZE DISTRIBUTION

Coal particle size distribution is the most important factor in determining the maximum loading of coal in the CWS fuel, and it affects both the stability and the rheological characteristics of the CWS fuel. The coal particle size was, therefore, varied to study the optimum distribution to provide good stability and pumping characteristics. The coal particle size was determined by a L & N Microtrac Particle Size Analyzer. Figure 2 shows the particle size analysis of Coal A, which was pulverized to 88% less than 75 Micron. Figure 3 gives the typical coal particle size distribution after blending coal A and Coal B (with particle size distribution 48% + 75 Micron, 100%-170 Micron). Several blends were prepared to study the effect of particle size distribution.

In view of the increased interest in the micronized coal-water slurries (MCWS) by the utilities, coal was ground to 95-98 percent -44 Microns and the slurries were prepared utilizing the C.C.I. The characteristics of the MCWS were determined and are also reported here-under.

CHARACTERISTICS OF CWS FUELS

Several samples of CWS fuel were prepared varying the particle size distribution of coal and the chemical additive package used for providing desirable stability and viscosity characteristics. The stability characteristics were determined until the CWS fuel settled into a hard-packed state. The stability criteria used in determining the sedimentation characteristics are:

- Coal settling at the bottom
- Type of settling; loose, compact
- Remixing potential
- Supernatant water at the top
- Fluidity

The viscosity of the samples was determined using a Brookfield RVTD viscometer and the various LV and RV spindles depending on the viscosity of the fuel. Viscosity measurements were made at various spindle revolutions to simulate the pumping conditions.

The rheological properties of the CWS fuels are very important for designing the pumps, piping system, valves, etc. Also these properties determine the feasibility of long distance transport to the user's facilities as well as ease of atomization in the burner during combustion. Also, viscosity of the various samples was determined at varying shear rates, using a Small Sample Adapter.

The coal particle size distribution in the CWS fuels prepared with 62 weight percent, 65 weight percent and 70 weight percent coal concentration are shown in Figures 4,5 and 6 respectively.

The stability characteristics of three typical CWS fuels are given in Table 3.

Rheological properties of various CWS fuels were determined as above and are shown in Figure 7, 8, and 9 for various coal concentrations and additive packages. The use of chemical additives greatly affects the rheology of the CWS fuels. As shown, with the proper choice, the apparent viscosity of the CWS fuel can be reduced considerably. Also, the effect of concentration of coal on the apparent viscosity can be controlled with proper choice of additive.

Figure 7 shows the viscosity characteristics of two slurries with nominal 62 weight percent coal with two different chemical additive packages. The slurry with additive package GIM-9 exhibited superior viscosity characteristics but did not remain as a stable mixture. Although the slurry with additive package GIM-8 was more viscous, its stability characteristics were very good and the fuel remained stable for over six weeks.

Unlike the previous case, the slurry with the best viscosity characteristics in the 65 weight percent coal range also exhibited the best uniformity and stability. Figure 8 illustrates the viscosity characteristics of four slurries in that coal concentration range. It is clearly shown in Figure 8 that the slurry containing the chemical additive package GIM-22 has better viscosity characteristics especially in the low RPM (and low shear rate) range. This slurry also remained stable for approximately four weeks.

Figure 9 gives the viscosities of some of the slurries prepared in the nominal 70 weight percent coal concentration range. In this range, the slurry containing additive package GIM-22, again, resulted in the best stability characteristics. However, this slurry also exhibites the most viscous behavior as compared to the other slurries represented in Figure 9.

It may be noted that all the slurries prepared in the program behave similarly in one aspect. In all the different coal concentration categories the slurries behaved in a pseudoplastic manner, i.e. the viscosity decreased with the increase in shear rate.

COAL-WATER SLURRY TEST LOOP

A coal-water Slurry Test Loop installed at the Columbia Chase Corporation, Holbrook facility was used for preparation and pumping of coal-water slurries to evaluate pumping characteristics.

The coal-water slurry Test Loop consists of a CWS fuel mixing tank together with an agitator, a recirculating pump and a C.C.I. with a test section about 50 ft. long with bends and tee connections. A schematic of the Test Loop is given in Figure 10. A gear pump with a capacity of about 60 g.p.m. was used for pumping the CWS fuel in 1½ inch and 2 inch diameter piping system. Several pressure and temperature gauges were installed at various locations in the Test Loop to assess the pressure drop characteristics.

Two CWS fuels, one with 65 wt.% coal concentration and another with 68 wt.% coal concentration, were prepared in the test loop. Both of these CWS fuels were circulated through the Test Loop and the flow-rate as well as pressure drops along the four main sections of the Loop were observed and recorded. The flow rates of the CWS were varied from 11 gpm to 46 gpm.

Samples of the CWS fuel were taken at each flow rate and tests were carried out to determine the stability, viscosity and particle attrition characteristics. The procedures for these tests were the same as for the CWS fuel prepared in the pilot plant.

The samples of both the pumped slurries i.e. 65 wt.% and 68 wt.% exhibited good stability characteristics for over 4 weeks. No significant settling of coal particles was observed. Also, the slurries showed excellent consistency, with no supernatant water separation.

Figures 11 and 12 show the viscosity characteristics of 65 wt.% and 68 wt.% CWS fuels at various flow rates through the pumping loop. The tests were carried out beginning with a high flow rate and the flow-rate was reduced gradually. As expected, the CWS fuel containing 68 wt.% coal has a higher viscosity than did the slurry containing 65 wt.% coal. Both slurries behaved in a pseudoplastic manner at low shear rates i.e. the viscosity decreased with increased shear rate. At higher shear rates, however, the viscosity was constant. Both the slurries increased in viscosity during the prolonged pumping in the Test Loop.

The particle-size attrition during the pumping operation of 65 wt.% and 68 wt.% CWS fuels is shown in Figures 13 and 14 respectively. A gradual particle size attrition was noted as the CWS fuels were pumped through the Test Loop over a period of time. The extent of particle size attrition was greater for the 68 wt.% CWS fuel than for the 65 wt.% CWS fuel.

Figure 15 shows the pressure drop characteristics of the two CWS fuels tested in the Test Loop. The pressure gradient of the 65 wt.% CWS fuel has linear characteristics indicating a laminar flow over the velocity range tested. For 68 wt.% CWS fuel, the pressure gradient increased with an increase in the velocity. Also, it was observed that the pressure gradients were about 15-25 percent higher in case of 68 wt.% CWS fuel than those for 65 wt.% CWS fuel.

MICRONIZED COAL-WATER SLURRY (MCWS)

In view of the increased potential of derating of oil or gas designed boilers, while burning conventional pulverized coal, in dry form or in a slurry, in which the coal is ground to a size distribution of 70/80 percent less than 200 mesh (74 Microns), there has veen increased interest in utilities to examine the use of micronized coal. Recent tests carried out at the Babcock and Wilcox test facility show that the derating may be reduced considerably by use of micronized coal in which the coal particle size is less than 325 mesh (44 Microns). Results from their test program indicated that the ash deposition rate is less for micronized coal than for pulverized coal. Also, the fly-ash from micronized coal has a finer particle size distribution and the deposits were easily removable by soot blowing with air. The micronized coal not only increased the rate of burning but it is also expected that there is less deposition and slagging in the furnace tubes, resulting in higher efficiency and reduced derating of the boiler.

The coal pulverized in a ball and race pulverizer was micronized using a jet mill in which compressed air is introduced through specially designed nozzles. Figure 16 shows the particle size distribution of coal. The coal was ground to 98 percent passing through 325 mesh (44 Micron) with a mass mean diameter of 8 microns.

The MCWS fuel was prepared in the pilot plant at Holbrook facility using the Micronized coal and GIM-22 additive package. The procedure for making the MCWS fuel was similar to that described for preparation of the CWS fuel.

CHARACTERISTICS OF MCWS FUEL

The stability characteristics of MCWS fuel was determined over a period of time. No coal settling or water separation was observed for over 8 weeks of storage of this fuel. The fuel has been extremely stable, with no sedimentation or supernatant water separation.

Although limited testing was performed with the MCWS fuel, a very interesting observation was made with regard to its

viscosity characteristics. The viscosity of the samples was determined using a Brookfield Viscometer and a Small Sample Adaptor. Viscosity measurements were made for both the MCWS fuel prepared in the laboratory and in the pilot plant, at various shear rates to simulate pumping conditions. The rheological properties of the MCWS fuel are shown in Figure 17, for a nominal 68 weight percent coal concentration and 0.6% GIM-22 additive package. The major difference in the characteristics of the two samples shown in Figures 17 is the method of preparation. Whereas the laboratory sample was prepared using a high shear laboratory Mixer, the MCWS fuel was prepared in the pilot plant using the Columbia Chase Integrator. It will be observed that both the laboratory sample and the pilot plant sample behave in a similar manner as far as the rheological characteristics are concerned, and the rate of decrease of viscosity with the increase of shear rate is same. The sample prepared in the pilot plant with the use of the C.C.I., however, exhibits much lower viscosity in the range of the shear rate tested.

Figure 18 shows the rheological characteristics of 70 wt.% MCWS fuel prepared in the pilot plant using the C.C.I. The viscosity at a shear rate of approximately 10 Sec^{-1} is on the order of 700 cps.

Figure 19 shows the effect of varying temperature on the viscosity of the MCWS fuel. The MCWS fuel sample containing 68 wt.% coal was tested using a Small Sample Adapter in a Brookfield RVTD Viscometer. The viscometer was set at a shear rate of 9.3 Sec^{-1}, equivalent to 10 rpm. Tests were carried out at temperatures varying from 60°F to 110°F. It was observed that the MCWS fuel sample exhibited a decrease in viscosity as the temperature was increased, the viscosity varying from 645 cps at 60°F to 440 cps at 100°F. At a temperature beyond 100°F, evaporation of the sample was noted.

In order to simulate the freezing conditions during the storage and pumping of MCWS fuel, freeze/thaw tests were carried out on a sample. After freezing the sample, containing 68 wt.% coal, for about 12 hours, the sample was thawed in a warm water bath for about one hour. The sample was checked both for stability and rheological characteristics, after remixing. The stability of the sample was checked over a period of four weeks. No coal settling was observed in the process and the MCWS fuel exhibited excellent stability during the freeze/thaw process. The viscosity of the sample before and after the freeze/thaw process was observed at varying shear rates and is shown in Figure 20. It was observed that the sample after freeze/thaw process exhibited a higher viscosity than the sample before freezing. The shape of the viscosity/shear rate curves in both the cases was similar to each other.

CONCLUSIONS

From the results of the pilot plant and the pumping test loop test programs, it is concluded that stable and pumpable CWS fuels can be formulated with high coal concentration by proper selection of the chemical additives, and use of Columbia Chase Integrator .

The rheological properties of the CWS fuels are very dependent upon the rank of coal, particle size distribution and the type of chemical additive used in the preparation of CWS fuel. The data presented in this paper would be useful for comparative purposes and also for understanding the relative influence of these variables on the rheological properties of CWS fuels.

The rheograms obtained in the program exhibit a profound pseudoplastic behavior, with very low yield stress at low shear rates. Also, the effect of varying the temperature on the viscosity of the CWS fuel was found to be minimal.

In general, the anionic and non-ionic class of chemical additives along with the C.C.I. provided desirable stability and viscosity characteristics required for long term storage, pumping and atomization of CWS fuels for combustion.

Micronized Coal-Water Slurry fuels prepared using the chemical additives and C.C.I. were found to be very stable with practically no settling and no supernatant water separation during the test program.

Although limited testing was performed on the rheological characteristics of MCWS fuel, the viscosities were observed to be much lower than the CWS fuels having the same concentration of coal and prepared with the same chemical additives.

Similar to the CWS fuels, the MCWS fuel behaved in a psudoplastic manner.

REFERENCES

1. Batra, S.K., et al, "Stability and Rheological Characteristics of Coal-Water Slurry Fuels", Proc. 8th International Technical Conference on Slurry Transportation, San Francisco, CA, March 15-18, 1983.

2. Morris, T.A., et al, "Micronized Coal Alternative Fuel for Oil Gas Fired Boilers", Proc. 5th International Coal Utilization Exhibition & Conference", Houston, Texas, December 7-9, 1982.

3. Donnelly, Richard G., "Formulation, Handling & Combustion Characteristics of Coal-Water Mixtures", Proc. 5th International Coal Utilization Exhibition & Conference, Houston, Texas, December 7-9, 1982.

4. Batra, S.K. and Batra, R.K., "Characterization of Coal-Water Slurry Fuels for Utility and Industrial Boilers", Proc. Coal Technology Europe '82 Conference, Copenhagen, Denmark September 22-24, 1982.

5. Naka, Akihiro, et al, "Development of Additive for High-Content Coal-Water Slurry", Proc. Fourth International Symposium on Coal Slurry Combustion, Orlando, Florida, May 10-12, 1982.

6. Batra, S.K., "Use of Coal-Oil and Coal-Water Mixtures for Industrial Fuels", Deutsche Glastechnische Gesellschaft E.V. Hanover, West Germany, February 17, 1982.

7. Batra, S.K., "Coal-Water Mixture Technology State-of-the-Art Report", GIMRET International, Inc., January, 1982.

8. Scheffe, R.S., et al, "Development and Burning of coal/Water Slurries", Proc. Third International Symposium on Coal-Oil-Mixture Combustion, Orlando, Florida, April 1-3, 1981.

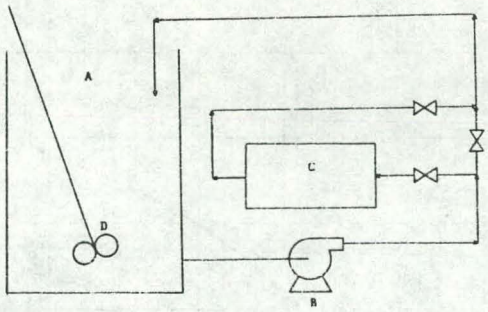

Figure 1. Schematic of CWS Pilot Plant

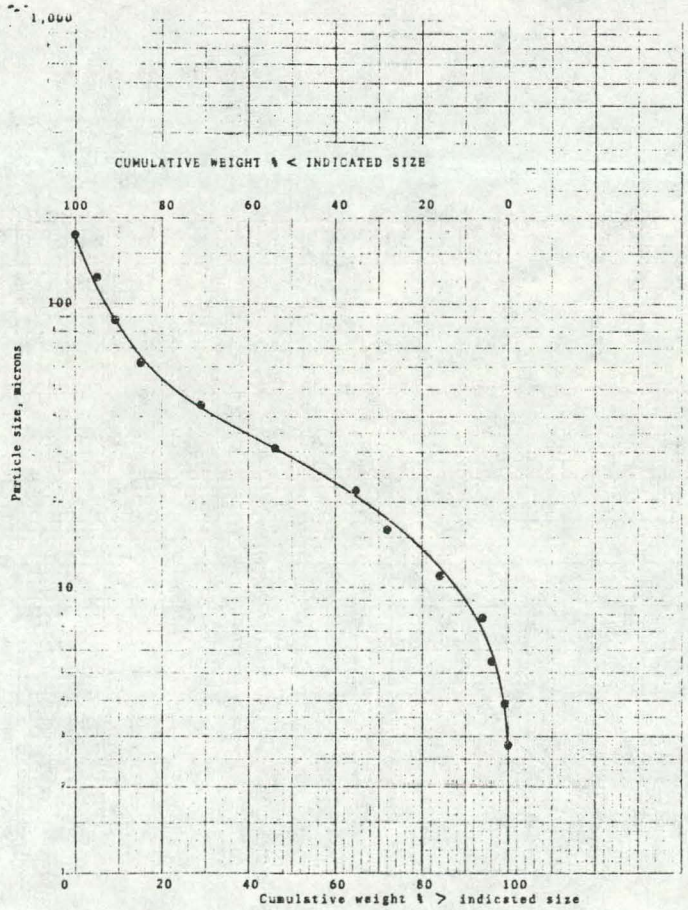

Figure 2. Particle Size Analysis "A" Coal

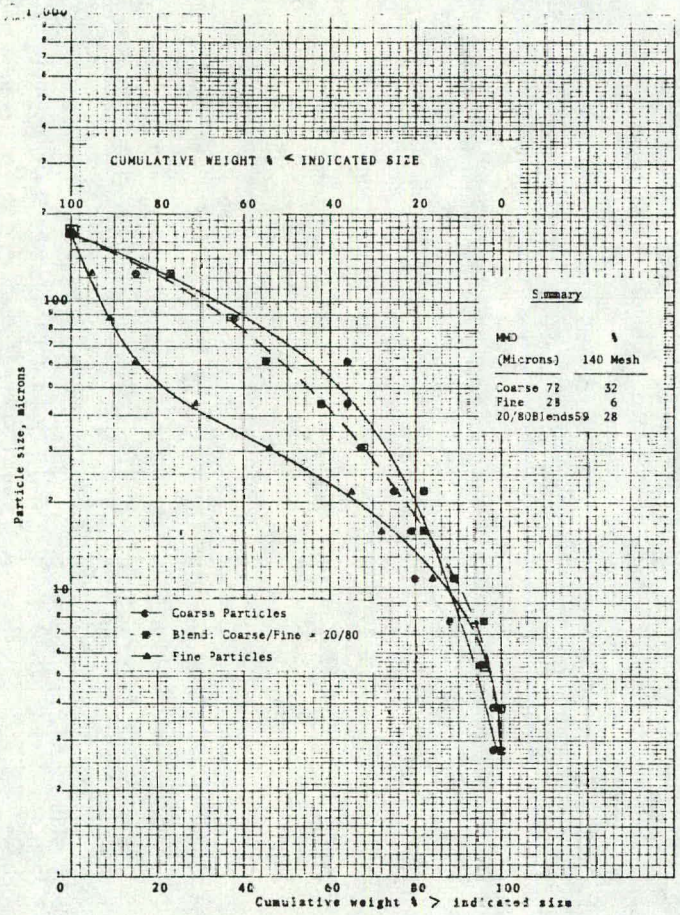

Figure 3. Effect of blending on coal Particle Size Distribution

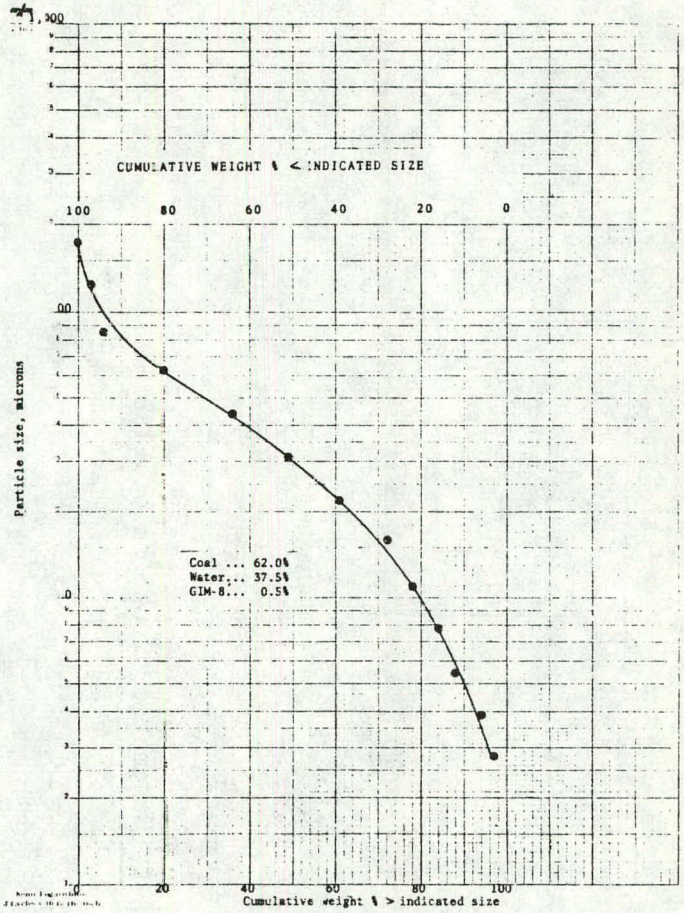

Figure 4. Particle size Distribution of Nominal 62 Weight % CWS

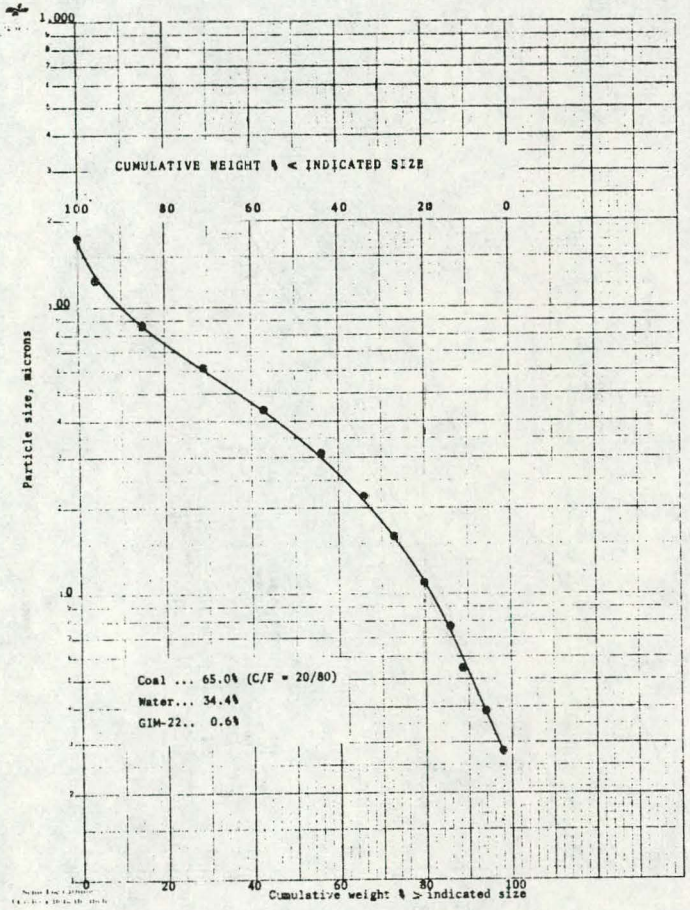

Figure 5. Particle Size Distribution of Nominal 65 Weight % CWS

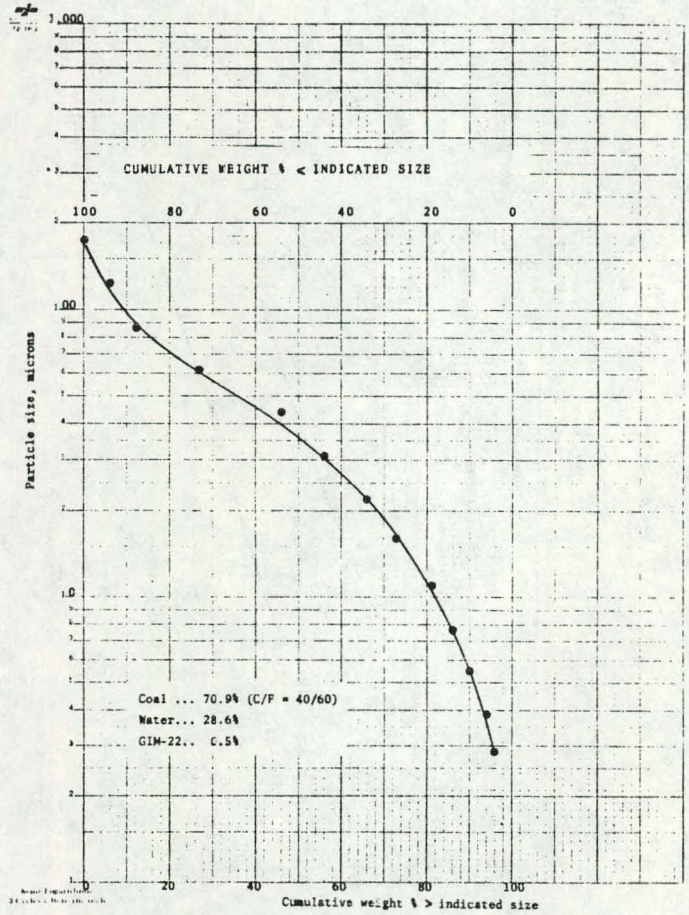

Figure 6. Particle Size Distribution of Nominal 70 Weight % CWS

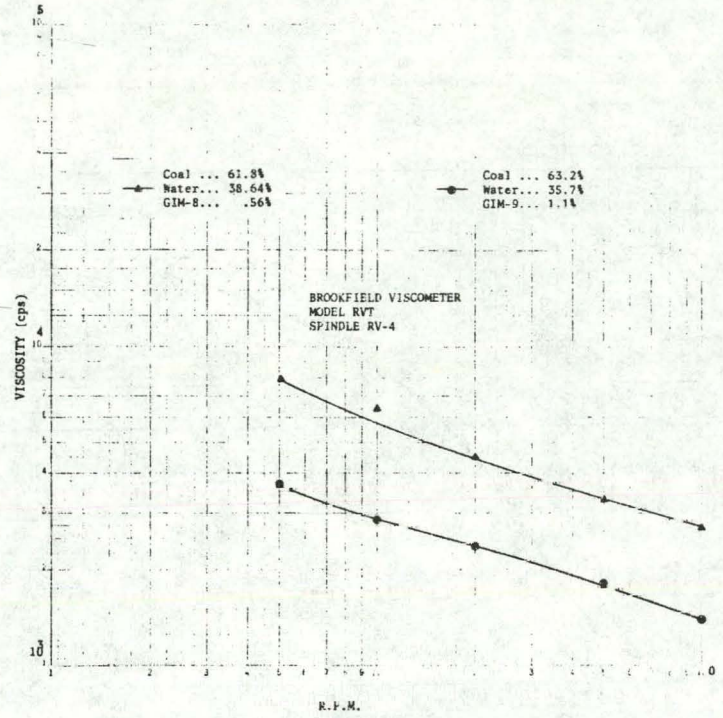

Figure 7. Effect of Chemical Additives on the Viscosity Characteristics of Nominal 62 Weight % CWS Fuels

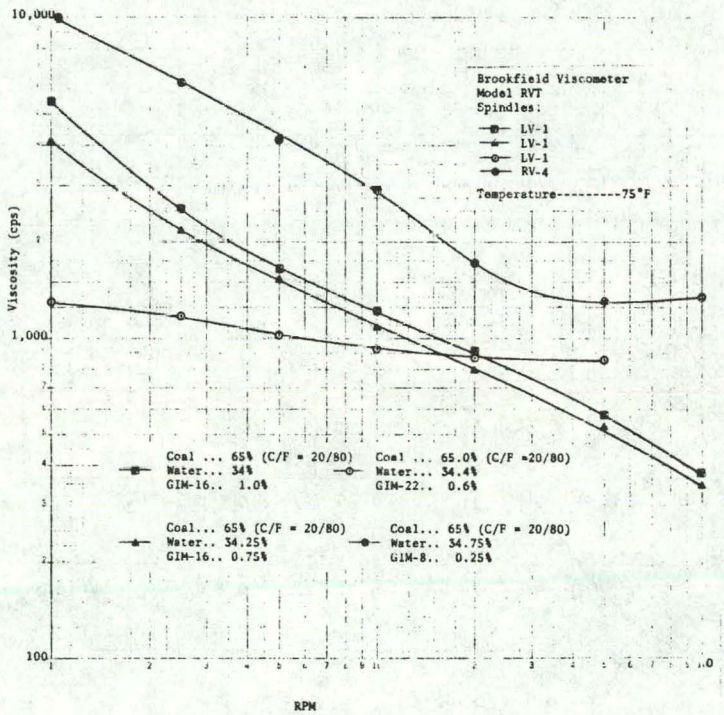

Figure 8. Effect of Chemical Additives on the Viscosity Characteristics of Nominal 65 Weight % CWS Fuels

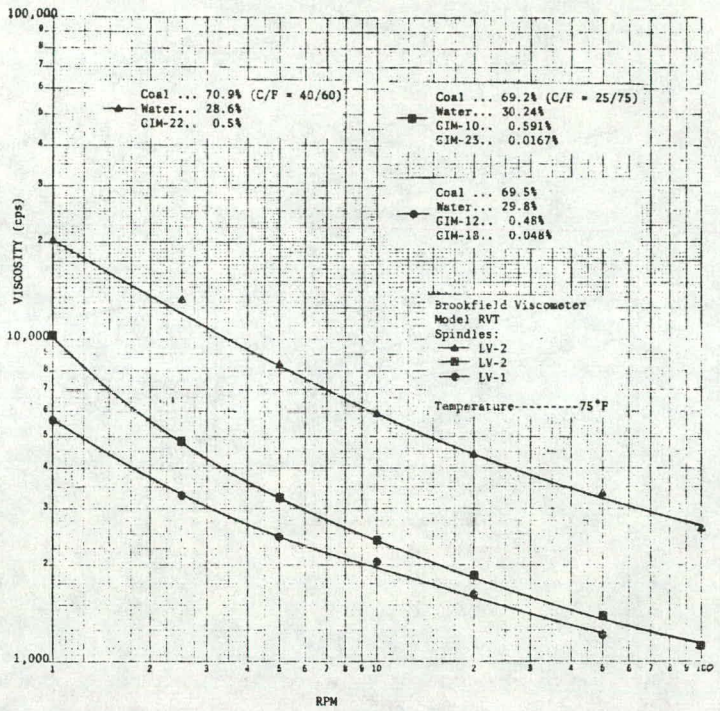

Figure 9. Effect of Chemical Additives on the Viscosity Characteristics of Nominal 70 Weight % CWS Fuels

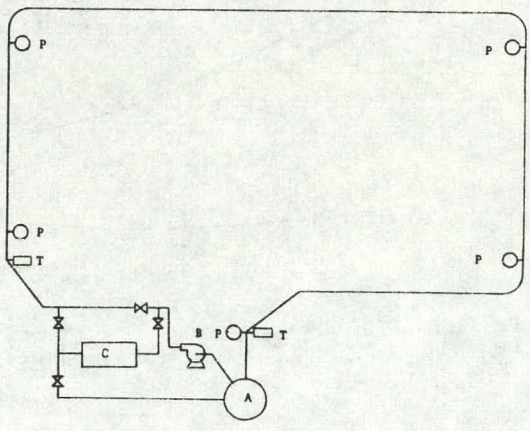

A- Mixing Tank P- Pressure Gauge
B- Pump T- Thermometer
C- Columbia Chase Integrator (C.C.I.)

Figure 10. Schematic of CWS Pumping Test Loop

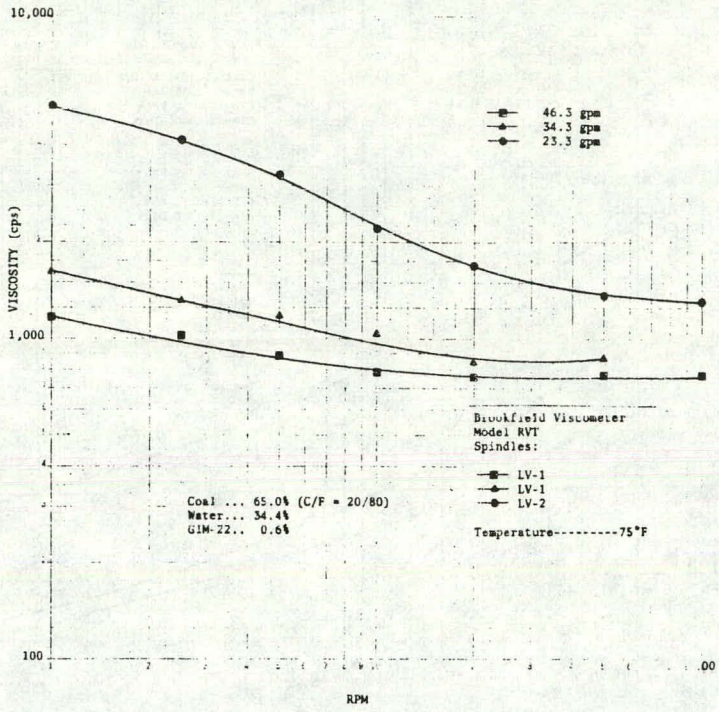

Figure 11. Effect of Pumping on Viscosity of Nominal 65 Weight % CWS Fuel

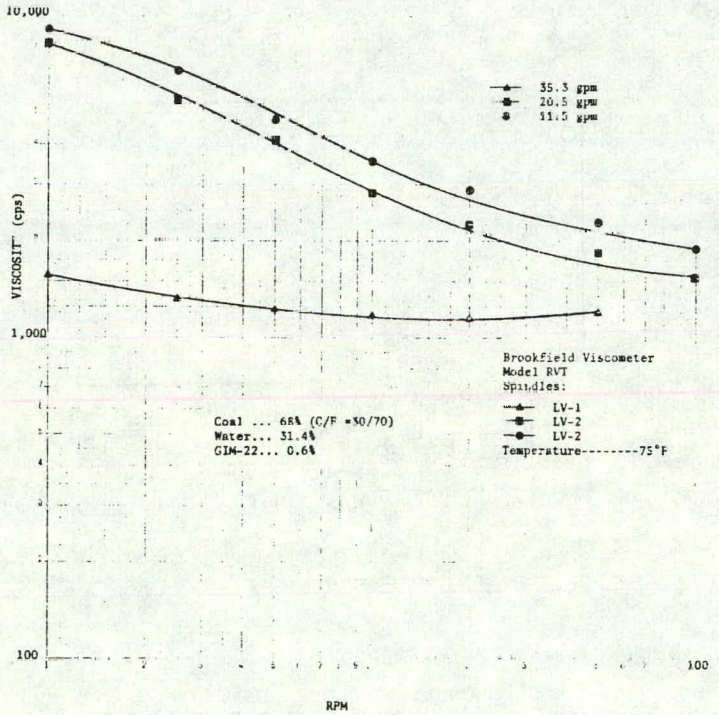

Figure 12. Effect of Pumping on Viscosity of Nominal 68 Weight % CWS Fuel

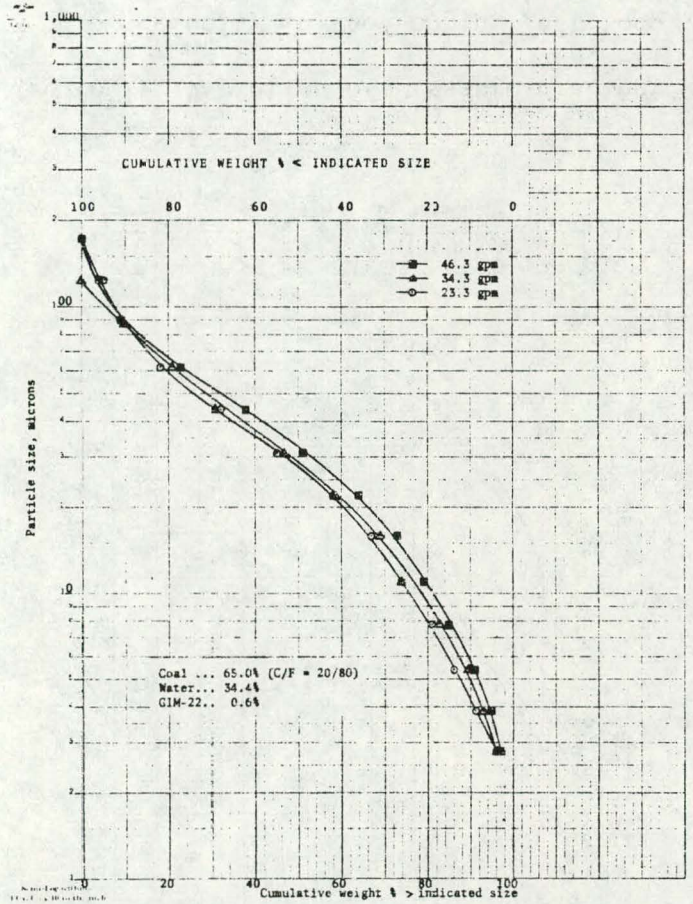

Figure 13. Effect of Pumping on Coal Particle Attrition of Nominal 65 Weight % CWS Fuel

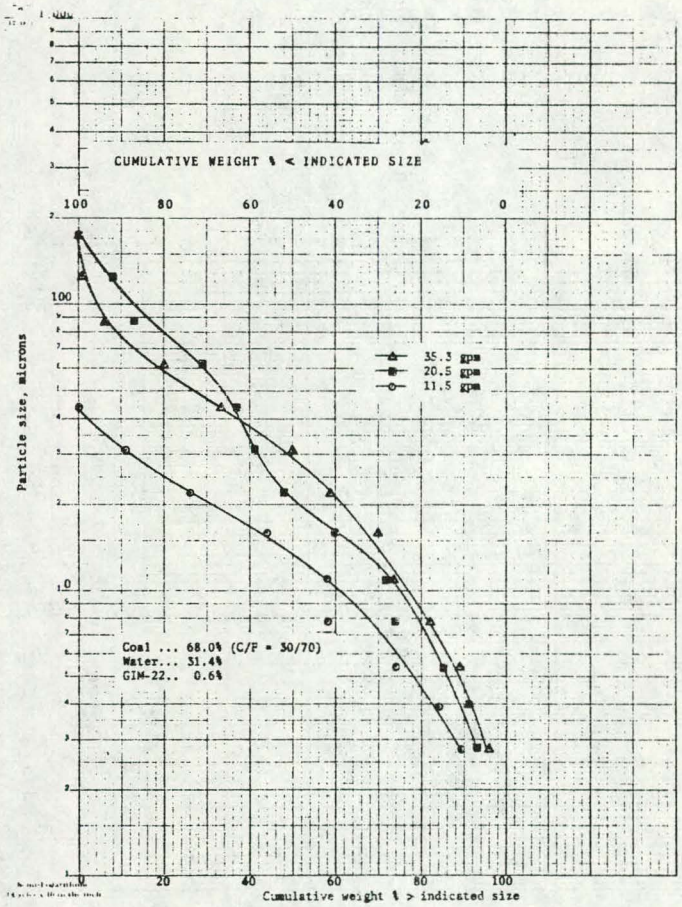

Figure 14. Effect of Pumping on Coal Particle Attrition of Nominal 68 Weight % CWS Fuel

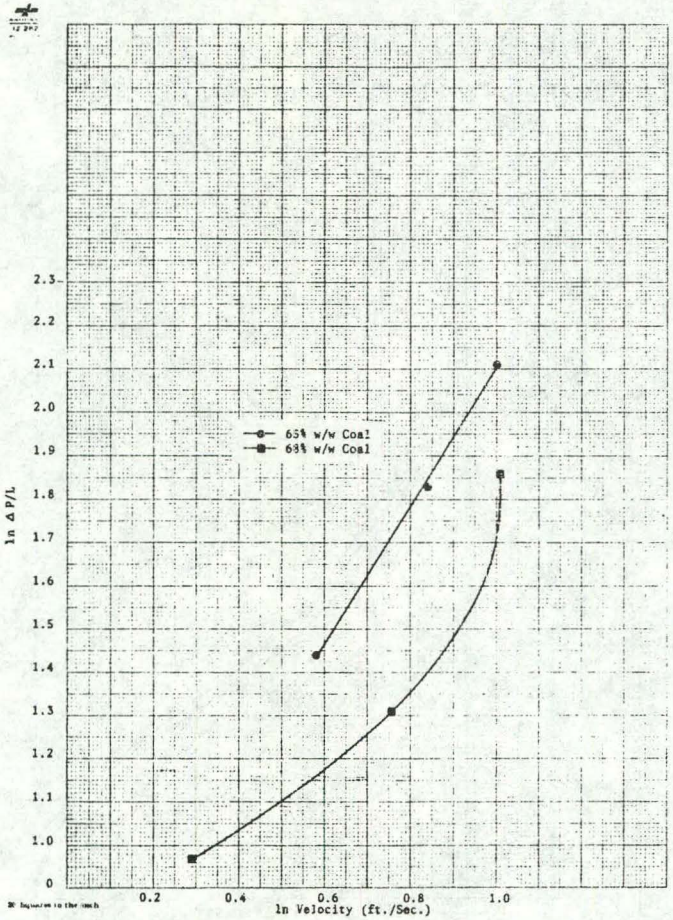

Figure 15. Variation of Pressure Gradient with Flow Velocity in the Pumping Test Loop

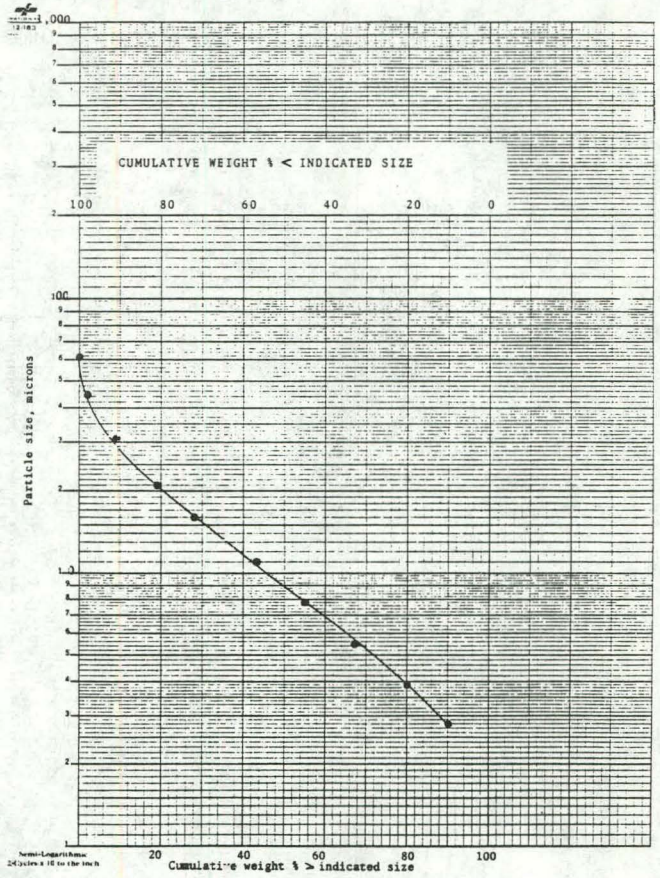

Figure 16. Particle Size Distribution of Micronized Coal

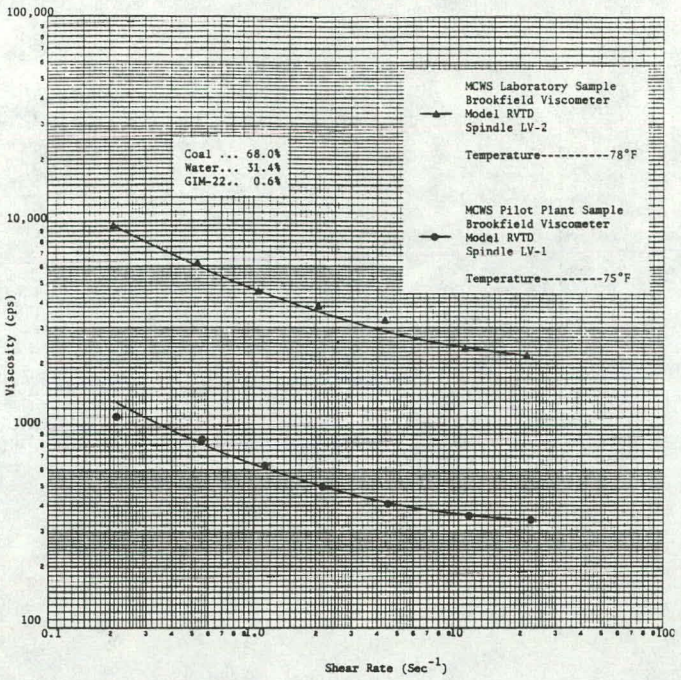

Figure 17. Viscosity Characteristics of 68 Weight % MCWS Fuel

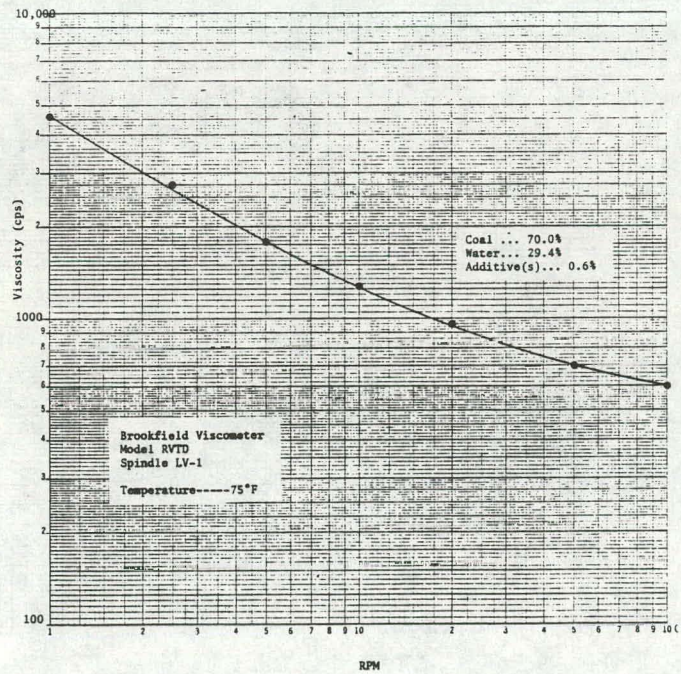

Figure 18. Viscosity Characteristics of 70 Weight % MCWS Fuel

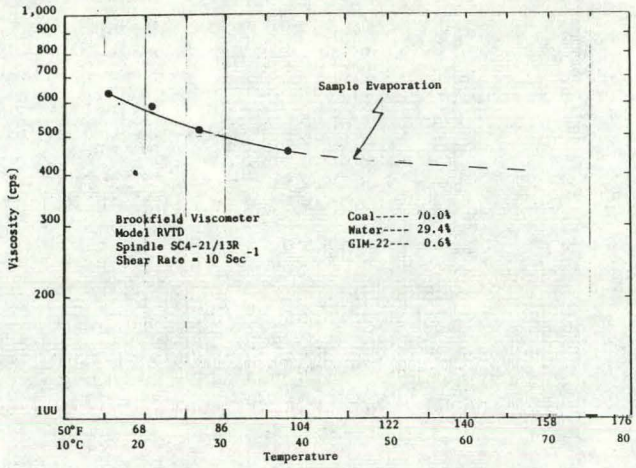

Figure 19. Effect of Temperature on Viscosity of 70 Weight % MCWS Fuel

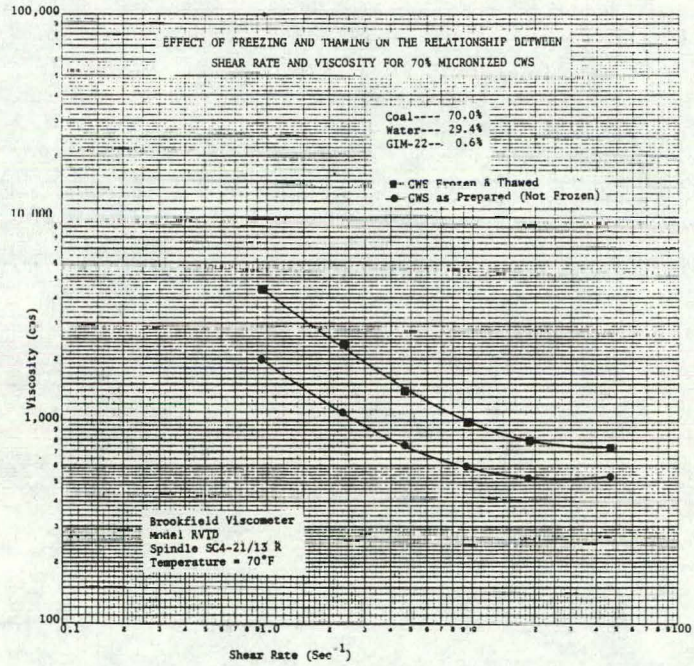

Figure 20. Effect of Freezing and Thawing on the Relationship Between Shear Rate and Viscosity for 70 Weight % MCWS Fuel

	Coal A	Coal B	Coal C
Volatile matter (%)	36.9	36.7	33.44
Fixed carbon (%)	50.5	52.8	55.07
Moisture (%)	1.7	3.3	3.03
Ash (%)	10.9	7.2	8.46
Heating value (Btu/lb)	12,802	13,370	13,811

Table 1. Proximate Analysis of Various Coals

- Sodium salt of condensed napthalene sulfonic acid
  - GIM-6
- Hydroxyoethyl cellulose
  - GIM-8; GIM-20; GIM-21; GIM-22
- Calcium lignosulfonate
  - GIM-9
- Condensed napthalene formaldehyde sulfonate
  - GIM-10; GIM-12; GIM-14
- Modified natural gum
  - GIM-11
- Hydroxypropylated corn starch
  - GIM-15; GIM-16
- Guar gum
  - GIM-18
- Sodium salt of condensed arysulfonic acid
  - GIM-19
- Xanthan gum
  - GIM-23

Table 2. List of Chemical Additives

o Nominal 62 % CWS

- Sample No. 007082-107; Additive - GIM-8
- No settling in 4 weeks
- Slight settling in 6 weeks
- Water Separation in 8 weeks

o Nominal 65 % CWS

- Sample No. 010082-2042; Additive - GIM-22
- Slight settling in 2 weeks
- Settling in 4 weeks

o Nominal 79 % CWS

- Sample No. 010082-2044; Additive - GIM-22
- Slight settling in 2 weeks
- Moderate settling in 4 weeks

Tabel 3. Stability Characteristics of Typical CWS Fuels

HANDLING PROPERTIES OF COAL/WATER SLURRIES

John Dooher, Barbara Gilmartin, Donald Albert, Nancy Chuisano, Daniel Cote, John Gozelski, Marie Grasso, Terry Kanabrocki Phillip Malicki, Donald Wright

Adelphi Center for Energy Studies, Adelphi University, Garden City, New York

Martin Mullarkey - Long Island Lighting Company, Hicksville, New York

This work was funded by the Long Island Lighting Company (LILCO), contracts #853770, 869562; the Empire State Electrical Energy Research Corporation (ESEERCO), project EP82-20; the New York State Energy Research and Development Authority (NYSERDA), contract #536-FFES-FUC-83; and the Electric Power Research Institute (EPRI), agreement RP1895-10.

The Adelphi Center for Energy Studies would like to thank the CWS suppliers for their cooperation in this project.

PURPOSE

In light of the national goal to reduce the use of imported oil and to utilize this country's vast coal reserves, the Long Island Lighting Company (LILCO) has been investigating the feasibility of converting some of its oil fired power plants to direct coal firing. Recent studies have shown, however, that this conversion at the Northport power plant is not technically, finacially, or environmentally feasible. The use of coal-containg liquid fuels, especially highly loaded coal/water slurries (CWS), is a possible alternative approach to direct coal conversion. Since CWS can be handled in fuel forwarding systems similar to those presently used with oil, a major obstacle to coal conversion, i.e., handling and storage of coal, is avoided. In order to evaluate the technical feasibility of handling CWS in conventional fuel feed systems, LILCO engaged the Adelphi Center for Energy Studies (ACES) to perform rheological and pumping tests on commercially available slurries. As a follow-up to this program, similar testing on CWS is now being performed for the Empire State Electric Energy Research Corporation (ESEERCO), the New York State Energy Research and Development Authority (NYSERDA), the Electric Power Research Institute (EPRI), and LILCO.

SCOPE

The major technical objectives of the ACES CWS program are:

- To delineate and quantify the flow properties of coal/water

slurries from various CWS suppliers.

- To determine the effect of pumping and recirculation on CWS.
- To evaluate the use of various pumps, fittings, and measuring instruments for use with CWS.

Four producers of coal/water slurries participated in the study: Gulf and Western Advanced Fuels Technology, Atlantic Research Corporation, Slurrytech, and Occidental Research Corporation. In order to preserve the anonymity of the producers of specific samples, the suppliers will be identified as A, B, C, and D. The slurries were produced with both beneficiated and non-beneficiated bituminous coals; all coals had sulfur contents less than 2%, dry basis, and volatile matter greater than 32%. The CWS all had solids contents of approximately 70% and a top particle size of 300 microns. No detailed chemical or particle size analyses were performed on the slurries.

The laboratory testing of the CWS samples included: measurement of heat content, solids content, specific gravity, ash characteristics, ash fusion temperature, rheological analyses, and stability testing. In the test loop, the rheological properties of the slurries and control equipment were evaluated.

EXPERIMENTAL PROCEDURES

Flow Properties

ACES uses a Haake RV3 concentric cylinder viscometer to determine the rheological properties of the CWS. In this device, the slurry is sheared in the annular gap between a rotating bob and a stationary cup. The torque necessary to rotate the bob at a given speed is measured by a torsion spring. The stator is surrounded by a temperature tempering vessel connected with a constant temperature bath. Most testing was conducted at 20 ^{0}C (68 ^{0}F). The viscometer is integrated with a Hewlett Packard HP-87 data acquisition and analysis system. Viscosity as a function of shear rate is computed and the raw data is stored on floppy discs.

The shear stress - shear rate relationship for the majority of the slurries tested in the laboratory were evaluated using a power law model:

$$\tau = k\,\dot{\gamma}^{n} \qquad (1)$$

where:

τ = shear stress, measured in dPa (deciPascals)
$\dot{\gamma}$ = shear rate, measured in s^{-1}
k = flow consistency index, measured in $dPa \cdot s^{n}$
n = flow behavior index, dimensionless

If the flow behavior index, n, is equal to 1 in the shear rate range covered, the slurry is behaving as a Newtonian fluid; if $n < 1$, the fluid is shear thinning; if $n > 1$, the fluid is dilatant. For a

power law fluid, the apparent viscosity, $\eta(\dot{\gamma})$, is given by:

$$\eta(\dot{\gamma}) = k\ \dot{\gamma}^{n-1} \times 100 \qquad (2)$$

where viscosity is measured in mPa·s (milliPascal-seconds, equivalent to centiPoise).

The time dependent behavior of the CWS was also investigated. The testing of the slurries was accomplished by steadily increasing the shear rate to which the sample was subjected from zero to approximately 250 s^{-1}, steadily decreasing $\dot{\gamma}$ back to zero, and then repeating the cycle. The data from the third flow curve, generated at increasing shear rate, were deemed to be the equilibrium values for the slurries, representing their behavior after being sheared, e.g., after going through a pump. If the initial flow curve showed higher viscosities than the equilibrium flow curve, the CWS is thixotropic; if higher equilibrium values are seen, rheopectic.

Stability

Based on a design from the Bureau of Mines, ACES developed a sophisticated method to determine the static stability of coal-containing fuels. Figure 1 shows a block diagram of the pendulum settling apparatus (PSA). The fuel is contained in a test tube, which is inserted into the pendulum apparatus. The pendulum swings on two pins and breaks a collimated light beam as it passes through the mid point of its swing. Using a frequency counter, the period for ten oscillations is determined. Because the PSA is a physical pendulum, two sets of measurements must be taken, so that the center of mass and moment of inertia can be determined. When not being tested, the tubes of fuel are covered and stored in constant temperature baths. The frequency counter is integrated with the HP data acquisition system, computer, and floppy disc storage unit. The computer calculates the center of mass of the CWS and this information is stored on floppy discs.

Most of the samples were tested over a one week interval with the center of mass of the CWS being determined initially, and after one hour, one day, two days, three days, and seven days. A shift in center of mass of about 0.15 cm at any time indicates a severly settled slurry which would need to be remixed before it could be used.

Besides testing the static stability of the fuels stored at 2 ^{0}C, 20 ^{0}C, and 48.9 ^{0}C (36 ^{0}F, 68 ^{0}F, and 120 ^{0}F), a freeze/thaw test was also performed on the CWS. The center of mass of a sample is determined and then the CWS is stored at -16 ^{0}C (3 ^{0}F) for 16 hours. The CWS is thawed at 20 ^{0}C for 8 hours and its center of mass determined. This cycle is repeated three times. A larger sample also undergoes the temperature cycling and is tested for viscosity after the third cycle.

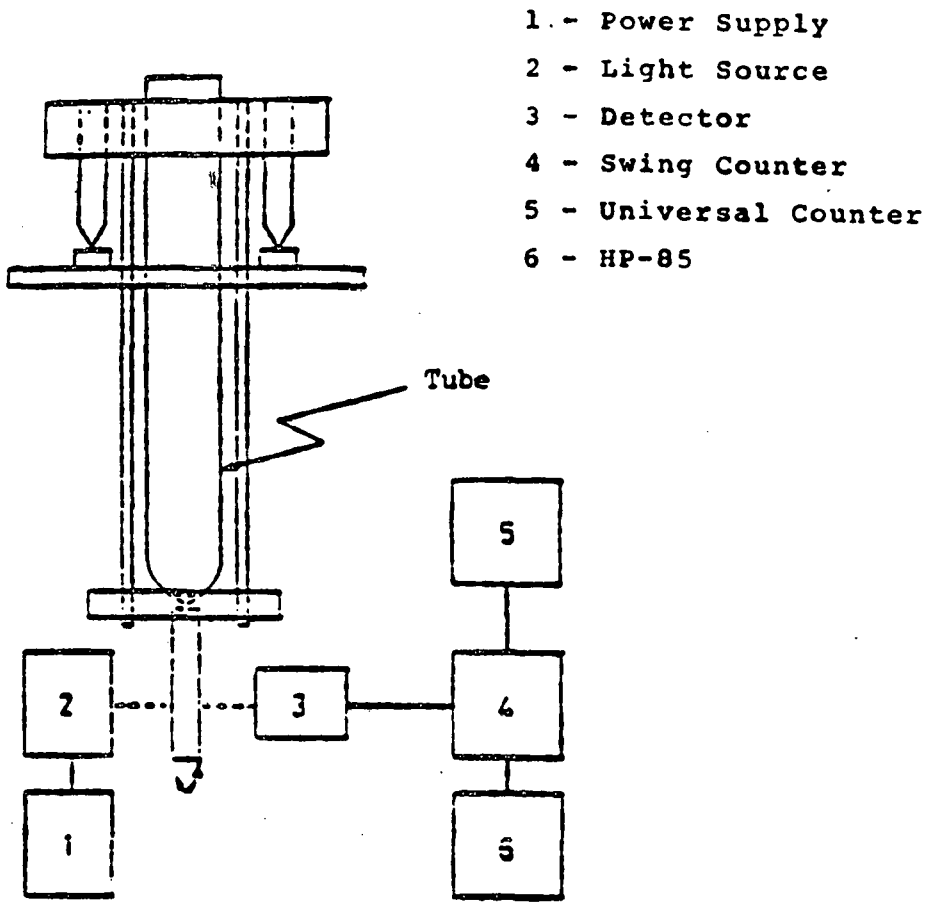

Figure 1. Pendulum Settling Apparatus

Test Loop

The ACES loop, Figure 2, was designed to simulate the fuel feed system of a typical utility power plant. The loop contains 1", 1½", 2", and 3" lines, and for this program flow rates of 10 to 150 gpm were used. In order for the flow parameters obtained in the loop to be valid for a larger fuel feed system, equivalent shear rates must be present in both systems.

The pump used in this program was a Moyno progressing cavity pump. It has a maximum output of 175 gpm at 150 psi. The rotor was made of tool steel; the stator of Buna-N. This pump was chosen because of its general suitability for use with high viscosity coal-containing fuels, and its good performance with coal/oil mixtures and coal/water/oil emulsions previously tested at ACES.

Flow rate measurements were performed with a Micro-Motion Mass Flow Meter, Model B200. Because of the high solids content and variable viscosity of CWS, standard flow measuring devices cannot be used. This meter, which measures the Coriolis force on the CWS, is not affected by viscosity, air entrainment, or multi-phase fluids. Differential and total pressures were measured using standard strain gauge pressure transducers. To prevent coal from becoming trapped in the transducers and the pressure transmission lines, isolation spools were used. The loop contains a shell and tube heat exchanger, used to keep the temperature of the CWS to 20± 0.1 ^{0}C. The temperature of the CWS was monitored using a copper-constantan thermocouple with an electronic ice point reference. The flow rate was varied using a variable speed drive on the Moyno pump. A DC motor controller was also used for part of the program. The signals from the thermocouple, the mass flow meter, and the pressure transducers were fed into a Hewlett-Packard HP-85 computer and data acquisition system.

Because of temporal and financial limitations, a non-Newtonian flow analysis was only performed on some of the loop samples. Since the majority of the CWS were fairly Newtonian, not using the Rabinowitsch-Mooney correction resulted in errors of less than 10% in the shear rate. The apparent viscosities of the CWS were calculated using Poiseuille's equation, unless otherwise noted.

Two different series of tests were performed on the CWS. Some slurries were pumped for several hours of constant shear at approximately 100 s^{-1}, and then subjected to variable shear rates up to 1100 s^{-1}. Other samples, which had not undergone constant shear testing, were subjected to variable shear rates up to 150 s^{-1}.

RESULTS

Fuel Analysis

Because of confidentiality agreements between ACES and the CWS suppliers, no in-depth chemical analyses were performed on the slurries. The heat contents of the mixtures were approximately 70% of the values of the parent coals, showing that the additives used

Note: Thermocouple, Mass Flow Meter, Pressure Transducers are integrated with an HP-85 Data Acquisition and Computer System

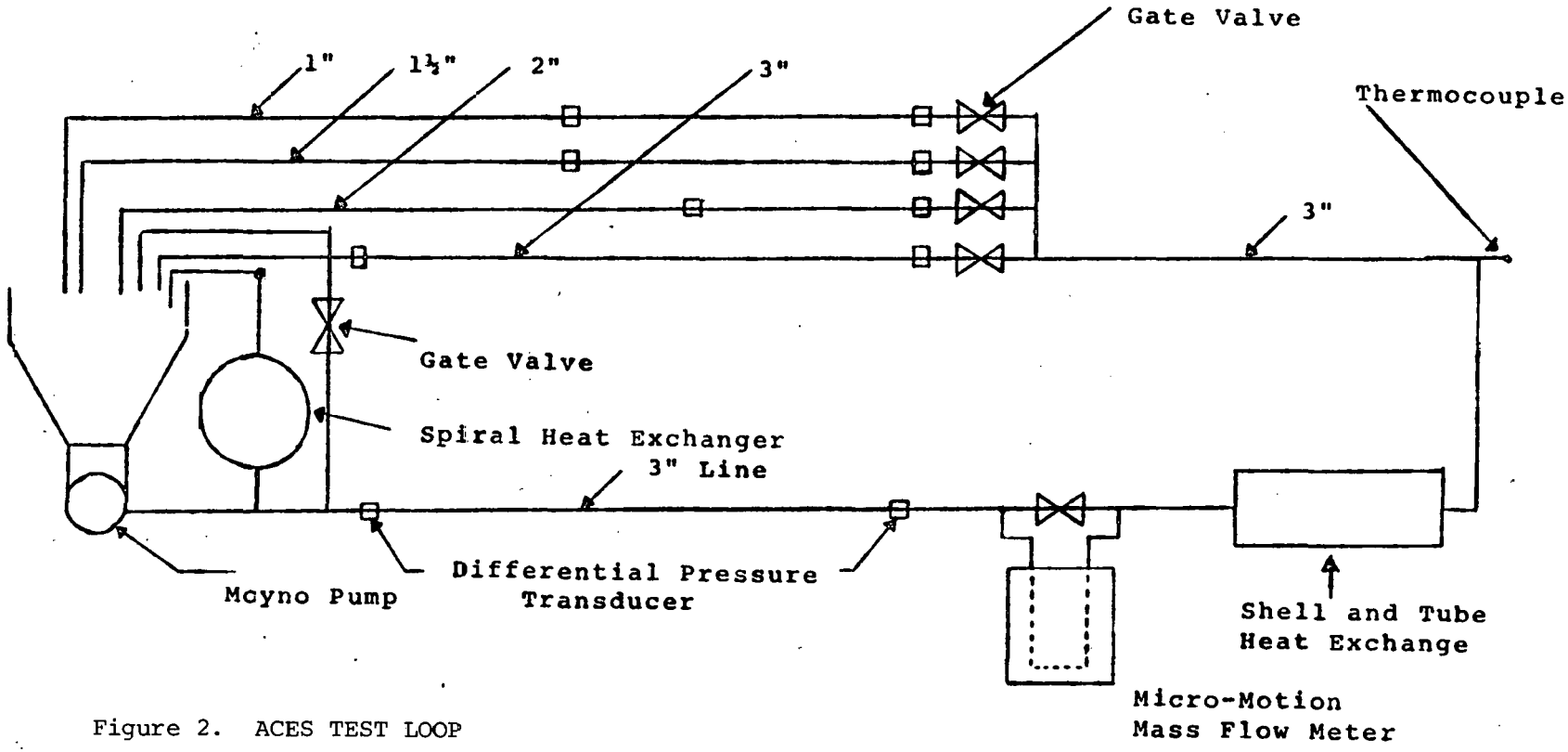

Figure 2. ACES TEST LOOP

in CWS preparation did not significantly affect the overall heat content of the fuels. However, some additives did alter the ash properties of the fuels. The fouling index of four of the eight CWS tested went from low fouling for the parent coals to high fouling for the prepared slurries. In three of the samples, large decreases were also seen in the ash fusion temperatures.

Rheology

Table 1 presents the rheological properties of the CWS, as determined in the concentric cylinder viscometer. Moderate thixotropy or rheopexy indicates a greater than 10% difference between the apparent viscosities at 100 s^{-1} determined from the initial and equilibrium flow curves. Samples B-2, B-3, C-1 and C-2 also exhibited little time dependence when pumped at variable shear in the loop. Samples C-1 and C-2 were tested after eight hours of constant shear; sample B-3 was a fresh sample. The results of the loop tests on the CWS which exhibited time dependent phenomena will be discussed in a later section. Eight slurries were tested for viscosity after undergoing three cycles of freezing and thawing. Two of the three samples tested from supplier D showed little change in viscosity; the third increased by 22%. The other slurries all decreased in viscosity after the freezing and thawing. In general, a loss in viscosity was accompanied by a slight loss in stability. This phenomenon is presently being investigated. The slurries were also tested for the effect of temperature on viscosity. Most CWS showed a decrease in viscosity with temperature similar to that of water, i.e., a 53% decrease between 10 ^{0}C and 60 ^{0}C, Figure 3.

Stability

The majority of the coal/water slurries showed excellent stability when tested in the pendulum settling apparatus at 20 ^{0}C for one week. Only one sample, which according to the supplier was made with contaminated stabilizer, settled completely in the testing period. At elevated temperatures, many of the slurries exhibit rises in their centers of mass. This behavior was also seen when the slurries were placed in a four foot long three inch diameter, settling column. High coal concentrations were seen at the top and bottom, with a low concentration in the center of the column. At 2 ^{0}C, three of the six slurries showed rises in their centers of mass while the other three remained stable. Typical CWS settling behaviors are seen in Figures 4 and 5. After undergoing three cycles of freezing and thawing, the slurries were placed in a 20 ^{0}C bath and tested four days later. In comparison to the CWS which had been stored at constant temperature, only one sample showed a large difference in settling.

Liter samples of CWS were also stored under laboratory conditions without agitation for two to six months. Almost all of the slurries showed settling and approximately 20% of the CWS became hard packed. Any long term storage of CWS would require agitation and/or recirculation.

Table 1

Rheological Properties - Viscometer Measurement

Sample	n	Viscosity @ 100 s^{-1} (mPa·s)	Time Dependence
A - 1	1.21	2910	moderately thixotropic
A - 2	0.91	1210	moderately thixotropic
B - 1	1.28	1760	slightly thixotropic
B - 2	1.00	2550	negligible
B - 3	0.88	2260	negligible
C - 1	0.93	1420	negligible
C - 2	0.97	1470	negligible
D - 1	0.79	1320	moderately rheopectic
D - 2	1.12	1070	moderately rheopectic
D - 3	1.28	1350	moderately rheopectic
D - 4	1.10	1890	moderately rheopectic

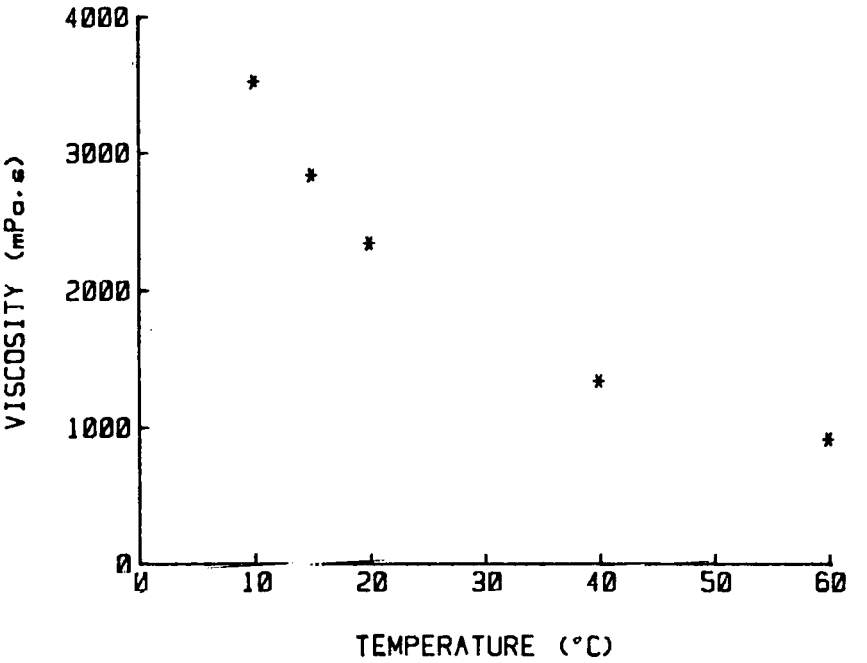

Figure 3. Effect of Temperature on Viscosity, Sample B-3

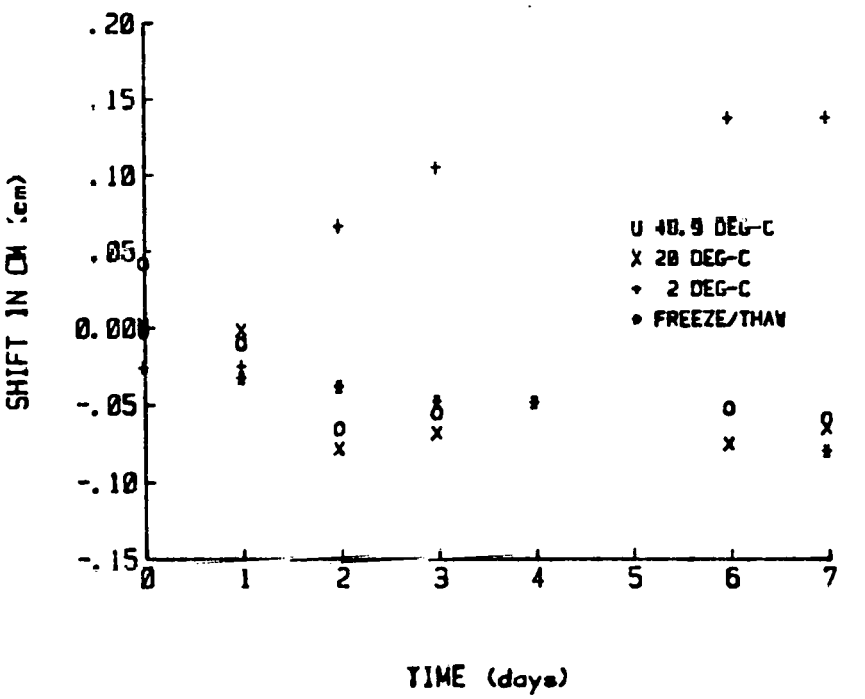

Figure 4. Stability Versus Temperature and Freeze/thaw, Sample B-2.

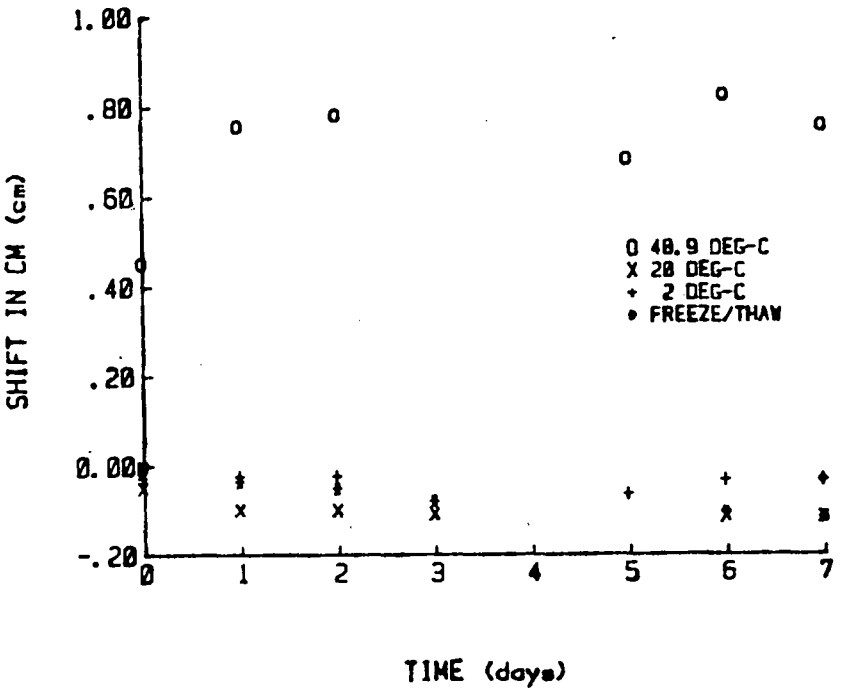

Figure 5. Stability versus Temperature and Freeze/thaw, Sample C-2.

Loop Testing

Thus far, eleven CWS have been evaluated for their flow properties in the ACES test loop. Testing is continuing on the effect of pumping on CWS, the use of various types of control valves with CWS, and the erosion/corrosion potential of these fuels.

Several types of behavior have been seen with the slurries tested. Figures 6 and 7 show the behavior of two slurries when pumped at constant low shear. As can be seen, there is a rapid increase in apparent viscosity in less than half an hour. Most CWS, however, showed more acceptable behavior. Figure 8 shows the apparent viscosity of a sample from supplier D over the twenty hour test period. During the first eight hours of constant shear testing, at approximately 100 s^{-1}, the apparent viscosity remained fairly constant. At point A, variable shear testing up to 1000 s^{-1}, was begun. The viscosity, as measured at 100 s^{-1}, began to increase rapidly, however, not as quickly as seen with the first two samples. Point B represents a point of pump start-up after 65 hours of shutdown. The viscosity had almost decreased to its original value, but then quickly increased during constant shear testing. The behavior shown by this sample, i.e., an increase in viscosity when subjected to high shear, was seen with several of the CWS tested. Other CWS

reached an equilibrium viscosity during constant shear testing and were not deleteriously affected by high shear. A slurry from supplier B had been pumped for twenty hours at constant shear before the variable shear testing was begun. Figure 9 shows the results from the four lines in the test loop as well as from the viscometer. There is good agreement among all the measurements. This slurry was Newtonian as received, however, it became slightly dilatant after twenty hours in the loop. This slight dilatancy caused no pumping problems.

Two of the CWS were subjected to variable shear testing before being circulated for any length of time. Figures 10 and 11 show the results for these slurries. The tests were conducted by increasing the flow rate from 0 to 100 gpm (0 to 150 s^{-1}), curve 1, and then decreasing the flow rate back to zero, curve 2. This cycle is repeated three times. The test sequence takes one and a half hours. The slurry from supplier B showed a gradual decrease in viscosity towards an equilibrium value, while the CWS from supplier D still exhibited a strong time dependency. This sample reached equilibrium after two and a half additional hours of pumping.

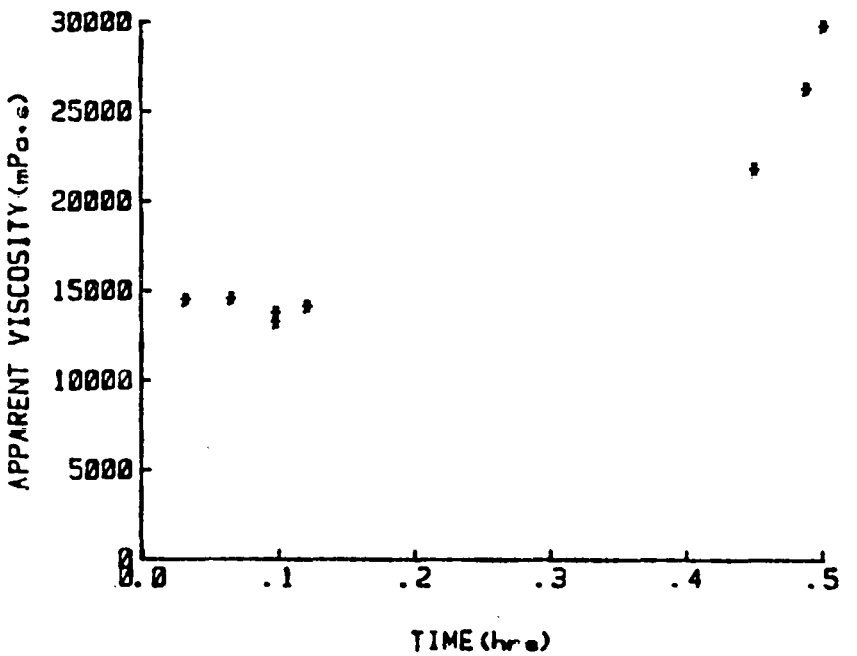

Figure 6. Apparent Viscosity Versus Time, Sample A-1.

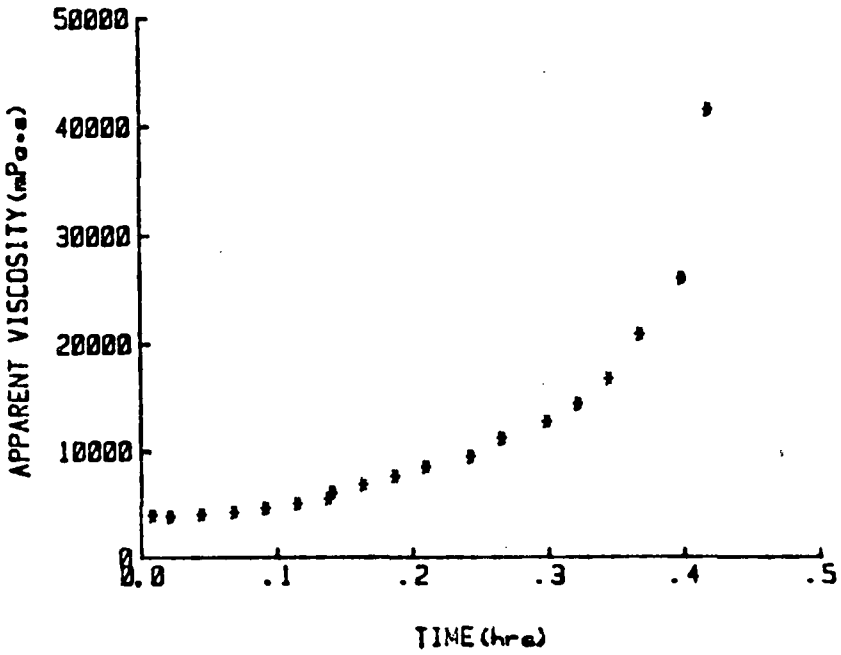

Figure 7. Apparent Viscosity Versus Time, Sample B-1.

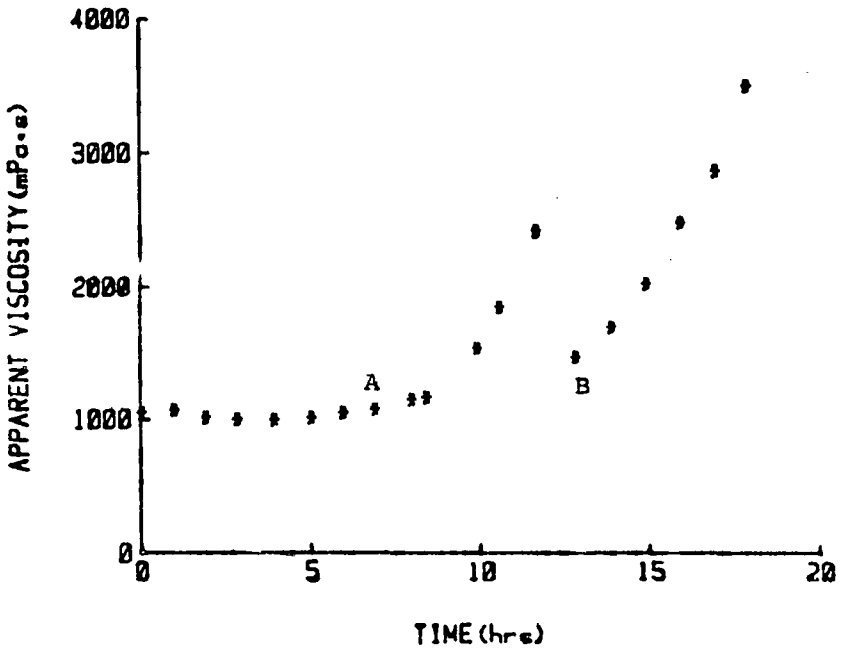

Figure 8. Apparent Viscosity Versus Time, Sample D-1.

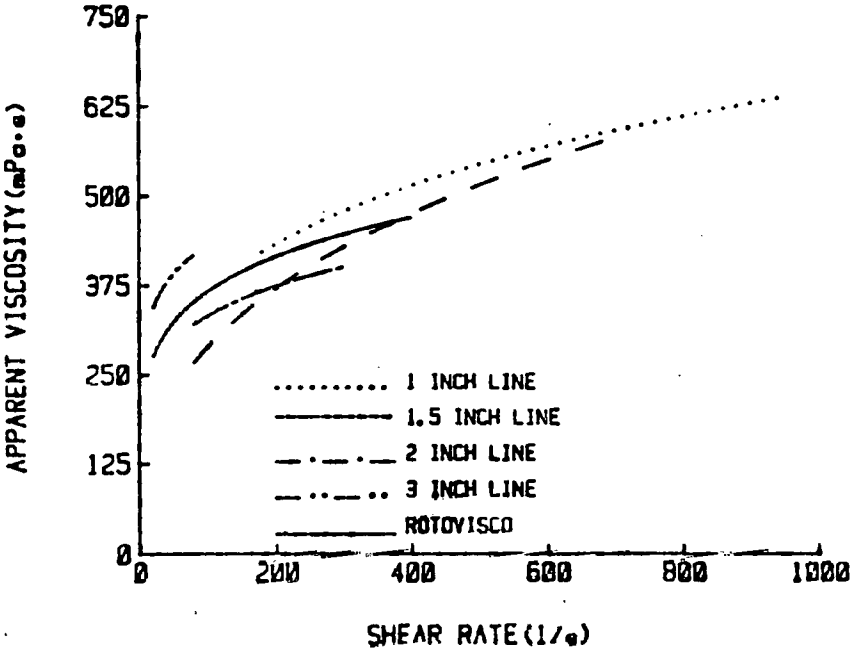

Figure 9. Apparent Viscosity Versus Shear Rate, Sample B-2.

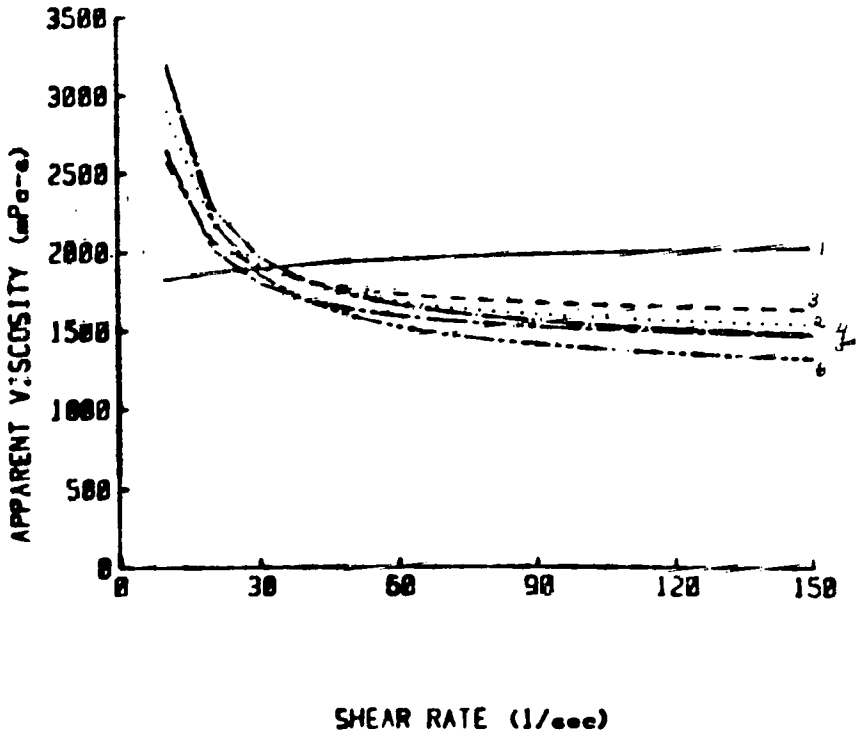

Figure 10. Apparent Viscosity Versus Shear Rate, Sample B-3.

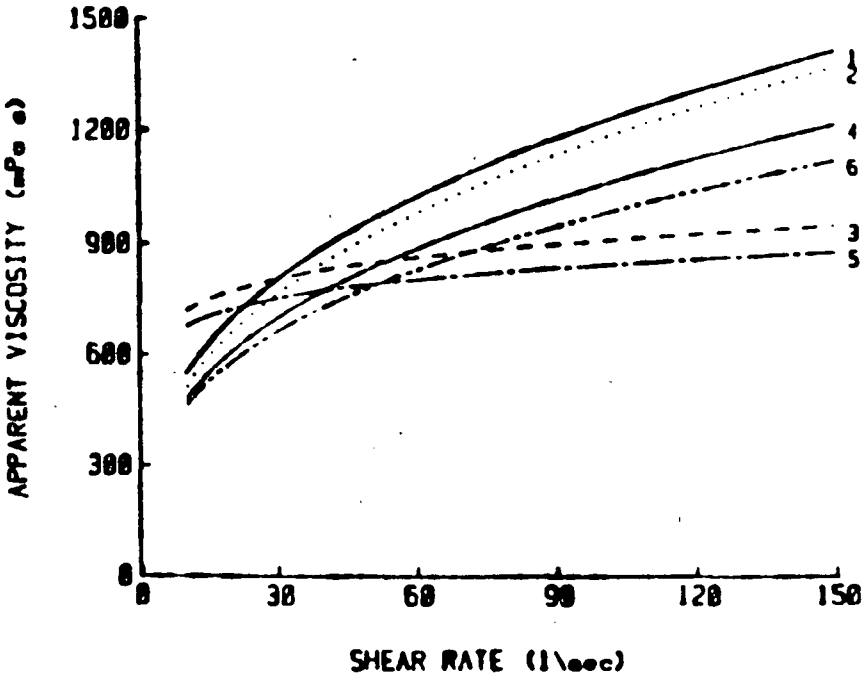

Figure 11. Apparent Viscosity Versus Shear Rate, Sample D-4.

CONCLUSIONS

From the samples which were examined during this program, some general statements can be made about the handling properties of these fuels. More testing must be performed before coal/water slurries can be successfully used as a fuel in a utility power plant.

- Each of the suppliers has demonstrated that they are capable of producing a technically acceptable utility fuel, however, due to secrecy agreements, it cannot be determined whether or not the specific fuels tested can be produced in large quantities at attractive prices.

- Quality control of the CWS delivered to the plant is critical. Wide variations in slurry properties were seen in the samples tested, some of which were unacceptable for utility use.

- The seventy percent weight coal slurry seems to be, for some suppliers, the borderline level for producing an acceptable slurry. A lowering of the concentration requirement would decrease the viscosity of the CWS and perhaps minimize some of the changes in the slurry after pumping and circulation.

- The additives used by some suppliers greatly altered the ash properties of the CWS, i.e., from a low fouling index to a high fouling index. These additives cannot be used in a commercially available slurry.

- The flow behavior of the CWS in a concentric cylinder viscometer closely matched that seen in the loop used for testing. However, viscometer testing cannot yet predict the changes that some slurries undergo during pumping.

- Some amount of agitation will be required to keep the fuels uniformly mixed, however, the power required will be much less than that needed for initial mixing. Since complete settling must be avoided, long-term storage tanks should have a back-up agitation or recirculation system.

- The rheological behavior of most of the slurries were evaluated in the loop after eight or more hours of pumping. Some of the slurries behaved as nearly Newtonian fluids, however, others became dilatant or had flow properties which rapidly changed with time. In order to correctly design a fuel forwarding system, both the initial and equilibrium behavior of the slurries must be taken into account.

- The high shear to which most of the CWS were subjected in the loop seemed to adversely affect most of the slurries tested. Shear rates should be kept to a minimum, perhaps less than 150 s^{-1}, to avoid problems.

- The Micro-Motion mass flow meter performed well during this test program and accurately measured the flow rate of seventy percent by weight slurries.

- The Moyno progressing cavity pump performed well with CWS, even with viscosities up to 40,000 mPa·s. The flow rate of the slurries could be easily controlled using the variable speed pump control.

- Gate valves were used for flow cut-off and performed satisfactorily.

Fifth International Symposium on Coal Slurry Combution

RHEOLOGICAL CHARACTERISTICS OF COAL WATER MIXTURE

Yasuhiro Kiyonaga : Lion Corp.
Shin-ichi Watanabe : Kao Corp.

RHEOLOGICAL CHARACTERISTICS OF COAL WATER MIXTURE

Yasuhiro Kiyonaga, Lion Corp.
Shin-ichi Watanabe, Kao Corp.

ABSTRACT

The stability of Coal-Water-Mixture (CWM) can be evaluated by measuring the magnitude of structural viscosity of CWM and the area of the hysteresis loop of shear stress at comparatively low shear rate with a double cylinder type rheometer.

The excellent performance of ACC-700, which was developed by Lion Corporation, was confirmed by rheology measurement; its concentration limit of CWM was as high as 70% as well as its capability for CWM stability.

1. INTRODUCTION

Application techniques and the effective transportation systems for coal have to be established due to the current demand for oil-free energy sources. Lion Corporation and Kao Corporation took part in the Advanced Coal Chain (ACC) Project, which was led by Electric Power Development Co., and have been contributing to the development of software including additives.

The research on CWM additives was reported at the last symposium and the dispersant, ACC=100 was introduced.

At this symposium, Lion Corp. will introduce an improved dispersant, ACC-700 and the studies on the rehological behaviour of CWM for the earliest prediction of CWM stability. The studies on Coal-Oil-Mixture (COM) can assist studies on the rheological behaviour of CWM. CWM was compared with COM to understand the basic rheological characteristics of CWM. The fluid characteristics of COM and CWM reflect the characteristics of respective dispersion media. COM is difficult to be concentrated due to the high viscosity of dispersion media, heavy oil. The CWM can provide a higher concentration and can be packed with coal as high as 70% and over.

The rheology was measured by a rheometer under continuous fluctuation (increasing and decreasing) of shear rate to understand respective rheological characteristics. As shown in Fig. 1, COM proved to be a weak psudo-plastic fluid or Newtonian fluid before any dispersant was added. The addition of stabilizer improved the static stability of

COM with the higher apparent viscosity, due to the increased stress, at a low shear rate. Since the area of the hysteresis loop was small, the structure rapidly recovered after shear was applied at a fluctuating rate. Since the fluid characteristics of COM are excellent, the stability can be easily evaluated by such measurements as the Casson plot yield value.

The CWM can be prepared to a high concentration, although the dispersion stability is inferior to COM. Fig. 2 is the rheogram of Tatung coal slurry with no additive and shows that the stress decreases rapidly at low shear rate and remarkably destroys the structure. The static stability period of this slurry was shorter than a week. The higher coal concentration makes it a dilatant fluid and the 65% coal concentration is difficult to achieve with CWM without an additive.

The fluid characteristics of CWM with no additive are inferior to COM and accordingly provides such rheological characteristics. However, CWM is required to be of high quality, with a coal concentration higher than 70%, of good dispersion and fluid characteristics as well as a static stability longer than a month. Lion Corp. developed the CWM dispersant ACC-700, which is superior to ACC-100, for the achievement of the required quality. The addition of ACC-700 provides better dispersion stability to prepare a slurry with better fluid characteristics. Lion Corp. rheologically studied the ACC-700 added CWM in relation to stability.

2. EXPERIMENT

2-1 Coal

Tatung coal with smaller ash content and Warkworth coal with larger ash content were employed to represent bituminous coal.

Beluga coal was selected for a sub-bituminous coal.

2-2 Coal Pulverizing

(1) Dry milling with a Cross Beater Mill (Retsch)
The largest particle size was limited to 200 μm.
(2) Dry milling with a Ball Mill
Coal powders of different average particle sizes were mixed to provide a fine coal powder of wide particle distribution.

2-3 CWM preparation

The slurry was prepared by adding fine coal powders into the additive solution with a "Labo-Disper" (Tokushu Kika Kogyo), after pre-mixing.

2-4 Particle size distribution measurement of fine coal powder

For particle size over 44 μm: by wet sifting with JIS sieves
For particle size under 44 μm: with laser particle size distribution measuring equipment (CILAS)

2-5 Observation of fine coal powder surface (EMX analysis)

The observation was made by electron micro-probe X-ray analysis equipment (Shimadzu).

2-6 CWM evaluation

(1) Viscosity characteristics - Rheology

The viscosity characteristics were measured by a double cylinder type rheometer "Rotovisco" (Haake).

The CWM sampling system was "MV-IIP" with a specific structure to prevent glide at the fluid contact.

(2) Viscosity characteristics - Apparent viscosity

Apparent viscosity was measured by the Brookfield viscometer.

(3) Static stability

The static stability was evaluated by the rod penetration test (rod diameter: 5 mm, rod weight: 50g). The evaluation was made each week and CWM was evaluated stable if the rod penetrated quickly down to the bottom.

3. RESULTS

3-1 Additive

The following provides the results of studies on various performance characteristics of ACC-700.

(1) High concentration dispersion

Higher concentration was tried with Tatung coal using a prepared particle size. As illustrated in Fig. 3, ACC-700 proved to be a quality CWM dispersant with the preparation limit 4-5% higher than ACC-100.

(2) Fluidity (pH adjustment)

It is common knowledge that pH affects the fluid characteristics of the slurry. To study the pH effect, the viscosity of the CWM, with ACC-700 added, was measured under various pH conditions adding sodium hydroxide or sulfuric acid.

As shown in Fig. 4, the viscosity of CWM on the alkaline side was 1/2 - 1/3 as low as CWM on the acid side. Therefore, the fluidity should improve if CWM, with ACC-700 added, is prepared as neutral or weak alkali.

(3) Stability

The CWM static stability was studied in conjunction with the rheology of ACC-700 alone and ACC-700 plus commercial stabilizers.

(a) Effect of amount of ACC-700
The rheology was measured to understand the effect of amount of ACC-700 in the range of 0.5 - 1.0% versus coal by preparing the slurry with a Labo-Disper. Fig. 5 shows the results with Tatung coal. The apparent stress of rheogram at a low shear rate became larger with a decrease in the amount added. The area of the stress hysteresis loop conversely increased. The stable period was not reduced with a decrease in the amount added, in the static stability evaluation.

(b) Effect by combined use of stabilizers with ACC-700
The study was carried out adding ACC-700 and several stabilizers said to be effective in improving CWM stability.

(Water-soluble polymer)
Commercial soluble polymers (xnthan gums) for CWM stabilization were applied. No marked improvement was observed by adding 0.1% versus coal. Fig. 6 shows the result.

(Inorganic salt)
Sodium hexametaphosphate is said to be effective for dispersion stability of fine particles. However, it proved to have no influence on the rheology and static stability.

3-2 Stirring Effect

When considering the dispersion stability with a dispersant, it is needless to say that the adsorption speed and amount of dispersant influence greatly for slurry preparation and stabilization of CWM.

It was thought the stability could be improved by stirring the slurry after CWM was prepared. The stirring effect was studied by low speed stirring and high shear rate stirring after preparing the CWM with ACC-700 added.

(1) Low speed stirring

The stirring effect was observed with the rheology measurement along a time scale for low speed stirring with a turbine agitator (200 rpm). As shown in Fig. 7, the rheogram showing high viscosity and a big hysteresis gap right after slurry preparation changed to what showed a low viscosity and a small hysteresis gap and apparently, big yield value appeared gradually, after stirring for 10 hours.

The static stability of the 66% concentration of the CWM with Tatung coal was improved by further 2 weeks after stirring it for 30 hours. The CWM with 72% Warkworth Coal Concentration of comparatively inferior stability changed to a stable CWM, in which the water did not separate for longer than 3 weeks, with the same 30 hours stirring.

However, when the CWM rheology was measured by broadening the rheology measurement range and applying high shear rates up to 88 sec^{-1}, the rheogram pattern was disturbed at the high shear rate to indicate the tendency of CWM structural failure. The dynamic stability was rather dubious when the high shear was applied to CWM. (Fig. 8)

(2) High shear rate stirring

CWM changed to provide the same rheological behaviour obtained by the 30 hours low speed stirring, after stirring approximately for 10 minutes with a homogenizer (3000 rpm). The rheology measurement at 88 sec^{-1} proved no disturbance in the rheogram pattern. The CWM was improved to be useful enough for pumping (Fig. 9, 10)

The static stability was improved to longer than 5 weeks with the CWM with 72% Warkworth coal concentration with a 10 minutes high shear rate stirring.

A statically and dynamically stable CWM can be prepared by adding ACC-700 alone with the incorporation of a high shear rate stirrer in a CWM production process.

3-3 Coal Types

The dispersion stability of the CWM with ACC-700 added was rheologically studied and the relation between the rheology characteristics and stability was confirmed. Lion Corp. found that rheological analysis can be applied to various coal types and the particle structure both of which are known to affect CWM stability.

The following coal types were rheologically analyzed. Bituminous coal (Tatung coal and Warkworth coal) and sub-bituminous coal (Beluga coal) were pulverized for one step with a cross beater mill under the same conditions. The particle size distribution of pulverised coal is provided in the fig. 15. The amount of purverized coal through the 200 mesh sieve was different according to the Hardgrove Grindability Index (HGI).

Slurries with each fine coal powder were prepared adding ACC-700 dispersant, and the rheology was measured at particular concentrations (Fig. 11). Since the particle distribution was not adjustment, the slurry threshold concentration was not necessarily high. The study did not involve stirring after CWM preparation.

(1) Tatung coal

It became dilatant fluid at the 68% coal concentration.

Even below 66% where the rheology measurement was possible, it provided neither clear pseude-plasticity nor yield value.

The static stability period of the CWM was approximately a week.

(2) Warkworth coal

It did not become a dilatant fluid at even the 72% coal concentration. It was a good pseudeo-plastic fluid at low concentration and had a yield value at high concentration. Its static stability was also good. The CWM of the 68%-70% coal concentration separated into only a little water at the top, but no settled layer was observed for longer than 4 weeks. At the 72% concentration it provided a rheogram with a big hysteresis loop gap and the static stability period was 2 weeks. Fig. 12 illustrates the rheogram change by coal concentration fluctuation.

(3) Beluga coal

At the 62% coal concentration the CWM was dilatant fluid. Even with the 60% concentration, the stress conspicuously deteriorated at a low shear rate, destroying the structure and indicating difficulties in building a stable dispersion structure.

The effect by coal type has been studied in compliance with the improvement of the CWM concentration. As can be understood from this report, the coal type influences the CWM static stability. The rheology characteristics provided clear distinction to the coal types, as predicted. Lion Corp. understood that rheology was useful for the prediction of static stability regarding coal types.

A slurry of good static stability could provide pseudo-plasticity and definite yield value even at a coal concentration higher than 70%.

Lion Corp. studied the reasons for conspicuous differences as mentioned due to coal types with two bituminous coals, i.e. Warkworth and Tatung coal. As shown in Fig. 13 and 14, the EMX observation of the coal surface found the Warkworth coal contains more silicon atoms, which is comprised of ash, than the Tatung coal. Their distribution is almost uniform, although a little difference is noticeable between the shorn and the cloven survfaces. Since the ash is generally hydrophilic, the slurry with fine Warkworth coal powder is thought to have provided easier preparation due to better wetting qauality.

The electron microscopic picture shows that the fine coal powder surface was smoother to indicate the specific surface area was not so large.

The fact leads to the increased adsorption of ACC-700 by unit area of fine coal powder, for the more effective dispersion stability by ACC-700.

As can be understood from the particle size distribution shown in Fig. 15, a considerable amount of fine particles below 10 μm diameter existed in the Warkworth coal slurry. This could be one of the reason that it rheologically provided pseudeo-plasticity. This can also be seen from the poor pseudeo-plasticity of Beluga coal which contained few fine particles.

3-4 CWM Stability from the Viewpoint of Rheology

The results are classified from the viewpoint of rheology and static stability.

The rheogram of static-stable CWM provided a large stress at low shear rate and the pattern of a pseudo-plastic fluid. These rheological characteristics indicate that CWM has structural viscosity. It is generally said that the structural viscosity correlates with the stability of the dispersion.

Similar correlation was proven in CWM. It has been said that the structure is unstable and the structural recovery characteristics are poor for those which provide a big hysteresis loop gap by shear stress with the shear rate fluctuation and a big loop area in the rheology measurement.

Lion Corp. took up this point and obtained the hysteresis loop area by integration making the increase/decrease curves a function of the shear stress and the shear rate. The loop area of the CWM with 72% Workworth coal concentration of inferior stability was enlarged to 13 times as large as that of the 68% CWM of superior stability. Conversely, the hysteresis loop area of the CWM with ACC-700 added was reduced to 1/2 - 1/3, being stabilized by stirring.

These results clarified that the hysteresis loop area of the rheogram correlates with CWM stability. A simple evaluation of CWM stability is seen to be possible in terms of energy per unit volume which is the multiple of the difference of shear stresses at the same shear rate by the shear rate.

Lion Corp. will study the above possiblity.

4. CONCLUSION

Through the studies on the rheological behaviour and the static stability, ACC-700 from Lion Corp's development was verified to be a superior CWM dispersant to ACC-100, providing dispersion stabilizing quality for many coal types.

Useful knowledge was also obtained on the correlation between CWM stability and rheological characteristics. Many factors (e.g. coal types, particle size constitution, additives, methods of slurry

preparation) influence the stability. However, the stability could be predicted from the CWM rheological characteristics by limiting those factors to a certain degree.

The result of the study are itemized as follows:

(1) From the rheology measurement and the evaluation of static stability of CWM, it was understood that a correlation existed between the magnitude of structural viscosity, which is a rheological characteristics of CWM, and the static stability of CWM and that the bigger the structural viscosity is, the better the static stability. CWM with a excessively large hysteresis loop area of stress due to the fluctuation of shear rate proved to have inferior static stability.

(2) ACC-700 was verified to be an excellent dispersant for the CWM preparation of coal concentrations over 70%. The rheology measurement confirmed that viscosity of the CWM is decreased and fluidity is improved by preparing CWM neutral to weak alkali during the preparation process.

It also confirmed that ACC-700 had such superior performance not requiring other stabilizers and the CWM stability was remarkably improved and the viscosity was further decreased only by stirring.

High shear rate stirring is especially effective for that purpose.

(3) Commercial stabilizers betrayed our expectations in improving the stability of the CWM with ACC-700 added. For instance, such water-soluble polymers as xanthan gums improved the stability. However, it stabilizes slurry via increased viscosity and has the drawback of poorer fluidity.

Lion Corp. are confident that the above knowledge is very useful for the quick evaluation of CWM characteristics in pilot plant tests etc. and are researching rheology inclusive of the correlation between the yield value and the structural viscosity for further quantitative correlation between the rheological characteristics and stability. We believe this research will greatly help the establishment of extensive stability and effective preparation of CWM.

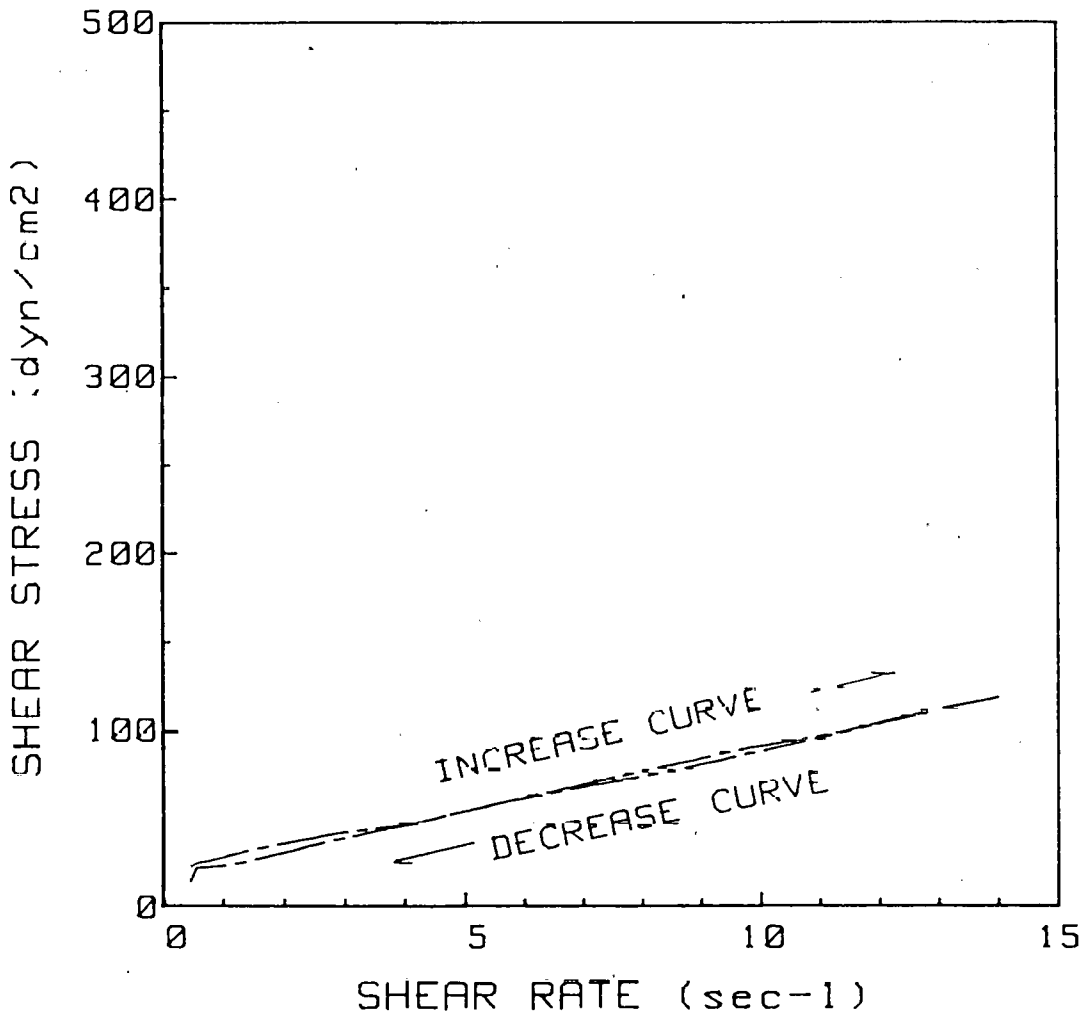

COM -- Tatung coal / Mid-east heavy oil

Coal conc. -- 50% Meas. temp. -- 70 °C

Fig.1 Rheogram of COM -- No additive

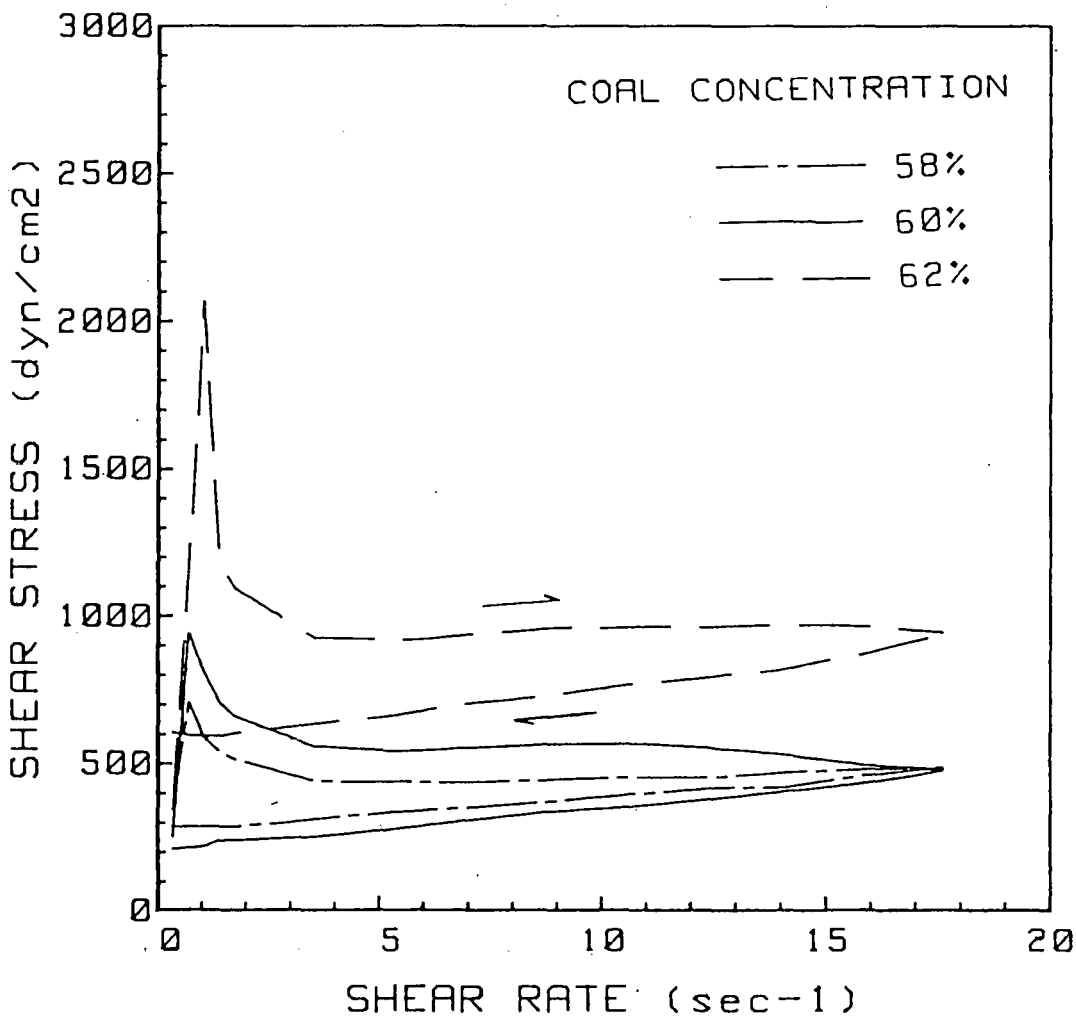

Fig.2 Rheogram of CWM -- No additive

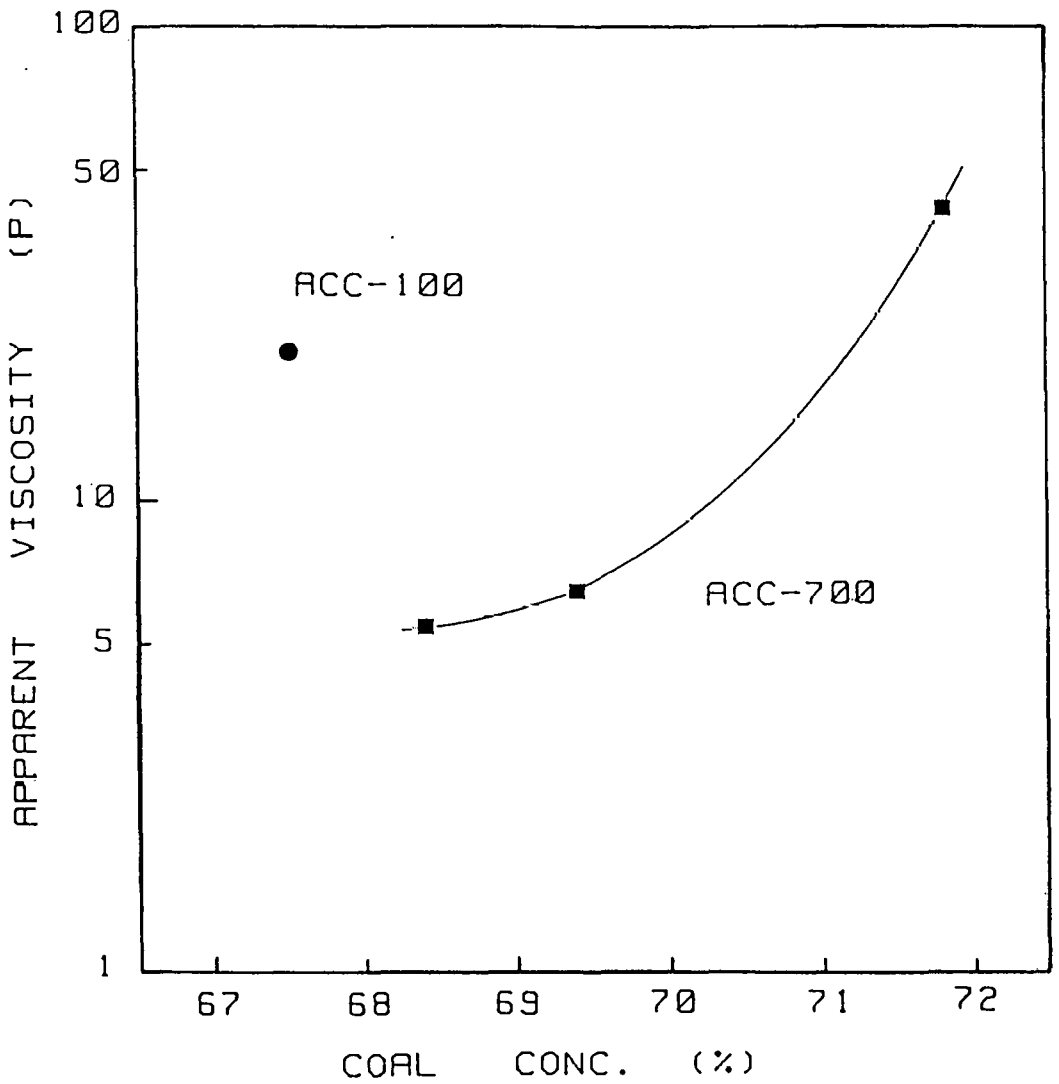

Coal -- Tatung coal (prepared particle size)

Fig.3 Viscosity of CWM

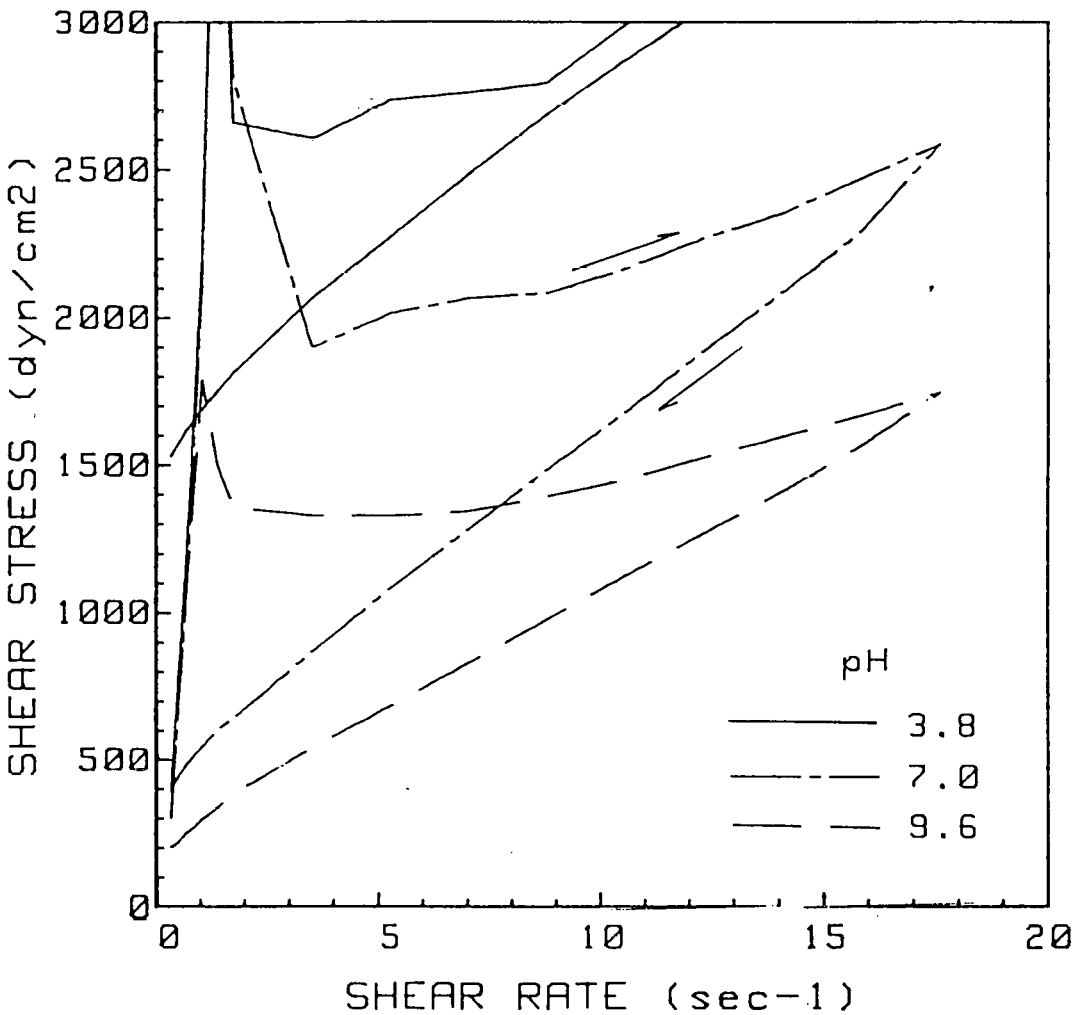

Fig.4 Rheogram of CWM -- Effect of pH

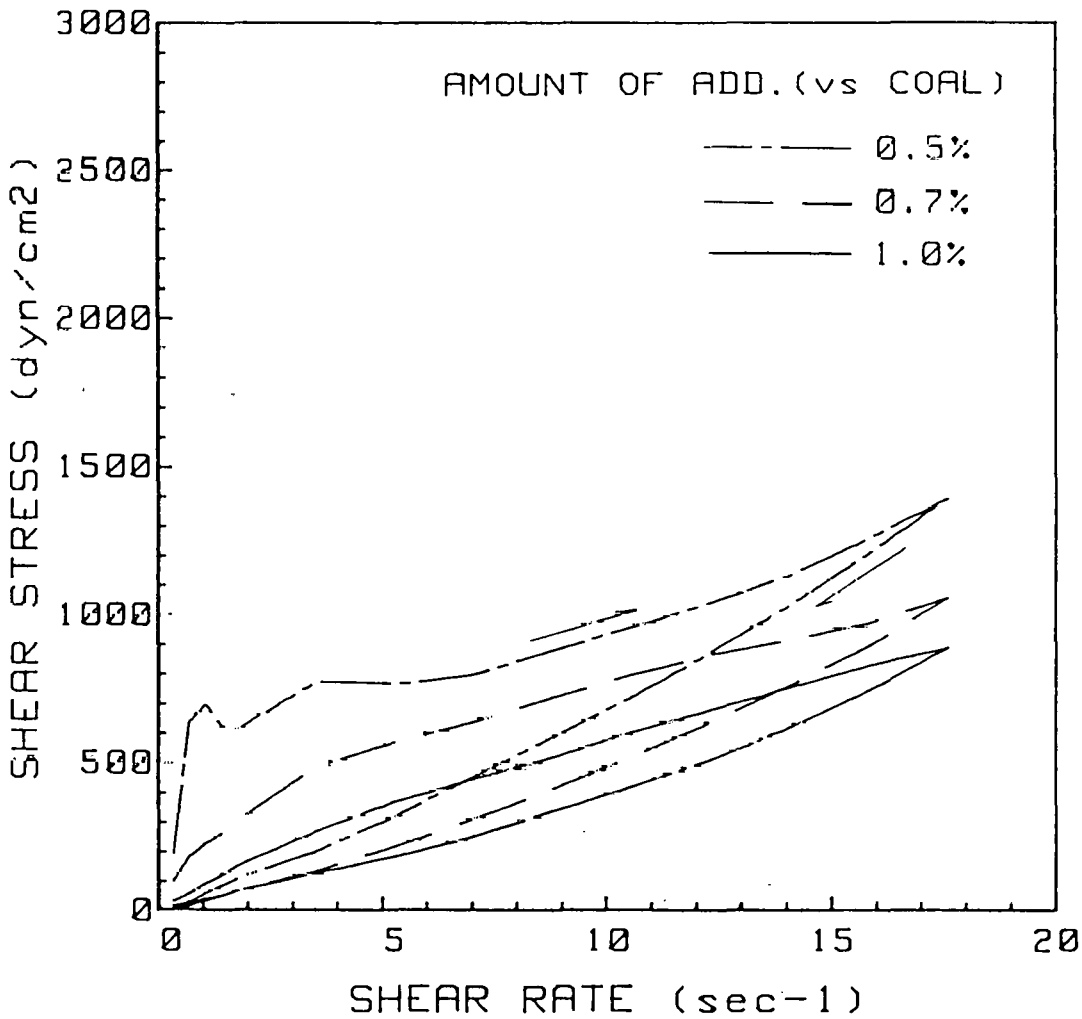

Tatung coal (c.c.66%)

Additive -- ACC-700

Fig.5 Rheogram of CWM

-- Effect of amount of ACC-700

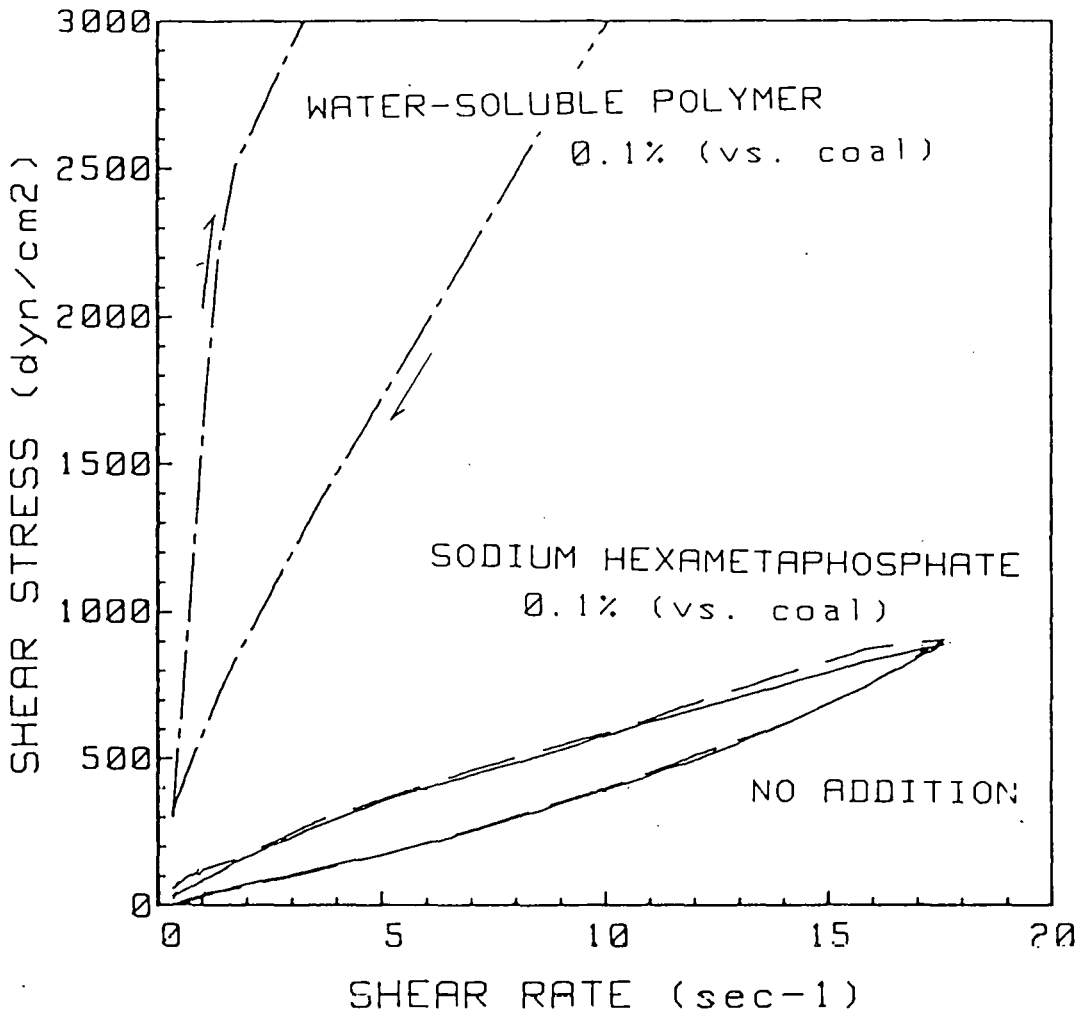

Tatung coal (c.c.66%)

Additive -- ACC-700 1%(vs. coal)

Fig.6 Rheogram of CWM

-- Effect by combined use of stabilizer

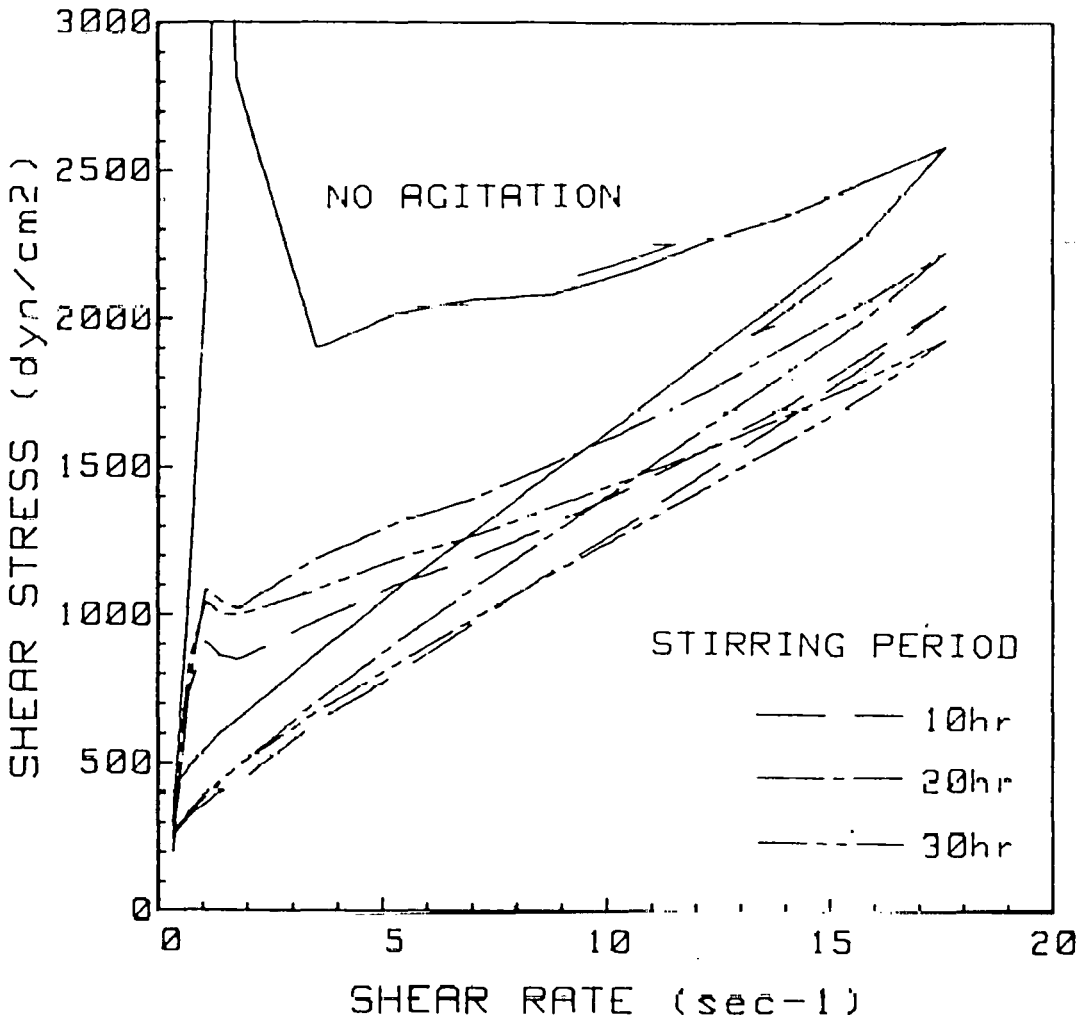

Warkworth coal (c.c.72%)

Additive -- ACC-700 1%(vs. coal)

Fig.7 Rheogram of CWM

-- Stirring effect (low speed)

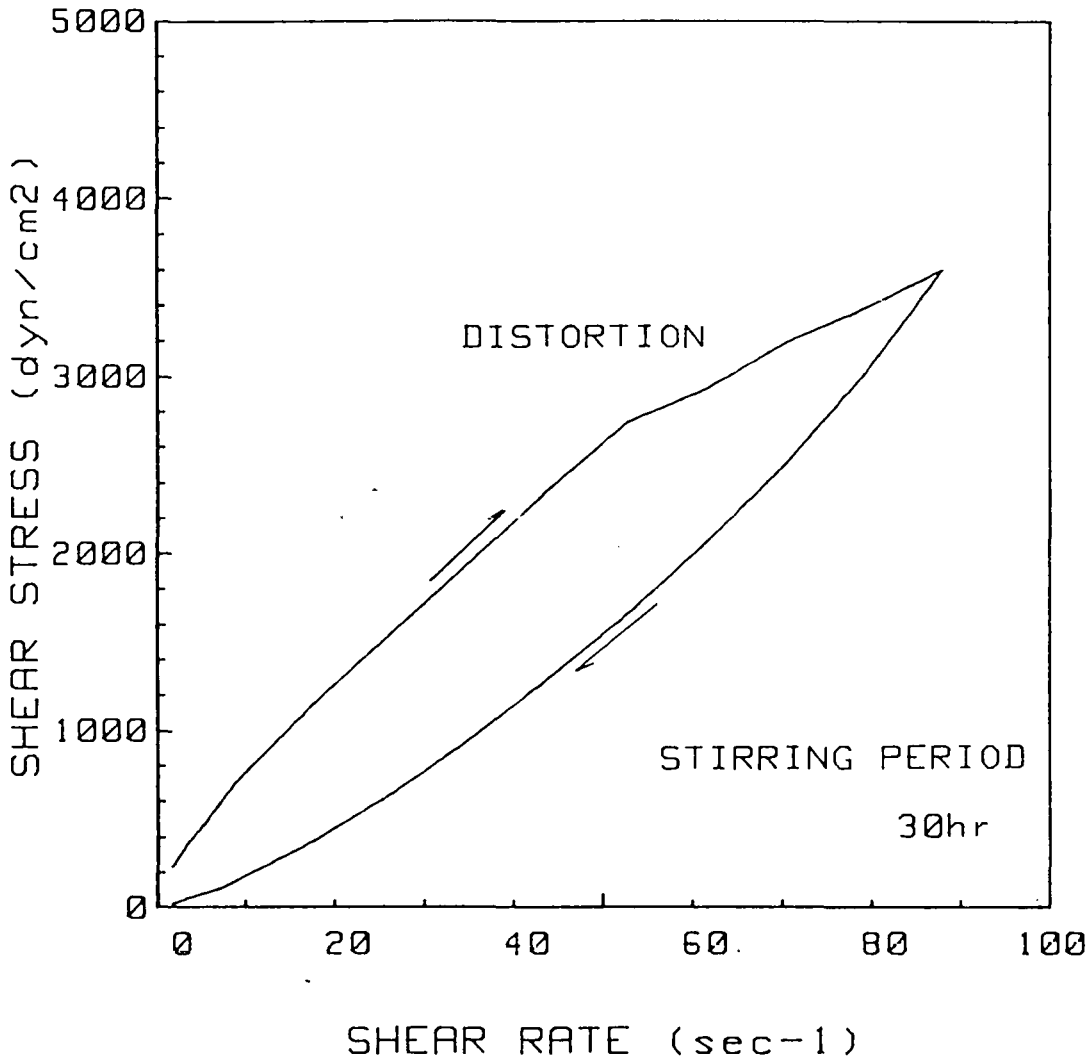

Tatung coal (c.c.66%)

Hddítive -- HCC-700 1%(vs. coal)

Fig.8 Rheogram of CWM

-- Stirring effect (low speed)

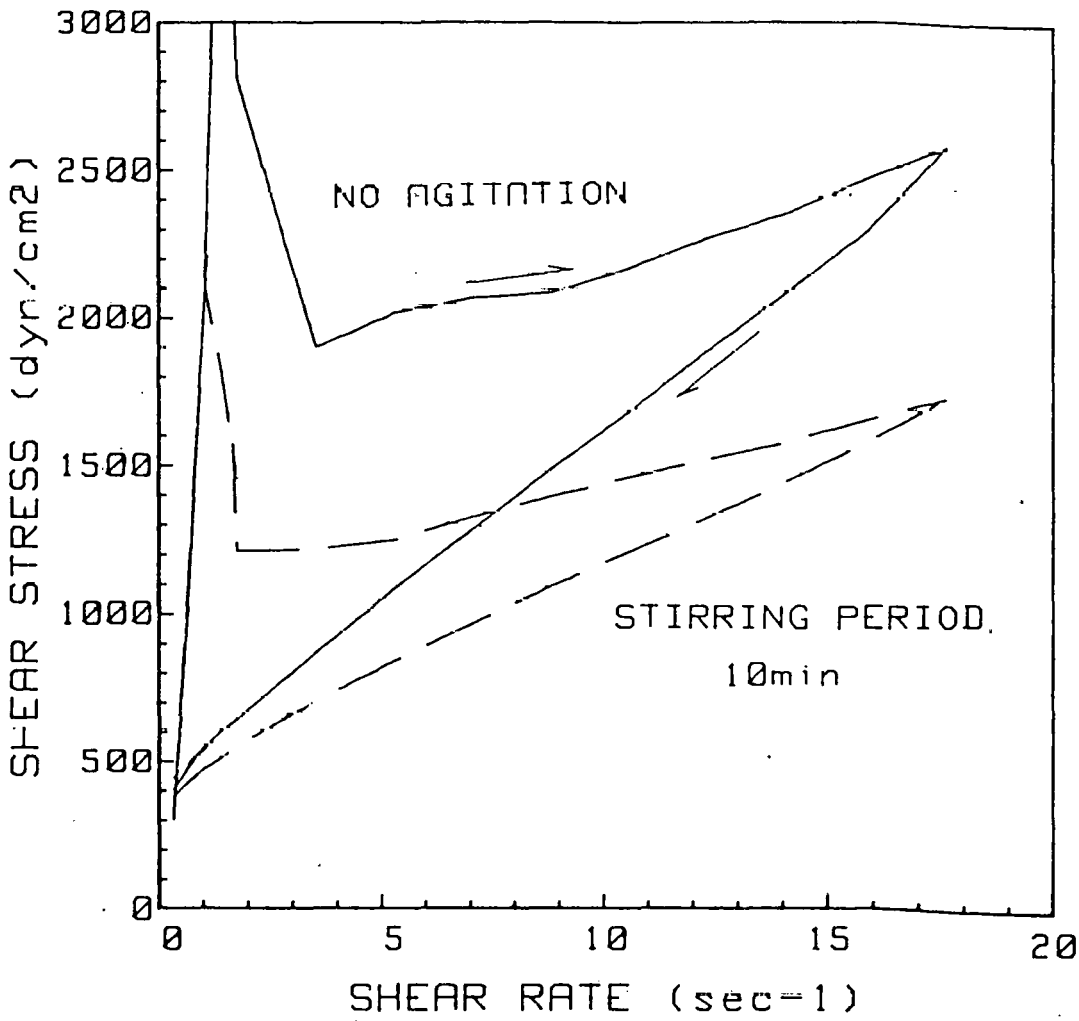

Warkworth coal (c.c.72%)

Additive -- ACC-700 1%(vs. coal)

Fig.9 Rheogram of CWM

-- Stirring effect (high shear rate)

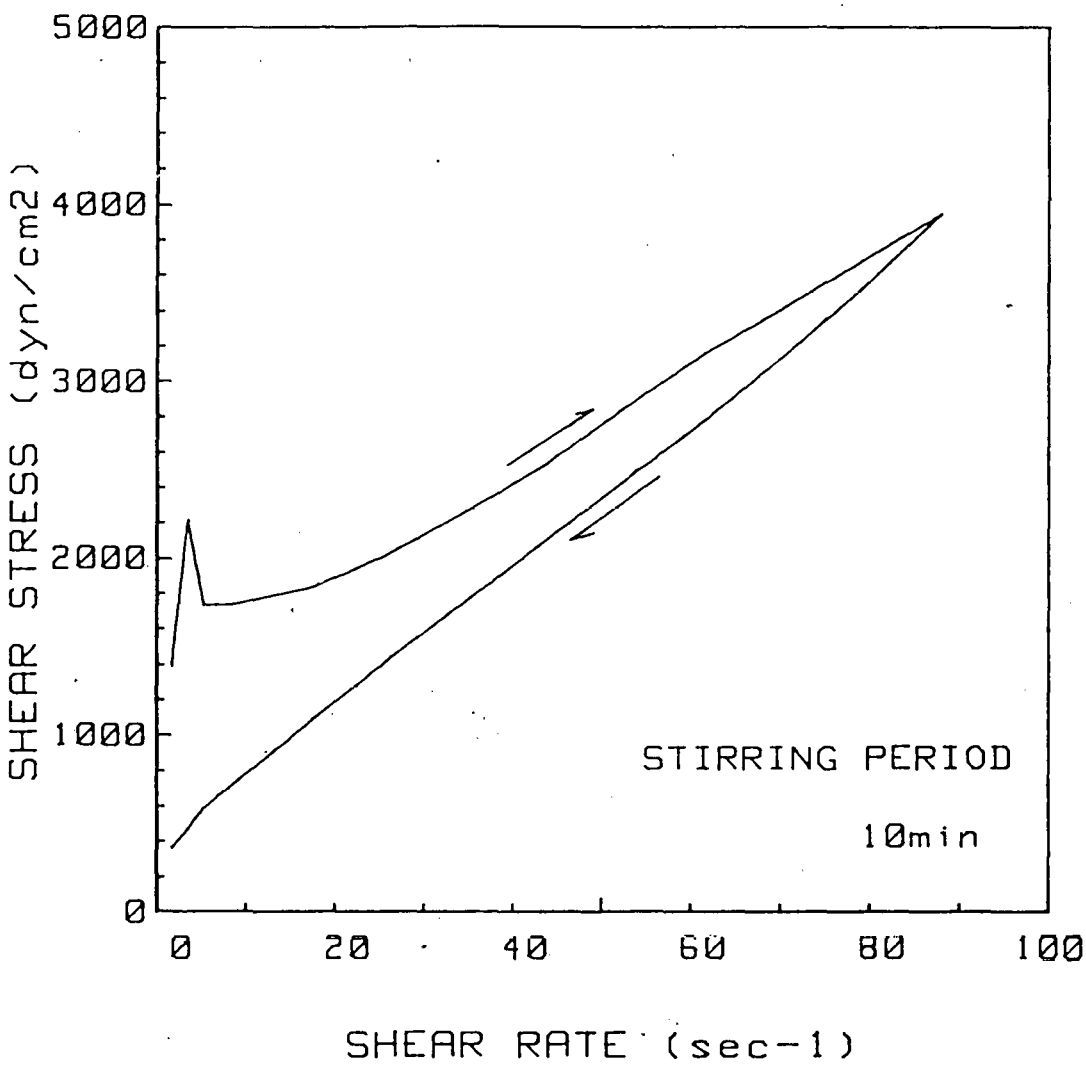

Warkworth coal (c.c.72%)

Additive -- HCC-700 1%(vs. coal)

Fig.10 Rheogram of CWM

-- Stirring effect (high shear rate)

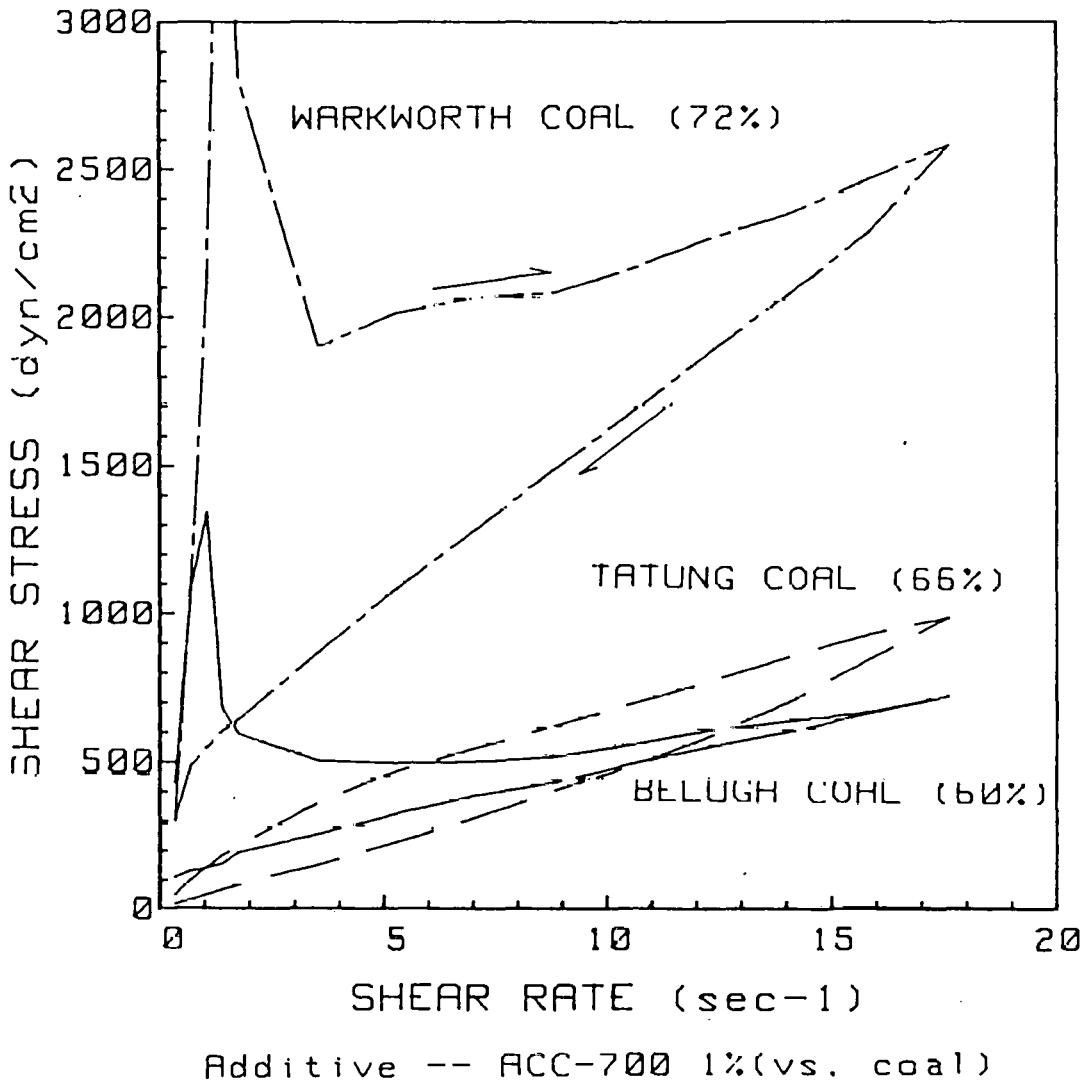

Fig.11 Rheogram of CWM -- Kinds of coal

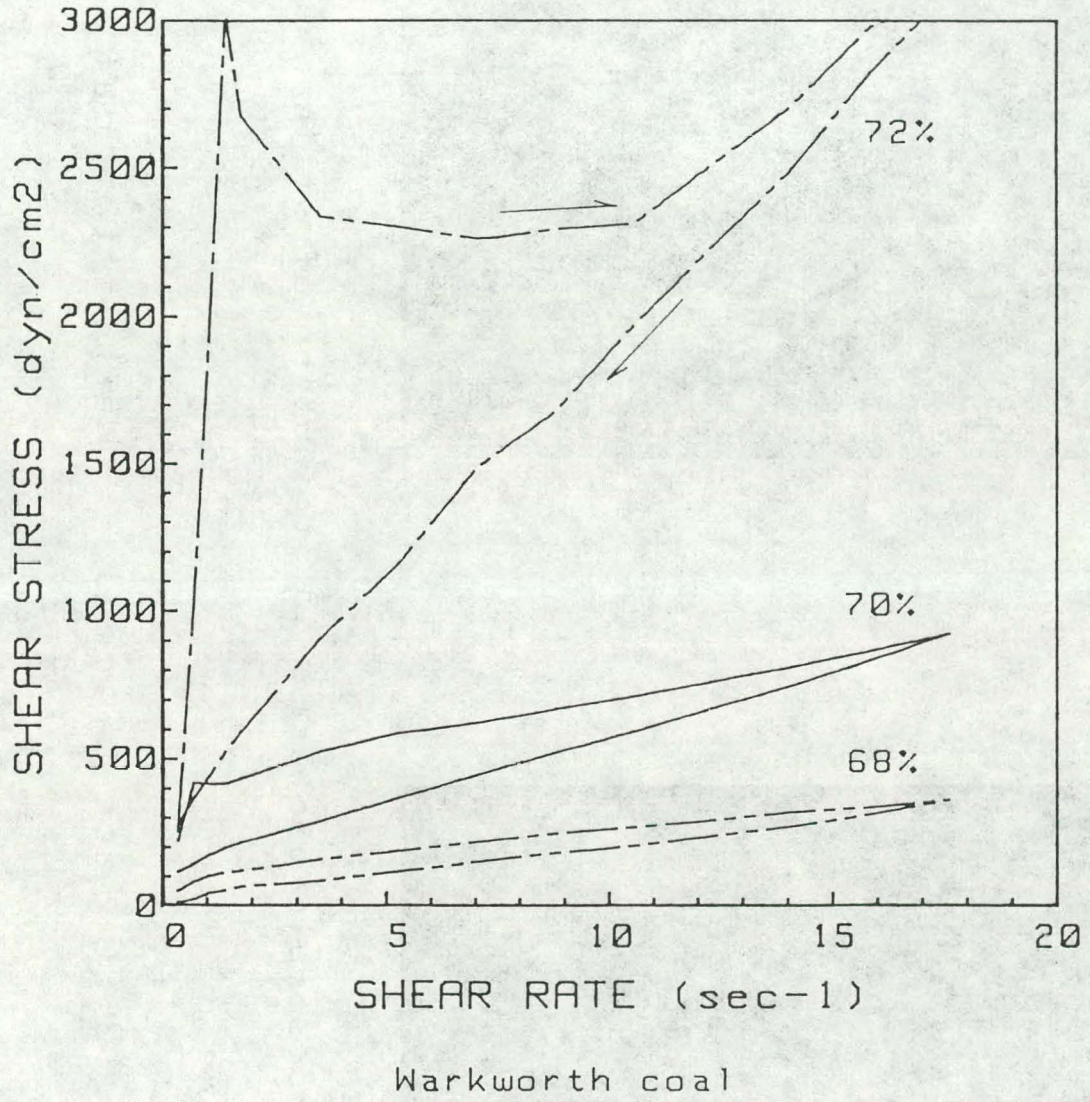

Fig.12 Rheogram of CWM

-- Effect of concentration of CWM

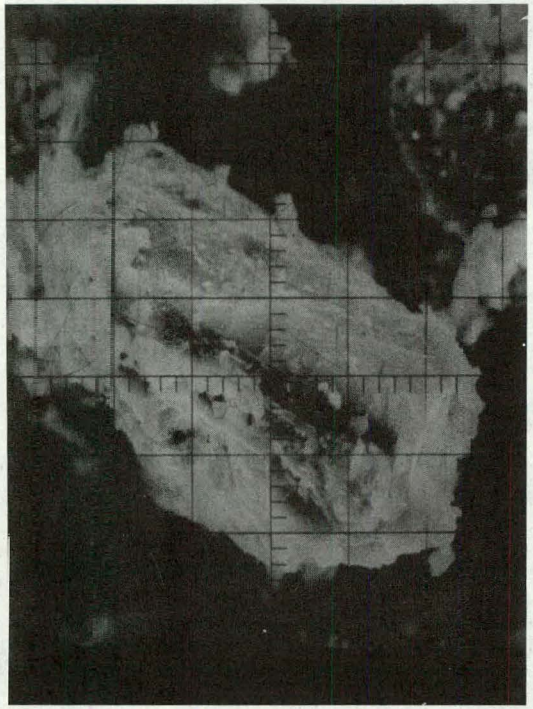

Electron micro-scopic picture

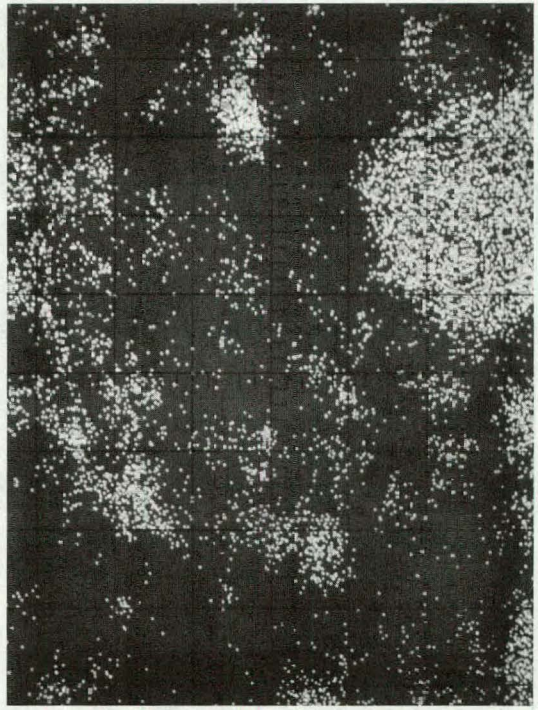

Distribution of silicon atoms (ash)

Fig.13 Surface of coal -- Warkworth coal

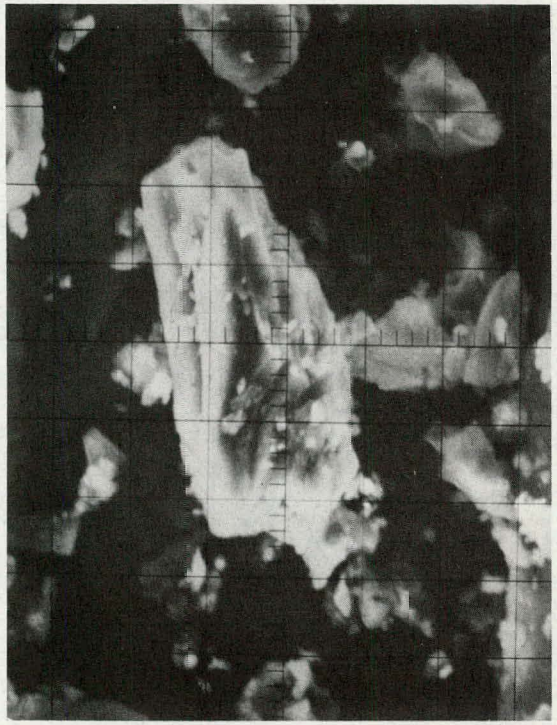

Electron micro-scopic picture

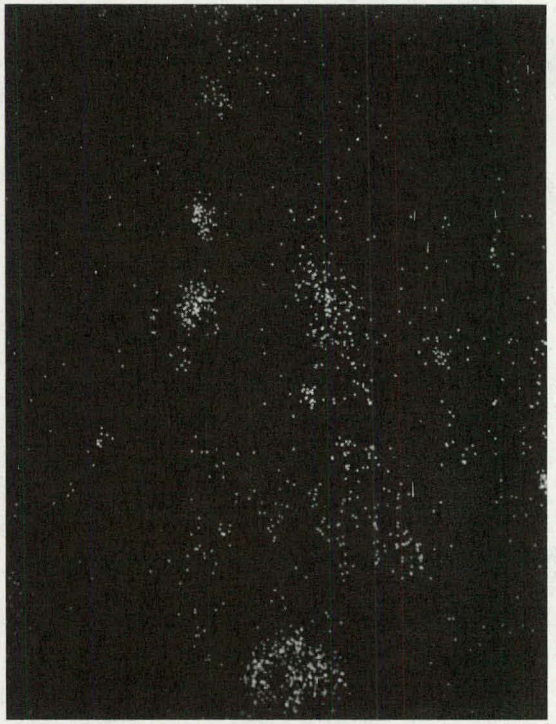

Distribution of silicon atoms (ash)

Fig.14 Surface of coal -- Tatung coal

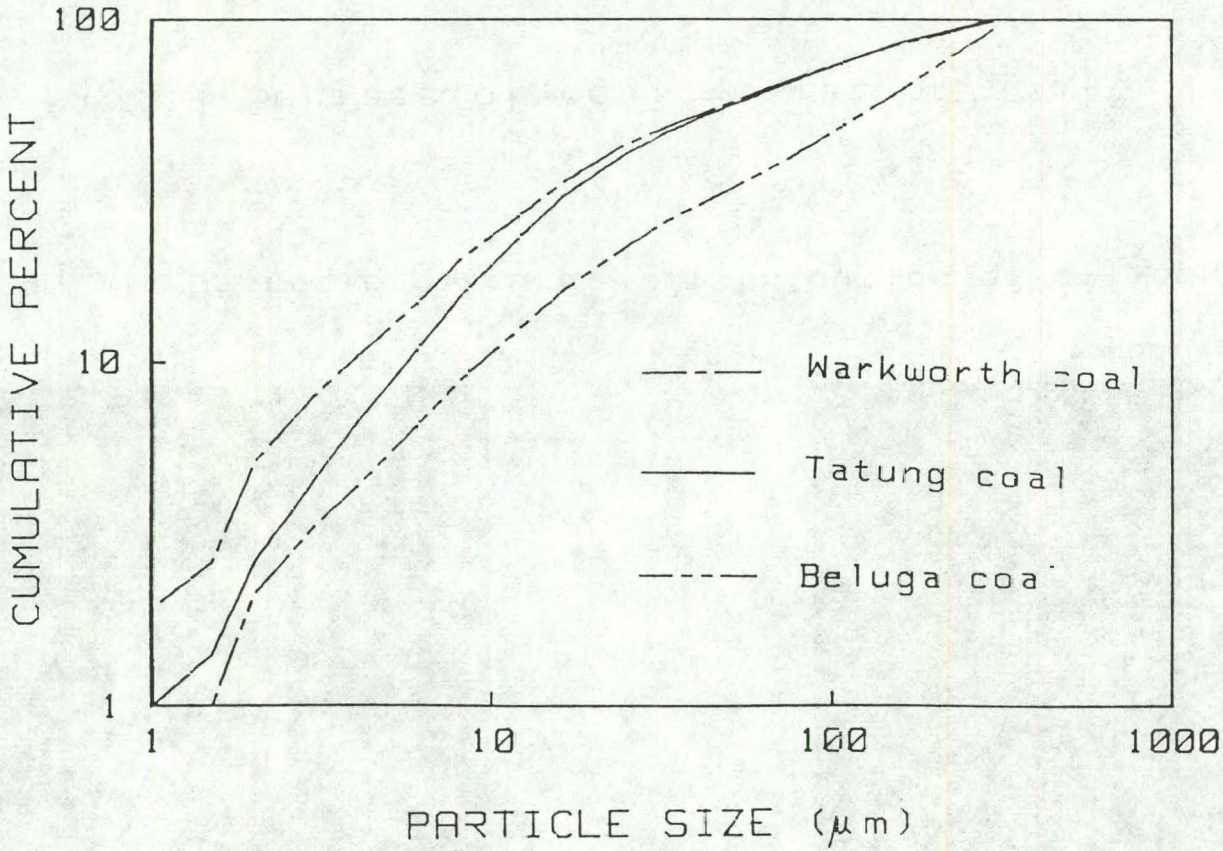

Fig.15 Particle size distribution of coals

The following manuscript was unavailable at time of publication:

Rheology of Highly Concentrated Coal Slurries

G. D. Botsaris and Y. Glazman
Tufts University

DO NOT MICROFILM THIS PAGE

COAL/WATER SLURRY ROTATING CUP ATOMIZATION

Ronald J. Marnicio* and Holger T. Sommer**

Carnegie-Mellon University
Pittsburgh, PA 15213

1 ABSTRACT

A rotary cup atomizer design for coal/water slurries is examined which provides for continuous centrifugal separation of the coal and water while effectively preparing the mixture for droplet break-up and combustion. A literature review of rotary atomization and centrifugal flow regimes has identified a number of design and operational variables and flow parameters determinate to the effectiveness of the rotary atomization system. The fluid density and viscosity were also found to directly influence the cup internal flow regime. In recognition of the importance of this flow regime to both centrifugal separation and atomization, an extensive effort was undertaken to define the limits to predictive capability based on theory.

The early theoretical work of Hinze and Milborn [1], which addressed the flow within a rotary cup for a homogeneous liquid, was critically reviewed with particular emphasis paid to the expressions for the film's thickness, the surface and mean velocities, and velocity profile due to their pertinence to the separation and atomization processes.

The Hinze and Milborn analysis neglected the effects of gravitational forces and used thin film assumptions that were justified given their postulated conditions. Given the goals of the present study, other flow conditions and modes of operation became interesting, most notably, low speed operation. Under these conditions, the assumptions of the Hinze and Milborn analysis were believed to become binding.

The present analysis was developed from the spherical coordinate Navier-Stokes equations of motion for a constant property fluid. Following an order of magnitude analysis of the Navier-Stokes terms, a second order differential equation for the radial velocity was obtained which incorporated the effects of gravity and was less constrained by the geometrical thin film approximations. The velocity expression was subject to the boundary conditions of no slip at the cup wall and no shear at the film's free surface. Analytical expressions were developed for the film thickness, surface and mean velocities, and velocity profile. The pertinence of the six parameters

---

*Graduate Student, Mechanical Engineering Dept. and Dept. of Engineering and Public Policy

**Assistant Professor of Mechanical Engineering

recognized by Hinze and Milborn was confirmed and the cup's orientation with respect to gravity was also found to be influential under certain conditions.

2 INTRODUCTION

Ways to reduce coal transportation costs from mines to power plants have been investigated in many coal producing countries for a number of years. The first industrially used slurry pipeline was installed in 1947 in Lothringen, near the German-French border. In this 9km long pipeline, slurry containing primarily 300 μm or smaller coal particles with some large particles of 10mm, was transported [2,3]. The first coal slurry transportation project in the USA was initiated in 1961 and resulted in a 175km slurry pipeline from Cadir, Ohio to Eastlake, Ohio near Cleveland. A 45% by weight slurry consisting of coal particles less than 240 μm was transported through this trans-Ohio pipeline [3-7].

Both of these projects, however, required processing the coal after its transport through the pipelines. Mechanical dewatering and drying of the slurry made this mode of transporting coal over long distances economically unattractive. The amount of energy required to separate the water from the coal prior to combustion was prohibitive as railroad transportation costs were lower than the combined cost of transporting the slurry through the pipeline, and dewatering it once on site.

Though not practical in themselves, these projects stimulated research on how to directly burn heavily coal loaded slurries in power plants and industrial furnaces. A program was established in 1961 to study the technical and economic feasibility of direct coal-water slurry combustion [8]. This project involved testing the coal-water slurry preparations and combustion processes on an industrial scale, as well as investigating global material properties and slurry rheology, in order to provide the necessary design parameters not formerly available.

As mentioned above, the combined system of transportation and combustion becomes economically viable when a coal-water separation or drying process is unnecessary, and direct combustion of coal-water slurries is technically possible under steady conditions. It is known from liquid fuel combustion that atomization or spray formation of the fuel has a critical influence on the combustion and ignition processes. The process of atomization prepares the fuel for combustion by providing a larger surface area for radiation-ignition. In addition, it produces smaller volumes of the fuel material for faster burnout, and together with the aerodynamics of the combustion air, atomization influences the global flame shape within the combustion chamber of a boiler. Therefore, knowledge of the details and mechanisms involved in the atomization process itself will provide the tools and necessary engineering design criteria for the construction of utility boilers and industrial furnaces.

In the fall of 1961, the Werner Station power plant of the New Jersey Central Power and Light Company successfully fired one of their boilers for one continuous month on a 70%-30% (by weight) coal/water slurry [9-11]. The

test, using a conventional spray atomizer, was considered a breakthrough in coal utilization and many economic and operational advantages were identified with the use of slurry combustion instead of conventional pulverized coal combustion. Surprisingly, coal-water combustion activity was never followed up in the United States until quite recently. In Germany however, the work of Schwarz and Merten [12-14] explored many aspects of coal-water slurries, from preparation to combustion. Schwarz [12] examined the effect of the fuel's higher moisture content on the combustion process and outlined some of the advantages to direct slurry firing. In later works, Schwarz and Merten [13,14] described the successful retrofit of pulverized coal industrial boilers with slurry burners employing rotary cup atomizers. They preferred the rotating cup design over pressure-type atomizers due to lower erosion and no requirement of high pressure feed lines. They noted a separation effect of the coal and water as the slurry flowed towards the edge of the rotating cup. During this flow, radial forces formed two concentric layers on the inner walls of the cup, one of coal and one of water. They concluded that it was possible to separate the coal from the water before the slurry enters the combustion chamber, thus substantially increasing boiler efficiency and providing the potential to conserve water. A negative pressure zone developed in the cup's interior during operation, drawing in hot combustion gases which evaporated some water and pre-heated the coal. Unlike oil atomizers, the authors found that the droplet size in the spray was restricted by the size of the suspended coal particles and that the spray consisted of a combination of either water droplets or coal particles. Their rotary cup atomizer incorporated a special bearing arrangement which automatically compensated for eccentric slurry loading. The burner was tested for 2000 hours. Based on the success of their rotary cup atomizer in field tests, the authors anticipated further retrofits using their design for attaining better performance. In Russia [15], work has centered on the preparation and stabilization of coal-water slurries and economic analyses of integrated mining-transportation-combustion slurry systems.

Rotary cup atomizers were first developed for industrial and residential oil furnaces, with design rules established in a piecemeal, trial and error fashion. Even so, a number of currently relevant design parameters and practices have been identified. Steiner [16-18] noted the importance of the cup's speed of rotation, length and angle of taper in the preparation and motion of the fluid film inside the cup. He also qualitatively described the role of the speed, direction and volume of the primary and secondary air used to shear the film, shape the spray and provide the proper stoichiometry. Steiner also identified design features which augment the operational reliability of the rotary cup atomizer, such as cup detachability for cleaning, unobstructive fuel delivery lines and good cup/shaft axial alignment. Burkhardt [19,20] and Trinks and Mawhinney [21] discussed the applications most suited to rotary cup atomizers and added further qualitative description of their operation. Giffen and Muraszew [22], in their comprehensive review of liquid spray atomization theory, cited only the work of Hinze and Milborn [1]. The work of the latter represents the best fundamental analysis of the rotary cup atomization of single phase liquids up to now. Hinze and Milborn used fluid analysis and photographic diagnostics to quantitatively identify the effect of many of the variables identified by Steiner and Burkhardt on the atomization process. They also noted the dependence of performance on the fluid's density, viscosity and surface tension and identified different regimes of droplet

formation under various operating conditions. Rotary cup atomization was found to yield droplets of remarkable size uniformity.

Thus, as of this date, coal-water combustion has been successfully demonstrated at the industrial scale. Slurry atomization has been identified as an important link between slurry transport and combustion. Investigators have shown advantages to the use of rotary cup atomizers over pressure-type atomizers in some slurry applications.

3 THEORETICAL DEVELOPMENT

The present theoretical analysis of the flow within a rotating cup was begun in hopes of refining the analysis performed by Hinze and Milborn in support of their 1949 Experimental work at Delft Laboratory in Holland. This exercise was aimed at assessing the theory's ability to predict the physical behavior within a rotating cup atomizer and the potential to harness the separation effect of the coal and water observed by Schwartz and Merten [13,14].

The analysis is developed from an examination of the Navier-Stokes equations of motion and the continuity equation written in spherical coordinates for an incompressible fluid with constant properties. The coordinate system, defined and oriented as in Figure 1, allowed the convenient and sufficient specification of the system boundaries.

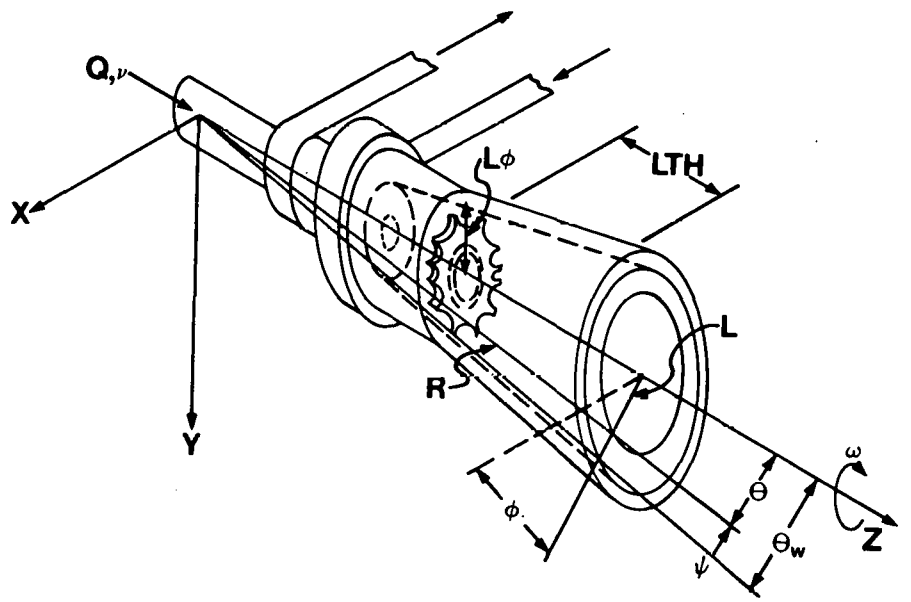

Figure 1: Rotating Cup Geometry and Coordinate System.

To simplify the equation and make the problem amenable to solution the following assumptions were made:

1. Constant fluid properties of density and viscosity.

2. The thickness of the fluid layer is very small relative to the dimensions of the cup.

3. Steady flow analysis.

4. Flow within the cup is rotationally symmetric.

5. Velocities are relative to the non-accelerating spinning cup.

Imposing the constraints associated with these assumptions onto the set of equations left them somewhat more tractable. An order of magnitude analysis of the various remaining terms of the equations was then undertaken by defining the cup diameter and the film thickness as two characteristic system lengths and a characteristic system velocity in the radial direction. This analysis yielded the following results:

1. From considerations of continuity, the fluid velocity on the θ or ψ direction was negligible relative to the fluid velocity in the R direction.

2. Within a fairly wide range of parameters, the viscous terms of the Navier-Stokes equations for all three directions were about two orders of magnitude larger than the convective terms. Thus, the convective terms were considered to be negligible relative to the viscous terms, and the rotating cup flow regime to resemble creep flow.

3. The body force terms of the equations of motion were found to consist of contributions of both centrifugal and gravitational origin weighted according to cup geometry. In the θ direction, the gravitational contributions were roughly three orders of magnitude smaller than the centrifugal contributions, and thus were considered to be negligible by comparison. In contrast, the gravitational contributions in the R direction fell within the range of 1% to 10% of centrifugal contributions, and, as such, could not be considered to be negligible.

4. Static pressure variations were found to be negligible based on the order of magnitude analysis and the characteristics of the system.

The ramifications of these findings further simplified the set of equations. Having justified the elimination from concern of the θ and ϕ velocity components, the resulting R direction equation became:

$$0 = Lw^2 \sin\theta \pm g \cos\theta + \frac{\mu}{\rho R^2 \sin\theta} \frac{d}{d\theta}\left(\sin\theta \frac{dV_R}{d\theta}\right) \tag{1}$$

This equation can be solved for V_R by direct integration to yield:

$$V_R = E\left(\sin\theta - \left(\theta + \frac{\theta^3}{18} + \frac{7\theta^5}{1800} + \ldots + \frac{2(2^{2n-1} - 1)}{(2n+1)!} B_n \theta^{2n+1} + \ldots\right)\right) \tag{2}$$

$$+ F\cos\theta + K1\left(\ln(\tan\frac{\theta}{2})\right) + K2$$

where : B_n is the n^{th} Bernoulli Number [23] given by the following:

$$1 + \frac{1}{2^{2n}} + \frac{1}{3^{2n}} + \frac{1}{4^{2n}} + \ldots + \frac{1}{K^{2n}} + \ldots = \frac{\pi^{2n} 2^{2n-1}}{(2n)!} B_n \tag{3}$$

The radial velocity of Equation 2 is subject to the following boundary conditions:

B.C. # 1: $V_R = 0 \; @ \; \theta = \theta_w$ (No slip condition) (4)

B.C. # 2: $\frac{\mu}{R}\frac{dV_R}{d\theta} = 0 \; @ \; \theta = \theta_s$ (5)

(No shear at the free surface)

Applying B.C. # 2 to Equation 2 defines K1 as:

$$K1 = E\left(\theta_s - \frac{\sin(2\theta_s)}{2}\right) + F\sin^2(\theta_s) \tag{6}$$

Subsequently applying B.C. # 1 to Equation 2 defines K2 as:

$$K2 = -E\left(\sin\theta_w - (\theta_w + \frac{\theta_w^3}{18} + \frac{7\theta_w^5}{1800} + \ldots\right.$$

$$\left. + \frac{2(2^{2n-1} - 1)}{(2n+1)!} B_n \theta_w^{2n+1} + \ldots)\right)$$

(7)

$$- F \cos\theta_w - K1\left(ln(\tan \frac{\theta_w}{2})\right)$$

The surface angle, θ_s, is found using the continuity constraint that the total quantity of liquid flowing through the layer toward the brim of the cup must equal the quantity supplied to the cup. This condition can be written:

$$Q = \int_{\theta_s}^{\theta_w} V_R(\theta) dA(\theta) \tag{8}$$

where

$$dA(\theta) = 2\pi R^2 \sin\theta_s \, d\theta \tag{9}$$

This condition can be rewritten in the form:

$$0 = \int_{\theta_s}^{\theta_w} V_R(\theta) dA\theta - \frac{Q}{2\pi R^2 \sin\theta_s} \tag{10}$$

or

$$0 = -E\left(\cos\theta + \frac{\theta^2}{2} + \frac{\theta^4}{72} + \frac{7\theta^6}{10800} + \ldots \right.$$

$$\left. + \frac{2(2^{2n-1}-1)}{(2n+1)!} B_n \frac{\theta^{2n+2}}{(2n+2)} + \ldots\right) \Big|_{\theta_s}^{\theta_w} + F(\sin\theta)\Big|_{\theta_s}^{\theta_w}$$

$$+ K1\left(\theta ln \frac{\theta}{2} - \theta + \frac{\theta^3}{36} + \frac{14\theta^5}{14{,}400} + \ldots \right. \tag{11}$$

$$\left. + \frac{(2^{2n-1}-1)}{n(2n+1)!} B_n \theta^{2n+1} + \ldots\right) \Big|_{\theta_s}^{\theta_w} + K2(\theta)\Big|_{\theta_s}^{\theta_w}$$

$$- \left(\frac{Q}{2\pi R^2}\right) \csc\theta_s$$

Although Equation 11 is a function only of the variable θ_s, it can not be solved explicitly. Application of the Newton-Raphson method for iterative solution of equations of the form $f(\theta_s) = 0$, where f is differentiable [24] works well for this system, providing rapid convergence on the surface angle, θ_s. The analytical derivative of the function identified in Equation 11 with respect to θ_s is given by:

$$
\begin{aligned}
f'(\theta_s) = E\Big(\sin\theta - \Big(\theta + \frac{\theta^3}{18} + \frac{7\theta^5}{1800} + \ldots \\
+ \frac{2(2^{2n-1}-1)}{(2n+1)!} B_n \theta^{2n+1} + \ldots\Big)\Big)\Big|_{\theta_s}^{\theta_w} \\
+ F(\cos\theta)\Big|_{\theta_s}^{\theta_w} \\
+ K1\Big(ln\,\frac{\theta}{2} + \frac{\theta^2}{12} + \frac{7\theta^4}{1440} + \ldots \\
+ \frac{(2n+1)(2^{2n-1}-1)}{n(2n+1)!} B_n \theta^{2n} + \ldots\Big)\Big|_{\theta_s}^{\theta_w} \\
+ \Big(\theta ln\,\frac{\theta}{2} - \theta + \frac{\theta^3}{36} + \frac{14\theta^5}{14{,}400} + \ldots \\
+ \frac{(2^{2n-1}-1)}{n(2n+1)!} B_n \theta^{2n+1} + \ldots\Big)\frac{dK1}{d\theta_s}\Big|_{\theta_s}^{\theta_w} \\
+ \Big(K2 + (\theta_w - \theta_s)\frac{dK2}{d\theta_s}\Big)\Big|_{\theta_s}^{\theta_w} \\
+ \Big(\frac{Q}{2\pi R^2}\Big)(\csc\theta\,\cot\theta)\Big|_{\theta_s}^{\theta_w}
\end{aligned}
\tag{12}
$$

where:

$$\frac{dK1}{d\theta_s} = E(1 - \cos(2\theta_s)) + 2F \sin\theta_s \cos\theta_s \tag{13}$$

$$\frac{dK2}{d\theta_s} = -\ln\left(\tan\left(\frac{\theta_w}{2}\right)\right) \frac{dK1}{d\theta_s} \tag{14}$$

Using equations 11-14 in the general Newton-Raphson algorithm

$$\theta_{s_{k+1}} = \theta_{s_k} - \frac{f(\theta_{s_k})}{f'(\theta_{s_k})} \quad (k = 0,1,2,\ldots) \tag{15}$$

with a first guess for θ_{s_0}, the value of θ_s satisfying the continuity constraint can be quickly determined.

Having determined this value of θ_s, the flow characteristics of the system can be completely specified. The most pertinent characteristics to slurry dewatering and atomization are:

1. The Film Thickness:
$$\delta = R(\theta_w - \theta_s) \tag{16}$$
2. The Velocity Profile Across the Film: Given by Equation 2 with θ sweeping from θ_s to θ_w.
3. The Film Surface Velocity, V_{R_s}: Given by Equation 2 with $\theta = \theta_s$.
4. The Mean Velocity Across the Film X-Section, V_{R_M}

$$V_{R_M} = \left(\frac{1}{\theta_w - \theta_s}\right)\left[-E\left(\cos\theta + \frac{\theta^2}{2} + \frac{\theta^4}{72} + \frac{7\theta^6}{10{,}800} + \ldots + \frac{2(2^{2n-1}-1)}{(2n+1)!} B_n \frac{\theta^{2n+2}}{(2n+2)} + \ldots\right)\Big|_{\theta_s}^{\theta_w} + F(\sin\theta)\Big|_{\theta_s}^{\theta_w}\right.$$
$$\left. + K1\left(\theta \ln\frac{\theta}{2} - \theta + \frac{\theta^3}{36} + \frac{14\theta^5}{14{,}400} + \ldots + \frac{(2^{2n-1}-1)}{n(2n+1)!} B_n \theta^{2n+1} + \ldots\right)\Big|_{\theta_s}^{\theta_w} + K2(\theta)\Big|_{\theta_s}^{\theta_w}\right] \tag{17}$$

As can be seen these important characteristics were found to depend on

many of the same fluid characteristics, cup design, and operational parameters identified earlier by Steiner and Burkhardt [16-19] which include:

1. The cup's speed of revolution, angle of taper, and characteristic radius.

2. The slurry density and absolute viscosity.

3. The slurry volumetric flow rate.

4. The cup's orientation with respect to gravity.

3.1 CONTRAST TO HINZE AND MILBORN ANALYSIS

Following the order of magnitude analysis of the terms of the Navier-Stokes equations of motion, the present analysis diverged from that of Hinze and Milborn, primarily for two reasons. First, calculations indicated that the geometric approximations adopted by Hinze and Milborn (enabling the second order differential equation to be treated as having constant coefficients) may not be appropriate under certain situations of potential interest, such as larger angle cups. Second, lower angular velocity applications were also of interest. In these cases the gravitational components of the body force terms of the Navier-Stokes equations were found to be potentially significant. Thus, the present analysis proceeded, incorporating the gravitational effects at various orientations, and without making the geometric simplifications.

The resulting second order differential equation resembled the Hinze and Milborn equation, as can be seen in equations 18 and 19, but the required 3 successive integrations with respect to the independent variable in the present analysis proved to be analytically challenging.

Hinze & Milborn:

[18A]

$$\frac{1}{R^2}\frac{d^2V_R}{d\theta^2} + \frac{\rho\omega^2 R \sin^2\theta_w}{\mu} = 0$$

(FORM):

[18B]

$$\frac{d^2V_R}{d\theta^2} + \text{constant} = 0$$

Present Analysis:

[19A]

$$\frac{1}{R^2}\frac{d}{d\theta}\left(\sin\theta\,\frac{dV_R}{d\theta}\right) + \frac{\rho\omega^2 L}{\mu}\sin^2\theta \pm \frac{\rho g}{\mu}\sin\theta\cos\theta = 0$$

(FORM):

[19B]

$$\frac{d}{d\theta}\left(\sin\theta \frac{dV_R}{d\theta}\right) + \text{constant}_1 \sin^2\theta \pm \text{constant}_2 \sin\theta\cos\theta = 0$$

The present analysis, albeit more computationally demanding, provides greater flexibility and accuracy to the rotary system designer and provides a more suitable foundation for future work by the authors.

4 DESCRIPTION OF THE COMPUTER PROGRAM

A Fortran computer program has been developed to perform the many calculations and iterations involved with both the Hinze and Milborn analysis and the present study. A flowchart of the program's logic appears in Figure 2.

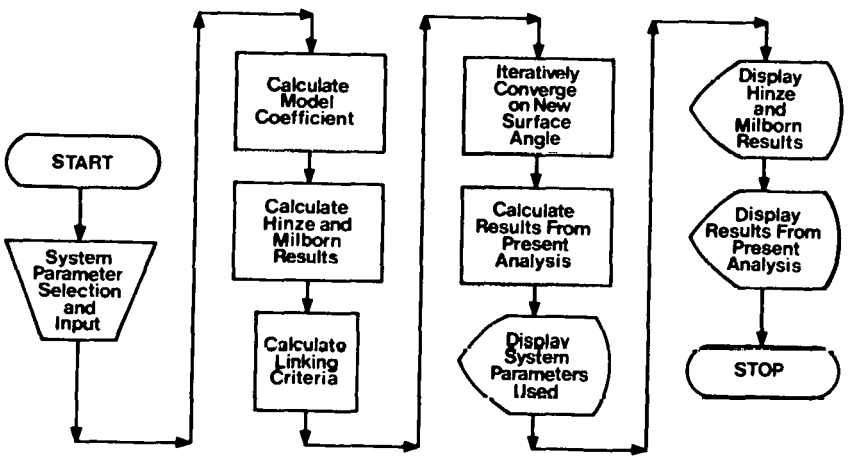

Figure 2: Flow Chart for Rotary Cup Flow Simulation Program.

The program is interactive and user friendly in the input of any of six major program variables, which are:

Q = the liquid volumetric flow rate

ν = μ/ρ = the liquid kinematic viscosity

ω = the cup rotational velocity

θ_w = the cup taper angle

L_o = the cup entrance rotational radius, and

LTH = the overall cup length along the axis of revolution.

The user also chooses how the cup is to be oriented so that the gravitational effects can be properly incorporated. The program calculates and displays the following outputs for both the Hinze and Milborn solution technique and that of the present analysis at the cup's entrance, its mid-length, and its exit:

1. the rotational radius
2. the radial spherical coordinate
3. the liquid film thickness
4. the film's surface velocity
5. the film's mean cross-sectional velocity; and
6. the velocity profile of the liquid across the film.

In addition, the Hinze and Milborn output contains the value of the thin film criterion used to judge the appropriateness of the thin film assumption and the output of the present analysis lists the percentages of the total velocities attributable to centrifugal terms and gravitational terms.

The subroutines of the program are all written in the double precision format. This was found necessary due to the system's mathematical sensitivity to small differences in angles which in part follows from the conical geometry.

5 FINDINGS AND DISCUSSION

A parametric study of the primary system variables was performed using this Fortran program. The results, discussed below, are displayed graphically in Figures 3-9. Based on the literature review, a representative value was chosen for each of the parameters to provide a base case above and below which each parameter was varied, one at a time, while the others were held constant. These base case values and the range of variation are shown in Table 1.

The parameter study was performed with the goal of providing a quantitative measure of each parameter's effect on the flow within the cup and on the velocity and thickness of the film layer at the cup exit, since these characteristics directly impact the film break-up and atomization processes. Consequently, Figures 3-8 contain results for the cup exit and, arbitrarily, for the cup in the gravity enhancing orientation. It should be reiterated that the model can predict the flow at all positions within the cup and for various orientations, as is evidenced by Figure 9.

The first two plots in the series show the system parameters generally considered requirements imposed externally by an atomization application: the total volumetric flow rate of slurry and its kinematic viscosity (generally a

Table 1: Summary of Parameter Study

PARAMETER	LOWER VALUE	BASE CASE VALUE	HIGHER VALUE
1. Volumetric Flow Rate, Q (GPM) - Figure 3	0.1	0.5	2.5
2. Kinematic Viscosity, ν (m^2/sec)	1.0×10^{-5}	1.1×10^{-3}	1.4×10^{0}
(as coal weight %) Figure 4	40	65	90
3. Cup Rotational Speed, ω, (RPM) - Figure 5	1200	3600	9600
4. Cup Angle of Taper, θ_w, (Degrees) - Figure 6	5	25	45
5. Radius of Rotation at Cup Inlet, $L\phi$, (CM) - Figure 7	0.43	1.27	2.12
6. Cup Length, LTH, (CM) - Figure 8	4.23	12.7	21.2
7. Cup Orientation	Gravity Enhanced	Gravity Enhanced	Gravity Enhanced

function of the coal loading). Figure 3 shows that increasing the volumetric flow rate serves to increase both the film thickness and mean velocity as might be guessed from considerations of continuity. The present analysis has the mean film velocity increasing as $Q^{0.667}$ and the film thickness as $Q^{0.334}$. This is virtually identical to Hinze and Milborn's 2/3 and 1/3, respectively. The dependence of the film thickness on Q is significant in that increasing the slurry throughput might lead to the formation of a liquid sheet at the cup exit which is too thick to be satisfactorily broken into droplets. Thus, to maintain an optimal or maximum film thickness for atomization purposes, increases in the slurry throughput would have to be accompanied by other compensating design or operational adjustments (discussed below). Figure 4 shows that increasing the slurry's coal mass loading, and consequently its kinematic viscosity, drastically increases the film thickness and slows it down. The present analysis once again concurs with the Hinze and Milborn analysis in finding that the mean film velocity falls and the film thickness grows as $\nu^{1/3}$. It should be noted that the highest viscosity run on Figure 4 is more of a mathematical limit than a reality since the fluid-like nature of a 90% by weight coal slurry is highly dubious.

Taken together, Figures 3 and 4 indicate that the more appealing scenarios of high slurry throughput at high coal loadings could present atomization problems since very thick film layers at the cup exit can be expected. However, the remaining system parameters can provide sufficient flexibility and control over the flow within the rotating cup to eliminate the atomization problems caused by these external requirements.

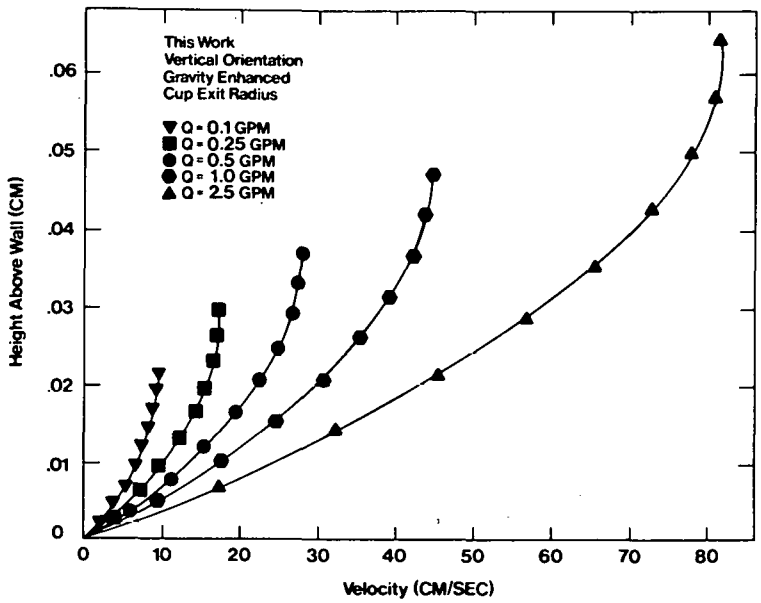

Figure 3: Results: Effect of Volumetric Flow on Velocity Profile.

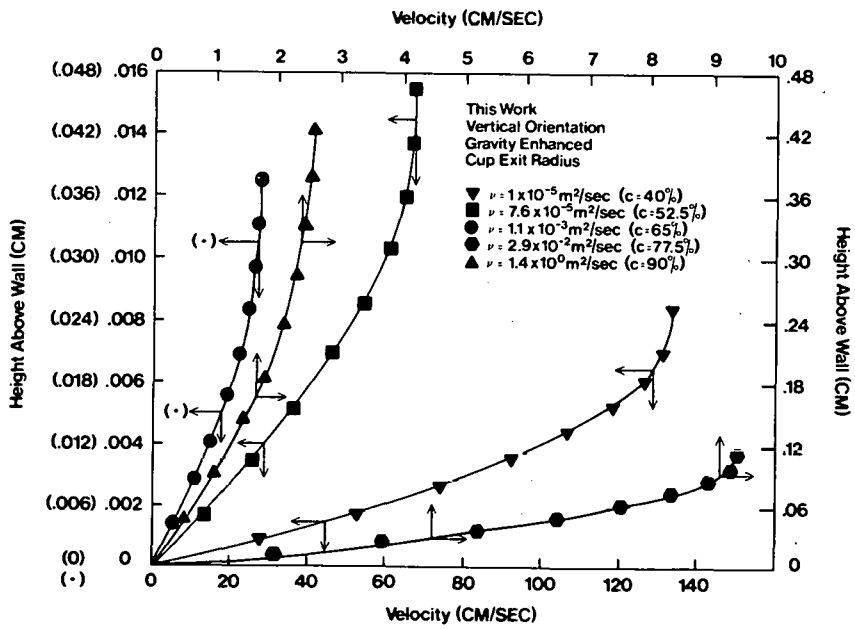

Figure 4: Results: Effect of Viscosity on Velocity Profile.

The first such parameter is the cup rotational speed. Figure 5 shows that increasing the cup RPMs decreases the film thickness, varying as $\omega^{-0.666}$, and increases the slurry mean velocity, as $\omega^{0.663}$. These quantitative dependencies agree well with those of the Hinze and Milborn analysis, who found -2/3 and +2/3, respectively. It then follows that increasing the cup RPMs directly offsets the atomization-retarding effects of increased slurry throughput or loading. The limit to the effectiveness of this scheme of

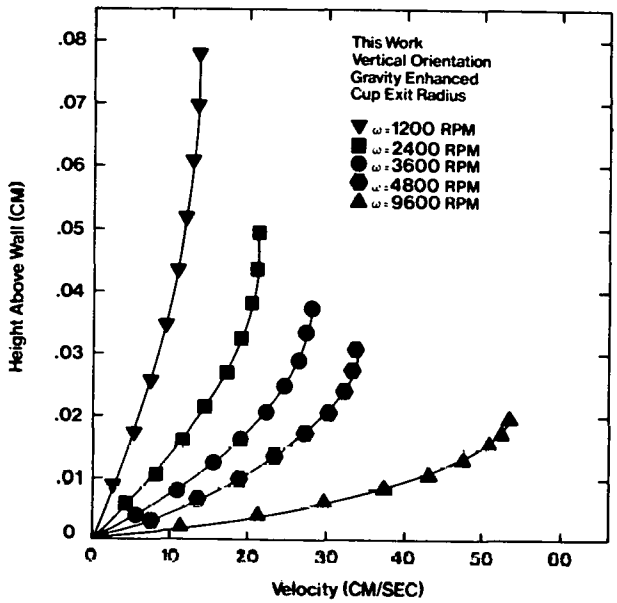

Figure 5: Results: Effect of Rotational Speed on Velocity Profile.

control arises from engineering considerations such as the vibration, cup misalignment, and energy and material costs associated with high RPM systems. These not withstanding, variation of the cup rotational speed provides a simple and effective tool for controlling the film thickness and facilitating atomization.

A second useful parameter is the cup angle of taper, whose effect is shown in Figure 6. It can be seen that increasing this design geometry parameter has little effect on the mean film velocity. But it can decrease the film thickness significantly. The present analysis found that the film thickness varied as the $[\sin(\theta_w)]^{-0.907}$ while the Hinze and Milborn analysis was found to vary as $[\sin(\theta_w)]^{-1}$. The Hinze and Milborn analysis found the mean velocity to be insensitive to changes in the wall angle while this analysis shows an effect of varying direction and magnitude, going as roughly $[\sin(\theta_w)]^{0.10}$ for cup angles less than 20 degrees. The film thickness effect would appear to result from the rapidly increasing flow circumference at the cup exit for the larger angles requiring ever decreasing film heights to accommodate a fixed throughput. Increasing the cup angle also provides an effective means of decreasing a film thickness inflated by high Q or ν. However, it does not provide the degree of velocity control offered by cup RPM adjustments. The differences between the present model and that of Hinze and Milborn concerning the effects of this geometry variable are undoubtedly due to the approximations employed in the earlier analysis.

Figure 7 shows that increasing the rotational radius at the cup inlet, holding all other parameters constant, has little effect on either the film thickness or mean velocity. Thus, this variable would not appear to be important from purely atomization considerations. For dewatering, however, this parameter grows in importance since it is believed to proportionally affect the rate of settling of coal through the slurry layer.

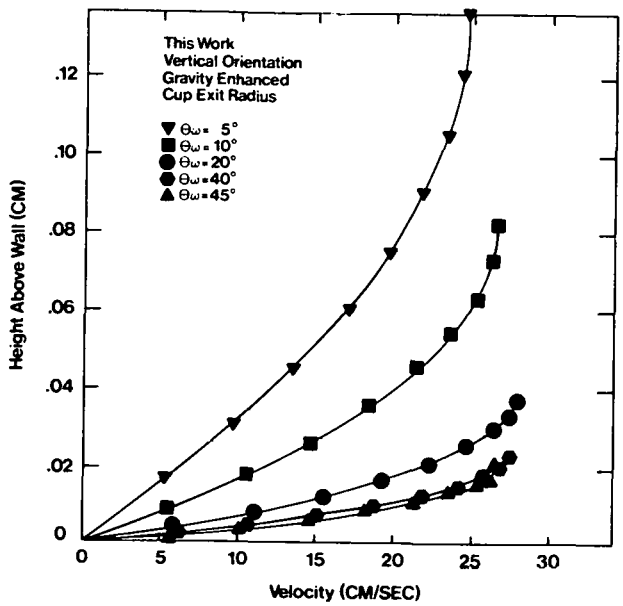

Figure 6: Results: Effect of Cup Angle on Velocity Profile.

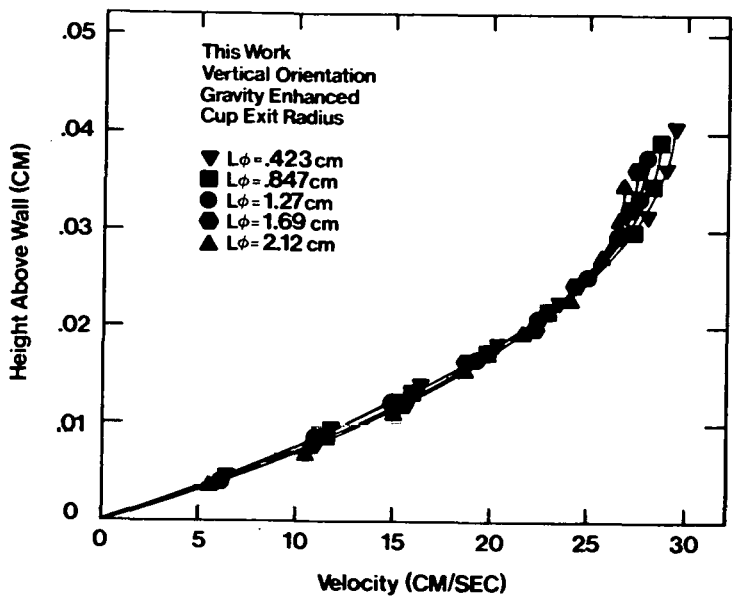

Figure 7: Results: Effect of Inlet Rotational Radius on Velocity Profile.

Figure 8 shows the effect of cup length on the slurry's velocity profile at the cup exit. Increasing the cup length is seen to decrease the mean film velocity, varying as $LTH^{-0.259}$, and also decreasing the film thickness, having a $LTH^{-0.516}$ dependence. Due to the difference in format, no comparison can be made with the Hinze and Milborn analysis concerning this parameter. The impact of cup length shown in Figure 8 would seem to be explained by a lengthening flow circumference coupled with the continuity constraint and a

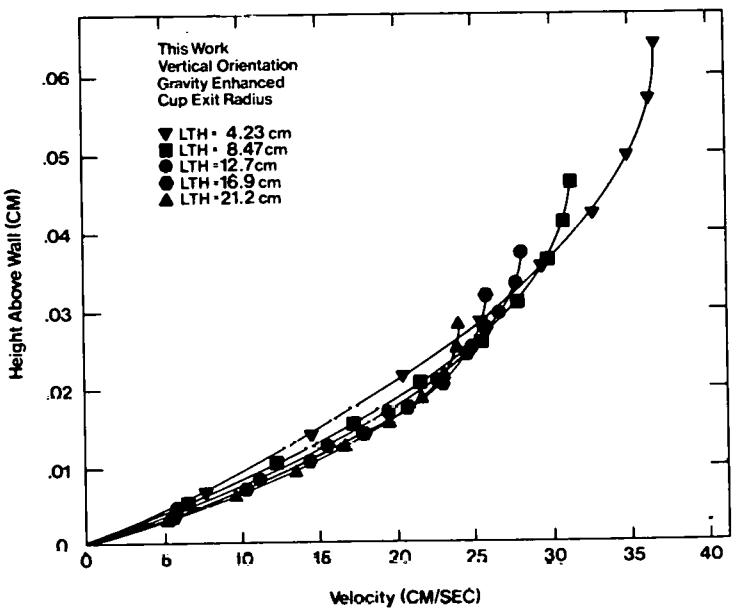

Figure 8: Results: Effect of Cup Length on Velocity Profile.

balancing of centrifugal acceleration and frictional forces. Thus, varying the cup length can provide a fairly strong means of control over both the film thickness and the slurry velocity. What is more, a combination of increased cup length and cup RPMs would provide a means to decrease the film thickness, for enhanced atomization, while having little effect on the mean velocity, which might be an important operational consideration.

Figure 9 shows the effect of the cup's orientation with respect to gravity for a system with the base case parameter values, except for ω = 1200 RPMs. As can be seen, gravitational effects are most noticeable, being as high as 10%, at the cup inlet where the centrifugal acceleration complements are smallest. The differences disappear by the time the cup exit is reached. As is expected, when gravity enhances the flow, the film is thinner and faster and when it retards the flow, the film is thicker and slower. A direct comparison can be made of the Hinze and Milborn velocity profile at the cup exit and the present study's horizontal orientation profile, since both neglect gravity. The more exact geometry assumptions of the present analysis would lead to predictions of slightly thicker and faster films relative to Hinze and Milborn. Thus, cup orientation should be of little use in the tailoring of the slurry film for atomization since no significant effect can be seen at the cup exit. However, the inclusion of gravitational effects will be important to considerations of coal settling and slurry dewatering which are intimately tied to the flow history along the entire cup length.

6 CONCLUSION

A slurry application externally imposes two driving effects on a rotary atomization system. The first is the slurry's viscosity, which is non-linearly tied to the coal loading, and the second is a slurry volumetric flow rate to

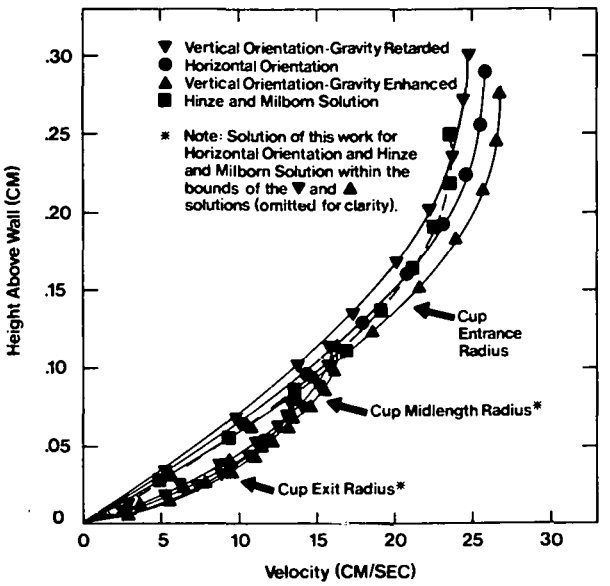

Figure 9: Results: Effect of Cup Orientation on Velocity Profile.

accommodate a certain boiler size. The most appealing combinations of these parameters tend to result in film layer thicknesses at the cup exit which are not conducive to good atomization. However, the remaining parameters provide a number of ways in which to adjust the system's design or operation to yield good atomization characteristics. A summary of options and effects appears in Table 2. In addition, enough flexibility exists in rotating cup systems to provide this tailoring without encountering excessive cost or operational constraints. Using the results of the present analysis, one can develop the design criteria necessary to construct a rotating cup atomizer for coal-water slurries.

Table 2: Summary of Rotary Atomization Control Options

PARAMETER	EFFECT ON THE FILM THICKNESS DUE TO AN INCREASE IN THE PARAMETER	EFFECT ON THE FILM MEAN VELOCITY DUE TO AN INCREASE IN THE PARAMETER
EXTERNAL SYSTEM REQUIREMENTS		
• Volumetric Flow rate (Figure 3)	$Q^{0.334}$	$Q^{0.667}$
• Kinematic Viscosity (Figure 4)	$\nu^{0.333}$	$\nu^{-0.333}$
DESIGN AND OPERATIONAL PARAMETERS		
• Rotational Speed (Figure 5)	$\omega^{-0.666}$	$\omega^{0.663}$
• Angle of Taper (Figure 6)	$[\sin(\theta_w)]^{-0.907}$	$[\sin(\theta_w)]^{0.10*}$
• Inlet Radius of Rotation (Figure 7)	Little Influence	Little Influence
• Cup Length (Figure 8)	$LTH^{-0.516}$	$LTH^{-0.259}$
• Cup Orientation (Figure 9)	Little Influence	Little Influence

*For θ_w < 20 degrees (negative exponent for θ_w > 25 degrees).

7 REFERENCES

1. Hinze, J.O. and H. Milborn, "Atomization of Liquids by Means of a Rotating Cup", *J. Applied Mech.*, 17, June, 145-153, 1950.

2. Aubathier, P., "Le Traitement des Schlams Transportes Hydrauliquement a'la Centrale Emile Huchet", *Ann. Min. Belg.*, Mai 1958.

3. Gibrat, R. and F. Chemin, "Transport and Utilization of Colliery Tailings at the Emil Hudet Power Station", *Inst. Elec. Engrs.*, Feb. 24, 1954.

4. Reichl, E., "Some Comments on Coal Pipelines", Energy Transportation Conf., St. Louis, Mo., November 1963.

5. Perry, H., *Revolution in Coal Transport Mechanization*, May 1963.

6. Wasp, E., *et al.*, "Cross Country Coal Pipeline", *Pipe Line News*, July 1963.

7. Bain, A., "Hydraulic Transport of Coal Over Long Distances", *J. I, EE*, August 1962.

8. Merten, H. and M. Honer, "Verfeurung von Kohle/Wasser-Suspensionen im Kraftwerk", Final Report, Steinkohlen Bergbauzerein Essen, 1972.

9. "Coal-and-Water Slurry Burned as Delivered by Pipeline", *Electrical World*, 52-53, November 20, 1961.

10. "Direct Firing of Coal Slurry", *Coal Age*, 12, 56-58, December 1961.

11. Schwarz, O. and K. Lemke, "Steinkohle wird wie Heroel Gepumpt und Verbrannt (Coal is pumped and burned like fuel oil)", *Chemie-Ing.-Techn.*, 34, 6, Jahra., 1962.

12. Schwarz, O., "Verbrennung von Staubkohle und Kohle/Wasser-Suspension in Wasserrohrkesseln (Comparison of Pulverized Fuel and Slurry Firing in a Water Tube Boiler Plant)", *Brennst.-Warme-Kraft*, 16, 6, 273-277, June 1964.

13. Schwarz, O. and H. Merten, "Herstellung, Transport, und Verbrennung von Kohle/Wasser-Suspension (Production, Transport, and Combustion of Coal/Water Suspension)", *Brennst.-Warme-Kraft*, 18, 10, 474-478, October 1966.

14. Schwarz, O. and H. Merten, "Direkte Verbrennung von Kohle-Wasser-Suspension im Kraftwek (Direct Combustion of Coal/Water Suspensions in Power Plants)", *Glukauf*, Heft 5, 225-231, March 1967.

15. Marnell, P., "Direct Firing of Coal-Water Suspensions: State of the Art Review", BNL-28575, CONF-80114.2-2, Department of Energy and

Environment, Brookhaven National Laboratory, Upton, NY, November 1980.

16. Steiner, K., *Fuels and Fuel Burners*, McGraw-Hill Book Co., Inc., New York, 1946.

17. Steiner, K., *Oil Burners*, McGraw-Hill Book Co., Inc., New York, 1950.

18. Steiner, K. and F. Ravensbeck, *Oil Burner Service Manual*, First Edition, McGraw-Hill Book Co., Inc., New York, 1942.

19. Burkhardt, C.H., *Domestic Oil Burners - Installation and Servicing*, First Edition, McGraw-Hill Book Co., Inc., New York, 1951.

20. Burkhardt, C.H., *Domestic Oil Burners - Installation and Servicing*, Second Edition, McGraw-Hill Book Co., Inc., New York, 1951.

21. Trinks, W. and M.H. Mawhinney, *Industrial Furnaces*, Vol. II, Fourth Edition, John Wiley & Sons, Inc., New York, 1967.

22. Giffen, E. and A. Muraszew, *The Atomization of Liquid Fuels*, John Wiley & Sons, Inc., New York, 1953.

23. Bronstein, I.N. and K.A. Semendjajew, *Taschenbuch der Mathematik*, Verlag Harri Deutsch, Zurich und Frankfurt/M., 254, 1970.

24. Kreyszig, E., *Advanced Engineering Mathematics*, Third Edition, John Wiley & Sons, Inc., New York, 641, 1972.

8 NOMENCLATURE

L = The rotational radius (cm)

ω = The cup rotational speed (radians/second)

θ = The angle off the cup axis of rotation (radians)

g = The gravitational acceleration constant (cm/sec^2)

$\pm$ = + if gravity enhances the flow
- if gravity retards the flow

μ = The slurry absolute viscosity (gm/cm-sec)

ρ = The slurry density (gm/cm^3)

R = The radial coordinate (cm)

V_R = The radial velocity component (cm/sec)

E = Centrifugal coefficient
= $\rho R^2 L\omega^2/2\mu$ (cm/sec)

F = Gravitational coefficient
= $\pm\rho R^2 g/2\mu$ (cm/sec)

B_n = Bernoulli number, nth order

$K1$ = First constant of integration (cm/sec)

$K2$ = Second constant of integration (cm/sec)

θ_w = Angle off the axis of rotation to the wall of the cup (radians)

θ_s = Angle off the axis of rotation to the film surface (radians)

Q = Volumetric fluid flow rate (cm^3/sec)

δ = Film thickness (cm)

V_{R_s} = The radial surface velocity (cm/sec)

V_{R_m} = The mean radial velocity (cm/sec)

The following manuscript was unavailable at time of publication:

Properties and Performance Characteristics of Coal-Water Fuels

G. A. Farthing, Jr., R. D. Daley, S. J. Vecci, E. R. Michaud and R. Manfred
The Babcock & Wilcox Company, Electric Power Research Institute

RHEOLOGY OF COAL/WATER SLURRIES

E.Z. Casassa, G.D. Parfitt, A.S. Rao and E.W. Toor
Department of Chemical Engineering
Carnegie-Mellon University
Pittsburgh, Pennsylvania 15213

ABSTRACT

The effect of solid concentration, pH, particle charge, temperature and the presence of added electrolytes on the rheology of 50% (wt) coal/water slurries of four bituminous coals (Pittsburgh Seam #8, Illinois #6, San Juan and Hiawatha) has been examined.

Shear rates were in the range 10-100 sec^{-1}. The pH of the slurries was varied from 2.5 to 12 and the slurry temperature from 8° to 48°C. Four different electrolytes (10^{-1}-10^{-3} mol dm^{-3}) were added to some of the slurries.

For all four coals the viscosity of slurries increased with coal concentration and showed pH dependence and pseudoplastic flow behavior with low yield values. Coal particles showed high surface charge in the pH regions where the viscosity of the slurries was low. Addition of mono-, di-, and tri-valent ions caused a shift in the viscosity maxima on the pH scale. Increase in slurry temperature resulted in a decrease in slurry viscosity which appears to be mainly due to the fluid.

INTRODUCTION

It has been suggested(1) that concentrated coal/water slurries can be utilized as an economical means for the transportation of coal over long distances or as substitute fuel for oil or coal/oil mixtures for electric power generation. Since coal is a complicated mixture of carbonaceous and inorganic matter, the physico-chemical properties of each coal must be understood in order to optimize the rheology of the slurries. Although in recent years there have been a number of reports(2) on the rheology of coal/water mixtures, no consistent picture has emerged from the published data on the relationship between slurry rheology and the chemistry of the coals in terms of polydis-

persity of particle size, the surface chemistry of the coal, the effect of the chemical nature of the suspending fluid, slurry temperature, the effect of added electrolyte, etc. This is the focus of our current studies at Carnegie-Mellon University.

Four bituminous coals were selected for this work and the effect of solid concentration, pH, particle surface charge, slurry temperature and addition of electrolytes on the rheology of 50% (wt) slurries has been investigated.

EXPERIMENTAL

The coals (Pittsburgh Seam #8, Illinois #6, San Juan (New Mexico), and Hiawatha (Utah) were supplied by the Pittsburgh Energy and Technology Center as nominally 100% < 100 mesh, 80% < 200 mesh coal powders. Particle size distributions were measured by sieving with a Sonic Sifter (sieve openings between 149 and 7 μm), and with the Coulter Counter (in 0.15 mol dm^{-3} NaCl and Coulter Type IA dispersing agent). Particle size, shape and surface topography were examined by scanning electron microscopy. Proximate analysis was carried out by Conti Testing Labs., Pittsburgh. The extent of the solubility of surface contaminants in the suspending fluid of a 10% (wt) slurry was determined by Atomic Absorption (NUS Corporation, Pittsburgh) and volumetric analysis (Water Chem. Lab., Dept. of Civil Eng., Carnegie-Mellon University).

The slurries were prepared by mixing known amounts of coal and distilled water in a (Hamilton Beach) domestic blender. The volume of the slurries was 200 cm^{-3} and after each measurement the slurries were kept in sealed bottles for further examination at a later date. Some Pittsburgh Seam #8 coal was washed five times with distilled water to remove soluble surface contaminants. The washed coal was dried and stored in sealed bottles until the slurries were prepared. Slurry pH was adjusted with either sodium hydroxide or hydrochloric acid to achieve a range of initial pH 3-12. The densities of the coals in water were measured using a pycnometer.

The electrophoretic mobility of the coal particles in 50% (wt) slurries was measured using a Micromeritics Mass Transport Analyzer. Most of the viscosity measurements were made at low shear rates (10-100 sec^{-1}) with a Brookfield Digital Viscometer. Since the Brookfield instrument design is based on the assumption that the sheared fluid is Newtonian, necessary corrections for shear rates were made using the standard procedure(3,4). A Haake Rotovisco viscometer (Pittsburgh Energy and Technology Center) was used for shear rates of 100-1000 sec^{-1} for some Pittsburgh Seam #8 slurries. The temperature of the slurries in the Brookfield viscometer was maintained constant by circulating water through a jacket attached to the sample holder; a Haake FK constant-temperature bath controlled the water temperature to $\pm$ 1°C.

THEORETICAL

Einstein showed that the viscosity (η) of a very dilute dispersion of

uncharged rigid spheres is related to the volume fraction (ϕ) by

$$\eta = \eta_o(1 + 2.5\ \phi + 4\phi^2 + \ldots) \qquad (1)$$

where η_o is the viscosity of the medium. This equation was derived assuming that the particles do not interact hydrodynamically, and therefore applies to volume fractions close to zero. For $\phi > 0.01$ the viscosity is increased due to the formation of temporary doublets, triplets, etc. which enhance the rate of energy dissipation.

A large number of equations, both empirical and theoretical, have been used to describe the viscosity of disperse systems at $\phi > 0.01$. A useful general power-series equation is

$$\eta = \eta_o(1 + k_1\phi + k_2\phi^2 + k_3\phi^3 + \ldots) \qquad (2)$$

k_1 is related to the intrinsic viscosity $[\eta]$ in that as $\phi \rightarrow 0$, $k_1 \rightarrow [\eta]$. Goodwin(5) suggests that the magnitude of $[\eta]$ can be related to particle shape, and comparing with experimental data found $[\eta] = 4.0$ for rods, 3.2 for ellipsoids and 2.9 for discs, these being average values for different axial ratios ($[\eta] = 2.5$ for spheres).

The constant k_2 is dependent on the perturbation of the streamlines by collision doublets, and k_3, etc. are used to describe higher-order collisions. The lower bound for k_2 must be 4, and various authors using a variety of assumptions have predicted values between 7 and 14. No rigorous hydrodynamic solutions for k_3, etc. are available due to the difficulty of handling higher-order collisions, even for uncharged rigid spheres. For this reason other equations which have been proposed to describe behavior in concentrated dispersions(6) have usually been modifications of that proposed by Arrhenius in 1885,

$$\eta = \eta_o \exp(k_1\phi) \qquad (3)$$

where k_1 is a constant which is equal to 2.5 at infinite dilution.

To determine $[\eta]$ from experimental results, the Dougherty and Krieger equation(7) may be used to relate viscosity to the volume fraction of the suspended solid as

$$\eta = \eta_o(1 - \phi/\phi_\infty)^{-[\eta]\phi_\infty} \qquad (4)$$

where ϕ_∞ is the maximum packing fraction at which flow can occur.

The rheological behavior of a suspension is usually depicted as a plot of shear stress (τ) against rate of shear ($\dot{\gamma}$). The shape of this plot generally conforms to one of the following mathematical formulations:

$\tau = \eta\dot{\gamma}$	Newtonian	(5)
$\tau = K\dot{\gamma}^n$	$n < 1$ pseudoplastic $n > 1$ dilatant	(6)
$\tau = \tau_o + \eta_{pl}\dot{\gamma}$	plastic/Bingham	(7)
$\tau = \tau_o + K\dot{\gamma}^n$	$n < 1$ pseudoplastic with yield value $n > 1$ dilatant with yield value	(8)

where K is the flow consistency number, n the flow behavior index, τ_o the yield stress and η_{pl} the plastic viscosity. Equation (6) is

often referred to as the power law or the Ostwald-de Waele equation(8), and equation (8) as the power law with yield or the Herschel-Bulkley equation (9). The values of τ_o and n reflect the magnitude of the deviation from Newtonian flow (equation (5)) and are dependent upon the state of dispersion of the particles.

RESULTS

Particle size distributions from sieve and Coulter Counter analysis, are given in Table 1, together with the densities (g cm^{-3}) of the coals.

Table 1. Particle Size Distribution and Coal Density

	Pittsburgh #8		Illinois #6		San Juan		Hiawatha	
Diam. (μm)	Sieve anal. %(wt)	Coulter Counter %(vol)	Sieve anal. %(wt)	Coulter Counter %(vol)	Sieve anal. %(wt)	Coulter Counter %(vol)	Sieve anal. %(wt)	Coulter Counter %(vol)
>150	0	0	7	7	8	6	7	8
> 75	13	12	39	40	42	38	42	44
> 37	58	54	67	68	67	66	72	66
> 20	80	75	93	82	88	80	96	81
< 20	20	25	7	18	12	20	4	19
Mean diam. (μm)	43	41	57	57	58	55	65	56
Density	1.37		1.40		1.44		1.35	

Log-normal plots of the Coulter Counter data suggest that all four coals have about 0.3% by volume of particles < 2.0 μm in diameter. The Pittsburgh #8 coal was ground at a different time and using different equipment than the other coals, for which the size distributions are similar, but flatter, than that for Pittsburgh #8.

In scanning electron micrographs the particles of Pittsburgh #8 and Illinois #6 resemble small rocks or pebbles, those of Hiawatha coal are plate- or disc-like, and those for San Juan are intermediate between the two. The surfaces of Pittsburgh #8 particles contain sharp edges and cracks, but the other coals have smooth surfaces.

Proximate analyses for the four coals are given in Table 2.

Table 2. Proximate Analysis

	Pittsburgh #8	Illinois #6	San Juan	Hiawatha
Moisture (%)	1.61	5.31	10.09	8.26
Ash (%)	10.46	9.74	22.15	7.51
Sulfur (%)	1.96	3.80	0.79	0.80
Volatiles (%)	40.3	42.3	35.8	43.7
Heating Value (Btu/lb)	12887	11822	8976	11596

10% (wt) slurries of all four coals were left to stand for four days, and the supernatant was analyzed for ions removed from the coal surface. The results are given in Table 3.

Table 3. Water Soluble Surface Contaminants (mg dm^{-3})

	Pittsburgh #8	Illinois #6	San Juan	Hiawatha
Si	4.0	2.0	2.0	5.0
Al	4.6	< 0.1	< 0.1	< 0.1
Fe	50	14.3	< 0.04	0.18
Ca	30	204	187	43.5
Mg	75	4.24	12.7	12.7
K	4.4	2.8	2.5	2.9
Na	8.5	68	50.5	11.5
SO_4	340	540	490	140
Cl	40	60	50	65
NO_3	< 0.3	< 0.5	< 0.5	< 0.5

We see that significant amounts of Ca^{2+}, SO_4^{2-}, and Cl^- were dissolved from all the coals, Fe^{2+}/Fe^{3+} dissolved from the Eastern but not the Western coals, and only small amounts of Si^{4+} and Al^{3+} were removed by washing.

When a powdered coal is immersed in pure water a "natural" pH will be observed, a consequence of the acid/base character of the surface. The pH might change with time due to dissolution of surface contaminants and their subsequent oxidation and hydrolysis. pH values of 50% (wt) slurries of the four coals immediately after preparation and one week later are given in Table 4. Identical values were obtained for the respective supernatant liquids.

Table 4. Slurry pH

	Pittsburgh #8	Illinois #6	San Juan	Hiawatha
Initial slurry pH	2.85	4.1	6.3	5.2
After 1 week	2.75	3.9	7.2	5.8

Figure 1 shows the initial viscosity (Brookfield) of coal/water slurries as a function of the coal concentration (a) including moisture and (b) moisture free. Plotting on a moisture-free basis brings the viscosity curves together, although that for Hiawatha remains slightly lower than the others. No other parameter had the same normalizing effect. The dramatic increase in viscosity at concentrations in excess of 50% (wt) is in agreement with earlier reports for coal/oil(10-13) and coal/water(14-17) slurries.

Equation (2) expresses the viscosity of a suspension in terms of the volume fraction of the dispersed phase. Plots of this equation in the form $[(\eta/\eta_o)-1]/\phi$ versus ϕ are not linear for any of the coals for $\phi > 0.1$. The Brookfield viscometer could not be used for ϕ much below 0.2 because of high sedimentation rates.

In Figure 2 $\ln(\eta/\eta_o)$ is plotted versus ϕ for all four coals, corresponding to an equation of the type

$$\eta = \eta_o \exp(k' + k''\phi) \qquad (9)$$

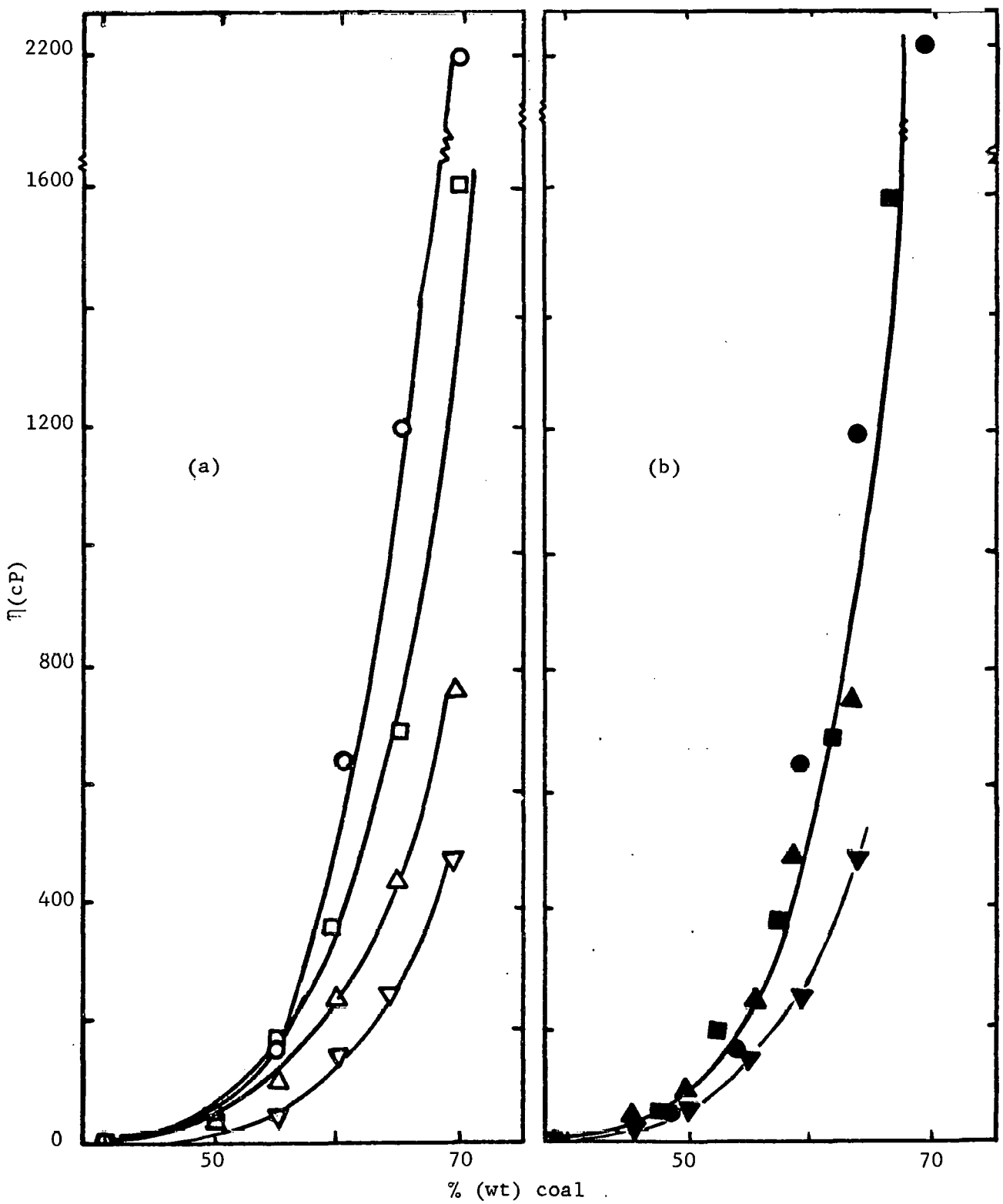

Figure 1. Viscosity of coal/water slurries. Pittsburgh #8 (●), Illinois #6 (□), San Juan (△), Hiawatha (▽). Shear rate 90 s^{-1}. Concentration based on (a) actual weight of coal, (b) without moisture.

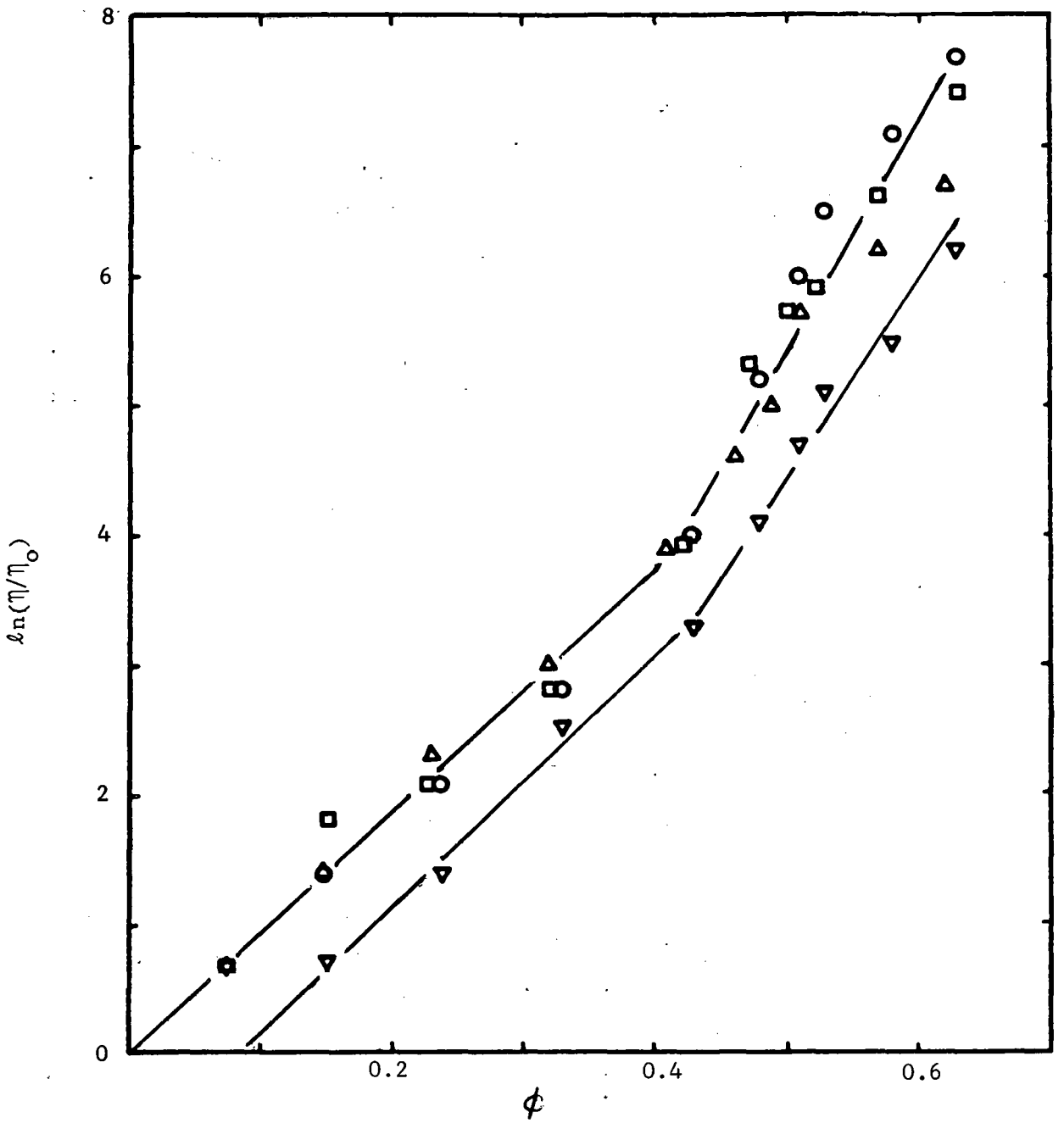

Figure 2. Viscosity of coal/water slurries. Pittsburgh #8 (○), Illinois #6 (□), San Juan (△), Hiawatha (▽). Shear rate 90 s^{-1}.

which is a modification of equation (3); ϕ values are based on the actual weight of coal. The plots for each coal show two linear regions, one for $\phi < 0.4$ and the other for $\phi > 0.4$. The values of k' and k" are given in Table 5.

Table 5. Values of k' and k" from Plots of Equation (9)

	Pittsburgh #8		Illinois #6		San Juan		Hiawatha	
	k'	k"	k'	k"	k'	k"	k'	k"
$\phi < 0.4$	0	8.7	0	9.7	0	9.2	-1.0	10.0
$\phi > 0.4$	-2.8	16.8	-3.0	17.1	-3.1	16.8	-2.0	12.9

The change in the values of k' and k" occurs for all four coals at about the ϕ value where the slurry behavior ceases to be Newtonian. Indeed, if a higher shear rate were to be used, lower values of (η/η_o) would be expected at high ϕ. k' and k" change least for Hiawatha coal which deviates least from Newtonian behavior. When k' = 0 equation (9) becomes the Arrhenius equation and k" = k_1 in a series expansion. This suggests that for $\phi < 0.4$ values of $[\eta]$ for Pittsburgh #8, Illinois #6 and San Juan are about 9. k' $\neq$ 0 for Hiawatha and the meaning of this result is not clear.

Equation (4) also relates viscosity to concentration. From a plot of $\ell n\ (\eta/\eta_o)$ versus $\ell n[1 - (\phi/\phi_\infty)]$ the intrinsic viscosity can be determined. For the four coals this equation is best fitted if the maximum packing fraction (ϕ_∞) at which flow can occur is taken as 0.7 (equivalent to 76-77% (wt)). These plots are shown in Figure 3, and the values of intrinsic viscosity derived from this analysis are given in Table 6.

Table 6. Intrinsic Viscosity from Plots of Equation (4)

Pittsburgh #8	$[\eta] = 6.5$
Illinois #6	$[\eta] = 6.3$
San Juan	$[\eta] = 6.5$
Hiawatha	$[\eta] = 5.2$

These values are somewhat lower than those obtained from equation (9) at $\phi < 0.4$, and the reasons for the discrepancy are not known. To fit the data to equation (4) a value of $\phi_\infty = 0.7$ was used, which is higher than the maximum concentration for which we measured flow ($\phi \sim 0.62$), or the value of $\phi \sim 0.58$ which was determined from sedimentation measurements (to be reported elsewhere). With such lower ϕ_∞ values, the plots were reasonably linear but did not pass through the origin.

Plots of shear stress versus shear rate according to equations (5)-(8) provide values of the constants τ_o, n, and K which reflect deviation from Newtonian flow and the effect of flocculation. Most of the coal/water systems studied obey the Herschel-Bulkley equation (equation (8)), exhibiting pseudoplastic flow with a yield value. Figure 4(a) shows a shear stress versus shear rate plot for a 50% (wt) slurry of Pittsburgh #8 coal in water at pH 2.85 based on Brookfield and Haake data obtained as soon as possible after preparation. Figure 4(b) shows a log-log plot of the data from which n and K in equation (8) are derived. Values of the constants in equation (8)

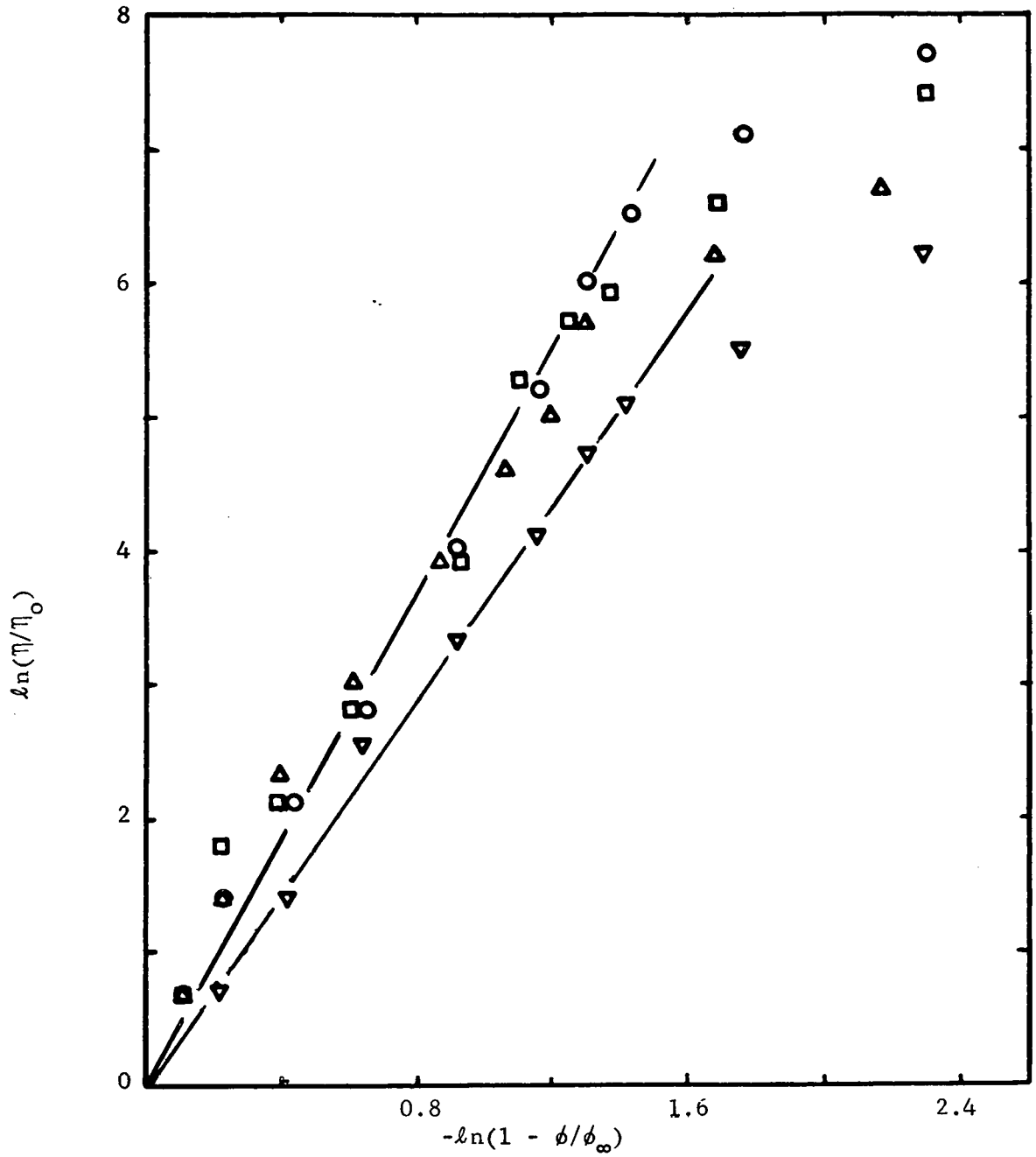

Figure 3. Plot of Dougherty and Krieger equation with $\phi_\infty = 0.70$. Pittsburgh #8 (○), Illinois #6 (□), San Juan (△), Hiawatha (▽). Shear rate 90 s^{-1}.

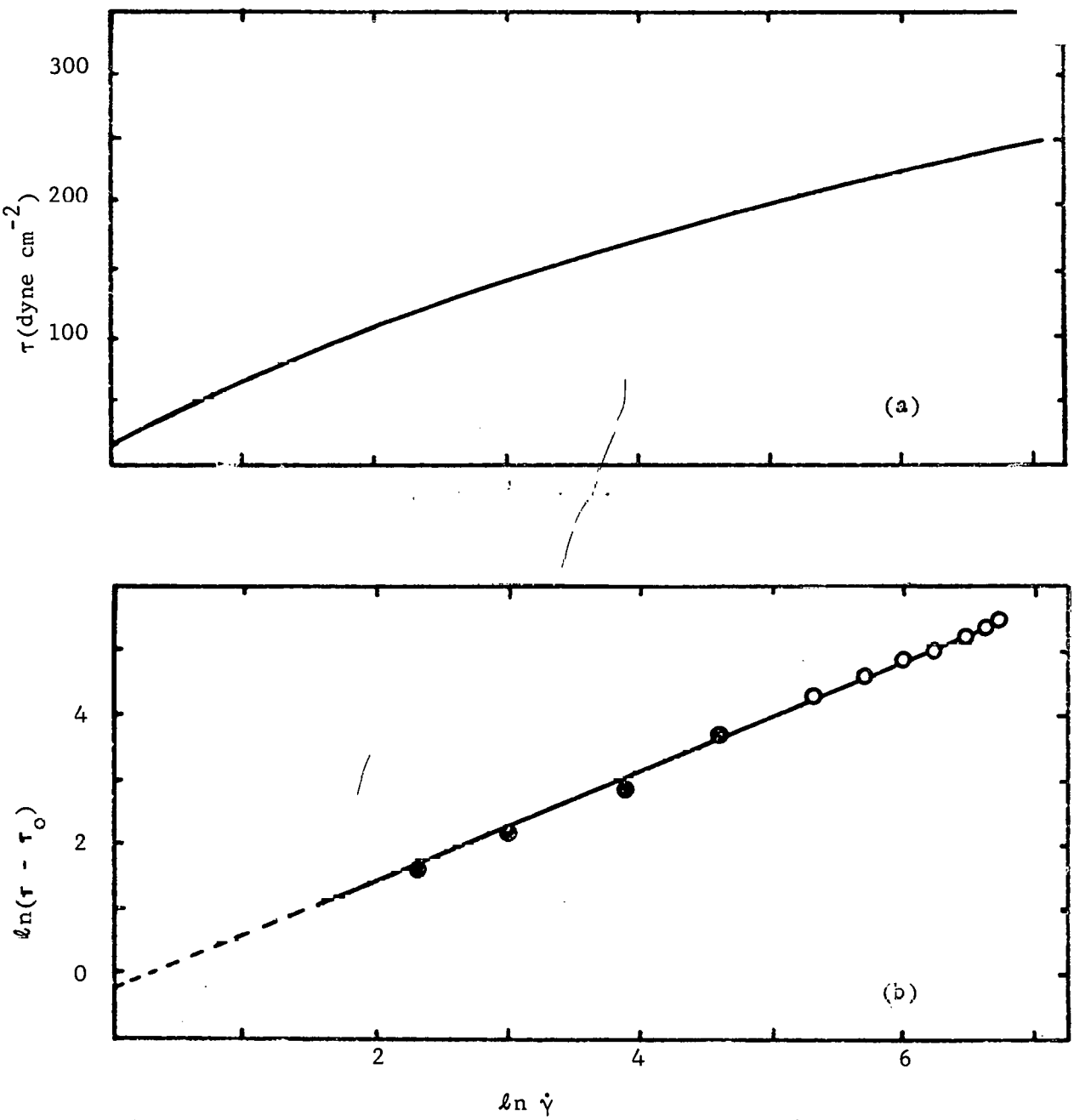

Figure 4. Flow behavior of 50% (wt) Pittsburgh #8 coal/water slurry at pH 3.0. (a) Shear stress versus shear rate (Brookfield and Haake data). (b) Plot of Herschel-Bulkley equation (equation 8). Brookfield data (●), Haake data (○) (points obtained from selected values of recorder trace).

for 50% (wt) coal/water slurries at their natural pH are given in Table 7.

Table 7. Herschel-Bulkley Constants for Coal/Water Slurries

	τ_o(dyne cm^{-2})	n	K(poise)	pH
Pittsburgh #8	18	0.89	0.74	2.85
Illinois #6	18	0.80	0.75	4.1
San Juan	15	0.78	0.66	6.3
Hiawatha	3.8	0.96	0.24	5.2

For Newtonian systems n = 1 and K = η. Hiawatha coal slurries are almost Newtonian with a negligible yield value and low viscosity. The other coal slurries are pseudoplastic but with relatively low yield values.

The pH dependence of viscosity at shear rate 45 s^{-1} of 50% (wt) slurries of the four coals, measured shortly after preparation, is shown in Figure 5; similar profiles were obtained at 9, 18 and 90 s^{-1}. Values of τ_o, n and K were obtained from plots of the Herschel-Bulkley equation and are given in Figure 6. Electrophoretic mobilities are plotted in Figure 7. The pH range for San Juan coal is restricted since 50% (wt) slurries have very high viscosities above pH ~ 7. Also in the high pH range (>7) Hiawatha coal settled so rapidly that electrophoresis measurements are impossible.

There is a close correlation between viscosity and electrophoretic mobility. In most cases the viscosity is highest around the pH at which the electrophoretic mobility is zero (the isoelectric point (iep)), and lowest when the mobility is high (either positive or negative). These complex changes with pH, which reflect the heterogeneous character of the coal surface, are also apparent with the Hershel-Bulkley constants (Figure 6). Hiawatha coal slurries are well dispersed (nearly Newtonian) over the pH range 3-10, with a small deviation around pH 7, at which the particles have their smallest (negative) charge. The variations in the constants for the other coals also reflect the surface charge behavior, but overall they are similar in magnitude and relate to the pseudoplasticity of all the slurries.

Figure 8 shows the viscosity and electrophoretic mobility of the 50% (wt) Pittsburgh #8 coal/water slurries one week after the measurements recorded in Figures 5-7. During this time significant amounts of Fe^{2+}, Ca^{2+}, Mg^{2+}, SO_4^{2-} and $C\ell^-$ have dissolved from the coal, and the original slurry pH at the upper end of the range has declined to about pH 8.5. Similar pH changes were observed with the other coals, particularly San Juan for which the pH range contracts to pH 5.5-7 from both the acid and base side.

The effect of thorough washing of Pittsburgh #8 coal on the electrophoretic mobility and viscosity is shown in Figure 9. The viscosity data presented were recorded at a shear rate of 9 s^{-1} - a similar profile was seen at higher shear rates (18, 45, 90 s^{-1}) but the peaks and troughs were less prominent. We again see a correlation between

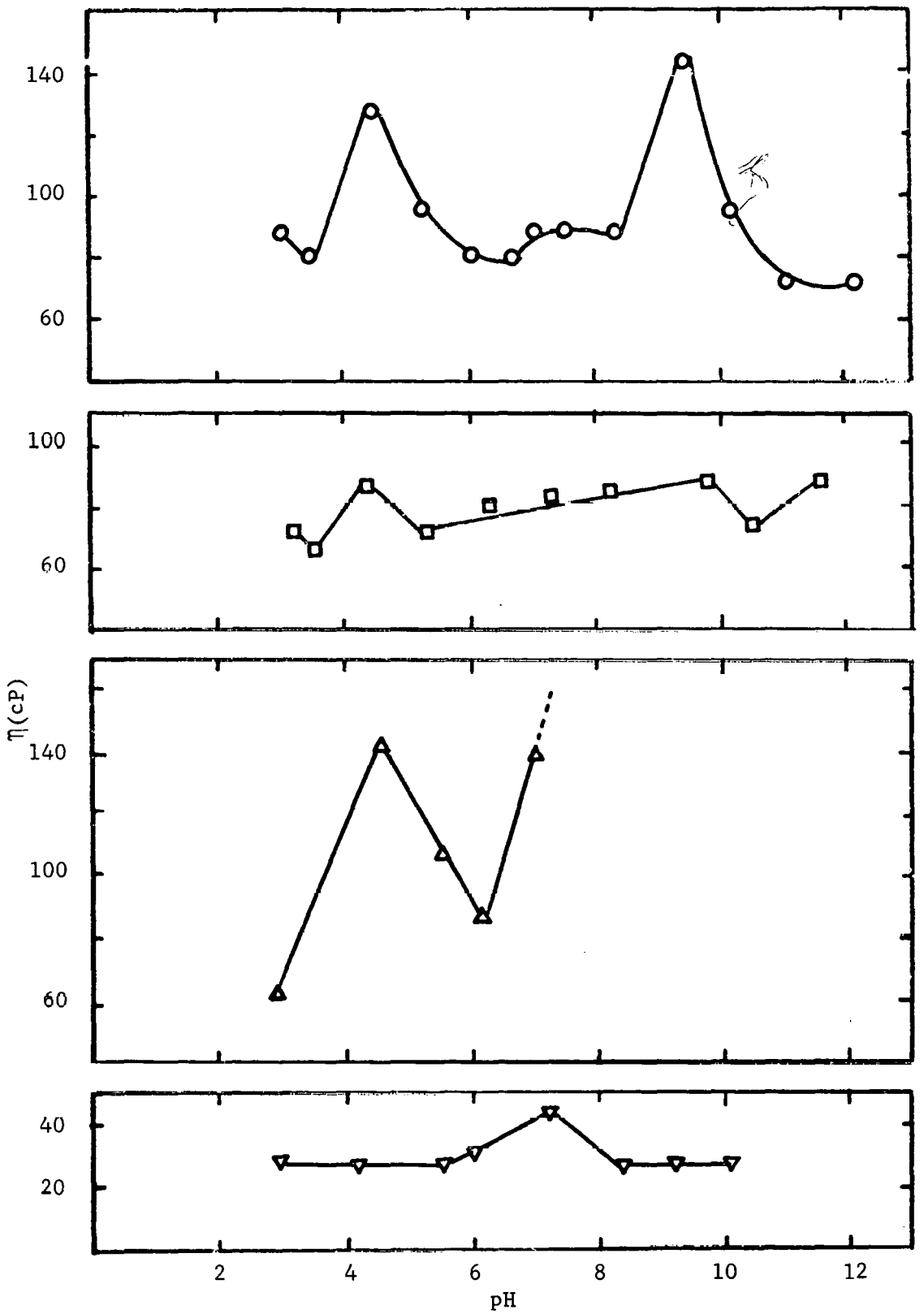

Figure 5. Viscosity of 50% (wt) coal/water slurries. Shear rate 45 s^{-1}. Pittsburgh #8 (○), Illinois #6 (□), San Juan (△), Hiawatha (▽).

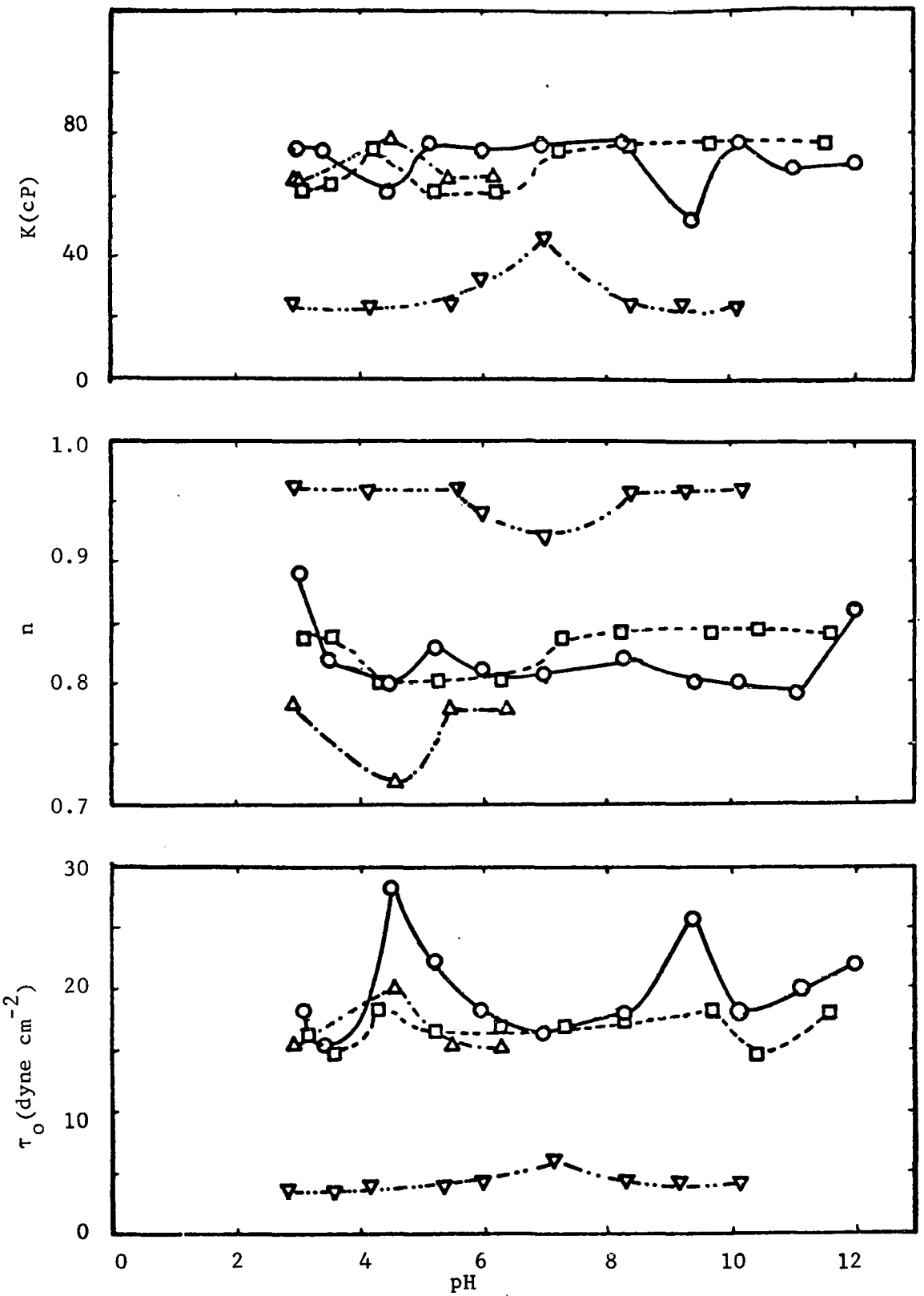

Figure 6. Rheological data (Herschel-Bulkley Equation) for 50% (wt) Coal/Water Slurries. Pittsburgh #8 (○), Illinois #6 (□), San Juan (△), Hiawatha (▽).

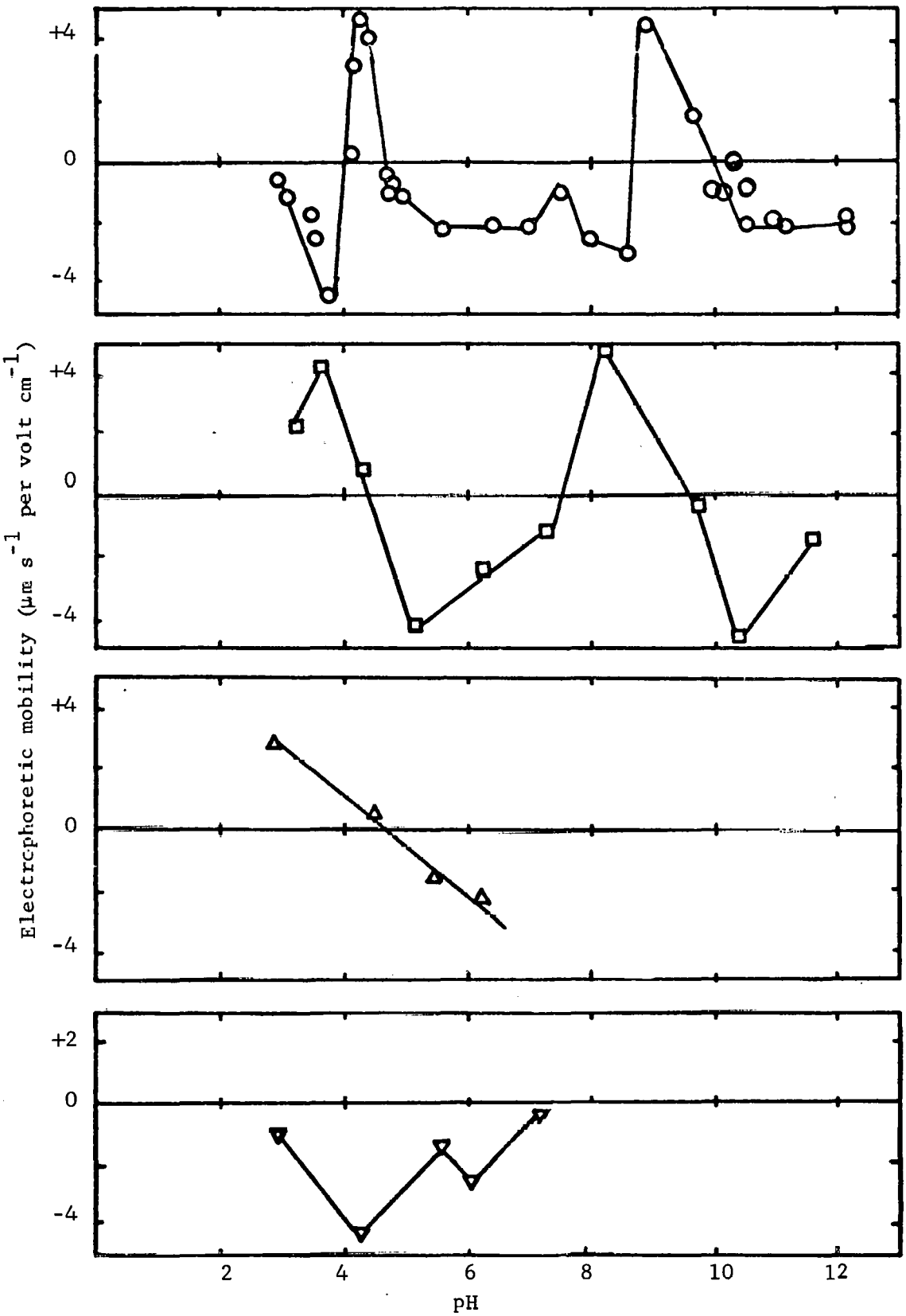

Figure 7. Electrophoretic mobility of 50% (wt) coal/water slurries Pittsburgh #8 (○), Illinois #6 (□), San Juan (△), Hiawatha (▽).

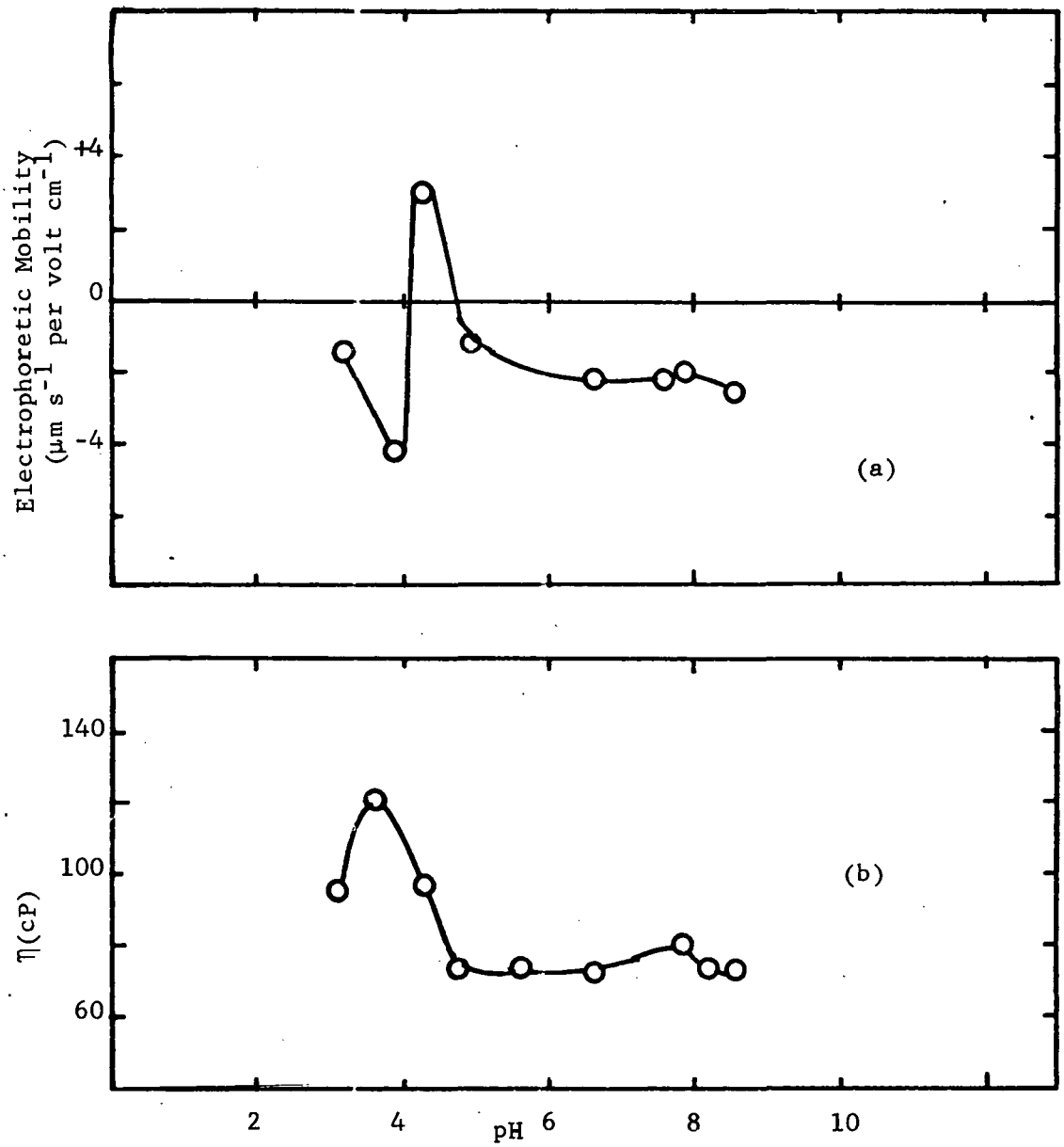

Figure 8. (a) Electrophoretic mobility, (b) viscosity of 50% (wt) Pittsburgh #8 coal/water slurries, one week after preparation. Shear rate 45 s^{-1}.

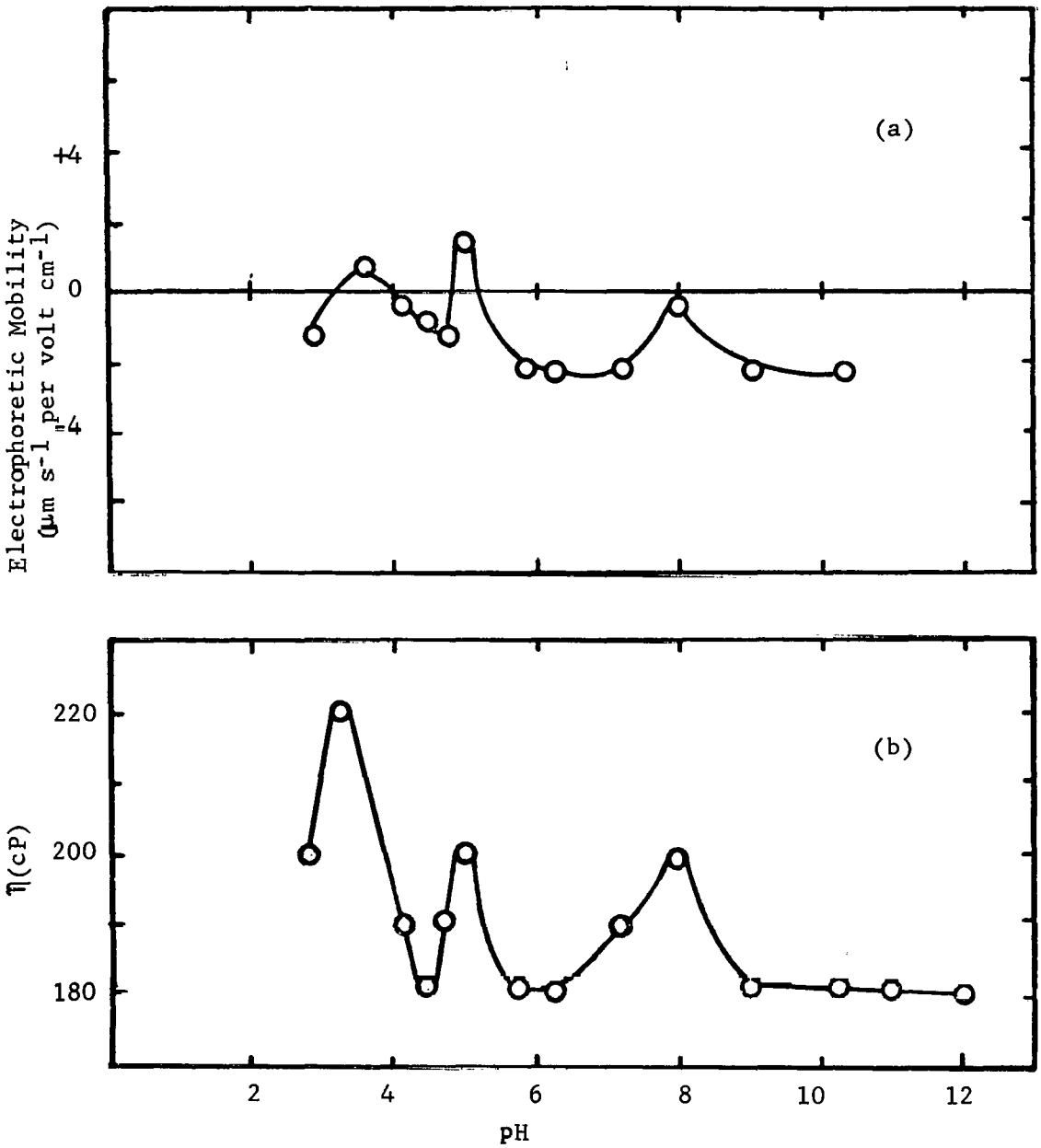

Figure 9. (a) Electrophoretic mobility, (b) viscosity of 50% (wt) washed Pittsburgh #8 coal/water slurries. Shear rate 9 s^{-1}.

the effect of pH on electrophoresis (surface charge) and viscosity. Washing the coal has caused a shift in the isoelectric points and reduced the magnitude of the mobility at the peaks in the pH range 2.5-5.0, and the isoelectric point at pH ~ 10 has disappeared.

The effect of addition of electrolytes on the rheological behavior has been studied using KNO_3, $Mg(NO_3)_2$. K_2SO_4, and $La(NO_3)_3$ at concentrations of 10^{-3}-10^{-1} mol dm^{-3}. Data for K_2SO_4 and $La(NO_3)_3$, representing the effects of adding multivalent anions and cations, are shown in Figures 10 and 11 respectively for 50% (wt) Pittsburgh #8 coal/water slurries. The addition of multivalent ions reduces the number of peaks in the viscosity versus pH plot, especially at higher concentrations. Several effects may be responsible. The increase in ionic strength causes compression of the electric double layer, and consequent reduction in inter-particle repulsion. The multivalent ions may also adsorb on particle surfaces, changing the magnitude and even the sign of charge. Furthermore, the dissolution of soluble surface contaminants may be suppressed by addition of these electrolytes. Flocculation is apparent at pH ~ 7 with 10^{-1} mol dm^{-3} K_2SO_4 and at pH ~ 8 for 10^{-2} and 10^{-1} mol dm^{-3} $La(NO_3)_3$. This is consistent with charge neutralization and the isoelectric point at pH 7-8.

The constants in the Herschel-Bulkley equation for Pittsburgh #8 in 50% (wt) slurries with addition of KNO_3, $Mg(NO_3)_2$, $La(NO_3)_3$, and K_2SO_4 show some general trends:
(a) At pH close to the natural pH (2.8), τ_o and K decrease and n increases with increasing electrolyte concentration for the nitrates, but the changes are in the opposite direction for K_2SO_4, although in no case are these effects large. Compared to the system without added electrolyte, the addition of SO_4^{2-}, Mg^{2+} and La^{3+} has little effect on τ_o, increases n and decreases K, hence these slurries are tending toward Newtonian flow (n=1) once the yield value has been exceeded. This suggests that even though compression of the electrical double layer is causing some flocculation the energy required to initiate flow, as reflected in τ_o, is about the same in all cases.
(b) In the pH range 4-10, τ_o and K increase and n decreases with increasing KNO_3 concentration. At low KNO_3 concentration τ_o increases but K and n remain relatively constant with increasing pH, but at high concentration τ_o and K increase and n decreases significantly as the pH is increased. This suggests increased agglomeration in the higher pH range. For the other electrolytes the effect of pH is relatively small, particularly for $La(NO_3)_3$. Across the pH range we see high n, low K and τ_o similar to that for the slurry at the natural pH.

The effect of temperature on the viscosity of 50% (wt) coal/water slurries for the four coals, the slurries being prepared at room temperature at their natural pH, is shown in Figure 12. This can be simply explained in terms of the effect of temperature on the properties of the aqueous medium.

DISCUSSION

The rapid increase in viscosity of coal slurries at high solids concentration is well known. Such behavior determines the maximum loading

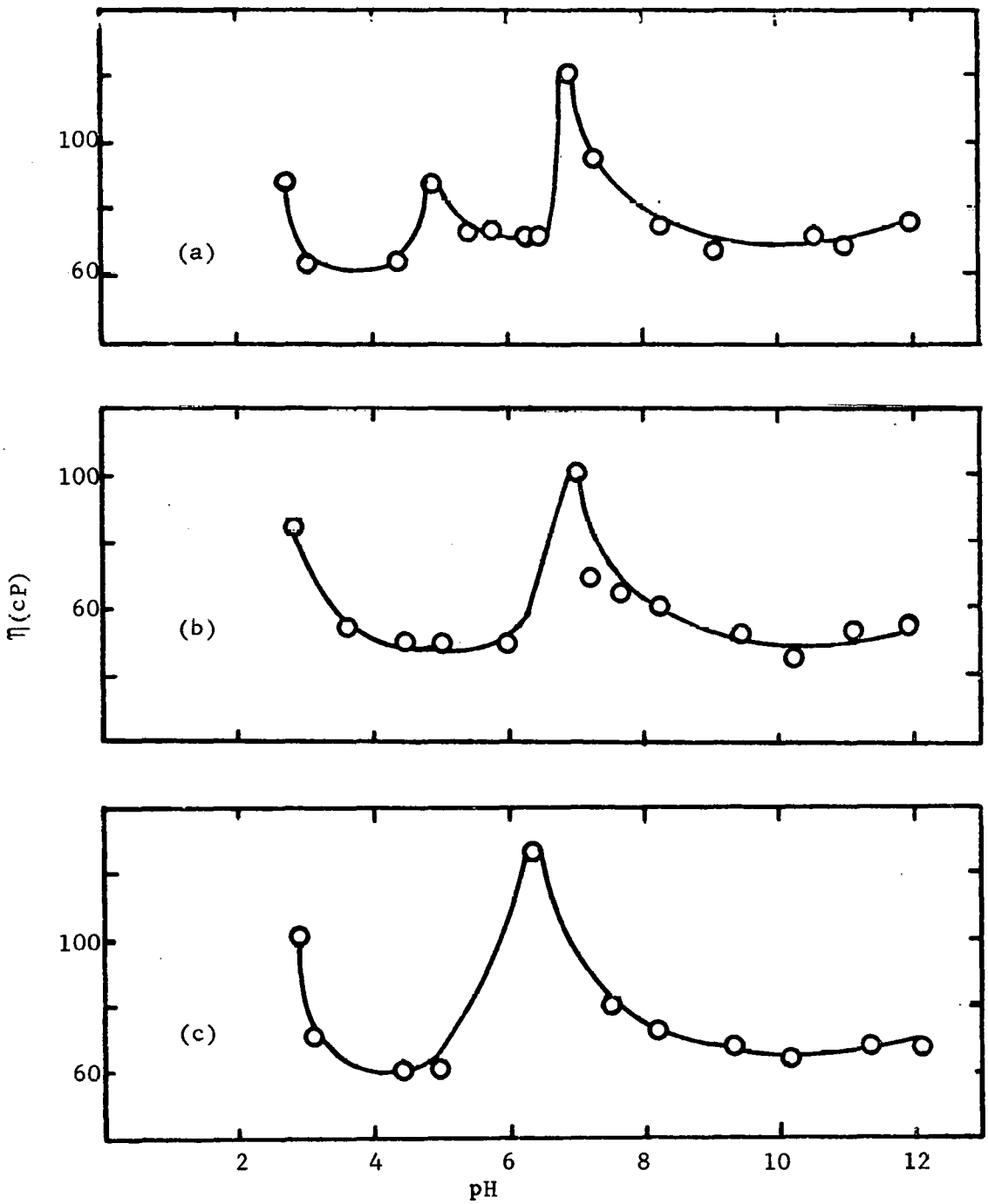

Figure 10. Viscosity of 50% (wt) Pittsburgh #8 coal/water slurries in (a) 10^{-3} mol dm^{-3}, (b) 10^{-2} mol dm^{-3}, (c) 10^{-1} mol dm^{-3} K_2SO_4 solution. Shear rate 45 s^{-1}.

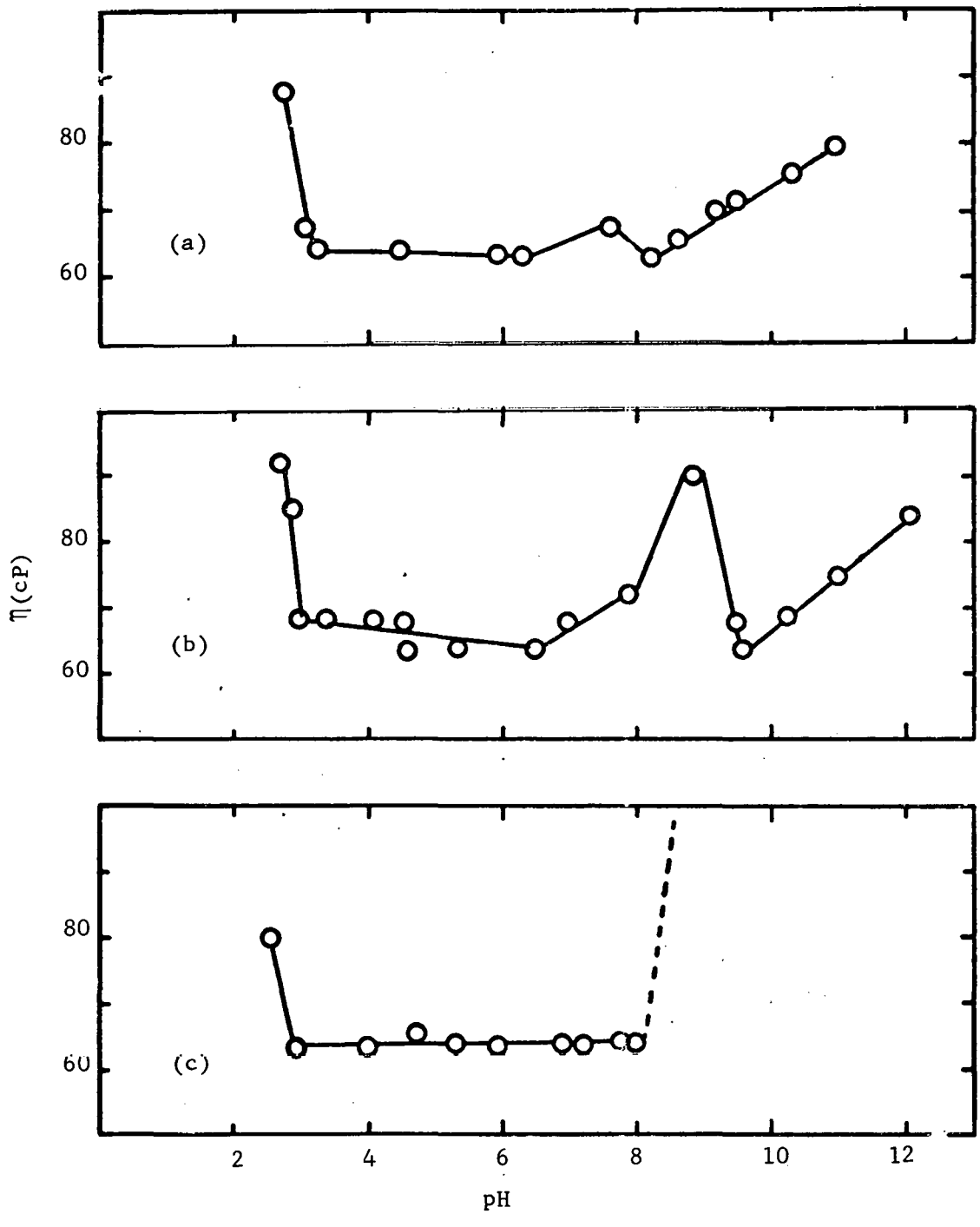

Figure 11. Viscosity of 50% (wt) Pittsburgh #8 coal/water slurries in (a) 10^{-3} mol dm^{-3}, (b) 10^{-2} mol dm^{-3}, (c) 10^{-1} mol dm^{-3} $La(NO_3)_3$ solutions. Shear rate 45 s^{-1}.

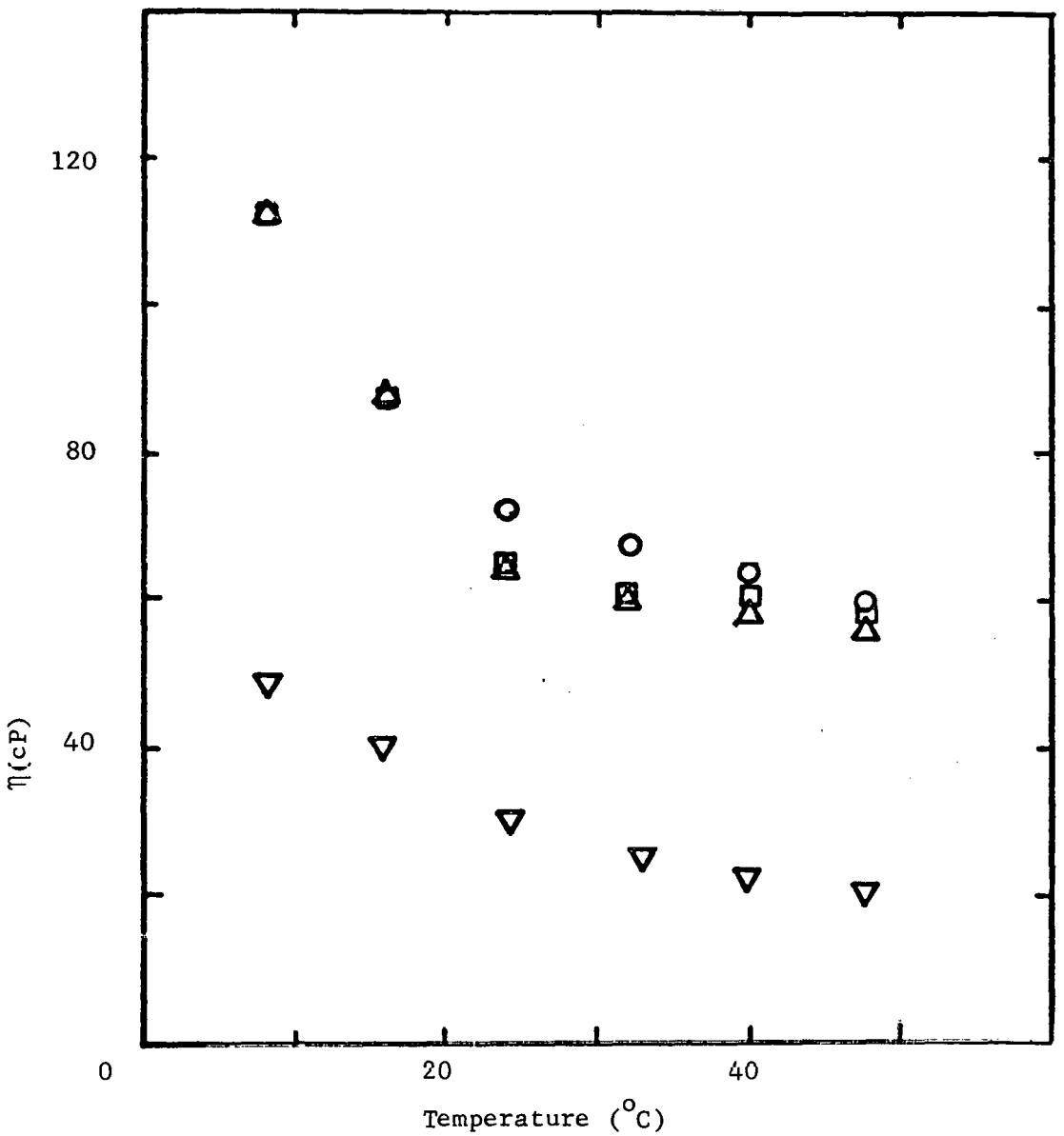

Figure 12. Temperature dependence of viscosity at shear rate 45 s^{-1} for 50% (wt) coal/water slurries Pittsburgh #8 (○), Illinois #6 (□), San Juan (△), Hiawatha (▽).

of coal for acceptable flow characteristics. As might be expected, the viscosity-concentration curve varies with coal type, as shown in Figure 1(a), since the packing of the particles in suspension is determined by their size distribution and the particle-particle interactions that cause structure formation (flocculation). The size distributions of the coals used in this study differ somewhat (Table 1) but probably not enough to account for the large viscosity differences at high coal concentration. The magnitude of the particle-particle interactions and the degree of flocculation in the slurry is also related to the size distribution in that the attractive and repulsive forces between particles depend on their relative size. But the major difference between the coals reflect their chemistry, and in particular that of the surface, since the particle charge is determined by the type and concentration of ionizable surface species as well as the electrochemistry of the aqueous medium (pH, electrolyte concentration and type). Both the surface chemistry and the ionic species in the slurry fluid differ markedly from coal to coal, as suggested by the analytical data in Tables 2 and 3. It is therefore surprising that for three of the coals (Pittsburgh #8, Illinois #6, and San Juan) the viscosity versus concentration curves are superimposable if plotted on a moisture-free basis for the coals (Figure 1(b) although the total concentration of dissolved species is about the same for each of the three - Hiawatha coal is distinctly different and has a much lower total concentration of dissolved species. We see from Figure 1 that the maximum concentration of coal which can be incorporated into water to give an acceptable viscosity for normal flow is 65-70% (wt), with Hiawatha coal somewhat above the rest, suggesting that for this coal there is the least structuring of the particles in the slurry.

Many equations, both theoretically based and empirical, have been developed and used to relate the viscosity of dispersions of fine particles to the volume fraction (ϕ) of the dispersed phase. As ϕ increases, so the number of complicating factors increase, and it would be unlikely that one particular equation could be used to describe the behavior over a range of concentration as wide as that (ϕ = 0.1-0.65) we have studied with our coal/water slurries. The data do not fit the power series equation (equation (2)), but plots of $\log(\eta/\eta_o)$ versus ϕ are linear (Figure 2) with a distinct change in slope at $\phi \approx 0.4$. It is at about this concentration that the slurries become non-Newtonian and strictly speaking, equations relating η/η_o to ϕ do not apply when there is a shear rate dependence. Below 0.4 the simple Arrhenius equation (equation (3)) is applicable for three of the coals (Pittsburgh #8, Illinois #6, and San Juan), and a value of ~9 is derived for the intrinsic viscosity $[\eta]$ of their slurries. For Hiawatha at $\phi < 0.4$ and all of the coals above ϕ = 0.4, the data fit equation (9) with negative intercepts on the $\ln(\eta/\eta_o)$ versus ϕ plot. Although several authors have reported(6) on the use of this equation, we cannot at present derive any meaning for it in terms of the physical characteristics of the coal/water slurries. Use of equation (4) to determine $[\eta]$ involves obtaining a value for the maximum ϕ at which flow can occur, and this is difficult to establish precisely from our data. Nevertheless using ϕ_∞= 0.7 in equation (4) leads to linear plots and values of $[\eta]$ of ~6.4 are obtained for the Pittsburgh #8, Illinois #6 and San Juan coal/water slurries while that for Hiawatha is lower (Table 6).

The intrinsic viscosities derived from plots of equations (3) and (4) are not in good agreement, and more precise and more detailed data would be needed to investigate the reason. But both sets of values are significantly higher than that (2.5) predicted for rigid, uniform, uncharged spheres which suggests that charge, shape and polydispersity markedly affect the rheological behavior of coal/water slurries, as would be expected.

Useful information can be obtained from plots of shear stress versus shear rate at fixed solid concentration. The shape of such plots indicates the type of rheological behavior, i.e., whether it is Newtonian or non-Newtonian (shear thinning or shear thickening, with or without a yield value). All the data presented in this paper were obtained for slurries at a concentration of 50% (wt) coal, and were analyzed using the Herschel-Bulkley equation to give values of the yield value (τ_o), the flow behavior index (n) and the flow consistency number (K). The values for these constants for slurries prepared at their natural pH (Table 4) are given in Table 7. Again Hiawatha coal stands apart from the others in that its slurry is almost Newtonian with a negligible yield value and low viscosity, suggesting that the coal particles are well dispersed. Slurries of the other coals are pseudoplastic and the viscosity decreases with increasing shear, but the yield values are relatively low. This is probably due to minor flocculation which increases with time, as indicated by sedimentation data (to be reported elsewhere), which is presumably a result of the dissolution of multivalent ions from the coal surface.

The effect of pH is very important since the acidity of the slurries prepared at the natural pH would be unacceptable, particularly for Pittsburgh #8 and Illinois #6 coals. The major parameter that is controlled by pH is the particle charge which arises from the ionic dissociation of acidic and basic groups on the surface. For pure substances this is relatively well defined and the zero point charge (zpc) is the pH at which the net charge on the particle is zero. At pH values less than the zpc the particles are positively charged and above the zpc they are negative. The zpc is characteristic of the material and defines the acid/base nature of the surface. For a heterogeneous surface containing more than one type of surface group the situation is more complex and a number of zero points are feasible depending on the relative dissociation constants of the surface species. This has been demonstrated(18) by electrophoresis measurements on silica dispersed in a solution containing a hydrolyzable metal ion, e.g., Co, for which three zero points were observed. The first is at pH 2 and is the iep of the silica surface - silica hydroxyl groups are strongly acidic. On increasing the pH there is a charge reversal at about pH 8 due to precipitation of $Co(OH)_2$, and at about pH 10 there is another which is associated with the basic character of the precipitated hydroxide. We observed even more complex behavior with Pittsburgh #8 and Illinois #6 coals (Figure 7), and this probably reflects the widely different dissociation constants of the surface contaminants. Comparing with literature values for the various species present (based on dissolution analysis, Table 3) we propose that for Pittsburgh #8 the isoelectric points at pH 3, 4.7, 7.5 and 10 correspond to coal, iron oxide, aluminum oxide and calcium/magnesium

oxides respectively. Such behavior will obviously vary from coal to coal and needs to be established for each coal type before an analysis of the dispersion characteristics can be contemplated.

Comparing the viscosity (Figure 5) and electrophoretic mobility (Figure 7) data we see a correlation in that the maximum viscosities usually occur at pH values close to the isoelectric points, and this is to some extent reflected in the yield values (Figure 6). It is reasonable to assume that flocculation is occurring in these regions although it is on a minor scale. The addition of multivalent ions to Pittsburgh #8 slurries has a profound effect on the viscosity, particularly with $La(NO_3)_3$ at high pH at which gross flocculation occurs.

It is difficult to interpret these changes with pH, electrolyte type and concentration in terms of the agglomeration/flocculation in the system. Addition of multivalent ions brings about a change from pseudoplastic towards Newtonian behavior, associated with flocculation on a minor scale. Gross flocculation (high viscosity) occurs at high pH with high $La(NO_3)_3$ concentration. With KNO_3 we see the opposite effect (increasing pseudoplasticity). It seems likely that the effect of monovalent ions is related to double layer compression only, whereas the multivalent ions are adsorbed and change the surface charge.

REFERENCES

1. Proc. of 4th Int. Tech. Conf. on Slurry Transportation, Las Vegas, Nevada, 1979.

2. Proc. of the 4th Int. Symp. on Coal Slurry Combustion, Orlando, Florida, 1982.

3. A.B. Metzner and R.E. Otto, AIChE J., 3, 3 (1957).

4. R.E. Smith, J. Coatings Technol., 54, 21 (1982).

5. J.W. Goodwin in "Colloidal Dispersions," Editor J.W. Goodwin, Roy. Soc. Chem. Spec. Pub., 43, 165 (1982).

6. R. Rutgers, Rheol. Acta, 4, 305 (1962).

7. I.M. Krieger, Adv. Colloid Interface Sci., 3, 111 (1972).

8. W. Ostwald, Kolloid Zeits., 25, 26 (1925); A. de Waale, J. Amer. Chem. Soc., 48, 2760 (1960).

9. W.H. Herschel and R. Bulkley, Kolloid Zeits., 39, 291 (1926).

10. C. Moreland, Can. J. Chem. Eng., 48, 24 (1963).

11. M.E. Sacks, M.J. Romney and J.F. Jon, Ind. Eng. Chem. Process Res. Dev., 9, 148 (1970).

12. M. Adams Viola, G.D. Botsaris, W.G. Filmyer, Jr., Y.M. Glazman and K.D. King, in Proc. of 4th Int. Symp. on Coal Slurry Combustion,

Orlando, Florida, 1982.

13. M. Adams Viola, G.D. Botsaris, W.G. Filmyer, Jr., Y.M. Glazman and K.D. King, Colloids and Surfaces, 4, 225 (1982).

14. K.C. Adiga, R. Rangnekar, B. Moudgil and D.O. Shah in Proc. of 4th Int. Symp. on Coal Slurry Combustion, Orlando, Florida, 1982.

15. J.E. Funk, U.S. Patent No. 4,288,006, 1981.

16. L.D. Smoot, Paper presented at the DOE Contractors Meeting on Pulverized Coal Combustion, Pittsburgh, 1982.

17. R.R. Faddick, "Properties of Coal-Water Slurries," Bur. Mines Report OFR 53-76, 1974.

18. R.O. James and T.W. Healy, J. Colloid Interface Sci., 40, 53 (1972).

ACKNOWLEDGMENT

This work was supported by the Department of Energy under contract FG22-81PC40285.

SOME RHEOLOGICAL DATA AND ATOMIZATION BEHAVIOUR OF CWM'S CONTAINING 68 to 83 % COAL

Lars Gillberg
Nils Larsson
Mihkel Mathiesen
Olle Nyström
Jan-Erik Persson

AB Carbogel, Helsingborg, Sweden.

A concentrated CWM mixture was prepared based on air dried filter cake from pilot plant milling at 6 tons/hour. The CWM was diluted in increments for determination of rheological properties and atomization behaviour whereby both particle size distribution and the ratio of dispersing agent over coal content were kept constant.

In addition, CWM samples with high water content were prepared with various concentrations of stabilizer. The rheological properties and atomization behaviour are discussed and a relationship between slurry viscosity and mass median diameter of atomized droplets is proposed.

1. Sample Preparation

Coal water slurry samples with varying moisture contents were prepared by diluting an 80 kg master batch to varying degrees from the original total moisture content of 16.7 % by weight of slurry (As determined with a Mettler PC440 balance with drying unit LP15). The coal used was a medium volatile bituminous coal ex United Coal Companies, Virginia (Widow Kennedy seam, 6 % mineral matter and 28 % volatiles on dry basis). It was milled in a pilot operation at 6 tons/hour in a circuit comprising primary rod mill and secondary ball mill. The size distribution was as follows:

99.9 %	- 200 µm
90.0 %	- 132 µm
75.0 %	- 80 µm
50.0 %	- 44 µm
24.0 %	- 15 µm

Portions - approximately 7 kgs - of the master batch were diluted with deionized water to form dispersions with increasing moisture contents; 19.4 %, 22.4 %, 25.2 %, 28.2 %, 30.2 % and 32.3 % . The dilute slurry portion containing 32.3 % moisture was made into a larger batch and divided into three portions, two of which were further admixed with different amounts of stabilizer, to obtain viscosities corresponding to the slurry portions with 28.2 % and 22.4 % moisture respectively.

This method of slurry preparation ensured that the coal/dispersant ratio and the particle size distribution were kept identical in all nine samples. In addition to these one further sample was prepared using the same ground coal product and a lower molecular weight dispersant, hereinafter denoted "B". This 31.9 % moisture content slurry had to be stabilized in order to avoid rapid settling and was given a viscosity roughly corresponding to that of the 22.4 % moisture slurry. The dispersant used in the master batch will be denoted dispersant "A".

2. Slurry Properties

2.1 Rheology

Slurry flow curves were obtained by shearing small samples in a Contraves Rheomat 115 cup and bob viscometer according to DIN standard. Measuring system 125 was used. The precision of the measurements varied with the shear history and instrumental settings from 0.004 to 0.15 Pas. The procedure included low shear stirring prior to pouring slurry into viscometer cup, whereupon rheograms were taken during a 13 minute shear acceleration from 0 to 450 s^{-1}, followed by deceleration for an equal time. Viscosity change with time at constant shear rate was determined at 31 and 450 s^{-1} respectively. The results are given in tables 1 to 3. Some curves in Table 1 are also given in Figure 1, in order to better clarify the differences.

2.1 Atomizability

The resulting droplet sizes of atomized slurry were obtained from an atomization test rig comprising a Malvern particle analyzer (Model

2200; with 300 mm lens for droplet sizes ranging from 5.8 to 564 μm) using a modified Delavan Airo Nozzle (30615 -56; 50 gph) air assisted internal type atomizer. The modifications done to the commercially available atomizer result in reduced fuel feed pressure and narrowed spray angle; in this case an angle of 20°. Beyond the equipment mentioned above, the test rig comprised a pressure vessel from which the slurry was fed to the atomizer, a critical nozzle for the measurement of the atomizing air, pressure gauges and a collection system, vented by a fan and drained into a well, for confinement of the spray - all according to Figure 2.

With the exception of slurry properties the only parameter actively changed during the measurements was the slurry feed pressure and hence the flow rate, which was obtained by measuring the level in the vessel (depressurized) through time. The compressed air was kept at a constant 1.2 bar at the nozzle.

Evaluation of the results was made by comparing the spray size distributions given by the log-normal and the model independent Malvern programs. If when using the log-normal distribution the percentage above the maximum particle size given in the print out (320 μm) was above approximately 20 % and the model independent distribution did not yield a peak below the maximum detectable particle size (564 μm), the log error value of that particular test run indicated a misfit to the data and the test was discarded. The MMD (mass median diameter) value was an output from the log-normal program.

All ten test slurries were atomized except the slurry from the master batch which was judged to have too high a viscosity for the particular equipment used. Figure 3 shows the feed pressure vs. slurry moisture at 30, 60 and 90 kgs/hour respectively. Figure 4 shows the mass median diameter (MMD) of droplets vs. slurry moisture content (no: 1 - 6) at varied air to slurry ratios and Figure 5 shows the MMD vs. air/slurry feed ratios for slurries 1,4,6,8,9 and 10.

3. Discusssions and Conclusions

3.1 Rheology

The object was to study rheology as a function of slurry moisture content. The method chosen made this possible with the obvious exception of slight differences in coal particle surface coverage with dispersant which is a function of the relative volume of free aqueous phase. In the viscosity vs. shear rate measurements both viscosity and degree of pseudoplasticity decreased with increasing water content. Over the shear accceleration/deceleration cycle the initial viscosity was always higher than the final viscosity indicating that an internal structure was broken by the shearing action and this structure was not re-established in the final stages on low shear deceleration.

When measuring the viscosity at constant shear rate (31 s^{-1}) the slurries with the lowest moisture contents had the largest drop in viscosity vs. time The slurries with a water content above 24 % displayed constant viscosity after 30 minutes shearing while the other

slurries were thixotropic during the whole measuring period.

The results from higher shear rate (450 s^{-1}) distinctly show three phases of slurry behaviour:

i) initial thixotropy ($d\eta/dt < 0$)

ii) transition phase ($d\eta/dt = 0$)

iii) rheopexy ($d\eta/dt > 0$)

Here the slurries with the lowest moisture contents displayed the shortest phases of initial thixotropy followed by transition phase and thereafter a phase of rheopexy. Slurries with moisture contents above 25.2 % all showed a 20 minute initial thixotropy and did not reach rheopexy within the 60 minute measurement time.

Considering also that slurries with more than 30 % moisture displayed no differences in thixotropy (Figure 6) it becomes evident that the thixotropy observed was caused by shear imposed destruction of internal structure. This also influences the observed viscosity changes in the acceleration/deceleration cycles. This internal structure was more pronounced in slurries with low moisture contents. It was more rapidly broken down at higher shear rates at each given moisture content. The rheopexy is believed to be a result of particle sliding, migration and rotation. These effects increase in magnitude with increasing shear rates and lead to an increasing inter-particle volume. The water required to fill this volume is increasingly scarce with decreasing slurry moisture content, which leads to an increasing rheopexy with decreasing slurry moisture contents. Comminution of the particles during the measurement is also an effect which may play a rôle in the development of rheopexy.

An important aspect of the study was to relate slurry water content and extent of internal structure to atomization behaviour. Slurries no. 8 to 10 were prepared for this purpose with high water contents and additional stabilizer (8, 9) and different dispersant-stabilizer (10). The viscosities of these slurries at 450 s^{-1} were near those of slurries 3 (8) and 5 (9, 10) respectively.

Figure 3 classifies the atomizer and slurries used. The approximate shear rates at 30, 60 and 90 kgs/hr were 1100, 2200 and 3000 s^{-1} respectively.

Figure 4 summarizes the spray data for the systems without stabilizer. There is some uncertainty in the data obtained for mass median diameters exceeding 110-120 µm, owing to restrictions in maximum detectable MMD of the particular lens used. This notwithstanding, a relationship was found between the MMD and the viscosities of these slurries at 450 s^{-1}:

$$d_{50} \propto \eta_{450}^{0.3}$$

where: d_{50} denotes MMD

η_{450} denotes viscosity at 450 s^{-1}

The relationship is valid for the particular slurries used in this study and cannot be transferred to other slurries. It is expected however, that similar relations can be found for other slurry types which are likewise dispersed or do not contain soluble constituents which structure the aqueous phase, i.e. slurries which display a structure caused by inter-particle interaction only. The relationship between atomization behaviour and slurry viscosity when a free water structuring agent is present is suggested by the curves (Figure 4) but requires further investigation to be quantified. It must be noted that as moisture content is decreased to bring the slurry closer to its critical coal concentration the exponent 0.3 tends to increase considerably, indicating that at high solids loadings the atomization process is increasingly influenced by effects other than those prevalent at higher moisture contents - in this specific study above approximately 22 % moisture.

Figure 5 and Table 4 illustrate some further relations between rheological properties and atomization behaviour indicated by the study. The slurries are divided into three different groups in Table 4:

I - Slurries without stabilizer (dispersant A) Viscosity increase at 450 s^{-1} achieved by decreasing moisture content (no: 1, 4 and 5)

II - Slurries with identical moisture content, dispersed with A. Viscosity increase at 450 s^{-1} achieved by adding increasing concentrations of hydrocolloid (no: 1, 8 and 9)

III - Slurries with near identical moisture content, dispersed with A and B respectively and with low hydrocolloid additions in both (no: 8 and 10)

In Figure 5, three groups of curves can be identified according to the measured MMD. The lowest MMD readings are achieved with slurry number 1. Slurry number 1 therefore will be considered to belong to group "F" (for fine). Slurries 4, 8 and 10 fall into an intermediate group, "M" (medium) and slurries 6 and 9 are identified as belonging to the coarsest group "C".

Slurry Groupings.

Table 4's right column shows at which moisture content slurries containing dispersant "A" as the only additive display similar viscosities at 450 s^{-1} as the slurries listed.

It is evident that the mass median diameter increases with reduced moisture content (Group I) as discussed above and by adding a hydrocolloid to the slurry which adds structure to the slurry by further structuring the aqueous phase (Group II).

It may also be concluded that in the instances where viscosity was increased to a certain level as measured (at 450 s^{-1}) by reducing moisture content the atomization process resulted in significantly

finer sprays than if the same viscosity increase was achieved by hydrocolloid addition. This tendency appears to be enhanced at lower actual/equivalent moisture contents. The observations suggest that successful atomization requires a sufficient volume fraction (in this study $\gtrsim$ 22 % w/w) of free aqueous phase with a minimum of dissolved structuring constituents.

Both slurries within Group III had a similar moisture content, similarly low hydrocolloid content and yielded very similar atomization results but displayed very different viscosities. The difference was due primarily to the difference in dispersants used. This difference manifests itself in the viscosity measurements but is not noticeable in the process of atomization. This again suggests that slurries with sufficient volume fraction of free aqueous phase with low concentrations of structuring constituents will atomize well. It also shows that viscosity data alone are not sufficient for the prediction of their atomization behaviour. Knowledge of the type of dispersants used, other additives present in the slurry and moisture content vs. moisture content at the critical coal concentration of the particular slurry is also required.

Slurry number	Total moisture [wt %]	Density [g/cm³]	VISCOSITY [Pas]									
			ACCELERATED					DECELERATED				
			32.3	100	200	300	450	32.3	100	200	300	450
1	32.3	1.208	0.074	0.067	0.063	0.057	0.051	0.057	0.044	0.044	0.046	0.051
2	30.2	1.213	0.099	0.084	0.081	0.076	0.068	0.067	0.058	0.059	0.062	0.068
3	28.2	1.219	0.145	0.137	0.124	0.111	0.101	0.099	0.083	0.086	0.091	0.101
4	25.2	1.231	0.290	0.274	0.245	0.217	0.202	0.177	0.157	0.167	0.180	0.202
5	22.4	1.240	0.593	0.593	0.507	0.440	0.399	0.311	0.310	0.319	0.347	0.399
6	19.4	1.254	1.58	1.64	1.43	1.19	1.05	0.749	0.739	0.819	0.904	1.05
7	16.7	1.264	4.87	5.39	4.78	n.a.	n.a.	2.90	2.77	2.88	n.a.	n.a.

Table 1.

Viscosity at various shear rates, density and moisture content of the master batch and slurries diluted therefrom.
Note: shear rates given in reciprocal seconds.

Slurry number	Total moisture [wt %]	Density [g/cm³]	VISCOSITY [Pas]										Stabilizer [wt %]	Dispersant
			ACCELERATED					DECELERATED						
			32.3	100	200	300	450	32.3	100	200	300	450		
8	32.2	1.203	0.219	0.171	0.143	0.126	0.108	0.117	0.104	0.098	0.099	0.108	0.040	A
9	32.2	1.215	1.41	0.82	0.59	0.48	0.37	1.13	0.62	0.46	0.40	0.37	0.250	A
10	31.9	1.217	1.53	1.05	0.74	0.56	0.45	0.73	0.55	0.46	0.45	0.45	0.060	B

Table 2.

Viscosity, density and moisture content of slurries containing stabilizer.

Table 3.

Viscosity of slurries numbers 1 to 7 measured at constant shear rates for a period of 60 minutes.

Slurry number	Total moisture [wt %]	Shear rate [s^{-1}]	VISCOSITY [Pas]			OBSERVATIONS
			Initial	Lowest	Final	
1	32.3	31	0.08	0.04	0.04	Thixotropy dominates
2	30.2	31	0.12	0.09	0.09	" "
3	28.2	31	0.15	0.11	0.11	" "
4	25.2	31	0.29	0.19	0.19	" "
5	22.4	31	0.64	0.37	0.37	" "
6	19.4	31	1.63	0.95	0.95	" "
7	16.7	31	4.70	2.94	2.94	" "
1	32.3	450	0.10	0.04	0.04	Thixotropic for 20 min
2	30.2	450	0.13	0.07	0.07	" " "
3	28.2	450	0.17	0.09	0.09	" " "
4	25.2	450	0.40	0.17	0.17	Thixotropic for 18 min
5	22.4	450	0.77	0.36	0.37	Faintly rheopectic after 30 min
6	19.4	450	2.25	1.01	1.10	Rheopectic after 16 min
7	16.7	450	n.a.	n.a.	n.a.	

Table 4.

Groups of slurries the atomization behaviour of which is described in Figure 5.

Group number	Slurry number	MMD group	Actual moisture % w/w	Dispersant	Hydro colloid % w/w	Equivalent moisture % w/w
I	6	C	19.4	A	–	(19.4)
	4	M	25.2	A	–	(25.2)
	1	F	32.3	A	–	(32.3)
II	9	C	32.2	A	0.25	22
	8	M	32.2	A	0.04	28
	1	F	32.3	A	–	(32.3)
III	10	M	31.9	B	0.06	22
	8	M	32.2	A	0.04	28

Note: The right column shows at which moisture content slurries containing dispersant "A" as the only additive, display similar viscosities at 450 s^{-1} as the slurries listed.

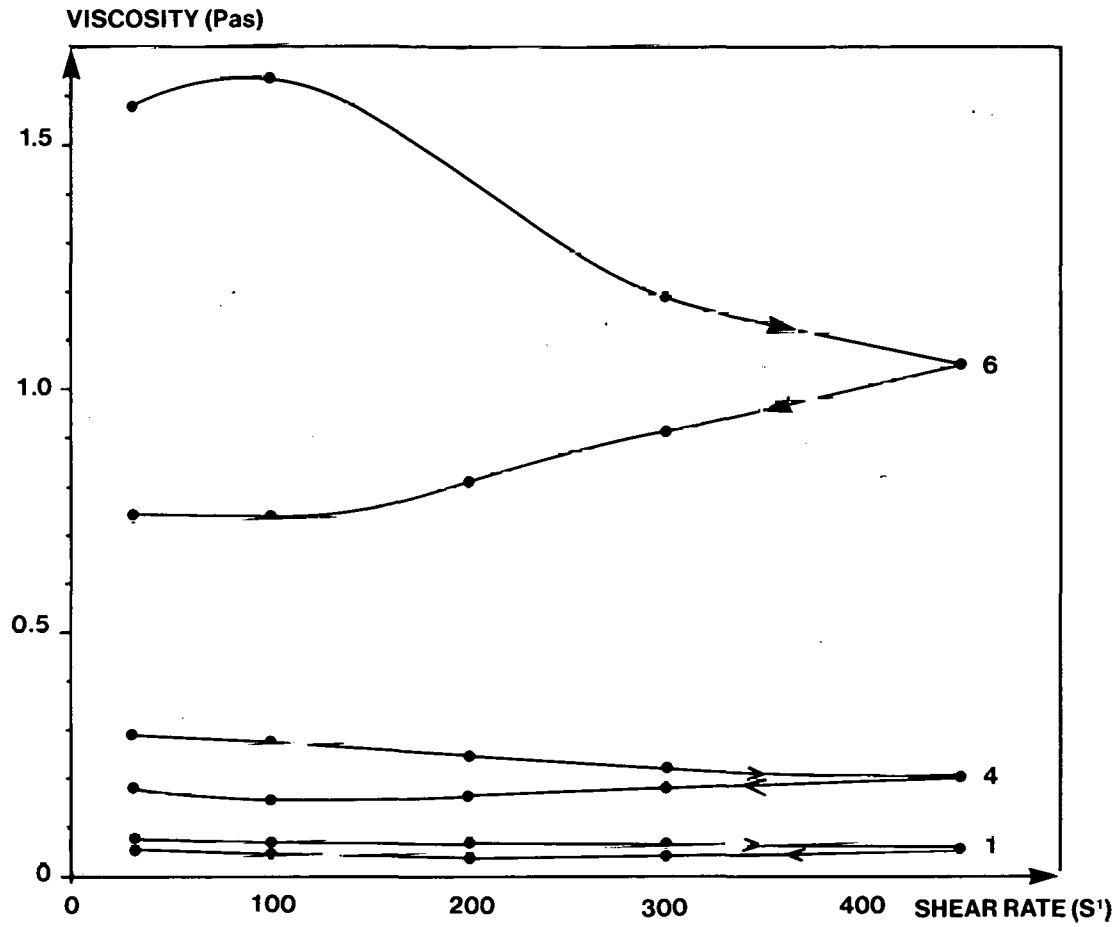

Figure 1.

Viscosity (Pas) vs. shear rate (s-1) for slurries number 1, 4 and 6.

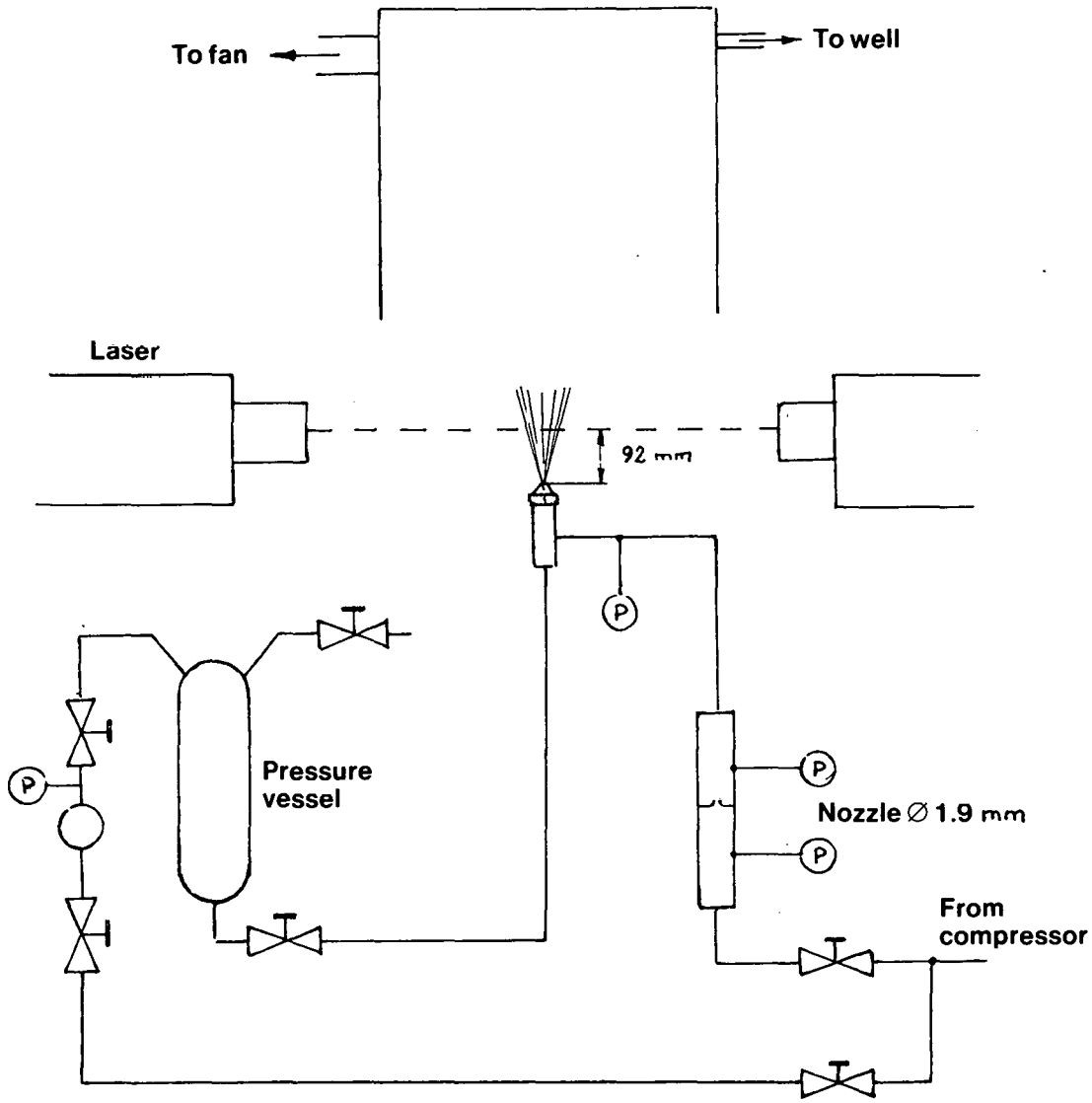

Figure 2.

Atomization test facility.

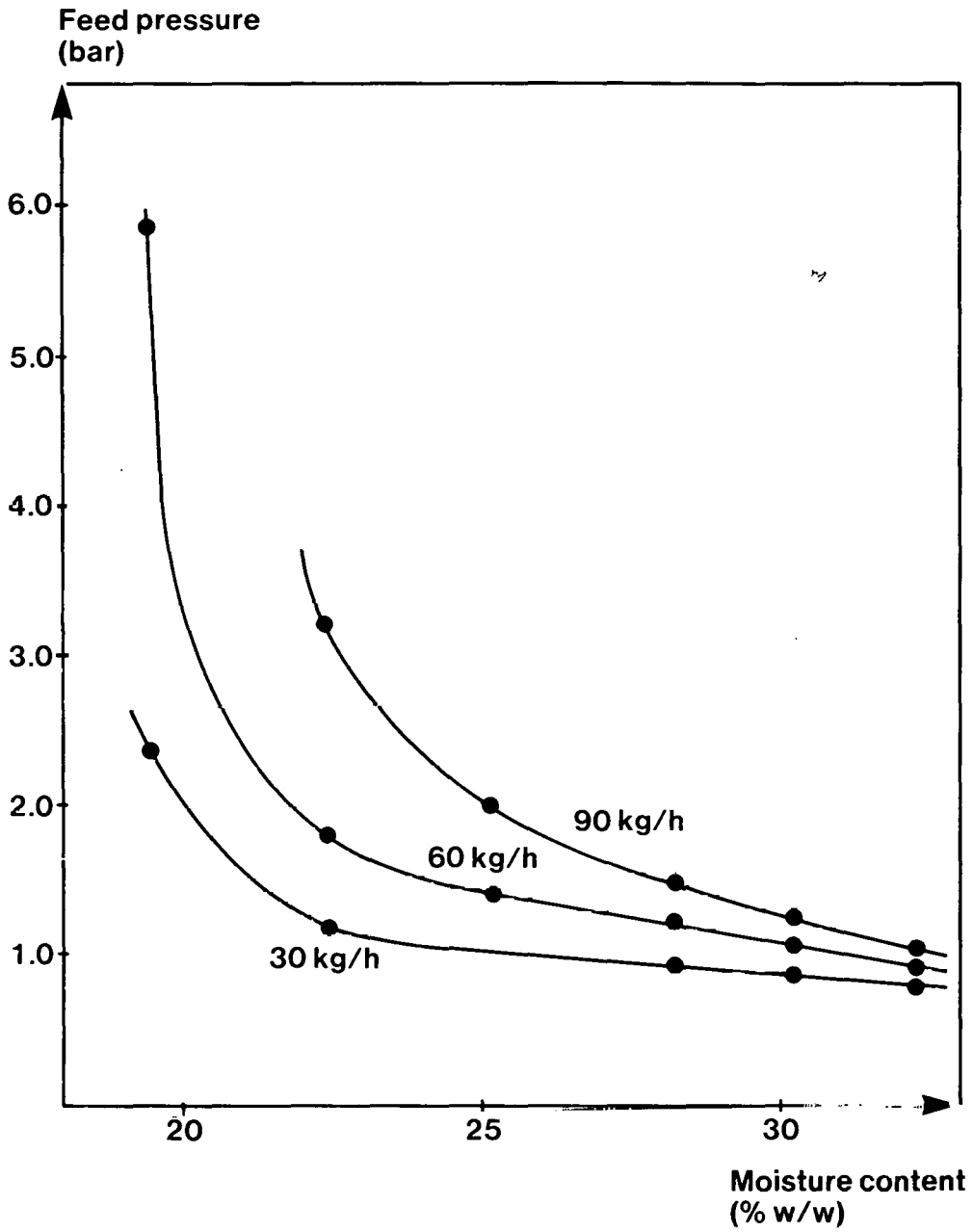

Figure 3.

Feed pressure vs. moisture content at
1.2 bar atomization air pressure and
30, 60 and 90 kg/hr slurry feed respectively.

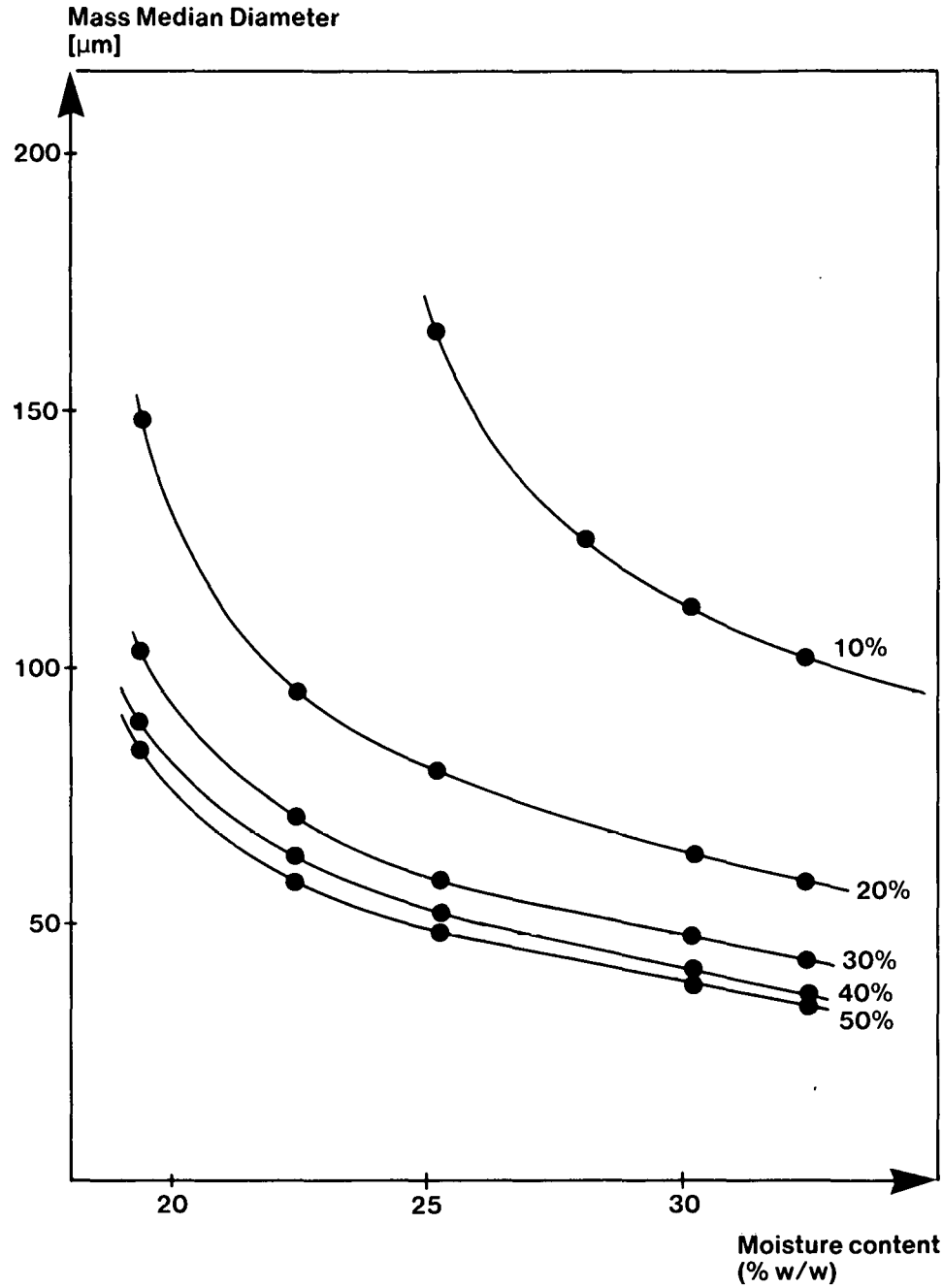

Figure 4.

Mass Median Diameter (µm) vs. moisture content at 1.2 bar atomization air pressure and 10, 20, 30, 40 and 50 % air to slurry ratios

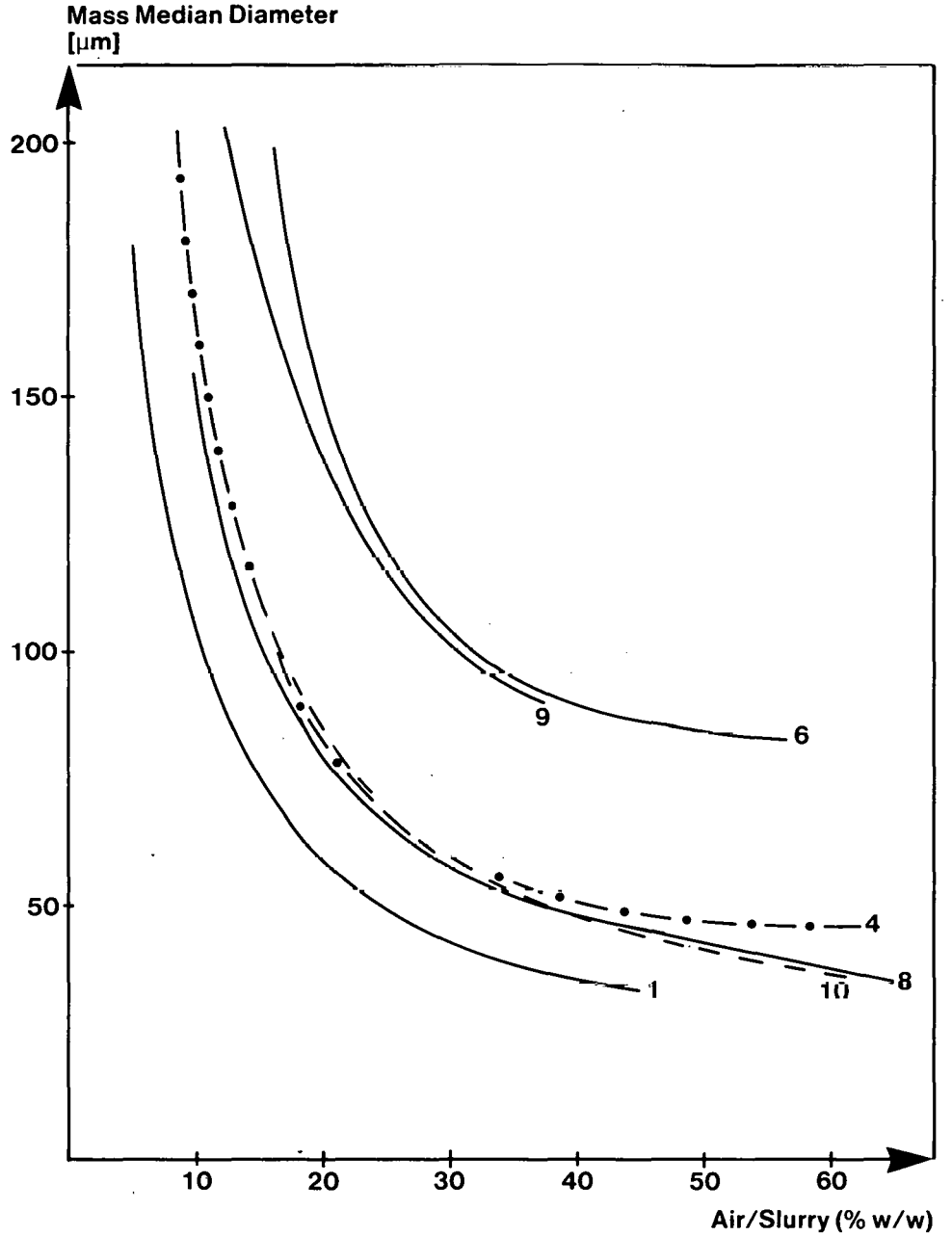

Figure 5.

Mass Median Diameter vs. air to slurry ratio for six slurries, four of which (1, 8, 9 and 10) with a moisture content of 32.2 % and formulated differently. Air pressure at 1.2 bar.

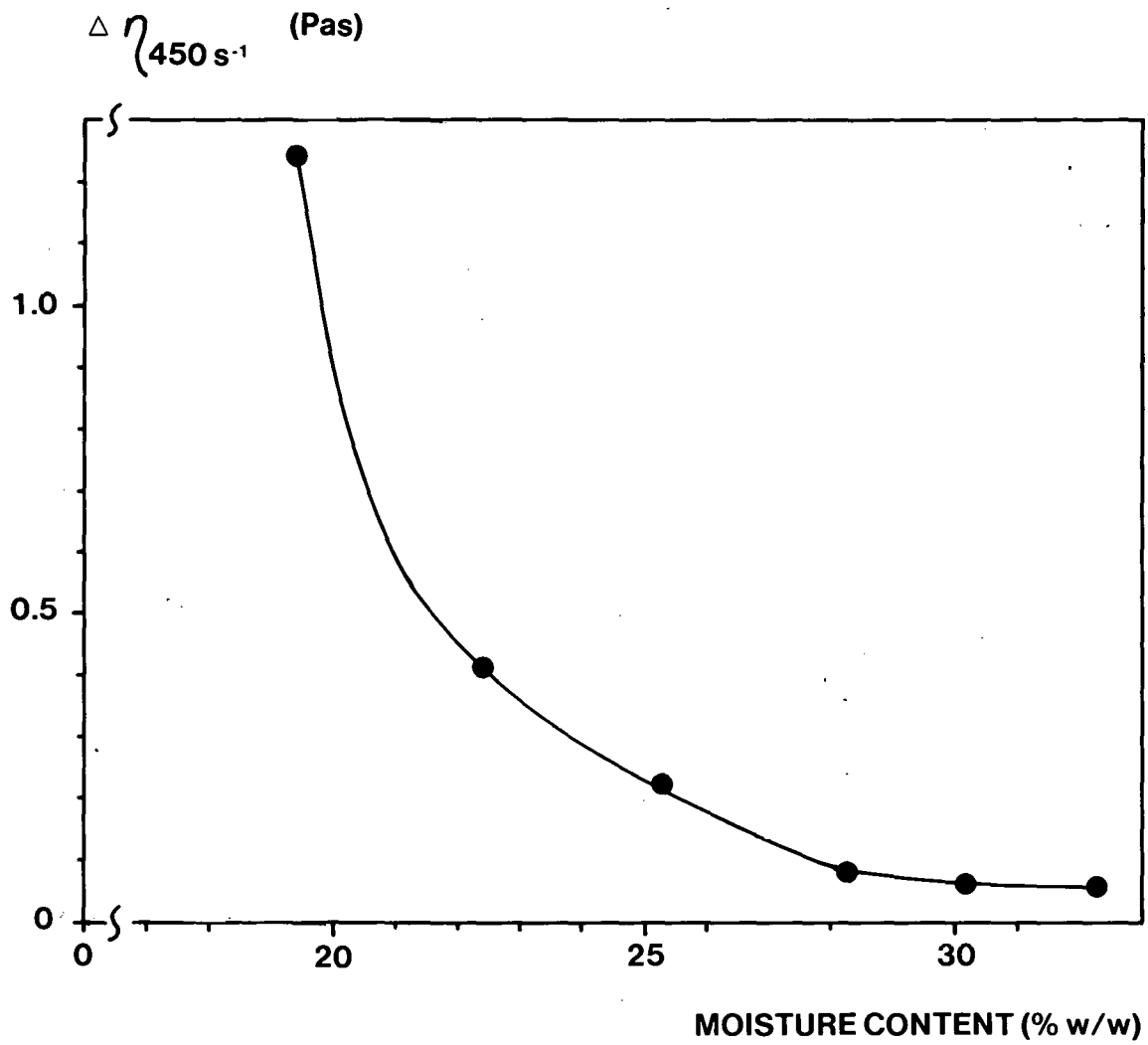

Figure 6.

Initial viscosity - Lowest viscosity at 450 s^{-1}
(Pas) vs. moisture content (% w/w)

Author Index

Page No.

A

ADAMS, D. R. - Island Creek Coal Sales Company 361
ADIGA, K. C. - University of Florida 1070
ALABAF, J. S. - University of Surrey 718
ALBERT, D. - Adelphi Center for Energy Studies, Adelphi University 1142
ANASTASI, J. L. - TRW Inc. 595
ANDERSON, R. J. - Morgantown Energy Technology Center 692, 693
ARIKAWA, Y. - Babcock-Hitachi, K.K., Kure Research Laboratory 151

B

BAJURA, R. A. - Morgantown Energy Technology Center 358
BANDOPADHAYAY, P. C. - CSIRO 46
BARRETT, R. E. - Battelle Columbus Laboratories 872
BATRA, S. K. - GIMRET International, Inc. 625, 1119
BEDROSSIAN, A. - Iron Ore Company of Canada 489
BELLAS, G. T. - Pittsburgh Energy Technology Center 695, 972
BENNETT, A. - National Research Council of Canada 659
BERKSHIRE, L. H. - Morgantown Energy Technology Center 358
BESHORE, D. G. - Cities Service Research and Development Company 283
BETHELL, P. J. - A. T. Massey Coal Company 238
BOTSARIS, G. D. - Tufts University 1181
BRUMMER, J. - General Electric Environmental Services ... 336
BUCKINGHAM, F. P. - Forney Engineering Company 525
BUELL, D. T. - Florida Power Corporation 323
BURGESS, L. - Gulf+Western 255
BURGESS, J. S. - Iron Ore Company of Canada 489
BURRILL, K. F. - Scotia Liquicoal Ltd. 659

C

CAPES, C. E. - National Research Council of Canada 659
CASASSA, E. Z. - Carnegie-Mellon University 1205
CHEN, S. L. - Energy and Environment Research Corporation 756
CHO, S. H. - Korea Institute of Energy and Resources 757
CHONGQING, Lu-Zhejiang University 1092
CHUISANO, N. - Adelphi Center for Energy Studies, Adelphi University 1142
CLEMENTS, J. T. - Standard Havens Research Corporation 280
COSSEE, R. P. - Shell/NCB Coal Technology Research Group, University of Sheffield 949
COTE, D. - Adelphi Center for Energy Studies, Adelphi University 1142
COVILL, I. D. - Nova Scotia Power Commission 809
CROWE, C. T. - Washington State University 677
CUTTING, J. C. - Gilbert/Commonwealth 337

D

DALEY, R. D. - The Babcock & Wilcox Company 1204
DAVIS, B. E. - Gulf Research and Development Company ... 1023
DeMICHELE, G. - Enel-CRTN Pisa 1053
DESHOU, Lu - Zhejiang University 1092
DIEHL, S. P. - Brigham Young University 973
DILLON, M. L. - Robbins & Myers, Inc. 542
DOOHER, J. - Adelphi Center for Energy Studies, Adelphi University 1091, 1142
DOWNIE, R. J. - CSIRO 46
DUDLEY, W. E. - Florida Power Corporation 318
DURET, Y. - Iron Ore Company of Canada 489

Page No.

E

ECKHART, C. F. - The Babcock & Wilcox Company 381
EKMANN, A. C. - Pittsburgh Energy Technology Center 214
EKMANN, J. - Pittsburgh Energy Technology Center 694
EN-HAI, Hou - Xian Thermal Power Research Institute 478

F

FADDICK, R. R. - Colorado School of Mines 826
FANG-JIE, Xu - Xian Thermal Power Research Institute 478
FARTHING, Jr., G. A. - The Babcock & Wilcox Company 1204
FORD, F. - Occidental Research Corporation 75
FOX, W. K. - Standard Havens Research Corporation 280
FUJII, K. - Kawasaki Heavy Industries, Ltd. 842
FURMAN, R. C. - Consulting Engineer 579

G

GALLAGHER, D. R. - Gallagher Asphalt Company 280
GANDOLFI, A. J. - University of Toronto & General Comminution, Inc. 656
GAUSACHS, M. - Iron Ore Company of Canada 489
GERMANE, G. J. - Brigham Young University 973
GETTINGER, G. - University of Florida 1070
GIAMMAR, R. D. - Battelle Columbus Laboratories 872
GILLBERG, L. - AB Carbogel 1229
GILMARTIN, B. - Adelphi Center for Energy Studies, Adelphi University 1142
GIULI, M. - Centro Sperimentale Metallurgico 606
GLAZMAN, Y. - Tufts University 1181
GOZELSKI, J. - Adelphi Center for Energy Studies, Adelphi University 1142
GRASSO, M. - Adelphi Center for Energy Studies, Adelphi University 1142
GRAZIADIO, M. - Enel-CRTN Pisa 1053
GRESKOVICH, E. J. - Air Products and Chemicals, Inc. 109
GRIMM, U. - Morgantown Energy Technology Center 692
GUOQUAN, Huang - Zhejiang University 1092

H

HAAG, A. - The Swedish National Board for Energy Source Development 777
HARGROVE, M. J. - Combustion Engineering, Inc. 356, 1023
HAWKINS, G. T. - CoaLiquid, Inc. 3
HEDLEY, A. B. - SHELL/NCB Coal Technology Research Group, University of Sheffield 949
HENDERSON, C. B. - Atlantic Research Corporation 279
HERMAN, D. - Gulf+Western 255
HICKMAN, R. H. - Forney Engineering Company 525
HIGGINS, M. E. - Florida Power Corporation 314, 318
HIGUCHI, H. - Nippon Oil & Fats Co., Ltd. 151
HISHINUMA, Y. - Hitachi Research Laboratory, Hitachi, Ltd. 151
HONG-NIAN, Yun - Institute of Photographic Chemistry 79
HUANG, Y. S. - Imperial Dynasty, Inc. 127

I

IBA, T. - Sumitomo Metal Industries, Ltd. 362
IGARASHI, T. - Nippon Oil & Fats Co., Ltd. 151

J

JONASSON, K. A. - National Research Council of Canada .. 659
JONES, J. F. - TRW, Inc. 595
JOUBERT, J. I. - Pittsburgh Energy Technology Center 695,

Page No.

K

KAJI, R. - Hitachi Research Laboratory, Hitachi, Ltd. 151
KAMIJO, Y. - Tsukishima Kikai Co., Ltd. 179
KANABROCKI, T. - Adelphi Center for Energy Studies, Adelphi University 1091, 1142
KANG, S. K. - Korea Institute of Energy and Resources 757
KATABE, Ken-ichi - Kao Corporation 88
KAWAMURA, T. - Hitachi, Ltd. 151
KEFA, Cen - Zhejiang University 1092
KELLER, Jr., D. V. - Otisca Industries, Ltd. 269
KENNEY, R. B. - GIMRET International, Inc. 1119
KIKKAWA, H. - Kure Research Laboratory, Babcock-Hitachi, K.K. 151
KIM, D. C. - Korea Institute of Energy and Resources 757
KIM, S. J. - Washington State University 677
KIMEL, E. - Burns and Roe, Inc. 897
KIYONAGA, Y. - Lion Corporation 88, 1157
KOJIMA, M. - Sumitomo Metal Industries, Ltd. 362
KOVACH, J. J. - Morgantown Energy Technology Center 693
KOWALCZEWSKI, J. J. - CSIRO 46
KOYAMA, I. - Babcock Hitachi K.K. 409
KUO, H. - Imperial Dynasty, Inc. 127
KURASHIGE, I. - Sumitomo Metal Industries, Ltd. 362
KURODA, H. - Kure Works, Babcock-Hitachi, K.K. 502
KURTZROCK, R. - Pittsburgh Energy Technology Center 897

L

LAPWOOD, K. J. - Fuels and Energy Research Group, University of Surrey 924
LARSSON, N. - AB Carbogel 1229
LEE, S. L. - Imperial Dynasty, Inc. 127
LEVASSEUR, A. A. - Combustion Engineering, Inc. 1023
LI, X. - Institute of Coal Chemistry 112
LI-JUN, Gao - Institute of Engineering Thermophysics 1038
LIGASACCHI, S. - Enel-CRTN Pisa 1053
LILJEDAHL, G. N. - Combustion Engineering Inc. 356
LIPPOLD, J. H. - Atlantic Research Corporation 279
LONG, Jiang - Institute of Photographic Chemistry 79
LOVE, W. C. - Florida Power Corporation 336
LUO, C. - Institute of Coal Chemistry 112
LUO, J. - Institute of Coal Chemistry 533

M

MADGAVKAR, A. J. - Occidental Research Corporation 75
MAIER, G. A. - Florida Power and Light Company 872
MALGARINI, G. - Centro Sperimentale Metallurgico 606
MALICKI, P. - Adelphi Center for Energy Studies, Adelphi University 1142
MANFRED, R. - Electric Power Research Institute 1204
MARNICIO, R. J. - Carnegie-Mellon University 1182
MASAI, T. - Kure Works, Babcock-Hitachi, K.K. 502
MATHIESEN, M. - AB Carbogel 1229
MATSUURA, Y. - Electric Power Development Co., Ltd. 179, 409
McCLANATHAN, L. C. - TRW Inc. 595
McCORMICK, R. J. - Occidental Research Corporation 75
McGARRY, P. - Gulf+Western 255
McHALE, E. T. - Atlantic Research Corporation 279
MENGON, A. M. - Ohio University 37
MEYER, D. K. - Florida Power Corporation 318
MEYERS, R. A. - TRW Inc. 595
MICHAUD, E. R. - The Babcock & Wilcox Company 1204
MINGJIANG, Ni - Zhejiang University 1092
[illegible]KI, T. - Sumitomo Metal Industries, Ltd. 362
[illegible]), Y. - Neos Co., Ltd. 58

Page No.

M

MOLES, F. D. - Fuels and Energy Research Group, University of Surrey 924
MOORE, R. - Occidental Research Corporation 75
MORELAND, W. C. - Morgantown Energy Technology Center 358
MORRIS, W. - General Electric Environmental Services 336
MOUDGIL, B. M. - University of Florida 1070
MOULDER, G. R. - Energy & Minerals Research Company 256
MULLARKEY, M. - Long Island Lighting Company 1142
MURANAKA, Y. - Hitachi Research Laboratory, Hitachi, Ltd. 151
MURATA, M. - Babcock-Hitachi, K.K., ... 151
MUROI, K. - Hitachi, Ltd. 179

N

NAKA, A. - Dai-Ichi Kogyo Seiyaku Co., Ltd. 58
NAKABAYASHI, Y. - Electric Power Development Co., Ltd. .. 842
NAKAMURA, Y. - Hitachi, Ltd. 179
NEIDERT, J., Jr. - Babcock & Wilcox Company 323
NICHOLSON, R. P. - Cape Breton Development Corporation 809
NISHIZAWA, M. - Hitachi Zosen Corporation 409
NOTESTEIN, J. E. - Morgantown Energy Technology Center 358
NYSTROM, O. - AB Carbogel 1229

O

O'TOOLE, A. - Columbus Chase Corporation 1119
OTSUKA, K. - Hitachi Research Laboratory, Hitachi, Ltd. 151

P

PALLELLA, S. - Centro Sperimentale Metallurgico 606
PALUMBO, L. - Centro Sperimentale Metallurgico 606
PAN, Y.S. - Pittsburgh Energy Technology Center 695, 972
PAPACHRISTODOULOU, G. - General Comminution, Inc. ... 656
PARFITT, G. D. - Carnegie-Mellon University 1205
PASSMAN, R. A. - Atlantic Research Corporation 357
PAYNE, R. - Energy and Environmental Research Corporation 756
PERSSON, J. - AB Carbogel 1229
PETERSEN, G. L. - Florida Power Corporation 323
PIA VERNEKER, V. R. - University of Florida 1070
POUNDSTONE, W. N. - Consultant to the Mining Industry ... 280

R

RANKIN, D. M. - New Brunswick, Electric Power 809
RAO, A. S. - Carnegie-Mellon University 1205
RAWLINS, D. C. - Brigham Young University 973
READ, W. R. - CSIRO 46
REUTHER, J. J. - The Pennsylvania State University 109
RHEINFRANK, L., Jr. - Standard Havens Research Corporation 280
RICHARDSON, K. H. - Brigham Young University 973
RICHTER, W. - Energy and Environmental Research Corporation 756
RISING, B. W. - Battelle Columbus Laboratories 872
ROMANOSKY, Jr., R. R. - Morgantown Energy Technology Center 693
ROWELL, R. L. - University of Massachusetts 1111

Page No.

S

SACCENTI, G. - Enel-CRTN Pisa 1053
SALVI, G. - SNAMPROGETTI 1053
SATO, N. - Kawasaki Heavy Industries, Ltd. 179, 842
SATOH, K. - Sumitomo Metal Industries, Ltd. 362
SAVAGE, R. L. - Ohio University 37
SCAVUZZO, S. A. - Babcock & Wilcox Company 323
SCHALL, G. - Draiswerke, Inc. 558
SCHEFFEE, R. S. - Atlantic Research Corporation 279
SELL, F. R. - COMCO 238
SHAH, D. O. - University of Florida 1070
SHILLING, N. - General Electric Environmental Services 336
SHIN, D. H. - Korea Institute of Energy and Resources 757
SHINANO, K. - Sumitomo Heavy Industries, Ltd. 179
SHINOHARA, T. - Tsukishima Kikai Co., Ltd. 409
SINGH, V. P. - Ontario Hydro 17
SKOLNIK, E. G. - Atlantic Research Corporation 279
SMOOT, L. D. - Brigham Young University 973
SNEDDEN, R. B. - Pittsburgh Energy Technology Center 695, 972
SOMMER, H. T. - Carnegie-Mellon University 1182
SONG, Y. - Institute of Coal Chemistry 112
ST. CLAIR, K. A. - Robbins & Myers, Inc. 542
STIGSSON, L. - Fluidcarbon Sweden AB 522
STREET, P. J. - Marchwood Engineering Laboratories, Central Electricity Generating Board 924
STROM, S. S. - Gilbert/Commonwealth, Combustion Engineering 337
SUGINO, Y. - Electric Power Development Co., Ltd. 179, 409
SUZUKI, N. - Electric Power Development Co., Ltd., Kawasaki Heavy Industries, Ltd. 842

T

TAKAHASHI, Y. - Kure Works, Babcock-Hitachi, K.K. ... 151, 502
TAKAO, S. - Electric Power Development Co., Ltd., Kawasaki Heavy Industries, Ltd. 842
TARPLEY, Jr., W. B. - Energy & Minerals Research Company 256
TAYLOR, S. R. - Energy & Minerals Research Company 256
THAYER, W. L. - National Research Council of Canada 659
THOMPSON, Jr., J. F. - U.S. Army Corps of Engineers 304
TOOR, E. W. - Carnegie-Mellon University 1205
TRASS, O. - University of Toronto & General Comminution Inc. 656

V

VECCI, S. J. - The Babcock & Wilcox Company 1204

Page No.

W

WAGONER, C. L. - The Babcock & Wilcox Company 381
WALSH, Jr., W. A. - The Lezzon Group 625
WALTERMIRE, D. M. - Morgantown Energy Technology Center 692
WARFIELD, W. R. - Ohio University 37
WARYACZ, R. E. - Combustion Engineering, Inc. 337
WATANABE, S. - Kure Works, Babcock-Hitachi, K.K. 502
WATANABE, Shin-ichi - Kao Corporation 88, 1157
WEI, T. - Institute of Coal Chemistry 112
WENHUI, Zhai - Institute of Chemistry, Academia Sinica 1000
WHALEY, H. - Energy, Mines and Resources Canada 809
WHITEWAY, S. G. - National Research Council of Canada .. 659
WILBORN, J. - Southern California Edison 756
WILDA, J. C. - COMCO 305
WILLMAN, D. J. - Pittsburgh Energy Technology Center 694, 695
WRIGHT, D. - Adelphi Center for Energy Studies, Adelphi University 1091, 1142

X

XIAO, Zhao - Yang Shupu Power Plant 478
XING-CHANG, Li - Institute of Photographic Chemistry 79
XINYU, Cao - Zhejiang University 1092

Y

YA-NAN, Zhang - Institute of Engineering Thermophysics ... 1038
YAGIELA, A. S. - COMCO 283
YAMAGUCHI, K. - Kawasaki Heavy Industries, Ltd. 409
YAMAMURA, Masaaki - Kao Corporation 88
YANG, X. - Institute of Coal Chemistry 532
YIFENG, Wu - Institute of Engineering Thermophysics, Academia Sinica 1000
YING-SHI, Wang - Institute of Engineering Thermophysics, Academia Sinica 1038
YIZHEN, Wang - Institute of Engineering Thermophysics, Institute of Chemistry 1000
YUNSIEN, Chen - Zhejiang University 1092
YUYING, L. - Institute of Coal Chemistry 533

Z

ZEITZ, V. - Scotia Liquicoal Ltd. 659
ZHANG, C. - Institute of Coal Chemistry 112
ZHANGJIE, Li - Institute of Engineering Thermophysics, Academia Sinica 1000
ZHAOXIANG, Huang - Institute of Engineering Thermophysics, Academia Sinica 1000
ZHENFU, Yuan - Zhejiang University 1092
ZRONEK, S. C. - Ohio University 37